MODEL ORGANISMS: A PRECIOUS RESOURCE FOR UNDERSTANDING OF THE MOLECULAR MECHANISMS UNDERLYING HUMAN PHYSIOLOGY AND DISEASE

EDITED BY: Maria Grazia Giansanti and Roberta Fraschini

PUBLISHED IN: Frontiers in Genetics

frontiers Research Topics

frontiers

ISSN 1664-8714
ISBN 978-2-88963-183-4
DOI 10.3389/978-2-88963-183-4

About Frontiers

Frontiers is more than just an open-access publisher of scholarly articles: it is a pioneering approach to the world of academia, radically improving the way scholarly research is managed. The grand vision of Frontiers is a world where all people have an equal opportunity to seek, share and generate knowledge. Frontiers provides immediate and permanent online open access to all its publications, but this alone is not enough to realize our grand goals.

Frontiers Journal Series

The Frontiers Journal Series is a multi-tier and interdisciplinary set of open-access, online journals, promising a paradigm shift from the current review, selection and dissemination processes in academic publishing. All Frontiers journals are driven by researchers for researchers; therefore, they constitute a service to the scholarly community. At the same time, the Frontiers Journal Series operates on a revolutionary invention, the tiered publishing system, initially addressing specific communities of scholars, and gradually climbing up to broader public understanding, thus serving the interests of the lay society, too.

Dedication to Quality

Each Frontiers article is a landmark of the highest quality, thanks to genuinely collaborative interactions between authors and review editors, who include some of the world's best academicians. Research must be certified by peers before entering a stream of knowledge that may eventually reach the public - and shape society; therefore, Frontiers only applies the most rigorous and unbiased reviews.
Frontiers revolutionizes research publishing by freely delivering the most outstanding research, evaluated with no bias from both the academic and social point of view. By applying the most advanced information technologies, Frontiers is catapulting scholarly publishing into a new generation.

What are Frontiers Research Topics?

Frontiers Research Topics are very popular trademarks of the Frontiers Journals Series: they are collections of at least ten articles, all centered on a particular subject. With their unique mix of varied contributions from Original Research to Review Articles, Frontiers Research Topics unify the most influential researchers, the latest key findings and historical advances in a hot research area! Find out more on how to host your own Frontiers Research Topic or contribute to one as an author by contacting the Frontiers Editorial Office: researchtopics@frontiersin.org

MODEL ORGANISMS: A PRECIOUS RESOURCE FOR UNDERSTANDING OF THE MOLECULAR MECHANISMS UNDERLYING HUMAN PHYSIOLOGY AND DISEASE

Topic Editors:
Maria Grazia Giansanti, National Research Council (CNR), Italy
Roberta Fraschini, University of Milano-Bicocca, Italy

Citation: Giansanti, M. G., Fraschini, R., eds. (2019). Model Organisms: A Precious Resource for Understanding of the Molecular Mechanisms Underlying Human Physiology and Disease. Lausanne: Frontiers Media. doi: 10.3389/978-2-88963-183-4

Table of Contents

frontiers in Genetics

EDITORIAL
published: 10 September 2019
doi: 10.3389/fgene.2019.00822

Editorial: Model Organisms: A Precious Resource for the Understanding of Molecular Mechanisms Underlying Human Physiology and Disease

Maria Grazia Giansanti[1]* *and Roberta Fraschini*[2]*

[1] *Istituto di Biologia e Patologia Molecolari del CNR, Dipartimento di Biologia e Biotecnologie, Università Sapienza di Roma, Roma, Italy,* [2] *Dipartimento di Biotecnologie e Bioscienze, Università degli Studi di Milano-Bicocca, Milano, Italy*

Keywords: model organisms, human diseases, human physiological model, DNA damage, human disorders

Editorial on the Research Topic

Model Organisms: A Precious Resource for the Understanding of Molecular Mechanisms Underlying Human Physiology and Disease

OPEN ACCESS

Edited and Reviewed by:
Inês Barroso,
University of Cambridge,
United Kingdom

***Correspondence:**
Maria Grazia Giansanti
mariagrazia.giansanti@uniroma1.it
Roberta Franschini
roberta.fraschini@unimib.it

Specialty section:
This article was submitted to Genetic Disorders, a section of the journal Frontiers in Genetics

Received: *05 July 2019*
Accepted: *08 August 2019*
Published: *10 September 2019*

Citation:
Giansanti MG and Fraschini R (2019) Editorial: Model Organisms: A Precious Resource for the Understanding of Molecular Mechanisms Underlying Human Physiology and Disease. Front. Genet. 10:822. doi: 10.3389/fgene.2019.00822

INTRODUCTION

This issue includes eight reviews and five research articles, which highlight how research in model organisms lays the foundations for the comprehension of molecular mechanisms underlying human diseases. Although budding yeast and humans are separated by a billion years of evolutionary history, more than 400 essential yeast genes can be replaced with their human orthologs. Pioneering genetic studies in yeast have contributed to understand the mechanisms involved in autophagy and vesicle trafficking, two processes involved in cancer and neurodegenerative disorders (Novick et al., 1980; Takeshige et al., 1992; Mizushima et al., 1998). More recently, production of yeast strains expressing human genes ("humanized yeast") has been essential for the detailed analysis of normal and pathogenic variants (Laurent et al., 2016). *Drosophila melanogaster* provides an extremely valid resource to investigate the mechanisms involved in organ formation and in the pathology of human diseases. Nearly 65% of human genes have orthologs in *D. melanogaster*, and nearly 75% of the genes involved in human disease have functional orthologs in flies (Reiter et al., 2001; Chien et al., 2002). The sophisticated genetic tools offered by *Drosophila* allow rapid generation of models for human disease, assaying the functional effects of human variant alleles and testing new therapeutic drugs (Moulton and Letsou, 2016; Wangler et al., 2017). *Danio rerio* shares vertebrate-conserved characteristics with human including very similar organs and is a highly suitable model system for investigating gene functions involved in hematopoiesis and screening for novel potential drugs (Wangler et al., 2017). Mouse models of human diseases are the most commonly used, reflecting the genetic and physiological similarities between humans and mice (Perlman, 2016).

Using Budding Yeast to Study the Molecular Pathways That Are Altered in Human Diseases

Orlandi et al. used yeast as a model system to study aging of post-mitotic mammalian cells. Their data describe a connection between nicotinamide adenine dinucleotide (NAD^+) content,

mitochondrial functionality, and chronological life span. They show that, during chronological aging, an altered expression of the specific mitochondrial NAD^+ carriers deeply influences the metabolic reprogramming that enables cells to acquire features required to maintain viability during aging.

Ohkuni et al. used yeast as a cellular model of neurodegenerative disorders such as Huntington's disease (HD). They show that the SUMO-targeted ubiquitin ligase (STUbL) Slx5 reduces the toxicity and abnormal transcriptional activity associated with a mutant fragment of huntingtin (Htt) that induces aggregation, the causative agent of HD. Importantly, RNF4, the human ortholog of Slx5, limits the aberrant transcriptional activity of aggregation-prone Htt in yeast and in several cultured human cell lines. Thus, this study uncovers a conserved pathway that counteracts the accumulation of aggregating, transcriptionally active Htt, on chromatin in both yeast and in mammalian cells.

Fraschini's review is focused on the molecular pathways and proteins involved in the control mitotic spindle morphogenesis and function, which are highly conserved from yeast to humans and whose impairment is connected with the development of human diseases. Fraschini illustrates the processes of spindle formation and orientation in yeast and in humans and includes many examples of misregulation that lead to the development of cancer and other human diseases.

Smurova and De Wulf report the role of centromeres and kinetochores in preserving genetic stability; in particular, they describe how centromere transcription contributes to faithful kinetochore function, how pericentromeric chromatin is silenced by RNA processing, and the transcriptional misregulation of (peri)centromeres during stress, natural aging, and disease.

Bonetti et al. illustrate how DNA ends are processed in budding yeast in order to maintain genome stability. DNA double-strand breaks (DSBs) are dangerous lesions that can be repaired by homologous recombination (HR) that occurs after DNA ends are correctly processed by several nucleases by a process called DNA end resection. The same nucleases function also during DNA replication in the processing of replication fork structures. The authors describe current knowledge of the mechanism of resection at DNA DSBs and replication forks.

Natali and Rancati describe the mutator phenotype in budding yeast. The mutator phenotype enhances genome instability and generation of phenotypic variation in a population of cells and increases the probability that some of these variations undergo selection and clonal expansion in challenging environments. This issue is particularly relevant for human health since cancer cells experience an increased mutational charge during early steps of carcinogenesis. The authors discuss the activity of the DNA replication and repair machineries and how mutations can confer increased genome instability. In addition, they describe recent clinical evidences in cancer biology indicating that these lessons can be applied to tumor development.

Using Model Organisms to Model Tumor Formation and Progression

Sollazzo et al. used *Drosophila* larval wing epithelium to investigate the impact of MYC upregulation on cells carrying mutations in neoplastic tumor suppressor genes (nTSGs). MYC overexpression confers to cells mutant for different nTSGs, the ability to initiate multifocal, three-dimensional growth, a hallmark of mammalian pre-cancerous fields.

By using three different models of Ras induction and tumor formation in zebrafish, Anelli et al. demonstrate that six microRNAs increase following expression of a constitutively active $HRAS^{G12V}$ allele. Two Ras-induced microRNAs, namely, miR-146a and miR93a, target the Jmjd6 gene, which encodes a JumonjiC domain protein. Results in this study show that Jmjd6 plays a critical role in zebrafish melanoma development and that miR-146a and miR93a function as tumor suppressors, antagonizing Jmjd6 activation.

Mirzoyan et al. provide a comprehensive insight into the signaling pathways involved in tumorigenesis that are conserved in flies and highlight the ease to genetically manipulate these circuits to study cancer biology. In addition, they describe examples of *Drosophila* cancer models and their use to identify new therapeutic strategies.

Merigliano et al. describe the link between vitamin B6, diabetes, and cancer. Although several data indicate that diabetes and cancer are correlated, the molecular mechanisms involved remain to be clarified. Recent results obtained in *Drosophila* indicate that vitamin B6 deficiency causes hyperglycemia and increases DNA damage. These data suggest that, in diabetic patients, high PLP levels should increase the frequency of DNA damage thus contributing to cancer formation and progression.

Using Model Organisms to Study the Neurological Defects Associated With Human Diseases

Burla et al. (2018) demonstrate that mutant mice with progeroid traits, caused by reduced expression of the *Ft1* gene (the ortholog of human *AKTIP*), display repeated seizures not linked to overt brain morphological alterations or severe neurodegeneration. However, Ft1 reduction is associated with the activation of the inflammatory markers IL-6 and TGF-β. Remarkably, reduction of the guardian of the genome p53 rescues the epileptic behavior and reverses back the expression of IL-6 and TGF-β in *Ft1* mutant mice, suggesting an involvement of DNA damage response in these phenotypes.

Two reviews describe the use of *D. melanogaster* for dissecting the molecular mechanisms underlying the neurological defects in inherited human diseases. Congenital disorders of glycosylation (CDGs) are multisystemic diseases caused by mutations in genes controlling the glycosylation pathways (Freeze et al., 2015). Most CDGs are associated with neurological defects, including mental retardation and seizures. As described by Frappaolo et al. *D. melanogaster* is emerging as a well-suited model organism for modeling congenital disorders of N-linked glycoprotein glycosylation due to a well-characterized glycome and a plethora of electrophysiological and behavioral assays that can be used to test neurological alterations in the whole organism.

The fragile-X (Fra-X) syndrome, caused by mutations in the fragile-X mental retardation (*Fmr1*) is associated with intellectual disability, autism, hyperactivity and language delay, long face and large ears, macroorchidism, and irregular spermatids (Santoro et al., 2012). The *Drosophila* Fra-X disease model recapitulates many phenotypic aspects of the Fra-X syndrome including

defective neuronal architecture and synaptic function and altered germline development. Specchia et al. describe the involvement of dFmr1/FMRP protein in the piRNA pathway and in the DNA genome response, which may open up new perspectives in the search of potential therapeutic targets.

AUTHOR CONTRIBUTIONS

MGG and RF wrote the editorial.

FUNDING

RF researches are supported by grants from PRIN (Progetti di Ricerca di Interesse Nazionale) and from the University of Milano Bicocca (FA). Financial support from the Italian Ministry of University and Research (MIUR) through grant "Dipartimenti di Eccellenza- 2017 "to University of Milano Bicocca, Department of Biotechnology and Biosciences is also acknowledged. Research in MG lab is supported by a grant from Fondazione AIRC per la ricerca sul Cancro (AIRC), grant IG 2017, Id 20779.

REFERENCES

Chien, S., Reiter, L. T., Bier, E., and Gribskov, M. (2002). Homophila: human disease gene cognates in *Drosophila*. *Nucleic Acids Res.* 30 (1), 149–151. doi: 10.1093/nar/30.1.149

Freeze, H. H., Eklund, E. A., Ng, B. G., and Patterson, M. C. (2015). Neurological aspects of human glycosylation disorders. *Annu. Rev. Neurosci.* 38, 105–125. doi: 10.1146/annurev-neuro-071714-034019

Laurent, J. M., Young, J. H., Kachroo, A. H., and Marcotte, E. M. (2016). Efforts to make and apply humanized yeast. *Brief Funct. Genomics.* 15 (2), 155–163. doi: 10.1093/bfgp/elv041

Mizushima, N., Noda, T., Yoshimori, T., Tanaka, Y., Ishii, T., George, M. D., et al. (1998). A protein conjugation system essential for autophagy. *Nature* 395, 395–398. doi: 10.1038/26506

Moulton, M. J., and Letsou, A. (2016). Modeling congenital disease and inborn errors of development in *Drosophila melanogaster. Dis. Model Mech.* 9 (3), 253–269. doi: 10.1242/dmm.023564

Novick, P., Field, C., and Schekman, R. (1980). Identification of 23 complementation groups required for post-translational events in the yeast secretory pathway. *Cell* 21 (1), 205–215. doi: 10.1016/0092-8674(80)90128-2

Perlman, R. L. (2016). Mouse models of human disease: an evolutionary perspective. *Evol. Med. Public Health* (1), 170–176. doi: 10.1093/emph/eow014

Reiter, L. T., Potocki, L., Chien, S., Gribskov, M., and Bier, E. (2001). A systematic analysis of human disease-associated gene sequences in *Drosophila* melanogaster. *Genome Res.* 11 (6), 1114–1125. doi: 10.1101/gr.169101

Santoro, M. R., Bray, S. M., and Warren, S. T. (2012). Molecular mechanisms of fragile X syndrome: a twenty-year perspective. *Annu. Rev. Pathol.* 7, 219–245. doi: 10.1146/annurev-pathol-011811-132457

Takeshige, K., Baba, M., Tsuboi, S., Noda, T., and Ohsumi, Y. (1992). Autophagy in yeast demonstrated with proteinase-deficient mutants and conditions for its induction. *J. Cell Biol.* 119, 301–311. doi: 10.1083/jcb.119.2.301

Wangler, M. F., Yamamoto, S., Chao, H. T., Posey, J. E., Westerfield, M., Postlethwait, J., et al. (2017). Model organisms facilitate rare disease diagnosis and therapeutic research. *Genetics* 207 (1), 9–27. doi: 10.1534/genetics.117.203067

Conflict of Interest Statement: The authors declare that the research was conducted in the absence of any commercial or financial relationships that could be construed as a potential conflict of interest.

frontiers in Genetics

MINI REVIEW
published: 06 August 2019
doi: 10.3389/fgene.2019.00713

The Mutator Phenotype: Adapting Microbial Evolution to Cancer Biology

Federica Natali[1,2] *and Giulia Rancati*[1]*

[1] *Institute of Medical Biology (IMB), Agency for Science, Technology and Research (A*STAR), Singapore, Singapore,* [2] *School of Biological Sciences, Nanyang Technological University, Singapore, Singapore*

The mutator phenotype hypothesis was postulated almost 40 years ago to reconcile the observation that while cancer cells display widespread mutational burden, acquisition of mutations in non-transformed cells is a rare event. Moreover, it also suggested that cancer evolution could be fostered by increased genome instability. Given the evolutionary conservation throughout the tree of life and the genetic tractability of model organisms, yeast and bacterial species pioneered studies to dissect the functions of genes required for genome maintenance (caretaker genes) or for cell growth control (gatekeeper genes). In this review, we first provide an overview of what we learned from model organisms about the roles of these genes and the genome instability that arises as a consequence of their dysregulation. We then discuss our current understanding of how mutator phenotypes shape the evolution of bacteria and yeast species. We end by bringing clinical evidence that lessons learned from single-cell organisms can be applied to tumor evolution.

Keywords: mutator phenotype, cell-to-cell heterogeneity, adaptation, selective pressure, asexually reproducing organisms

OPEN ACCESS

Edited by:
Roberta Fraschini, University of Milano-Bicocca, Italy

Reviewed by:
Michael McDonald, Monash University, Australia
Sylvester Holt, INSERM U1081 Institut de recherche sur le cancer et le Vieillissement, France

***Correspondence:**
Giulia Rancati
giulia.rancati@imb.a-star.edu.sg

Specialty section:
This article was submitted to Genetic Disorders, a section of the journal Frontiers in Genetics

Received: *15 October 2018*
Accepted: *05 July 2019*
Published: *06 August 2019*

Citation:
Natali F and Rancati G (2019) The Mutator Phenotype: Adapting Microbial Evolution to Cancer Biology. Front. Genet. 10:713. doi: 10.3389/fgene.2019.00713

INTRODUCTION

The mutator phenotype was proposed by Loeb almost 40 years ago to reconcile the observations that while cancer cells display widespread DNA and chromosomal changes (Alexandrov et al., 2013; Loeb, 2016), the rate of spontaneous mutation in somatic cells is low (Milholland et al., 2017). This hypothesis also suggested that an increased genome instability favors cancer evolution. Indeed, by reshuffling cancer cell genomes, the mutator phenotype generates cell-to-cell heterogeneity, which is the presence of cells with different genotypes and phenotypes within a population (Loeb, 2016). Since clonal competition within a tumor mass favors the expansion of fitter cells, the presence of cells with different phenotypes within a cancer sample increases the likelihood that some of them might be more aggressive and ultimately leads to poor patient survival (Greaves, 2015; McGranahan and Swanton, 2017). Thanks to the ease with which they can be grown in the laboratory and the wealth of genetic resources, in the last decades, model organisms have been extensively used to identify and dissect the function of genes required for genome stability. For instance, some of the available yeast genome-wide libraries include the systematic knockout collection (Winzeler et al., 1999; Giaever et al., 2002), the green fluorescent protein-tagged collection (Huh et al., 2003), and loss-of-function alleles for essential genes (Ben-Aroya et al., 2008; Breslow et al., 2008; Li et al., 2011). Though progress in our ability to perform high-throughput screens and to manipulate mammalian cells has greatly improved (Behan et al., 2019), it is still difficult to envision a close future in which large-scale screens performed in model organisms could be easily and cost-effectively

reproduced in mammalian cells. A more effective way is to directly translate findings of interesting candidates from model organisms to mammalian cells. For instance, a recent screen in budding yeast showed that, contrary to what was previously thought, heterozygous mutations in gatekeeper genes can cause genome instability (Coelho et al., 2019). Introduction of these mutations in human orthologs triggered genome instability also in human cells (Coelho et al., 2019). Interestingly, only some of the identified genes have been previously found mutated in cancer cells, supporting the idea that findings in budding yeast hold great potential for cancer cell biology.

CELLS LOSING BALANCE

Studies on model organisms have been instrumental to understand mechanisms generating cell-to-cell heterogeneity and its consequence in evolutionary outcomes. While an important route to heterogeneity in yeast is sexual outbreeding (Long et al., 2015; Vazquez-Garcia et al., 2017; Li et al., 2019), this point will not be discussed as evolution of cancer cells is comparable to evolution of asexually reproducing organisms. A route to heterogeneity common between single-cell model organisms and cancer cells involves the dysregulation of the genome integrity network. Initial identification of players of this network in yeast and bacteria was soon followed by the realization that cancer cells carry recurrent mutations in their respective human orthologs and provided ground for key findings. Some popular examples include the identification in cancer cells of cohesion mutations (Hill et al., 2016), of the links between microsatellite instability and the mismatch repair pathway (Kolodner and Marsischky, 1999), and of predicting novel therapeutic targets based on synthetic lethality (Ashworth et al., 2011; Beijersbergen et al., 2017). Though most of the core machinery required for genome maintenance and replication is conserved throughout evolution, there are important exceptions. The most notable differences include the lack of a well-defined nucleotide sequence of the origin of replication in human cells (Gerhardt et al., 2006) and the presence of the human DNA replication inhibitor, geminin (Symeonidou et al., 2012). Yeast cells also lack obvious orthologs of key human DNA repair enzymes, such as breast related cancer antigens 1/2 (BRCA1/2) or poly (ADP-ribose) polymerase (PARP) (Morales et al., 2014; Walsh, 2015). Given the therapeutic importance of some of these proteins, "humanized" yeast strains carrying cancer-associated mutations in BRCA genes have been generated (Guaragnella et al., 2014; Maresca et al., 2018) and used to screen for novel therapeutics.

Due to space constraints, we briefly summarize the role of key DNA repair genes and DNA replication genes. For a detailed overview of the field, please refer to the reviews by Kunkel and Erie (2015), Lujan et al. (2016), and Liu et al. (2017). For a summary of the genes discussed in this paragraph, please refer to **Table 1**.

Mutations Affecting DNA Polymerases

DNA replication of the lagging and the leading strands depends on the activity of two high-fidelity DNA polymerases, DNA polymerases δ (Polδ) and ε (Polε), respectively (Maslowska et al., 2018). The faithfulness of the process relies on the accuracy of nucleotide incorporation coupled with the 3′–5′ exonuclease proofreading activity (Pavlov and Shcherbakova, 2010). Indeed, biochemical assays showed that while purified human Polδ catalyzes one base substitution error every 22,000 nucleotides, the error rate decreased at least 10-fold in presence of a functional proofreading domain (Schmitt et al., 2009). Mouse models lacking a functional Polδ proofreading activity develop spontaneous cancers at high frequency (Goldsby et al., 2002), confirming *in vivo* the importance of the domain for genome stability and cancer formation. Moreover, germline mutations in the proofreading domain of Polδ and Polε have been identified in a number of families with increased susceptibility to colorectal adenomas and carcinomas (Palles et al., 2013; Heitzer and Tomlinson, 2014). Accordingly with an inability to repair mispaired bases inserted during DNA replication, tumors from affected patients increased the rate of base substitution mutations while maintaining microsatellite stability (Palles et al., 2013). Mutations in the proofreading activity of *S. cerevisiae* that mimic mutations in tumors resulted in a mutator phenotype and elevated spontaneous base substitution rates (Murphy et al., 2006; Nick McElhinny et al., 2007).

However, Polδ and Polε mutations outside of the proofreading domain were also mapped in sporadic cancers and cancer cell lines (Briggs and Tomlinson, 2013). Introduction of one of such variant, pol3-R696W (human POLD1-R689W), in heterozygosity in *S. cerevisiae* increased 30-fold the rate of forward mutations. At a biochemical level, pol3-R696W was shown to be an error-prone DNA polymerase with an increased nucleotide misinsertion rate and a specific mutational pattern (Daee et al., 2010) that is consistent with the one observed in colorectal cancer lines bearing the POLD1-R689W variant (Mertz et al., 2017). Collectively, these observations suggest that mutations affecting both the polymerase and the 3'–5' exonuclease domains confer a mutator phenotype that can be translated from bacteria and yeast to human cells.

Mutations Affecting Mismatch Repair Genes

The mismatch repair (MMR) pathway is a conserved surveillance system that recognizes and resolves misincorporated bases (Fishel, 2015). In prokaryotes, the MMR machinery is relatively simple and involves proteins detecting DNA mismatches (MutS), processing the damage (MutH), and bridging these two proteins together (MutL) (Fukui, 2010). While mutations in *mutS* and *mutL* human orthologs were found in the germline of patients with hereditary nonpolyposis colorectal cancer/Lynch syndrome (HNPCC/LS), and other cancer-predisposing Lynch variant syndromes (Lynch and de la Chapelle, 2003; Morales-Burgos et al., 2008; Wimmer and Kratz, 2010), they also somatically occur in up to 15% of sporadic colorectal, gastric, or endometrial carcinomas (Boland et al., 1998). Experimentally, engineered mice lacking functional MMR proteins are genomically unstable and predisposed to spontaneous cancer onset (Lee et al., 2016). Modeling cancer-related MMR mutations in yeast has been instrumental to dissect the consequences on cellular physiology

TABLE 1 | The table reports a list of mutations discussed in the section "Cells losing balance" and details phenotypic consequences arising from such mutations.

Gene	*S. cerevisiae* mutator allel	Type of mutation	Mutated domain	Affected function	Phenotype	Human mutator allele	Clinical relevance
POL3	pol3-D321G (Murphy et al., 2006)	Amino acid substitution (Murphy et al., 2006)	ExoI motif (Murphy et al., 2006)	Exonuclease proofreading activity (Murphy et al., 2006)	Increased forward mutation rate at *CAN1* gene (33-fold), reversion at trp1 locus (13-fold), and reversion at his2 locus (100-fold) compared to WT (Murphy et al., 2006)	POLD1-D316G (Barbari and Shcherbakova, 2017)	Mutation identified in colorectal cancer and endometrial cancer (Barbari and Shcherbakova, 2017)
	pol3-C324Y (Murphy et al., 2006)	As above (Murphy et al., 2006)	As above (Murphy et al., 2006)	As above (Murphy et al., 2006)	As above (Murphy et al., 2006)	POLD1-C319Y (Barbari and Shcherbakova, 2017)	Mutation observed in multiple myeloma and brain tumor (Barbari and Shcherbakova, 2017)
	pol3-L612M (Nick McElhinny et al., 2007)	As above (Nick McElhinny et al., 2007)	DNA polymerase motif (Nick McElhinny et al., 2007)	Partitioning of mismatches to the exonuclease active site (Nick McElhinny et al., 2007)	Increased forward mutation rate at *CAN1* gene (10-fold), compared to WT (Nick McElhinny et al., 2007)	L606M (Shlien et al., 2015)	Mutation observed in biallelic mismatch repair deficiency child brain tumor (Shlien et al., 2015)
	pol3-R696W (Daee et al., 2010)	As above (Daee et al., 2010)	DNA polymerase motif (Daee et al., 2010)	Fidelity of nucleotide incorporation (Daee et al., 2010)	Increased forward mutations at *CAN1* locus (65- to 200-fold) compared to WT (Daee et al., 2010)	POLD1-R689W (Mertz et al., 2017)	Mutation identified in the colon cancer cell line DLD1 (Mertz et al., 2017)
MSH2	msh2-G693S (Drotschmann et al., 1999)	As above (Drotschmann et al., 1999)	Walker A motif of *MSH2* (Drotschmann et al., 1999)	Recognition of base–base mispairs and indels of various size (Drotschmann et al., 1999)	Increase in reverse mutations at lys2::InsE-A14 locus (44- to 10,000-fold) compared to WT (Drotschmann et al., 1999)	hMSH2-G674S (Gammie et al., 2007)	Mutation associated with hereditary nonpolyposis colorectal cancer (HNPCC) (Gammie et al., 2007)
MSH2–MSH6	*MSH2–MSH6* co-overexpression (Chakraborty et al., 2018)	Overexpression (Chakraborty et al., 2018)		Efficiency of other DNA damage repair pathways due to sequestration of factors, such as PCNA (Chakraborty et al., 2018)	As above (Chakraborty et al., 2018)	hMSH2–hMSH6 copy number amplification (Wagner et al., 2016)	Overexpression of MSH2 and MAH6 in oral squamous cell carcinoma from patient's biopsy correlates with poor prognosis (Wagner et al., 2016)
MLH1	mlh1-G64R (Clyne et al., 2009)	Amino acid substitution (Clyne et al., 2009)	ATP binding domain of *MLH1* (Clyne et al., 2009)	Exonuclease activity (Clyne et al., 2009)	Increase in forward -mutations at *CAN1* locus (4- to 8-fold) and reverse mutations at -lys2::InsE-A14 locus (4,000 to 8,000-fold) compared to WT (Clyne et al., 2009)	hMLH1-G67R (Clyne et al., 2009)	Mutation identified in patients with HNPCC (Clyne et al., 2009)
	mlh1-G64E (Clyne et al., 2009)	As above (Clyne et al., 2009)	As above (Clyne et al., 2009)	As above (Clyne et al., 2009)	As above (Clyne et al., 2009)	hMLH1-G67E (Clyne et al., 2009)	Mutation identified in a patient with a family history of atypical cancers, carrying male breast cancer, leiomyosarcoma of the thigh, colon cancer, and prostate cancer (Clyne et al., 2009)

(Continued)

TABLE 1 | Continued

MLH1	*MLH1* overexpression (Shcherbakova and Kunkel, 1999)	Overexpression from the natural promoter or from ADH1 promoter (Shcherbakova and Kunkel, 1999)	Formation of MMR complexes due to excessive binding with Mlh1 (Shcherbakova and Kunkel, 1999)	Increase in forward mutations at *CAN1* locus (2- to 26-fold), reverse mutations at lys2::InsE-A14 (100 to 8,500-fold) and his7-2 (5- to 170-fold) compared to WT (Shcherbakova and Kunkel, 1999)	Overexpression of *MLH1* is triggered by increased genomic damage (Wilczak et al., 2017)	Mlh1 overexpression correlated with genetic instability, advanced tumor stage, and poor outcome in patients with prostatic cancer (Wilczak et al., 2017)
	Δ mlh1 (Shcherbakova and Kunkel, 1999)	Homozygous deletion (haploid) (Shcherbakova and Kunkel, 1999)	Exonuclease activity (Shcherbakova and Kunkel, 1999)	As above (Shcherbakova and Kunkel, 1999)	Reduced expression of *MLH1* due to promoter hypermethylation (Gausachs et al., 2012)	Downregulation of MLH1 associated with the promoter hypermethylation observed in Lynch syndrome patients (Gausachs et al., 2012)
	MLH1/Δ mlh1 (12)	Heterozygous deletion (diploid) (Shcherbakova and Kunkel, 1999)	As above (Shcherbakova and Kunkel, 1999)	As above (Shcherbakova and Kunkel, 1999)	As above (Gausachs et al., 2012)	As above (Gausachs et al., 2012)

ADH1, alcohol dehydrogenase 1; PCNA, proliferating cell nuclear antigen; WT, wild type.

of a non-functional mismatch repair pathway. For instance, mimicking MMR mutations found in HNPCC (Kurzawski et al., 2002) in yeast cells caused an increase in the rate of spontaneous (Drotschmann et al., 1999) and forward mutations (Clyne et al., 2009). Moreover, consistent with the observation that human cancer cell lines with dysregulation in the expression of the MMR proteins are genomically unstable (Ryan et al., 2017; Wilczak et al., 2017), tinkering with the expression levels of the yeast orthologs in *S. cerevisiae* resulted in significant increase of repeats' instability and forward mutations (Shcherbakova and Kunkel, 1999; Chakraborty et al., 2018).

THE RISE AND THE FALL OF THE MUTATOR PHENOTYPE

While maintenance of genome stability is key for reproductive success of prokaryotes and eukaryotes, laboratory and clinical evidence suggests that tinkering with such pathways favors cellular adaptation and population expansion during exposure to challenges. Below we discuss some such evidence.

Lessons from Model Organisms

Several clinical isolates and natural populations of pathogenic bacteria and fungi were reported to have an enhanced mutation rate mostly mapped to defects in the methyl-directed mismatch repair system (Oliver et al., 2000; Bjorkholm et al., 2001; Chopra et al., 2003; Wang et al., 2013; Healey et al., 2016), suggesting that a mutator phenotype could be selected in fluctuating or hostile environments, such as the presence of drugs or adaptation to new ecological niches. Experimental studies have supported this idea. For instance, *MSH2*-defective *Cryptococcus neoformans*, *Candida glabrata*, and *Cryptococcus deuterogattii* strains increased mutation rates and underwent rapid adaptation to antifungal drugs (Healey et al., 2016; Billmyre et al., 2017; Boyce et al., 2017). Similarly, hypermutator *Staphylococcus aureus* bacteria strains impaired in the DNA mismatch repair pathway developed vancomycin resistance more rapidly than control strains (Schaaff et al., 2002). Moreover, mutant strains defective in DNA repair and characterized by increased mutation rates outcompeted wild-type strains and were fixed in 6 out of 12 *E. coli* populations in the Long-Term Evolution Experiment (Tenaillon et al., 2016). A link between increased mutation rates and adaptability comes also from observations that impairment in the activity of DNA repair pathways was often found to co-segregate with mutations conferring antibiotic resistance (Gould et al., 2007). At the theoretical level, a mutator phenotype potentially endows populations with a higher adaptability by generating cell-to-cell heterogeneity and a pool of allelic variants on which selection could select upon (**Figure 1**). Accordingly, mutator *msh2Δ S. cerevisiae* strains acquired resistance to the toxic arginine analog canavanine up to 20-fold faster than wild type (Bowers et al., 1999). Adaptive mutations encompassed single-nucleotide misincorporations and deletions of the canavanine influx pump gene (Sokolsky and Alani, 2000). Since such mutations are edited by the MMR pathway, these observations suggest that crippling with DNA replication or repair pathways could generate beneficial

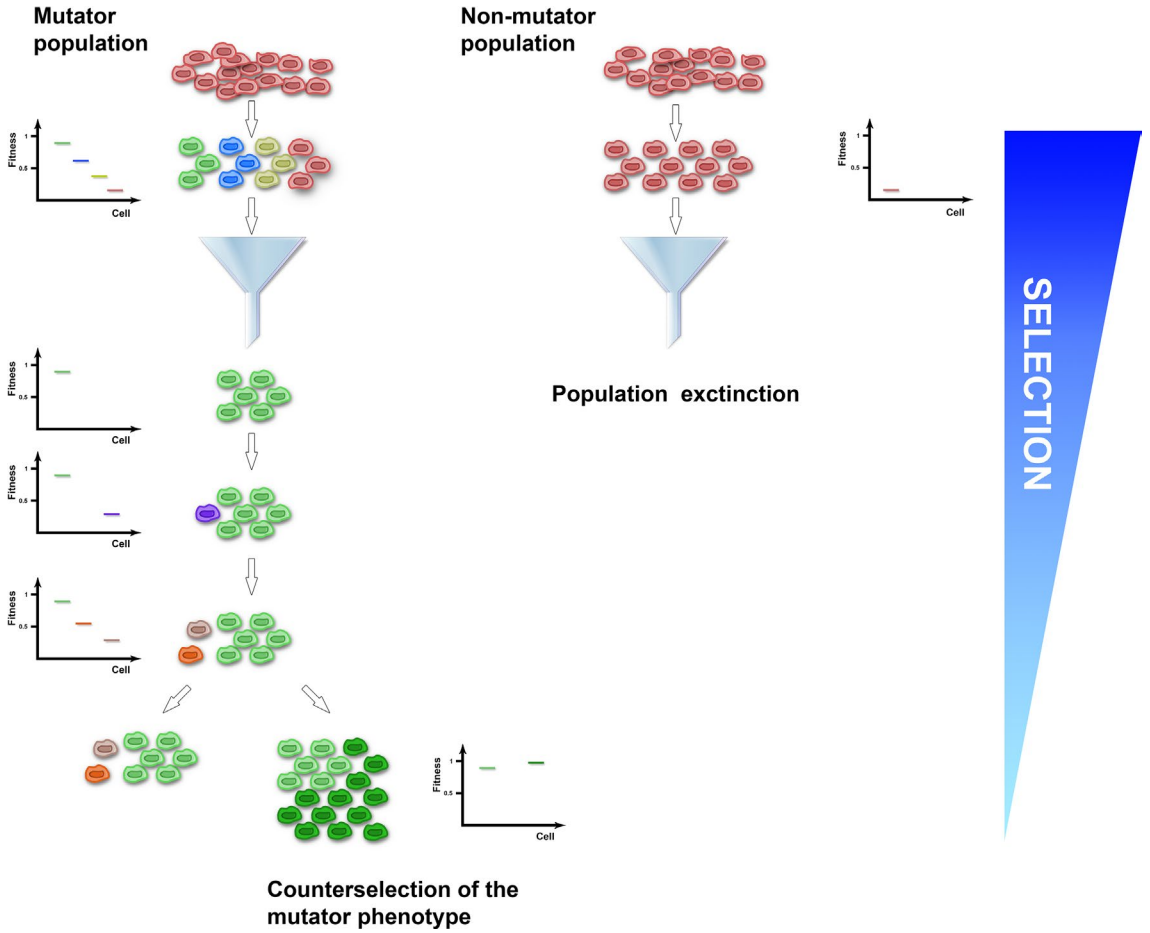

FIGURE 1 | The mutator population (left) experiences enhanced genome instability and acquires cell-to-cell heterogeneity, while the non-mutator population (right) expands clonally. Upon application of selection, the mutator-induced phenotypic variation increases the probability of the population to have cells with a selective advantage (green cells) that could be fixed. Conversely, the clonal non-mutator population has higher probability of becoming extinct (red cells). Once adaptive mutations have been fixed and the population reaches a local optimum, acquisition of additional variation is detrimental and selected against (purple, orange, and grey cells). To increase adaptation in non-selective conditions, the mutator population can evolve a suppressor of the genome instability phenotype (dark green cells).

allelic variants. However, mutators with no direct effect on cellular fitness in asexually evolving unicellular organisms could sweep in a population if they are linked to beneficial mutations, a process called mutator hitchhiking. A large body of evidence coming from theoretical and experimental studies in both bacteria and yeast showed that the probability of hitchhiking has been linked to the population size and the fitness effects of beneficial mutations in complex-to-predict scenarios (Taddei et al., 1997; Notley-McRobb et al., 2002; Shaver et al., 2002; Wahl et al., 2002; Andre and Godelle, 2006; Thompson et al., 2006; Gerrish et al., 2007; Gentile et al., 2011; Raynes et al., 2014; Bui et al., 2015; Good and Desai, 2016). For instance, large population sizes are known to increase clonal interference, which has been shown to either delay or enhance fixation of mutators in different conditions (Raynes et al., 2014; Good and Desai, 2016). However, in populations at local fitness minima or experiencing fluctuating environments, mutators can hitchhike to a higher frequency when linked to strong beneficial mutations. It comes, therefore, as no surprise that mutator multidrug-resistant bacterial strains are a common feature of chronic infections, like cystic fibrosis or urinary tract infections (Oliver et al., 2000; Labat et al., 2005; Feliziani et al., 2010; Macia et al., 2014), where bacterial strains endure pulses of antibiotic treatments. In the laboratory, coupling of cycles of antibiotic or carbon source selection with mutagenesis increased the percentage of strains carrying mutations in mismatch repair genes up to 50–100% (Mao et al., 1997), further supporting the notion that fluctuating environments positively select for mutator strains. However, since the vast majority of mutations are detrimental, genome instability in populations at their fitness peaks comes with a cost (**Figure 1**). Indeed, a general role for asexual pathogenic mutators in the emergence of drug resistance is still being debated, possibly because mutators are selected against once beneficial mutations have been acquired. For instance, *mutS* mutant *S. aureus* laboratory strains characterized by a 78-fold increased mutation frequency did not increase the rate of adaptation to vancomycin (O'Neill and Chopra, 2002). Also, *MSH2* mutations in *C. glabrata* clades were shown to be present as polymorphisms within different natural populations that were equally sensitive or resistant to antifungal drugs (Carrete et al., 2018). At the same

time, *C. glabrata* clinical isolates carrying *MSH2* mutations did not show increased resistance to azole or echinocandin (Singh et al., 2018). Lastly, an *in vivo* model for chronic bone infection in the rat showed that *MSH2* mutant *S. aureus* strains carried a decreased fitness and did not acquire antibiotic resistance (Daurel et al., 2007). The reported discrepancies on the effect of mutators on evolving populations of asexual singe-cell organisms could be linked to clonal interference, mutation effects, or population fitness or could be the result of the negative selection that mutators face once beneficial mutations have been acquired. Indeed, laboratory evidence showed that while mutator strains were initially selected for, both bacteria and yeast mutants experienced reduced transmission and recolonization abilities as well as rapid fitness decline upon prolonged passaging (Giraud et al., 2001; Trindade et al., 2010). These observations suggest that mutator strains could be counterselected once adaptation to the novel environment is achieved. Accordingly, mathematical modeling of *E. coli* population dynamics showed a sharp decline in the frequency of mutator strains once adaptation was achieved (Taddei et al., 1997). At a molecular level, experimental evolution correlated fitness drop of evolving strains with acquisition of detrimental mutations in genes required for optimal fitness (Andersson and Hughes, 1996; Funchain et al., 2000), suggesting that the mutational load of mutator strains could become a selective pressure itself. Accordingly, decreased cellular fitness after prolonged passaging of *msh2Δ* mutator *S. cerevisiae* strains in non-challenging environments was followed by restoration of genome stability by increasing the buffering ability of heat shock proteins (McDonald et al., 2012). Alternatively, restoration of genome stability arose either by acquisition of antimutator suppressor alleles or by replacing the mutator alleles with functional ones through horizontal gene transfer (Denamur et al., 2000; Wielgoss et al., 2013). Taken together, all of this evidence suggests that while the mutator phenotype is initially selected for during adaptation, it could be selected against once adaptive mutations are fixed.

Evidence From Cancer Evolution

Intra- and inter-tumor heterogeneity has been observed in early (Jamal-Hanjani et al., 2017) as well as in advanced stages of tumor progression (Caswell and Swanton, 2017; Jamal-Hanjani et al., 2017). Its presence suggests that cancer proceeds through a branched evolutionary pathway (Nowell, 1976; McGranahan and Swanton, 2017). Specifically, single-cell–derived clones carrying different genomes, epigenomes, and karyotypes compete in a non-linear model that favors the expansion and the coexistence of clones containing distinct beneficial mutations under challenging environments (Merlo et al., 2006). The presence of cell-to-cell heterogeneity promotes cancer progression (Gerlinger et al., 2012; Loeb, 2016; McGranahan and Swanton, 2017) by potentially increasing the number of clones with penetrant driver mutations (Jamal-Hanjani et al., 2017), with resistance to drugs or poor environmental conditions (Scalerandi et al., 1999; Calcagno et al., 2010), or immune to interaction with host immune cells (Seliger, 2005).

Cancer cell populations evolve as asexually reproducing organisms and can be modeled as bacteria or mating-type locked laboratory yeast strains. As discussed above, studies on mutator populations in these model organisms indicate that while a mutator phenotype can initially promote adaptation to a variety of selective pressures, it has detrimental effects once adaptive mutations have been fixed. Does this dynamic also occur during cancer progression? We would like to propose this to be the case. In recent years, the tumultuous advances of deep-sequencing technologies increased our ability to perform and analyze large single-cell sequencing data sets (Gerlinger et al., 2012). By looking at mutations present in cancer cells in spatially distinct regions at different stages of cancer progression, a few lessons have emerged. First, consistent with a positive contribution of genome instability to cancer development and evolution in response to challenges, cancer cells display a high level of intra- and inter-tumor heterogeneity (McGranahan and Swanton, 2017). Experimentally, several mouse models of genome instability display an increased spontaneous incidence of cancer onset (Liu et al., 2007; Weaver et al., 2007) and increased tumor relapse when challenged by oncogene withdrawal (Sotillo et al., 2010). This suggests that mutator phenotype could increase aggressiveness or drug resistance of cancer cells. Second, early evolution stages of different types of cancers display genome instability. Thanks to the long latency and frequent biopsies patients are subjected to, one of the cancer types that undergoes the most frequent longitudinal sampling is Barrett's esophagus. This neoplastic lesion frequently gives rise to esophageal adenocarcinoma and is associated with a high level of genomic instability (Reid et al., 2001). Consistent with the idea that mutator phenotype is an enabling characteristic of tumor development, heterogeneity of premalignant Barrett's esophagus populations is a prognostic marker that correlates with increased probability of esophageal adenocarcinoma development (Maley et al., 2006). Another line of evidence that a mutator phenotype is an early event comes from clinical evidence that mutations in mismatch repair genes and genome instability occur early in HNPCC and colon cancer evolution. For instance, microsatellite instability was found in premalignant adenomas (Shibata et al., 1996), consistent with the idea that mutations in mismatch repair genes occur prior to hallmark mutation markers for colon cancer (Huang et al., 1996). Lastly, mathematical modeling favors a positive contribution of mutator phenotype in early events of cancer progression leading to rapid tumor growth (Beckman, 2009). Therefore, similarly to yeast and bacteria adaptation to hostile environments, the mutator phenotype can facilitate early stages as well as later stages of cancer evolution. Consistently, it was recently shown that metastatic cells have higher mutations rates than non-metastatic cancer cells (Bertucci et al., 2019). However, extreme genomic instability was reported to have a negative effect on tumor growth, leading to massive cancer cell death (Kops et al., 2004; Janssen et al., 2009). Similarly to what observed in model organisms, it was proposed that excessive mutational burden decreased cellular fitness as cells cannot tolerate high levels of genome instability (Komarova and Wodarz, 2004). Accordingly, clinical evidence suggests that high levels of chromosomal instability are a marker for better prognosis than intermediate ones in non-small-cell lung carcinoma (Jamal-Hanjani et al., 2015). Similar observations have been made in other epithelial tumors, such as ovarian and squamous non-small-cell lung cancer and gastric adenocarcinoma (Birkbak et al., 2011). Taken together, all of this clinical evidence suggests that cancer cells, pretty much like mutator

yeasts, can evolve adaptive mechanisms to decrease the rate of genome instability once fitter and more aggressive cancer clones have emerged. This view is also supported by recent studies showing that at different stages of tumor progression, cancer cells exhibit distinct types of genome instability (Nik-Zainal et al., 2012). For instance, sequencing of spatially distant clear-cell renal carcinoma masses within patients showed that, while the bulk of the primary tumor was stable and diploid, cells from metastatic regions derived from a tetraploid intermediate and were genomically unstable (Gerlinger et al., 2012). Moreover, phylogenetic reconstruction of breast cancer tissues carrying BRCA mutations showed that while early mutations during cancer development were consistent with patients' germline mutations, late-stage genome instability had a significantly different mutational pattern consistent with localized hypermutation with specific base substation (Nik-Zainal et al., 2012). Taken together, all of this clinical evidence suggests that different types of genome instability of tumor cells can be selected to better adapt to cycles of selective and non-selective environments as well as different selective pressures.

FUTURE PERSPECTIVE

As speculated above, to better adapt to a variety of different selective and non-selective environments, cancer cells could tinker with their genome instability to either generate cell-to-cell heterogeneity or stabilize fitter clones or change their mutational landscape. Since different types of mutations could allow cells to differently hike the fitness landscape (Pavelka et al., 2010), the ability of cancer cells to switch between different mutational patterns could equip them with different "gears" to successfully adapt to challenges. Therefore, to successfully eradicate cancer cells, strategies to curb their incredible genome plasticity should be found. Given the similarity in the evolution of mutator phenotypes between single-cell model organisms and cancer cells, we predict that dissecting the molecular mechanisms that allow yeast or bacteria to fine-tune their genome instability will pinpoint targets to curb cancer genome plasticity.

AUTHOR CONTRIBUTIONS

FN and GR conceived and wrote the manuscript.

FUNDING

This study is funded by the NRF Investigatorship (ref. no. NRF-NRFI05-2019-0008) awarded to GR.

ACKNOWLEDGMENTS

We thank Dr. Sebastien Teissier and Realite Design for assisting with Figure 1.

REFERENCES

Alexandrov, L. B., Nik-Zainal, S., Wedge, D. C., Campbell, P. J., and Stratton, M. R. (2013). Deciphering signatures of mutational processes operative in human cancer. *Cell. Rep.* 3 (1), 246–259. doi: 10.1016/j.celrep.2012.12.008

Andersson, D. I., and Hughes, D. (1996). Muller's ratchet decreases fitness of a DNA-based microbe. *Proc. Natl. Acad. Sci. U.S.A.* 93 (2), 906–907. doi: 10.1073/pnas.93.2.906

Andre, J. B., and Godelle, B. (2006). The evolution of mutation rate in finite asexual populations. *Genetics* 172 (1), 611–626. doi: 10.1534/genetics.105.046680

Ashworth, A., Lord, C. J., and Reis-Filho, J. S. (2011). Genetic interactions in cancer progression and treatment. *Cell.* 145 (1), 30–38. doi: 10.1016/j.cell.2011.03.020

Barbari, S. R., and Shcherbakova, P. V. (2017). Replicative DNA polymerase defects in human cancers: consequences, mechanisms, and implications for therapy. *DNA Repair (Amst.)* 56, 16–25. doi: 10.1016/j.dnarep.2017.06.003

Beckman, R. A. (2009). Mutator mutations enhance tumorigenic efficiency across fitness landscapes. *PLoS One* 4 (6), e5860. doi: 10.1371/journal.pone.0005860

Behan, F. M., Iorio, F., Picco, G., Goncalves, E., Beaver, C. M., Migliardi, G., et al. (2019). Prioritization of cancer therapeutic targets using CRISPR–Cas9 screens. *Nature* 568 (7753), 511–516. doi: 10.1038/s41586-019-1103-9

Beijersbergen, R. L., Wessels, L. F. A., and Bernards, R. (2017). Synthetic lethality in cancer therapeutics. *Annu. Rev. Cancer Biol.* 1 (1), 141–161. doi: 10.1146/annurev-cancerbio-042016-073434

Ben-Aroya, S., Coombes, C., Kwok, T., O'Donnell, K. A., Boeke, J. D., and Hieter, P. (2008). Toward a comprehensive temperature-sensitive mutant repository of the essential genes of *Saccharomyces cerevisiae*. *Mol. Cell* 30 (2), 248–258. doi: 10.1016/j.molcel.2008.02.021

Bertucci, F., Ng, C. K. Y., Patsouris, A., Droin, N., Piscuoglio, S., Carbuccia, N., et al. (2019). Genomic characterization of metastatic breast cancers. *Nature* 569 (7757), 560–564. doi: 10.1038/s41586-019-1056-z

Billmyre, R. B., Clancey, S. A., and Heitman, J. (2017). Natural mismatch repair mutations mediate phenotypic diversity and drug resistance in *Cryptococcus deuterogattii*. *Elife* 6, e28802. doi: 10.7554/eLife.28802

Birkbak, N. J., Eklund, A. C., Li, Q., McClelland, S. E., Endesfelder, D., Tan, P., et al. (2011). Paradoxical relationship between chromosomal instability and survival outcome in cancer. *Cancer Res.* 71 (10), 3447–3452. doi: 10.1158/0008-5472.CAN-10-3667

Bjorkholm, B., Sjolund, M., Falk, P. G., Berg, O. G., Engstrand, L., and Andersson, D. I. (2001). Mutation frequency and biological cost of antibiotic resistance in *Helicobacter pylori*. *Proc. Natl. Acad. Sci. U.S.A.* 98 (25), 14607–14612. doi: 10.1073/pnas.241517298

Boland, C. R., Thibodeau, S. N., Hamilton, S. R., Sidransky, D., Eshleman, J. R., Burt, R. W., et al. (1998). A National Cancer Institute Workshop on Microsatellite Instability for cancer detection and familial predisposition: development of international criteria for the determination of microsatellite instability in colorectal cancer. *Cancer Res.* 58 (22), 5248–5257.

Bowers, J., Sokolsky, T., Quach, T., and Alani, E. (1999). A mutation in the MSH6 subunit of the *Saccharomyces cerevisiae* MSH2–MSH6 complex disrupts mismatch recognition. *J. Biol. Chem.* 274 (23), 16115–16125. doi: 10.1074/jbc.274.23.16115

Boyce, K. J., Wang, Y., Verma, S., Shakya, V. P. S., Xue, C., and Idnurm, A. (2017). Mismatch repair of DNA replication errors contributes to microevolution in the pathogenic fungus *Cryptococcus neoformans*. *MBio* 8 (3), e00595–17. doi: 10.1128/mBio.00595-17

Breslow, D. K., Cameron, D. M., Collins, S. R., Schuldiner, M., Stewart-Ornstein, J., Newman, H. W., et al. (2008). A comprehensive strategy enabling high-resolution functional analysis of the yeast genome. *Nat. Methods* 5 (8), 711–718. doi: 10.1038/nmeth.1234

Briggs, S., and Tomlinson, I. (2013). Germline and somatic polymerase epsilon and delta mutations define a new class of hypermutated colorectal and endometrial cancers. *J. Pathol.* 230 (2), 148–153. doi: 10.1002/path.4185

Bui, D. T., Dine, E., Anderson, J. B., Aquadro, C. F., and Alani, E. E. (2015). A genetic incompatibility accelerates adaptation in yeast. *PLoS Genet.* 11 (7), e1005407. doi: 10.1371/journal.pgen.1005407

Calcagno, A. M., Salcido, C. D., Gillet, J. P., Wu, C. P., Fostel, J. M., Mumau, M. D., et al. (2010). Prolonged drug selection of breast cancer cells and enrichment of

cancer stem cell characteristics. *J. Natl. Cancer Inst.* 102 (21), 1637–1652. doi: 10.1093/jnci/djq361

Carrete, L., Ksiezopolska, E., Pegueroles, C., Gomez-Molero, E., Saus, E., Iraola-Guzman, S., et al. (2018). Patterns of genomic variation in the opportunistic pathogen *Candida glabrata* suggest the existence of mating and a secondary association with humans. *Curr. Biol.* 28 (1), 15–27 e17. doi: 10.1016/j.cub.2017.11.027

Caswell, D. R., and Swanton, C. (2017). The role of tumour heterogeneity and clonal cooperativity in metastasis, immune evasion and clinical outcome. *BMC Med.* 15 (1), 133. doi: 10.1186/s12916-017-0900-y

Chakraborty, U., Dinh, T. A., and Alani, E. (2018). Genomic instability promoted by overexpression of mismatch repair factors in yeast: a model for understanding cancer progression. *Genetics* 209 (2), 439–456. doi: 10.1534/genetics.118.300923

Chopra, I., O'Neill, A. J., and Miller, K. (2003). The role of mutators in the emergence of antibiotic-resistant bacteria. *Drug Resist. Updat.* 6 (3), 137–145. doi: 10.1016/S1368-7646(03)00041-4

Clyne, M., Offman, J., Shanley, S., Virgo, J. D., Radulovic, M., Wang, Y., et al. (2009). The G67E mutation in hMLH1 is associated with an unusual presentation of Lynch syndrome. *Br. J. Cancer* 100 (2), 376–380. doi: 10.1038/sj.bjc.6604860

Coelho, M. C., Pinto, R. M., and Murray, A. W. (2019). Heterozygous mutations cause genetic instability in a yeast model of cancer evolution. *Nature* 566 (7743), 275–278. doi: 10.1038/s41586-019-0887-y

Daee, D. L., Mertz, T. M., and Shcherbakova, P. V. (2010). A cancer-associated DNA polymerase delta variant modeled in yeast causes a catastrophic increase in genomic instability. *Proc. Natl. Acad. Sci. U.S.A.* 107 (1), 157–162. doi: 10.1073/pnas.0907526106

Daurel, C., Prunier, A. L., Chau, F., Garry, L., Leclercq, R., and Fantin, B. (2007). Role of hypermutability on bacterial fitness and emergence of resistance in experimental osteomyelitis due to *Staphylococcus aureus*. *FEMS Immunol. Med. Microbiol.* 51 (2), 344–349. doi: 10.1111/j.1574-695X.2007.00310.x

Denamur, E., Lecointre, G., Darlu, P., Tenaillon, O., Acquaviva, C., Sayada, C., et al. (2000). Evolutionary implications of the frequent horizontal transfer of mismatch repair genes. *Cell.* 103 (5), 711–721. doi: 10.1016/S0092-8674(00)00175-6

Drotschmann, K., Clark, A. B., Tran, H. T., Resnick, M. A., Gordenin, D. A., and Kunkel, T. A. (1999). Mutator phenotypes of yeast strains heterozygous for mutations in the MSH2 gene. *Proc. Natl. Acad. Sci. U.S.A.* 96 (6), 2970–2975. doi: 10.1073/pnas.96.6.2970

Feliziani, S., Lujan, A. M., Moyano, A. J., Sola, C., Bocco, J. L., Montanaro, P., et al. (2010). Mucoidy, quorum sensing, mismatch repair and antibiotic resistance in *Pseudomonas aeruginosa* from cystic fibrosis chronic airways infections. *PLoS One* 5 (9), e12669. doi: 10.1371/journal.pone.0012669

Fishel, R. (2015). Mismatch repair. *J. Biol. Chem.* 290 (44), 26395–26403. doi: 10.1074/jbc.R115.660142

Fukui, K. (2010). DNA mismatch repair in eukaryotes and bacteria. *J. Nucleic Acids* 2010, 260512. doi: 10.4061/2010/260512

Funchain, P., Yeung, A., Lee Stewart, J., Lin, R., Slupska, M. M., and Miller, J. H. (2000). The consequences of growth of a mutator strain of *Escherichia coli* as measured by loss of function among multiple gene targets and loss of fitness. *Genetics* 154 (3), 959–970.

Gammie, A. E., Erdeniz, N., Beaver, J., Devlin, B., Nanji, A., and Rose, M. D. (2007). Functional characterization of pathogenic human MSH2 missense mutations in *Saccharomyces cerevisiae*. *Genetics* 177 (2), 707–721. doi: 10.1534/genetics.107.071084

Gausachs, M., Mur, P., Corral, J., Pineda, M., González, S., Benito, L., et al. (2012). MLH1 promoter hypermethylation in the analytical algorithm of Lynch syndrome: a cost-effectiveness study. *Eur. J. Hum. Genet.* 20 (7), 762–768. doi: 10.1038/ejhg.2011.277

Gentile, C. F., Yu, S. C., Serrano, S. A., Gerrish, P. J., and Sniegowski, P. D. (2011). Competition between high- and higher-mutating strains of *Escherichia coli*. *Biol. Lett.* 7 (3), 422–424. doi: 10.1098/rsbl.2010.1036

Gerhardt, J., Jafar, S., Spindler, M. P., Ott, E., and Schepers, A. (2006). Identification of new human origins of DNA replication by an origin-trapping assay. *Mol. Cell. Biol.* 26 (20), 7731–7746. doi: 10.1128/MCB.01392-06

Gerlinger, M., Rowan, A. J., Horswell, S., Math, M., Larkin, J., Endesfelder, D., et al. (2012). Intratumor heterogeneity and branched evolution revealed by multiregion sequencing. *N. Engl. J. Med.* 366 (10), 883–892. doi: 10.1056/NEJMoa1113205

Gerrish, P. J., Colato, A., Perelson, A. S., and Sniegowski, P. D. (2007). Complete genetic linkage can subvert natural selecti.on. *Proc. Natl. Acad. Sci. U.S.A.* 104 (15), 6266–6271. doi: 10.1073/pnas.0607280104

Giaever, G., Chu, A. M., Ni, L., Connelly, C., Riles, L., Veronneau, S., et al. (2002). Functional profiling of the *Saccharomyces cerevisiae* genome. *Nature* 418 (6896), 387–391. doi: 10.1038/nature00935

Giraud, A., Matic, I., Tenaillon, O., Clara, A., Radman, M., Fons, M., et al. (2001). Costs and benefits of high mutation rates: adaptive evolution of bacteria in the mouse gut. *Science* 291 (5513), 2606–2608. doi: 10.1126/science.1056421

Goldsby, R. E., Hays, L. E., Chen, X., Olmsted, E. A., Slayton, W. B., Spangrude, G. J., et al. (2002). High incidence of epithelial cancers in mice deficient for DNA polymerase delta proofreading. *Proc. Natl. Acad. Sci. U.S.A.* 99 (24), 15560–15565. doi: 10.1073/pnas.232340999

Good, B. H., and Desai, M. M. (2016). Evolution of mutation rates in rapidly adapting asexual populations. *Genetics* 204 (3), 1249–1266. doi: 10.1534/genetics.116.193565

Gould, C. V., Sniegowski, P. D., Shchepetov, M., Metlay, J. P., and Weiser, J. N. (2007). Identifying mutator phenotypes among fluoroquinolone-resistant strains of *Streptococcus pneumoniae* using fluctuation analysis. *Antimicrob. Agents Chemother.* 51 (9), 3225–3229. doi: 10.1128/AAC.00336-07

Greaves, M. (2015). Evolutionary determinants of cancer. *Cancer Discov.* 5 (8), 806–820. doi: 10.1158/2159-8290.CD-15-0439

Guaragnella, N., Palermo, V., Galli, A., Moro, L., Mazzoni, C., and Giannattasio, S. (2014). The expanding role of yeast in cancer research and diagnosis: insights into the function of the oncosuppressors p53 and BRCA1/2. *FEMS Yeast Res.* 14 (1), 2–16. doi: 10.1111/1567-1364.12094

Healey, K. R., Zhao, Y., Perez, W. B., Lockhart, S. R., Sobel, J. D., Farmakiotis, D., et al. (2016). Prevalent mutator genotype identified in fungal pathogen *Candida glabrata* promotes multi-drug resistance. *Nat. Commun.* 7, 11128. doi: 10.1038/ncomms11128

Heitzer, E., and Tomlinson, I. (2014). Replicative DNA polymerase mutations in cancer. *Curr. Opin. Genet. Dev.* 24, 107–113. doi: 10.1016/j.gde.2013.12.005

Hill, V. K., Kim, J. S., and Waldman, T. (2016). Cohesin mutations in human cancer. *Biochim. Biophys. Acta* 1866 (1), 1–11. doi: 10.1016/j.bbcan.2016.05.002

Huang, J., Papadopoulos, N., McKinley, A. J., Farrington, S. M., Curtis, L. J., Wyllie, A. H., et al. (1996). APC mutations in colorectal tumors with mismatch repair deficiency. *Proc. Natl. Acad. Sci. U.S.A.* 93 (17), 9049–9054. doi: 10.1073/pnas.93.17.9049

Huh, W. K., Falvo, J. V., Gerke, L. C., Carroll, A. S., Howson, R. W., Weissman, J. S., et al. (2003). Global analysis of protein localization in budding yeast. *Nature* 425 (6959), 686–691. doi: 10.1038/nature02026

Jamal-Hanjani, M., A'Hern, R., Birkbak, N. J., Gorman, P., Gronroos, E., Ngang, S., et al. (2015). Extreme chromosomal instability forecasts improved outcome in ER-negative breast cancer: a prospective validation cohort study from the TACT trial. *Ann. Oncol.* 26 (7), 1340–1346. doi: 10.1093/annonc/mdv178

Jamal-Hanjani, M., Wilson, G. A., McGranahan, N., Birkbak, N. J., Watkins, T. B. K., Veeriah, S., et al. (2017). Tracking the evolution of non-small-cell lung cancer. *N. Engl. J. Med.* 376 (22), 2109–2121. doi: 10.1056/NEJMoa1616288

Janssen, A., Kops, G. J., and Medema, R. H. (2009). Elevating the frequency of chromosome mis-segregation as a strategy to kill tumor cells. *Proc. Natl. Acad. Sci. U.S.A.* 106 (45), 19108–19113. doi: 10.1073/pnas.0904343106

Kolodner, R. D., and Marsischky, G. T. (1999). Eukaryotic DNA mismatch repair. *Curr. Opin. Genet. Dev.* 9 (1), 89–96. doi: 10.1016/S0959-437X(99)80013-6

Komarova, N. L., and Wodarz, D. (2004). The optimal rate of chromosome loss for the inactivation of tumor suppressor genes in cancer. *Proc. Natl. Acad. Sci. U.S.A.* 101 (18), 7017–7021. doi: 10.1073/pnas.0401943101

Kops, G. J., Foltz, D. R., and Cleveland, D. W. (2004). Lethality to human cancer cells through massive chromosome loss by inhibition of the mitotic checkpoint. *Proc. Natl. Acad. Sci. U.S.A.* 101 (23), 8699–8704. doi: 10.1073/pnas.0401142101

Kunkel, T. A., and Erie, D. A. (2015). Eukaryotic mismatch repair in relation to DNA replication. *Annu. Rev. Genet.* 49, 291–313. doi: 10.1146/annurev-genet-112414-054722

Kurzawski, G., Suchy, J., Kladny, J., Safranow, K., Jakubowska, A., Elsakov, P., et al. (2002). Germline MSH2 and MLH1 mutational spectrum in HNPCC families from Poland and the Baltic states. *J. Med. Genet.* 39 (10), E65. doi: 10.1136/jmg.39.10.e65

Labat, F., Pradillon, O., Garry, L., Peuchmaur, M., Fantin, B., and Denamur, E. (2005). Mutator phenotype confers advantage in *Escherichia coli* chronic urinary tract infection pathogenesis. *FEMS Immunol. Med. Microbiol.* 44 (3), 317–321. doi: 10.1016/j.femsim.2005.01.003

Lee, K., Tosti, E., and Edelmann, W. (2016). Mouse models of DNA mismatch repair in cancer research. *DNA Repair (Amst.)* 38, 140–146. doi: 10.1016/j.dnarep.2015.11.015

Li, J., Vazquez-Garcia, I., Persson, K., Gonzalez, A., Yue, J. X., Barre, B., et al. (2019). Shared molecular targets confer resistance over short and long evolutionary timescales. *Mol. Biol. Evol.* 36 (4), 691–708. doi: 10.1093/molbev/msz006

Li, Z., Vizeacoumar, F. J., Bahr, S., Li, J., Warringer, J., Vizeacoumar, F. S., et al. (2011). Systematic exploration of essential yeast gene function with temperature-sensitive mutants. *Nat. Biotechnol.* 29 (4), 361–367. doi: 10.1038/nbt.1832

Liu, D., Keijzers, G., and Rasmussen, L. J. (2017). DNA mismatch repair and its many roles in eukaryotic cells. *Mutat. Res.* 773, 174–187. doi: 10.1016/j.mrrev.2017.07.001

Liu, X., Holstege, H., van der Gulden, H., Treur-Mulder, M., Zevenhoven, J., Velds, A., et al. (2007). Somatic loss of BRCA1 and p53 in mice induces mammary tumors with features of human BRCA1-mutated basal-like breast cancer. *Proc. Natl. Acad. Sci. U.S.A.* 104 (29), 12111–12116. doi: 10.1073/pnas.0702969104

Loeb, L. A. (2016). Human cancers express a mutator phenotype: hypothesis, origin, and consequences. *Cancer Res.* 76 (8), 2057–2059. doi: 10.1158/0008-5472.CAN-16-0794

Long, A., Liti, G., Luptak, A., and Tenaillon, O. (2015). Elucidating the molecular architecture of adaptation *via* evolve and resequence experiments. *Nat. Rev. Genet.* 16 (10), 567–582. doi: 10.1038/nrg3937

Lujan, S. A., Williams, J. S., and Kunkel, T. A. (2016). DNA polymerases divide the labor of genome replication. *Trends Cell. Biol.* 26 (9), 640–654. doi: 10.1016/j.tcb.2016.04.012

Lynch, H. T., and de la Chapelle, A. (2003). Hereditary colorectal cancer. *N. Engl. J. Med.* 348 (10), 919–932. doi: 10.1056/NEJMra012242

Macia, M. D., Rojo-Molinero, E., and Oliver, A. (2014). Antimicrobial susceptibility testing in biofilm-growing bacteria. *Clin. Microbiol. Infect.* 20 (10), 981–990. doi: 10.1111/1469-0691.12651

Maley, C. C., Galipeau, P. C., Finley, J. C., Wongsurawat, V. J., Li, X., Sanchez, C. A., et al. (2006). Genetic clonal diversity predicts progression to esophageal adenocarcinoma. *Nat. Genet.* 38 (4), 468–473. doi: 10.1038/ng1768

Mao, E. F., Lane, L., Lee, J., and Miller, J. H. (1997). Proliferation of mutators in A cell population. *J. Bacteriol.* 179 (2), 417–422. doi: 10.1128/jb.179.2.417-422.1997

Maresca, L., Lodovichi, S., Lorenzoni, A., Cervelli, T., Monaco, R., Spugnesi, L., et al. (2018). Functional interaction between BRCA1 and DNA repair in yeast may uncover a role of RAD50, RAD51, MRE11A, and MSH6 somatic variants in cancer development. *Front. Genet.* 9, 397. doi: 10.3389/fgene.2018.00397

Maslowska, K. H., Makiela-Dzbenska, K., Mo, J. Y., Fijalkowska, I. J., and Schaaper, R. M. (2018). High-accuracy lagging-strand DNA replication mediated by DNA polymerase dissociation. *Proc. Natl. Acad. Sci. U.S.A.* 115 (16), 4212–4217. doi: 10.1073/pnas.1720353115

McDonald, M. J., Hsieh, Y. Y., Yu, Y. H., Chang, S. L., and Leu, J. Y. (2012). The evolution of low mutation rates in experimental mutator populations of *Saccharomyces cerevisiae*. *Curr. Biol.* 22 (13), 1235–1240. doi: 10.1016/j.cub.2012.04.056

McGranahan, N., and Swanton, C. (2017). Clonal heterogeneity and tumor evolution: past, present, and the future. *Cell.* 168 (4), 613–628. doi: 10.1016/j.cell.2017.01.018

Merlo, L. M., Pepper, J. W., Reid, B. J., and Maley, C. C. (2006). Cancer as an evolutionary and ecological process. *Nat. Rev. Cancer* 6 (12), 924–935. doi: 10.1038/nrc2013

Mertz, T. M., Baranovskiy, A. G., Wang, J., Tahirov, T. H., and Shcherbakova, P. V. (2017). Nucleotide selectivity defect and mutator phenotype conferred by a colon cancer–associated DNA polymerase delta mutation in human cells. *Oncogene* 36 (31), 4427–4433. doi: 10.1038/onc.2017.22

Milholland, B., Dong, X., Zhang, L., Hao, X., Suh, Y., and Vijg, J. (2017). Differences between germline and somatic mutation rates in humans and mice. *Nat. Commun.* 8, 15183. doi: 10.1038/ncomms15183

Morales-Burgos, A., Sanchez, J. L., Figueroa, L. D., De Jesus-Monge, W. E., Cruz-Correa, M. R., Gonzalez-Keelan, C., et al. (2008). MSH-2 and MLH-1 protein expression in Muir Torre syndrome–related and sporadic sebaceous neoplasms. *P. R. Health Sci. J.* 27 (4), 322–327.

Morales, J., Li, L., Fattah, F. J., Dong, Y., Bey, E. A., Patel, M., et al. (2014). Review of poly (ADP-ribose) polymerase (PARP) mechanisms of action and rationale for targeting in cancer and other diseases. *Crit. Rev. Eukaryot. Gene. Expr.* 24 (1), 15–28. doi: 10.1615/CritRevEukaryotGeneExpr.2013006875

Murphy, K., Darmawan, H., Schultz, A., Fidalgo da Silva, E., and Reha-Krantz, L. J. (2006). A method to select for mutator DNA polymerase deltas in *Saccharomyces cerevisiae*. *Genome* 49 (4), 403–410. doi: 10.1139/g05-106

Nick McElhinny, S. A., Stith, C. M., Burgers, P. M., and Kunkel, T. A. (2007). Inefficient proofreading and biased error rates during inaccurate DNA synthesis by a mutant derivative of *Saccharomyces cerevisiae* DNA polymerase delta. *J. Biol. Chem.* 282 (4), 2324–2332. doi: 10.1074/jbc.M609591200

Nik-Zainal, S., Van Loo, P., Wedge, D. C., Alexandrov, L. B., Greenman, C. D., Lau, K. W., et al. (2012). The life history of 21 breast cancers. *Cell.* 149 (5), 994–1007. doi: 10.1016/j.cell.2012.04.023

Notley-McRobb, L., Seeto, S., and Ferenci, T. (2002). Enrichment and elimination of mutY mutators in *Escherichia coli* populations. *Genetics* 162 (3), 1055–1062.

Nowell, P. C. (1976). The clonal evolution of tumor cell populations. *Science* 194 (4260), 23–28. doi: 10.1126/science.959840

O'Neill, A. J., and Chopra, I. (2002). Insertional inactivation of mutS in *Staphylococcus aureus* reveals potential for elevated mutation frequencies, although the prevalence of mutators in clinical isolates is low. *J. Antimicrob. Chemother.* 50 (2), 161–169. doi: 10.1093/jac/dkf118

Oliver, A., Canton, R., Campo, P., Baquero, F., and Blazquez, J. (2000). High frequency of hypermutable *Pseudomonas aeruginosa* in cystic fibrosis lung infection. *Science* 288 (5469), 1251–1254. doi: 10.1126/science.288.5469.1251

Palles, C., Cazier, J. B., Howarth, K. M., Domingo, E., Jones, A. M., Broderick, P., et al. (2013). Germline mutations affecting the proofreading domains of POLE and POLD1 predispose to colorectal adenomas and carcinomas. *Nat. Genet.* 45 (2), 136–144. doi: 10.1038/ng.2503

Pavelka, N., Rancati, G., and Li, R. (2010). Dr Jekyll and Mr Hyde: role of aneuploidy in cellular adaptation and cancer. *Curr. Opin. Cell Biol.* 22 (6), 809–815. doi: 10.1016/j.ceb.2010.06.003

Pavlov, Y. I., and Shcherbakova, P. V. (2010). DNA polymerases at the eukaryotic fork-20 years later. *Mutat. Res.* 685 (1-2), 45–53. doi: 10.1016/j.mrfmmm.2009.08.002

Raynes, Y., Halstead, A. L., and Sniegowski, P. D. (2014). The effect of population bottlenecks on mutation rate evolution in asexual populations. *J. Evol. Biol.* 27 (1), 161–169. doi: 10.1111/jeb.12284

Reid, B. J., Prevo, L. J., Galipeau, P. C., Sanchez, C. A., Longton, G., Levine, D. S., et al. (2001). Predictors of progression in Barrett's esophagus II: baseline 17p (p53) loss of heterozygosity identifies a patient subset at increased risk for neoplastic progression. *Am. J. Gastroenterol.* 96 (10), 2839–2848. doi: 10.1111/j.1572-0241.2001.04236.x

Ryan, E., Sheahan, K., Creavin, B., Mohan, H. M., and Winter, D. C. (2017). The current value of determining the mismatch repair status of colorectal cancer: a rationale for routine testing. *Crit. Rev. Oncol. Hematol.* 116, 38–57. doi: 10.1016/j.critrevonc.2017.05.006

Scalerandi, M., Romano, A., Pescarmona, G. P., Delsanto, P. P., and Condat, C. A. (1999). Nutrient competition as a determinant for cancer growth. *Phys. Rev. E* 59 (2), 2206–2217. doi: 10.1103/PhysRevE.59.2206

Schaaff, F., Reipert, A., and Bierbaum, G. (2002). An elevated mutation frequency favors development of vancomycin resistance in *Staphylococcus aureus*. *Antimicrob. Agents Chemother.* 46 (11), 3540–3548. doi: 10.1128/AAC.46.11.3540-3548.2002

Schmitt, M. W., Matsumoto, Y., and Loeb, L. A. (2009). High fidelity and lesion bypass capability of human DNA polymerase delta. *Biochimie* 91 (9), 1163–1172. doi: 10.1016/j.biochi.2009.06.007

Seliger, B. (2005). Strategies of tumor immune evasion. *BioDrugs* 19 (6), 347–354. doi: 10.2165/00063030-200519060-00002

Shaver, A. C., Dombrowski, P. G., Sweeney, J. Y., Treis, T., Zappala, R. M., and Sniegowski, P. D. (2002). Fitness evolution and the rise of mutator alleles in experimental *Escherichia coli* populations. *Genetics* 162 (2), 557–566.

Shcherbakova, P. V., and Kunkel, T. A. (1999). Mutator phenotypes conferred by MLH1 overexpression and by heterozygosity for mlh1 mutations. *Mol. Cell. Biol.* 19 (4), 3177–3183. doi: 10.1128/MCB.19.4.3177

Shibata, D., Navidi, W., Salovaara, R., Li, Z.-H., and Aaltonen, L. A. (1996). Somatic microsatellite mutations as molecular tumor clocks. *Nat. Med.* 2 (6), 676–681. doi: 10.1038/nm0696-676

Shlien, A., Campbell, B. B., de Borja, R., Alexandrov, L. B., Merico, D., Wedge, D., et al. (2015). Combined hereditary and somatic mutations of replication error repair genes result in rapid onset of ultra-hypermutated cancers. *Nat. Genet.* 47 (3), 257–262. doi: 10.1038/ng.3202

Singh, A., Healey, K. R., Yadav, P., Upadhyaya, G., Sachdeva, N., Sarma, S., et al. (2018). Absence of azole or echinocandin resistance in *Candida glabrata* isolates in India despite background prevalence of strains with defects in the DNA mismatch repair pathway. *Antimicrob. Agents Chemother.* 62 (6), e00195–18. doi: 10.1128/AAC.00195-18

Sokolsky, T., and Alani, E. (2000). EXO1 and MSH6 are high-copy suppressors of conditional mutations in the MSH2 mismatch repair gene of *Saccharomyces cerevisiae*. *Genetics* 155 (2), 589–599.

Sotillo, R., Schvartzman, J. M., Socci, N. D., and Benezra, R. (2010). Mad2-induced chromosome instability leads to lung tumour relapse after oncogene withdrawal. *Nature* 464 (7287), 436–440. doi: 10.1038/nature08803

Symeonidou, I. E., Taraviras, S., and Lygerou, Z. (2012). Control over DNA replication in time and space. *FEBS Lett.* 586 (18), 2803–2812. doi: 10.1016/j.febslet.2012.07.042

Taddei, F., Radman, M., Maynard-Smith, J., Toupance, B., Gouyon, P. H., and Godelle, B. (1997). Role of mutator alleles in adaptive evolution. *Nature* 387 (6634), 700–702. doi: 10.1038/42696

Tenaillon, O., Barrick, J. E., Ribeck, N., Deatherage, D. E., Blanchard, J. L., Dasgupta, A., et al. (2016). Tempo and mode of genome evolution in a 50,000-generation experiment. *Nature* 536 (7615), 165–170. doi: 10.1038/nature18959

Thompson, D. A., Desai, M. M., and Murray, A. W. (2006). Ploidy controls the success of mutators and nature of mutations during budding yeast evolution. *Curr. Biol.* 16 (16), 1581–1590. doi: 10.1016/j.cub.2006.06.070

Trindade, S., Perfeito, L., and Gordo, I. (2010). Rate and effects of spontaneous mutations that affect fitness in mutator *Escherichia coli*. *Philos. Trans. R. Soc. Lond., B, Biol. Sci.* 365 (1544), 1177–1186. doi: 10.1098/rstb.2009.0287

Vazquez-Garcia, I., Salinas, F., Li, J., Fischer, A., Barre, B., Hallin, J., et al. (2017). Clonal heterogeneity influences the fate of new adaptive mutations. *Cell. Rep.* 21 (3), 732–744. doi: 10.1016/j.celrep.2017.09.046

Wagner, V. P., Webber, L. P., Salvadori, G., Meurer, L., Fonseca, F. P., Castilho, R. M., et al. (2016). Overexpression of MutSalpha complex proteins predicts poor prognosis in oral squamous cell carcinoma. *Medicine (Baltimore)* 95 (22), e3725. doi: 10.1097/MD.0000000000003725

Wahl, L. M., Gerrish, P. J., and Saika-Voivod, I. (2002). Evaluating the impact of population bottlenecks in experimental evolution. *Genetics* 162 (2), 961–971.

Walsh, C. S. (2015). Two decades beyond BRCA1/2: homologous recombination, hereditary cancer risk and a target for ovarian cancer therapy. *Gynecol. Oncol.* 137 (2), 343–350. doi: 10.1016/j.ygyno.2015.02.017

Wang, S., Wang, Y., Shen, J., Wu, Y., and Wu, C. (2013). Polymorphic mutation frequencies in clinical isolates of *Staphylococcus aureus*: the role of weak mutators in the development of fluoroquinolone resistance. *FEMS Microbiol. Lett.* 341 (1), 13–17. doi: 10.1111/1574-6968.12085

Weaver, B. A., Silk, A. D., Montagna, C., Verdier-Pinard, P., and Cleveland, D. W. (2007). Aneuploidy acts both oncogenically and as a tumor suppressor. *Cancer Cell.* 11 (1), 25–36. doi: 10.1016/j.ccr.2006.12.003

Wielgoss, S., Barrick, J. E., Tenaillon, O., Wiser, M. J., Dittmar, W. J., Cruveiller, S., et al. (2013). Mutation rate dynamics in a bacterial population reflect tension between adaptation and genetic load. *Proc. Natl. Acad. Sci. U.S.A.* 110 (1), 222–227. doi: 10.1073/pnas.1219574110

Wilczak, W., Rashed, S., Hube-Magg, C., Kluth, M., Simon, R., Buscheck, F., et al. (2017). Up-regulation of mismatch repair genes MSH6, PMS2 and MLH1 parallels development of genetic instability and is linked to tumor aggressiveness and early PSA recurrence in prostate cancer. *Carcinogenesis* 38 (1), 19–27. doi: 10.1093/carcin/bgw116

Wimmer, K., and Kratz, C. P. (2010). Constitutional mismatch repair-deficiency syndrome. *Haematologica* 95 (5), 699–701. doi: 10.3324/haematol.2009.021626

Winzeler, E. A., Shoemaker, D. D., Astromoff, A., Liang, H., Anderson, K., Andre, B., et al. (1999). Functional characterization of the *S. cerevisiae* genome by gene deletion and parallel analysis. *Science* 285 (5429), 901–906. doi: 10.1126/science.285.5429.901

Conflict of Interest Statement: The authors declare that the research was conducted in the absence of any commercial or financial relationships that could be construed as a potential conflict of interest.

frontiers in Genetics

REVIEW
published: 01 March 2019
doi: 10.3389/fgene.2019.00051

Drosophila melanogaster: A Model Organism to Study Cancer

*Zhasmine Mirzoyan[1], Manuela Sollazzo[2], Mariateresa Allocca[1], Alice Maria Valenza[3], Daniela Grifoni[2] and Paola Bellosta[1,2,3,4]**

[1] Department of Cellular, Computational and Integrative Biology, University of Trento, Trento, Italy, [2] Department of Pharmacy and Biotechnology, University of Bologna, Bologna, Italy, [3] Department of Biosciences, University of Milan, Milan, Italy, [4] Department of Medicine, NYU Langone Medical Center, New York, NY, United States

Cancer is a multistep disease driven by the activation of specific oncogenic pathways concomitantly with the loss of function of tumor suppressor genes that act as sentinels to control physiological growth. The conservation of most of these signaling pathways in *Drosophila*, and the ability to easily manipulate them genetically, has made the fruit fly a useful model organism to study cancer biology. In this review we outline the basic mechanisms and signaling pathways conserved between humans and flies responsible of inducing uncontrolled growth and cancer development. Second, we describe classic and novel *Drosophila* models used to study different cancers, with the objective to discuss their strengths and limitations on their use to identify signals driving growth cell autonomously and within organs, drug discovery and for therapeutic approaches.

Keywords: *Drosophila cancer modeling*, cancer biology, oncogene, tumor suppressor, tissue growth, signaling, metabolism, therapeutic approaches

OPEN ACCESS

Edited by:
Maria Grazia Giansanti, Consiglio Nazionale Delle Ricerche (CNR), Italy

Reviewed by:
Alysia Vrailas-Mortimer, Illinois State University, United States
Fiammetta Verni, Sapienza University of Rome, Italy

***Correspondence:**
Paola Bellosta
paola.bellosta@unitn.it

Specialty section:
This article was submitted to Genetic Disorders, a section of the journal Frontiers in Genetics

Received: *19 September 2018*
Accepted: *21 January 2019*
Published: *01 March 2019*

Citation:
Mirzoyan Z, Sollazzo M, Allocca M, Valenza AM, Grifoni D and Bellosta P (2019) Drosophila melanogaster: A Model Organism to Study Cancer. Front. Genet. 10:51. doi: 10.3389/fgene.2019.00051

INTRODUCTION

The fruit fly, *Drosophila melanogaster*, is used as a model organism to study disciplines ranging from fundamental genetics to the development of tissues and organs. *Drosophila* genome is 60% homologous to that of humans, less redundant, and about 75% of the genes responsible for human diseases have homologs in flies (Ugur et al., 2016). These features, together with a brief generation time, low maintenance costs, and the availability of powerful genetic tools, allow the fruit fly to be eligible to study complex pathways relevant in biomedical research, including cancer. Indeed, publications that use flies to model cancer have exponentially increased in the last 10 years, as shown in the graph of **Figure 1**, suggesting the relevance of this model to cancer research.

In this review we first describe the basic biological mechanisms responsible for uncontrolled growth conserved between humans and flies. We placed a particular emphasis on the characterization of epithelial tumors from most studied models (gut and brain), to novel approaches for studying tumor-induced angiogenesis, prostate, thyroid and lung cancers, with the goal to discuss their strengths and limitations. In the second part, we analyze few physiological mechanisms that uncover potential non-autonomous mechanisms controlling growth, including the relation between the immune cells (macrophages) and the growth of epithelial cells, or the function of lipid metabolism in cancer growth. Finally, we discuss how *Drosophila* models are used to find novel interesting therapeutic approaches.

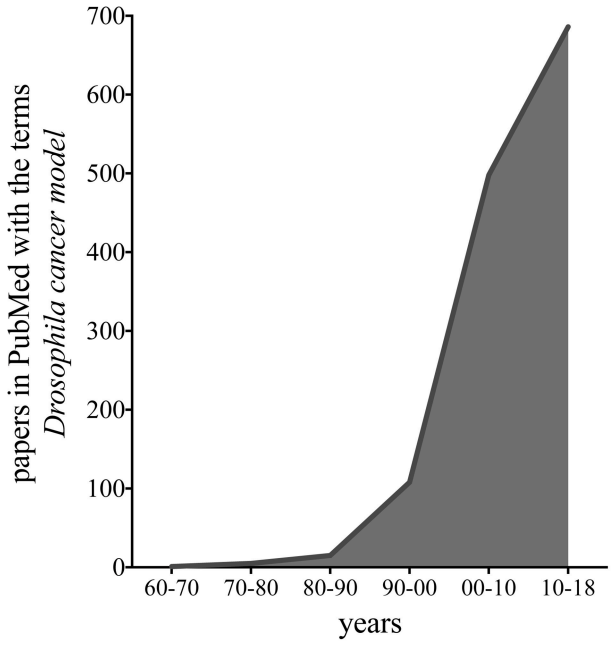

FIGURE 1 | Graph representing the number of publications in PubMed found with the terms "*Drosophila* cancer model," in the last 48 years.

PROPERTIES OF EPITHELIAL CANCER CELLS

Cancer cells are characterized by unrestrained proliferation that results from defects in signaling driving cellular growth, apoptosis and changes in metabolic pathways. At cellular level, the hyperproliferative status of cancer cells is mainly due to the activation of growth signals induced by proto-oncogenes (e.g., the RAS/RAF/MAPK axis), which function downstream of receptor signaling cascades, and are deregulated in 25% of human tumors (Samatar and Poulikakos, 2014). Tumor cells escape the anti-proliferative effect of tumor suppressor genes, such as *RB* (retinoblastoma-associated) and *TP53* genes (Duronio and Xiong, 2013), through mutations in these genes, which result in uncontrolled growth (Hanahan and Weinberg, 2000, 2011; Hariharan and Bilder, 2006). Apoptotic cell death represents another physiological mechanism to maintain cellular homeostasis, and cancer cells have developed strategies to evade apoptosis, i.e., by increasing the activity of anti-apoptotic genes (*Bcl-2, Bcl-xL, Bcl-w*) and of pro-survival factors (*Igf-1, Igf-2*) or by downregulating the action of pro-apoptotic genes (*Bax, PUMA, Bin*) (Hanahan and Weinberg, 2011). Another characteristic of cancer cells is the reactivation of telomerase, present in 90% of human cancers, that allows them to replicate unlimitedly (Kumar et al., 2016).

Cancer cells also exhibit alterations in metabolic pathways that contribute to their survival. Rapidly proliferating cells have a high metabolic rate and suffer from low oxygen conditions (hypoxia). In epithelial tumors, this condition triggers the so-called angiogenic "switch" where the quiescent vascular network is induced to proliferate by the secretion of pro-angiogenic factors, such as VEGF (Vascular Endothelial Growth Factor) and FGF (Fibroblast Growth Factor) (Hida et al., 2018), allowing the formation of new vessels that penetrate into the tumor mass to supply oxygen and nutrients (Carmeliet and Jain, 2011). Cancers cells also exhibit a metabolic switch where they reprogram their metabolism to use an alternative and less abundant anabolic pathway to sustain their growth. In particular they switch from oxidative phosphorylation to anaerobic glycolysis, where glucose is used to produce lactate, through a process called the "Warburg effect" (Pavlova and Thompson, 2016; Vander Heiden and DeBerardinis, 2017). This metabolic switch is not yet completely characterized but is supported by the activation of oncogenes, including Myc that also activates glutaminolysis to fuel the TCA cycle with anaplerotic reactions to produce the intermediates necessary for cellular biosynthesis (Hsieh and Dang, 2016).

The last stage of tumorigenesis is represented by the invasive and metastatic capabilities of tumor cells to disrupt the apical-basal cell polarity, a process that is associated with the downregulation of cell-cell contact molecules and the release of metalloproteases (MMP1), lytic enzymes that degrade the extracellular matrix (ECM) allowing tumor cells to escape and colonize an environment that suites them and to acquire new oncogenic properties (Massague and Obenauf, 2016; Lambert et al., 2017). A variety of studies are now focused on how the tumor micro environment (TME), a specific niche composed of fibroblasts, lymphocytes and immune cells, that may shape pre-cancer cells for their progression into cancer cells and it may select the development of metastasis (Massague and Obenauf, 2016). Emergent evidence suggests also a key role for non-autonomous signals released by the cells composing the niche, particularly from cancer-associated fibroblasts (CAFs), that are essential to support the growth of cancer cells in this "new" metabolic environment (Lambert et al., 2017).

CANCER MODELING IN *DROSOPHILA*

Most of the signaling pathways controlling cell growth and invasion in mammals have a conserved function in flies allowing their modulation into models that mimic tumor's biology in a simple model organism like *Drosophila* (Millburn et al., 2016). The combination of genetic screens with the availability of powerful recombination techniques enabled also a rapid characterization of the primary function of conserved oncogenes and of tumor suppressor genes in a whole animal (Sonoshita and Cagan, 2017). In addition, recent studies using *Drosophila* imaginal discs explored the mechanisms that govern growth in epithelial tumors and their interaction with the local TME and stromal cells, including some steps in the recruitment of the immune cells (macrophages) to the tumor mass (Herranz et al., 2016; Muzzopappa et al., 2017).

EPITHELIAL TUMORS IN *DROSOPHILA*

About 90% of human cancers are of epithelial origin (Hanahan and Weinberg, 2000). Epithelial tissues are characterized by a specific cell architecture composed of junctions and apical and baso-lateral membrane domains that are crucial for the

maintenance of cell-physiological functions. Loss of cell adhesion and cell polarity, with an increase of cell motility, are indeed characteristic early cancer traits. In this context, *Drosophila* larval imaginal discs are a monolayer epithelium that is limited apically by a squamous epithelium (peripodial membrane) and, basally to the notum, by a layer of myoblasts embedded in Extracellular Matrix, and constitute a perfect system in which to model the onset of epithelial cancer progression. These larval organs are indeed morphologically and biochemically comparable to mammalian epithelia (Wodarz and Nathke, 2007). Moreover, the prominent signaling pathways that regulate growth in humans are conserved in the fruit fly (**Figure 2**), allowing the use of this animal model to examine the hallmarks of cancer (St. Johnston, 2002). During the last few years, the imaginal wing and eye discs have been used successfully to study tumor growth and invasion, to investigate the function of cancer genes, and to perform chemical screenings (Tipping and Perrimon, 2014). The imaginal discs also represent an excellent model to analyze oncogenic cooperation: thanks to the use of the MARCM system (Lee and Luo, 1999), it is feasible to induce simultaneously in single cells mutations in tumor suppressor genes (e.g., mutations in cell polarity genes and Hippo pathway components and interactors) and oncogenic activating mutations, or to overexpress specific genes (e.g., EGFR, Ras, Myc, Yorki), resulting in tissue overgrowth, alteration of the normal tissue architecture, disruption of the basement membrane, and invasive/metastatic behavior (Brumby and Richardson, 2003; Pagliarini and Xu, 2003; Wu et al., 2010).

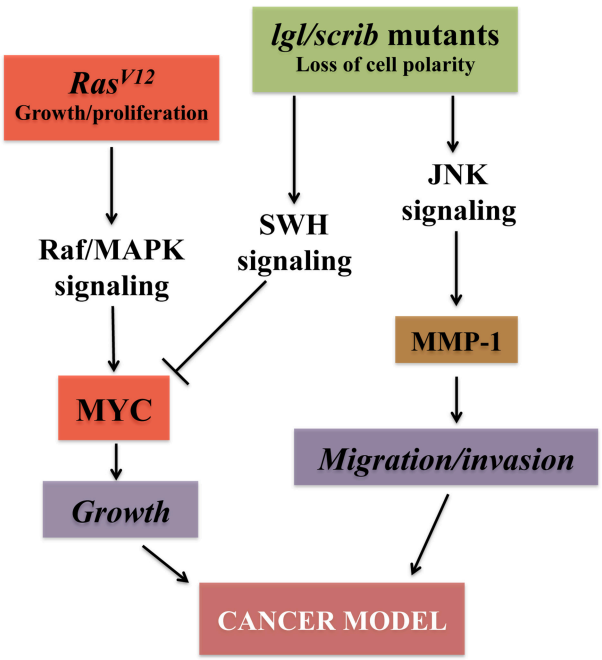

FIGURE 2 | Major pathways converging on uncontrolled growth in *Drosophila* epithelial cells. The signaling pathways outlined confer growth, migration and invasive capabilities to epithelial cells both in vertebrates and flies. Models that mimic the growth of epithelial cancer cells and their ability to undergo metastasis in *Drosophila* have been established by inducing the cooperation between oncogenes (RED) like the active form of Ras (Ras^{V12}) together with the loss of function of cell polarity genes (GREEN) (Brumby and Richardson, 2003; Pagliarini and Xu, 2003). Alteration of cell polarity with the downregulation of the SWH (Salvador-Hippo-Warts) pathway, together with Ras^{V12}, triggers downstream events, including activation of the MAPK signaling that stabilize Myc protein (Galletti et al., 2009) resulting in robust cellular growth. Activation of the JNK signaling, with the concomitant loss of cell polarity, induces metalloproteases (MMP-1) and confers to the epithelial cells the distinct characteristics of migration and invasion, hallmarks of tumor growth (Uhlirova et al., 2005; Igaki et al., 2006; Ma et al., 2017).

Marks of Alteration in Epithelial Cells

Loss of Cell Polarity

Cellular junctions and a proper apical-basal cell polarity are fundamental for the maintenance of epithelial tissue architecture and function. During early cancer stages, tissues lose these properties and cells subvert their normal growth rate and acquire invasive and migratory behaviors (Wodarz and Nathke, 2007; Bryant and Mostov, 2008). In *Drosophila*, three complexes establish and maintain epithelial polarity: the Crumbs/Stardust/PATJ/Bazooka, the Par6/aPKC (atypical protein kinase-C) and the Scrib/Dlg/Lgl (Scribble/Discs large/Lethal giant larvae) complexes, which are respectively placed at the apical, subapical and baso-lateral membrane domains. Alterations in these proteins provoke continued cell proliferation, loss of differentiation and complete loss of tissue architecture, resulting in neoplastic overgrowth (Bilder, 2004; Grzeschik et al., 2010; Johnson and Halder, 2014). *lgl* was the first neoplastic tumor suppressor gene discovered in *Drosophila* and its loss leads to an abnormal growth of the imaginal structures and the larval brain. In addition, *lgl* mutant tissues, and tissues bearing *dlg* or *scrib* mutation, have the ability to form secondary tumors in the thorax, brain, wings, muscles, intestine and ovaries (Woodhouse et al., 1998). The loss of cell polarity impacts cell proliferation through the deregulation of the Hippo (Hpo) pathway, a signaling cascade involved in organ size maintenance (Lu et al., 2010). It is not yet fully known how *lgl* activity interacts with the Hpo cascade, but it was observed that its downregulation up-regulates cell cycle genes (such as Cyclin E and E2F1) (Grzeschik et al., 2007) and permits the nuclear translocation of Yorkie (Yki), the downstream effector of the Hippo pathway, causing the activation of its target genes, including MYC, that was found to be important for the growth of *lgl* mutant clones in a competitive environment (Froldi et al., 2010). In humans, two *lgl* homologs have been discovered, *HUGL-1* and *HUGL-2*, with *HUGL-1* rescuing all the defects of the fly *lgl* mutant (Grifoni et al., 2004). *HUGL-1* loss of function has been associated with a series of human malignancies (Schimanski et al., 2005; Grifoni et al., 2007; Lu et al., 2009). Finally, while the human genome encodes for only one homolog of the tumor suppressor *scrib*, a number of homologs are known for *dlg* which have been implicated in different types of cancer (Halaoui and McCaffrey, 2015).

Growth Signaling

The **Salvador-Warts-Hippo (SWH)** tumor suppressor pathway was discovered first in *Drosophila* as a regulator of organ

size (Pan, 2010; Yu et al., 2015) and later in humans, where it was found to be fundamental in the regulation of cancer growth (Harvey et al., 2013). The physiological activation of the Hippo (HPO) kinase, (MST1/2 in human) (Harvey et al., 2003) consists in the phosphorylation of Warts (WTS), (LATS1/2 in human) (Genevet et al., 2010; Yu et al., 2010) and in the activation of the phosphorylated core complex, that includes Salvador (SAV in human) (Tapon et al., 2002) and Mob/MATS, that in turn, phosphorylate Yki (YAP/TAZ in humans) (Oh and Irvine, 2008). Phosphorylated Yki is sequestered and degraded in the cytoplasm, resulting in the inhibition of its nuclear transcriptional activity and oncogenic function (Harvey et al., 2013). Upstream, the Hippo cascade is regulated by components of cell junctions, including cell adhesion molecules such as Merlin, a homolog of the human Neurofibromatosis Type 2 (NF2) (Genevet et al., 2010; Yu et al., 2010), which acts as tumor suppressor; the cadherin Fat in complex with Dachsous; and by cell polarity regulators such as Crumbs (Robinson et al., 2010; Harvey et al., 2013). Alterations in the composition of the core proteins (HPO, WTS, SAV, MATS) of the pathway trigger Yki translocation into the nucleus that binds tissue-specific partners and induces the expression of its target genes, among them: CyclinE, dIAP1 and MYC (Harvey et al., 2003; Pantalacci et al., 2003; Neto-Silva et al., 2010; Ziosi et al., 2010). This articulated system is also tightly regulated by other signaling pathways: for example, in the *Drosophila* imaginal wing disc, Lgl or aPKC deregulation results in JNK activation to promote Yki nuclear translocation via phosphorylation of Ajuba (Jub), an upstream regulator of the cascade that binds to and inhibits Wts kinase activity (Sun and Irvine, 2013). In addition to the regulation of cell-cell interaction signals, components of the Hippo pathway have been found to be sensitive to mechanical stress (Panciera et al., 2017). This mechanotransduction function is critical in the control of physiological pathways, and its deregulation may contribute to the abnormal cell behavior in diseases such as cancer, where the cells in the tumor have to sustain physical forces generated by tissue overgrowth. Interestingly, this last function has shown differences in the behavior of Yki between human and flies: indeed, in *Drosophila* the Yki protein does not respond to integrin stimulation, while in mammals integrin signaling promotes YAP/TAZ activity. One possible explanation for this different behavior may be that the N-terminus of Yki is missing a domain necessary to bind PDZ-containing proteins, which is found in its human counterpart YAP, and is necessary for the activation of the integrin-Src adhesion branch of the pathway (Elbediwy and Thompson, 2018). However, an interesting and potential explanation for this difference comes from a comparative analysis of the Yki protein and the evolution of the different epithelia: this analysis outlines how in *Drosophila* the apical membrane of the columnar epithelium is well differentiated in its function to activate the Hippo pathway, whereas in mammals the multilayer of cells lacks a functional apical domain, and the activation of YAP/TAZ relies on the activation/signal from the integrin adhesion pathways of the stem cells on the basal layer of the epithelium (Elbediwy and Thompson, 2018).

The **RAS/RAF/ERK** signaling cascade is one of the most conserved pathways in all organisms, including *Drosophila*. This pathway is part of the MAP kinase signaling that, in addition to ERK1/2, also includes JNK1/2/3, p38/MAPK, and ERK5, which mainly respond to stress activators (Morrison, 2012). Highly conserved in flies, ERK1/2 are activated by growth factors such as EGF or FGFs. These ligands bind to receptor tyrosine kinases (RTKs) to activate downstream signaling, in particular its core complex, which is represented by the guanidine exchange factor Son of Sevenless (SOS) that, in turn, activates the small G proteins RAS on the cell membrane. This leads to RAF activation and to the formation of the complex with the kinase D-Sor also called MAPKK or MEK that, upon phosphorylation of Rolled, the fly homolog of MAPK or ERK kinases, induces the activation of its final targets (Shilo, 2014). ERK in flies has much fewer targets than those described in vertebrates, the most common being the ETS-domain protein Pointed (Pnt). In particular PntP2, needs to be phosphorylated for its activation and is the principal activator of transcription downstream of many RTKs, and PntP1 is transcriptionally induced by MAPK (Shilo, 2014). A second transcriptional repressor is Capicua (Cic), an HMG box-containing protein highly conserved in vertebrates (Simon-Carrasco et al., 2018). Interestingly, in the last couple of years, this protein was found to possess oncogenic properties and be overexpressed in many tumors (Simon-Carrasco et al., 2018). In addition, Cic activity regulates co-target genes upon Yki activation, placing this protein at the crossroads of RTKs and SWH pathways (Simon-Carrasco et al., 2018).

Even though MAPK targets in *Drosophila* are less abundant than in mammals, its activation and translocation to the nucleus results in a growth phenotype mimicking a few characteristic steps of growth in tumor cells (Brumby et al., 2011). Activation of Ras is considered a cancer distinctive trait both in *Drosophila* and humans, and it represents one of the strategies to model human cancer in flies. In *Drosophila* there are three *Ras* genes but only *Ras1* has functional homology with mammalian *RAS*. In the epithelial cells of the wing imaginal disc, Ras1 activation triggers hyperproliferation but also determines cell fate (Prober and Edgar, 2000). Ras activation is at the crossroads of other growth factor signaling cascades: recently, a link to Hpo function was shown in *Drosophila* epithelial cells, where Ras activation was able to induce the tissues to switch from a pro-differentiative to a pro-growth program by modulating SWH's transcriptional output (Pascual et al., 2017). Ras increases cell proliferation also through the transcriptional regulation of growth factors and their receptors. For example, it helps promote angiogenesis-like mechanisms in tracheal development through secretion of the FGF/EGFR molecules (Petit et al., 2002; Grifoni et al., 2015); its activation stabilizes pro-growth signals including MYC (Prober and Edgar, 2000), and inhibits pro-apoptotic molecules like Hid (Bergmann et al., 1998). Because of all these functional homologies to human RAS, its activation in *Drosophila* is considered a good method to establish models that mimic tumor growth.

The **JNK Signaling Pathway** is activated mainly by oxidative stress, producing reactive oxygen species (ROS), and by Eiger, the *Drosophila* homolog of TNF-α. Its function is variable and

depends also on the cellular environment: it can indeed induce cell proliferation and migration, but its major role is to induce apoptosis (Igaki, 2009). The signaling core is characterized by Hemipterus/Hep (JNKK) (Glise et al., 1995), Basket/Bsk (JNK) (Stronach, 2005) and the AP-1 complex, that functions as negative feedback by up-regulating the expression of the Puckered phosphatase (Martin-Blanco et al., 1998). The AP-1 complex is composed of Fra (Fos-Related Antigen) and dJun (*Drosophila* Jun) and is the final effector of the cascade (Kockel et al., 2001). Upstream Hep is phosphorylated by many JNKK kinases (Tak1-12, Mekk1, Ask1, Slpr) and can also be activated by different indirect stimuli (e.g., RAS, JNKKKK/Msn, and Eiger). Cell death is induced by the expression of the pro-apoptotic genes *hid, reaper* and *grim*, whose activity inhibits the pro-survival protein dIAP1 (Weston and Davis, 2007). In *Drosophila* cancer cells, the JNK pathway plays a dual role, by suppressing or promoting growth depending on the context (Brumby and Richardson, 2003; Uhlirova et al., 2005; Cordero et al., 2010). *lgl, scrib*, and *dlg* mutant cells undergo JNK-mediated apoptosis resulting in a mechanism of tumor suppression (Brumby and Richardson, 2003; Uhlirova et al., 2005; Igaki et al., 2006). On the contrary, in tumor cells with active RAS, apoptosis is blocked and JNK signaling acts as a tumor promoter transcribing genes involved in growth and invasion such as MMP1 (Igaki et al., 2006; Uhlirova and Bohmann, 2006). The overexpression of activated RAS together with Hep ($ras^{v12}hep^{wt}$) gives cells invasive and metastatic abilities, highlighting how these pathways converge to induce transformation in epithelia.

The **PI3K/Target of rapamycin (TOR)** signaling pathway is a highly conserved key regulator of growth. The binding of insulin-like peptides (ILPs) (fly's insulin) to the receptor (InR) results in the phosphorylation of *chico*/IRS1-4, and the production of phosphatidylinositol-3, 4,5-triphosphate (PIP3) by PI3K, a reaction that is counteracted by the lipid phosphatase PTEN (Grewal, 2009). PIP3 recruits several Ser/Thr kinases to the plasma membrane, including Akt/PKB and PDK1 (3′-phosphoinosite-dependent protein kinase-1), while its activation results in the inhibition of Glycogen Synthase Kinase-beta (GSK3-β), a conserved kinase that not only controls energy metabolism by inactivation of Glycogen Synthase, but also regulates Wnt signaling by controlling β-catenin/*armadillo* (Xu et al., 2009) and Myc stability (Bellosta and Gallant, 2010). Activation of Akt also inhibits Tuberous Sclerosis Complex 1 and 2 (TSC1/2), a tumor suppressor binary complex that negatively regulates Rheb, a GTPase upstream of TOR kinase responsible for the activation of TORC1. TOR is found in two complexes: TORC1, which includes Raptor and LST8 adaptor molecules, is sensitive to amino acids and is inhibited by rapamycin; and TORC2, that is composed of LST8 and Rictor adaptor molecules, and does not respond to amino acids or rapamycin (Saxton and Sabatini, 2017). Activation of TORC1 results in phosphorylation of ribosomal protein kinase p-70-S6 (S6K) and of eukaryotic translation initiation factor 4E-binding protein-1(4E-BP1), thereby triggering protein synthesis and initiation of translation. Insulin and TOR activities are also balanced by a negative feedback mechanism that is activated when S6K is hyper-activated to counteract insulin activity. Under this condition, S6K phosphorylates IRS1-4/*chico* triggering its internalization and subsequent proteasomal degradation. This feedback mechanism is reduced in pathological conditions, such as the Tuberous Sclerosis Complex syndrome (TSC), where cells carrying *tsc1* or *tsc2* mutations display an abnormal increase in size and exhibit constitutive phosphorylation of S6K (Saxton and Sabatini, 2017). As members of PI3Ks and TOR signaling are frequently activated in human tumors, they are attractive targets for cancer treatment.

Myc and Cell Competition

MYC is one of the most studied oncogenes, and its misexpression is associated with various tumor types including meningioma, Burkitt's lymphoma, medulloblastoma and hepatocellular carcinoma (Hsieh and Dang, 2016). *Drosophila* Myc is the sole fly member of the family of transcription factors that in mammals is composed of three genes (N-, L-, and *c-MYC*) (Gallant et al., 1996; Schreiber-Agus et al., 1997). Hypomorphic alleles of *myc* in flies are developmentally delayed and show a reduction in cell size resulting in smaller flies (hence the name of the mutant as *diminutive* = small) (Johnston et al., 1999), while null mutants die during larval stage (Pierce et al., 2004). Notably, ubiquitous expression of *myc* increases cell mass resulting in enrichment of genes encoding components of the nucleolus and of the ribosome; this evidence, concomitantly with Myc's ability to indirectly stimulate RNA pol I and III (Grewal et al., 2005; Hulf et al., 2005; Orian et al., 2005), contribute to revealing its role in the control of ribosomal biogenesis, thus mass and size. Myc activity is finely regulated, and while its expression is required at physiological levels during development, an excess of its activity triggers autonomous cell death and unbalanced growth (Grifoni and Bellosta, 2015). Therefore, Myc is strictly controlled both transcriptionally and post-translationally, where its protein stability is controlled by phosphorylation events downstream of RAS/ERK and GSK3β kinases with a signaling conserved in flies and mammals (Galletti et al., 2009; Parisi et al., 2011). Myc regulation of the cellular metabolic milieu is highly similar in *Drosophila* to the regulation found in tumor cells (DeBerardinis et al., 2008), indeed it was shown that in cells undergoing to a metabolic stress (starvation or competitive environment), expression of Myc switched their metabolism to increase glycolysis, glutaminolysis (Parisi et al., 2013; de la Cova et al., 2014; Hsieh et al., 2015), or lipid metabolism to favor survival by inducing autophagy (Parisi et al., 2013; Paiardi et al., 2017). Fascinatingly, these evolutionary functions of Myc to control mass and metabolism, resulted in the selective advantage of growth of epithelial cells described as cell competition and characterized in the monolayer epithelia composing *Drosophila's* imaginal discs (Johnston, 2014). Briefly, cells expressing Myc create a competitive environment and they grow at the expense of *wild-type* cells that are killed by non cell-autonomous apoptosis (de la Cova et al., 2004; Moreno and Basler, 2004). Myc cells thus behave as "winners" and they are able to repopulate the space of the dying "loser" cells that are killed by unidentified Myc-dependent mechanisms (Johnston, 2014). Myc-induced cell competition was also shown to be necessary in vertebrates

to eliminate unfit cells (losers) during early embryogenesis (Claveria and Torres, 2016). More recently, evidence that sustains a central role for Myc-induced cell competition in the early steps of tumor formation have shown Myc present at high levels in cells surrounding the tumor near dying cells, potentially allowing the winner cells to expand and to eliminate the surrounding *wild-type* cells, thus establishing the first evidence of Myc involved in a tumor growth competitive environment (Johnston, 2014; Di Giacomo et al., 2017). Another form of cell competition is regulated by cell polarity genes *(lgl, scrib, dlg)* and by endocytic genes (such as *Rab5*). Cells mutant for these genes behave as losers and were eliminated by *wild-type* cells (Brumby and Richardson, 2003; Menendez et al., 2010); notably the expression of oncogenes in those loser clones provided them with super-competitive characteristics, i.e., *lgl* mutant cells over-expressing MYC send death signals to the adjacent *wild-type* proliferating cells (Froldi et al., 2010), suggesting the presence of another mechanism of cell competition driven by different growth forces working in combination with cell polarity genes and oncogenic signals.

ORGANOTYPIC *DROSOPHILA* CANCER MODELS

Gut Cancer

Similar to mammalian counterparts, the *Drosophila* adult gut is specialized in the digestion of food, the absorption of nutrients, and for controlling the defense response against infection (Tian et al., 2018). Based on these distinct functions, the *Drosophila* gut is composed of three parts: foregut, midgut, and hindgut. Among them, the midgut has a distinct architecture that resembles the digestive tract of vertebrates. The epithelium is a monolayer that is replenished by Intestinal Stem Cells (ISCs) that differentiate to either enteroblasts (EB) or pre-enteroendocrine cells (pre-EE), that then differentiate into absorptive enterocytes (EC) or secretory enteroendocrine cells (EE). Thanks to significant similarities in the physiology between the *Drosophila* gut and the intestine of vertebrates (Apidianakis and Rahme, 2011), *Drosophila* adult midgut epithelium has been used to study the contribution of signaling pathways (i.e., EGFR, Notch, Hedgehog, and Wg/Wnt) to Intestinal Stem Cells (ISCs) renewal (Jiang and Edgar, 2009; Biteau and Jasper, 2011; Jiang et al., 2011).

In vertebrates, the majority of sporadic cases of colorectal cancer and familial adenomatous polyposis (FAP) cancer syndrome are associated with activation of Wnt signaling (Bienz and Clevers, 2000). In humans, abnormal expression of Wnt in ISCs promotes adenoma formation, while deletions in mouse ISCs of the tumor suppressor *adenomatous polyposis coli* gene *APC* triggers the initial step of colon-adenoma formation (Barker et al., 2009), underlying the relevance of both mutations in this malignancy. In *Drosophila,* loss of the *Apc* gene, leads to the over proliferation of ISCs in the gut, resulting in loss of epithelial cell polarity, hyperplasia and epithelial overgrowth resembling that of intestinal adenomas induced by the loss of *APC* (Yu et al., 1999). Remarkably, the over-proliferation of the *Apc* $^{-/-}$ cells was rescued by *lof* mutation of *Ras* (Wang et al., 2013). On the contrary $Apc^{-/-}$ cells expressing an active form of Ras^{v12} showed a malignant transformation including loss of cell polarity and invasive phenotype, highlighting the conserved functional cooperation between RAS and APC in controlling proper growth in the gut. In *Drosophila*, intestinal progenitors mutant for the *Apc* gene expand at the expense of the surrounding *wild-type* cells that die by apoptosis; because of this behavior these cells have been defined as "super-competitors" (Suijkerbuijk et al., 2016). *Apc* mutant cells exhibit higher Yki/YAP activity and increased JNK signaling, that was also detected at the border between $Apc^{-/-}$ and *wild-type* cell; moreover, inhibition of apoptosis prevented *Apc* mutant cells from further expansion, suggesting that a competitive behavior in these cells is controlling *Apc* dependent tumor growth (Suijkerbuijk et al., 2016).

The JNK-Wg signaling is important to control the physiology and regeneration of intestinal cells, as ISCs damage leads to an overactivation of the JNK pathway and an increase in Wg ligand (Biteau et al., 2008; Cordero et al., 2012b). Wg activity in the enterocytes (ECs) indirectly drives the expansion of the ISCs by upregulating the JAK-STAT ligands Upd2 and Upd3, acting non-autonomously on ISCs proliferation (Tian et al., 2018). Moreover, activation of Wnt drives Myc upregulation in ISCs leading to non-autonomous upregulation of Upd3 in the ECs (Cordero et al., 2012a). Similarly, loss of *Apc1* in the midgut (ISCs) also results in JAK-STAT and EGFR pathway hyper-activation, and their removal suppresses the intestinal hyperplasia resulting from *Apc1* loss, revealing an underlying conserved signaling between flies and mammals that controls ISCs proliferation and gut homeostasis (Cordero et al., 2012a).

Another aggressive oncogene that is hyper-activated upon *Apc* loss, in mouse and human intestinal adenomas is the non-receptor tyrosine kinase *c-Src* (Yeatman, 2004). This proto-oncogene is amplified or activated in more than 20% of human tumors, and its activity has been demonstrated to play a central role in the formation of colorectal cancer (CRC). In mice, expression of *c-Src* increases in the proliferative progenitor cells of the "cripta" favoring hyperplastic adenoma formation (Cordero et al., 2014). In *Drosophila* the expression of *c-Src* orthologs (*Src42A* and *Src62B*) induces proliferation of the ISCs cells in *wild-type* animals, and reduction of their expression is sufficient to inhibit ISCs' hyper-proliferation of *Apc* mutant cells (Cordero et al., 2014). Notably, these results recapitulate an important part of the function of mammalian c-Src in the progenitor cells of the intestine during homeostasis and adenoma formation, suggesting a conserved role of this gene in flies in controlling proper ISCs proliferation.

Recently, *Drosophila* was also used to generate multigenic models of colon cancer using data from patients from The Cancer Genome Atlas. Interestingly, the outcomes of these models mimicked important properties of human cancers, and can be explored and used in chemical screens to find new combinations of cancer-relevant drugs (Bangi et al., 2016). Studies, using *Drosophila* models, to characterize intestinal human pathophysiology, revealed the high conservation between these species of the mechanisms underlaying colorectal tumorigenesis (Christofi and Apidianakis, 2013), and further revealed also the mechanisms that control

the processes leading to bacterial-mediated inflammation (Lemaitre and Hoffmann, 2007).

Brain Cancer

Meningioma are the most common intracranial tumors (Claus et al., 2005; Rogers et al., 2015) and frequently linked with mutations in the PI3K catalytic subunit p110α isoform encoded by the gene (*PI3KCA*), or in the *v-akt murine thymoma viral oncogene homolog 1* (*AKT1*) gene. Complex interactions were found between members of the PI3K/AKT/mTOR pathway and MAPK-, JAK/STAT, and Notch-1-mediated pathways that contribute to meningioma progression (El-Habr et al., 2014). Increased risk of meningiomas was associated also with neurofibromatosis type II syndrome, where mutations within the tumor suppressor gene *Suppressor of fused* (*SUFU*) was associated with hereditary meningiomas (Aavikko et al., 2012) and with medulloblastomas (Taylor et al., 2002). In *Drosophila* SUFU regulates Hedgehog (Hh) signaling (Ohlmeyer and Kalderon, 1998), with a similar function in humans, where loss of *SUFU* results in the aberrant activation of the Hedgehog (Hh) pathway (Aavikko et al., 2012).

Of all glioblastomas, the glioblastoma multiforme (GBM) is the most aggressive form of gliomas, accounting for approximately 50% of all glial tumors (Phillips et al., 2006). In GBM, Notch activity is associated with the control of Glioma Stem Cell (GSC), since its activity regulates asymmetric cell division and Notch unbalanced expression leads to uncontrolled growth and high malignancy (Mukherjee et al., 2016), Several studies demonstrate a role for Notch signal in controlling growth and stem cell maintenance of the brain also in flies (Song and Lu, 2011). Because of its conserved function, Notch pathway is now an important target for therapeutic intervention in brain cancer treatment (Yuan et al., 2015).

The current understanding of asymmetric cell division and its relation to tumorigenesis is largely derived from studies on *Drosophila* neuroblasts (NBs), where mutation of a single gene, *brain tumor* (*brat*), was shown to alter asymmetric stem cell division in larval development, and to generate massive neoplastic growth and enlarged adult brain formed entirely of neoplastic NBs (Caussinus and Gonzalez, 2005; Betschinger et al., 2006). Suppression of *brat* expression was used to establish a model of glioma stemness in *Drosophila*, where the upregulation of Notch, induced by reducing *brat,* was the critical node to maintain self-renewal and proper stemness (Mukherjee et al., 2016). This observation was also confirmed in glioblastomas where the human ortholog of *brat*, the tripartite motif-containing protein-3 (TRIM3), was shown to be necessary to suppress NOTCH1 signaling and to control stem cell activity during development to reduce tumor growth (Chen et al., 2014; Mukherjee et al., 2016). Glioma stem cells divide asymmetrically under the guidance of cell polarity complexes that control the proper apical and basolateral polarization and cell division, a process that was originally identified in *Drosophila* and later confirmed for the mechanism driving differentiation in human glia for members of the *Hugl-1/Llgl-1* complexes (Prehoda, 2009). We recently developed a neurogenic brain tumor model by impairing asymmetric cell division through the loss of function of *lethal giant larvae* (*lgl*) the *Drosophila* ortholog of *Hugl-1*, in the type II NBs of the central brain (Paglia et al., 2017). In our model, PI3K activation mimics PTEN loss of function and hampers Lgl localization at the apical membrane by aPKC cortical recruitment (Paglia et al., 2017). These data connect the function of *HUGL-1* in the maintenance of glioma stem cells with the loss of function of the tumor suppressor *PTEN* (Gont et al., 2013) and together with those in glioma (Read et al., 2009) show a conserved function for PI3K and EGFR overexpression in these tumors recapitulating many features of the neurogenic subtype of human glioblastoma. Inhibition of PI3K/Akt activity is currently used as a therapy in GBM (Zhao et al., 2017).

Other brain tumors such as oligodendrogliomas, that account for 10% of all cancers of the central nervous system, are characterized by mutations in the *capicua* (*cic*) gene (Bettegowda et al., 2011), a conserved transcriptional repressor that regulates MAPK effector genes downstream of receptor tyrosine kinase (RTK) (Simon-Carrasco et al., 2018). The development of correct animal model also for these tumors will be essential to develop specific treatments that can tackle these different brain tumors *in vivo*.

The Paradigm for Angiogenesis

In the fruit fly, the circulatory system is open, the heart pumps the hemolymph into the body cavities and the exchange of gases takes place directly within the organs (Medioni et al., 2009). Moreover, *Drosophila* is equipped with a complex branched system of interconnected tubules that is responsible for the oxygen transport, the tracheal system, an organ that is comparable in structure and function to the circulatory system of mammals (Affolter et al., 2009). In *Drosophila*'s epithelia, the induction of clones bearing *lgl, Ras*^{V12} mutations identified how tumors are able to recruit vessels to oxygenate the growing mass (Grifoni et al., 2015; Calleja et al., 2016). These tumor cells showed ectopic expression of *Bnl* (*branchless*), the *Drosophila* homolog of Fibroblast Growth Factors (FGFs,), and suffered from oxygen shortage (hypoxia). In addition, it was observed a trans-differentiation of tumor cells into pseudo-tracheal cells with and the formation of new vessels, mimicking human FGF-mediated vascularization in cancer (Grifoni et al., 2015).

Cell under hypoxia condition changes their cellular metabolism to favor growth, particularly in solid tumors (Pavlova and Thompson, 2016; Vander Heiden and DeBerardinis, 2017). Interesting studies in flies showed how reduction of the SCF (Skp/Cullin/F-box)-type ubiquitin ligase *Ago*, homolog of human *Fbw7,* increased tracheogenesis through up-regulation of the hypoxia-inducible transcription factor Sima/dHIF and of its target, the FGF ligand Bnl (Mortimer and Moberg, 2013). Fbw7 is known to inhibit tumor growth by targeting proteins to the proteasome pathways, and is mutated in a wide range of primary human cancers, this data suggests that its role as a tumor suppressor may be conserved also in the modulation of HIF-regulated angiogenesis in the tracheal system of the fly (Mortimer and Moberg, 2013). This process of neo-tracheogenesis is now considered a novel cancer

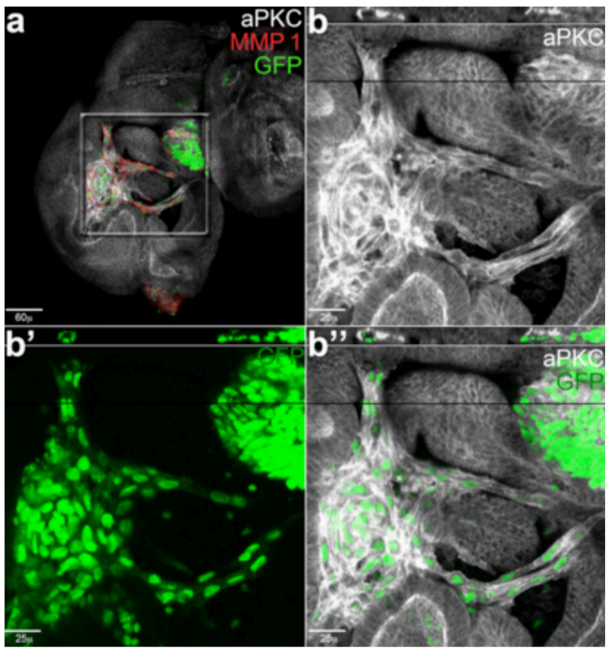

FIGURE 3 | Cancer cells form branched and tubule-shaped structures (reproduced from Grifoni et al., 2015) with permission). **(a)** An imaginal wing disc bearing *lgl*^{4}, Ras^{V12} clones induced in a wild-type background. **(b–b")** Magnifications of the central region squared in **(a)**. Migrating tumor cells (GFP) are positive for the junctional marker aPKC (white) and secrete MMP1 (red). The reconstruction along the z-axis shown in the upper part of the magnified images reveals a tubule-shaped structure encircling a lumen, indicating these cells are forming tracheal-like structures.

hallmark in fly, which may help to explore the relation between angiogenesis and tumor growth in humans (Herranz et al., 2016; **Figure 3**).

Lung Cancer

Lung cancer is a major cause of death in the world, and the standard therapeutic strategy used is chemotherapy because target therapies only decrease tumor growth and result in high toxicity. Recently, a new *Drosophila* lung cancer model was developed exploiting the tubular structure of the tracheal network (Levine and Cagan, 2016), and considered functionally and anatomically comparable to the vertebrate airways (Andrew and Ewald, 2010). Both in *Drosophila* and mammals, airways are formed by interconnected branches that depends on the secretion of Bnl/FGFs by the neighboring cells (Ghabrial et al., 2003; Grifoni et al., 2015). Using a binary system, *Ras*^{V12} was ectopically expressed specifically in the tracheal cells while downregulating *PTEN*, a negative regulator of the PI3K/AKT signaling (Hafen, 2004; Ortega-Molina and Serrano, 2013). As a result, the cells of the tracheal branches over-proliferated to form tumors that ultimately killed the animals (Levine and Cagan, 2016). This model was successfully used in a screen for chemical compounds approved by the Food and Drug Administration (FDA), which resulted in the identification of several compounds able to reduce cell over-proliferation and to improve tracheal physiological functions (Levine and Cagan, 2016), further highlighting the strong potential of the use of fruit fly models for cancer-related chemical screens.

Prostate and Thyroid Cancer

The prostate is an exocrine gland of the male reproductive system responsible for the maturation and production of the seminal fluid, with its activity depending on androgens mostly produced by the testis. During organogenesis, the differentiation of the prostate's epithelium occurs along with that of stroma and depends on the complex coordination of many transcription factors and hormones that control the maturation of the quiescent organ (Toivanen and Shen, 2017). The adult prostate epithelium has a low turnover rate and its hyperplasia characterizes the majority of benign prostatic tumors. On the contrary, adenocarcinoma of the prostate is an aggressive tumor that rapidly progresses to a metastatic stage that can be partially blocked by androgen therapy (Shiao et al., 2016). Studies on flies' male accessory gland revealed many parallels with the physiology of human prostate epithelium (Wilson et al., 2017), i.e., a genetic screen using the *Drosophila* accessory gland identified genes that promote growth and migration of the secondary cells as homologs of genes expressed in human prostate cancer (Ito et al., 2014).

Like in human prostate, *Drosophila's* accessory gland presents a secondary layer of epithelial cells that continue to proliferate; this homology allowed the development of models that mimic tumors of endocrine origin, including human prostate and thyroid adenomas (Das and Cagan, 2013, 2018). For example, the multiple endocrine neoplasia type 2 (MEN2) syndrome, is characterized by different mutant-translocations involving the RET genes that result in multiple cancer phenotypes, including pheochromocytoma, parathyroid adenoma and the aggressive medullary thyroid carcinoma (MTC) (Das and Cagan, 2013). A recent study demonstrated that the papillary carcinoma of the thyroid (PTC), also caused by another genomic mutations of RET gene, can be profitably studied using the accessory gland of *Drosophila* to delineate and understand the mechanisms that characterize PTC in the context of the whole animal, including the relationship between tumor and normal cells in an environment that mimics tumor of endocrine origin in humans (Levinson and Cagan, 2016).

The prostate epithelium is characterized by the abundance of exosomes, microvesicles secreted from the endosomal multivesicular body (MVB) that fuse with sperm to modulate its activity and protect its homeostasis (Wilson et al., 2017). The exosomes are particularly relevant in cancer biology for their implication in tumor progression and survival, since they deliver survival factors, metabolites and miRNAs, that help creating a favorable microenvironment for cancer growth; in addition they also favor drug-resistance by activating mechanisms that favor the elimination of toxic chemicals such as chemotherapeutic products (Ruivo et al., 2017; Namee and O'Driscoll, 2018). Since the accessory gland has a similar structure as the prostate

epithelium, characterized by the abundance of exosomes, it could be an optimal model to better study exosome biology in tumors of endocrine origins.

LIQUID TUMORS

The signaling pathways regulating blood cell differentiation are conserved from *Drosophila* to humans (Lebestky et al., 2003; Jung et al., 2005). In addition, fly macrophages originate via self-renewal from progenitor cells localized in the lymph gland, a specialized hematopoietic organ that can be compared to the hematopoietic stem cell niche of the mammalian bone marrow (Krzemien et al., 2007; Mandal et al., 2007). These similarities with vertebrate hematopoiesis outline the utility of using fly models to elucidate the basic mechanisms of hematopoietic differentiation and homeostasis responsible for severe diseases, including leukemia. *Drosophila* has already been used to study Acute Myeloid Leukemia (AML), a widespread form of leukemia, and to identify the genes responsible for the disease. AML1 is a transcription factor, responsible for activating myeloid differentiation, which has a counterpart in the fly (Sinenko et al., 2010). In vertebrate tumors, the fusion of AML1 with the repressor ETO inhibits the differentiation of the multilineage progenitor cells, while their proliferation is activated, leading to AML1. Interestingly, AML1 fused with ETO in *Drosophila* also causes the inhibition of hematopoietic cell differentiation, confirming that the fly is a good genetic model to study the mechanisms that drive leukemia in humans (Osman et al., 2009; Sinenko et al., 2010). Myeloproliferative neoplasms (MPNs) have also been reproduced in the fly through gain-of-function mutations in the JAK pathway, finding a role for the downstream effector of the SWH pathway Yki in priming the expansion of *Drosophila* blood cells, which undergo malignant behavior following JAK activation (Anderson et al., 2017).

CANCER AND IMMUNE SYSTEM

Inflammation in tumor development acts as "tug and war" since it may promote survival of tumor cells by favoring angiogenesis, by reducing the natural immune responses and by altering responses to chemotherapeutic agents (Mantovani et al., 2008; Wu and Zhou, 2009). The inflammatory response of cancer cells has been attributed to a response of the immune system to eradicate the tumor, but it can also be seen as a way to provide growth and survival, as inflammation contributes to genomic instability by releasing cytokines and through production of reactive oxygen species (ROS) that may induce genetic and genomic alterations (Negrini et al., 2010). Normal cells detect and repair DNA damage, ensuring the maintenance of the correct number of chromosomes and tissue homeostasis, instead often cancer cells have increased mutation-rates leading to high chromosomal instability (CIN) that triggers aneuploidy and advances tumorigenesis (Negrini et al., 2010). Chromosomal instability is a process conserved also in *Drosophila,* and it was shown to contribute to the invasive behavior of epithelial cells, with a mechanism called "compensatory proliferation" activated to counteract CIN-induced cell death (Clemente-Ruiz et al., 2016; Benhra et al., 2018).

The mechanisms controlling cancer immune response are somehow conserved also in flies as studies in *Drosophila* have shown that infiltration of macrophages (called hemocytes) in cancer cells requires the activation of the JAK-STAT, JNK, TNF-α, and Toll/Imd/TLR signaling pathways (Bangi, 2013). Of particular interest is TNF-α that plays an important role in controlling apoptosis and the inflammation processes (Ham et al., 2016). TNF-α in tumors has distinct and overlapping functions to promote tumor growth and proliferation and to activate cell death, functions that are mainly mediated by the activation of TNFR1 that is ubiquitously expressed while TNFR2, mainly expressed in immune cells, is less well understood. Thus these opposite signaling pathways activated by TNF signals depend on the adaptor complexes recruited by the receptors and by the cellular context, and they may create a problem for the development of therapeutic strategies that target TNF signaling in tumors (Ham et al., 2016). In *Drosophila* the sole TNF-α, called Eiger (Egr), binds two receptors called Wengen (Kanda et al., 2002) and Grindelwald (Andersen et al., 2015), the latter shown necessary for the growth of $Ras^{V12}/scribble^{-/-}$ tumors (Andersen et al., 2015). An interesting mechanism links the possibility that ROS, induced by stress or local inflammation, triggers Egr expression in the hemocytes, to control JNK signaling, in a phenomenon called Apoptosis-Induced Proliferation (AIP), a sort of compensatory proliferative response of the epithelial cells that responds to cues from local "activated" hemocytes (Fogarty et al., 2016). Other studies highlighted the role of hemocytes in the interplay between inflammation and cancer, i.e., using a classic cancer model that recapitulates the hallmarks of epithelial cancer cells ($Ras^{v12}/scribble^{-/-}$), it was shown that cancer cells induce hemocyte's recruitment and proliferation *in vivo* by activating JNK signaling to cause the expression of JAK/STAT cytokines (Pastor-Pareja et al., 2008). Using a similar model it was shown that Egr expression was higher in the hemocytes derived from cancer animals, and that its activity was necessary to stimulate invasive migration of tumor cells (Cordero et al., 2010). On the contrary, Egr acts as a tumor suppressor to drive apoptosis in cancer cells upon activation of Toll/NF-κB signaling by the fat body (adipocytes) in response to the secretion of Egr by the circulating "activated" hemocytes (Parisi et al., 2014). Work using allograft transplantation experiments, identify also a function for the hemocytes in tumor initiation, that is independent on Eiger, but relays rather on the activation by external stimuli (i.e., CIN, abnormal growth) of JNK pathway and on the complex of non-autonomous and autonomous signals between tumor cells and those composing the tumor microenvironment; a similar mechanism has been proposed in vertebrates suggesting a conserved response for JNK signaling in fly to control initial tumor growth (Muzzopappa et al., 2017).

In summary, all these data suggest the existence of conserved mechanisms between the immune and tumor cells in flies that may recapitulate some of the most evolutionary conserved aspects described in cancer cells.

CANCER AND LIPID METABOLISM, OBESITY

In tumor biology, evidences highlight the relevance of lipid metabolism in influencing tumor growth (Katheder and Rusten, 2017; Weber et al., 2017). In this context, a recent role was identified for adipose triglyceride lipase (ATGL) whereby it hydrolyzes triacylglycerols into fatty acids (FAs) that may act as signaling molecules to induce growth both cell autonomously and in neighboring cells (Walther and Farese, 2012). The contribution of ATGL to cancer growth is controversial, indeed several studies showed that its depletion reduced proliferation in colorectal cancer cells and in non-small-cell lung carcinoma (Ou et al., 2014; Zagani et al., 2015), and in breast and pancreatic carcinoma its upregulation contributed to tumorigenesis (Grace et al., 2017; Wang et al., 2017). On the contrary, lack of *ATGL* favored pulmonary neoplasia in mice, and in few human tumors *ATGL* expression was found reduced highlighting the complex role of lipids in tumorigenesis (Al-Zoughbi et al., 2016). Cancer cells activate *de novo* lipogenesis by upregulation of key enzymes in lipid metabolism, some of which, such as AcetylCo-A Lyase (ACLY), AcetylCo-A Carboxylase (ACC) and Stearoyl-CoA desaturase-1 (SCD), are targets of pharmacological inhibitors to decrease cancer proliferation (Zaidi et al., 2012; Zu et al., 2013; Peck and Schulze, 2016; Stoiber et al., 2018). Recent work associated the mechanism of lypolysis with the induction of autophagy, a mechanism used by the cells to re-cycle part of their cytoplasm or cellular content to survive when nutrients are reduced (Dall'Armi et al., 2013). The relevance in cancer of the link between lipids and autophagy was shown when ATGL-mediated lipolysis in a peritumoral area, increased autophagy and tumor survival using a non-autonomous mechanisms (Martinez-Outschoorn et al., 2011; Gnerlich et al., 2013). Interestingly, we observed that Myc in *Drosophila* induced autophagy in the fat body and this was enough to enhance survival of the whole animals upon starvation (Parisi et al., 2013). We linked this effect with the ability of Myc to increase desat1, a Stearoyl-CoA desaturase-1 (SCD1) key enzyme in the synthesis of lipids, that we found co-expressed with Myc in human prostatic tumors (Paiardi et al., 2017).

Metabolic disorders and obesity are associated with cardiovascular disease and type II diabetes (T2D), however numerous cohort studies reported that overweight people are more likely to develop certain types of cancer including endometrial, breast, liver, and ovarian cancer (Cancer, 2012; Chen et al., 2012; Riboli, 2014; Wang and Xu, 2014; Dougan et al., 2015; Hirabayashi, 2016). Obese people have often increased levels of circulating hormones like insulin that has been associated to higher levels of IGF-1 in colon, kidney, prostate and endometrial cancer (Roberts et al., 2010; Gallagher and LeRoith, 2015). Another hormone, leptin, a cytokine produced by the adipocytes to control satiety in a signaling circuit of the brain, has also been found up-regulated in tissues from obese people, particularly in women post-menopause, and increased levels of leptin have been associated with higher incidence of breast and other tumors (Ray, 2018). The adipose tissue produces pro-inflammatory cytokines including IL-6, IL-8, IFNγ, and TNF-α among others (Scheller et al., 2011; Arango Duque and Descoteaux, 2014), and their over-production in fats from obese, activates the infiltration of macrophages into the adipose tissue inducing a low level of chronic inflammation or adipocyte tissue macrophage infiltration called ATM (Lafontan, 2014; Kuroda and Sakaue, 2017). This low level of inflammation increases the levels of ROS and induces DNA and protein damage that may increase the risk of cancer (Lafontan, 2014; Mraz and Haluzik, 2014). The role of the inflammatory response to combat infection and tissue injury, through the activation of the immune cells, is conserved also in *Drosophila's* circulating hemocytes (Lemaitre and Hoffmann, 2007), where most of the signals activated in the fat body results also in ROS production (Dionne, 2014; Vlisidou and Wood, 2015). Indeed, we showed, using a genetic model that harbors an inflammation state in the fat body of larvae that mimic ATM, that reduction of ROS, using exogenous anti-oxidants components like flavonoids and anthiocianins, decreased hemocyte's migration and JNK activation in the cells of fat body (Valenza et al., 2018), suggesting that the converging signaling between the fat body and hemocytes on lipid metabolism and ROS/cytokines in response to stress is conserved also in *Drosophila*.

CANCER STEM CELLS

Cancer stem cells (CSCs) have more features than tissue stem cells because they are able to initiate the tumor growth and fuel its maintenance and metastasis (Malanchi et al., 2011; Kreso and Dick, 2014). In addition, CSCs are highly resistant to conventional therapy, both radiation and chemotherapy, and they are responsible for the recurrence of disease (Mueller et al., 2009). Since the mechanisms underlying the ability of stem cells to support cancer progression are still unclear, *Drosophila* is convenient to use as it provides many tools for genetic and molecular investigations. Adult stem cells are required for tissue homeostasis and repair after injury and in adult flies, populations of stem cells are present in the posterior midgut, testis, and ovarian follicle rendering it again a good system to dissect these stem cell programs (Hou and Singh, 2017). *Drosophila* was used to better understand the functions of the centrosome and microtubule-organizing center (MTOC) in the division of stem cells (Tillery et al., 2018). *Drosophila* and mammalian stem cells are similar and they are regulated by homologous signals corroborating the use of the fly in this field of tumor biology. CSCs can arise from normal stem cells whose long lifespan favors the accumulation of genetic mutations responsible for the malignant phenotype. The progression from normal progenitors to stem-like cancer cells was first explored in leukemia, although nowadays we know that several solid tumors such as brain, breast, lung and colon cancer originate from cells with stem features (Krivtsov et al., 2006). Several *Drosophila* models of stem cell tumors are now available, and a drug screening was successfully carried out highlighting several compounds active on the signaling promoting cancer growth (Markstein et al., 2014).

DROSOPHILA CANCER MODELS FOR THE IDENTIFICATION OF THERAPEUTIC DRUGS

Therapeutic drug discovery requires chemical screening, a procedure allowing for the identification of potential new drugs. The spread of sequencing, automation, and miniaturization has made High Throughput Screening (HTS) the leading contributor to early-stage drug discovery. HTS consists of random screening of chemicals to find an affinity for a specific protein or biological activity characteristic of a disorder. Once identified *in vitro*, the compounds need to be validated *in vivo* to assess efficacy and toxicity during a long and expensive period of drug development. The high throughput assays depend on the existence of a specific target, assuming an in depth understanding of a disease that is not always available. Phenotype screening is an eligible option when the knowledge about the mechanisms underlying a disease process is not well defined. It is a process by which small molecules are screened for their effect on the phenotype in cells, tissue or whole animals, where a more physiological environment better describes the pharmacokinetics and toxicological effects of a drug. The great availability of genetic tools and the low cost of maintenance makes the fruit fly an ideal to model to study human diseases including cancer, in fact the fly has considerably contributed to understand tumor biology.

Chemical screens have been successfully performed in *Drosophila* for several disorders affecting the central nervous system, kidney and metabolism (Whitworth et al., 2006; Gasque et al., 2013; Hofherr et al., 2016), as well as for a type of thyroid cancer, the multiple endocrine neoplasia type 2A and 2B (MEN2) (Vidal et al., 2005). Regarding cancer, JAK- STAT, APC, Wnt, Notch and other signaling molecules, deeply characterized in *Drosophila* and shared with humans, are precious for cancer drug development. The availability of *Drosophila* models for multiple cancer types makes pharmacological screens possible against several drugs that aim to restrict proliferation and metastasis. The identification of anticancer compounds is possible using the adult fly, but also larvae, embryos and cells. The combined effect of anti-cancer drugs with radiation has been investigated in *Drosophila* larvae, producing similar findings to those observed in human cancer cells (Edwards et al., 2011). Moreover, *Drosophila* avatars, consisting of patient-specific tumors modeled in transgenic flies, are very promising for personalized medicine. *Drosophila* and other small model organisms are helpful to quickly analyze the mode of action of several active compounds *in vivo,* nevertheless mammalian models are indispensable in the successive phase of drug development to define important pharmacokinetic parameters such as absorption, distribution and metabolism.

DISCUSSION

The communication between tumor cells and their microenvironment is largely implicated in neoplastic growth, hence the substantial difficulty to recapitulate the features of malignant transformation in cellular systems. Cancer research needs *in vivo* investigations, and the use of model organisms contributes to answer this request. In this review we described most relevant approaches in *Drosophila*, used to explore cancer mechanisms and therapeutics that contribute to our understanding on tumor initiation and progression. In spite of some limitations, because of the anatomical differences between flies and humans, the use of *Drosophila*'s cancer models has been fundamental to understand some basic processes that regulate human cancers, such as the competitiveness of cancer stem cells (CSCs), the importance of tumor microenvironment, cancer cachexia, drug resistance and tumor-associated vasculogenesis, which was recently found to be functionally conserved in fly's cancer. Additional cancer hallmarks such as genomic instability, resistance to cell death, cell metabolism reprogramming, tumor-promoting inflammation and evasion from the immune system, have been studied and extensively characterized in *Drosophila*. Finally, although the evolutionary difference between *Drosophila* and humans certainly represents a restriction to the use of the fruit fly in drug discovery and development, phenotypic screenings have proven relevant to identify potential drugs that would elude the classic screens in the absence of targets. *Drosophila* is also offering a significant contribution to the investigation of organotypic cancers, since despite the evident differences at the macroscopic level, organ cells and functional units are usually well conserved at the biochemical and structural levels respectively. This conservation allowed to develop thyroid, lung, prostate, gut, brain and blood cancer models starting from the most characteristic genetic lesions found in the same human cancers. These models, as described in the review, are greatly helping in dissecting the contribution of specific molecular pathways to the final cancer phenotype. Given the heterogeneous nature of mammalian solid cancers, new strategies are being developed to decipher cancers at single-cell resolution. The international *Drosophila* community has always been engaged in the development of novel, sophisticated genetic tools, which allowed in the last 30 years to revolutionate functional gene analysis. For this reason, we anticipate that the use of the fruit fly will move fast into the field of precision medicine, contributing to seminal findings in this new era of cancer research.

AUTHOR CONTRIBUTIONS

All authors listed have made a substantial, direct and intellectual contribution to the work, and approved it for publication.

FUNDING

Funding was provided from the Cariplo Foundation 2014–0703 and EHDN 689 for PB and AV, AIRC-IG17252 for DG and MS.

ACKNOWLEDGMENTS

We apologize to colleagues whose work was not cited in this manuscript due to space limitations. We thank all members of Bellosta's and Grifoni's laboratories and Sheri Zola for their comments on the review.

REFERENCES

Aavikko, M., Li, S. P., Saarinen, S., Alhopuro, P., Kaasinen, E., Morgunova, E., et al. (2012). Loss of SUFU function in familial multiple meningioma. *Am. J. Hum. Genet.* 91, 520–526. doi: 10.1016/j.ajhg.2012.07.015

Affolter, M., Zeller, R., and Caussinus, E. (2009). Tissue remodelling through branching morphogenesis. *Nat. Rev. Mol. Cell Biol.* 10, 831–842. doi: 10.1038/nrm2797

Al-Zoughbi, W., Pichler, M., Gorkiewicz, G., Guertl-Lackner, B., Haybaeck, J., Jahn Stephan, W., et al. (2016). Loss of adipose triglyceride lipase is associated with human cancer and induces mouse pulmonary neoplasia. *Oncotarget* 7, 33832–33840. doi: 10.18632/oncotarget.9418

Andersen, D. S., Colombani, J., Palmerini, V., Chakrabandhu, K., Boone, E., Rothlisberger, M., et al. (2015). The *Drosophila* TNF receptor Grindelwald couples loss of cell polarity and neoplastic growth. *Nature* 522, 482–486. doi: 10.1038/nature14298

Anderson, A. M., Bailetti, A. A., Rodkin, E., De, A., and Bach, E. A. (2017). A genetic screen reveals an unexpected role for yorkie signaling in JAK/STAT-dependent hematopoietic malignancies in *Drosophila melanogaster*. *G3* 7, 2427–2438. doi: 10.1534/g3.117.044172

Andrew, D. J., and Ewald, A. J. (2010). Morphogenesis of epithelial tubes: insights into tube formation, elongation, and elaboration. *Dev. Biol.* 34, 34–55. doi: 10.1016/j.ydbio.2009.09.024

Apidianakis, Y., and Rahme, L. G. (2011). *Drosophila melanogaster* as a model for human intestinal infection and pathology. *Dis. Model. Mech.* 4, 21–30. doi: 10.1242/dmm.003970

Arango Duque, G., and Descoteaux, A. (2014). Macrophage cytokines: involvement in immunity and infectious diseases. *Front. Immunol.* 5:491. doi: 10.3389/fimmu.2014.00491

Bangi, E. (2013). *Drosophila* at the intersection of infection, inflammation, and cancer. *Front. Cell. Infect. Microbiol.* 3:103. doi: 10.3389/fcimb.2013.00103

Bangi, E., Murgia, C., Teague, A. G., Sansom, O. J., and Cagan, R. L. (2016). Functional exploration of colorectal cancer genomes using *Drosophila*. *Nat. Commun.* 7:13615. doi: 10.1038/ncomms13615

Barker, N., Ridgway, R. A., van Es, J. H., van de Wetering, M., Begthel, H., van den Born, M., et al. (2009). Crypt stem cells as the cells-of-origin of intestinal cancer. *Nature* 457, 608–611. doi: 10.1038/nature07602

Bellosta, P., and Gallant, P. (2010). Myc Function in *Drosophila*. *Genes Cancer* 1, 542–546. doi: 10.1177/1947601910377490

Benhra, N., Barrio, L., Muzzopappa, M., and Milan, M. (2018). Chromosomal instability induces cellular invasion in epithelial tissues. *Dev. Cell* 47, 161 e164–174 e164. doi: 10.1016/j.devcel.2018.08.021

Bergmann, A., Agapite, J., McCall, K., and Steller, H. (1998). The *Drosophila* gene hid is a direct molecular target of ras-dependent survival signaling. *Cell* 95, 331–341. doi: 10.1016/S0092-8674(00)81765-1

Betschinger, J., Mechtler, K., and Knoblich, J. A. (2006). Asymmetric segregation of the tumor suppressor brat regulates self-renewal in *Drosophila* neural stem cells. *Cell* 124, 1241–1253. doi: 10.1016/j.cell.2006.01.038

Bettegowda, C., Agrawal, N., Jiao, Y., Sausen, M., Wood, L. D., Hruban, R. H., et al. (2011). Mutations in CIC and FUBP1 contribute to human oligodendroglioma. *Science* 333, 1453–1455. doi: 10.1126/science.1210557

Bienz, M., and Clevers, H. (2000). Linking colorectal cancer to Wnt signaling. *Cell* 103, 311–320. doi: 10.1016/S0092-8674(00)00122-7

Bilder, D. (2004). Epithelial polarity and proliferation control: links from the *Drosophila* neoplastic tumor suppressors. *Genes Dev.* 18, 1909–1925. doi: 10.1101/gad.1211604

Biteau, B., Hochmuth, C. E., and Jasper, H. (2008). JNK activity in somatic stem cells causes loss of tissue homeostasis in the aging *Drosophila* gut. *Cell Stem Cell* 3, 442–455. doi: 10.1016/j.stem.2008.07.024

Biteau, B., and Jasper, H. (2011). EGF signaling regulates the proliferation of intestinal stem cells in *Drosophila*. *Development* 138, 1045–1055. doi: 10.1242/dev.056671

Brumby, A. M., Goulding, K. R., Schlosser, T., Loi, S., Galea, R., Khoo, P., et al. (2011). Identification of novel Ras-cooperating oncogenes in *Drosophila melanogaster*: a RhoGEF/Rho-family/JNK pathway is a central driver of tumorigenesis. *Genetics* 188, 105–125. doi: 10.1534/genetics.111.127910

Brumby, A. M., and Richardson, H. E. (2003). scribble mutants cooperate with oncogenic Ras or Notch to cause neoplastic overgrowth in *Drosophila*. *EMBO J.* 22, 5769–5779. doi: 10.1093/emboj/cdg548

Bryant, D. M., and Mostov, K. E. (2008). From cells to organs: building polarized tissue. *Nat. Rev. Mol. Cell Biol.* 9, 887–901. doi: 10.1038/nrm2523

Calleja, M., Morata, G., and Casanova, J. (2016). Tumorigenic properties of *Drosophila* epithelial cells mutant for lethal giant larvae. *Dev. Dyn.* 245, 834–843. doi: 10.1002/dvdy.24420

Cancer, C. G. o. E. S. o. O. (2012). Ovarian cancer and body size: individual participant meta-analysis including 25,157 women with ovarian cancer from 47 epidemiological studies. *PLoS Med.* 9:e1001200. doi: 10.1371/journal.pmed.1001200

Carmeliet, P., and Jain, R. K. (2011). Molecular mechanisms and clinical applications of angiogenesis. *Nature* 473, 298–307. doi: 10.1038/nature10144

Caussinus, E., and Gonzalez, C. (2005). Induction of tumor growth by altered stem-cell asymmetric division in *Drosophila melanogaster*. *Nat. Genet.* 37, 1125–1129. doi: 10.1038/ng1632

Chen, G., Kong, J., Tucker-Burden, C., Anand, M., Rong, Y., Rahman, F., et al. (2014). Human Brat ortholog TRIM3 is a tumor suppressor that regulates asymmetric cell division in glioblastoma. *Cancer Res.* 74, 4536–4548. doi: 10.1158/0008-5472.CAN-13-3703

Chen, Y., Wang, X., Wang, J., Yan, Z., and Luo, J. (2012). Excess body weight and the risk of primary liver cancer: an updated meta-analysis of prospective studies. *Eur J Cancer* 48, 2137–2145. doi: 10.1016/j.ejca.2012.02.063

Christofi, T., and Apidianakis, Y. (2013). Ras-oncogenic *Drosophila* hindgut but not midgut cells use an inflammation-like program to disseminate to distant sites. *Gut Microbes* 4, 54–59. doi: 10.4161/gmic.22429

Claus, E. B., Bondy, M. L., Schildkraut, J. M., Wiemels, J. L., Wrensch, M., and Black, P. M. (2005). Epidemiology of intracranial meningioma. *Neurosurgery* 57, 1088–1095; discussion 1088–1095. doi: 10.1227/01.NEU.0000188281.91351.B9

Claveria, C., and Torres, M. (2016). Cell competition: mechanisms and physiological roles. *Annu. Rev. Cell Dev. Biol.* 32, 411–439. doi: 10.1146/annurev-cellbio-111315-125142

Clemente-Ruiz, M., Murillo-Maldonado, J. M., Benhra, N., Barrio, L., Perez, L., Quiroga, G., et al. (2016). Gene dosage imbalance contributes to chromosomal instability-induced tumorigenesis. *Dev. Cell* 36, 290–302. doi: 10.1016/j.devcel.2016.01.008

Cordero, J. B., Macagno, J. P., Stefanatos, R. K., Strathdee, K. E., Cagan, R. L., and Vidal, M. (2010). Oncogenic ras diverts a host TNF tumor suppressor activity into tumor promoter. *Dev. Cell* 18, 999–1011. doi: 10.1016/j.devcel.2010.05.014

Cordero, J. B., Ridgway, R. A., Valeri, N., Nixon, C., Frame, M. C., Muller, W. J., et al. (2014). c-Src drives intestinal regeneration and transformation. *EMBO J.* 33, 1474–1491. doi: 10.1002/embj.201387454

Cordero, J. B., Stefanatos, R. K., Myant, K., Vidal, M., and Sansom, O. J. (2012a). Non-autonomous crosstalk between the Jak/Stat and Egfr pathways mediates Apc1-driven intestinal stem cell hyperplasia in the *Drosophila* adult midgut. *Development* 139, 4524–4535. doi: 10.1242/dev.078261

Cordero, J. B., Stefanatos, R. K., Scopelliti, A., Vidal, M., and Sansom, O. J. (2012b). Inducible progenitor-derived Wingless regulates adult midgut regeneration in *Drosophila*. *EMBO J.* 31, 3901–3917. doi: 10.1038/emboj.2012.248

Dall'Armi, C., Devereaux, K. A., and Di Paolo, G. (2013). The role of lipids in the control of autophagy. *Curr. Biol.* 23, R33–R45. doi: 10.1016/j.cub.2012.10.041

Das, T. K., and Cagan, R. L. (2013). A *Drosophila* approach to thyroid cancer therapeutics. *Drug Discov. Today Technol.* 10, e65–71. doi: 10.1016/j.ddtec.2012.09.004

Das, T. K., and Cagan, R. L. (2018). Non-mammalian models of multiple endocrine neoplasia type 2. *Endocr. Relat. Cancer* 25, T91–T104. doi: 10.1530/ERC-17-0411

de la Cova, C., Abril, M., Bellosta, P., Gallant, P., and Johnston, L. A. (2004). *Drosophila* myc regulates organ size by inducing cell competition. *Cell* 117, 107–116. doi: 10.1016/S0092-8674(04)00214-4

de la Cova, C., Senoo-Matsuda, N., Ziosi, M., Wu, D. C., Bellosta, P., Quinzii, C. M., et al. (2014). Supercompetitor status of *Drosophila* Myc cells requires p53 as a fitness sensor to reprogram metabolism and promote viability. *Cell Metab.* 19, 470–483. doi: 10.1016/j.cmet.2014.01.012

DeBerardinis, R. J., Lum, J. J., Hatzivassiliou, G., and Thompson, C. B. (2008). The biology of cancer: metabolic reprogramming fuels cell growth and proliferation. *Cell Metab.* 7, 11–20. doi: 10.1016/j.cmet.2007.10.002

Di Giacomo, S., Sollazzo, M., de Biase, D., Ragazzi, M., Bellosta, P., Pession, A., et al. (2017). Human cancer cells signal their competitive fitness through MYC activity. *Sci. Rep.* 7, 12568. doi: 10.1038/s41598-017-13002-1

Dionne, M. (2014). Immune-metabolic interaction in *Drosophila*. *Fly (Austin)*. 8, 75–79. doi: 10.4161/fly.28113

Dougan, M. M., Hankinson, S. E., Vivo, I. D., Tworoger, S. S., Glynn, R. J., and Michels, K. B. (2015). Prospective study of body size throughout the life-course and the incidence of endometrial cancer among premenopausal and postmenopausal women. *Int. J. Cancer* 137, 625–637. doi: 10.1002/ijc.29427

Duronio, R. J., and Xiong, Y. (2013). Signaling pathways that control cell proliferation. *Cold Spring Harb. Perspect. Biol.* 5:a008904. doi: 10.1101/cshperspect.a008904

Edwards, A., Gladstone, M., Yoon, P., Raben, D., Frederick, B., and Su, T. T. (2011). Combinatorial effect of maytansinol and radiation in *Drosophila* and human cancer cells. *Dis. Model. Mech.* 4, 496–503. doi: 10.1242/dmm.006486

Elbediwy, A., and Thompson, B. J. (2018). Evolution of mechanotransduction via YAP/TAZ in animal epithelia. *Curr. Opin. Cell Biol.* 51, 117–123. doi: 10.1016/j.ceb.2018.02.003

El-Habr, E. A., Levidou, G., Trigka, E. A., Sakalidou, J., Piperi, C., Chatziandreou, I., et al. (2014). Complex interactions between the components of the PI3K/AKT/mTOR pathway, and with components of MAPK, JAK/STAT and Notch-1 pathways, indicate their involvement in meningioma development. *Virchows Arch.* 465, 473–485. doi: 10.1007/s00428-014-1641-3

Fogarty, C. E., Diwanji, N., Lindblad, J. L., Tare, M., Amcheslavsky, A., Makhijani, K., et al. (2016). Extracellular reactive oxygen species drive apoptosis-induced proliferation via *Drosophila* macrophages. *Curr. Biol.* 26, 575–584. doi: 10.1016/j.cub.2015.12.064

Froldi, F., Ziosi, M., Garoia, F., Pession, A., Grzeschik, N. A., Bellosta, P., et al. (2010). The lethal giant larvae tumour suppressor mutation requires dMyc oncoprotein to promote clonal malignancy. *BMC Biol.* 8:33. doi: 10.1186/1741-7007-8-33

Gallagher, E. J., and LeRoith, D. (2015). Obesity and diabetes: the increased risk of cancer and cancer-related mortality. *Physiol. Rev.* 95, 727–748. doi: 10.1152/physrev.00030.2014

Gallant, P., Shiio, Y., Cheng, P. F., Parkhurst, S. M., and Eisenman, R. N. (1996). Myc and max homologs in *Drosophila*. *Science* 274, 1523–1527. doi: 10.1126/science.274.5292.1523

Galletti, M., Riccardo, S., Parisi, F., Lora, C., Saqcena, M. K., Rivas, L., et al. (2009). Identification of domains responsible for ubiquitin-dependent degradation of dMyc by glycogen synthase kinase 3β and casein kinase 1 kinases. *Mol. Cell. Biol.* 29, 3424–3434. doi: 10.1128/MCB.01535-08

Gasque, G., Conway, S., Huang, J., Rao, Y., and Vosshall, L. B. (2013). Small molecule drug screening in *Drosophila* identifies the 5HT2A receptor as a feeding modulation target. *Sci. Rep.* 3:srep02120. doi: 10.1038/srep02120

Genevet, A., Wehr, M. C., Brain, R., Thompson, B. J., and Tapon, N. (2010). Kibra is a regulator of the Salvador/Warts/Hippo signaling network. *Dev. Cell* 18, 300–308. doi: 10.1016/j.devcel.2009.12.011

Ghabrial, A., Luschnig, S., Metzstein, M. M., and Krasnow, M. A. (2003). Branching morphogenesis of the *Drosophila* tracheal system. *Annu. Rev. Cell Dev. Biol.* 19, 623–647. doi: 10.1146/annurev.cellbio.19.031403.160043

Glise, B., Bourbon, H., and Noselli, S. (1995). hemipterous encodes a novel *Drosophila* MAP kinase kinase, required for epithelial cell sheet movement. *Cell* 83, 451–461. doi: 10.1016/0092-8674(95)90123-X

Gnerlich, J. L., Yao, K. A., Fitchev, P. S., Goldschmidt, R. A., Bond, M. C., Cornwell, M., et al. (2013). Peritumoral expression of adipokines and fatty acids in breast cancer. *Ann. Surg. Oncol.* 20(Suppl. 3), S731–S738. doi: 10.1245/s10434-013-3274-1

Gont, A., Hanson, J. E., Lavictoire, S. J., Parolin, D. A., Daneshmand, M., Restall, I. J., et al. (2013). PTEN loss represses glioblastoma tumor initiating cell differentiation via inactivation of Lgl1. *Oncotarget* 4, 1266–1279. doi: 10.18632/oncotarget.1164

Grace, S. A., Meeks, M. W., Chen, Y., Cornwell, M., Ding, X., Hou, P., et al. (2017). Adipose triglyceride lipase (ATGL) expression is associated with adiposity and tumor stromal proliferation in patients with pancreatic ductal adenocarcinoma. *Anticancer Res.* 37, 699–703. doi: 10.21873/anticanres.11366

Grewal, S. S. (2009). Insulin/TOR signaling in growth and homeostasis: a view from the fly world. *Int. J. Biochem. Cell Biol.* 41, 1006–1010. doi: 10.1016/j.biocel.2008.10.010

Grewal, S. S., Li, L., Orian, A., Eisenman, R. N., and Edgar, B. A. (2005). Myc-dependent regulation of ribosomal RNA synthesis during *Drosophila* development. *Nat. Cell Biol.* 7, 295–302. doi: 10.1038/ncb1223

Grifoni, D., and Bellosta, P. (2015). *Drosophila* Myc: a master regulator of cellular performance. *Biochim. Biophys. Acta* 1849, 570–581. doi: 10.1016/j.bbagrm.2014.06.021

Grifoni, D., Garoia, F., Bellosta, P., Parisi, F., De Biase, D., Collina, G., et al. (2007). aPKCζ cortical loading is associated with Lgl cytoplasmic release and tumor growth in *Drosophila* and human epithelia. *Oncogene* 26, 5960–5965. doi: 10.1038/sj.onc.1210389

Grifoni, D., Garoia, F., Schimanski, C. C., Schmitz, G., Laurenti, E., Galle, P. R., et al. (2004). The human protein Hugl-1 substitutes for *Drosophila* lethal giant larvae tumour suppressor function *in vivo*. *Oncogene* 23, 8688–8694. doi: 10.1038/sj.onc.1208023

Grifoni, D., Sollazzo, M., Fontana, E., Froldi, F., and Pession, A. (2015). Multiple strategies of oxygen supply in *Drosophila* malignancies identify tracheogenesis as a novel cancer hallmark. *Sci. Rep.* 5:9061. doi: 10.1038/srep 09061

Grzeschik, N. A., Amin, N., Secombe, J., Brumby, A. M., and Richardson, H. E. (2007). Abnormalities in cell proliferation and apico-basal cell polarity are separable in *Drosophila* lgl mutant clones in the developing eye. *Dev. Biol.* 311, 106–123. doi: 10.1016/j.ydbio.2007.08.025

Grzeschik, N. A., Parsons, L. M., and Richardson, H. E. (2010). Lgl, the SWH pathway and tumorigenesis: It's a matter of context & competition! *Cell Cycle* 9, 3202–3212. doi: 10.4161/cc.9.16.12633

Hafen, E. (2004). Cancer, type 2 diabetes, and ageing: news from flies and worms. *Swiss Med. Wkly.* 134, 711–719. doi: 10.4414/smw.2004.09885

Halaoui, R., and McCaffrey, L. (2015). Rewiring cell polarity signaling in cancer. *Oncogene* 34, 939–950. doi: 10.1038/onc.2014.59

Ham, B., Fernandez, M. C., D'Costa, Z., and Brodt, P. (2016). The diverse roles of the TNF axis in cancer progression and metastasis. *Trends Cancer Res.* 11, 1–27.

Hanahan, D., and Weinberg, R. A. (2000). The hallmarks of cancer. *Cell* 100, 57–70. doi: 10.1016/S0092-8674(00)81683-9

Hanahan, D., and Weinberg, R. A. (2011). Hallmarks of cancer: the next generation. *Cell* 144, 646–674. doi: 10.1016/j.cell.2011.02.013

Hariharan, I. K., and Bilder, D. (2006). Regulation of imaginal disc growth by tumor-suppressor genes in *Drosophila*. *Annu. Rev. Genet.* 40, 335–361. doi: 10.1146/annurev.genet.39.073003.100738

Harvey, K. F., Pfleger, C. M., and Hariharan, I. K. (2003). The *Drosophila* Mst ortholog, hippo, restricts growth and cell proliferation and promotes apoptosis. *Cell* 114, 457–467. doi: 10.1016/S0092-8674(03)00557-9

Harvey, K. F., Zhang, X., and Thomas, D. M. (2013). The Hippo pathway and human cancer. *Nat. Rev. Cancer* 13, 246–257. doi: 10.1038/nr c3458

Herranz, H., Eichenlaub, T., and Cohen, S. M. (2016). Cancer in *Drosophila*: imaginal discs as a model for epithelial tumor formation. *Curr. Top. Dev. Biol.* 116, 181–199. doi: 10.1016/bs.ctdb.2015.11.037

Hida, K., Maishi, N., Annan, D. A., and Hida, Y. (2018). Contribution of tumor endothelial cells in cancer progression. *Int. J. Mol. Sci.* 19. doi: 10.3390/ijms19051272

Hirabayashi, S. (2016). The interplay between obesity and cancer: a fly view. *Dis. Model. Mech.* 9, 917–926. doi: 10.1242/dmm.025320

Hofherr, A., Wagner, C. J., Watnick, T., and Kottgen, M. (2016). Targeted rescue of a polycystic kidney disease mutation by lysosomal inhibition. *Kidney Int.* 89, 949–955. doi: 10.1016/j.kint.2015.11.015

Hou, S. X., and Singh, S. R. (2017). Stem-cell-based tumorigenesis in adult *Drosophila*. *Curr. Top. Dev. Biol.* 121, 311–337. doi: 10.1016/bs.ctdb.2016.07.013

Hsieh, A. L., and Dang, C. V. (2016). MYC, metabolic synthetic lethality, and cancer. *Recent Results Cancer Res.* 207, 73–91. doi: 10.1007/978-3-319-42118-6_4

Hsieh, A. L., Walton, Z. E., Altman, B. J., Stine, Z. E., and Dang, C. V. (2015). MYC and metabolism on the path to cancer. *Semin. Cell Dev. Biol.* 43, 11–21. doi: 10.1016/j.semcdb.2015.08.003

Hulf, T., Bellosta, P., Furrer, M., Steiger, D., Svensson, D., Barbour, A., et al. (2005). Whole-genome analysis reveals a strong positional bias of conserved dMyc-dependent E-boxes. *Mol. Cell. Biol.* 25, 3401–3410. doi: 10.1128/MCB.25.9.3401-3410.2005

Igaki, T. (2009). Correcting developmental errors by apoptosis: lessons from *Drosophila* JNK signaling. *Apoptosis* 14, 1021–1028. doi: 10.1007/s10495-009-0361-

Igaki, T., Pagliarini, R. A., and Xu, T. (2006). Loss of cell polarity drives tumor growth and invasion through JNK activation in *Drosophila*. *Curr. Biol.* 16, 1139–1146. doi: 10.1016/j.cub.2006.04.042

Ito, S., Ueda, T., Ueno, A., Nakagawa, H., Taniguchi, H., Kayukawa, N., et al. (2014). A genetic screen in *Drosophila* for regulators of human prostate cancer progression. *Biochem. Biophys. Res. Commun.* 451, 548–555. doi: 10.1016/j.bbrc.2014.08.015

Jiang, H., and Edgar, B. A. (2009). EGFR signaling regulates the proliferation of *Drosophila* adult midgut progenitors. *Development* 136, 483–493. doi: 10.1242/dev.026955

Jiang, H., Grenley, M. O., Bravo, M. J., Blumhagen, R. Z., and Edgar, B. A. (2011). EGFR/Ras/MAPK signaling mediates adult midgut epithelial homeostasis and regeneration in *Drosophila*. *Cell Stem Cell* 8, 84–95. doi: 10.1016/j.stem.2010.11.026

Johnson, R., and Halder, G. (2014). The two faces of Hippo: targeting the Hippo pathway for regenerative medicine and cancer treatment. *Nat. Rev. Drug Discov.* 13, 63–79. doi: 10.1038/nrd4161

Johnston, L. A. (2014). Socializing with MYC: cell competition in development and as a model for premalignant cancer. *Cold Spring Harb. Perspect Med.* 4:a014274. doi: 10.1101/cshperspect.a014274

Johnston, L. A., Prober, D. A., Edgar, B. A., Eisenman, R. N., and Gallant, P. (1999). *Drosophila* myc regulates cellular growth during development. *Cell* 98, 779–790. doi: 10.1016/S0092-8674(00)81512-3

Jung, S. H., Evans, C. J., Uemura, C., and Banerjee, U. (2005). The *Drosophila* lymph gland as a developmental model of hematopoiesis. *Development* 132, 2521–2533. doi: 10.1242/dev.01837

Kanda, H., Igaki, T., Kanuka, H., Yagi, T., and Miura, M. (2002). Wengen, a member of the *Drosophila* tumor necrosis factor receptor superfamily, is required for Eiger signaling. *J. Biol. Chem.* 277, 28372–28375. doi: 10.1074/jbc.C200324200

Katheder, N. S., and Rusten, T. E. (2017). Microenvironment and tumors-a nurturing relationship. *Autophagy* 13, 1241–1243. doi: 10.1080/15548627.2017.1310361

Kockel, L., Homsy, J. G., and Bohmann, D. (2001). *Drosophila* AP-1: lessons from an invertebrate. *In Oncogene, pp*. 2347–2364. doi: 10.1038/sj.onc.1204300

Kreso, A., and Dick, J. E. (2014). Evolution of the cancer stem cell model. *Cell Stem Cell* 14, 275–291. doi: 10.1016/j.stem.2014.02.006

Krivtsov, A. V., Twomey, D., Feng, Z., Stubbs, M. C., Wang, Y., Faber, J., et al. (2006). Transformation from committed progenitor to leukaemia stem cell initiated by MLL-AF9. *Nature* 442, 818–822. doi: 10.1038/nature 04980

Krzemien, J., Dubois, L., Makki, R., Meister, M., Vincent, A., and Crozatier, M. (2007). Control of blood cell homeostasis in *Drosophila* larvae by the posterior signalling centre. *Nature* 446, 325–328. doi: 10.1038/nature05650

Kumar, M., Lechel, A., and Gunes, C. (2016). Telomerase: the devil inside. *Genes (Basel)* 7:E43. doi: 10.3390/genes7080043

Kuroda, M., and Sakaue, H. (2017). Adipocyte death and chronic inflammation in obesity. *J. Med. Invest.* 64, 193–196. doi: 10.2152/jmi.64.193

Lafontan, M. (2014). Adipose tissue and adipocyte dysregulation. *Diabetes Metab.* 40, 16–28. doi: 10.1016/j.diabet.2013.08.002

Lambert, A. W., Pattabiraman, D. R., and Weinberg, R. A. (2017). Emerging biological principles of metastasis. *Cell* 168, 670–691. doi: 10.1016/j.cell.2016.11.037

Lebestky, T., Jung, S. H., and Banerjee, U. (2003). A Serrate-expressing signaling center controls *Drosophila* hematopoiesis. *Genes Dev.* 17, 348–353. doi: 10.1101/gad.1052803

Lee, T., and Luo, L. (1999). Mosaic analysis with a repressible cell marker for studies of gene function in neuronal morphogenesis. *Neuron* 22, 451–461. doi: 10.1016/S0896-6273(00)80701-1

Lemaitre, B., and Hoffmann, J. (2007). The host defense of *Drosophila melanogaster*. *Annu. Rev. Immunol.* 25, 697–743. doi: 10.1146/annurev.immunol.25.022106.141615

Levine, B. D., and Cagan, R. L. (2016). *Drosophila* lung cancer models identify trametinib plus statin as candidate therapeutic. *Cell Rep.* 14, 1477–1487. doi: 10.1016/j.celrep.2015.12.105

Levinson, S., and Cagan, R. L. (2016). *Drosophila* Cancer models identify functional differences between ret fusions. *Cell Rep.* 16, 3052–3061. doi: 10.1016/j.celrep.2016.08.019

Lu, L., Li, Y., Kim, S. M., Bossuyt, W., Liu, P., Qiu, Q., et al. (2010). Hippo signaling is a potent *in vivo* growth and tumor suppressor pathway in the mammalian liver. *Proc. Natl. Acad. Sci. U.S.A.* 107, 1437–1442. doi: 10.1073/pnas.0911427107

Lu, X., Feng, X., Man, X., Yang, G., Tang, L., Du, D., et al. (2009). Aberrant splicing of Hugl-1 is associated with hepatocellular carcinoma progression. *Clin. Cancer Res.* 15, 3287–3296. doi: 10.1158/1078-0432.CCR-08-2078

Ma, X., Wang, H., Ji, J., Xu, W., Sun, Y., Li, W., et al. (2017). Hippo signaling promotes JNK-dependent cell migration. *Proc. Natl. Acad. Sci. U.S.A.* 114, 1934–1939. doi: 10.1073/pnas.1621359114

Malanchi, I., Santamaria-Martinez, A., Susanto, E., Peng, H., Lehr, H. A., Delaloye, J. F., et al. (2011). Interactions between cancer stem cells and their niche govern metastatic colonization. *Nature* 481, 85–89. doi: 10.1038/nature10694

Mandal, L., Martinez-Agosto, J. A., Evans, C. J., Hartenstein, V., and Banerjee, U. (2007). A Hedgehog- and Antennapedia-dependent niche maintains *Drosophila* haematopoietic precursors. *Nature* 446, 320–324. doi: 10.1038/nature05585

Mantovani, A., Allavena, P., Sica, A., and Balkwill, F. (2008). Cancer-related inflammation. *Nature* 454, 436–444. doi: 10.1038/nature07205

Markstein, M., Dettorre, S., Cho, J., Neumuller, R. A., Craig-Muller, S., and Perrimon, N. (2014). Systematic screen of chemotherapeutics in *Drosophila* stem cell tumors. *Proc. Natl. Acad. Sci. U.S.A.* 111, 4530–4535. doi: 10.1073/pnas.1401160111

Martin-Blanco, E., Gampel, A., Ring, J., Virdee, K., Kirov, N., Tolkovsky, A. M., et al. (1998). puckered encodes a phosphatase that mediates a feedback loop regulating JNK activity during dorsal closure in *Drosophila*. *Genes Dev.* 12, 557–570. doi: 10.1101/gad.12.4.557

Martinez-Outschoorn, U. E., Pestell, R. G., Howell, A., Tykocinski, M. L., Nagajyothi, F., Machado, F. S., et al. (2011). Energy transfer in "parasitic" cancer metabolism: mitochondria are the powerhouse and Achilles' heel of tumor cells. *Cell Cycle* 10, 4208–4216. doi: 10.4161/cc.10.24.18487

Massague, J., and Obenauf, A. C. (2016). Metastatic colonization by circulating tumour cells. *Nature* 529, 298–306. doi: 10.1038/nature17038

Medioni, C., Senatore, S., Salmand, P. A., Lalevee, N., Perrin, L., and Semeriva, M. (2009). The fabulous destiny of the *Drosophila* heart. *Curr. Opin. Genet. Dev.* 19, 518–525. doi: 10.1016/j.gde.2009.07.004

Menendez, J., Perez-Garijo, A., Calleja, M., and Morata, G. (2010). A tumor-suppressing mechanism in *Drosophila* involving cell competition and the Hippo pathway. *Proc. Natl. Acad. Sci. U.S.A.* 107, 14651–14656. doi: 10.1073/pnas.1009376107

Millburn, G. H., Crosby, M. A., Gramates, L. S., Tweedie, S., and FlyBase, C. (2016). FlyBase portals to human disease research using *Drosophila* models. *Dis. Model. Mech.* 9, 245–252. doi: 10.1242/dmm.023317

Moreno, E., and Basler, K. (2004). dMyc transforms cells into super-competitors. *Cell* 117, 117–129. doi: 10.1016/S0092-8674(04)00262-4

Morrison, D. K. (2012). MAP kinase pathways. *Cold Spring Harb. Perspect. Biol.* 4:a011254. doi: 10.1101/cshperspect.a011254

Mortimer, N. T., and Moberg, K. H. (2013). The archipelago ubiquitin ligase subunit acts in target tissue to restrict tracheal terminal cell branching and hypoxic-induced gene expression. *PLoS Genet.* 9:e1003314. doi: 10.1371/journal.pgen.1003314

Mraz, M., and Haluzik, M. (2014). The role of adipose tissue immune cells in obesity and low-grade inflammation. *J. Endocrinol.* 222, R113–127. doi: 10.1530/JOE-14-0283

Mueller, M. T., Hermann, P. C., Witthauer, J., Rubio-Viqueira, B., Leicht, S. F., Huber, S., et al. (2009). Combined targeted treatment to eliminate tumorigenic cancer stem cells in human pancreatic cancer. *Gastroenterology* 137, 1102–1113. doi: 10.1053/j.gastro.2009.05.053

Mukherjee, S., Tucker-Burden, C., Zhang, C., Moberg, K., Read, R., Hadjipanayis, C., et al. (2016). *Drosophila* brat and human ortholog TRIM3 maintain stem cell equilibrium and suppress brain tumorigenesis by attenuating notch nuclear transport. *Cancer Res.* 76, 2443–2452. doi: 10.1158/0008-5472.CAN-15-2299

Muzzopappa, M., Murcia, L., and Milan, M. (2017). Feedback amplification loop drives malignant growth in epithelial tissues. *Proc. Natl. Acad. Sci. U.S.A.* 114, E7291–E7300. doi: 10.1073/pnas.1701791114

Namee, N. M., and O'Driscoll, L. (2018). Extracellular vesicles and anti-cancer drug resistance. *Biochim. Biophys. Acta Rev. Cancer* 1870, 123–136. doi: 10.1016/j.bbcan.2018.07.003

Negrini, S., Gorgoulis, V. G., and Halazonetis, T. D. (2010). Genomic instability–an evolving hallmark of cancer. *Nat. Rev. Mol. Cell Biol.* 11, 220–228. doi: 10.1038/nrm2858

Neto-Silva, R. M., de Beco, S., and Johnston, L. A. (2010). Evidence for a growth-stabilizing regulatory feedback mechanism between Myc and Yorkie, the *Drosophila* homolog of Yap. *Dev. Cell* 19, 507–520. doi: 10.1016/j.devcel.2010.09.009

Oh, H., and Irvine, K. D. (2008). *In vivo* regulation of Yorkie phosphorylation and localization. *Development* 135, 1081–1088. doi: 10.1242/dev.015255

Ohlmeyer, J. T., and Kalderon, D. (1998). Hedgehog stimulates maturation of Cubitus interruptus into a labile transcriptional activator. *Nature* 396, 749–753. doi: 10.1038/25533

Orian, A., Grewal, S. S., Knoepfler, P. S., Edgar, B. A., Parkhurst, S. M., and Eisenman, R. N. (2005). Genomic binding and transcriptional regulation by the *Drosophila* Myc and Mnt transcription factors. *Cold Spring Harb. Symp. Quant. Biol.* 70, 299–307. doi: 10.1101/sqb.2005.70.019

Ortega-Molina, A., and Serrano, M. (2013). PTEN in cancer, metabolism, and aging. *Trends Endocrinol. Metab.* 24, 184–189. doi: 10.1016/j.tem.2012.11.002

Osman, D., Gobert, V., Ponthan, F., Heidenreich, O., Haenlin, M., and Waltzer, L. (2009). A *Drosophila* model identifies calpains as modulators of the human leukemogenic fusion protein AML1-ETO. *Proc. Natl. Acad. Sci. U.S.A.* 106, 12043–12048. doi: 10.1073/pnas.0902449106

Ou, J., Miao, H., Ma, Y., Guo, F., Deng, J., Wei, X., et al. (2014). Loss of abhd5 promotes colorectal tumor development and progression by inducing aerobic glycolysis and epithelial-mesenchymal transition. *Cell Rep.* 9, 1798–1811. doi: 10.1016/j.celrep.2014.11.016

Paglia, S., Sollazzo, M., Di Giacomo, S., de Biase, D., Pession, A., and Grifoni, D. (2017). Failure of the PTEN/aPKC/Lgl axis primes formation of adult brain tumours in *Drosophila*. *Biomed Res. Int.* 2017, 2690187. doi: 10.1155/2017/2690187

Pagliarini, R. A., and Xu, T. (2003). A genetic screen in *Drosophila* for metastatic behavior. *Science* 302, 1227–1231. doi: 10.1126/science.1088474

Paiardi, C., Mirzoyan, Z., Zola, S., Parisi, F., Vingiani, A., Pasini, M. E., et al. (2017). The stearoyl-CoA desaturase-1 (Desat1) in *Drosophila* cooperated with Myc to induce autophagy and growth, a potential new link to tumor survival. *Genes* 8:E131. doi: 10.3390/genes8050131

Pan, D. (2010). The hippo signaling pathway in development and cancer. *Dev. Cell* 19, 491–505. doi: 10.1016/j.devcel.2010.09.011

Panciera, T., Azzolin, L., Cordenonsi, M., and Piccolo, S. (2017). Mechanobiology of YAP and TAZ in physiology and disease. *Nat. Rev. Mol. Cell Biol.* 18, 758–770. doi: 10.1038/nrm.2017.87

Pantalacci, S., Tapon, N., and Léopold, P. (2003). The salvador partner Hippo promotes apoptosis and cell-cycle exit in *Drosophila*. *Nat. Cell Biol.* 5, 921–927. doi: 10.1038/ncb1051

Parisi, F., Riccardo, S., Daniel, M., Saqcena, M., Kundu, N., Pession, A., et al. (2011). *Drosophila* insulin and target of rapamycin (TOR) pathways regulate GSK3 beta activity to control Myc stability and determine Myc expression *in vivo*. *BMC Biol.* 9, 65. doi: 10.1186/1741-7007-9-65

Parisi, F., Riccardo, S., Zola, S., Lora, C., Grifoni, D., Brown, L. M., et al. (2013). dMyc expression in the fat body affects DILP2 release and increases the expression of the fat desaturase Desat1 resulting in organismal growth. *Dev. Biol.* 379, 64–75. doi: 10.1016/j.ydbio.2013.04.008

Parisi, F., Stefanatos, R. K., Strathdee, K., Yu, Y., and Vidal, M. (2014). Transformed epithelia trigger non-tissue-autonomous tumor suppressor response by adipocytes via activation of Toll and Eiger/TNF signaling. *Cell Rep.* 6, 855–867. doi: 10.1016/j.celrep.2014.01.039

Pascual, J., Jacobs, J., Sansores-Garcia, L., Natarajan, M., Zeitlinger, J., Aerts, S., et al. (2017). Hippo reprograms the transcriptional response to ras signaling. *Dev. Cell* 42, 667.e664–680.e664. doi: 10.1016/j.devcel.2017.08.013

Pastor-Pareja, J. C., Wu, M., and Xu, T. (2008). An innate immune response of blood cells to tumors and tissue damage in *Drosophila*. *Dis. Model. Mech.* 1, 144–154; discussion 153. doi: 10.1242/dmm.000950

Pavlova, N. N., and Thompson, C. B. (2016). The emerging hallmarks of cancer metabolism. *Cell Metab.* 23, 27–47. doi: 10.1016/j.cmet.2015.12.006

Peck, B., and Schulze, A. (2016). Lipid desaturation-the next step in targeting lipogenesis in cancer? *FEBS J.* 283, 2767–2778. doi: 10.1111/febs.13681

Petit, V., Ribeiro, C., Ebner, A., and Affolter, M. (2002). Regulation of cell migration during tracheal development in *Drosophila melanogaster*. *Int. J. Dev. Biol.* 46, 125–132.

Phillips, H. S., Kharbanda, S., Chen, R., Forrest, W. F., Soriano, R. H., Wu, T. D., et al. (2006). Molecular subclasses of high-grade glioma predict prognosis, delineate a pattern of disease progression, and resemble stages in neurogenesis. *Cancer Cell* 9, 157–173. doi: 10.1016/j.ccr.2006.02.019

Pierce, S. B., Yost, C., Britton, J. S., Loo, L. W., Flynn, E. M., Edgar, B. A., et al. (2004). dMyc is required for larval growth and endoreplication in *Drosophila*. *Development* 131, 2317–2327. doi: 10.1242/dev.01108

Prehoda, K. E. (2009). Polarization of *Drosophila* neuroblasts during asymmetric division. *Cold Spring Harb. Perspect. Biol.* 1:a001388. doi: 10.1101/cshperspect.a001388

Prober, D. A., and Edgar, B. A. (2000). Ras1 promotes cellular growth in the *Drosophila* wing. *Cell* 100, 435–446. doi: 10.1016/S0092-8674(00)80679-0

Ray, A. (2018). Cancer and comorbidity: the role of leptin in breast cancer and associated pathologies. *World J. Clin. Cases* 6, 483–492. doi: 10.12998/wjcc.v6.i12.483

Read, R. D., Cavenee, W. K., Furnari, F. B., and Thomas, J. B. (2009). A *Drosophila* model for EGFR-Ras and PI3K-dependent human glioma. *PLoS Genet.* 5:e1000374. doi: 10.1371/journal.pgen.1000374

Riboli, E. (2014). The cancer-obesity connection: what do we know and what can we do? *BMC Biol.* 12:9. doi: 10.1186/1741-7007-12-9

Roberts, D. L., Dive, C., and Renehan, A. G. (2010). Biological mechanisms linking obesity and cancer risk: new perspectives. *Annu. Rev. Med.* 61, 301–316. doi: 10.1146/annurev.med.080708.082713

Robinson, B. S., Huang, J., Hong, Y., and Moberg, K. H. (2010). Crumbs regulates Salvador/Warts/Hippo signaling in *Drosophila* via the FERM-domain protein Expanded. *Curr. Biol.* 20, 582–590. doi: 10.1016/j.cub.2010.03.019

Rogers, L., Barani, I., Chamberlain, M., Kaley, T. J., McDermott, M., Raizer, J., et al. (2015). Meningiomas: knowledge base, treatment outcomes, and uncertainties. A RANO review. *J. Neurosurg.* 122, 4–23. doi: 10.3171/2014.7.JNS131644

Ruivo, C. F., Adem, B., Silva, M., and Melo, S. A. (2017). The biology of cancer exosomes: insights and new perspectives. *Cancer Res.* 77, 6480–6488. doi: 10.1158/0008-5472.CAN-17-0994

Samatar, A. A., and Poulikakos, P. I. (2014). Targeting RAS-ERK signalling in cancer: promises and challenges. *Nat. Rev. Drug Dis.* 13, 928–942. doi: 10.1038/nrd4281

Saxton, R. A., and Sabatini, D. M. (2017). mTOR signaling in growth, metabolism, and disease. *Cell* 168, 960–976. doi: 10.1016/j.cell.2017.02.004

Scheller, J., Chalaris, A., Schmidt-Arras, D., and Rose-John, S. (2011). The pro- and anti-inflammatory properties of the cytokine interleukin-6. *Biochim. Biophys. Acta* 1813, 878–888. doi: 10.1016/j.bbamcr.2011.01.034

Schimanski, C. C., Schmitz, G., Kashyap, A., Bosserhoff, A. K., Bataille, F., Schafer, S. C., et al. (2005). Reduced expression of Hugl-1, the human homologue of *Drosophila* tumour suppressor gene lgl, contributes to progression of colorectal cancer. *Oncogene* 24, 3100–3109. doi: 10.1038/sj.onc.1208520

Schreiber-Agus, N., Stein, D., Chen, K., Goltz, J. S., Stevens, L., and DePinho, R. A. (1997). *Drosophila* Myc is oncogenic in mammalian cells and plays a role in the diminutive phenotype. *Proc. Natl. Acad. Sci. U.S.A.* 94, 1235–1240. doi: 10.1073/pnas.94.4.1235

Shiao, S. L., Chu, G. C., and Chung, L. W. (2016). Regulation of prostate cancer progression by the tumor microenvironment. *Cancer Lett.* 380, 340–348. doi: 10.1016/j.canlet.2015.12.022

Shilo, B. Z. (2014). The regulation and functions of MAPK pathways in *Drosophila*. *Methods* 68, 151–159. doi: 10.1016/j.ymeth.2014.01.020

Simon-Carrasco, L., Jimenez, G., Barbacid, M., and Drosten, M. (2018). The Capicua tumor suppressor: a gatekeeper of Ras signaling in development and cancer. *Cell Cycle* 17, 702–711. doi: 10.1080/15384101.2018.1450029

Sinenko, S. A., Hung, T., Moroz, T., Tran, Q. M., Sidhu, S., Cheney, M. D., et al. (2010). Genetic manipulation of AML1-ETO-induced expansion of hematopoietic precursors in a *Drosophila* model. *Blood* 116, 4612–4620. doi: 10.1182/blood-2010-03-276998

Song, Y., and Lu, B. (2011). Regulation of cell growth by Notch signaling and its differential requirement in normal vs. *tumor-forming stem cells in Drosophila*. *Genes Dev* 25, 2644–2658. doi: 10.1101/gad.171959.111

Sonoshita, M., and Cagan, R. L. (2017). Modeling human cancers in *Drosophila*. *Curr. Top. Dev. Biol.* 121, 287–309. doi: 10.1016/bs.ctdb.2016.07.008

St. Johnston, D. (2002). The art and design of genetic screens: *Drosophila melanogaster*. *Nat. Rev. Genet.* 3, 176–188. doi: 10.1038/nrg751

Stoiber, K., Naglo, O., Pernpeintner, C., Zhang, S., Koeberle, A., Ulrich, M., et al. (2018). Targeting de novo lipogenesis as a novel approach in anti-cancer therapy. *Br. J. Cancer* 118, 43–51. doi: 10.1038/bjc.2017.374

Stronach, B. (2005). Dissecting JNK signaling, one KKKinase at a time. *Dev. Dyn.* 232, 575–584. doi: 10.1002/dvdy.20283

Suijkerbuijk, S. J., Kolahgar, G., Kucinski, I., and Piddini, E. (2016). Cell competition drives the growth of intestinal adenomas in *Drosophila*. *Curr. Biol.* 26, 428–438. doi: 10.1016/j.cub.2015.12.043

Sun, G., and Irvine, K. D. (2013). Ajuba family proteins link JNK to hippo signaling. *Sci. Signal.* 6:ra81. doi: 10.1126/scisignal.2004324

Tapon, N., Harvey, K. F., Bell, D. W., Wahrer, D. C., Schiripo, T. A., Haber, D., et al. (2002). salvador Promotes both cell cycle exit and apoptosis in *Drosophila* and is mutated in human cancer cell lines. *Cell* 110, 467–478. doi: 10.1016/S0092-8674(02)00824-3

Taylor, M. D., Liu, L., Raffel, C., Hui, C. C., Mainprize, T. G., Zhang, X., et al. (2002). Mutations in SUFU predispose to medulloblastoma. *Nat. Genet.* 31, 306–310. doi: 10.1038/ng916

Tian, A., Benchabane, H., and Ahmed, Y. (2018). Wingless/Wnt signaling in intestinal development, homeostasis, regeneration and tumorigenesis: a *Drosophila* perspective. *J. Dev. Biol.* 6:E8. doi: 10.3390/jdb6020008

Tillery, M. M. L., Blake-Hedges, C., Zheng, Y., Buchwalter, R. A., and Megraw, T. L. (2018). Centrosomal and non-centrosomal microtubule-organizing centers (MTOCs) in *Drosophila melanogaster*. *Cells* 7:E121. doi: 10.3390/cells7090121

Tipping, M., and Perrimon, N. (2014). *Drosophila* as a model for context-dependent tumorigenesis. *J. Cell. Physiol.* 229, 27–33. doi: 10.1002/jcp.24427

Toivanen, R., and Shen, M. M. (2017). Prostate organogenesis: tissue induction, hormonal regulation and cell type specification. *Development* 144, 1382–1398. doi: 10.1242/dev.148270

Ugur, B., Chen, K., and Bellen, H. J. (2016). *Drosophila* tools and assays for the study of human diseases. *Dis. Model. Mech.* 9, 235–244. doi: 10.1242/dmm.023762

Uhlirova, M., and Bohmann, D. (2006). JNK- and Fos-regulated Mmp1 expression cooperates with Ras to induce invasive tumors in *Drosophila*. *EMBO J.* 25, 5294–5304. doi: 10.1038/sj.emboj.7601401

Uhlirova, M., Jasper, H., and Bohmann, D. (2005). Non-cell-autonomous induction of tissue overgrowth by JNK/Ras cooperation in a *Drosophila* tumor model. *Proc. Natl. Acad. Sci. U.S.A.* 102, 13123–13128. doi: 10.1073/pnas.0504170102

Valenza, A., Bonfanti, C., Pasini, M. E., and Bellosta, P. (2018). Anthocyanins function as anti-inflammatory agents in a. *Biomed Res. Int.* 2018:6413172. doi: 10.1155/2018/6413172

Vander Heiden, M. G., and DeBerardinis, R. J. (2017). Understanding the intersections between metabolism and cancer biology. *Cell* 168, 657–669. doi: 10.1016/j.cell.2016.12.039

Vidal, M., Wells, S., Ryan, A., and Cagan, R. (2005). ZD6474 suppresses oncogenic RET isoforms in a *Drosophila* model for type 2 multiple endocrine neoplasia syndromes and papillary thyroid carcinoma. *Cancer Res.* 65, 3538–3541. doi: 10.1158/0008-5472.CAN-04-4561

Vlisidou, I., and Wood, W. (2015). *Drosophila* blood cells and their role in immune responses. *FEBS J.* 282, 1368–1382. doi: 10.1111/febs.13235

Walther, T. C., and Farese, R. V. Jr. (2012). Lipid droplets and cellular lipid metabolism. *Annu. Rev. Biochem.* 81, 687–714. doi: 10.1146/annurev-biochem-061009-102430

Wang, C., Zhao, R., Huang, P., Yang, F., Quan, Z., Xu, N., et al. (2013). APC loss-induced intestinal tumorigenesis in *Drosophila*: roles of ras in Wnt signaling activation and tumor progression. *Dev. Biol.* 378, 122–140. doi: 10.1016/j.ydbio.2013.03.020

Wang, F., and Xu, Y. (2014). Body mass index and risk of renal cell cancer: a dose-response meta-analysis of published cohort studies. *Int. J. Cancer* 135, 1673–1686. doi: 10.1002/ijc.28813

Wang, Y. Y., Attane, C., Milhas, D., Dirat, B., Dauvillier, S., Guerard, A., et al. (2017). Mammary adipocytes stimulate breast cancer invasion through metabolic remodeling of tumor cells. *JCI Insight* 2:e87489. doi: 10.1172/jci.insight.87489

Weber, R. J., Desai, T. A., and Gartner, Z. J. (2017). Non-autonomous cell proliferation in the mammary gland and cancer. *Curr. Opin. Cell Biol.* 45, 55–61. doi: 10.1016/j.ceb.2017.02.009

Weston, C. R., and Davis, R. J. (2007). The JNK signal transduction pathway. *Curr. Opin. Cell Biol.* 19, 142–149. doi: 10.1016/j.ceb.2007.02.001

Whitworth, A. J., Wes, P. D., and Pallanck, L. J. (2006). *Drosophila* models pioneer a new approach to drug discovery for Parkinson's disease. *Drug Discov. Today* 11, 119–126. doi: 10.1016/S1359-6446(05)03693-7

Wilson, C., Leiblich, A., Goberdhan, D. C., and Hamdy, F. (2017). The *Drosophila* accessory gland as a model for prostate cancer and other pathologies. *Curr. Top. Dev. Biol.* 121, 339–375. doi: 10.1016/bs.ctdb.2016.06.001

Wodarz, A., and Nathke, I. (2007). Cell polarity in development and cancer. *Nat. Cell Biol.* 9, 1016–1024. doi: 10.1038/ncb433

Woodhouse, E., Hersperger, E., and Shearn, A. (1998). Growth, metastasis, and invasiveness of *Drosophila* tumors caused by mutations in specific tumor suppressor genes. *Dev. Genes Evol.* 207, 542–550. doi: 10.1007/s004270050145

Wu, M., Pastor-Pareja, J. C., and Xu, T. (2010). Interaction between Ras(V12) and scribbled clones induces tumour growth and invasion. *Nature* 463, 545–548. doi: 10.1038/nature08702

Wu, Y., and Zhou, B. P. (2009). Inflammation: a driving force speeds cancer metastasis. *Cell Cycle* 8, 3267–3273. doi: 10.4161/cc.8.20.9699

Xu, C., Kim, N. G., and Gumbiner, B. M. (2009). Regulation of protein stability by GSK3 mediated phosphorylation. *Cell Cycle* 8, 4032–4039. doi: 10.4161/cc.8.24.10111

Yeatman, T. J. (2004). A renaissance for SRC. *Nat. Rev. Cancer* 4, 470–480. doi: 10.1038/nrc1366

Yu, F. X., Zhao, B., and Guan, K. L. (2015). Hippo pathway in organ size control, tissue homeostasis, and cancer. *Cell* 163, 811–828. doi: 10.1016/j.cell.2015.10.044

Yu, J., Zheng, Y., Dong, J., Klusza, S., Deng, W. M., and Pan, D. (2010). Kibra functions as a tumor suppressor protein that regulates Hippo signaling in conjunction with Merlin and Expanded. *Dev. Cell* 18, 288–299. doi: 10.1016/j.devcel.2009.12.012

Yu, X., Waltzer, L., and Bienz, M. (1999). A new *Drosophila* APC homologue associated with adhesive zones of epithelial cells. *Nat. Cell Biol.* 1, 144–151. doi: 10.1038/11064

Yuan, X., Wu, H., Xu, H., Xiong, H., Chu, Q., Yu, S., et al. (2015). Notch signaling: an emerging therapeutic target for cancer treatment. *Cancer Lett.* 369, 20–27. doi: 10.1016/j.canlet.2015.07.048

Zagani, R., El-Assaad, W., Gamache, I., and Teodoro, J. G. (2015). Inhibition of adipose triglyceride lipase (ATGL) by the putative tumor suppressor G0S2 or a small molecule inhibitor attenuates the growth of cancer cells. *Oncotarget* 6, 28282–28295. doi: 10.18632/oncotarget.5061

Zaidi, N., Swinnen, J. V., and Smans, K. (2012). ATP-citrate lyase: a key player in cancer metabolism. *Cancer Res.* 72, 3709–3714. doi: 10.1158/0008-5472.CAN-11-4112

Zhao, H. F., Wang, J., Shao, W., Wu, C. P., Chen, Z. P., To, S. T., et al. (2017). Recent advances in the use of PI3K inhibitors for glioblastoma multiforme: current preclinical and clinical development. *Mol. Cancer* 16, 100. doi: 10.1186/s12943-017-0670-3

Ziosi, M., Baena-Lopez, L. A., Grifoni, D., Froldi, F., Pession, A., Garoia, F., et al. (2010). dMyc functions downstream of Yorkie to promote the supercompetitive behavior of hippo pathway mutant cells. *PLoS Genet.* 6:e1001140. doi: 10.1371/journal.pgen.1001140

Zu, X., Zhong, J., Luo, D., Tan, J., Zhang, Q., Wu, Y., et al. (2013). Chemical genetics of acetyl-CoA carboxylases. *Molecules* 18, 1704–1719. doi: 10.3390/molecules18021704

Conflict of Interest Statement: The authors declare that the research was conducted in the absence of any commercial or financial relationships that could be construed as a potential conflict of interest.

frontiers in Genetics

REVIEW
published: 13 February 2019
doi: 10.3389/fgene.2019.00010

Drosophila melanogaster as a Model to Study the Multiple Phenotypes, Related to Genome Stability of the Fragile-X Syndrome

*Valeria Specchia[1], Antonietta Puricella[1], Simona D'Attis[1], Serafina Massari[1], Angela Giangrande[2,3,4,5] and Maria Pia Bozzetti[1]**

[1]*Dipartimento di Scienze e Tecnologie Biologiche ed Ambientali, DiSTeBA, Università del Salento, Lecce, Italy,* [2]*Institut de Génétique et de Biologie Moléculaire et Cellulaire, Illkirch, France,* [3]*Centre National de la Recherche Scientifique, UMR7104, Illkirch, France,* [4]*Institut National de la Santé et de la Recherche Médicale, U964, Illkirch, France,* [5]*Université de Strasbourg, Illkirch, France*

OPEN ACCESS

Edited by:
Maria Grazia Giansanti, Consiglio Nazionale Delle Ricerche (CNR), Italy

Reviewed by:
Ezio Rosato, University of Leicester, United Kingdom
Sergio Pimpinelli, Sapienza University of Rome, Italy
Fabian M. Feiguin, International Centre for Genetic Engineering and Biotechnology, Italy

***Correspondence:**
Maria Pia Bozzetti
maria.bozzetti@unisalento.it

Specialty section:
This article was submitted to Genetic Disorders, a section of the journal Frontiers in Genetics

Received: *01 October 2018*
Accepted: *11 January 2019*
Published: *13 February 2019*

Citation:
Specchia V, Puricella A, D'Attis S, Massari S, Giangrande A and Bozzetti MP (2019) Drosophila melanogaster as a Model to Study the Multiple Phenotypes, Related to Genome Stability of the Fragile-X Syndrome. Front. Genet. 10:10. doi: 10.3389/fgene.2019.00010

Fragile-X syndrome is one of the most common forms of inherited mental retardation and autistic behaviors. The reduction/absence of the functional FMRP protein, coded by the X-linked *Fmr1* gene in humans, is responsible for the syndrome. Patients exhibit a variety of symptoms predominantly linked to the function of FMRP protein in the nervous system like autistic behavior and mild-to-severe intellectual disability. Fragile-X (FraX) individuals also display cellular and morphological traits including branched dendritic spines, large ears, and macroorchidism. The *dFmr1* gene is the Drosophila ortholog of the human *Fmr1* gene. *dFmr1* mutant flies exhibit synaptic abnormalities, behavioral defects as well as an altered germline development, resembling the phenotypes observed in FraX patients. Therefore, *Drosophila melanogaster* is considered a good model to study the physiopathological mechanisms underlying the Fragile-X syndrome. In this review, we explore how the multifaceted roles of the FMRP protein have been addressed in the *Drosophila* model and how the gained knowledge may open novel perspectives for understanding the molecular defects causing the disease and for identifying novel therapeutical targets.

Keywords: FMRP/dFmr1, Fragile-X syndrome, piRNA pathway, DNA damage response, transposon elements, neurological diseases

INTRODUCTION

Fragile-X syndrome (FXS, MIM300624) is the most common form of mental retardation in the human population. This affects approximately 1/7,000 males and 1/11,000 females (Hunter et al., 2014), and patients exhibit intellectual disability, autism, hyperactivity, long face, large ears, language delay, hyper arousal anxiety (Johannisson et al., 1987; O'Donnell and Warren, 2002; Santoro et al., 2012) macroorchidism, and malformed spermatids (Johannisson et al., 1987; Slegtenhorst-Eegdeman et al., 1998). The most frequent cause of the syndrome is a CGG trinucleotide repeat expansion (greater than 200 repeats) in the 5′ of the Fragile-X locus in Xq27.3, which leads to the hypermethylation of the gene promoter. The final effect is the transcriptional silencing of the Fragile-X Mental Retardation (*Fmr1*) gene, with a consequent loss of the encoded FMRP protein (Godler et al., 2010).

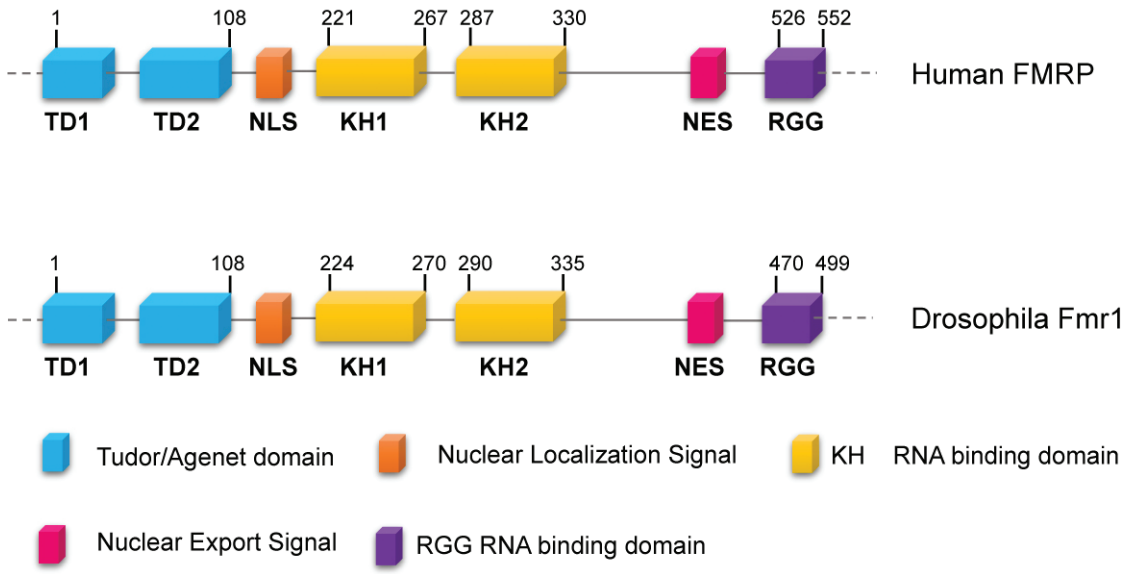

FIGURE 1 | Conserved domains of FMRP/dFmr1 proteins. The drawings are not to scale; the exact positions of the amino acids are indicated; the domains are indicated with different colors.

FMRP is a complex protein that displays distinct motifs: a nuclear localization signal (NLS) and a nuclear export signal (NES), two tandem Tudor domains that are likely involved in protein-protein interactions and/or in the DNA binding, as well as three RNA-binding domains including two KH domains and one Arg-Gly-Gly (RGG) box (**Figure 1**) (O'Donnell and Warren, 2002; Ramos et al., 2006; Santoro et al., 2012). In mammals, FMRP is nearly ubiquitous, but it is heavily expressed in neurons, particularly in the cortex, hippocampus, and Purkinje cells where it regulates specific messenger targets. FMRP is also expressed at high levels in testes. Accordingly, the main effects of the FMRP loss in humans are in the nervous system and in the gonads (Santoro et al., 2012). In neurons, the absence of FMRP may alter the processing, the localization, and/or the translational regulation of mRNAs encoding pre- and postsynaptic proteins. These defects can account for the abnormal maturation of dendritic spines in FXS patients, which are longer, thinner, and denser than the normal ones (Swanger and Bassell, 2011; Bardoni et al., 2012; Maurin et al., 2014), representing the cellular defects underpinning the neuronal dysfunctions characterizing the Fragile-X disorder.

In addition to CGG triplet expansion, different mutations in the *Fmr1* gene, leading to FXS, have been reported. They include deletions and missense and nonsense mutations, which are listed in the Human Gene Mutation Database for FXS[1]. Mutations occur all along the coding sequences and affect different domains, which may explain why the FraX patients display common as well as specific defects (Reeve et al., 2008; Santoro et al., 2012; Alpatov et al., 2014; Okray et al., 2015; Suhl and Warren, 2015; Quartier et al., 2017).

[1]http://www.hgmd.cf.ac.uk/ac/gene.php?gene=FMR1

Two autosomal homologs of *Fmr1* have been identified in the human genome: the Fragile-X mental retardation autosomal homolog 1 (FXR1) and 2 (FXR2), together with the *Fmr1* gene, form the Fragile-X gene family (Siomi et al., 1995; Zhang et al., 1995). Both homologs encode for RNA-binding proteins, FXR1P and FXR2P, with similar and/or complementary functions to those of FMRP, respectively (Penagarikano et al., 2007; Ascano et al., 2012).

A particular aspect linked to FXS is that individuals with a number of CGG repeats from 55 to 200 present a condition known as premutation and display an increased amount of *Fmr1* mRNA. It was proposed that the symptoms, exhibited by these subjects, are related to the *Fmr1* mRNA overproduction. Males with the premutation are at risk to developing Fragile-X-associated tremor/ataxia syndrome (FXTAS, MIM300623), whereas females with the premutation have an increased probability to develop Fragile-X-associated primary ovary insufficiency (FXPOI) (Amiri et al., 2008; Kronquist et al., 2008; Rossetti et al., 2017).

The function of FMRP has been primarily studied in the nervous system of mammals and *Drosophila*, focusing on its role as a translational regulator acting: either by repressing translational initiation (Schenck et al., 2003; Napoli et al., 2008; Aitken and Lorsch, 2012) or by interacting with the translating ribosomes (Siomi et al., 1996; Tamanini et al., 1996; Feng et al., 1997; Ishizuka et al., 2002; Darnell et al., 2005). It has also been proposed that FMRP may exert its translational control through the miRNA pathway (Siomi et al., 1996; Caudy et al., 2002; Ishizuka et al., 2002; Jin et al., 2004; Xu et al., 2008). Many screenings, aiming at identifying FMRP targets (mRNAs and proteins), contributed to the understanding of the role of FMRP, mainly in the nervous system. Many of these targets are involved in synaptic activity, which may account

for the FXS phenotypes, such as defects in the development of neuronal architecture and in synaptic dysfunction (Darnell et al., 2011; Ascano et al., 2012).

FMRP regulates the local translation of a subset of mRNAs at synapses following the activation of the metabotropic glutamate receptors (mGluRs) (Huber et al., 2002; Bear et al., 2004; McBride et al., 2005). Deregulation of local protein synthesis is considered a core mechanism in FXS, underlying altered synaptic plasticity and consequent cognitive impairment. The role of FMRP in the regulation of translation was better characterized in the Drosophila quiescent oocyte in which the translation of stored mRNAs is a crucial point for the correct development of embryos (Greenblatt and Spradling, 2018).

Animal models of FXS have been developed in zebrafish, mouse, and rat (Tucker et al., 2004; McBride et al., 2005, 2012; Hamilton et al., 2014). Over the last decades, *Drosophila* has also provided key contributions to further understand the molecular pathways defective in FXS, thanks to the many advantages in the use of this versatile organism (Tessier and Broadie, 2012; Sears and Broadie, 2017; Drozd et al., 2018; Dockendorff and Labrador, 2019). The resulting imprecise excisions provided *Fmr1* alleles that lack dFmr1 expression, a situation comparable to the loss of function mutations observed in FXS patients (Wan et al., 2000). dFmr1 is equally similar to the three mammalian gene products (~35% identity, ~60% similarity) and shows particularly high sequence conservation (~70% identity) in critical domains such as the Tudor/Agenet domain that is involved in DNA binding, the RNA-binding domains, and the nuclear localization signals (Zalfa et al., 2007; Zhang et al., 2007; Xu et al., 2008).

The *Drosophila melanogaster* dFmr1 protein is expressed from embryonic stages to adult, and it is enriched in the nervous system (Morales et al., 2002). In the brain, dFmr1 is highly expressed in the mushroom bodies, the main structure of the brain involved in cognitive functions. dFmr1 highly accumulates in the dendrites and in the axons of Kenyon cells, the intrinsic neurons of the mushroom bodies (**Figure 2A**). Its expression is ubiquitous in the neurons of the adult brain, whereas very low levels have been detected in glial cells (Wan et al., 2000; Zhang et al., 2001; Morales et al., 2002; Coffee et al., 2010). Outside the nervous system, dFmr1 is presented at a high level in larval and adult testes with a strong expression in spermatocytes (Zhang et al., 2004; Bozzetti et al., 2015). dFmr1 is also a component of the polar granules of the embryo where it interacts with other specific proteins present in these structures such as Vasa, Cup, and Hsp83 (Verrotti and Wharton, 2000; Cziko et al., 2009; Pisa et al., 2009; Lasko, 2013).

The *Drosophila* animals that completely lack dFmr1 recapitulate many of the phenotypes exhibited by patients with the Fragile-X syndrome. At the cellular level, mutants present defective neuronal architecture and synaptic function. The neurons of *dFmr1* null mutant animals exhibit abnormally organized synapses in both the peripheral and central nervous systems. The neuromuscular junctions (NMJs) of the *Drosophila* larva are simple synapses that represent a good model to study synaptic plasticity. The lack of *dFmr1* causes pronounced synaptic overgrowth at the NMJs (Zhang et al., 2001; Schenck et al., 2003; Pan et al., 2004). Mutant flies display altered behaviors, such as reduced courtship activity of males and irregular circadian rhythms, like the eclosion timing, even though the mRNAs for the two clock elements Per and Tim are not affected. In addition, *dFmr1* mutants exhibit defects in locomotor activity and an acute impairment of long-term memory (Sehgal et al., 1994; Dockendorff et al., 2002; Morales et al., 2002; Bolduc et al., 2008, 2010).

In the ovary, dFmr1 plays a role in translational regulation (Costa et al., 2005), where it controls germ stem cell differentiation through the miRNA-mediated pathway (Yang et al., 2007) and cell proliferation through the proto-oncogene *cbl* (Epstein et al., 2009).

Interestingly, dFmr1 is also involved in the piRNA pathway in the *Drosophila* gonads as well as in the DNA damage response in *Drosophila* and mouse (Zhang et al., 2012; Alpatov et al., 2014; Bozzetti et al., 2015) These findings provide a direct link between dFmr1/FMRP (from here onward, we will name dFmr1 the Drosophila protein as FMRP the mammalian protein) and genome instability, which may represent the common denominator for the multiple phenotypes described in the Fragile-X syndrome and in animal models for the disease.

In this review, we will predominantly treat the roles of dFmr1 related to the genome instability in the gonads and in the nervous system.

THE ROLE OF dFmr1 IN THE piRNA PATHWAY

dFmr1 Mutations Affect the Regulation of the *Crystal-Stellate* System and of the Transposable Elements in the Gonads

In 2015, our group demonstrated, for the first time, the role of dFmr1 in the piRNA-mediated silencing of transposable elements and repetitive sequences in the *Drosophila* gonads (Bozzetti et al., 2015). Piwi-interacting RNAs or piRNAs are small RNA molecules protecting animal germ cells and their somatic precursors from the insertion of transposons and other repetitive elements hence preserving genome stability (Malone et al., 2009; Patil and Kai, 2010; Zhang et al., 2011; Anand and Kai, 2012; Specchia et al., 2017). The genomic clusters that act as sources of piRNAs contain multiple and also defective transposon sequences. Most of the piRNA clusters produce piRNAs from both genomic strands, and the other clusters produce piRNAs only from one genomic strand.

The molecular mechanism underlying the silencing of transposable elements reached a deep level of knowledge following studies performed in the ovaries. Argonaute proteins, belonging to the Piwi subfamily groups (P-element-induced Wimpy Testes or Piwi, Aubergine or Aub, and Ago3), play a crucial role in these processes (Aravin et al., 2007). Aub and Ago3 localize to the nuage (**Figure 2B**), a perinuclear structure found in animal germ cells. Piwi localizes predominantly in the nucleus of both germ and somatic cells of the ovary.

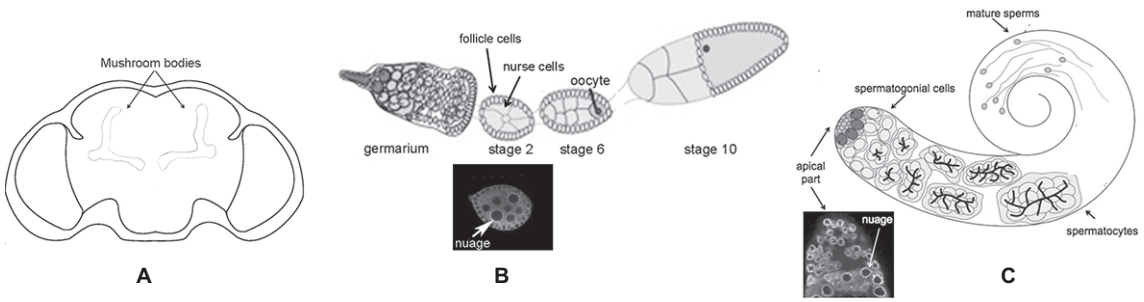

FIGURE 2 | Schematic of different body parts of a *Drosophila melanogaster* adult. **(A)** Head, the mushroom bodies are indicated. **(B)** Upper part: ovariole; lower part: immunolabeling of a stage 2 oocyte; the white arrow indicates the perinuclear nuage. **(C)** Upper part: adult testis; lower part: immunolabeling of the apical part of the testis is indicated; the white arrow indicates the perinuclear nuage.

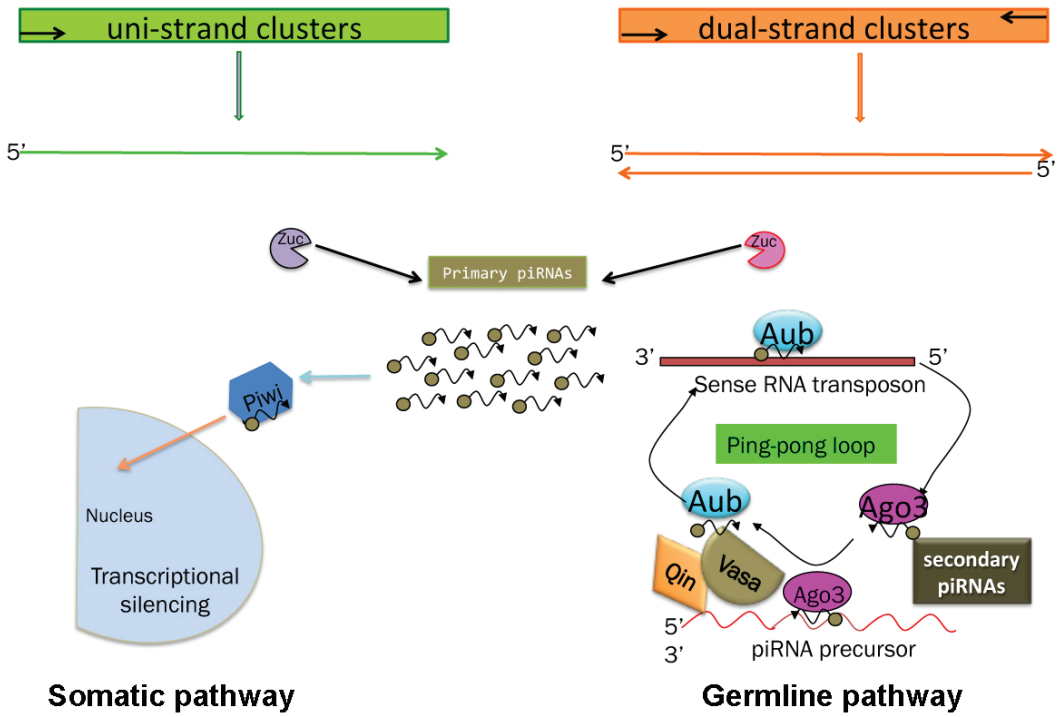

FIGURE 3 | Schematic of the piRNA's biogenesis. Somatic and germline pathways are indicated. Zuc stands for Zucchini protein (see text). In the germline pathway, Qin is a partner of Vasa, which behaves like a molecular platform for the piRNA pathway (see text and Specchia et al., 2017).

Two pathways for piRNA biogenesis and function have been established the primary and the ping-pong pathways (**Figure 3**) (Aravin et al., 2007; Malone et al., 2009).

In the primary pathway, transcript precursors, arising from specific genomic clusters, are processed into primary piRNAs that are bound by specific Piwi proteins. *Drosophila* ovarian somatic cells use exclusively the primary pathway. In these cells, the process occurs in perinuclear Yb bodies, which are discrete cytoplasmic compartments that take their name from the principal player in the process, the protein Yb, in the somatic cells of the ovary and testis (Szakmary et al., 2009). piRNA factors, such as Armitage, Shutdown, and Vreteno, accumulate in the Yb bodies. Upon the formation of the 3′ end of the precursors by Zucchini, the mature primary piRNAs are loaded onto Piwi, which then enters the nucleus and induces transcriptional transposon silencing (Saito et al., 2010).

Germ cells use predominantly the ping-pong amplification process in which the primary piRNAs are subjected to an amplification loop that increases their amount. In this case, the Piwi subfamily proteins, Aub and Ago3, bind the piRNAs and use the sequence homology to recognize the corresponding transposon transcript. Aub and Ago3 cooperate in the ping-pong pathway to amplify the piRNAs (Aravin et al., 2007).

The primary and the ping-pong pathways are also present in *Drosophila* testes (**Figure 2C**). In this tissue, the most

abundant piRNAs associated with Aub and Ago3 correspond to the "*crystal*" piRNAs (Aravin et al., 2001, 2003; Vagin et al., 2006; Nishida et al., 2007; Bozzetti et al., 2012). The *crystal-Stellate* system represents the first reported natural case of piRNA-mediated regulation, where the repetitive euchromatic *Stellate* sequences are silenced by the piRNAs produced by the heterochromatic *crystal* locus. *Stellate* and *crystal* are composed of tens to hundreds of copies of repetitive sequences organized in tandem (Livak, 1984; Palumbo et al., 1994; Belloni et al., 2002; Tritto et al., 2003; Egorova et al., 2009; Bozzetti et al., 2012). At the molecular level, the loss of the *crystal* region or the "loss of function" mutations of genes involved in the *crystal-Stellate* regulation, called *crystal-Stellate* modifiers, results in the production of a testes-specific *Stellate* mRNA of 750 bases, coding for the Stellate protein. This results in the formation of needle or star-shaped crystalline aggregates that can be revealed by using a specific antibody (Bozzetti et al., 1995). The phenotype induced by *crystal-Stellate* misregulation has provided an efficient tool to identify several genes involved in the piRNA pathway. The majority of the *crystal-Stellate* modifiers has a role in the silencing of germinal and somatic transposons and participates in the primary as well as in the ping-pong pathway. Interestingly, mutants for these genes affect fertility, at various degrees, both in females and males (Pane et al., 2007; Specchia et al., 2008, 2017; Specchia and Bozzetti, 2009; Bozzetti et al., 2012; Sahin et al., 2016).

Null *dFmr1* mutations affect the piRNA pathway in the gonads and the fertility of males and females (Zhang et al., 2004; Bozzetti et al., 2015). In the mutant testes, the levels of the "*crystal*" specific piRNAs are reduced, leading to the formation of the crystalline aggregates. In addition, dFmr1 was demonstrated to have a role in the piRNA-mediated silencing of both germline and somatic transposable elements (TEs) (Bozzetti et al., 2015). For all these reasons, dFmr1 should be considered as a *bona fide* component of the piRNA pathway, at least in the gonads. More recently, the role in the silencing of TEs was confirmed by the work of Jiang et al. who demonstrated that the expression of selfish genetic elements increases in the ovaries of *dFmr1* mutant females (Jiang et al., 2016).

dFmr1 Genetic and Biochemical Interaction With Argonaute Proteins in the Gonads and in the Nervous System

The Argonaute proteins are key players of the small RNA-mediated silencing pathway, being the components of the RNA-induced silencing complex (RISC). By using small RNA molecules, they mediate the post-transcriptional control of repetitive sequences, transposons, and genes in different tissues (Kalmykova et al., 2005; Brennecke et al., 2007; Klattenhoff and Theurkauf, 2008; Zhou et al., 2008; Li et al., 2009; Malone et al., 2009). The *Drosophila melanogaster* genome contains five genes coding for proteins of Argonaute family: Ago1 and Ago2 belong to the Ago subfamily and work in the miRNA (micro RNA) and siRNA (small interfering RNA) pathways. As mentioned above, Ago3, Piwi, and Aub act predominantly in the gonad-specific piRNA pathway (Li et al., 2009; Thomson and Lin, 2009).

Ago1 is commonly associated to the miRNA pathway, but data from our lab assign to this protein an additional role in the piRNA pathway as well. Indeed, Ago1 affects the silencing of the transposons in the gonads of both sexes, is involved in *crystal-Stellate* regulation in the *Drosophila* testis (Bozzetti et al., 2015; Specchia et al., 2017), and localizes at the "nuage" in the subcellular compartment in which other piRNA components localize, at least in testes (Kibanov et al., 2011; Nagao et al., 2011). Accordingly, an Ago1-mediated function was demonstrated to be required for the formation of piRNAs in follicle cells, linking together the two pathways (Mugat et al., 2015). The Ago1 protein, hence, has a promiscuous role in small RNA regulation.

A strong argument supporting the role of dFmr1 in the small RNA-mediated pathways is the finding that dFmr1 interacts with the Argonaute proteins. One of the first evidence was provided by the biochemical interaction of dFmr1 with Ago2 and with the components of the RISC in S2 *Drosophila* cells (Caudy et al., 2002; Ishizuka et al., 2002).

Since this discovery, many efforts were made to clarify the molecular role of FMRP in the RNA-mediated silencing pathways based on the genetic and biochemical interactions with the Argonaute proteins. Almost all the Argonaute proteins of both subfamilies have been connected to dFmr1 in the gonads as well as in the nervous system. We here present the main findings related to the specific role of FMRP in the small RNA pathways in the two tissues, disclosing multifaceted connections.

dFmr1 interacts with Ago1 and with the *bantam* microRNA in the *Drosophila* ovary to regulate the fate of germline stem cells (Yang et al., 2007, 2009). Ago1 was also implicated in terminal dendrites elongation (Lee et al., 2015) and is required for a correct function of dFmr1 at the NMJ (Jin et al., 2004; Bozzetti et al., 2015).

dFmr1 also interacts genetically with Aub, whose overexpression in the germline, as well as in the somatic tissues of the *dFmr1* mutant animals, rescues the phenotypes related to the regulation of transposable elements and to the *crystal-Stellate* interaction mediated by piRNAs (Bozzetti et al., 2015). dFmr1 is widely distributed in the gonads, and it overlaps with Aub at the nuage and at the "piRNA nuage giant bodies" (piNG bodies) (**Figure 4**), a giant structure in the nuage of testes where the piRNA components are located and function (Bozzetti et al., 2015). The biochemical interaction between dFmr1 and Aub, in S2 cells, also supports the data obtained with the genetic experiment (Bozzetti et al., 2015). Aub and dFmr1 were demonstrated also to genetically interact in the larval neuromuscular junctions, as the neuronal overexpression of *aub* rescues the *dFmr1* defective NMJs (Bozzetti et al., 2015). Since the presence of Aub in the nervous system is still debated (see the following paragraphs), it has been proposed that the overexpressed Aub may work by taking on the function of Ago1, a protein that is definitely present and has a well-studied role in the nervous system (Lee et al., 2015).

Another crucial Argonaute interactor of dFmr1 is Piwi. A recent study from Jiang et al. in 2016 reported that dFmr1

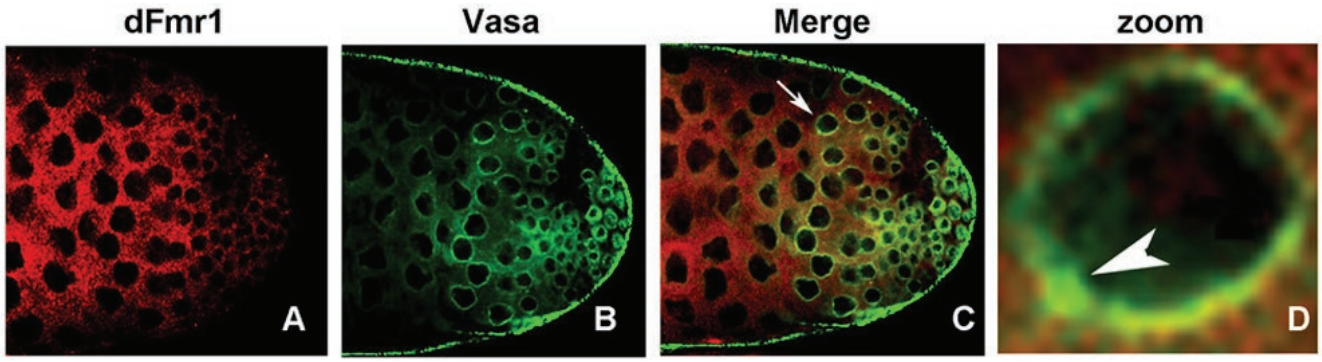

FIGURE 4 | dFmr1 and Vasa immunolocalization in wt (wild type) adult testes. **(A)** Single confocal section of a wt testis labeled with anti-dFmr1, **(B)** anti-Vasa, and **(C)** merge; magnification 40×. **(D)** Photographic zoom of the cells indicated by arrow in **(C)**; the white arrowhead shows the colocalization of dFmr1 and Vasa in the piNG body.

and Piwi are present in the same complex in ovarian extracts and act together in the piRNA-mediated transcriptional silencing on the transposable elements in both somatic and germline tissues of the *Drosophila* ovary (Jiang et al., 2016). *dFmr1* mutations also influence the amount of a specific piRNA regulating the *roo* transposable elements. The N-terminal region of dFmr1, where the Tudor/Agenet domain is present (Ramos et al., 2006; Adams-Cioaba et al., 2010; Bozzetti et al., 2015; Iwasaki et al., 2015), is required for the interaction with Piwi.

Finally, no interaction has been reported between dFmr1 and mammalian FMRP with Ago3, another Argonaute protein that operates in the biogenesis of piRNAs in combination with Aubergine (Li et al., 2009).

piRNA-Related dFmr1 Interactors Other Than Argonaute Proteins

The role of dFmr1 in the piRNA pathway is supported by its interaction with other components of the piRNA pathway, including Vasa, which is considered a molecular platform for the key components of the piRNA machinery, the so-called Amplifier complex (Xiol et al., 2014; Specchia et al., 2017). **Figure 4** shows the colocalization of dFmr1 and Vasa at the nuage in testes, in particular at the piNG bodies. Emblematic examples have been described above where the direct interaction with four Argonaute proteins has been reported.

The zinc finger protein RP-8 (Zfrp8) also stands out as a very interesting interactor of dFmr1, even though its role in the piRNA pathway or in the human syndrome is still poorly understood.

Zfrp8 was initially identified for its fundamental role in the lymph glands, the site of larval hematopoiesis in *Drosophila* (Minakhina et al., 2007). In this tissue, Zfrp8 controls cell proliferation. Zfrp8 has also an essential role in follicle cells and in germline (Minakhina and Steward, 2010; Minakhina et al., 2014). This function is conserved during evolution, and the vertebrate Zfrp8 homolog, Pdcd2, is required for stem cell maintenance (Mu et al., 2010; Granier et al., 2014). Zfrp8 genetically interacts with several components of the piRNA pathway in the ovary including *vasa, ago3, spindle-E*, and *squash* (Stapleton et al., 2001; Pane et al., 2007; Li et al., 2009; Lasko, 2013; Tan et al., 2016). In addition, the distribution of Maelstrom, one of the known components of the piRNA pathway, is strongly affected in *Zfrp8* KD (Knock Down) ovaries and in germ stem cell (GSC) clones, in which the Zfrp8 protein had been silenced. The argument that strongly supports the role of Zfrp8 in the piRNA pathway is that its reduction affects the expression of the transposable elements in the ovaries (Minakhina et al., 2014), as also seen in animals, that are mutant for the member of the piRNA pathway. Notably, dFmr1 was found as a component of the Zfrp8 protein complex together with Nufip (nuclear FMRP interacting protein) and Trailer hitch (Tral) (Minakhina et al., 2014). Both these proteins were already identified as dFmr1 interactors: Nufip is one of the known interactors of FMRP in mammals (Bardoni et al., 2003), whereas Tral is a component of the RNP granules in *Drosophila* neurons (Barbee et al., 2006). Zfrp8 may have a role in the early assembly of ribosomes with translational repressors and, as a consequence, influences different processes during oogenesis, including transposons silencing (Tan et al., 2016). Very intriguingly, Hsp83, a known component of piRNA-mediated silencing pathway in the *Drosophila* gonads (Specchia et al., 2010; Gangaraju et al., 2011; Tan et al., 2016), was found in the Zfrp8 complex as well (Tan et al., 2016).

Finally, the TDP-43 protein involved in amyotrophic lateral sclerosis (ALS) also interacts with dFmr1. The physical association of these two proteins in ribonucleoproteic complexes was observed *in vivo*, in an ALS *Drosophila* model, and *in vitro*, in neuronal derived cells. FMRP deficit causes developmental defects and autistic behavior, whereas lack of TDP-43 leads to age-dependent neurodegeneration (Fallini et al., 2012; Yu et al., 2012; Coyne et al., 2015, 2017; Majumder et al., 2016). The unexpected link between TDP-43 and FMRP opens novel perspectives to understand the physiopathological mechanisms underlying these seemingly different pathologies.

piRNA and TEs in the Nervous System

Although piRNAs were first identified in the gonads of mouse and *Drosophila* as regulators of transposable elements and repetitive sequences (Girard et al., 2006; Grivna et al., 2006; Vagin et al., 2006; Watanabe et al., 2006; Gunawardane et al., 2007; Nishida et al., 2007; Li et al., 2009; Malone et al., 2009), a specific set of piRNAs was found in the mouse hippocampus and in neuronal cultures (Lee et al., 2011). In addition, Ghildiyal et al. (2008) identified small RNA molecules in *Drosophila* heads displaying features resembling piRNAs (piRNA-like RNA molecules, pil-RNAs) (Ghildiyal et al., 2008). More recently, piRNAs with a role in the regulation of learning-related synaptic plasticity were also identified in the nervous system of *Aplysia* (Rajasethupathy et al., 2012). These discoveries represented the starting point for studies demonstrating the presence of piRNAs in somatic tissues and in particular in the brain of several organisms including *Drosophila* and humans (Baillie et al., 2011; Thomas et al., 2012; Perrat et al., 2013; Reilly et al., 2013; Ross et al., 2014; Weick and Miska, 2014). Furthermore, RNA-seq analyses revealed the presence of thousands of retrotransposon-derived piRNA-like molecules as well as the presence of factors, involved in the piRNA biogenesis, such as Mili and Maelstrom in hippocampal mammalian neurons. Mice lacking one or the other protein exhibit defects in locomotor activity and behavior (Matsumoto et al., 2015; Nandi et al., 2016). The presence of piRNAs in the nervous system suggests a role in the transposon silencing and hence in genome stability, which may impact on brain heterogeneity, aging, and also neurological diseases. Using different organisms, it was demonstrated that the deregulated expression of the transposable elements can induce their mobilization, which causes *de novo* insertions in the genome and hence triggers genomic variability in neuronal cells (Muotri et al., 2005; Coufal et al., 2009; Baillie et al., 2011; Evrony et al., 2012; Rajasethupathy et al., 2012; Perrat et al., 2013; Ross et al., 2014; Weick and Miska, 2014; Upton et al., 2015; Jachowicz et al., 2017).

Long-interspersed line-1 element (L1) is the only active element in the human genome (Beck et al., 2011) and can transpose in the neuronal precursor stem cells of the rat hippocampus. The new insertions were found in neuronal protein coding genes (Muotri et al., 2005). Engineered human L1 *in vitro* mobilization was also reported in neuronal precursor cells isolated from human fetal brains and embryonic stem cells. These discoveries strongly suggest that L1-mediated transposition has the potential to contribute to genotypic variation in neurons.

Whole genome sequencing and the analysis of the new insertions of a *gypsy*-construct support the idea that piRNA-mediated transposition also triggers cellular heterogeneity in the neurons of the *Drosophila* mushroom bodies, which are considered as the functional homolog of the mammalian hippocampus (Li et al., 2013; Perrat et al., 2013). The mobilization of the TEs occurs in a specific neuronal population, the αβ neurons, which contain a lower amount of Aub and Ago3 compared to the γδ neurons (Perrat et al., 2013), raising the concrete hypothesis that transposition may have a functional role in brain physiology. More recent data, however, do not seem to confirm the correlation between the increment in the expression of TEs and new integration sites in aging (Treiber and Waddell, 2017).

Clearly, the field is still very young and more studies will be required to firmly reach a consensus. However, even though the number of new genomic insertions does not exactly correlate with that expected from the remarkable increment of TE expression, a role of transposition in the nervous system must be considered, due to the growing amount of data on the topic.

Recent reports from many laboratories, conducted in *Drosophila*, in postmortem human tissues and in mammalian cells, support the relation between retrotransposition and neurological disorders (Muotri et al., 2010; Douville et al., 2011; Li et al., 2012; Tan et al., 2012; Rajan and Ramasamy, 2014; Krug et al., 2017; Morandi et al., 2017; Prudencio et al., 2017; Faulkner and Billon, 2018; Guo et al., 2018; Short et al., 2018). Significant examples are reported below. Parkinson's disease (PD) is a neurodegenerative disorder that strongly affects movements. Aging represents a risk factor for the occurrence of sporadic PD (Martin, 2011). piRNAs and piRNA-like molecules are differentially expressed in "induced Pluripotent Stem Cells" (iPSCs) from patients during differentiation (Schulze et al., 2018).

Alzheimer disease (AD) is the neurodegenerative disorder that represents the most common cause of dementia. As a remarkable feature, the analysis of postmortem brains from Alzheimer patients reveals the presence of misfolded proteins, namely the β-amyloid peptide and the Tau protein. In addition, transposable elements are also deregulated in these tissues compared with normal brains and in adult brains of *Drosophila* expressing human Tau protein associated with AD (Qiu et al., 2017; Roy et al., 2017; Guo et al., 2018). Intriguingly, the Tau-induced neurological phenotypes can be partially rescued by manipulating DNA damage response key factors, providing a further link between transposition, genomic instability, and DNA (Guo et al., 2018).

Amyotrophic lateral sclerosis and frontotemporal dementia (FTD) are neurological disorders exhibiting a specific phenotypic spectrum causing dementia and cognitive impairment. They have been associated to a defect in TAR-DNA-binding protein 43 (TDP-43) (Douville et al., 2011; Li et al., 2015; Prudencio et al., 2017). Retrotransposition of one of the peculiar TEs with a functional similarity to viruses possessing also a "capsid," whose name is *gypsy*, has been associated to ALS and FTD in a model expressing human TDP-43 (Krug et al., 2017). Even in the model of ALS, the modulation of DNA damage response (DDR) factors partially rescues the neurological phenotypes as occurs in Alzheimer's disease model.

Finally, Fragile-X-associated tremor/ataxia syndrome (FXTAS) is a progressive neurological disorder associated to the premutation in the *Fmr1* gene reported before (expansion up to 90 RGG repeats in the regulatory region) (Amiri et al., 2008; Kronquist et al., 2008). Transgenic *Drosophila* lines that carry the FXTAS-associated expansion exhibit an increased expression of *gypsy*, hence providing the first link between the activation of transposons and neurodevelopmental disorders (Tan et al., 2012).

DNA DAMAGE RESPONSE AND FRAGILE-X IN *DROSOPHILA* AND MAMMALS

Damage to DNA can arise for different reasons and can generate multiple lesions including single- and double-strand breaks (SSBs and DSBs). These lesions set in motion the DNA repair machine that repairs the damage and prevents massive genome instability. This involves changes in the chromatin structure and cell cycle arrest.

Different factors are sequentially involved in the repairing process like the MRN complex, which is a eukaryotic protein complex consisting of Mre11, Rad 50 and Nbs1 proteins, followed by the ATM kinase, in turn phosphorylating several targets including p53 Chk2, BRCA1, and the key histone variant H2AX in mammals (Lou et al., 2006; Matsuoka et al., 2007; Lavin, 2008; Ciccia and Elledge, 2010). Proteins and processes participating in "DNA Damage Response" (DDR) cascade are conserved during evolution. In *Drosophila*, the majority of the information comes from studies on the meiotic checkpoint in ovaries, whose defects affect the fate of the embryonic dorsal cells (Ghabrial and Schupbach, 1999; Abdu et al., 2002; Staeva-Vieira et al., 2003; Cotta-Ramusino et al., 2011). Females displaying defects in this checkpoint process produce embryos with fused dorsal appendages and the mutations affect the so-called spindle class genes (Gonzalez-Reyes et al., 1997).

Interestingly, piRNA mutants also display defects in embryonic axis specification, which are thought to be a consequence of DNA damage mediated by the activation of transposable elements (Chen et al., 2007; Klattenhoff et al., 2007; Pane et al., 2007 Klattenhoff and Theurkauf, 2008). Mutations in *aub* and in other genes of the piRNA pathway such as *armitage* (Cook et al., 2004), *spindle-E* (Stapleton et al., 2001), *zucchini*, and *squash* (Pane et al., 2007), which belong to the spindle class genes, lead to the accumulation of the H2Av histone variant (Klattenhoff et al., 2007).

DDR, Transposons, and Neurological Diseases

DNA lesions have been linked to neuronal decline in aging, oxidative stress conditions, and in neurological diseases (Ferrante et al., 1997; Adamec et al., 1999; Lu et al., 2004; Rass et al., 2007; Dobbin et al., 2013), even though the underlying molecular mechanisms remain poorly understood. Recently, the hyperactivation of the PARP-mediated DNA repair of single-strand breaks has been reported to be associated with neurodegeneration and ataxia in humans and mice (Nouspikel and Hanawalt, 2003; Katyal et al., 2014; Hoch et al., 2017).

As described above, transposable elements represent a considerable fraction of the eukaryotic genome and are regulated by the small RNA pathways, in particular the piRNA pathway. Defects in the small RNA-mediated regulation trigger their activation in the germline and in the somatic tissues of the *Drosophila* gonads, hence generating genome instability (Sarot et al., 2004; Kalmykova et al., 2005; Vagin et al., 2006; Chen et al., 2007; Pane et al., 2007; Specchia et al., 2010; Piacentini et al., 2014). A strong correlation between transposon mobilization and the DNA damage response also exists in human cells where the insertion of the Line-1 non-LTR retrotransposon depends on the DNA repair machine (Belgnaoui et al., 2006; Gasior et al., 2006). In addition, enhanced L1 mobilization has been reported in ataxia telangiectasia, a neurological disorder due to mutations in the ATM gene implicated in DNA repair (Coufal et al., 2011). These observations, linking the transposable elements and the DNA damage response, have led to the hypothesis that DNA breaks accumulate in piRNA mutants, where the transposons are massively activated (Klattenhoff and Theurkauf, 2008). This opens novel perspectives in understanding the causes of devastating neurological diseases, which, in the long term, will result in better therapeutical targets.

DDR Has a Physiological Role in Neuronal Development

Emerging evidence support the hypothesis that activation of the DDR mediated by the double-strand breaks plays a physiological role in neuronal activity, by promoting the expression of the so-called early response genes in mice (Madabhushi et al., 2015). In neurons, the "early-response genes" code for transcription factors that are activated soon after the stimulation and regulate the cellular response by activating the expression of the "late response genes" (West and Greenberg, 2011). The "early" genes play a key role in synapse development and maturation and are hence required for learning and memory (Perez-Cadahia et al., 2011). Madabhushi et al. (2015) demonstrated that DSBs occur after neuronal activity at the transcriptional start sites of the early genes (and are related to the TopoII β activity). This facilitates the rapid response of these genes, whose promoters are bound to the "paused" RNA pol II in basal condition, that is, in the absence of stimuli (Kim et al., 2010). It is interesting to note that RNA pol II pausing is also observed at the promoters of genes that are expressed in response to environmental stimuli, and these genes are targeted by the *Drosophila* "HSP90 chaperone" (Sawarkar et al., 2010). This finding represents an intriguing link among "early" gene activation, HSP90, and DNA breaks.

The activation/movement of the transposable elements in the nervous system may induce genome instability, which in turn could connect DDR machinery and synaptic activity.

dFmr1/FMRP Has a Role in the DNA Damage Response

FMRP may have a crucial role in this scenario because it has been related to the DNA damage response. Liu and collaborators demonstrated that *dfmr1* mutant flies display disproportioned cell death, related to DNA breaks and to marked genome instability, upon inducing DNA lesions (Liu et al., 2012). dFmr1 and FMRP had been previously shown to regulate cell cycle progression and differentiation in the germline as well as in the brain (Epstein et al., 2009; Yang

et al., 2009; Callan et al., 2010; Papoulas et al., 2010), exerting their function in the early DDR through its Agenet and KH domains (Zhang et al., 2014). Soon after this observation, a result in mouse also supported a role of FMRP in the DNA damage response, regulating H2Ax phosphorylation, BRCA complex formation, and accumulation in embryonic fibroblasts and in mouse spermatocyte (Alpatov et al., 2014). This role is thought to be independent of the canonical function in the translational control of mRNAs involved in the synaptic plasticity (Brown et al., 2001; O'Donnell and Warren, 2002; Bassell and Warren, 2008) and requires FMRP N-terminal Tudor/Agenet domain for its binding to the H3 histone (Alpatov et al., 2014). All these discoveries assign a role to FMRP/dFmr1 in the DDR cascade, identifying this multifaceted protein as a hub for multiple cellular processes. Clearly, one of the most exciting and difficult features of FMRP is the presence of multiple domains involved in a variety of molecular processes, from the nuclear localization domain, the RNA-binding domains, and the Tudor/Agenet domain. This implies that a single protein has distinct roles depending on its localization in the different subcellular compartments. Future efforts will aim at disentangling the diverse functions of this molecular "Swiss knife" in development and physiology.

CONCLUSIONS AND FUTURE PERSPECTIVES

A growing number of studies report the identification of piRNAs, piRNA-related proteins, and piRNA-mediated transposition as key factors ensuring heterogeneity in mammalian neurons. Transposable elements are indeed emerging as novel players in neuronal development, and they may function through the DNA damage response pathway. In parallel, it has been shown that the *Drosophila* ortholog of the Fragile-X gene in humans, *dFmr1*, interacts with 4 of 5 Argonaute proteins in the gonads and in somatic tissues (Caudy et al., 2002; Ishizuka et al., 2002; Bozzetti et al., 2015; Jiang et al., 2016) and plays a role in the piRNA-mediated silencing of the repetitive sequences and transposon in the gonads (Bozzetti et al., 2015; Specchia et al., 2017). **Figure 5** illustrates the potential role of dFmr1 in the protein network involved in genome stability. These discoveries

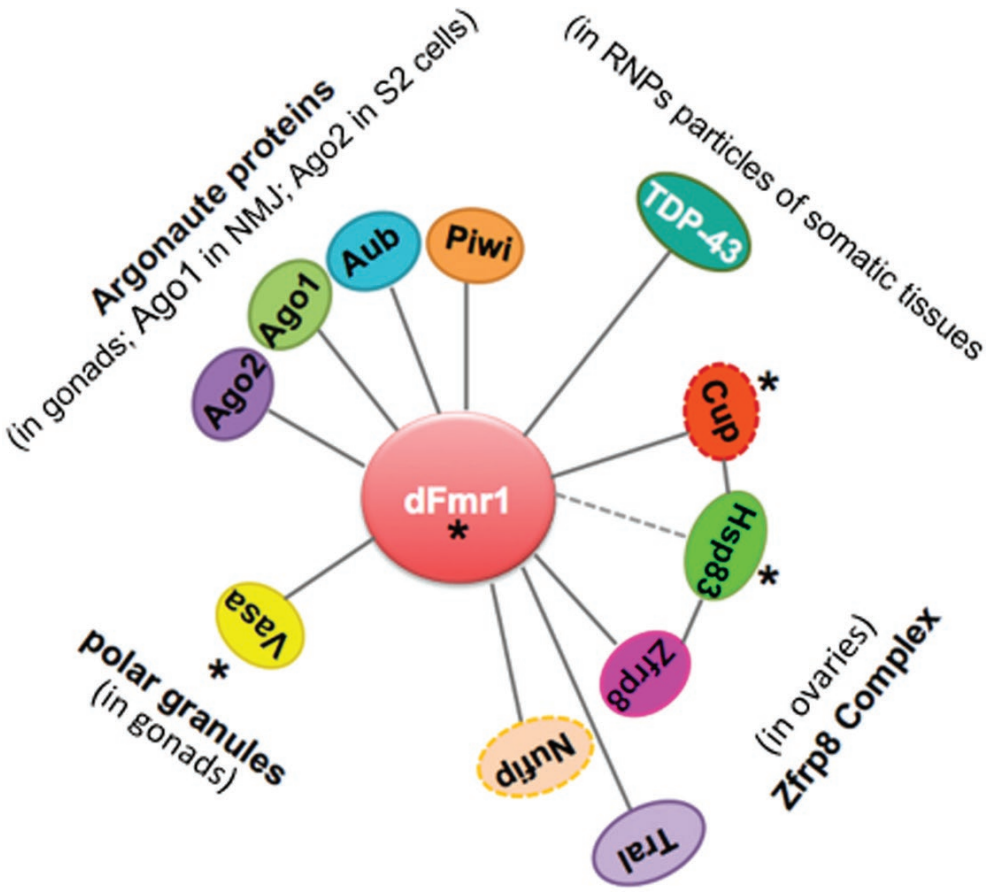

FIGURE 5 | Scheme displaying the network of genetic and biochemical interactors of dFmr1 related to its role in genome stability. The tissues in which the genetic and/or biochemical interaction occurs are indicated (see text). Cup and Nufip are indicated by a dotted line, because they have not been yet tested for their role in the piRNA-mediated silencing of TEs. Hsp83 is connected to dFmr1 by a dotted line, because its interaction has not yet been demonstrated. Asterisks indicate the proteins that are part of the polar granules.

open new perspectives for understanding the role and the mode of action of the dFmr1 protein in genome stability and pave the way to address its role in the piRNA pathway operating in the nervous system.

Key questions need now to be addressed: Does dFmr1 has a piRNA-mediated role in the brain and, if so, does its role in genome stability account for the multiple neurological phenotypes exhibited by *dFmr1* mutants and by the FraX patients? Typically, is the dFmr1 pathway linked to piRNAs involved in synaptic plasticity, learning and memory, and circadian behaviors? Should this role of dFmr1 be exerted in a specific temporal window during development as suggested by recent studies? (Weisz et al., 2015; Doll and Broadie, 2016; Doll et al., 2017).

Drosophila represents an attractive model for studying the Fragile-X syndrome and will help to address these questions because of the short generation time; the different types of genetic, cellular and molecular tools available; and the easy phenotype evaluation and rescue. *Drosophila melanogaster* offers a suitable *in vivo* model to prescreen numerous potential therapeutic molecules (McBride et al., 2005; Choi et al., 2010; Kanellopoulos et al., 2012; Hagerman et al., 2014), and clinical trials have been performed in human FraX patients, even though the results are not convincing. If the role of dFmr1 in the piRNA-mediated regulation of transposons is confirmed in the nervous system as well, new therapeutic possibility will open up. We are confident that dFmr1/FMRP will still surprise us and will help us in searching and finding potential therapeutical targets for the treatment of this devastating disease.

AUTHOR CONTRIBUTIONS

MB prepared the initial version of the manuscript. VS, SM, and AG significantly revised the manuscript. All authors provided intellectual contribution, edited, and approved the manuscript for publication in its complete version.

FUNDING

We acknowledge the financial support of Telethon-Italy (grant number GG14181) and MIUR (grant number RBFR10V8K6). The laboratory of AG is funded by INSERM, CNRS, UDS, Ligue Régionale contre le Cancer, Hôpital de Strasbourg, ARC, and ANR grants. The IGBMC was also supported by a French state fund through the ANR labex.

REFERENCES

Abdu, U., Brodsky, M., and Schupbach, T. (2002). Activation of a meiotic checkpoint during Drosophila oogenesis regulates the translation of Gurken through Chk2/Mnk. *Curr. Biol.* 12, 1645–1651. doi: 10.1016/S0960-9822(02)01165-X

Adamec, E., Vonsattel, J. P., and Nixon, R. A. (1999). DNA strand breaks in Alzheimer's disease. *Brain Res.* 849, 67–77. doi: 10.1016/S0006-8993(99)02004-1

Adams-Cioaba, M. A., Guo, Y., Bian, C., Amaya, M. F., Lam, R., Wasney, G. A., et al. (2010). Structural studies of the tandem Tudor domains of fragile X mental retardation related proteins FXR1 and FXR2. *PLoS One* 5:e13559. doi: 10.1371/journal.pone.0013559

Aitken, C. E., and Lorsch, J. R. (2012). A mechanistic overview of translation initiation in eukaryotes. *Nat. Struct. Mol. Biol.* 19, 568–576. doi: 10.1038/nsmb.2303

Alpatov, R., Lesch, B. J., Nakamoto-Kinoshita, M., Blanco, A., Chen, S., Stutzer, A., et al. (2014). A chromatin-dependent role of the fragile X mental retardation protein FMRP in the DNA damage response. *Cell* 157, 869–881. doi: 10.1016/j.cell.2014.03.040

Amiri, K., Hagerman, R. J., and Hagerman, P. J. (2008). Fragile X-associated tremor/ataxia syndrome: an aging face of the fragile X gene. *Arch. Neurol.* 65, 19–25. doi: 10.1001/archneurol.2007.30

Anand, A., and Kai, T. (2012). The tudor domain protein kumo is required to assemble the nuage and to generate germline piRNAs in Drosophila. *EMBO J.* 31, 870–882. doi: 10.1038/emboj.2011.449

Aravin, A. A., Hannon, G. J., and Brennecke, J. (2007). The Piwi-piRNA pathway provides an adaptive defense in the transposon arms race. *Science* 318, 761–764. doi: 10.1126/science.1146484

Aravin, A. A., Lagos-Quintana, M., Yalcin, A., Zavolan, M., Marks, D., Snyder, B., et al. (2003). The small RNA profile during Drosophila melanogaster development. *Dev. Cell* 5, 337–350. doi: 10.1016/S1534-5807(03)00228-4

Aravin, A. A., Naumova, N. M., Tulin, A. V., Vagin, V. V., Rozovsky, Y. M., and Gvozdev, V. A. (2001). Double-stranded RNA-mediated silencing of genomic tandem repeats and transposable elements in the *D. melanogaster* germline. *Curr. Biol.* 11, 1017–1027. doi: 10.1016/S0960-9822(01)00299-8

Ascano, M. Jr., Mukherjee, N., Bandaru, P., Miller, J. B., Nusbaum, J. D., Corcoran, D. L., et al. (2012). FMRP targets distinct mRNA sequence elements to regulate protein expression. *Nature* 492, 382–386. doi: 10.1038/nature11737

Baillie, J. K., Barnett, M. W., Upton, K. R., Gerhardt, D. J., Richmond, T. A., De Sapio, F., et al. (2011). Somatic retrotransposition alters the genetic landscape of the human brain. *Nature* 479, 534–537. doi: 10.1038/nature10531

Barbee, S. A., Estes, P. S., Cziko, A. M., Hillebrand, J., Luedeman, R. A., Coller, J. M., et al. (2006). Staufen- and FMRP-containing neuronal RNPs are structurally and functionally related to somatic P bodies. *Neuron* 52, 997–1009. doi: 10.1016/j.neuron.2006.10.028

Bardoni, B., Abekhoukh, S., Zongaro, S., and Melko, M. (2012). Intellectual disabilities, neuronal posttranscriptional RNA metabolism, and RNA-binding proteins: three actors for a complex scenario. *Prog. Brain Res.* 197, 29–51. doi: 10.1016/B978-0-444-54299-1.00003-0

Bardoni, B., Willemsen, R., Weiler, I. J., Schenck, A., Severijnen, L. A., Hindelang, C., et al. (2003). NUFIP1 (nuclear FMRP interacting protein 1) is a nucleocytoplasmic shuttling protein associated with active synaptoneurosomes. *Exp. Cell Res.* 289, 95–107. doi: 10.1016/S0014-4827(03)00222-2

Bassell, G. J., and Warren, S. T. (2008). Fragile X syndrome: loss of local mRNA regulation alters synaptic development and function. *Neuron* 60, 201–214. doi: 10.1016/j.neuron.2008.10.004

Bear, M. F., Huber, K. M., and Warren, S. T. (2004). The mGluR theory of fragile X mental retardation. *Trends Neurosci.* 27, 370–377. doi: 10.1016/j.tins.2004.04.009

Beck, C. R., Garcia-Perez, J. L., Badge, R. M., and Moran, J. V. (2011). LINE-1 elements in structural variation and disease. *Annu. Rev. Genomics Hum. Genet.* 12, 187–215. doi: 10.1146/annurev-genom-082509-141802

Belgnaoui, S. M., Gosden, R. G., Semmes, O. J., and Haoudi, A. (2006). Human LINE-1 retrotransposon induces DNA damage and apoptosis in cancer cells. *Cancer Cell Int.* 6:13. doi: 10.1186/1475-2867-6-13

Belloni, M., Tritto, P., Bozzetti, M. P., Palumbo, G., and Robbins, L. G. (2002). Does stellate cause meiotic drive in Drosophila melanogaster? *Genetics* 161, 1551–1559.

Bolduc, F. V., Bell, K., Cox, H., Broadie, K. S., and Tully, T. (2008). Excess protein synthesis in Drosophila fragile X mutants impairs long-term memory. *Nat. Neurosci.* 11, 1143–1145. doi: 10.1038/nn.2175

Bolduc, F. V., Bell, K., Rosenfelt, C., Cox, H., and Tully, T. (2010). Fragile x mental retardation 1 and filamin a interact genetically in Drosophila long-term memory. *Front. Neural Circuits* 3:22. doi: 10.3389/neuro.04.022.2009

Bozzetti, M. P., Fanti, L., Di Tommaso, S., Piacentini, L., Berloco, M., Tritto, P., et al. (2012). The "Special" crystal-stellate system in Drosophila melanogaster reveals mechanisms underlying piRNA pathway-mediated canalization. *Genet. Res. Int.* 2012:324293. doi: 10.1155/2012/324293

Bozzetti, M. P., Massari, S., Finelli, P., Meggio, F., Pinna, L. A., Boldyreff, B., et al. (1995). The Ste locus, a component of the parasitic cry-Ste system of Drosophila melanogaster, encodes a protein that forms crystals in primary spermatocytes and mimics properties of the beta subunit of casein kinase 2. *Proc. Natl. Acad. Sci. U. S. A.* 92, 6067–6071. doi: 10.1073/pnas.92.13.6067

Bozzetti, M. P., Specchia, V., Cattenoz, P. B., Laneve, P., Geusa, A., Sahin, H. B., et al. (2015). The Drosophila fragile X mental retardation protein participates in the piRNA pathway. *J. Cell Sci.* 128, 2070–2084. doi: 10.1242/jcs.161810

Brennecke, J., Aravin, A. A., Stark, A., Dus, M., Kellis, M., Sachidanandam, R., et al. (2007). Discrete small RNA-generating loci as master regulators of transposon activity in Drosophila. *Cell* 128, 1089–1103. doi: 10.1016/j.cell.2007.01.043

Brown, V., Jin, P., Ceman, S., Darnell, J. C., O'Donnell, W. T., Tenenbaum, S. A., et al. (2001). Microarray identification of FMRP-associated brain mRNAs and altered mRNA translational profiles in fragile X syndrome. *Cell* 107, 477–487. doi: 10.1016/S0092-8674(01)00568-2

Callan, M. A., Cabernard, C., Heck, J., Luois, S., Doe, C. Q., and Zarnescu, D. C. (2010). Fragile X protein controls neural stem cell proliferation in the Drosophila brain. *Hum. Mol. Genet.* 19, 3068–3079. doi: 10.1093/hmg/ddq213

Caudy, A. A., Myers, M., Hannon, G. J., and Hammond, S. M. (2002). Fragile X-related protein and VIG associate with the RNA interference machinery. *Genes Dev.* 16, 2491–2496. doi: 10.1101/gad.1025202

Chen, Y., Pane, A., and Schupbach, T. (2007). Cutoff and aubergine mutations result in retrotransposon upregulation and checkpoint activation in Drosophila. *Curr. Biol.* 17, 637–642. doi: 10.1016/j.cub.2007.02.027

Choi, C. H., McBride, S. M., Schoenfeld, B. P., Liebelt, D. A., Ferreiro, D., Ferrick, N. J., et al. (2010). Age-dependent cognitive impairment in a Drosophila fragile X model and its pharmacological rescue. *Biogerontology* 11, 347–362. doi: 10.1007/s10522-009-9259-6

Ciccia, A., and Elledge, S. J. (2010). The DNA damage response: making it safe to play with knives. *Mol. Cell* 40, 179–204. doi: 10.1016/j.molcel.2010.09.019

Coffee, R. L. Jr., Tessier, C. R., Woodruff, E. A., 3rd, and Broadie, K. (2010). Fragile X mental retardation protein has a unique, evolutionarily conserved neuronal function not shared with FXR1P or FXR2P. *Dis. Model. Mech.* 3, 471–485. doi: 10.1242/dmm.004598

Cook, H. A., Koppetsch, B. S., Wu, J., and Theurkauf, W. E. (2004). The Drosophila SDE3 homolog armitage is required for oskar mRNA silencing and embryonic axis specification. *Cell* 116, 817–829. doi: 10.1016/S0092-8674(04)00250-8

Costa, A., Wang, Y., Dockendorff, T. C., Erdjument-Bromage, H., Tempst, P., Schedl, P., et al. (2005). The Drosophila fragile X protein functions as a negative regulator in the orb autoregulatory pathway. *Dev. Cell* 8, 331–342. doi: 10.1016/j.devcel.2005.01.011

Cotta-Ramusino, C., McDonald, E. R., 3rd, Hurov, K., Sowa, M. E., Harper, J. W., and Elledge, S. J. (2011). A DNA damage response screen identifies RHINO, a 9-1-1 and TopBP1 interacting protein required for ATR signaling. *Science* 332, 1313–1317. doi: 10.1126/science.1203430

Coufal, N. G., Garcia-Perez, J. L., Peng, G. E., Marchetto, M. C., Muotri, A. R., Mu, Y., et al. (2011). Ataxia telangiectasia mutated (ATM) modulates long interspersed element-1 (L1) retrotransposition in human neural stem cells. *Proc. Natl. Acad. Sci. U. S. A.* 108, 20382–20387. doi: 10.1073/pnas.1100273108

Coufal, N. G., Garcia-Perez, J. L., Peng, G. E., Yeo, G. W., Mu, Y., Lovci, M. T., et al. (2009). L1 retrotransposition in human neural progenitor cells. *Nature* 460, 1127–1131. doi: 10.1038/nature08248

Coyne, A. N., Lorenzini, I., Chou, C. C., Torvund, M., Rogers, R. S., Starr, A., et al. (2017). Post-transcriptional inhibition of Hsc70-4/HSPA8 expression leads to synaptic vesicle cycling defects in multiple models of ALS. *Cell Rep.* 21, 110–125. doi: 10.1016/j.celrep.2017.09.028

Coyne, A. N., Yamada, S. B., Siddegowda, B. B., Estes, P. S., Zaepfel, B. L., Johannesmeyer, J. S., et al. (2015). Fragile X protein mitigates TDP-43 toxicity by remodeling RNA granules and restoring translation. *Hum. Mol. Genet.* 24, 6886–6898. doi: 10.1093/hmg/ddv389

Cziko, A. M., McCann, C. T., Howlett, I. C., Barbee, S. A., Duncan, R. P., and Luedemann, R. (2009). Genetic modifiers of dFMR1 encode RNA granule components in Drosophila. *Genetics* 182, 1051–1060. doi: 10.1534/genetics.109.103234

Darnell, J. C., Fraser, C. E., Mostovetsky, O., Stefani, G., Jones, T. A., Eddy, S. R., et al. (2005). Kissing complex RNAs mediate interaction between the Fragile-X mental retardation protein KH2 domain and brain polyribosomes. *Genes Dev.* 19, 903–918. doi: 10.1101/gad.1276805

Darnell, J. C., Van Driesche, S. J., Zhang, C., Hung, K. Y., Mele, A., Fraser, C. E., et al. (2011). FMRP stalls ribosomal translocation on mRNAs linked to synaptic function and autism. *Cell* 146, 247–261. doi: 10.1016/j.cell.2011.06.013

Dobbin, M. M., Madabhushi, R., Pan, L., Chen, Y., Kim, D., Gao, J., et al. (2013). SIRT1 collaborates with ATM and HDAC1 to maintain genomic stability in neurons. *Nat. Neurosci.* 16, 1008–1015. doi: 10.1038/nn.3460

Dockendorff, T. C., and Labrador, M. (2019). The Fragile X protein and genome function. *Mol. Neurobiol.* 56, 711–721. doi: 10.1007/s12035-018-1122-9

Dockendorff, T. C., Su, H. S., McBride, S. M., Yang, Z., Choi, C. H., Siwicki, K. K., et al. (2002). Drosophila lacking dfmr1 activity show defects in circadian output and fail to maintain courtship interest. *Neuron* 34, 973–984. doi: 10.1016/S0896-6273(02)00724-9

Doll, C. A., and Broadie, K. (2016). Neuron class-specific requirements for Fragile X mental retardation protein in critical period development of calcium signaling in learning and memory circuitry. *Neurobiol. Dis.* 89, 76–87. doi: 10.1016/j.nbd.2016.02.006

Doll, C. A., Vita, D. J., and Broadie, K. (2017). Fragile X mental retardation protein requirements in activity-dependent critical period neural circuit refinement. *Curr. Biol.* 27, 2318–2330 e3. doi: 10.1016/j.cub.2017.06.046

Douville, R., Liu, J., Rothstein, J., and Nath, A. (2011). Identification of active loci of a human endogenous retrovirus in neurons of patients with amyotrophic lateral sclerosis. *Ann. Neurol.* 69, 141–151. doi: 10.1002/ana.22149

Drozd, M., Bardoni, B., and Capovilla, M. (2018). Modeling Fragile X syndrome in Drosophila. *Front. Mol. Neurosci.* 11:124. doi: 10.3389/fnmol.2018.00124

Egorova, K. S., Olenkina, O. M., Kibanov, M. V., Kalmykova, A. I., Gvozdev, V. A., and Olenina, L. V. (2009). Genetically derepressed nucleoplasmic stellate protein in spermatocytes of *D. melanogaster* interacts with the catalytic subunit of protein kinase 2 and carries histone-like lysine-methylated mark. *J. Mol. Biol.* 389, 895–906. doi: 10.1016/j.jmb.2009.04.064

Epstein, A. M., Bauer, C. R., Ho, A., Bosco, G., and Zarnescu, D. C. (2009). Drosophila Fragile X protein controls cellular proliferation by regulating cbl levels in the ovary. *Dev. Biol.* 330, 83–92. doi: 10.1016/j.ydbio.2009.03.011

Evrony, G. D., Cai, X., Lee, E., Hills, L. B., Elhosary, P. C., Lehmann, H. S., et al. (2012). Single-neuron sequencing analysis of L1 retrotransposition and somatic mutation in the human brain. *Cell* 151, 483–496. doi: 10.1016/j.cell.2012.09.035

Fallini, C., Bassell, G. J., and Rossoll, W. (2012). The ALS disease protein TDP-43 is actively transported in motor neuron axons and regulates axon outgrowth. *Hum. Mol. Genet.* 21, 3703–3718. doi: 10.1093/hmg/dds205

Faulkner, G. J., and Billon, V. (2018). L1 retrotransposition in the soma: a field jumping ahead. *Mob. DNA* 9:22. doi: 10.1186/s13100-018-0128-1

Feng, Y., Absher, D., Eberhart, D. E., Brown, V., Malter, H. E., and Warren, S. T. (1997). FMRP associates with polyribosomes as an mRNP, and the I304N mutation of severe fragile X syndrome abolishes this association. *Mol. Cell* 1, 109–118. doi: 10.1016/S1097-2765(00)80012-X

Ferrante, R. J., Browne, S. E., Shinobu, L. A., Bowling, A. C., Baik, M. J., MacGarvey, U., et al. (1997). Evidence of increased oxidative damage in both sporadic and familial amyotrophic lateral sclerosis. *J. Neurochem.* 69, 2064–2074. doi: 10.1046/j.1471-4159.1997.69052064.x

Gangaraju, V. K., Yin, H., Weiner, M. M., Wang, J., Huang, X. A., and Lin, H. (2011). Drosophila Piwi functions in Hsp90-mediated suppression of phenotypic variation. *Nat. Genet.* 43, 153–158. doi: 10.1038/ng.743

Gasior, S. L., Wakeman, T. P., Xu, B., and Deininger, P. L. (2006). The human LINE-1 retrotransposon creates DNA double-strand breaks. *J. Mol. Biol.* 357, 1383–1393. doi: 10.1016/j.jmb.2006.01.089

Ghabrial, A., and Schupbach, T. (1999). Activation of a meiotic checkpoint regulates translation of Gurken during Drosophila oogenesis. *Nat. Cell Biol.* 1, 354–357. doi: 10.1038/14046

Ghildiyal, M., Seitz, H., Horwich, M. D., Li, C., Du, T., Lee, S., et al. (2008). Endogenous siRNAs derived from transposons and mRNAs in Drosophila somatic cells. *Science* 320, 1077–1081. doi: 10.1126/science.1157396

Girard, A., Sachidanandam, R., Hannon, G. J., and Carmell, M. A. (2006). A germline-specific class of small RNAs binds mammalian Piwi proteins. *Nature* 442, 199–202. doi: 10.1038/nature04917

Greenblatt, E. J., and Spradling, A. C. (2018). Fragile X mental retardation 1 gene enhances the translation of large autism-related proteins. *Science* 361, 709–712. doi: 10.1126/science.aas9963

Godler, D. E., Tassone, F., Loesch, D. Z., Taylor, A. K., Gehling, F., Hagerman, R. J., et al. (2010). Methylation of novel markers of fragile X alleles is inversely correlated with FMRP expression and FMR1 activation ratio. *Hum. Mol. Genet.* 19, 1618–1632. doi: 10.1093/hmg/ddq037

Gonzalez-Reyes, A., Elliott, H., and St Johnston, D. (1997). Oocyte determination and the origin of polarity in Drosophila: the role of the spindle genes. *Development* 124, 4927–4937.

Granier, C. J., Wang, W., Tsang, T., Steward, R., Sabaawy, H. E., Bhaumik, M., et al. (2014). Conditional inactivation of PDCD2 induces p53 activation and cell cycle arrest. *Biol. Open* 3, 821–831. doi: 10.1242/bio.20148326

Grivna, S. T., Beyret, E., Wang, Z., and Lin, H. (2006). A novel class of small RNAs in mouse spermatogenic cells. *Genes Dev.* 20, 1709–1714. doi: 10.1101/gad.1434406

Gunawardane, L. S., Saito, K., Nishida, K. M., Miyoshi, K., Kawamura, Y., Nagami, T., et al. (2007). A slicer-mediated mechanism for repeat-associated siRNA 5′end formation in Drosophila. *Science* 315, 1587–1590. doi: 10.1126/science.1140494

Guo, C., Jeong, H. H., Hsieh, Y. C., Klein, H. U., Bennett, D. A., De Jager, P. L., et al. (2018). Tau activates transposable elements in Alzheimer's disease. *Cell Rep.* 23, 2874–2880. doi: 10.1016/j.celrep.2018.05.004

Hagerman, R. J., Des-Portes, V., Gasparini, F., Jacquemont, S., and Gomez-Mancilla, B. (2014). Translating molecular advances in fragile X syndrome into therapy: a review. *J. Clin. Psychiatry* 75, e294–e307. doi: 10.4088/JCP.13r08714

Hamilton, S. M., Green, J. R., Veeraragavan, S., Yuva, L., McCoy, A., Wu, Y., et al. (2014). Fmr1 and Nlgn3 knockout rats: novel tools for investigating autism spectrum disorders. *Behav. Neurosci.* 128, 103–109. doi: 10.1037/a0035988

Hoch, N. C., Hanzlikova, H., Rulten, S. L., Tetreault, M., Komulainen, E., Ju, L., et al. (2017). XRCC1 mutation is associated with PARP1 hyperactivation and cerebellar ataxia. *Nature* 541, 87–91. doi: 10.1038/nature20790

Huber, K. M., Gallagher, S. M., Warren, S. T., and Bear, M. F. (2002). Altered synaptic plasticity in a mouse model of fragile X mental retardation. *Proc. Natl. Acad. Sci. U. S. A.* 99, 7746–7750. doi: 10.1073/pnas.122205699

Hunter, J., Rivero-Arias, O., Angelov, A., Kim, E., Fotheringham, I., and Leal, J. (2014). Epidemiology of fragile X syndrome: a systematic review and meta-analysis. *Am. J. Med. Genet. A* 164A, 1648–1658. doi: 10.1002/ajmg.a.36511

Kanellopoulos, A. K., Semelidou, O., Kotini, A. G., Anezaki, M., and Skoulakis, E. M. (2012). Learning and memory deficits consequent to reduction of the fragile X mental retardation protein result from metabotropic glutamate receptor-mediated inhibition of cAMP signaling in Drosophila. *J. Neurosci.* 32, 13111–13124. doi: 10.1523/JNEUROSCI.1347-12.2012

Ishizuka, A., Siomi, M. C., and Siomi, H. (2002). A Drosophila fragile X protein interacts with components of RNAi and ribosomal proteins. *Genes Dev.* 16, 2497–2508. doi: 10.1101/gad.1022002

Iwasaki, Y. W., Siomi, M. C., and Siomi, H. (2015). PIWI-Interacting RNA: its biogenesis and functions. *Annu. Rev. Biochem.* 84, 405–433. doi: 10.1146/annurev-biochem-060614-034258

Jachowicz, J. W., Bing, X., Pontabry, J., Boskovic, A., Rando, O. J., and Torres-Padilla, M. E. (2017). LINE-1 activation after fertilization regulates global chromatin accessibility in the early mouse embryo. *Nat. Genet.* 49, 1502–1510. doi: 10.1038/ng.3945

Jiang, F., Lu, F., Li, P., Liu, W., Zhao, L., Wang, Q., et al. (2016). Drosophila homolog of FMRP maintains genome integrity by interacting with Piwi. *Int. J. Genet. Genomics* 43, 11–24. doi: 10.1016/j.jgg.2015.11.001

Jin, P., Zarnescu, D. C., Ceman, S., Nakamoto, M., Mowrey, J., Jongens, T. A., et al. (2004). Biochemical and genetic interaction between the fragile X mental retardation protein and the microRNA pathway. *Nat. Neurosci.* 7, 113–117. doi: 10.1038/nn1174

Johannisson, R., Rehder, H., Wendt, V., and Schwinger, E. (1987). Spermatogenesis in two patients with the fragile X syndrome. I. Histology: light and electron microscopy. *Hum. Genet.* 76, 141–147. doi: 10.1007/BF00284911

Kalmykova, A. I., Klenov, M. S., and Gvozdev, V. A. (2005). Argonaute protein PIWI controls mobilization of retrotransposons in the Drosophila male germline. *Nucleic Acids Res.* 33, 2052–2059. doi: 10.1093/nar/gki323

Katyal, S., Lee, Y., Nitiss, K. C., Downing, S. M., Li, Y., Shimada, M., et al. (2014). Aberrant topoisomerase-1 DNA lesions are pathogenic in neurodegenerative genome instability syndromes. *Nat. Neurosci.* 17, 813–821. doi: 10.1038/nn.3715

Kibanov, M. V., Egorova, K. S., Ryazansky, S. S., Sokolova, O. A., Kotov, A. A., Olenkina, O. M., et al. (2011). A novel organelle, the piNG-body, in the nuage of Drosophila male germ cells is associated with piRNA-mediated gene silencing. *Mol. Biol. Cell* 22, 3410–3419. doi: 10.1091/mbc.E11-02-0168

Kim, H., Erickson, B., Luo, W., Seward, D., Graber, J. H., Pollock, D. D., et al. (2010). Gene-specific RNA polymerase II phosphorylation and the CTD code. *Nat. Struct. Mol. Biol.* 17, 1279–1286. doi: 10.1038/nsmb.1913

Klattenhoff, C., Bratu, D. P., McGinnis-Schultz, N., Koppetsch, B. S., Cook, H. A., and Theurkauf, W. E. (2007). Drosophila rasiRNA pathway mutations disrupt embryonic axis specification through activation of an ATR/Chk2 DNA damage response. *Dev. Cell* 12, 45–55. doi: 10.1016/j.devcel.2006.12.001

Klattenhoff, C., and Theurkauf, W. (2008). Biogenesis and germline functions of piRNAs. *Development* 135, 3–9. doi: 10.1242/dev.006486

Kronquist, K. E., Sherman, S. L., and Spector, E. B. (2008). Clinical significance of tri-nucleotide repeats in Fragile X testing: a clarification of American College of Medical Genetics guidelines. *Genet. Med. Off. J. Am. Coll. Med. Genet.* 10, 845–847. doi: 10.1097/GIM.0b013e31818b0c8a

Krug, L., Chatterjee, N., Borges-Monroy, R., Hearn, S., Liao, W. W., Morrill, K., et al. (2017). Retrotransposon activation contributes to neurodegeneration in a Drosophila TDP-43 model of ALS. *PLoS Genet.* 13:e1006635. doi: 10.1371/journal.pgen.1006635

Lasko, P. (2013). The DEAD-box helicase Vasa: evidence for a multiplicity of functions in RNA processes and developmental biology. *Biochim. Biophys. Acta* 1829, 810–816. doi: 10.1016/j.bbagrm.2013.04.005

Lavin, M. F. (2008). Ataxia-telangiectasia: from a rare disorder to a paradigm for cell signalling and cancer. *Nat. Rev. Mol. Cell Biol.* 9, 759–769. doi: 10.1038/nrm2514

Lee, E. J., Banerjee, S., Zhou, H., Jammalamadaka, A., Arcila, M., Manjunath, B. S., et al. (2011). Identification of piRNAs in the central nervous system. *RNA* 17, 1090–1099. doi: 10.1261/rna.2565011

Lee, J., Peng, Y., Lin, W. Y., and Parrish, J. Z. (2015). Coordinate control of terminal dendrite patterning and dynamics by the membrane protein Raw. *Development* 142, 162–173. doi: 10.1242/dev.113423

Li, W., Prazak, L., Chatterjee, N., Gruninger, S., Krug, L., Theodorou, D., et al. (2013). Activation of transposable elements during aging and neuronal decline in Drosophila. *Nature Neuroscience* 16, 529–531. doi: 10.1038/nn.3368

Li, C., Vagin, V. V., Lee, S., Xu, J., Ma, S., Xi, H., et al. (2009). Collapse of germline piRNAs in the absence of Argonaute3 reveals somatic piRNAs in flies. *Cell* 137, 509–521. doi: 10.1016/j.cell.2009.04.027

Li, W., Jin, Y., Prazak, L., Hammell, M., and Dubnau, J. (2012). Transposable elements in TDP-43-mediated neurodegenerative disorders. *PLoS One* 7:e44099. doi: 10.1371/journal.pone.0044099

Li, W., Lee, M. H., Henderson, L., Tyagi, R., Bachani, M., Steiner, J., et al. (2015). Human endogenous retrovirus-K contributes to motor neuron disease. *Sci. Transl. Med.* 7:307ra153. doi: 10.1126/scitranslmed.aac8201

Liu, W., Jiang, F., Bi, X., and Zhang, Y. Q. (2012). Drosophila FMRP participates in the DNA damage response by regulating G2/M cell cycle checkpoint and apoptosis. *Hum. Mol. Genet.* 21, 4655–4568. doi: 10.1093/hmg/dds307

Livak, K. J. (1984). Organization and mapping of a sequence on the Drosophila melanogaster X and Y chromosomes that is transcribed during spermatogenesis. *Genetics* 107, 611–634.

Lou, Z., Minter-Dykhouse, K., Franco, S., Gostissa, M., Rivera, M. A., Celeste, A., et al. (2006). MDC1 maintains genomic stability by participating in the amplification of ATM-dependent DNA damage signals. *Mol. Cell* 21, 187–200. doi: 10.1016/j.molcel.2005.11.025

Lu, T., Pan, Y., Kao, S. Y., Li, C., Kohane, I., Chan, J., et al. (2004). Gene regulation and DNA damage in the ageing human brain. *Nature* 429, 883–891. doi: 10.1038/nature02661

Madabhushi, R., Gao, F., Pfenning, A. R., Pan, L., Yamakawa, S., Seo, J., et al. (2015). Activity-induced DNA breaks govern the expression of neuronal early-response genes. *Cell* 161, 1592–1605. doi: 10.1016/j.cell.2015.05.032

Majumder, P., Chu, J. F., Chatterjee, B., Swamy, K. B., and Shen, C. J. (2016). Co-regulation of mRNA translation by TDP-43 and Fragile X syndrome protein FMRP. *Acta Neuropathol.* 132, 721–738. doi: 10.1007/s00401-016-1603-8

Malone, C. D., Brennecke, J., Dus, M., Stark, A., McCombie, W. R., Sachidanandam, R., et al. (2009). Specialized piRNA pathways act in germline and somatic tissues of the Drosophila ovary. *Cell* 137, 522–535. doi: 10.1016/j.cell.2009.03.040

Martin, F. C. (2011). Falls risk factors: assessment and management to prevent falls and fractures. *Can. J. Aging* 30, 33–44. doi: 10.1017/S0714980810000747

Matsumoto, N., Sato, K., Nishimasu, H., Namba, Y., Miyakubi, K., Dohmae, N., et al. (2015). Crystal structure and activity of the endoribonuclease domain of the piRNA Pathway Factor Maelstrom. *Cell Rep.* 11, 366–375. doi: 10.1016/j.celrep.2015.03.030

Matsuoka, S., Ballif, B. A., Smogorzewska, A., McDonald, E. R., 3rd, Hurov, K. E., Luo, J., et al. (2007). ATM and ATR substrate analysis reveals extensive protein networks responsive to DNA damage. *Science* 316, 1160–1166. doi: 10.1126/science.1140321

Maurin, H., Chong, S. A., Kraev, I., Davies, H., Kremer, A., Seymour, C. M., et al. (2014). Early structural and functional defects in synapses and myelinated axons in stratum lacunosum moleculare in two preclinical models for tauopathy. *PLoS One* 9:e87605. doi: 10.1371/journal.pone.0087605

McBride, S. M., Bell, A. J., and Jongens, T. A. (2012). Behavior in a Drosophila model of fragile X. *Results Probl. Cell Differ.* 54, 83–117.

McBride, S. M., Choi, C. H., Wang, Y., Liebelt, D., Braunstein, E., Ferreiro, D., et al. (2005). Pharmacological rescue of synaptic plasticity, courtship behavior, and mushroom body defects in a Drosophila model of fragile X syndrome. *Neuron* 45, 753–764. doi: 10.1016/j.neuron.2005.01.038

Minakhina, S., Changela, N., and Steward, R. (2014). Zfrp8/PDCD2 is required in ovarian stem cells and interacts with the piRNA pathway machinery. *Development* 141, 259–268. doi: 10.1242/dev.101410

Minakhina, S., Druzhinina, M., and Steward, R. (2007). Zfrp8, the Drosophila ortholog of PDCD2, functions in lymph gland development and controls cell proliferation. *Development* 134, 2387–2396. doi: 10.1242/dev.003616

Minakhina, S., and Steward, R. (2010). Hematopoietic stem cells in Drosophila. *Development* 137, 27–31. doi: 10.1242/dev.043943

Morales, J., Hiesinger, P. R., Schroeder, A. J., Kume, K., Verstreken, P., Jackson, F. R., et al. (2002). Drosophila fragile X protein, DFXR, regulates neuronal morphology and function in the brain. *Neuron* 34, 961–972. doi: 10.1016/S0896-6273(02)00731-6

Morandi, E., Tanasescu, R., Tarlinton, R. E., Constantinescu, C. S., Zhang, W., Tench, C., et al. (2017). The association between human endogenous retroviruses and multiple sclerosis: a systematic review and meta-analysis. *PLoS One* 12:e0172415. doi: 10.1371/journal.pone.0172415

Mu, W., Munroe, R. J., Barker, A. K., and Schimenti, J. C. (2010). PDCD2 is essential for inner cell mass development and embryonic stem cell maintenance. *Dev. Biol.* 347, 279–288. doi: 10.1016/j.ydbio.2010.08.026

Mugat, B., Akkouche, A., Serrano, V., Armenise, C., Li, B., Brun, C., et al. (2015). MicroRNA-dependent transcriptional silencing of transposable elements in Drosophila follicle cells. *PLoS Genet.* 11:e1005194. doi: 10.1371/journal.pgen.1005194

Muotri, A. R., Chu, V. T., Marchetto, M. C., Deng, W., Moran, J. V., and Gage, F. H. (2005). Somatic mosaicism in neuronal precursor cells mediated by L1 retrotransposition. *Nature* 435, 903–910. doi: 10.1038/nature03663

Muotri, A. R., Marchetto, M. C., Coufal, N. G., Oefner, R., Yeo, G., Nakashima, K., et al. (2010). L1 retrotransposition in neurons is modulated by MeCP2. *Nature* 468, 443–446. doi: 10.1038/nature09544

Nagao, A., Sato, K., Nishida, K. M., Siomi, H., and Siomi, M. C. (2011). Gender-specific hierarchy in nuage localization of PIWI-interacting RNA factors in Drosophila. *Front. Genet.* 2:55. doi: 10.3389/fgene.2011.00055

Nandi, S., Chandramohan, D., Fioriti, L., Melnick, A. M., Hebert, J. M., Mason, C. E., et al. (2016). Roles for small noncoding RNAs in silencing of retrotransposons in the mammalian brain. *Proc. Natl. Acad. Sci. U. S. A.* 113, 12697–12702. doi: 10.1073/pnas.1609287113

Napoli, I., Mercaldo, V., Boyl, P. P., Eleuteri, B., Zalfa, F., De Rubeis, S., et al. (2008). The fragile X syndrome protein represses activity-dependent translation through CYFIP1, a new 4E-BP. *Cell* 134, 1042–1054. doi: 10.1016/j.cell.2008.07.031

Nishida, K. M., Saito, K., Mori, T., Kawamura, Y., Nagami-Okada, T., Inagaki, S., et al. (2007). Gene silencing mechanisms mediated by Aubergine piRNA complexes in Drosophila male gonad. *RNA* 13, 1911–1922. doi: 10.1261/rna.744307

Nouspikel, T., and Hanawalt, P. C. (2003). When parsimony backfires: neglecting DNA repair may doom neurons in Alzheimer's disease. *BioEssays: News Rev. Mol. Cell. Dev. Biol.* 25, 168–173. doi: 10.1002/bies.10227

O'Donnell, W. T., and Warren, S. T. (2002). A decade of molecular studies of fragile X syndrome. *Annu. Rev. Neurosci.* 25, 315–338. doi: 10.1146/annurev.neuro.25.112701.142909

Okray, Z., de Esch, C. E., Van Esch, H., Devriendt, K., Claeys, A., Yan, J., et al. (2015). A novel fragile X syndrome mutation reveals a conserved role for the carboxy-terminus in FMRP localization and function. *EMBO Mol. Med.* 7, 423–437. doi: 10.15252/emmm.201404576

Palumbo, G., Bonaccorsi, S., Robbins, L. G., and Pimpinelli, S. (1994). Genetic analysis of Stellate elements of Drosophila melanogaster. *Genetics* 138, 1181–1197.

Pan, L., Zhang, Y. Q., Woodruff, E., and Broadie, K. (2004). The Drosophila fragile X gene negatively regulates neuronal elaboration and synaptic differentiation. *Curr. Biol.* 14, 1863–1870. doi: 10.1016/j.cub.2004.09.085

Pane, A., Wehr, K., and Schupbach, T. (2007). Zucchini and squash encode two putative nucleases required for rasiRNA production in the Drosophila germline. *Dev. Cell* 12, 851–862. doi: 10.1016/j.devcel.2007.03.022

Papoulas, O., Monzo, K. F., Cantin, G. T., Ruse, C., Yates, J. R., 3rd, Ryu, Y. H., et al. (2010). dFMRP and Caprin, translational regulators of synaptic plasticity, control the cell cycle at the Drosophila mid-blastula transition. *Development* 137, 4201–4209. doi: 10.1242/dev.055046

Patil, V. S., and Kai, T. (2010). Repression of retroelements in Drosophila germline via piRNA pathway by the Tudor domain protein Tejas. *Curr. Biol.* 20, 724–730. doi: 10.1016/j.cub.2010.02.046

Penagarikano, O., Mulle, J. G., and Warren, S. T. (2007). The pathophysiology of fragile x syndrome. *Annu. Rev. Genomics Hum. Genet.* 8, 109–129. doi: 10.1146/annurev.genom.8.080706.092249

Perez-Cadahia, B., Drobic, B., and Davie, J. R. (2011). Activation and function of immediate-early genes in the nervous system. *Biochem. Cell Biol.* 89, 61–73. doi: 10.1139/O10-138

Perrat, P. N., DasGupta, S., Wang, J., Theurkauf, W., Weng, Z., Rosbash, M., et al. (2013). Transposition-driven genomic heterogeneity in the Drosophila brain. *Science* 340, 91–95. doi: 10.1126/science.1231965

Piacentini, L., Fanti, L., Specchia, V., Bozzetti, M. P., Berloco, M., Palumbo, G., et al. (2014). Transposons, environmental changes, and heritable induced phenotypic variability. *Chromosoma* 123, 345–354. doi: 10.1007/s00412-014-0464-y

Pisa, V., Cozzolino, M., Gargiulo, S., Ottone, C., Piccioni, F., Monti, M., et al. (2009). The molecular chaperone Hsp90 is a component of the cap-binding complex and interacts with the translational repressor Cup during Drosophila oogenesis. *Gene* 432, 67–74. doi: 10.1016/j.gene.2008.11.025

Prudencio, M., Gonzales, P. K., Cook, C. N., Gendron, T. F., Daughrity, L. M., Song, Y., et al. (2017). Repetitive element transcripts are elevated in the brain of C9orf72 ALS/FTLD patients. *Hum. Mol. Genet.* 26, 3421–3431. doi: 10.1093/hmg/ddx233

Qiu, W., Guo, X., Lin, X., Yang, Q., Zhang, W., Zhang, Y., et al. (2017). Transcriptome-wide piRNA profiling in human brains of Alzheimer's disease. *Neurobiol. Aging* 57, 170–177. doi: 10.1016/j.neurobiolaging.2017.05.020

Quartier, A., Poquet, H., Gilbert-Dussardier, B., Rossi, M., Casteleyn, A. S., Portes, V. D., et al. (2017). Intragenic FMR1 disease-causing variants: a significant mutational mechanism leading to Fragile-X syndrome. *Eur. J. Hum. Genet.* 25, 423–431. doi: 10.1038/ejhg.2016.204

Rajan, K. S., and Ramasamy, S. (2014). Retrotransposons and piRNA: the missing link in central nervous system. *Neurochem. Int.* 77, 94–102. doi: 10.1016/j.neuint.2014.05.017

Rajasethupathy, P., Antonov, I., Sheridan, R., Frey, S., Sander, C., Tuschl, T., et al. (2012). A role for neuronal piRNAs in the epigenetic control of memory-related synaptic plasticity. *Cell* 149, 693–707. doi: 10.1016/j.cell.2012.02.057

Ramos, A., Hollingworth, D., Adinolfi, S., Castets, M., Kelly, G., Frenkiel, T. A., et al. (2006). The structure of the N-terminal domain of the fragile X mental retardation protein: a platform for protein-protein interaction. *Structure* 14, 21–31. doi: 10.1016/j.str.2005.09.018

Rass, U., Ahel, I., and West, S. C. (2007). Defective DNA repair and neurodegenerative disease. *Cell* 130, 991–1004. doi: 10.1016/j.cell.2007.08.043

Reeve, S. P., Lin, X., Sahin, B. H., Jiang, F., Yao, A., Liu, Z., et al. (2008). Mutational analysis establishes a critical role for the N terminus of fragile X mental retardation protein FMRP. *J. Neurosci.* 28, 3221–3226. doi: 10.1523/JNEUROSCI.5528-07.2008

Reilly, M. T., Faulkner, G. J., Dubnau, J., Ponomarev, I., and Gage, F. H. (2013). The role of transposable elements in health and diseases of the central nervous system. *J. Neurosci.* 33, 17577–17586. doi: 10.1523/JNEUROSCI.3369-13.2013

Ross, R. J., Weiner, M. M., and Lin, H. (2014). PIWI proteins and PIWI-interacting RNAs in the soma. *Nature* 505, 353–359. doi: 10.1038/nature12987

Rossetti, R., Ferrari, I., Bonomi, M., and Persani, L. (2017). Genetics of primary ovarian insufficiency. *Clin. Genet.* 91, 183–198. doi: 10.1007/s10815-014-0342-9

Roy, J., Sarkar, A., Parida, S., Ghosh, Z., and Mallick, B. (2017). Small RNA sequencing revealed dysregulated piRNAs in Alzheimer's disease and their probable role in pathogenesis. *Mol. BioSyst.* 13, 565–576. doi: 10.1039/c6mb00699j

Sahin, H. B., Karatas, O. F., Specchia, V., Tommaso, S. D., Diebold, C., Bozzetti, M. P., et al. (2016). Novel mutants of the aubergine gene. *Fly* 10, 81–90. doi: 10.1080/19336934.2016.1174355

Saito, K., Ishizu, H., Komai, M., Kotani, H., Kawamura, Y., Nishida, K. M., et al. (2010). Roles for the Yb body components Armitage and Yb in primary piRNA biogenesis in Drosophila. *Genes Dev.* 24, 2493–2498. doi: 10.1101/gad.1989510

Santoro, M. R., Bray, S. M., and Warren, S. T. (2012). Molecular mechanisms of fragile X syndrome: a twenty-year perspective. *Annu. Rev. Pathol.* 7, 219–245. doi: 10.1146/annurev-pathol-011811-132457

Sarot, E., Payen-Groschene, G., Bucheton, A., and Pelisson, A. (2004). Evidence for a piwi-dependent RNA silencing of the gypsy endogenous retrovirus by the Drosophila melanogaster flamenco gene. *Genetics* 166, 1313–1321. doi: 10.1534/genetics.166.3.1313

Sawarkar, R., Sievers, C., and Paro, R. (2010). HSP90 globally targets paused RNA Polymerase to regulate gene expression in response to environmental stimuli. *Cell* 149, 807–818. doi: 10.1016/j.cell.2012.02.061

Schenck, A., Bardoni, B., Langmann, C., Harden, N., Mandel, J. L., and Giangrande, A. (2003). CYFIP/Sra-1 controls neuronal connectivity in Drosophila and links the Rac1 GTPase pathway to the fragile X protein. *Neuron* 38, 887–898. doi: 10.1016/S0896-6273(03)00354-4

Schulze, M., Sommer, A., Plotz, S., Farrell, M., Winner, B., Grosch, J., et al. (2018). Sporadic Parkinson's disease derived neuronal cells show disease-specific mRNA and small RNA signatures with abundant deregulation of piRNAs. *Acta Neuropathol. Commun.* 6:58. doi: 10.1186/s40478-018-0561-x

Sears, J. C., and Broadie, K. (2017). Fragile X mental retardation protein regulates activity-dependent membrane trafficking and trans-synaptic signaling mediating synaptic remodeling. *Front. Mol. Neurosci.* 10:440. doi: 10.3389/fnmol.2017.00440

Sehgal, A., Price, J. L., Man, B., and Young, M. W. (1994). Loss of circadian behavioral rhythms and per RNA oscillations in the Drosophila mutant timeless. *Science* 263, 1603–1606. doi: 10.1126/science.8128246

Short, P. J., McRae, J. F., Gallone, G., Sifrim, A., Won, H., Geschwind, D. H., et al. (2018). De novo mutations in regulatory elements in neurodevelopmental disorders. *Nature* 555, 611–616. doi: 10.1038/nature25983

Siomi, M. C., Siomi, H., Sauer, W. H., Srinivasan, S., Nussbaum, R. L., and Dreyfuss, G. (1995). FXR1, an autosomal homolog of the fragile X mental retardation gene. *EMBO J.* 14, 2401–2408. doi: 10.1002/j.1460-2075.1995.tb07237.x

Siomi, M. C., Zhang, Y., Siomi, H., and Dreyfuss, G. (1996). Specific sequences in the fragile X syndrome protein FMR1 and the FXR proteins mediate their binding to 60S ribosomal subunits and the interactions among them. *Mol. Cell. Biol.* 16, 3825–3832. doi: 10.1128/MCB.16.7.3825

Slegtenhorst-Eegdeman, K. E., de Rooij, D. G., Verhoef-Post, M., van de Kant, H. J., Bakker, C. E., Oostra, B. A., et al. (1998). Macroorchidism in FMR1 knockout mice is caused by increased Sertoli cell proliferation during testicular development. *Endocrinology* 139, 156–162. doi: 10.1210/endo.139.1.5706

Specchia, V., Benna, C., Mazzotta, G. M., Piccin, A., Zordan, M. A., Costa, R., et al. (2008). Aubergine gene overexpression in somatic tissues of aubergine(sting) mutants interferes with the RNAi pathway of a yellow hairpin dsRNA in Drosophila melanogaster. *Genetics* 178, 1271–1282. doi: 10.1534/genetics.107.078626

Specchia, V., and Bozzetti, M. P. (2009). Different aubergine alleles confirm the specificity of different RNAi pathways in Drosophila melanogaster. *Fly* 3, 170–172.

Specchia, V., D'Attis, S., Puricella, A., and Bozzetti, M. P. (2017). dFmr1 plays roles in small RNA pathways of Drosophila melanogaster. *Int. J. Mol. Sci.* 18:E1066. doi: 10.3390/ijms18051066

Specchia, V., Piacentini, L., Tritto, P., Fanti, L., D'Alessandro, R., Palumbo, G., et al. (2010). Hsp90 prevents phenotypic variation by suppressing the mutagenic activity of transposons. *Nature* 463, 662–665. doi: 10.1038/nature08739

Staeva-Vieira, E., Yoo, S., and Lehmann, R. (2003). An essential role of DmRad51/SpnA in DNA repair and meiotic checkpoint control. *EMBO J.* 22, 5863–5874. doi: 10.1093/emboj/cdg564

Stapleton, W., Das, S., and McKee, B. D. (2001). A role of the Drosophila homeless gene in repression of Stellate in male meiosis. *Chromosoma* 110, 228–240. doi: 10.1007/s004120100136

Suhl, J. A., and Warren, S. T. (2015). Single-nucleotide mutations in FMR1 reveal novel functions and regulatory mechanisms of the Fragile X syndrome protein FMRP. *J. Exp. Neurosci.* 9, 35–41. doi: 10.4137/JEN.S25524

Szakmary, A., Reedy, M., Qi, H., and Lin, H. (2009). The Yb protein defines a novel organelle and regulates male germline stem cell self-renewal in Drosophila melanogaster. *J. Cell Biol.* 185, 613–627. doi: 10.1083/jcb.200903034

Swanger, S. A., and Bassell, G. J. (2011). Making and breaking synapses through local mRNA regulation. *Curr. Opin. Genet. Dev.* 21, 414–421. doi: 10.1016/j.gde.2011.04.002

Tamanini, F., Meijer, N., Verheij, C., Willems, P. J., Galjaard, H., Oostra, B. A., et al. (1996). FMRP is associated to the ribosomes via RNA. *Hum. Mol. Genet.* 5, 809–813. doi: 10.1093/hmg/5.6.809

Tan, H., Qurashi, A., Poidevin, M., Nelson, D. L., Li, H., and Jin, P. (2012). Retrotransposon activation contributes to fragile X premutation rCGG-mediated neurodegeneration. *Hum. Mol. Genet.* 21, 57–65. doi: 10.1093/hmg/ddr437

Tan, W., Schauder, C., Naryshkina, T., Minakhina, S., and Steward, R. (2016). Zfrp8 forms a complex with fragile-X mental retardation protein and regulates its localization and function. *Dev. Biol.* 410, 202–212. doi: 10.1016/j.ydbio.2015.12.008

Tessier, C. R., and Broadie, K. (2012). Molecular and genetic analysis of the Drosophila model of fragile X syndrome. *Results Probl. Cell Differ.* 54, 119–156.

Thomas, C. A., Paquola, A. C., and Muotri, A. R. (2012). LINE-1 retrotransposition in the nervous system. *Annu. Rev. Cell Dev. Biol.* 28, 555–573. doi: 10.1146/annurev-cellbio-101011-155822

Thomson, T., and Lin, H. (2009). The biogenesis and function of PIWI proteins and piRNAs: progress and prospect. *Annu. Rev. Cell Dev. Biol.* 25, 355–376. doi: 10.1146/annurev.cellbio.24.110707.175327

Treiber, C. D., and Waddell, S. (2017). Resolving the prevalence of somatic transposition in Drosophila. *elife* 6, pii: e28297. doi: 10.7554/eLife.28297

Tritto, P., Specchia, V., Fanti, L., Berloco, M., D'Alessandro, R., Pimpinelli, S., et al. (2003). Structure, regulation and evolution of the crystal-Stellate system of Drosophila. *Genetica* 117, 247–257. doi: 10.1023/A:1022960632306

Tucker, B., Richards, R., and Lardelli, M. (2004). Expression of three zebrafish orthologs of human FMR1-related genes and their phylogenetic relationships. *Dev. Genes Evol.* 214, 567–574. doi: 10.1007/s00427-004-0438-9

Upton, K. R., Gerhardt, D. J., Jesuadian, J. S., Richardson, S. R., Sanchez-Luque, F. J., Bodea, G. O., et al. (2015). Ubiquitous L1 mosaicism in hippocampal neurons. *Cell* 161, 228–239. doi: 10.1016/j.cell.2015.03.026

Vagin, V. V., Sigova, A., Li, C., Seitz, H., Gvozdev, V., and Zamore, P. D. (2006). A distinct small RNA pathway silences selfish genetic elements in the germline. *Science* 313, 320–324. doi: 10.1126/science.1129333

Verrotti, A. C., and Wharton, R. P. (2000). Nanos interacts with cup in the female germline of Drosophila. *Development* 127, 5225–5232.

Wan, L., Dockendorff, T. C., Jongens, T. A., and Dreyfuss, G. (2000). Characterization of dFMR1, a Drosophila melanogaster homolog of the fragile X mental retardation protein. *Mol. Cell. Biol.* 20, 8536–8547. doi: 10.1128/MCB.20.22.8536-8547.2000

Watanabe, T., Takeda, A., Tsukiyama, T., Mise, K., Okuno, T., Sasaki, H., et al. (2006). Identification and characterization of two novel classes of small RNAs inthe mouse germline: retrotransposon-derived siRNAs in oocytes and germline small RNAs in testes. *Genes Dev.* 20, 1732–1743. doi: 10.1101/gad.1425706

Weick, E. M., and Miska, E. A. (2014). piRNAs: from biogenesis to function. *Development* 141, 3458–3471. doi: 10.1242/dev.094037

Weisz, E. D., Monyak, R. E., and Jongens, T. A. (2015). Deciphering discord: how Drosophila research has enhanced our understanding of the importance of FMRP in different spatial and temporal contexts. *Exp. Neurol.* 274, 14–24. doi: 10.1016/j.expneurol.2015.05.015

West, A. E., and Greenberg, M. E. (2011). Neuronal activity-regulated gene transcription in synapse development and cognitive function. *Cold Spring Harb. Perspect. Biol.* 3, pii: a005744. doi: 10.1101/cshperspect.a005744

Xiol, J., Spinelli, P., Laussmann, M. A., Homolka, D., Yang, Z., Cora, E., et al. (2014). RNA clamping by Vasa assembles a piRNA amplifier complex on transposon transcripts. *Cell* 157, 1698–1711. doi: 10.1016/j.cell.2014.05.018

Xu, X. L., Li, Y., Wang, F., and Gao, F. B. (2008). The steady-state level of the nervous-system-specific microRNA-124a is regulated by dFMR1 in Drosophila. *J. Neurosci.* 28, 11883–11889. doi: 10.1523/JNEUROSCI.4114-08.2008

Yang, L., Duan, R., Chen, D., Wang, J., and Jin, P. (2007). Fragile X mental retardation protein modulates the fate of germline stem cells in Drosophila. *Hum. Mol. Genet.* 16, 1814–1820. doi: 10.1093/hmg/ddm129

Yang, Y., Xu, S., Xia, L., Wang, J., Wen, S., Jin, P., et al. (2009). The bantam microRNA is associated with drosophila fragile X mental retardation protein and regulates the fate of germline stem cells. *PLoS Genet.* 5:e1000444. doi: 10.1371/journal.pgen.1000444

Yu, Z., Fan, D., Gui, B., Shi, L., Xuan, C., Shan, L., et al. (2012). Neurodegeneration-associated TDP-43 interacts with fragile X mental retardation protein (FMRP)/Staufen (STAU1) and regulates SIRT1 expression in neuronal cells. *J. Biol. Chem.* 287, 22560–22572. doi: 10.1074/jbc.M112.357582

Zalfa, F., Eleuteri, B., Dickson, K. S., Mercaldo, V., De Rubeis, S., di Penta, A., et al. (2007). A new function for the fragile X mental retardation protein in regulation of PSD-95 mRNA stability. *Nat. Neurosci.* 10, 578–587. doi: 10.1038/nn1893

Zhang, M., Wang, Q., and Huang, Y. (2007). Fragile X mental retardation protein FMRP and the RNA export factor NXF2 associate with and destabilize Nxf1 mRNA in neuronal cells. *Proc. Natl. Acad. Sci. U. S. A.* 104, 10057–10062. doi: 10.1073/pnas.0700169104

Zhang, W., Cheng, Y., Li, Y., Chen, Z., Jin, P., and Chen, D. (2014). A feed-forward mechanism involving Drosophila fragile X mental retardation protein triggers a replication stress-induced DNA damage response. *Hum. Mol. Genet.* 23, 5188–5196. doi: 10.1093/hmg/ddu241

Zhang, Y., Brown, M. R., Hyland, C., Chen, Y., Kronengold, J., Fleming, M. R., et al. (2012). Regulation of neuronal excitability by interaction of fragile X mental retardation protein with slack potassium channels. *J. Neurosci.* 32, 15318–15327. doi: 10.1523/JNEUROSCI.2162-12.2012

Zhang, Y., O'Connor, J. P., Siomi, M. C., Srinivasan, S., Dutra, A., Nussbaum, R. L., et al. (1995). The fragile X mental retardation syndrome protein interacts with novel homologs FXR1 and FXR2. *EMBO J.* 14, 5358–5366. doi: 10.1002/j.1460-2075.1995.tb00220.x

Zhang, Y. Q., Bailey, A. M., Matthies, H. J., Renden, R. B., Smith, M. A., Speese, S. D., et al. (2001). Drosophila fragile X-related gene regulates the MAP1B homolog Futsch to control synaptic structure and function. *Cell* 107, 591–603. doi: 10.1016/S0092-8674(01)00589-X

Zhang, Y. Q., Matthies, H. J., Mancuso, J., Andrews, H. K., Woodruff, E., 3rd, Friedman, D., et al. (2004). The Drosophila fragile X-related gene regulates axoneme differentiation during spermatogenesis. *Dev. Biol.* 270, 290–307. doi: 10.1016/j.ydbio.2004.02.010

Zhang, Z., Xu, J., Koppetsch, B. S., Wang, J., Tipping, C., Ma, S., et al. (2011). Heterotypic piRNA Ping-Pong requires qin, a protein with both E3 ligase and Tudor domains. *Mol. Cell* 44, 572–584. doi: 10.1016/j.molcel.2011.10.011

Zhou, R., Hotta, I., Denli, A. M., Hong, P., Perrimon, N., and Hannon, G. J. (2008). Comparative analysis of argonaute-dependent small RNA pathways in Drosophila. *Mol. Cell* 32, 592–599. doi: 10.1016/j.molcel.2008.10.018

Conflict of Interest Statement: The authors declare that the research was conducted in the absence of any commercial or financial relationships that could be construed as a potential conflict of interest.

frontiers in Genetics

MINI REVIEW
published: 10 January 2019
doi: 10.3389/fgene.2018.00738

Divide Precisely and Proliferate Safely: Lessons From Budding Yeast

*Roberta Fraschini**

Dipartimento di Biotecnologie e Bioscienze, Università degli Studi di Milano-Bicocca, Milan, Italy

A faithful cell division is essential for proper cellular proliferation of all eukaryotic cells; indeed the correct segregation of the genetic material allows daughter cells to proceed into the cell cycle safely. Conversely, errors during chromosome partition generate aneuploid cells that have been associated to several human pathological conditions, including cancer. Given the importance of this issue, all the steps that lead to cell separation are finely regulated. The budding yeast *Saccharomyces cerevisiae* is a unicellular eukaryotic organism that divides asymmetrically and it is a suitable model system to study the regulation of cell division. Humans and budding yeast are distant 1 billion years of evolution, nonetheless several essential pathways, proteins, and cellular structures are conserved. Among these, the mitotic spindle is a key player in chromosome segregation and its correct morphogenesis and functioning is essential for genomic stability. In this review we will focus on molecular pathways and proteins involved in the control mitotic spindle morphogenesis and function that are conserved from yeast to humans and whose impairment is connected with the development of human diseases.

Keywords: SPB, centrosome, mitotic spindle, genomic stability, aneuploidy

OPEN ACCESS

Edited by:
Maria Grazia Giansanti, Consiglio Nazionale delle Ricerche (CNR), Italy

Reviewed by:
Matteo Barberis, University of Amsterdam, Netherlands
Ethel Queralt, Biomedical Research Institute of Bellvitge, Spain

***Correspondence:**
Roberta Fraschini
roberta.fraschini@unimib.it

Specialty section:
This article was submitted to Genetic Disorders, a section of the journal Frontiers in Genetics

Received: *16 July 2018*
Accepted: *22 December 2018*
Published: *10 January 2019*

Citation:
Fraschini R (2019) Divide Precisely and Proliferate Safely: Lessons From Budding Yeast. Front. Genet. 9:738. doi: 10.3389/fgene.2018.00738

INTRODUCTION

In the last decades budding yeast has been largely used as a model system to unravel molecular mechanisms of cell life. *Saccharomyces cerevisiae* is a unicellular eukaryotic organism, its cells have the same subcellular organization as those of multicellular organisms but they are easier to manipulate. In the budding yeast system several methodologies can be easily applied: genetic, biochemical, cytological, genomic approaches (Botstein and Fink, 1988), and high-throughput technologies. Several processes and proteins are conserved from yeast to human cells despite their distance from an evolutionary point of view and their misregulation is involved in disease development. The sequence of the genes and functional complementation studies have revealed that at least 20% of human genes known to have a role in disease have functional equivalents in yeast (Douzery et al., 2004). In addition, a systematic humanization analysis revealed that 47% of the yeast genes can be replaced by their human orthologs, indicative of conserved functions despite large sequence divergence (Kachroo et al., 2015).

The importance of basic research using budding yeast is highlight by three Nobel Prizes in Physiology or Medicine assigned to scientist for their discoveries of key proteins or processes in yeast. Professors L. Hartwell, J. Rothman, and Y. Ohsumi used classical forward budding yeast genetic approaches to reveal fundamental cell biological processes in eukaryotes; genetic analysis was conducted in parallel with microscopic analysis of the mutants and followed by biochemical

and cell biology studies. Importantly, the conservation of the basic cellular processes across eukaryotes explains the great impact of these studies for understanding biology and disease.

Studies in budding yeast have revealed the essential functions of the centromeres, DNA sequences that allow the assembly of specialized multiprotein complexes, called kinetochores, that connect chromosomal DNA with mitotic spindle fibers in a bipolar way and ensure proper chromosome segregation during mitosis. A surveillance mechanism called Spindle Assembly Checkpoint (SAC) has been described in yeast and is conserved throughout evolution; the SAC delays anaphase onset in case of lack of biorientation, that is the correct binding of the two sister chromatids kinetochores to opposite spindle poles. Importantly, altered SAC function allows premature mitotic exit and can cause chromosome missegregation thus leading to aneuploid daughter cells, i. e., with an abnormal chromosome number. Interestingly, both decreased and increased SAC gene expression are found in tumors in mice (Sotillo et al., 2007; Ricke et al., 2011), in addition mutations in *MAD1*, *MAD2*, *BUB1, BUBR1,* and *BUB3* are found in human cancers and over expression of the same genes is associated with elevated proliferation index and metastatic potential in several solid tumors (Yuan et al., 2006; Wang et al., 2015). These data link cancer occurrence with SAC function, chromosome segregation defects and aneuploidy (for a complete overview on this topic see Simonetti et al., 2018).

The mitotic spindle is essential to allow proper partitioning of the genetic material between the daughter cells, it has a conserved structure and its malfunctions are at the basis of several human diseases, as described below. In budding yeast a bipolar spindle is formed during S phase, concomitantly with DNA duplication, while in animal cells the spindle apparatus is built during mitosis. However, in all eukaryotic cells the mitotic spindle is formed by microtubules (MTs), cylindric structures made by protofilaments of α- and β-tubulin heterodimers assembled in a head-to-tail fashion. Each MT has a dynamic fast growing end (plus end) and a slow growing end (minus end). MTs are associated with several proteins involved in regulation of spindle dynamics and with motor proteins that allow spindle positioning in the cell and intracellular transport. Before sister chromatids separation in anaphase, MTs plus ends bind the chromosomes via their kinetochores in a bipolar way thus ensuring their correct segregation in the daughter cells.

MTOC STRUCTURE AND FUNCTION

Eukaryotic cells contain microtubule organizing centers (MTOC) or centrosomes that allow MT nucleation in coordination with cell cycle progression. In *S. cerevisiae* the mitotic spindle is build thanks to the spindle pole body (SPB), the functional equivalent of multicellular eukaryotes centrosome. SPBs are approximately 2 megadaltons complexes embedded in the nuclear envelope and are able to nucleate both nuclear and cytoplasmic MTs, thus SPBs play a critical role in mitotic spindle formation and positioning. The SPB has a multilayered structure that consists of an outer plaque that faces the cytoplasm and emanates cytoplasmic microtubules, a central plaque, and an inner plaque that faces the nucleoplasm and emits nuclear MTs (Byers and Goetsch, 1974; **Figure 1A**). Attached to one side of the central plaque there is the half-bridge, essential for SPB duplication as it serves for the assembly of the satellite, the precursor of the daughter SPB. Given the crucial function of SPB, its components are encoded by essential genes. SPBs and human MTOCs share conserved proteins with common functions (Cavanaugh and Jaspersen, 2017), therefore the yeast SPB is good model to study centrosome function.

The SPB cycle is tightly connected with other cell cycle events (**Figure 1B**). The SPB duplicates once each cell cycle, just like chromosomes: during S phase the MTs bind the kinetochores and the SPBs separate from each other, thus allowing the formation of a short bipolar spindle. After separation, each SPB inherits a half bridge, essential for its duplication in the following cell cycle. During anaphase the SPBs further move away from each other toward the cortex of the mother and the daughter cell (Fraschini, 2017). SPB duplication is restricted once per cell cycle thanks to an oscillation between the activities of Cdk1 kinase and Cdc14 phosphatase. Sfi1 is a Centrin/Cdc31 binding protein, conserved from yeast to humans, that plays a key role in SPB cycle. During S phase and early mitosis Sfi1 is phosphorylated by Cdk1 and by Cdc5 and blocks the process of SPB duplication. After anaphase onset, the protein phosphatase Cdc14 is active and dephosphorylates Sfi1 thus allowing the maturation of the half-bridge and therefore daughter SPB formation (Elserafy et al., 2014).

Spindle pole body function is regulated by multiple proteins during the cell cycle and several SPB components have been shown to be phosphorylated *in vivo* (Keck et al., 2011). A genome-wide screen for the substrates of the cyclin dependent kinase Cdk1 identified some SPB components (Spc42, Spc29, Mps2, Bbp1, Sfi1) and suggested that Spc110, Cnm67, Kar1 may be Cdk1 substrates as well (Ubersax et al., 2003). Mps1 is a protein kinase involved in regulation of SPB duplication and phosphorylates three SPB components: Spc98, Spc110, Spc42. The polo-like kinase Cdc5 localizes to SPBs and over expression of a version of Cdc5 lacking the polo-box results in the formation of Spc42-containing structures in the cytoplasm. Pericentrin/Spc110 might be phosphorylated by Cdc5, since one of its phosphorylation sites matches the Cdc5 kinase consensus sequence and an affinity capture-western experiment showed that Cdc5 and Spc110 interact. The protein kinase Swe1 is an important cell cycle regulator, as it blocks entry into mitosis through inhibitory phosphorylation of the catalytic subunit of the cyclin-dependent kinase Cdk1 (*S. cerevisiae* Cdc28) in case of replication stress and alterations in actin cytoskeleton or cytokinetic structures (Booher et al., 1993). Interestingly Swe1, homolog of human Wee1, localizes at SPBs (Bartholomew et al., 2001), it is involved in mitotic spindle dynamics and it interacts with the outer plaque component Centrosomin/Spc72 (Raspelli et al., 2015, 2018).

Studies on SPB helped to reveal the protein composition and function of animal cells MTOC, that have a partly different structure. Each centrosome contains a pair of nine-fold symmetrical centrioles embedded in a proteinaceous matrix known as the pericentriolar material (PCM), which comprises

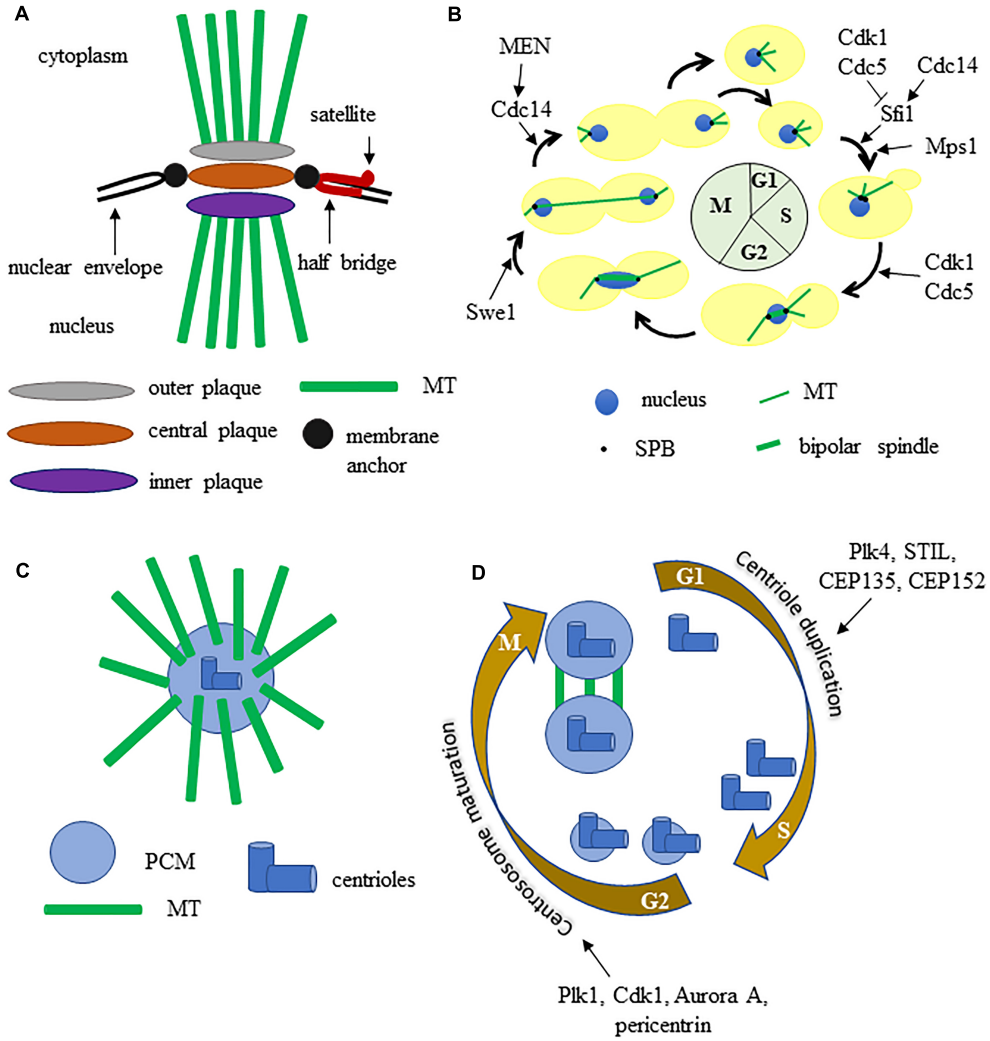

FIGURE 1 | (A) graphic representation of the budding yeast spindle pole body. **(B)** the SPB and spindle cycle in budding yeast, some key regulators are indicated. **(C)** schematic structure of a metazoan centrosome. **(D)** centrosome duplication and maturation cycle, some key regulators are indicated. See text for details.

proteins required for microtubule nucleation and cell cycle regulators (**Figure 1C**). Concomitantly with DNA replication, centrioles duplicate themselves to form a new centrosome then, during late G2 phase, centrosomes undergo maturation, which results in PCM expansion and recruitment of the conserved γ-tubulin rings. Polo-like kinase 1 (Plk-1) regulates the increase of PCM that accompanies mitotic entry by controlling the localization of γ-tubulin, Spd-2, and Cnn/CDK5RAP2. During prophase centrosomes separate, generate fibers and form a bipolar spindle (Nigg and Holland, 2018; **Figure 1D**).

MTOC MALFUNCTIONS AND GENETIC DISEASES

Studies in budding yeast have revealed the role of some proteins essential for SPB function and their homologs are involved in genetic diseases in human (**Table 1**). For example Spc110, the yeast homolog of pericentrin, is an essential component of the SPB inner plaque that stimulates binding with γ-tubulin and interacts with Cmd1, the homolog of human Calmodulin, a calcium sensor involved in the propagation of intracellular calcium signals. Missense mutations in one of the three genes coding for Calmodulin are associated with catecholaminergic polymorphic ventricular tachycardia (CPVT), early-onset severe long QT syndrome (esLQT), and idiopathic ventricular fibrillation (IVF) (Vassilakopoulou et al., 2015). Mutations that inactivate the *PCNT* gene, that encodes pericentrin, a structural component of the centrosome, can be found in all patients affected by Microcefalicosteodysplastic primordial dwarfism type II (MOPDII) (Ren et al., 2008). MOPDII is a rare and complex human autosomal recessive genetic disease, and individuals affected show primordial growth problems that are present before birth. Since pericentrin is

TABLE 1 | Summary of conserved genes involved in MTOC dynamics/signaling and the correlated genetic diseases.

S. cerevisiae	*H. sapiens*	Disease	Protein function	Localization yeast/human
CDC5	Plk1	Glioma, several types of carcinoma, melanoma, colorectal cancers, breast cancer, prostate cancer	MTOC separation	SPB outerplaque/centrosome
Sfi1	hSFI1	–	MTOC duplication	SPB half bridge/centriole
CDC31	Centrin	–	MTOC duplication	SPB half bridge/centriole
–	hPOC5	Idiopathic scoliosis	Binds Centrin and hSFI1	–
SPC72	Centrosomin CDK5RAP2/Cnn	Autosomal primary recessive microcephaly (MCPH)	MTOC organization	SPB outer plaque/centrosome
–	CEP63, CEP135, CEP152, CPAP/MCPH6, STIL/MCPH7	Autosomal primary recessive microcephaly (MCPH)	Centriole duplication	Centrosome
–	ASPM, WDR62	Autosomal primary recessive microcephaly (MCPH)	Centriole duplication	Spindle poles
SPC110	Pericentrin	Microcephalic osteodysplastic primordial dwarfism 2 (MOPD2)	MTOC maturation	SPB central plaque/centrosome
NUD1	Centriolin	Stem cell myeloproliferative disorder (MPD)	MTOC signaling	SPB outer plaque/centriole
CMD1	Calmodulin	CPV Tachycardia, early-onset severe long QT syndrome (esLQT), idiopathic ventricular fibrillation (IVF)	Calcium binding protein (MTOC structure)	SPB central plaque/nucleus and cytoplasm
TUB4	GCP1	Microcephaly, cortical dysplasia	γ-tubulin	SPB outer and inner plaque/centrosome
SPC97	GCP2	Dilated cardiomyopathy	γ-tubulin small complex	SPB outer and inner plaque/centrosome
SPC98	GCP3	Dilated cardiomyopathy	γ-tubulin small complex	SPB outer and inner plaque/centrosome
CDC15	MST1/2	Breast cancer, soft tissue sarcoma	Signaling kinase (Hippo pathway)	SPB/spindle poles
DBF2/DBF20	LATs/NDR	Breast cancer, astrocytoma	Signaling kinases (Hippo pathway)	SPB/spindle poles
MOB1	MOB1	Colorectal and lung cancers	Co-activator (Hippo pathway)	SPB/spindle poles

essential for mitotic spindle organization, mitotic progression and chromosome segregation, loss of its function causes defective recruitment of several proteins to the centrosome and inability to properly assemble microtubules, thus disrupting the mitotic cycle and cell division. These severe mitotic problems cause a dramatic reduction in the number of cells of both the growing embryo and the adult organism, resulting in small head, and body size (Delaval and Doxsey, 2010).

The homolog of Centrosomin (Cnn) is Spc72, an essential component of the SPB outer plaque, that interacts with Nud1, the yeast counterpart of human Centriolin. The SPBs components Cdc31 and Sf1 are the yeast counterparts of Centrin and hSFI1. Autosomal primary recessive microcephaly (MCPH) is a disorder in neurogenesis caused by at least nine genes, six of which encode centrosome components (CEP63, CEP135, CEP152, CDK5RAP2/Cnn, CPAP /MCPH6, and STIL/MCPH7) and two encode proteins associated with spindle poles (ASPM and WDR62) (Gilmore and Walsh, 2013). Mutations in these genes alter the precise centriole duplication process and therefore cause deregulation of centrosome number in cells. A translocation between chromosomes 8 and 9 disrupts Centriolin function and is associated with stem cell myeloproliferative disorder (MPD) (Ren et al., 2013). Idiopathic scoliosis is a complex disease with polygenic background that leads to a spinal deformity. Human POC5 dysfunction is associated with idiopathic scoliosis (Patten et al., 2015), being hPOC5 a protein that binds centrin and that is important for centriole duplication (Azimzadeh et al., 2009) together with Centrin and hSFI1 (Martinez-Sanz and Assairi, 2016).

CENTROSOME AMPLIFICATION AND CANCER

Centrosome amplification can cause the formation of multipolar spindle during mitosis, thus resulting in daughter cells with unbalanced genetic material. In yeast, SPB duplication is restricted by precise molecular mechanisms, as described above (Elserafy et al., 2014) and defective spindle or chromosome biorientation are sensed by the SAC, as described in the introduction (Stukenberg and Burke, 2015). The target of the checkpoint is the mitotic exit network (MEN), a pathway that

governs the transition from mitosis to the G1 phase of the cell cycle (Hotz and Barral, 2014). The MEN pathway is essential for proper coordination of nuclear division and exit from mitosis. Key MEN components are localized at the SPBs, that are therefore an important signaling platforms for mitosis progression. The MEN is conserved and in metazoan it is called the Hippo pathway; importantly, recently it has been shown that the core components of the Hippo pathway cooperate with p53 to suppress tumorigenesis (Furth et al., 2018). This cooperation occurs at multiple levels, for example in response to stress LATS2 blocks MDM2, a negative p53 regulator, thus causing p53 accumulation and activation (for a complete overview on this topic see Furth et al., 2018).

In the context of tumorigenesis, centrosome abnormalities and amplification are frequently detected in a wide range of solid cancers, myeloma, lymphomas and leukemias, and have been associated with multipolar cell divisions, chromosomal instability and aneuploidy (Chan, 2011). Cells with less or more than 2 centrosomes can form anastral, monopolar or multipolar spindles that can lead to chromosome missegregation and therefore aneuploidy. Centrosome defects can be found in early-low grade lesions, and are rarely observed in normal tissue, suggesting a possible role in tumor initiation. Recent studies show that centrosome aberrant number causes tumor formation in mice (Levine et al., 2017), centrosome amplification is correlated with high-grade tumors, disease progression and poor prognosis and also it enhances the aggressive nature of already transformed cells (Godinho and Pellman, 2014). Finally, several oncogenes and tumor suppressors have been localized to the centrosomes suggesting that they might contribute to centrosome anomalies (Tang et al., 2011). Centrosome alterations trigger a p53-response that arrest the cell cycle, indeed p53-proficient cells tolerate well variations of centrosomes copy number, while cancer cells defective in p53 frequently display centrosome anomalies (Lambrus et al., 2015).

Extracentrosomes can arise basically through two mechanisms: centriole overduplication or accumulation of mature centrosomes by aborted cell division, cell fusion, or centrosome clustering. It has been shown that the majority of centrosome aberrations in the primary tumor types are due to overduplication. However, in solid tumors other types of centrosome aberrations, originated from centrosome clustering or failed cytokinesis, are also found (Cosenza et al., 2017). Spindle multipolarity is strongly correlated with anaphase bridges, which cause DNA breaks that usually block cytokinesis, thus leading to centrosome amplification.

Centrosome amplification can be due to a deregulation of its duplication cycle that is controlled by many positive and negative regulators, such as members of the Cdk, Aurora/Ipl1, Polo-like, and NIMA families of conserved cell cycle kinases (Brownlee and Rogers, 2013). Some of these kinases are likely hyperactive in tumor tissue, since several centrosomal proteins are hyperphosphorylated in breast tumor cells compared to normal breast tissue (Lingle et al., 2005). Another key player is STIL, that interacts with the Polo-like kinase 4 (Plk4): its depletion leads to a decrease in centriole numbers while its excess activity causes extra centrioles (Habedanck et al., 2005). Cdk inhibitor $p27^{Kip1}$ levels and localization are highly regulated during the cell cycle and it acts to ensure proper centrosome amplification (Sharma et al., 2012). Recently, p27 involvement in centrosome duplication and cancer has also been studied at the systems levels (Barberis and Verbruggen, 2017), this kind of approach integrates experimental and computational data and allows the prediction of how perturbation of a protein can influence a biological process under analysis.

SPINDLE ALIGNMENT AND CELL POLARITY

Asymmetry is very important for the life of a cell: during development it drives the cellular fate, indeed in stem cells the asymmetric division discriminates the daughter cell that will differentiate and the other cell that will maintain the ability to proliferate. The asymmetry of a cell is built thanks to the polarization of several factors. In most eukaryotic cells astral MTs emanating from the centrosomes are captured by protein complexes at the cell cortex, align the mitotic spindle to the polarity axis of the cell and drive asymmetric division of the cell (Siller and Doe, 2009). Also budding yeast divides asymmetrically: the daughter cell originates from a bud that emerges from the mother cell, and the bud is the equivalent of the stem cells that retain the possibility to divide, while the mother gets old.

In budding yeast the localization of polarity factors determines the bud emergence site. At the beginning the bud grows in a polarized way, then the growth becomes isotropical and the bud becomes round shaped. The bud neck separates the mother from the daughter cell and it is the place where cells will divide. Since the division site is defined during late G1 phase, before DNA replication and mitotic spindle formation, in order to ensure proper chromosome partitioning during mitosis, the spindle must be correctly positioned and aligned with respect to the mother-bud axis (Lee et al., 2000). Yeast is the first model for which the mechanisms for spindle positioning have been described: an actin dependent and a dynein dependent pathway guide the process. In addition, the spindle orientation checkpoint (SPOC) blocks mitotic exit and cytokinesis in case of spindle mispositioning or misorientation (Caydasi and Pereira, 2012). If the checkpoint fails, cytokinesis occurs even if the nucleus divides into the mother cell, thus causing the formation of aneuploid cells.

The existing SPB is also called old SPB, while the one originated by duplication is called new SPB. Usually, the old SPB migrates into the bud thanks to cytoplasmatic MTs that contact the bud cortex. The two SPBs undergo different steps of regulation, for example differential Kar9 recruitment drives the movement of the selected SPB to the bud neck and helps spindle alignment (Liakopoulos et al., 2003). Several pathways contribute to SPB asymmetry: Kar9 is preferentially recruited to astral MTs emanated from the old SPB and this is governed by the SPB inheritance network (SPIN) and the MEN (Lengefeld et al., 2017). Recent data revealed that the asymmetry of the SPBs is due to spatial cues rather than different maturation

(Lengefeld et al., 2018). Similarly, in animal cells the old MTOC nucleates more astral MTs and is surrounded by more PCM than the new one, indicating that the new one is immature while the old one is mature and fully active (Lerit and Rusan, 2013).

Also in insect cells several data indicate that centrosome inheritance is consonant with cell fate decision. The stem cells of *Drosophila* male germline divide asymmetrically and produce a cell that differentiate and a cell that is totipotent. It has been observed that the old centrosome migrates in the cell that is able to renew while the new centrosome is inherited by the cell that is going to differentiate (Yamashita et al., 2007). Similar data were obtained in mouse radial glia progenitors and in *Drosophila* neuroblasts (Januschke et al., 2011), indicating that asymmetry of MTOCs and fate decision is a common feature of eukaryotic cells.

The centrosome plays an important role in brain development, indeed aberrant centrosome behavior is linked to inherited microcephaly. Microcephaly is the result of premature neural differentiation due to an insufficient number of symmetric division of neuroprogenitor cells before differentiation, that starts with the first asymmetric division, during cerebral cortex formation. Proper centrosome segregation ensures correct spindle orientation and the succession of several symmetric cell divisions before the beginning of differentiation (Morrison and Kimble, 2006). Several genes that encode for proteins implicated in centrosome function and spindle orientation are mutated in microcephaly in humans: MCPH5 or ASPM (abnormal spindle-like microcephaly associated), WDR62/MCPH2, and CEP63 (Thornton and Woods, 2009). However, not all forms of microcephaly are linked with spindle orientation defects, indicating that the causes of deficiencies in brain development are still partially unclear.

CLOSING REMARKS

The model organism *S. cerevisiae* offers powerful genetic tools to dissect the molecular pathways that control centrosome structure and number. In budding yeast the genetic analyses and manipulation are simple and fast, it is possible to synchronize cells in different cell cycle phases, to perform genetic screenings, and in addition the yeast two-hybrid assay allows detecting labile protein-protein interactions in the centrosome.

Despite structural differences, the yeast SPB carries many conserved proteins of the centriole and/or centrosome machinery in metazoans. Thus, it is becoming of growing interest to compare the structure and function of SPB with centrosomes and studies in budding yeast can elucidate the role of centrosomal proteins in physiological conditions. Altogether the knowledge provided by the studies on SPB structure and function in budding yeast will also improve our understanding of the molecular basis of important human diseases thus helping in developing new biomarkers and therapies.

AUTHOR CONTRIBUTIONS

RF wrote and revised the manuscript.

FUNDING

RF researches were supported by grants from PRIN (Progetti di Ricerca di Interesse Nazionale) and from the University of Milano-Bicocca (Fondo di Ateneo).

REFERENCES

Azimzadeh, J., Hergert, P., Delouvée, A., Euteneuer, U., Formstecher, E., Khodjakov, A., et al. (2009). hPOC5 is a centrin-binding protein required for assembly of full-length centrioles. *J. Cell Biol.* 185, 101–114. doi: 10.1083/jcb.200808082

Barberis, M., and Verbruggen, P. (2017). Quantitative Systems Biology to decipher design principles of a dynamic cell cycle network: the "Maximum Allowable mammalian Trade-Off-Weight" (MAmTOW). *NPJ Syst. Biol. Appl.* 3:26. doi: 10.1038/s41540-017-0028-x

Bartholomew, C. R., Woo, S. H., Chung, Y. S., Jones, C., and Hardy, C. F. (2001). Cdc5 interacts with the Wee1 kinase in budding yeast. *Mol. Cell. Biol.* 21, 4949–4959. doi: 10.1128/MCB.21.15.4949-4959.2001

Booher, R. N., Deshaies, R. J., and Kirschner, M. W. (1993). Properties of Saccharomyces cerevisiae wee1 and its differential regulation of p34CDC28 in response to G1 and G2 cyclins. *EMBO J.* 12, 3417–3426. doi: 10.1002/j.1460-2075.1993.tb06016.x

Botstein, D., and Fink, G. R. (1988). Yeast: an experimental organism for modern biology. *Science* 240, 1439–1443. doi: 10.1126/science.3287619

Brownlee, C. W., and Rogers, G. C. (2013). Show me your license, please: deregulation of centriole duplication mechanisms that promote amplification. *Cell Mol. Life Sci.* 70, 1021–1034. doi: 10.1007/s00018-012-1102-6

Byers, B., and Goetsch, L. (1974). Duplication of spindle plaques and integration of the yeast cell cycle. *Cold Spring Harb. Symp. Quant. Biol.* 38, 123–131. doi: 10.1101/SQB.1974.038.01.016

Cavanaugh, A. M., and Jaspersen, S. L. (2017). Big lessons from little yeast: budding and fission yeast centrosome structure, duplication, and function. *Annu. Rev. Genet.* 51, 361–383. doi: 10.1146/annurev-genet-120116-024733

Caydasi, A. K., and Pereira, G. (2012). SPOC alert when chromosomes get the wrong direction. *Exp Cell Res.* 318, 1421–1427. doi: 10.1016/j.yexcr.2012.03.031

Chan, J. Y. (2011). A clinical overview of centrosome amplification in human cancers. *Int. J. Biol. Sci.* 7, 1122–1144. doi: 10.7150/ijbs.7.1122

Cosenza, M. R., Cazzola, A., Rossberg, A., Schieber, N. L., Konotop, G., Bausch, E., et al. (2017). Asymmetric centriole numbers at spindle poles cause chromosome missegregation in cancer. *Cell Rep.* 20, 1906–1920. doi: 10.1016/j.celrep.2017.08.005

Delaval, B., and Doxsey, S. J. (2010). Pericentrin in cellular function and disease. *J. Cell Biol.* 188, 181–190. doi: 10.1083/jcb.200908114

Douzery, E. J., Snell, E. A., Bapteste, E., Delsuc, F., and Philippe, H. (2004). The timing of eukaryotic evolution: does a relaxed molecular clock reconcile proteins and fossils? *Proc. Natl. Acad. Sci. U.S.A.* 101, 15386–15391. doi: 10.1073/pnas.0403984101

Elserafy, M., Šarić, M., Neuner, A., Lin, T. C., Zhang, W., Seybold, C., et al. (2014). Molecular mechanisms that restrict yeast centrosome duplication to one event per cell cycle. *Curr. Biol.* 24, 1456–1466. doi: 10.1016/j.cub.2014.05.032

Fraschini, R. (2017). Factors that control mitotic spindle dynamics. *Adv. Exp. Med. Biol.* 925, 89–101. doi: 10.1007/5584_2016_74

Furth, N., Aylon, Y., and Oren, M. (2018). p53 shades of Hippo. *Cell Death Differ.* 25, 81–92. doi: 10.1038/cdd.2017.163

Gilmore, E. C., and Walsh, C. A. (2013). Genetic causes of microcephaly and lessons for neuronal development. *Wiley Interdiscip. Rev. Dev. Biol.* 2, 461–478. doi: 10.1002/wdev.89

Godinho, S. A., and Pellman, D. (2014). Causes and consequences of centrosome abnormalities in cancer. *Philos. Trans. R. Soc. Lond. B Biol. Sci.* 369, 1650. doi: 10.1098/rstb.2013.0467

Habedanck, R., Stierhof, Y. D., Wilkinson, C. J., and Nigg, E. A. (2005). The Polo kinase Plk4 functions in centriole duplication. *Nat. Cell Biol.* 7, 1140–1146. doi: 10.1038/ncb1320

Hotz, M., and Barral, Y. (2014). The mitotic exit network: new turns on old pathways. *Trends Cell Biol.* 24, 145–152. doi: 10.1016/j.tcb.2013.09.010

Januschke, J., Llamazares, S., Reina, J., and Gonzalez, C. (2011). Drosophila neuroblasts retain the daughter centrosome. *Nat. Commun.* 2:243. doi: 10.1038/ncomms1245

Kachroo, A. H., Laurent, J. M., Yellman, C. M., Meyer, A. G., Wilke, C. O., and Marcotte, E. M. (2015). Systematic humanization of yeast genes reveals conserved functions and genetic modularity. *Science* 348, 921–925. doi: 10.1126/science.aaa0769

Keck, J. M., Jones, M. H., Wong, C. C., Binkley, J., Chen, D., Jaspersen, S. L., et al. (2011). A cell cycle phosphoproteome of the yeast centrosome. *Science* 332, 1557–1561. doi: 10.1126/science.1205193

Lambrus, B. G., Uetake, Y., Clutario, K. M., Daggubati, V., Snyder, M., Sluder, G., et al. (2015). p53 protects against genome instability following centriole duplication failure. *J. Cell Biol.* 210, 63–77. doi: 10.1083/jcb.201502089

Lee, L., Tirnauer, J. S., Li, J., Schuyler, S. C., Liu, J. Y., and Pellman, D. (2000). Positioning of the mitotic spindle by a cortical-microtubule capture mechanism. *Science* 287, 2260–2262. doi: 10.1126/science.287.5461.2260

Lengefeld, J., Hotz, M., Rollins, M., Baetz, K., and Barral, Y. (2017). Budding yeast Wee1 distinguishes spindle pole bodies to guide their pattern of age-dependent segregation. *Nat. Cell Biol.* 19, 941–951. doi: 10.1038/ncb3576

Lengefeld, J., Yen, E., Chen, X., Leary, A., Vogel, J., and Barral, Y. (2018). Spatial cues and not spindle pole maturation drive the asymmetry of astral microtubules between new and preexisting spindle poles. *Mol. Biol. Cell.* 29, 10–28. doi: 10.1091/mbc.E16-10-0725

Lerit, D. A., and Rusan, N. M. (2013). PLP inhibits the activity of interphase centrosomes to ensure their proper segregation in stem cells. *J. Cell Biol.* 202, 1013–1022. doi: 10.1083/jcb.201303141

Levine, M. S., Bakker, B., Boeckx, B., Moyett, J., Lu, J., Vitre, B., et al. (2017). Centrosome amplification is sufficient to promote spontaneous tumorigenesis in mammals. *Dev. Cell* 40, 313.e–322.e. doi: 10.1016/j.devcel.2016.12.022

Liakopoulos, D., Kusch, J., Grava, S., Vogel, J., and Barral, Y. (2003). Asymmetric loading of Kar9 onto spindle poles and microtubules ensures proper spindle alignment. *Cell* 112, 561–574. doi: 10.1016/S0092-8674(03)00119-3

Lingle, W. L., Lukasiewicz, K., and Salisbury, J. L. (2005). Deregulation of the centrosome cycle and the origin of chromosomal instability in cancer. *Adv. Exp. Med. Biol.* 570, 393–421. doi: 10.1007/1-4020-3764-3_14

Martinez-Sanz, J., and Assairi, L. (2016). New insights into the interaction of centrin with Sfi1. *Biochim. Biophys. Acta* 1864, 319–330. doi: 10.1016/j.bbapap.2016.01.004

Morrison, S. J., and Kimble, J. (2006). Asymmetric and symmetric stem-cell divisions in development and cancer. *Nature* 441, 1068–1074. doi: 10.1038/nature04956

Nigg, E. A., and Holland, A. J. (2018). Once and only once: mechanisms of centriole duplication and their deregulation in disease. *Nat. Rev. Mol. Cell Biol.* 19, 297–312. doi: 10.1038/nrm.2017.127

Patten, S. A., Margaritte-Jeannin, P., Bernard, J. C., Alix, E., Labalme, A., Besson, A., et al. (2015). Functional variants of POC5 identified in patients with idiopathic scoliosis. *J. Clin. Invest*. 125, 1124–1128. doi: 10.1172/JCI77262

Raspelli, E., Cassani, C., Chiroli, E., and Fraschini, R. (2015). Budding yeast Swe1 is involved in the control of mitotic spindle elongation and is regulated by Cdc14 phosphatase during mitosis. *J. Biol. Chem.* 290, 1–12. doi: 10.1074/jbc.M114.590984

Raspelli, E., Facchinetti, S., and Fraschini, R. (2018). Novel insights into Swe1 and Mih1 role in the regulation of mitotic spindle dynamics. *J. Cell Science* 131:jcs.213520. doi: 10.1242/jcs.213520

Ren, C., Bao, Y. R., Meng, X. S., Diao, Y. P., and Kang, T. G. (2013). Comparison of the protective effects of ferulic acid and its drug-containing plasma on primary cultured neonatal rat cardiomyocytes with hypoxia/reoxygenation injury. *Pharmacogn. Mag.* 9, 202–209. doi: 10.4103/0973-1296.113264

Ren, M., Qin, H., Kitamura, E., and Cowell, J. K. (2008). Dysregulated signaling mutations in the pericentrin (PCNT) gene cause primordial dwarfism. *Science* 319, 816–819. doi: 10.1126/science.1151174

Ricke, R. M., Jeganathan, K. B., and van Deursen, J. M. (2011). Bub1 overexpression induces aneuploidy and tumor formation through aurora B kinase hyperactivation. *J. Cell Biol.* 193, 1049. doi: 10.1083/jcb.201012035

Sharma, S. S., Ma, L., Bagui, T. K., Forinash, K. D., and Pledger, W. J. (2012). A p27Kip1 mutant that does not inhibit CDK activity promotes centrosome amplification and micronucleation. *Oncogene* 31, 3989–3998. doi: 10.1038/onc.2011.550

Siller, K. H., and Doe, C. Q. (2009). Spindle orientation during asymmetric cell division. *Nat. Cell Biol.* 11, 365–374. doi: 10.1038/ncb0409-365

Simonetti, G., Bruno, S., Padella, A., Tenti, E., and Martinelli, G. (2018). Aneuploidy: cancer strength or vulnerability? *Int. J. Cancer* 144, 8–25. doi: 10.1002/ijc.31718

Sotillo, R., Hernando, E., Díaz-Rodríguez, E., Teruya-Feldstein, J., Cordón-Cardo, C., Lowe, S. W., et al. (2007). Mad2 overexpression promotes aneuploidy and tumorigenesis in mice. *Cancer Cell* 11, 9–23. doi: 10.1016/j.ccr.2006.10.019

Stukenberg, P. T., and Burke, D. J. (2015). Connecting the microtubule attachment status of each kinetochore to cell cycle arrest through the spindle assembly checkpoint. *Chromosoma* 124, 463–480. doi: 10.1007/s00412-015-0515-z

Tang, C. J., Lin, S. Y., Hsu, W. B., Lin, Y. N., Wu, C. T., Lin, Y. C., et al. (2011). The human microcephaly protein STIL interacts with CPAP and is required for procentriole formation. *EMBO J.* 30, 4790–4804. doi: 10.1038/emboj.2011.378

Thornton, G. K., and Woods, C. G. (2009). Primary microcephaly: do all roads lead to Rome? *Trends Genet.* 25, 501–510. doi: 10.1016/j.tig.2009.09.011

Ubersax, J. A., Woodbury, E. L., Quang, P. N., Paraz, M., Blethrow, J. D., Shah, K., et al. (2003). Targets of the cyclin-dependent kinase Cdk1. *Nature* 425, 859–864. doi: 10.1038/nature02062

Vassilakopoulou, V., Calver, B. L., Thanassoulas, A., Beck, K., Hu, H., Buntwal, L., et al. (2015). Distinctive malfunctions of calmodulin mutations associated with heart RyR2-mediated arrhythmic disease. *Biochim. Biophys. Acta* 1850, 2168–2176. doi: 10.1016/j.bbagen.2015.07.001

Wang, Z., Katsaros, D., Shen, Y., Fu, Y., Canuto, E. M., Benedetto, C., et al. (2015). Biological and clinical significance of MAD2L1 and BUB1 genes frequently appearing in expression signatures for breast Cancer prognosis. *PLoS One* 10:e0136246. doi: 10.1371/journal.pone.0136246

Yamashita, Y. M., Mahowald, A. P., Perlin, J. R., and Fuller, M. T. (2007). Asymmetric inheritance of mother versus daughter centrosome in stem cell division. *Science* 315, 518–521. doi: 10.1126/science.1134910

Yuan, B., Xu, Y., Woo, J. H., Wang, Y., Bae, Y. K., Yoon, D. S., et al. (2006). Increased expression of mitotic checkpoint genes in breast cancer cells with chromosomal instability. *Clin. Cancer Res.* 12, 405–410. doi: 10.1158/1078-0432.CCR-05-0903

Conflict of Interest Statement: The author declares that the research was conducted in the absence of any commercial or financial relationships that could be construed as a potential conflict of interest.

The handling Editor and author RF declared their involvement as co-editors in the Research Topic, and confirm the absence of any other collaboration.

frontiers in Genetics

REVIEW
published: 21 December 2018
doi: 10.3389/fgene.2018.00674

Centromere and Pericentromere Transcription: Roles and Regulation . . . in Sickness and in Health

*Ksenia Smurova and Peter De Wulf**

Centre for Integrative Biology, University of Trento, Trento, Italy

The chromosomal loci known as centromeres (CEN) mediate the equal distribution of the duplicated genome between both daughter cells. Specifically, centromeres recruit a protein complex named the kinetochore, that bi-orients the replicated chromosome pairs to the mitotic or meiotic spindle structure. The paired chromosomes are then separated, and the individual chromosomes segregate in opposite direction along the regressing spindle into each daughter cell. Erroneous kinetochore assembly or activity produces aneuploid cells that contain an abnormal number of chromosomes. Aneuploidy may incite cell death, developmental defects (including genetic syndromes), and cancer (>90% of all cancer cells are aneuploid). While kinetochores and their activities have been preserved through evolution, the CEN DNA sequences have not. Hence, to be recognized as sites for kinetochore assembly, CEN display conserved structural themes. In addition, CEN nucleosomes enclose a CEN-exclusive variant of histone H3, named CENP-A, and carry distinct epigenetic labels on CENP-A and the other CEN histone proteins. Through the cell cycle, CEN are transcribed into non-coding RNAs. After subsequent processing, they become key components of the CEN chromatin by marking the CEN locus and by stably anchoring the CEN-binding kinetochore proteins. CEN transcription is tightly regulated, of low intensity, and essential for differentiation and development. Under- or overexpression of CEN transcripts, as documented for myriad cancers, provoke chromosome missegregation and aneuploidy. CEN are genetically stable and fully competent only when they are insulated from the surrounding, pericentromeric chromatin, which must be silenced. We will review CEN transcription and its contribution to faithful kinetochore function. We will further discuss how pericentromeric chromatin is silenced by RNA processing and transcriptionally repressive chromatin marks. We will report on the transcriptional misregulation of (peri)centromeres during stress, natural aging, and disease and reflect on whether their transcripts can serve as future diagnostic tools and anti-cancer targets in the clinic.

Keywords: centromere, pericentromere, kinetochore, heterochromatin, long non-coding RNA, transcription

OPEN ACCESS

Edited by:
Roberta Fraschini, Università degli Studi di Milano-Bicocca, Italy

Reviewed by:
Tatsuo Fukagawa, Osaka University, Japan
Michael D. Blower, Harvard Medical School, United States

***Correspondence:**
Peter De Wulf
peter.dewulf@unitn.it

Specialty section:
This article was submitted to Genetic Disorders, a section of the journal Frontiers in Genetics

Received: *06 September 2018*
Accepted: *04 December 2018*
Published: *21 December 2018*

Citation:
Smurova K and De Wulf P (2018) Centromere and Pericentromere Transcription: Roles and Regulation . . . in Sickness and in Health. Front. Genet. 9:674. doi: 10.3389/fgene.2018.00674

CENTROMERES, KINETOCHORES, AND ANEUPLOIDY

During cell division, the replicated chromatids that are associated by cohesin rings bind to the microtubules of the metaphase spindle, which extend from two opposite spindle poles (**Figure 1**). This binding is mediated by kinetochores, each of which assembles on the centromere (CEN) of each chromatid. CENP-A/CenH3, a variant of histone protein H3, recruits all kinetochore subunits

and spindle assembly checkpoint (SAC) proteins to the centromeric nucleosome(s). To prevent aneuploidy, the SAC monitors chromosome-spindle attachment at each kinetochore. The SAC arrests the cell division process at the metaphase–anaphase transition when a single chromosome pair is found to be unbound or misbound to the mitotic spindle. The SAC kinase Aurora B then phosphorylates the outer kinetochore Ndc80 protein of each misbound sister pair to detach it from the spindle structure. The delay of mitosis allows for a correct re-attachment. Only when the SAC is satisfied will all sister chromosomes separate by enzymatic cleavage of the cohesin rings. Each kinetochore-bound chromatid then moves into the daughter cells by depolymerization of the spindle microtubules and, in some eukaryotes, by additonal motor protein activity. In the end, each cell receives a full complement of the maternal genome (**Figure 1**). Abnormal CEN or kinetochore activity has been linked with cancer initiation/progression, developmental defects, and genetic disease (Holland and Cleveland, 2009; Santaguida and Amon, 2015). For more detailed information about kinetochores we refer to Fukagawa and Earnshaw (2014); McKinley and Cheeseman (2016); and Musacchio and Desai (2017). Of note, during revision of this manuscript, an excellent review was published (Perea-Resa and Blower, 2018) partially overlaps with ours in subject matter.

CENTROMERES: EVOLUTIONARY DIVERGED SEQUENCES

The CEN was first identified as the central constriction of each chromosome during the light microscopic analysis of mitotic salamander cells (Flemming, 1880). Today, it is defined as the chromosomal region that underlies the stable transmission of the nuclear genomic content from one generation to the next. In the 1980s; the CEN of budding yeast *Saccharomyces cerevisiae* chromosome 3, and all three CEN of the fission yeast *Schizosaccharomyces pombe* were the first CEN loci to be characterized (Clarke and Carbon, 1980; Nakaseko et al., 1987; **Figures 2A,B**). The short budding yeast "point" CEN is ∼120 bp long and contains three DNA elements that wrap around a single CEN nucleosome. Alternate stretches of A and T residues, which cause DNA bending, comprise CDEII, which is bordered by palindromic motifs named CDEI and CDEIII (**Figure 2A**). In contrast to CDEII and CDEIII, CDEI is not essential for kinetochore activity but mutations in its sequence cause chromosome loss (Niedenthal et al., 1991). In *S. cerevisiae*, the CEN sequence *per se* defines CEN identity. In contrast and because of their 40–110 kb length, the CEN in fission yeast are designated as "regional." They comprise a 4–7 kb core sequence named *cnt* that encloses multiple CEN nucleosomes. The core is flanked by inverted, 6 kb-long innermost *imr* repeats that contain

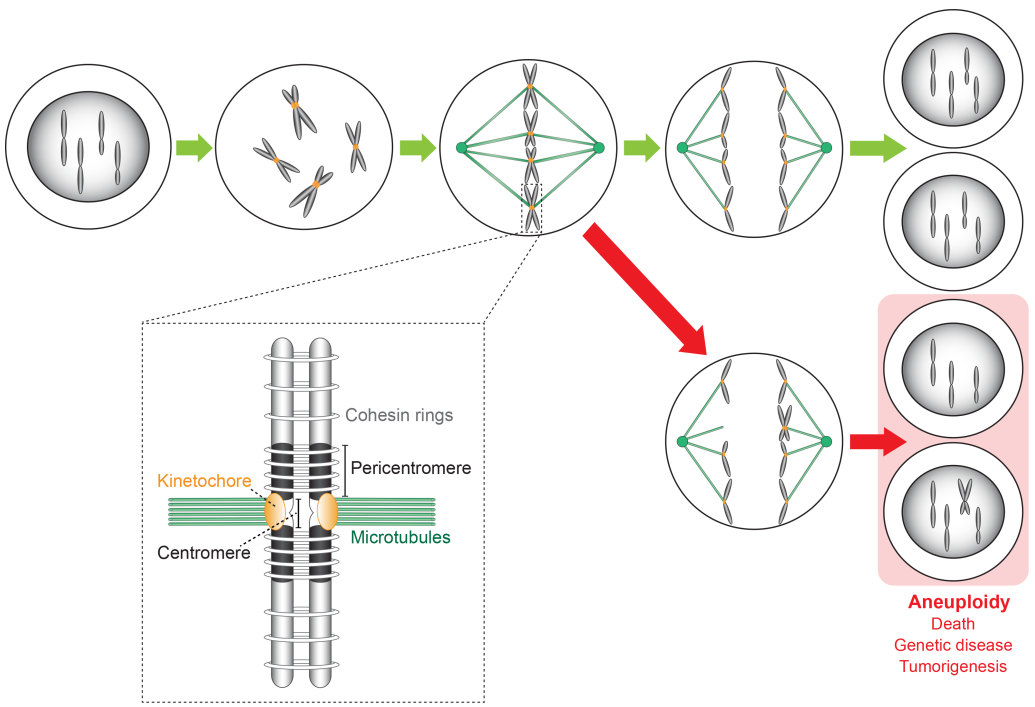

FIGURE 1 | Chromosome replication and segregation in a cell undergoing the mitotic cell division cycle. Kinetochores bi-orient the replicated chromosomes (forming sister chromatids) on the metaphase spindle along which they then segregate in opposite directions into the two daughter cells that receive a full complement of the maternal genome (green arrows). Errors made during the segregation process caused by CEN or kinetochore malfunction lead to aneuploid daughter cells (red arrows) carrying an abnormal number of chromosomes. Consequences are cell death, genetic disease (developmental defects), and cancer initiation/progression. The insert shows a more detailed representation of a sister chromosome pair whose chromosomes (original and copy) are linked by cohesion rings. The sister chromosomes are bound to the spindle microtubules via kinetochores that assemble on the CEN sequence of each chromosome.

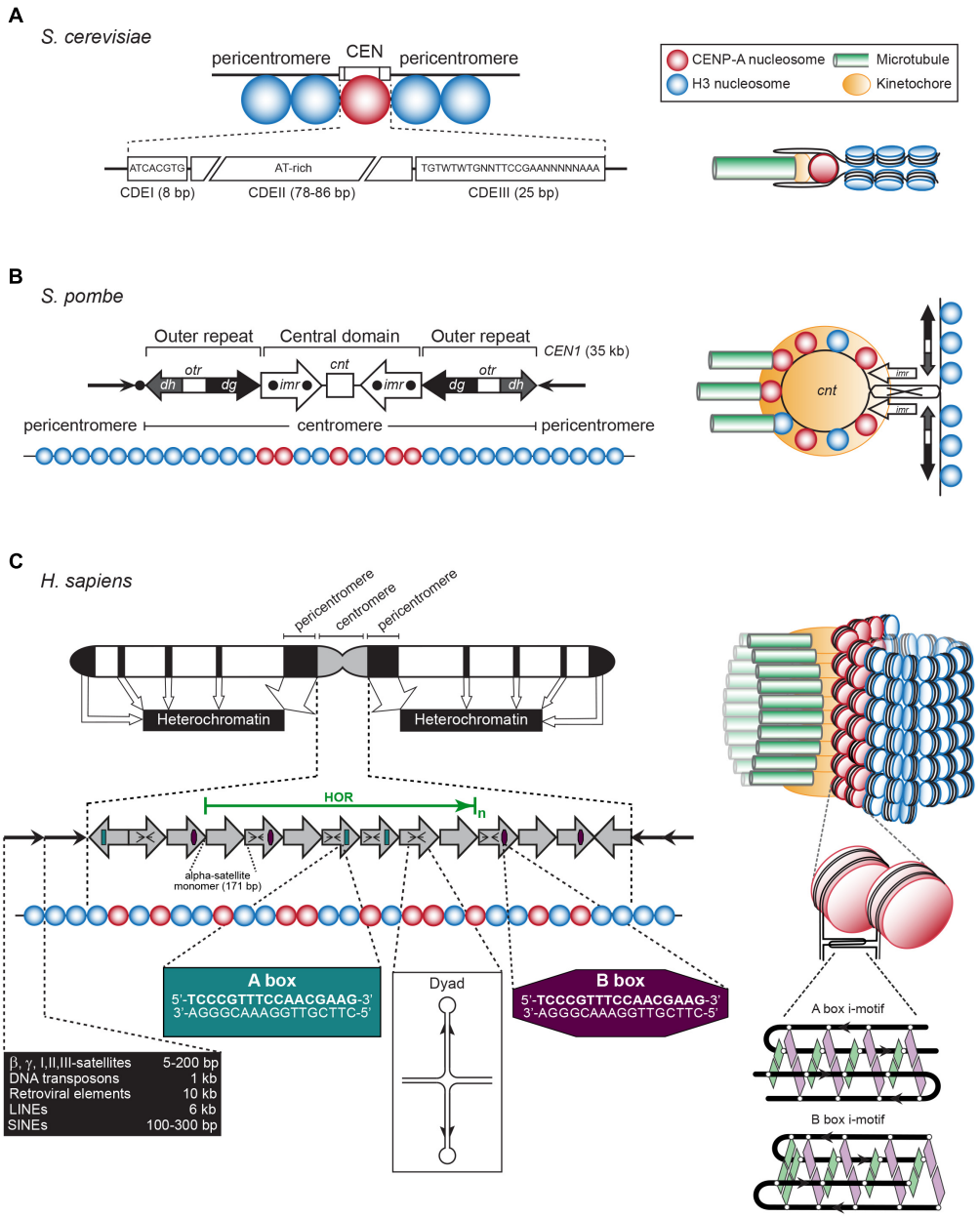

FIGURE 2 | (A) Left: The *S. cerevisiae* point CEN (the consensus CDEI and CDIII sequences are indicated; W = A or T, N = any base). Right: A single CENP-A containing nucleosome is bound to a single microtubule by a single kinetochore (based on Bloom and Costanzo, 2017). **(B)** Left: The *S. pombe* regional CEN. Black dots: tRNA clusters. See text for details. Right: A single, looped CEN harboring CENP-A- and histone H3-containing nucleosomes is bound to three microtubules via a single kinetochore (based on McFarlane et al., 2010). **(C)** Left: A typical human (*Homo sapiens*) chromosome. White regions: euchromatin, gray region: centromeric chromatin, black regions: heterochromatin. The latter represent the pericentromeres, telomeres, LINEs, SINEs, micro- and macrosatellites, β, γ, I, II, III-satellites, rDNA, and DNA transposons (approximate lengths are indicated in the black box). The gray arrows represent the CEN alpha-satellite monomers, organized in a head-to-tail fashion. HOR, high-order repeat of alpha-satellite monomers (green arrow). A-boxes (dark green) and B-boxes (purple) are indicated, as well as the cruciform configuration of a dyad sequence. Right: Human centromeric chromatin with the CENP-A containing nucleosomes clustered and exposed in amphipathic configuration at its outside is bound by numerous kinetochores to a bundle of microtubule fibers (based on Fukagawa and Earnshaw, 2014). See text for details.

clusters of tRNA genes. Together, these three elements form the central domain, which is flanked left and right by outer repeats, *otr*, named *dg* and *dh* (**Figure 2B**).

The regional CEN of most higher eukaryotes are comprised of retrotransposon repeats and repeats of a simple 171-bp CEN sequence, named alpha-satellite DNA, where the CENP-A nucleosomes reside (**Figure 2C**). The surrounding pericentromeric domains contain repeats that are less ordered. In humans and most primates, the alpha-satellite sequence is organized in back-to-back fashion, forming a high-order

repeat (HOR) (Manuelidis and Wu, 1978; Willard, 1985). Within a HOR, alpha-satellite monomers are 50–70% identical (Willard, 1985). Each HOR is repeated hundreds-to-thousands of times, producing 2–5 Mb-long arrays (Aldrup-MacDonald and Sullivan, 2014; **Figure 2C**). Different chromosomes are distinguished by variations within the alpha-satellite sequences, by the number of alpha-satellite monomers, and the overall size of the HOR. Not all alpha-satellite monomers contribute to human kinetochore activity, these are labeled as "inactive." Human CEN contain alpha-satellite monomers of the A and B type, while lower primates only have A-type satellites (Alexandrov et al., 2001). Both monomers differ in a 17-bp sequence called A or B box (**Figure 2C**). The latter, also named CENP-B box, binds CEN protein CENP-B (Masumoto et al., 1989). It is unclear if a specific protein binds to the A box. Human chromosomes, except the Y chromosome, contain B-type alpha-satellite monomers (Tyler-Smith and Brown, 1987). A third type of alpha-satellite monomers contains neither an A nor a B box. The CEN in mice consist of homogeneous arrays of 120-bp minor satellite (MinSat) repeats, that are flanked by repeats of less-ordered 234-bp major gamma-satellite (MajSat) sequences (Joseph et al., 1989). The CEN repeat units in higher eukaryotes are typically around 150 bp in length [178 bp in plants (Kumekawa et al., 2001; Nagaki et al., 2003)], each enclosing one CENP-A nucleosome. However, they can be much shorter as in *Drosophila melanogaster*, whose CEN (200–500 kb) are made up of 10-bp repeats followed by 11/12-bp tandem repeats (Garavís et al., 2015b).

Most eukaryotes are monocentric since their chromosomes contain one CEN. In contrast, moths and butterflies, as well as nematodes such as *Caenorhabditis elegans*, and arachnids contain holocentric CEN that cover the entire chromosome, except for the telomeric regions (Heckmann et al., 2011; Steiner and Henikoff, 2014). While the *C. elegans* genome comprises few tandem repeats (Hillier et al., 2007), ∼50% of the genome is associated with CENP-A in 20 CEN domains of variable size (Albertson and Thomson, 1982; Gassmann et al., 2012). Its kinetochores hence may assemble randomly or at specific regions. While the evolutionary forces that drove holocentrism are unknown, one benefit may lie in DNA breaks. In contrast to broken monocentric chromosomes, fragmented holocentric chromosomes can still segregate in mitotic anaphase because of the multiple microtubule attachments they may contain. Nevertheless, the prevalence of monocentrism suggests selective advantages, possibly related to difficulties in segregating recombined holocentric chromosomes during meiosis (Maddox et al., 2004). For more detailed information about CEN we refer to Aldrup-MacDonald and Sullivan (2014); Bloom and Costanzo (2017); and Fukagawa and Earnshaw (2014).

TRANSCRIPTIONALLY ENHANCED CENTROMERE FEATURES

Centromeres evolved rapidly due to homologous recombinations between stretches of tandemly repeated sequences. Even within one organism CEN sequences differ significantly between its chromosomes. Despite this divergence, most CEN-binding kinetochore proteins are conserved. This "CEN paradox" is explained by the maintenance of CEN-specific structural themes during the co-evolution of CEN DNA and the CEN-binding kinetochore proteins (Henikoff et al., 2001). The adaptive evolution of CENP-A and its orthologs involves regions within this protein that are predicted to contact the centromeric DNA (Talbert et al., 2004; Schueler et al., 2010). In turn, CEN may not have been selected based on their DNA sequence but rather on non-canonical structures that act as beacons for kinetochores and sustain the pulling forces that CEN nucleosomes undergo during chromosome segregation. Studies of CEN from numerous species have indicated a functional significance of non-B-form DNA structures including single-stranded (ss) DNA, hairpins, triplexes, i-motifs, and cruciform extrusions as observed *in vitro* and/or *in vivo* (Zhu et al., 1996; Ohno et al., 2002; Jonstrup et al., 2008; Garavís et al., 2015a,b; Aze et al., 2016; Kabeche et al., 2018). All CEN, except those of *S. cerevisiae*, maintain a high level of inter-repeat sequence property, suggestive of a recombination-based mechanism that produces covalently closed stem–loop structures, which may define CEN recognition and activity. A conserved stem–loop model would demand repeat DNA sequences, explaining the evolution of the CEN's repeat-array configuration (illustrated for the *S. pombe* CEN in **Figure 2B**). Metazoans might require a threshold number of these loop structures to produce a functional CEN (McFarlane et al., 2010). Possibly, the single-stranded loops could be formed temporarily during replication and/or transcription to seed kinetochores.

A neocentromere, being a new CEN that originates at a site that is not centromeric usually due to disruption of the natural CEN, lack centromeric alpha-satellite DNA, but are fully competent to generate a primary constriction and assemble a functional kinetochore (Marshall et al., 2008) indicating that alpha-satellite DNA *per se* is not a trigger for attracting CEN proteins. However, neocentromeres actually form at chromosomal sites that not only contain pre-existing repeats but further develop extensive repetitive DNA sequences over time, indicating the advantage of acquiring an extensive repeat configuration (Marshall et al., 2008). Epigenetic mechanisms are additionally required for maintaining neocentromere identity and activity.

Drosophila melanogaster CEN are made up of short satellite DNA repeats $(AATAACATAG)_n$ followed by doceda tandem repeats (CCCGTACT[C]GGT) that show an asymmetric distribution of G and C residues. *In vitro*, the C-rich dodeca satellite single strand produces an "i-motif"; a cubic structure that is formed by the head-to-tail association of two parallel strands combined in antiparallel fashion (Garavís et al., 2015b; **Figure 2C**). Similar i-motif structures arise *in vitro* between human alpha-satellite monomers in which the C-rich strand of one A-box associates with that of a neighboring A-box. CEN-B boxes also form i-motifs, while those produced from an A- and B-box strand are somewhat unstable *in vitro* (Garavís et al., 2015b). Murine Y CEN satellite DNA that lacks an A/B-box has a sequence capable of forming an i-motif in an equivalent position (Garavís et al., 2015a). As i-motifs can

form upon transcriptionally induced supercoiling (Sun and Hurley, 2009) and since the transcription of alpha-satellite DNA is required for CEN function (Chan et al., 2012), negative superhelicity may favor i-motif formation under physiological conditions.

In vivo evidence for the phasing of CENP-A nucleosomes showed that their positioning is a physical requirement for CEN function (Hasson et al., 2013; Zhang et al., 2013). In most higher eukaryotes CEN chromatin contains blocks of CENP-A that are interspersed with blocks of histone H3-containing nucleosomes (Bodor et al., 2014; Fukagawa and Earnshaw, 2014; **Figures 2A,C**). CENP-A nucleosomes may associate laterally and exclude the H3-containing nucleosomes. The flexibility observed in the chromatin that flanks the CENP-A nucleosomes facilitates these interactions (Panchenko et al., 2011; Hasson et al., 2013). In humans, the phasing of CENP-A nucleosomes on alpha-satellite DNA places the A- and B-boxes at the beginning and at the end of the nucleosome (Hasson et al., 2013). Models of CEN chromatin folding into an amphipathic helix, loop, or boustrophedon that expose the CENP-A nucleosomes at the chromatin surface have been suggested to facilitate kinetochore formation (Blower et al., 2002; Bloom and Costanzo, 2017). A hierarchical mechanism of chromatin folding based on A- and B-box interactions and i-motif formation may determine the 3D organization of the CEN. Although CENP-B null mice are viable (Kapoor et al., 1998), CENP-B is required for *de novo* CEN formation on artificial chromosomes (Ohzeki et al., 2002) and enhances chromosome segregation fidelity (Fachinetti et al., 2015). Possibly, B-box i-motifs contribute to a nucleosome environment that improves kinetochore assembly and activity.

While examining the CEN from different species, Kasinathan and Henikoff (2018) identified clade-specific variations in <10-bp dyad symmetries predicted to adopt stable non-B-form cruciform extrusions (**Figure 2C**). Satellites lacking CENP-B boxes were highly enriched in these palindromes. Non-B-form DNA regions were abundant in human alpha-satellite and murine MinSat sequences from activated B cells, while reduced levels were observed in non-proliferating cells, suggesting that replication induces cruciform extrusions at CEN in dividing cells (Kasinathan and Henikoff, 2018). The authors propose that CEN are either highly enriched with dyad sequences or less-enriched in dyads that flank a nearby binding site for a DNA-bending protein whose association may stimulate dyad cruciform formation. The four-way junctions of the cruciform could be recognized by the HJURP chaperone (Scm3 in yeast) that loads CENP-A into the centromeric nucleosome (Dunleavy et al., 2009; Foltz et al., 2009; Sanchez-Pulido et al., 2009). Non-B form elements may also facilitate CEN transcription initiation and elongation by RNA polymerase II (RNAPII), enabling the loading of CENP-A during nucleosome remodeling. Also, CENP-B may be dispensable for CEN where HJURP is recruited by CENP-C and the MIS18 complex (Nardi et al., 2016) (see below). Hence, A/B boxes and dyad sequences may organize and activate CENP-A loading into CEN nucleosomes.

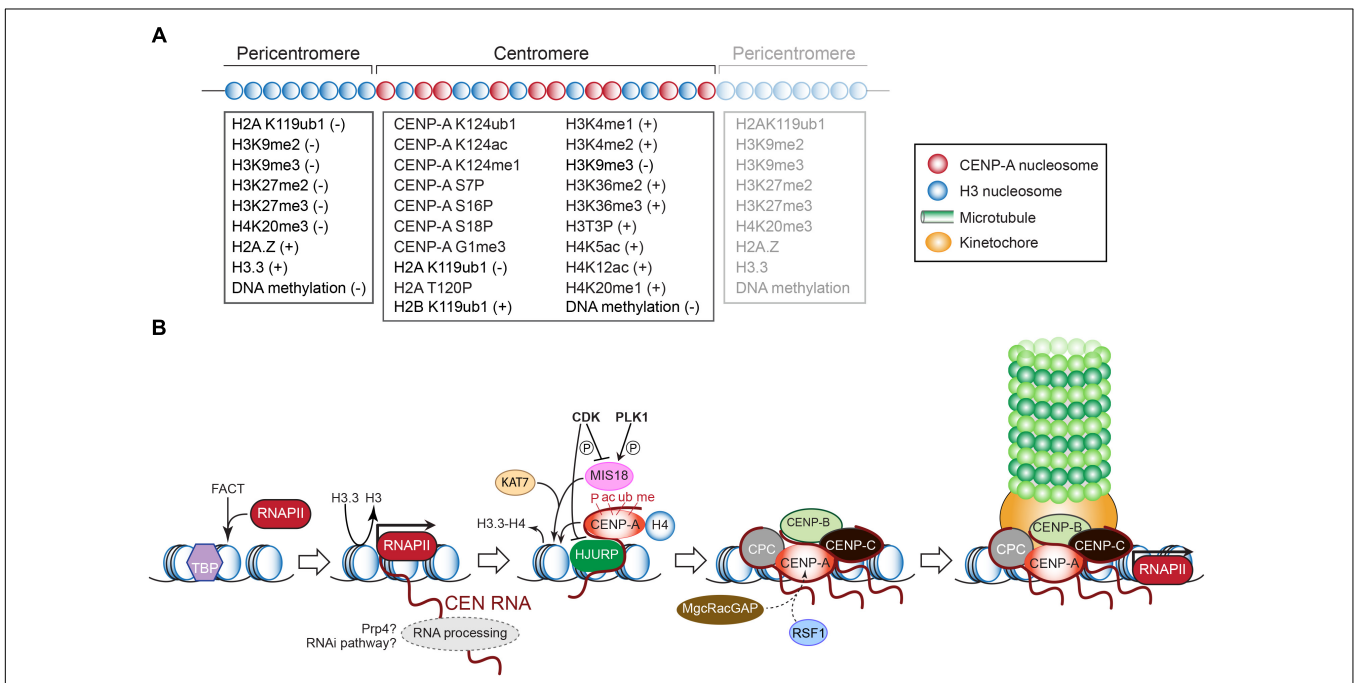

FIGURE 3 | (A) Epigenetic modifications that mark histones and DNA (cytosines) in the pericentric and centromeric domains. The positive or negative signs indicate whether the modification underlies transcriptional silence or activity, respectively. Modifications of CENP-A required for its deposition or maintenance are also listed. See text for explanations. **(B)** Schematic outline of transcription-dependent inclusion of histone H3 variant CENP-A at the CEN chromatin, and recruitment of downstream kinetochore components as in vertebrates. See text for details.

POST-TRANSLATIONAL MODIFICATIONS OF CENTROMERIC AND PERICENTROMERIC CHROMATIN

Within the CEN domain, CENP-A nucleosomes are interspersed with canonical nucleosomes whose histone H3 tails are methylated at Lys4 (H3K4me1, H3K4me2) and Lys36 (H3K36me2, H3K36me3) (**Figure 3A**). These modifications underlie open chromatin, promote RNAPII activity, and are essential for HJURP targeting and CENP-A assembly (Bergmann et al., 2011; Duda et al., 2017). They also differentiate the CEN chromatin from the surrounding pericentromere regions, which are marked differently (see below and **Figure 3A**) (Sullivan and Karpen, 2004; Eymery et al., 2009; Gopalakrishnan et al., 2009; Bergmann et al., 2011, 2012). Intriguingly, H3K9me3, typically associated with transcriptional repression, also labels the centromeric nucleosomes (Bergmann et al., 2012) indicating that CEN chromatin epitomizes both silent heterochromatin and transcribed euchromatin (Sullivan and Karpen, 2004).

Histone H4 mono-acetylation at Lys5 and Lys12, which correlates with transcribed chromatin, is enriched at CEN and is essential for CENP-A deposition in chicken cells (Shang et al., 2016; **Figure 3A**). H4 mono-methylation at Lys20, which marks human and chicken CENP-A nucleosomes, and is associated with transcriptional activation, is a prerequisite for kinetochore assembly (Sullivan and Karpen, 2004; Vakoc et al., 2006; Wang et al., 2008; Bergmann et al., 2011; Hori et al., 2014). Histone H2B mono-ubiquitination at Lys119, catalyzed by the E3 ubiquitin ligase RNF20/40 (Brl1 in *S. pombe*), is required for CEN transcription (Zhu et al., 2011; Sadeghi et al., 2014). Depleting RNF20 reduces CEN transcription and nucleosome turnover, and causes chromosome missegregation in human cells and *S. pombe* (Sadeghi et al., 2014; Zhang et al., 2017). The ubiquitin ligase BRCA1 preserves CEN identity by ubiquitinating histone H2A at Lys119, producing a repressive mark. BRCA1 depletion, led to CEN transcript overexpression, impaired CEN cohesion and SAC activity, and chromosome missegregation (Di Paolo et al., 2014).

CENTROMERE TRANSCRIPTION, PROMOTERS, AND TRANSCRIPTION FACTORS

Although electron microscopy-based studies had localized RNA at kinetochores in union and salamander cells in the 1970s (Braselton, 1975; Rieder, 1979), CEN were long considered transcriptionally silent since they are confined in transcriptionally inert heterochromatin. Today we know that CEN are actively transcribed by RNAPII, which has been detected at CEN in *S. pombe*, flies, and human cells, at centromeric chromatin on human artificial chromosomes (HACs), and at neocentromeres (Wong et al., 2007; Li et al., 2008; Chueh et al., 2009; Ferri et al., 2009; Bergmann et al., 2011; Choi et al., 2011; Ohkuni and Kitagawa, 2011; Lyn Chan and Wong, 2012; Quénet and Dalal, 2014; Rošić et al., 2014; Catania et al., 2015). Despite the evidence of RNAII polymerase transcribing the CEN, very little is known about the promoters and transcription factors involved.

In *S. cerevisiae*, RNAPII-mediated CEN transcription is driven by transcription factors Cbf1 and Ste12. Cbf1 promotes transcription from the sense strand, Ste12 from the antisense strand. Silencing protein Dig1 inhibits Ste12. Transcriptional silencers Sir1, Hst1–Sum1, and Cdc14–Net1 associate with the CEN sequence, possibly to antagonize RNAPII. While deleting *CBF1* or *STE12* did not prevent kinetochore assembly, each mutant experienced chromosome loss. This phenotype was rescued by driving CEN transcription from an inducible promoter introduced next to the Cbf1- or Ste12-binding site, illustrating that CEN transcription is imperative for kinetochore activity (Ohkuni and Kitagawa, 2011). CEN transcripts in *S. cerevisiae* remained unidentified until exosome activity (which degrades non-coding RNAs) was removed, indicating a fast turn over of these transcripts. This approach revealed a 1.2-kb CEN3 RNA species, revealing that RNAPII proceeds into the pericentromere (Houseley et al., 2007). Low-level CEN transcription is required for kinetochore activity in budding yeast. Disproportionate CEN expression driven by the galactose-inducible P_{GAL1} promoter placed adjacent to CEN3 on a plasmid caused plasmid loss (Hill and Bloom, 1987) since kinetochores were not able to assemble. When P_{GAL1} was positioned next to chromosomal CEN3 that was marked with a GFP-array, growth in galactose prevented spindle binding of labeled sister chromatids 3. Following glucose addition, the sisters bi-oriented on the metaphase spindle (Tanaka et al., 2005).

In *S. pombe*, the CENP-A binding region contains numerous transcription start sites and promoters on the forward and reverse strands. However, very low levels of transcripts are produced, due to transcript turnover as well as RNAPII stalling (Choi et al., 2011; Sadeghi et al., 2014), which could result from collisions with the replisome or transient H2B (de)ubiquitination activity that negatively affects chromatin accessibility (Chen et al., 2008; Sadeghi et al., 2014). In fission yeast mutants unable to restart stalled RNAPII, CENP-A became actively deposited on the CEN, suggesting that halting RNAPII, which results in a low-quality transcription environment, allows for CEN chromatin remodeling and/or CENP-A loading (Shandilya et al., 2014; Catania et al., 2015).

The PRAT CEN satellite monomer in the beetle *Palorus ratzeburgii* contains a putative RNAPII promoter site that overlaps with the most conserved part of the PRAT sequence. This concurrence could be the result of selection pressure to preserve the transcription activity of this satellite DNA. TATA-box-like motifs, multiple transcription initiation and termination sites were also mapped within the monomer. The presence of a 5′-RNA cap and 3′-poly(A) tails in a portion of the beetle CEN transcripts indicates RNAPII-dependent transcription. Indeed, treatment of larvae with alpha-amanitin at concentrations that selectively inhibit RNAPII activity reduced the amount of PRAT transcripts. These transcripts derived from one, two, or three monomers, and were produced from both strands (albeit 10 times less from the antisense strand) (Pezer and

Ugarković, 2008). Within the human alpha-satellite sequence, a candidate TATA box has been identified, as well as an SV40 enhancer-core sequence with spacing and orientation characteristic of RNAPII-transcribed genes (Vissel et al., 1992). In human cells, RNAPII has been found especially enriched at prometaphase, metaphase, and anaphase CEN, as well as at kinetochore-active neocentromeres. Consistent with active transcription, FCP1, a phosphatase that is specific for the carboxy-terminal domain of RNAP II and stimulates transcript elongation by RNAP II (Mandal et al., 2002), was identified at mitotic human and murine kinetochores (Chan et al., 2012).

TRANSCRIPTION AND POST-TRANSLATIONAL MODIFICATIONS PROMOTE CENP-A INCLUSION INTO CENTROMERIC CHROMATIN

While CENP-A represents the epigenetic mark of CEN identity in most eukaryotes (Vafa and Sullivan, 1997; Warburton et al., 1997) its presence *per se* is not enough for CEN formation since trypanosomes and insects with holocentric chromosomes lack a CENP-A ortholog (Akiyoshi and Gull, 2014; Drinnenberg et al., 2014). CENP-A nucleosomes in humans are also found at non-CEN sites, including neocentromeres (Bodor et al., 2014). Both observations underscore the need for additional CEN-specifying criteria, including structural themes embedded within the CEN DNA sequence (see above). Via its N- and C-terminal tails and through its central histone-fold domain, CENP-A recruits the other kinetochore proteins, including CENP-C with which it makes direct physical contact (Chen et al., 2000; van Hooser et al., 2001; Regnier et al., 2005; Liu et al., 2006; Carroll et al., 2009, 2010; Guse et al., 2011; Fachinetti et al., 2013; Kato et al., 2013; Folco et al., 2015; Logsdon et al., 2015; Westhorpe et al., 2015; **Figure 3B**). In contrast to histone H3, CENP-A may form a more rigid interface with its partner histone H4, which is further stabilized by CENP-C. Nucleosomes containing CENP-A bind less firmly to the DNA, profoundly affecting CEN transcription and distinghuishing it from the surrounding closed-state chromatin (Hasson et al., 2013; Falk et al., 2015). During chromosome replication, CENP-A becomes diluted 1:2 with histone H3 variant H3.3, which is deposited as a temporary placeholder allowing kinetochores to assemble in early metaphase (**Figure 3B**). In mammals, CENP-A becomes incorporated in late telophase/early G1, when its chaperone HJURP localizes to CEN and H3.3 is removed (Foltz et al., 2009; Dunleavy et al., 2011). CENP-A deposition also requires the MIS18 complex (MIS18α, MIS18β, MIS18-binding protein 1/KNL2) (Hayashi et al., 2004). In *D. melanogaster*, HJURP and MIS18 activities appear to be combined in the Cal1 protein (Erhardt et al., 2008; Chen et al., 2014).

In *S. cerevisiae*, the CEN nucleosomes are evicted and kinetochores disassembled at S-phase entry, allowing for the replication of the CEN sequences, which are the first loci to be replicated in budding yeast. It is unclear whether CEN transcription is downregulated during this process. The expelled CENP-A then becomes degraded. Within 5 min after passage of the replisome, the CEN nucleosomes reassemble by the inclusion of new CENP-A by the Scm3 chaperone (ortholog of HJURP). Kinetochores then reassemble to attach the still-replicating chromatids to the interphase spindle (Kitamura et al., 2007; Wisniewski et al., 2014).

During G1 in human cells, the MIS18 complex recruits the KAT7 histone acetyltransferase complex to maintain an acetylated CEN chromatin state, which facilitates the assembly of new CENP-A nucleosomes (Ohzeki et al., 2016). CENP-C contributes to CENP-A inclusion and stability by interacting directly with CENP-A, HJURP, and MIS18-binding protein 1 (Moree et al., 2011; Dambacher et al., 2012; McKinley and Cheeseman, 2014; Tachiwana et al., 2015; **Figure 3B**). Furthermore, CENP-C, the remodeling and spacing factor complex RSF, and the MgcRacGAP Male germ cell Rac GTPase-activating protein maintain CENP-A once incorporated (Perpelescu et al., 2009; Lagana et al., 2010; Falk et al., 2015). In contrast, cyclin-dependent kinase (CDK) activity negatively regulates CENP-A incorporation. In *D. melanogaster*, the turnover of S/G2 phase cyclin A in mitosis is key for the deposition of CENP-A (Erhardt et al., 2008; Mellone et al., 2011). In human cells, CDKs phosphorylate the MIS18-binding protein 1 to reduce its CEN localization (Silva et al., 2012) and to avert the recruitment of the MIS18α and MIS18β beyond G1 (McKinley and Cheeseman, 2014). CDK phosphorylation of HJURP also disrupts its CEN localization (Müller et al., 2014; **Figure 3B**). In contrast, the kinase PLK1 targets the MIS18 complex to promote its CEN localization and to license the CEN for CENP-A delivery. Bypassing both CDK and PLK1 activities led to CENP-A deposition throughout the cell cycle, causing severe mitotic defects (McKinley and Cheeseman, 2014). Clearly, CENP-A must be loaded only in G1 to ensure correct CEN function.

The *de novo* loading of CENP-A, as detailed above, requires CEN transcription as catalyzed by RNAPII (Lyn Chan and Wong, 2012; Quénet and Dalal, 2014; Rošić et al., 2014; Grenfell et al., 2016; **Figure 3B**). In *Drosophila*, Cal1 recruits RNAPII and the chromatin-remodeling complex FAcilitates Chromatin Transcription (FACT) (Foltz et al., 2006; Chen et al., 2015). Studies suggest that FACT activity weakens the histone core-DNA contact, facilitating the passage of RNAPII, and protecting the nucleosome from falling apart before it is remodeled and the new CENP-A nucleosome assembled. FACT also binds to the CEN CENP-T/W complex, possibly to promote also its deposition (Prendergast et al., 2016). Of note, FACT localizes at CEN at all stages of the cell cycle and is responsible for CENP-A loading in human cells (Okada et al., 2009). In fungi, FACT activity prevents the ectopic incorporation of CENP-A beyond CEN, rather than promoting CENP-A assembly at CEN nucleosomes (Deyter and Biggins, 2014). In *Drosophila*, CEN transcription and chromatin remodeling are required for

CENP-A to transition from an unstable chromatin-associated state to a stable nucleosome-incorporated state (Bobkov et al., 2018).

Alpha-satellite arrays amplified from human CEN and cloned into a BAC plasmid form a functional HAC that recruits kinetochores and stably propagates in HT1080 fibrosarcoma cells (Maloney et al., 2012). In HACs containing engineered tetO operator sequences within the alpha-satellite DNA, and cells expressing transcriptional activators or silencers fused with the tetO-binding TetR protein both destabilized kinetochore formation (Bergmann et al., 2011). Transcriptional silencing led to a gradual loss of CENP-A from the centromeric chromatin, due to reduced recruitment of HJURP. Enhancing alpha-satellite transcription ∼10-fold by tethering a minimal NF-κB p65 activation domain did not affect kinetochore formation or activity. However, tethering TetR with the activation domain of herpes virus transcription factor VP16 elevated transcription ∼150-fold, approaching the expression level of a housekeeping gene. The consequent increase in RNAPII occupancy provoked a loss of CENP-A, probably through nucleosome eviction (Bergmann et al., 2012).

Post-translational modifications of CENP-A are required for its loading (**Figure 3A**). Before becoming deposited, CENP-A is phosphorylated at Ser16 and Ser18 (Bailey et al., 2013); Ser18 is a substrate for the cyclin E1/CDK2 kinase (Takada et al., 2017). A loss or hyperphosphorylation of both sites causes chromosome missegregation (Bailey et al., 2013; Takada et al., 2017). *Drosophila* CENP-A is phosphorylated at Ser75 and Ser77, which could be the analogs of Ser16 and Ser18 in human CENP-A (Boltengagen et al., 2016). Biochemical evidence suggests that mono-ubiquitination of CENP-A at Lys124 by the E3 ligase activity of the CUL4A–RBX1–COPS8 complex promotes HJURP binding and CENP-A deposition (Niikura et al., 2015, 2017). However, disputing gene replacement experiments showed that non-ubiquitinatable mutant CENP-A still can replace endogenous CENP-A and support cell viability (Fachinetti et al., 2017). In humans, the starting methionine of pre-inclusion CENP-A is removed and the exposed Gly1 residue trimethylated by the enzyme NRMT1 (Bailey et al., 2013; Sathyan et al., 2017). Both this modification and phosphorylation of Ser16 and Ser18 persist after CENP-A loading (Bailey et al., 2013). Subsequent modifications of the incorporated CENP-A include Ser7 phosphorylation, which is responsible for the indirect recruitment of CENP-C, and ubiquitination of Lys124, shown to be involved in CENP-A binding to HJURP (Srivastava et al., 2018). Mutations in Ser7, Ser16, and Ser18 sites lead to chromosome missegregation, abnormal spindles, and errors in cytokinesis (Srivastava et al., 2018). Nevertheless, chromosomes carrying CENP-A mutants that cannot be phosphorylated at Ser68 or ubiquitinated at Lys124 establish functional CEN (Fachinetti et al., 2017). Since the same amount of CENP-A is renewed at each G1 stage, errors in CENP-A incorporation caused by abnormal CEN transcription, assembly factor activity, and/or post-translational modifications could permanently alter its levels at centromeric chromatin, contributing to chromosomal instability.

CENTROMERE TRANSCRIPTION THROUGH THE CELL CYCLE

Centromere transcription dynamics through the cell cycle have only been studied recently. The levels of alpha-satellite RNAs localizing at CEN did not change through the cell cycle, indicating a complex dynamic between CEN RNA synthesis, turnover, and stable incorporation in the CEN chromatin (McNulty et al., 2017). CEN RNA and DNA FISH experiments using identical HOR probes labeled with different fluorophores showed a co-localization of the transcripts to their originative CEN, indicating they are maintained in *cis* (McNulty et al., 2017). As discussed earlier, CEN transcription is required for CENP-A loading in human and *Drosophila* cells (Quénet and Dalal, 2014; Bobkov et al., 2018). Human CEN transcription mediated by RNAPII, in conjunction with the TATA-box binding protein, occurs through early G1 when mammalian CENP-A is deposited. When inhibiting transcription in G1, CENP-A levels dropped with ∼50% (Quénet and Dalal, 2014). Targeting the transcript with shRNA, while not impeding RNAPII activity, diminished CENP-A levels and induced mitotic defects (Quénet and Dalal, 2014). Reversely, depleting CENP-A reduced CENP-C concentrations at kinetochores, but CEN transcript levels were not affected, suggesting that CEN transcription occurs before the recruitment of CENP-A and CENP-C (McNulty et al., 2017). However, inhibiting active transcription resulted in CENP-C destabilization, suggesting that CEN transcription may also act downstream of CENP-A loading to promote CENP-C binding (Chan et al., 2012).

While most regions within condensed chromosomes are transcriptionally silent during mitosis, CEN are not (Chan et al., 2012; Lyn Chan and Wong, 2012; Liu et al., 2015), therewith differentiating them from the rest of the genome. Indeed, as indicated earlier, RNAPII localized at human and murine CEN from prometaphase through anaphase (Chan et al., 2012). Mild CEN transcription through the cell cycle ensures stable kinetochores and CEN cohesion (Liu et al., 2015).

In human cells, the cohesin-protecting protein Sgo1 (Shugoshin) is recruited to early mitotic kinetochores by the Bub1-phosphoryated centromeric histone H2A [phosphorylated at Thr120; (H2A T120P)]. Next, Sgo1 binds to RNAPII and travels along with it to the inner CEN (region between the two sister CEN) where it binds to the cohesin rings to protect them from precocious cleavage by the protease separase (Liu et al., 2015). Transcription by RNAPII and chromatin remodeling activities could open the chromatin, allowing Sgo1 access to cohesin. When transcription elongation was inhibited during mitosis with alpha-amanitin or when RNAPII subunit Rbp2 was degraded, Sgo1 still localized at kinetochores but did not relocate to the inner CEN. Besides RNAPII activity, the CEN RNAs themselves may facilitate Sgo1 relocation to the inner CEN. Indeed, since nonspecific RNA competed with H2A T120P for binding to Sgo1, CEN RNA could bind to Sgo1, releasing it

from H2A T120P and allowing Sgo1 to travel with RNAPol II toward the inner CEN.

In contrast to human alpha-satellite transcripts, murine MinSat transcripts are absent in G0/G1. They appear in S-phase, peak at G2/M, and become undetectable after mitosis, when cells re-enter the cell cycle (Ferri et al., 2009). This dynamic mirrors the accumulation of the chromosomal passenger complex (CPC) at the murine CEN, implicating a role of MinSat RNAs in CPC localization and activity. Indeed, MinSat RNAs accumulate at CENP-A chromatin and interact with CPC subunits Aurora B and Survivin at mitotic onset. We will describe the interactions between CEN RNA and the CPC components in detail further below.

Schizosaccharomyces pombe CEN are transcribed during DNA replication, which may generate transcription–replication conflicts. Encounters between RNAPII and the replisome may cause RNAPII to halt and produce immature transcripts (Lu and Gilbert, 2007; Chen et al., 2008). RNAPII stalling generates RNA–ssDNA hybrids, known as R-loops (Reddy et al., 2011), which have also been observed at human CEN chromatin (Kabeche et al., 2018). R-loops must be resolved; otherwise, they can provoke chromosome breaks and repeat-sequence recombinations. R-loops forming in centromeric chromatin (or at pericentromeres or across the genome) trigger Aurora B-mediated phosphorylation of local histone H3 at Ser10, as shown in yeast, *C. elegans*, and human cells. This mark stimulates confined chromatin condensation and restricts DNA replication and transcription (Castellano-Pozo et al., 2013; Oestergaard and Lisby, 2016). Since the FACT complex resolves R-loops in yeast and human cells (Herrera-Moyano et al., 2014), it could remove toxic R-loops prior to mitotic entry. FACT activities including the stimulation of CEN chromatin remodeling and transcription, the subsequent promotion of CENP-A assembly, and the resolution of R-loops may reflect the dynamic state of the CEN environment during cell cycle progression (Duda et al., 2017).

POST-TRANSCRIPTIONAL PROCESSING OF CENTROMERE TRANSCRIPTS

In *S. pombe*, 5′-capped and 3′-polyadenylated non-coding CEN RNAs that are produced from the central domain are quickly degraded by the exosome (Choi et al., 2011). No evidence exists for small CEN RNA processing products as documented for the transcripts derived from the pericentromeric chromatin (see below). The RNase activity of exosome subunit Dis3 is required for correct kinetochore assembly and kinetochore–microtubule interactions (Bühler and Moazed, 2007; Mukarami et al., 2007) suggesting that degradation of CEN transcripts independent of the RNA interference (RNAi) pathway contributes to CEN activity in fission yeast.

Genome-wide screens with *Drosophila* and human cells identified splicing factors that are required for cell division (Goshima et al., 2007; Kittler et al., 2007; Somma et al., 2008; Neumann et al., 2010). Also, purifications of the spliceosome from HeLa cell nuclear extracts revealed the presence of microtubule- and mitotic chromatin-interacting proteins (Makarov et al., 2002). The processing of CEN RNAs may occur in mitosis since splicing factors are co-transcriptionally recruited to the elongating RNAPII transcripts (Listerman et al., 2006; David et al., 2011) (and because RNA-splicing factor Prp4 localizes to mitotic kinetochores in HeLa cells (Montembault et al., 2007; **Figure 3B**). Splicing factors also interact with MinSat transcripts in murine cells (Maison et al., 2011). The co-transcriptional recruitment of the RNA processing machinery to nascent mitotic transcripts in *Xenopus* is an important step in kinetochore and spindle assembly. Indeed, long non-coding CEN RNAs localize to mitotic chromosomes, chromatin, and spindles (Blower, 2016). At spindles, the transcripts regulate Aurora B and MCAK activities (Grenfell et al., 2016). Inhibiting the spliceosome, which co-IPs with CEN transcripts and CENP-C, in metaphase-arrested *Xenopus* egg extracts caused an accumulation of long CEN antisense transcripts representing up to six *frc1* monomer repeats, which are much longer than the standard CEN RNAs containing one to two *frc1* repeats. A globally reduced recruitment of CENP-A, CENP-C, and Ndc80 was observed (Grenfell et al., 2016), suggesting that *fcr1* antisense RNA is processed and then freely diffuses between CEN *in trans*, similar to observations in *Drosophila* where CEN RNAs derived from the X chromosome also move to the CEN of autosomal chromosomes (Rošić et al., 2014). However, the RNA signals appear not to have been completely removed from the autosomes after RNase treatment (Rošić et al., 2014) suggesting that FISH detected CEN DNA rather than the CEN RNA *in trans* (Bobkov et al., 2018).

In maize, CEN RNAs identified in IPs of CENP-A are produced from both strands and derived from the 156-bp CentC satellite monomer and transposable elements that are arranged in nearly continuous, intermingled arrays, and clusters. The transcripts are heterogeneous in length (40–200 nt) but predominantly contain 40 and 75-nt species (Du et al., 2010). Although these transcripts lie outside the range of microRNAs or siRNAs (20–30 nt) generated by RNAi pathways, their sizes indicate processing. The CEN RNAs are maintained in a single-stranded state within the maize kinetochore and are firmly bound to centromeric histone protein H3 (Topp et al., 2004), which may protect them from Dicer double-strand cleavage activity. Importantly, genuine siRNAs present in total RNA extracted from maize were not associated with CENP-A chromatin (Du et al., 2010).

Mouse embryonic stem (ES) cells knocked out in *dicer-1* ($DCR^{\Delta/\Delta}$) are defective in global RNAi activity but retained ES cell characteristics. Although viable, they proliferated more slowly (Kanellopoulou et al., 2005). No aberrant chromosome structures or aneuploidy was observed but the cells displayed differentiation defects. The Dicer-negative cells contained increased levels of long, polyadenylated CEN MinSat, and pericentromere MajSat transcripts (>200 nt). Heterozygous mutant cells ($DCR^{\Delta/+}$) produced 150-nt MinSat and MajSat species, as well as 21–30 nt long specimen, suggesting the contribution of Dicer (Kanellopoulou et al., 2005). Further supporting the involvement of (peri)CEN RNA processing was the identification of protein WDHD1, which may stabilize the

association of Dicer with MinSat and MajSat RNAs (Hsieh et al., 2011).

In tammar wallaby cells, 34–42 nt double-stranded (ds) RNAs with homology to the CEN retroelement kLTR (Ferreri et al., 2011) were identified in small-RNA pools (Carone et al., 2009; Lindsay et al., 2012). In rice, RNAs of ∼40 nt derive from the CentO CEN satellites (Lee et al., 2006). These rice and tammar wallaby CEN RNA species have been termed crasiRNAs (CEN repeat-associated short interacting RNAs). Targeting the small RNAs produced from the kLTR disrupted CENP-A localization in late telophase (Carone et al., 2009; Lindsay et al., 2012). Tight regulation and processing of these crasiRNAs seem integral to the epigenetic framework that is required for CEN establishment.

Hammerhead ribozyme structures associated with transcribed satellite DNA sequences have been identified in salamanders (Epstein and Gall, 1987), schistostome flatworms (Ferbeyre et al., 1998), and *Dolichopoda* cave crickets (Rojas et al., 2000). All hammerhead ribozymes self-cleave multimeric satellite transcripts into monomer RNAs.

CENTROMERE PROTEINS THAT BIND TO CENTROMERE RNA

Centromere transcripts or small CEN RNA derivatives underlie the formation of ribonucleoprotein complexes that specify the CEN domains and establish correct kinetochore assembly and architecture. These complexes comprise CENP-A, HJURP, CENP-B, CENP-C, the CPC, and Sgo1. While it is not clear how each protein interacts with the CEN transcripts, CENP-B, CENP-C, Sgo1, and the CPC have in common that their RNA-binding capacity serves as a second chromatin-recruitment mechanism. Indeed, it complements their promiscuous DNA binding activity (CENP-C), their binding to a specific satellite monomer box (CENP-B), their recruitment by the CEN H2A T120P modification (Sgo1), and their recruitment by Thr3-phosphorylated CEN histone H3 and CEN H2A T120P (CPC).

CENP-A and HJURP

The interaction between CENP-A and CEN RNA was first observed at a human neocentromere. LINE-1 elements within the CENP-A-binding region of a neocentromere on 10q25 were transcribed into non-coding RNAs that integrate into the CENP-A chromatin (Chueh et al., 2009). Both CENP-A and HJURP interact with CEN RNA as shown in alpha-satellite transcript pull-down experiments (Quénet and Dalal, 2014). *In silico* predictions of potential RNA-binding sites indicated that 286 out of the 748 HJURP residues, and 79 out of the 140 CENP-A residues, have RNA-binding capacity. However, the vast majority of these CENP-A residues may well be buried inside the nucleosome and/or be bound by CENP-C and CENP-N. The predicted residues lie in the N-terminal half of CENP-A, the protein's most rapidly evolving part (Henikoff et al., 2001; Malik and Henikoff, 2001), which is required to stabilize CENP-A at centromeric nucleosomes (Logsdon et al., 2015). Possibly, the disparities in composition and length of the N-terminal halves of all CENP-A orthologs could allow for their interaction with the rapidly evolving CEN DNA and, consequently, CEN RNA sequences.

CENP-C

CENP-C, which acts as a dimer via its C-terminal dimerization domain (Cohen et al., 2008), binds to CENP-A, CEN DNA, and RNA (**Figure 3B**). Single-stranded alpha-satellite RNA localizes CENP-C to CEN in interphase, which then together with CENP-A recruits the other kinetochore proteins. Two regions in human CENP-C (one central and one C-terminal) preferably bind to CEN RNAs as shown in competition assays with rRNA, tRNA, and murine MajSat RNA (Wong et al., 2007). However, both sequences also bind to CEN DNA (Sugimoto et al., 1997; Yang et al., 1996). Each DNA-binding element contains a 21–22 amino acid motif via which CENP-C also contacts CENP-A (Kato et al., 2013). Mutating three lysine residues adjacent to CENP-A's central DNA-binding motif also abrogated RNA binding in that region (Wong et al., 2007). Noteworthy, CENP-C's central RNA-binding domain shares homology with the RNA-binding hinge domain region of the pericentromeric heterochromatin proteins (HP) HP1α, β, and γ (Du et al., 2010; Muchardt et al., 2002).

In maize, a C-terminal 122-residue CENP-C region encoded by exons 9–12 binds RNA and DNA, and is required for its CEN localization *in vivo*. While maize CENP-C binding to CEN RNA occurs without any sequence specificity (in contrast to human CENP-C), CEN DNA binding is stabilized by long ssRNA *in vitro*. The RNAs that stabilize this contact correspond to the ssCEN RNAs present in kinetochores (Du et al., 2010). Possibly, CEN ssRNA may stabilize CENP-C by enhancing its binding to CEN DNA, adjacent to where it interacts with the CENP-A nucleosome. Indeed, disrupting CEN RNA destabilizes CENP-C at the CEN. Treating mitotic human cells with alpha-amanitin lowered CENP-C levels at kinetochores and caused an increase in lagging chromosomes. A relatively greater reduction of CENP-C occurred on the lagging chromosomes compared to the chromosomes that segregated (Lyn Chan and Wong, 2012). Impeding transcription initiation or splicing also led to decreased CENP-C levels at kinetochores in *Xenopus* (Grenfell et al., 2016). In *Drosophila*, X chromosome-specific SatIII transcripts localize to CEN and associate with CENP-C (Rošić et al., 2014). Following CENP-C depletion, the SatIII RNA signals at CEN dropped. Reversely, when depleting SatIII RNAs, the presence of newly synthesized CENP-C and CENP-A at CEN was reduced. This negative effect cascaded up through the kinetochore (Rošić et al., 2014). Taken together, results with human cells, *Drosophila*, maize, and *Xenopus* suggest that the non-coding CEN RNAs recruit and stabilize CENP-C, supporting CENP-A deposition and stability.

CENP-C bound to CEN DNA and RNA also interacts with chromatin modifying proteins to create the unique epigenetic environment of the CEN domain. CENP-C recruits DNA methyltransferase 3A-B (DNMT3A-B) to reduce local transcription by promoting the methylation of CEN DNA and histone H3. Consequently, CENP-C depletion caused increased CEN transcription (Gopalakrishnan et al., 2009).

CENP-C also binds to MIS18 complex components MIS18α- and MIS18-binding protein 1 (Moree et al., 2011; Kim et al., 2012), which control CEN histone acetylation (Fujita et al., 2007). Mis18α through its interaction with DNMT3A-B can also control DNA methylation and histone modifications (Kim et al., 2012), whereas CENP-C through its interaction with M18BP1 promotes the recruitment of HJURP for CENP-A loading (Moree et al., 2011). Possibly, CEN RNA stabilizes CENP-C:DNMT3A-B:MIS18 to target HJURP:CENP-A.

The Chromosomal Passenger Complex

The binding of CENP-A and CENP-C to CEN DNA and alpha-satellite RNA promotes kinetochore assembly, including the recruitment of the 4-protein CPC (INCENP, Survivin, Borealin, and Aurora B), which regulates chromosome-spindle attachment and activates the SAC upon chromosome misalignment (Hindriksen et al., 2017). The CPC moves from the inner CEN to the spindle midzone in late anaphase to regulate cytokinesis (Warecki and Sullivan, 2018). Aurora B also phosphorylates CENP-A at Ser7 (Zeitlin et al., 2001). Both proteins coincide at the CEN in metaphase and move to the contractile ring in cytokinesis. Possibly, CEN RNA acts as a scaffold to promote their re-localization.

Knocking down alpha-satellite RNA in human cells (Ideue et al., 2014) or inhibiting transcription in *Xenopus* egg extracts (Blower, 2016) reduced the CEN levels of Aurora B, resulting in unaligned chromosomes caused by improper spindle attachment. Overexpressing MinSat RNA equally mislocalized Aurora B in murine cells, instigating chromosome misalignment and aneuploidy (Bouzinba-Segard et al., 2006). Moreover, Aurora B kinase activity was regulated by MinSat RNA levels (Ferri et al., 2009). Nonetheless, ectopic overexpression of satellite I RNA did not significantly affect chromosome segregation and CEN functions in human cells (Ideue et al., 2014).

The RNA-dependent inner kinetochore localization of the CPC is mediated by at least two RNA-binding domains: one that is present in Aurora B and one in Survivin or Borealin (Blower, 2016). Aurora B and recombinant CPC also bind to RNA *in vitro*. RNA stimulates Aurora B kinase activity *in vitro* and *in vivo*, and a positive feedback loop exists between its kinase activity and its metaphase localization (Wang et al., 2011; Jambhekar et al., 2014). CPC assembly and Aurora B activity were sensitive to RNase treatment. However, kinase activity was rescued with RNA, perhaps via allosteric effects on Aurora B binding (Ferri et al., 2009; Ideue et al., 2014; Jambhekar et al., 2014). Pull-downs of MinSat RNA from murine cells recovered CENP-A, Aurora B, Survivin, and INCENP (Ferri et al., 2009). Reciprocally, CEN RNAs of murine and human cells co-immunoprecipitated with CENP-A, Aurora B, Survivin, and INCENP (Ferri et al., 2009; Ideue et al., 2014).

Besides CEN RNA, *Xenopus* Aurora B also interacts with other RNAs (including mRNAs) to form ribonucleoprotein complexes, as observed in anti-Aurora B immunoprecipitation experiments with interphase and mitotic cells, followed by RNA-sequencing. Over 600 RNAs were identified, 465 of which were specific for mitosis, suggesting a cell cycle-regulated binding of target RNA. Identified RNAs encode proteins of the cytoskeleton, centrosome, transcription factors, and RNAs that are enriched on spindle microtubules (Jambhekar et al., 2014). While the RNA pool showed an overrepresentation of adenines, Aurora B interacted rather promiscuously with RNA, and bound *in vitro* only with minor preference to the *Xenopus fcr1* CEN satellite transcript (Blower, 2016).

HETEROCHROMATIC PERICENTROMERES INSULATE THE CENTROMERE

Centromeric chromatin in fission yeast and metazoans is flanked by constitutive heterochromatin. The pericentromeric domains bind specific proteins and carry epigenetic marks that keep them in a transcriptionally inert state thereby insulating themselves from the enclosed CEN. Pericentric chromatin stabilizes the CEN domain by preventing internal recombinations between intra-CEN repeat sequences (Hetrr and Allis, 2005). It also actively recruits cohesin (via the SUV4-20H2 methyltransferase enzymes that trimethylate histone H4 at Lys20) to promote the bi-orientation of and tension development between the sister chromatids (Bernard et al., 2001; Sakuno et al., 2009; Yamagishi et al., 2010; Yi et al., 2018).

Similar to the CEN sequence, pericentromeres comprise simple repeat sequences such as alpha-satellite DNA, beta-, gamma-, I, II, and III satellite sequences (5–200 bp). They further contain DNA transposons (1 kb), long terminal repeat (LTR)-endogenous retroviral elements (10 kb), non-LTR autonomous retrotransposons (transposons that are formed after reverse transcription of an intermediate RNAPIII-generated transcript) including long interspersed elements (LINEs, 6 kb) and short interspersed elements SINE (100–300 bp) (**Figure 2C**). Pericentromeres harbor promoter elements that recruit various transcription factors, including Ikaros in human cells (Gurel et al., 2008), the ubiquitous YY1 at murine gamma-satellites (Shestakova et al., 2004), Nanog and Sall1 in mouse ES cells (Lopes Novo and Rugg-Gunn, 2016) to regulate transcription by RNAPII or RNAPIII (Pezer and Ugarković, 2008). The repeat sequences are not conserved between or within a species, suggesting that pericentromere transcription is epigenetically controlled. Indeed, it contains histone H3 variants H3.3 and H2A.Z (Drané et al., 2010; Santenard et al., 2010) and binds the conserved HP1, which propagates the heterochromatic state and coordinates chromatin silencing, cohesion, and replication activities (Saksouk et al., 2015). The pericentric histones are hypoacetylated, resulting in chromatin fiber compaction. Methylation marks are enriched on histone H3; H3K9me2, H3K9me3 (recognized by HP1), H3K27me2, and H3K27me3, but also on histone H4; H4K20me2, H4K20Me3, and on cytosine and adenine (Gopalakrishnan et al., 2009; Rose and Klose, 2014; **Figure 3A**). Notwithstanding this repressive environment, pericentromeres are transcribed in many organisms. A delicate balance between pericentromere and CEN transcription ensures chromosomal stability (see next).

PERICENTROMERE TRANSCRIPTION AND TRANSCRIPT PROCESSING ENSURE ITS SILENT STATE

In *S. pombe*, repressive H3K9 methylation occurs at the outermost *dg* and *dh* pericentromere repeats and ends at the tRNA clusters inside the innermost repeats that surround the CEN's central domain. Their presence prevents the pericentromeric heterochromatin from expanding into the CENP-A chromatin (Cam et al., 2005; **Figure 4**). The tRNA clusters are transcribed by RNAPIII, which further delineates the CEN core domain from the flanking pericentromeres (Partridge et al., 2000; Scott et al., 2006). RNAPIII barrier transcription activity does not depend on the orientation of the tRNA genes, but on the DNA sequence that is required for formation of the RNAPIII complex (Scott et al., 2006, 2007). The retrotransposon SINE, found throughout the mammalian genome, is also transcribed by RNAPIII at pericentromeres. SINE expression has been linked to establishing boundary elements and chromatin insulators across the genome (Lunyak et al., 2007; Román et al., 2011). Similarly, SINE transcription and/or that of other pericentric DNA elements could insulate the CEN from the bulk chromatin.

Transcription of pericentromeric chromatin occurs in many species and, except for the tRNA genes in fission yeast, is largely devoid of protein-encoding sequences (Brown et al., 2012; Hall et al., 2012; Saksouk et al., 2015). In *S. pombe*, small-interfering RNAs (siRNAs) produced after the processing of longer transcripts are required for the propagation and maintenance of the heterochromatic identity of pericentromers (Volpe et al., 2002). The finding that transcription of pericentromeric chromatin is functionally significant led to a re-assessment of the definition of "silent" heterochromatin. Specifically, RNAPII bi-directionally produces pre-RNAs from cryptic and TATA-like promoter sequences within the *dh* and *dg* elements of the *otr* regions that border the central CEN (Reinhart and Bartel, 2002; Djupedal et al., 2005; Kato et al., 2005; **Figure 4**). Both *otr* elements are not required for CEN function during mitosis but provide a platform for the heterochromatin component of *S. pombe* CEN (Kagansky et al., 2009). The produced single-stranded polyadenylated transcripts are converted into dsRNA species by the RNA-directed RNA polymerase-containing RDRC complex, which Dicer (Dcr1) next processes into short siRNAs that are transferred by ARC (Argonaute siRNA chaperone complex) to the Argonaute (Ago1)-containing RNA-induced transcriptional silencing complex RITS (Volpe et al.,

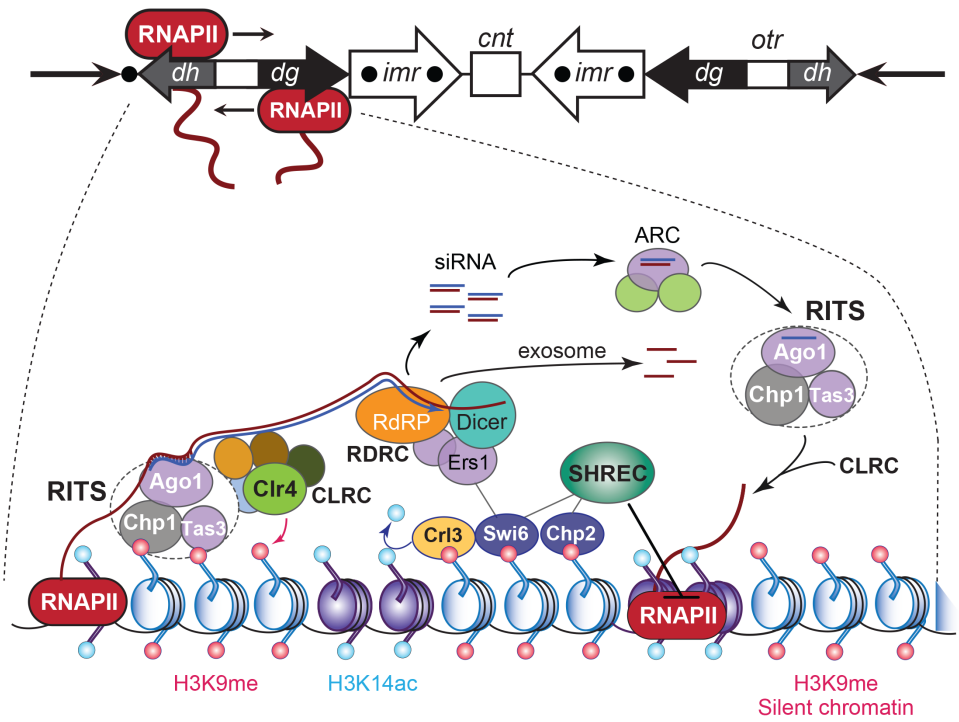

FIGURE 4 | RNA interference-based heterochromatin formation and maintenance at *S. pombe* CEN. Upper panel: the *S. pombe* CEN 1, indicating transcription by RNAPII of an outer repeat *otr* element that flanks the central core of the CEN. Lowe panel: Regulation of the heterochromatic state of CEN sequences that flank the central core domain. The RNA-induced transcriptional silencing (RITS) complex binds to ssRNA transcripts generated from the *otr* sequence repeats, by siRNA–RNA base pairing interactions and via nucleosomes by localizing to histone H3 methylated at Lys9 (H3K9me). RITS then recruits RDRC/Dicer activity, promotes dsRNA synthesis, the production of siRNAs, and CLRC H3K9 methyltransferase-mediated H3K9 methylation. The Argonaute siRNA chaperone complex (ARC) catalyzes the transfer of the siRNAs from RDRC/Dicer to the RITS complex. The transcript ssRNAs present in the siRNAs become degraded by the exosome. Chromodomain HP1 proteins Swi6 and Chp2 are recruited by the H3K9me mark and silence transcription of the chromatin by localizing the chromatin remodeling Snf2/HDAC repressive complex (SHREC), which inhibits RNAPII activity. Adapted from Holoch and Moazed (2015).

2002; Martienssen et al., 2005). Through their interaction with Ago1, the siRNAs load RITS onto the cognate pericentromeric chromatin via base-pairing with the nascent transcripts. The RITS complex then recruits the CLRC complex that contains the histone methyltransferase Clr4 (SUV39H in mammals), which methylates H3K9. The latter recruits chromodomain proteins Swi6 (*S. pombe* HP1 ortholog) and the SHREK-associated protein Chp2, as well as histone deacetylase Clr3 (HDAC1), which removes the local permissive H3K14ac marks. The SHREK complex inhibits RNAPII activity, resulting in silent heterochromatin (**Figure 4**).

Deleting RNAi pathway genes (*dcr1*, *ago1* or *RdP1*) caused chromosome missegregation due to defective silencing of the pericentromeric heterochromatin. *S. pombe* strains mutated in RNAPII subunits Rpb2 and Rpb7 also suffered from increased chromosomal instability, impaired transcriptional silencing, and a reduced association of H3K9me and Swi6 at *dg*/*dh* (Djupedal et al., 2005; Kato et al., 2005). Pericentromere transcription and siRNA production in *S. pombe* peak in S-phase. Hence, pericentromere silencing may be alleviated in S-phase as heterochromatin markers H3K9me and Swi6 become distributed on the replicated strands (Chen et al., 2008; Kloc et al., 2008). Without RNAi, homologous recombination repairs the stalled forks (Zaratiegui et al., 2011) suggesting that transcriptional silencing of pericentromeric heterochromatin prevents replication stress (Castel and Martienssen, 2013).

The importance of Dicer-dependent processing of pericentromere RNAs for heterochromatin assembly in vertebrates was demonstrated with chicken DT40 cells carrying a human chromosome (Fukagawa et al., 2004). Eliminating Dicer provoked an accumulation of long pericentric alpha-satellite and SatIII transcripts, and caused mitotic defects due to precocious sister chromatid separation; attributed to HP1 loss and a misregulation of cohesin and SAC protein BubR1. Similarly, conditionally depleting Dicer in mouse ES cells led to an accumulation of short MajSat transcripts (40 to >200 nt) and the normally repressed long interspersed repeated DNA and high-copy-number LTR retrotransposons. These findings indicated a role for Dicer in repressing pericentromere regions and other usually silent genetic elements (Kanellopoulou et al., 2005). Since the binding of HP1 to heterochromatin requires RNA (Maison et al., 2002; Muchardt et al., 2002), the Dicer-processed siRNAs were assumed to represent them. However, other than in chicken cells (Fukagawa et al., 2004), 21–25 nt siRNAs deriving from the pericentromeric domains have been difficult to identify in vertebrates. Irrespective of how or if the RNAi pathway contributes, pericentromere transcripts in mammals seem involved in the formation and maintenance of heterochromatin. For example in mice, protein WDHD1, which plays a role in RNAPII transcription and RNA processing, interacts with MajSat transcripts. Depleting WDHD1 enhanced MajSat levels and reduced pericentromeric heterochromatin condensation, resulting in proliferation defects (Hsieh et al., 2011). Additional work with mouse early embryos showed that injections of satellite dsRNAs can localize HP1β to pericentromeres revealing that HP1 is targeted in an RNA-dependent, sequence-specific manner. However, a functional association with the RNAi machinery was not assessed (Santenard et al., 2010).

Long non-coding transcripts corresponding to several MajSat satellite repeat units specifically associate with SUMOylated HP1, which is stabilized by H3K9me3, in murine cells. RNase treatment released HP1 and altered the spacing of the pericentromeric histones. HP1 preferentially binds to the forward strand of these RNAs, which remains bound to the site of transcription. Additional HP1 molecules then accumulate, connecting pericentromere transcription with heterochromatin formation (Maison et al., 2011). In primary mouse embryonic fibroblasts, pericentromeric heterochromatin transcription is proliferation- and cell cycle-dependent (Lu and Gilbert, 2007). A first pool of long, heterogeneous MajSat transcripts (1 kb to >8 kb) is produced by RNAPII through G1 and peaks in G1/S-phase, right before pericentromere replication (mid-to-late S-phase). Since the transcripts accumulate at the site of pericentromere replication, local transcription could promote heterochromatin reassembly at the replication fork. A pool of shorter transcripts (∼200 nt) is produced at mitotic onset, coinciding with transcription factors and other proteins becoming cleared from the heterochromatin. This transcript population/transcription activity could be involved in heterochromatin formation, maintenance, and reinforcement during the later stages of mitosis when cohesin at pericentromeres has been removed (Wu et al., 2006). Indeed, while HP1 is dispatched from heterochromatin during M-phase (Muchardt et al., 2002; Fischle et al., 2005), H3K9me3 and the short M-phase RNAs could contribute to the anaphase recruitment of HP1 (Saksouk et al., 2015). SUV39 (Suv39h) histone lysine methyltransferase promotes constitutive heterochromatin compaction and transcriptional repression by catalyzing the H3K9me2/3 modification in humans and mice. SUV39 is incorporated and stabilized in constitutive heterochromatin by chromatin-associated non-coding RNAs (Johnson et al., 2017; Velazquez Camacho et al., 2017).

Heterochromatin activity in *D. melanogaster* is also associated with histone H3K9 methylation by Su(var)3-9 and HP1 recruitment (Ebert et al., 2006). Involvement of siRNA pathways acting in heterochromatin formation in *Drosophila* has been hypothesized since a nuclear pool of transposable element-derived siRNAs (21 nt) was shown to promote heterochromatin formation in somatic cells of *Drosophila*. Components of the RNAi pathway contributed to heterochromatin maintenance (Fagegaltier et al., 2009). As in *S. pombe* and mammals, these siRNAs might tether complementary nascent transcripts of satellite DNAs and transposons, and guide chromatin-modifying enzymes, including Su(var)3-9. RNAi activity seems to help establish heterochromatin in the early embryo, which can then be maintained in the absence of RNAi in somatic tissues (Huisinga and Elgin, 2009). Contrary to *D. melanogaster*, plants often contain a significant portion of methylated repetitive DNA. In fact, siRNAs guiding the methylation of histones and DNA at the loci they were derived from (Zakrzewski et al., 2011). Processing

of satellite-derived transcripts by the RNAi pathway into siRNAs (21–24 nt) has been reported for *Arabidopsis*, rice, and sugar beet (May et al., 2005; Lee et al., 2006; Zakrzewski et al., 2011). Small RNAs with a predominant size of 24 nt cognate to the satellite TCAST (Ugarković et al., 1996; Feliciello et al., 2011) have been detected in the beetle *Tribolium castaneum* and are more abundant in embryos than in later developmental stages (Pezer and Ugarković, 2008; Pezer et al., 2012). The sequences of components of the RNAi pathway are present in the genome of *T. castaneum*, including Argonaute and Dicer, but not the RNA-dependent RNA polymerase gene (Tomoyasu et al., 2008), which insects and vertebrates appear to lack.

CENTROMERE AND PERICENTROMERE TRANSCRIPTION DURING DEVELOPMENT AND DIFFERENTIATION

Satellite DNA has been associated with differentiation and development. Repetitive DNA is not transcribed in adult tissues presumably because it is hypermethylated (Jeanpierre et al., 1993) while it is hypomethylated in fetal tissues (Miniou et al., 1997). Antisense MajSat transcripts accumulate in the central nervous system of mouse embryos 11.5 days post coitum (dpc), and become replaced by sense MajSat transcripts from 12.5 until 15.5 dpc. In adult mice, MajSat transcripts were identified only in highly proliferative tissues such as liver and testis (Rudert et al., 1995). In chicken and zebrafish, alpha-satellite expression from the sense and antisense strands occurs in a regulated pattern during embryogenesis, possibly to control gene expression following transcript processing (Li and Kirby, 2003). Before headfold formation in the chick and at 0–2 h post-fertilization (hpf) in zebrafish, blastodiscs expressed the alpha-repeat sequences. By stage 9 and at 6–8 hpf, respectively, the expression localized to the head mesoderm, myocardium, pharyngeal endoderm, and cardiac neural crest. Because the expression occurred so early in zebrafish, the authors looked for the alpha-repeat transcripts within the maternal RNAs in single-cell and four-cell stage embryos. These stages occur within minutes of fertilization and before the start of zygotic transcription at 3 hpf. High levels of the transcripts were found, supporting their maternal origin (Li and Kirby, 2003).

ANOMALOUS CENTROMERE AND PERICENTROMERE TRANSCRIPTION DURING STRESS AND DISEASE

Since the centromeric and pericentromeric regions are epigenetically controlled, any loss/reduction in repressive marks such as DNA and histone methylation or increased removal of active acetylation marks can provoke satellite overexpression from the centromeric and pericentromeric regions as observed during stress, senescence, aging, and in cancer cells. Pathological transcription of either region dramatically affects CEN insulation and activity, resulting in disturbed kinetochore formation and genetic instability.

(Peri)centromere Transcription During Stress

In human cells, the transcription of certain pericentromeric satellite sequences, in particular SatIII, is induced upon heat shock and exposure to heavy metals, chemicals, UV radiation, hyperosmotic, or oxidative conditions (**Figure 5A**). Importantly, while SatIII transcripts were up-regulated following heat shock, CEN transcripts were not, indicating that each domain is subject to different transcriptional control mechanisms (Jolly et al., 2004; Rizzi et al., 2004; Valgardsdottir et al., 2008; Eymery et al., 2009). SatIII expression levels also depend on the type of stress that is experienced: MMS, etoposide, aphidicolin, and oxidative stress are weak inducers; UV and hyperosmosis have a moderate effect; and heat shock and cadmium are very strong activators. In unstressed cells, SatIII sequences exist in a transcriptionally silent, closed heterochromatin conformation. Following heat shock or stress, SatIII transcription is induced (Valgardsdottir et al., 2008). Specifically, monomeric transcription factor Heat Shock transcription Factor 1 (HSF1) becomes upregulated and binds as a phosphorylated homotrimer to the SatIII sequences. HSF1 then recruits the histone acetylase CREB-binding protein CBP to trigger histone hyperacetylation while the death domain-associated protein DAXX, which acts as a chaperone for pericentromeric histone H3.3, promotes SatIII transcription by RNAPII. Upon DAXX depletion, SatIII expression levels in heat-shocked cells dropped, while less H3.3 was incorporated (Morozov et al., 2012). A set of RNA-binding and processing proteins associate with the SatIII transcripts. RNAi knock-downs of these transcripts that range between 2 and 5 kb (Jolly et al., 2004; Rizzi et al., 2004) reduced the recruitment of RNA processing factors, including the splicing factor SF2/ASF (Chiodi et al., 2004; Metz et al., 2004). The RNA-binding factors and SatIII transcripts produce ribonucleoprotein complexes that combine into many perichromatin granules. Together, they correspond to mature nuclear stress bodies that accumulate at the pericentromeres (Denegri et al., 2002; Jolly et al., 2004; **Figure 5A**). The number and size of the nuclear stress bodies correlate directly with SatIII expression (Valgardsdottir et al., 2008). During recovery from the stress, increased levels of heat shock protein HSP70 trigger the disassembly of the HSF1 trimers, which leave the nuclear stress bodies together with the histone acetyltransferase CBP and RNAPII. Next, the granule clusters dissociate, the RNA-binding proteins redistribute through the nucleoplasm but the SatIII transcripts stay bound to the granules. At the same time, granules that are H3K9 methylated appear adjacent to the disassembling nuclear stress bodies. The transcripts are then cleaved, and a complex similar to the *S. pombe* RITS complex may then localize the transcripts to the chromatin to silence the SatIII DNA arrays (Biamonti, 2004; Biamonti and Vourc'h, 2010; **Figure 5A**). Depending on the stress that is experienced, different transcription factors promote SatIII activation. For example, the tonicity-responsive enhancer binding protein TONEBP induces SatIII expression under hyperosmotic stress

(Valgardsdottir et al., 2008). Satellite transcript accumulation during heat stress also occurs in insects (Pezer et al., 2012) and plants (Tittel-Elmer et al., 2010). In the beetle *T. castaneum* pericentromere TCAST satellites are transcribed by RNAPII and processed into 21–30 nt siRNAs. The production of these siRNAs is developmentally regulated but is strongly induced upon heat shock. During recovery, siRNA expression and histone modifications are restored to normal. Transient heterochromatin remodeling seems part of a stress-activated gene-expression program in beetles (Pezer et al., 2012), and possibly other organisms as well. In *Arabidopsis*, a temperature upshift alleviated the silent state of CEN satellite sequences, pericentric 5S rDNA arrays, transposable elements, and 106B interspersed repeats. Surprisingly, the pattern of repressive epigenetic marks within the heterochromatin was not affected, suggesting that the temperature-stimulated transcription activity bypassed these regulatory modifications (Tittel-Elmer et al., 2010).

Centromere MinSat transcription increases when murine cells are exposed to chemical stress (DMSO, 5-aza-2′-deoxycytidine, apoptosis inducer staurosporine). Comparable ectopic overexpression of MinSat DNA led to decondensed CEN and mitotic defects such as multiple spindle attachments, loss of sister chromatid cohesion, aneuploidy, and cell death (Bouzinba-Segard et al., 2006).

Extensive evidence points to an interplay between the DNA damage response and satellite DNA expression. Ectopic expression of satellite RNA in cultured human mammary epithelial cells induced numerous foci of γ-H2A.X, the phosphorylated histone H2A.X variant that marks dsDNA breaks (Zhu et al., 2011). These cells also exhibited bridged and lagging chromosomes as well as disorganized metaphase spindles (Zhu et al., 2018). Similarly, MajSat RNA overexpression compromised DNA damage repair, resulting in high DNA mutation rates in cultured murine pancreatic cells (Kishikawa et al., 2016a, 2018). Elevated levels of γ-H2A.X were also observed after nuclear injection of satellite RNA in human cells, indicating that high transcription intensity *per se* does not trigger the DNA damage response (Zhu et al., 2018). CRISPR-mediated activation of MinSat and MajSat expression in murine cells incited chromosomal instability (Zhu et al., 2018). Vice versa, genotoxic etoposide treatment (causes dsDNA breaks) triggered MinSat transcription and CENP-A eviction from the mouse CEN, which relied on the p53-dependent DNA damage pathway and chromatin chaperone/remodeling factors (Hédouin et al., 2017). In the absence of functional p53, DNA demethylation as induced by 5-aza-2′-deoxycytidine resulted in massive transcription of MajSat RNA in mouse fibroblasts (Leonova et al., 2013). Moreover, ectopic overexpression of MajSat RNA stimulated by injection of sh-p53 RNA causing p53 knockdown led to tumor formation (Zhu et al., 2018).

How do (peri)centromere transcription/transcripts contribute to a stress response and recovery from it? The transcripts processed via an RNAi-dependent or -independent pathway could mediate heterochromatin reformation, as in *S. pombe*. Analogous to X-chromosome inactivation by the long non-coding Xist RNA, the transcripts might recruit chromatin remodelers and DNA methyltransferases to establish a silent pericentric state. Also, SatIII transcripts could protect a fragile region of the genome from stress-induced DNA damage (the SatIII-enriched 9q12 region is often rearranged in pathologies, including cancer). Possibly, the transcripts could regulate local RNA splicing during the stress response by sequestering splicing factors. Via a position-effect mechanism, they might counteract the repressive nature of heterochromatin and activate nearby genes in *cis* or *trans* (Eymery et al., 2009; Saksouk et al., 2015).

(Peri)centromere Transcription During Senescence and Aging

Heterochromatin structure and expression change during aging. An up-regulation of MajSat expression in senescent cardiac muscle cells of aging mice but not in their brain or kidneys may be linked to mitochondria-induced oxidative stress (Gaubatz and Cutler, 1990). Transcriptional activation of pericentromeres has been observed in replicative senescence and aging. Upon extensive passaging of human fibroblasts, the cells entered replicative senescence, which correlated with an increased expression of pericentromere transcripts. The pericentromeric heterochromatin was decondensed and exhibited reduced DNA methylation. Here, the produced transcripts may not have a specific biological role but rather be the consequence of a senescent state of the heterochromatin itself (Enukashvily et al., 2007). Aberrant overexpression of SatIII from 9q12 was observed in the Hutchinson–Gilford progeria syndrome (Shumaker et al., 2006). The latter arises from mutations in the laminA gene, which encodes a component of the nuclear lamina that maintains the structural integrity of the nucleus. Lamins are crucial for pericentromeric heterochromatin organization in interphase cells (Solovei et al., 2013).

Pericentromeric heterochromatin was show to lose H3K9me3 and HP1 proteins in older flies and human cells, leading to an anomalous expression of satellite sequences (Scaffidi and Misteli, 2006; Shumaker et al., 2006; Larson et al., 2012). Loss of pericentric silencing may drive age-related genome instability and death since the cells from older individuals or progeria patients are characterized by a global loss of heterochromatin marks, and increase in DNA damage (Scaffidi and Misteli, 2006; Shumaker et al., 2006; Leung et al., 2015). Inactivation of heterochromatin silencing components in flies cuts their lifespan in half whereas a moderate overexpression of HP1α extends their lifespan with 15%, suggesting that HP1α loss in older animals promotes aging (Larson et al., 2012). Finally, the transcriptional de-repression of satellite sequences has been linked to tau-induced neurodegeneration, as in Alzheimer's disease (Frost et al., 2014).

(Peri)centromere Transcription in Cancer and Disease

The transcriptional misregulation of the SatII and SatIII pericentromeric satellite sequences, and altered epigenetic state of pericentromeric chromatin characterizes many cancers and genetic disorders (Shumaker et al., 2006; Ehrlich, 2009; Eymery et al., 2009; Ting et al., 2011; Zhu et al., 2011; **Figure 5B**).

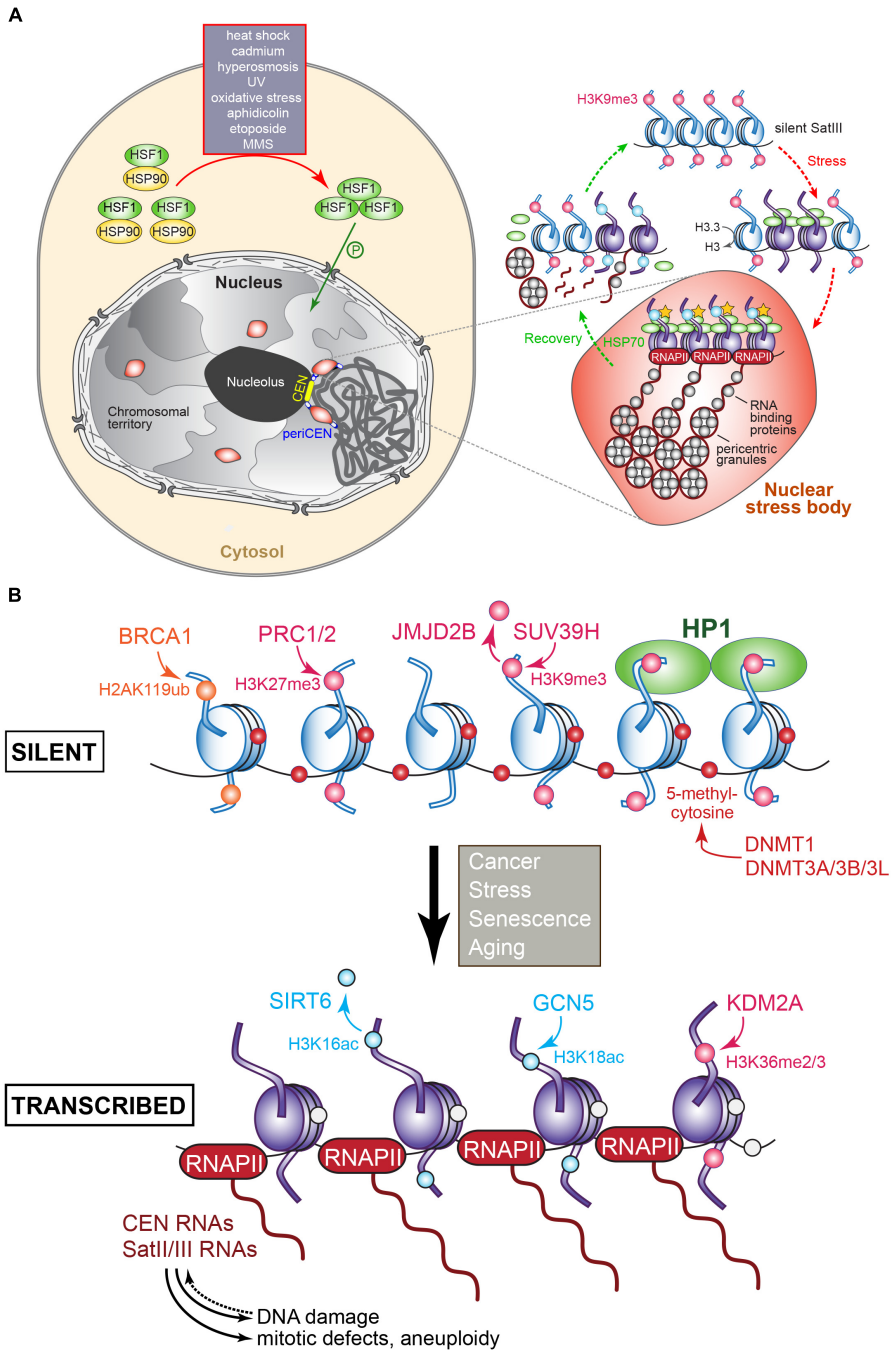

FIGURE 5 | (A) Regulation of pericentromere SatIII transcription in human cells following exposure to heat and other stresses. In the absence of stress, SatIII repeat sequences are epigenetically marked for silence (H3K9me, pink dot) and exist in a closed transcriptionally inert state (blue nucleosomes). Upon exposure to heat or other stresses, the monomeric HSF1 (shown in green) becomes upregulated, and forms homotrimers that after phosphorylation enter the nucleus. The HSF1 bind to the SatIII sequences and recruit the histone acetyltransferase (HAT) CREB-binding proteins to trigger histone hyperacetylation (yellow stars), which results in active SatIII transcription by RNAPII of one strand. A subset of RNA-binding/processing proteins is recruited to the SatIII transcripts, forming ribonucleoprotein complexes that associate into so-called perichromatin granules, which in turn produce clusters that correspond to a mature nuclear stress body (represented by the red oval structure). To recover from the inflicted stress, heat shock protein HSP70 induces the disassembly of the HSF1 trimers that leave the nuclear stress bodies, along with RNAPII and the HAT. The granules disassemble and the RNA-binding proteins redistribute throughout the nucleoplasm. SatIII transcripts may become processed into smaller fragments possibly by the RNAi machinery to protect and re-establish the heterochromatic state of the pericentromeric region comprising the SatIII repeats, possibly by recruiting epigenetic writing activity resulting in the establishment of the repressive H3K9me signals. Adapted from Biamonti and Vourc'h (2010) and Biamonti (2004). **(B)** Transcriptional regulation of (peri)centric repeat sequences as identified in various tumors. The epigenetic marks and the enzymes responsible for introducing or removing them at histones or cytosine are indicated. Blue nucleosomes: silent, purple nucleosomes: transcribed. The overproduction of (peri)centric transcripts can induce DNA damage, mitotic defects, genomic instability, and aneuploidy. See text for details.

In mouse models of pancreatic, colon, and lung cancers, satellite transcripts represent up to 50% of the total RNA, which was linked to deregulated DNA methylation. Specifically, in pancreatic ductal adenocarcinoma (PDAC) samples, 47% of all transcripts were produced from MajSat sequences. In contrast, in healthy reference tissues, only 0.02–0.4% of all transcripts originated from those repeats (Ting et al., 2011; Kishikawa et al., 2016a). The transcripts were highly heterogeneous (200–8,000 nt) and transcribed only from the forward strand. While PDAC murine cells expressed MajSats only minimally when cultured *ex vivo*, high expression levels similar to those observed in tumors *in vivo* were measured in immortalized PDAC tumor cells treated with 5-aza-2′-deoxycytidine, suggesting that transcription is regulated by DNA methylation, which might be re-established together with other epigenetic silencing mechanisms *ex vivo*. Furthermore, SatII expression showed a median 21-fold increase in human PDAC samples in comparison with "healthy" tissue samples (Ting et al., 2011). To determine what could be promoting SatII hyperexpression, linear regression analysis was performed to identify transcripts that were co-regulated with the mouse MajSat or human alpha-satellite sequences. Several genes involved in neuronal cell fate and stem cell pathways, that contained LINE1 transposable elements were highly expressed (Ting et al., 2011). A LINE1 insertion upstream of their transcription start sites can underlie their misregulation, contributing to cellular transformation. SatII RNA transcripts in colorectal cancer cells were reverse transcribed into DNA:RNA hybrids, and then generated dsDNAs, which were incorporated into the pericentromeric domains. Whole-genome sequencing showed that SatII copy number gain commonly characterizes human colon tumors, and is linked with low survival (Bersani et al., 2015). Healthy human testis tissue showed a high expression of pericentromeres, while in cancers their expression was silent (Eymery et al., 2009).

Methyltransferase DNMT3B, which methylates (peri)centromeric DNA at cytosines in CpG dinucleotides, is recruited by CENP-C. Impairment of this interaction causes an overproduction of CEN and pericentromere transcripts (Gopalakrishnan et al., 2009). Besides cancer, mutations in DNMT3B lead to the ICF syndrome (immunodeficiency, CEN instability, and facial anomalies) whose patients suffer from hypomethylated SatII and SatIII repeats (euchromatic gene methylation was at normal levels, Brun et al., 2011). The tumor-suppressing, heterochromatin-associating lysine demethylase 2A (KDM2A) is downregulated in prostate cancer (Frescas et al., 2008). Via its Jumonji domain, the enzyme demethylates the pericentromeric H3K36me2 modification to silence the heterochromatin. KDM2A depletion resulted in a loss of HP1 and elevated alpha-satellite and MajSat transcription in human and mouse cells, respectively. Phenotypes included genomic instability, sister chromatid misalignment, chromosome breaks, and anaphase bridges. The lower the level of KDM2A expression, the more severe the tumor grade in prostate cancer, linking hypermethylation and increased (peri)centromere transcription with cancer growth (Frescas et al., 2008; **Figure 5B**).

The histone demethylase JMJD2B acts as an oncogene in certain breast cancers (Slee et al., 2012). When overexpressed, its activity reduces H3K9me3 marks at CEN and causes chromosomal instability. While the levels of CEN and pericentromere transcripts in these tumors were not quantitated, their production was likely derepressed. A loss of SUV39H histone methyltransferase activity (mediates H3K9 methylation) facilitated the expression and/or stabilization of MinSat transcripts in mice, which accumulated as dsRNAs (Lehnertz et al., 2003; Martens et al., 2005). A forced accumulation of MinSat transcripts, in sense orientation, provoked a mislocalization of kinetochore proteins, affected chromosome segregation, sister chromatid cohesion, and induced modifications of CEN epigenetic hallmarks. Possibly, anomalous levels of CEN transcripts interfere with kinetochore and cohesin recruitment (Bouzinba-Segard et al., 2006). Of note, ectopic overexpression of alpha-satellite DNA in human cells led to chromosome loss but not to reduced methylation of the DNA. In contrast, DNA demethylation caused pathological alpha-satellite transcription and chromosome loss in human cells (Ichida et al., 2018).

SatII and SatIII transcripts were markedly overexpressed in human osteosarcoma cells depleted in tumor suppressor SIRT6, which deacetylates histone H3K16ac in pericentric heterochromatin. Its inactivation led to H3K18 hyperacetylation likely by the histone acetyltransferase GCN5, reversal of heterochromatin silencing, mitotic defects, genomic instability, and senescence. Importantly, depletion of the transcripts through RNAi rescued the phenotypes (Tasselli et al., 2016).

Mutations in the hereditary ovarian and breast cancer susceptibility gene BRCA1, which acts as a tumor suppressor, led to genomic instability. While BRCA1 acts in DNA replication and damage repair, control of the cell cycle, and many other regulatory functions, the protein was recently shown to also determine the epigenetic states of centromeric and pericentric chromatin (Zhu et al., 2011). Through its ubiquitin ligase activity, BRCA1 mono-ubiquitinates histone H2A at Lys119 (Chen et al., 2002; **Figure 5B**) to produce a repressive mark that prevents genomic instability and tumorigenesis (Zhu et al., 2011). When BRCA1 was knocked out in murine and human cells, a derepressed transcription of MinSat, MajSat, and alpha-satellite DNA was observed, respectively, concurrent with a loss of H2AK119 ubiquitination. While the latter may have produced defective heterochromatin (as indicated by reduced HP1 levels), it is unclear which factors promoted alpha-satellite transcription in the BRCA1-deficient cells. Ectopically expressing H2A fused to ubiquitin reversed the above BRCA1-loss phenotypes, whereas the ectopic expression of satellite DNA phenocopied it, resulting in DNA damage and genomic instability, cell cycle checkpoint defects, and centrosome amplification, indicating that overexpressed (peri)centromere transcripts could contribute to malignancy (Zhu et al., 2011).

The tumor-suppressing transcription factor Prep1 is associated with DNA damage control and the management of histone methylation levels (Iotti et al., 2011). Indeed, upon downregulating Prep1 in mouse or human cells, DNA damage increased. This phenotype, which is generated through an unknown mechanism, caused a widespread increase in

the repressive histone mark H3K9me3. Consequently, the transcription of MajSat in mouse, and alpha-satellite DNA in humans dropped with 62% and 45%, respectively, compared to wild-type control cells. Intriguingly, the decrease in CEN and pericentromere transcript production led to the same phenotypes as in cells overexpressing them, including aneuploidy, miniature chromosomes, Robertsonian translocations, and CEN duplications (Iotti et al., 2011).

Tumor-suppressing transcription factor p53 cooperates with DNA methylation activity to silence a large part of the mouse genome. A massive transcription of major classes of retroelements, near-CEN tandem repeat satellite DNAs, and numerous species of non-coding RNAs was observed in p53-deficient mouse fibroblasts treated with 5-aza-2′-deoxycytidine (not observed in treated p53 wild-type cells). The levels of these transcripts exceeded those of β-actin mRNA by more than 150-fold. Accumulation of these transcripts, which are capable of forming dsRNAs, was complemented by a potent apoptosis-inducing type I interferon response. The authors suggested a model in which the downregulation of these repeat sequences is controlled by p53-driven transcriptional silencing, DNA methylation-based suppression of transcription, and the suicidal type I interferon response, which eliminates the cells that escaped the first two lines of control (Leonova et al., 2013).

(Peri)centromere silencing is also regulated by the Polycomb repressive complexes PRC1 and PRC2, which are commonly misregulated in cancer (Blackledge et al., 2015). PRC2 lysine methyltransferase subunit EZH2 catalyzes the addition of one to three methyl groups to histone H3 at Lys27 (**Figure 5B**). In *Rb1* mutant mice, which are defective in recruiting EZH2 to repetitive sequences, a transcriptional derepression of satellite DNA was observed, which induced susceptibility to lymphoma (Ishak et al., 2016).

(PERI)CENTROMERE TRANSCRIPTS AS CANCER BIOMARKERS AND TARGETS IN THE CLINIC

SatII overexpression characterizes myriad cancerous and precancerous lesions, suggesting that SatII RNA levels might be a good predictor or indicator of cancer (Ting et al., 2011; Bersani et al., 2015; Tasselli et al., 2016; Hall et al., 2017). Indeed, RNA *in situ* hybridization analysis of SatII expression in biopsies proved a better diagnostic for pancreatic cancer than standard histopathological analysis (Ting et al., 2011). A convenient and highly sensitive method for quantitating circulating satellite repeat RNAs in blood serum (Kishikawa et al., 2016b) combines Tandem Repeat Amplification by nuclease Protector (TRAP) with droplet digital PCR. Patients with pancreatic ductal carcinoma (PDAC) were efficiently discriminated from healthy individuals, while patients with intraductal papillary mucinous neoplasm, a precancerous lesion of PDAC, could also be accurately identified. This simple and cheap test allows for early prognosis, quick screens, and regular follow-ups of PDAC progression. This method may well be adapted to quantitate additional (peri)centromere transcripts in other cancers as well.

Kinetochore subunit overexpression (Thiru et al., 2014; Zhang et al., 2016; Sun et al., 2016), CENP-A overproduction and mislocalization (Athwal et al., 2015), and de-silenced (peri)centromeric chromatin may all contribute to aneuploidy and promote cancer initiation/progression. The degree of overexpression of kinetochore protein-encoding genes, which associate with patient survival and response to therapy, could classify tumors, and serve as future prognostic cancer biomarkers (O'Brien et al., 2007; Sun et al., 2016; Zhang et al., 2016). Similarly, CEN and pericentromere transcript levels in conjunction with the (peri)centromeric methylation, acetylation, or ubiquitination state may serve as valuable readouts of cancer grade and survival. They may also represent novel therapeutic targets. In fact, various drugs inhibiting numerous epigenetic enzymes/regulators are in advanced developmental stages (Pfister and Ashworth, 2017). Nucleic acid therapeutics aimed at (peri)centromere repeats may provide alternative objectives for the future. They are transcribed in a cell- or tissue-specific manner, making them exceptional objectives. Powerful RNA structure determination assays can also map the secondary and tertiary structure of these RNAs (Wilkinson et al., 2006; Novikova et al., 2013; Lu et al., 2016). Clinical trials are already underway to similarly target highly structured bacterial or viral riboswitches using small-molecule inhibitors to treat bacterial and viral infections, respectively (Howe et al., 2015). Small-molecule ligands targeting structural elements in these CEN or pericentromere RNAs could potentially destabilize the transcript or interfere allosterically with CEN-protein binding to confer a therapeutic effect, although this remains purely hypothetical. With recent advances in genome editing methods, it is possible to achieve transcriptional silencing of (peri)centromere repeats via CRISPR interference (Gilbert et al., 2014; Koch, 2017). In a genome-wide CRISPR interference study, guide RNAs were developed to selectively and successfully inactivate >16,000 long non-coding RNA genes within the human genome (Liu et al., 2017). These experiments suggest that downregulating pathologically expressed (peri)centromeric elements could well be feasible (Zhang et al., 2016; Koch, 2017). The recently developed CRISPR/Cas13 system (Abudayyeh et al., 2017) represents another promising approach to knock down non-coding RNAs. However, only the future will tell to which extent these approaches will translate into clinical scenarios.

PERSPECTIVES

The continuous identification and functional characterization of new epigenetic activities (enzymes, histone modifications) that impinge on centromeric and pericentromere domains via ever more sensitive mass spectrometry approaches will take our understanding of CEN, kinetochore, and pericentromere biology to the next level. In addition, transcription factors that drive (peri)centromere transcription in healthy and diseased

cells must be identified as their biology and influences on the spatiotemporal regulation of the CEN and pericentric regions remains largely unknown. The same is true for regulators that act upon the RNAPII complex to orchestrate its activity (recruitment, elongation, termination) at (peri)centromeres. Kinases and phosphatase may be prime candidates. A better understanding of RNAi pathway involvement in mammalian biology would be welcomed as well. For sure, exciting (peri)centromere biology will continue to be "written" in laboratories worldwide, and hopefully at some point in cancer clinics as well.

AUTHOR CONTRIBUTIONS

KS and PDW wrote the paper and made the figures. Both authors have approved of the manuscript.

FUNDING

We acknowledge support from the Italian Association for Cancer Research (Investigator Grant IG19250) and the University of Trento (Intramural Grants 40202054 and 40201806).

REFERENCES

Abudayyeh, O. O., Gootenberg, J. S., Essletzbichler, P., Han, S., Joung, J., Belanto, J. J., et al. (2017). RNA targeting with CRISPR-CAS13. *Nature* 550, 280–284. doi: 10.1038/nature24049

Akiyoshi, B., and Gull, K. (2014). Discovery of unconventional kinetochores in kinetoplastids. *Cell* 156, 1247–1258. doi: 10.1016/J.CELL.2014.01.049

Albertson, D. G., and Thomson, J. N. (1982). The kinetochores of *Caenorhabditis elegans*. *Chromosoma* 86, 409–428. doi: 10.1007/BF00292267

Aldrup-MacDonald, M. E., and Sullivan, B. A. (2014). The past, present, and future of human centromere genomics. *Genes* 5, 33–50. doi: 10.3390/genes5010033

Alexandrov, I., Kazakov, A., Tumeneva, I., Shepelev, V., and Yurov, Y. (2001). Alpha-satellite DNA of primates: old and new families. *Chromosoma* 110, 253–266. doi: 10.1007/s004120100146

Athwal, R. K., Walkiewicz, M. P., Baek, S., Fu, S., Bui, M., Camps, J., et al. (2015). CENP-A nucleosomes localize to transcription factor hotspots and subtelomeric sites in human cancer cells. *Epigenetics Chromatin* 8:2. doi: 10.1186/1756-8935-8-2

Aze, A., Sannino, V., Soffientini, P., Bachi, A., and Costanzo, V. (2016). Centromeric DNA replication reconstitution reveals DNA loops and ATR checkpoint suppression. *Nat. Cell Biol.* 18, 684–691. doi: 10.1038/ncb3344

Bailey, A. O., Panchenko, T., Sathyan, K. M., Petkowski, J. J., Pai, P.-J., Bai, D. L., et al. (2013). Posttranslational modification of CENP-A influences the conformation of centromeric chromatin. *Proc. Natl. Acad. Sci. U.S.A.* 110, 11827–11832. doi: 10.1073/pnas.1300325110

Bergmann, J. H., Jakubsche, J. N., Martins, N. M., Kagansky, A., Nakano, M., Kimura, H., et al. (2012). Epigenetic engineering: histone H3K9 acetylation is compatible with kinetochore structure and function. *J. Cell Sci.* 125, 411–421. doi: 10.1242/jcs.090639

Bergmann, J. H., Rodríguez, M. G., Martins, N. M. C., Kimura, H., Kelly, D. A., Masumoto, H., et al. (2011). Epigenetic engineering shows H3K4ME2 is required for HJURP targeting and CENP-A assembly on a synthetic human kinetochore. *EMBO J.* 30, 328–340. doi: 10.1038/emboj.2010.329

Bernard, P., Maure, J. F., Partridge, J. F., Genier, S., Javerzat, J. P., and Allshire, R. C. (2001). Requirement of heterochromatin for cohesion at centromeres. *Science* 294, 2539–2542. doi: 10.1126/science.1064027

Bersani, F., Lee, E., Kharchenko, P. V., Xu, A. W., Liu, M., and Xega, K. (2015). Pericentromeric satellite repeat expansions through RNA-derived DNA intermediates in cancer. *Proc. Natl. Acad. Sci. U.S.A.* 112, 15148–15153. doi: 10.1073/pnas.1518008112

Biamonti, G. (2004). Nuclear stress bodies: a heterochromatin affair? *Nat. Rev. Mol. Cell Biol.* 5, 493–498. doi: 10.1038/nrm1405

Biamonti, G., and Vourc'h, C. (2010). Nuclear stress bodies. *Cold Spring Harb. Perspect. Biol.* 2:a000695. doi: 10.1101/cshperspect.a000695

Blackledge, N. P., Rose, N. R., and Klose, R. J. (2015). Targeting polycomb systems to regulate gene expression: modifications to a complex story. *Nat. Rev. Mol. Cell Biol.* 16, 643–649. doi: 10.1038/nrm4067

Bloom, K., and Costanzo, V. (2017). Centromere structure and function. *Prog. Mol. Subcell. Biol.* 56, 515–539. doi: 10.1007/978-3-319-58592-5_21

Blower, M. D. (2016). Centromeric transcription regulates aurora-B localization and activation. *Cell Rep.* 15, 1624–1633. doi: 10.1016/J.CELREP.2016.04.054

Blower, M. D., Sullivan, B. A., and Karpen, G. H. (2002). Conserved organization of centromeric chromatin in flies and humans. *Dev. Cell* 2, 319–330. doi: 10.1016/S1534-5807(02)00135-1

Bobkov, G. O. M., Gilbert, N., and Heun, P. (2018). Centromere transcription allows CENP-A to transit from chromatin association to stable incorporation. *J. Cell Biol.* 217, 1957–1972. doi: 10.1083/jcb.201611087

Bodor, D. L., Mata, J. F., Sergeev, M., David, A. F., Salimian, K. J., Panchenko, T., et al. (2014). The quantitative architecture of centromeric chromatin. *eLife* 3:e02137. doi: 10.7554/eLife.02137

Boltengagen, M., Huang, A., Boltengagen, A., Trixl, L., Lindner, H., Kremser, L., et al. (2016). A novel role for the histone acetyltransferase HAT1 in the CENP-A/CID assembly pathway in *Drosophila melanogaster*. *Nucleic Acids Res.* 44, 2145–2159. doi: 10.1093/nar/gkv1235

Bouzinba-Segard, H., Guais, A., and Francastel, C. (2006). Accumulation of small murine minor satellite transcripts leads to impaired centromeric architecture and function. *Proc. Natl. Acad. Sci. U.S.A.* 103, 8709–8714. doi: 10.1073/pnas.0508006103

Braselton, J. P. (1975). Ribonucleoprotein staining of *Allium cepa* kinetochores. *Cytobiologie* 12, 148–151.

Brown, J. D., Mitchell, S. E., and Neill, R. J. O. (2012). Making a long story short: noncoding RNAs and chromosome change. *Heredity* 108, 42–49. doi: 10.1038/hdy.2011.104

Brun, M.-E., Lana, E., Rivals, I., Lefranc, G., Sarda, P., Claustres, M., et al. (2011). Heterochromatic genes undergo epigenetic changes and escape silencing in immunodeficiency, centromeric instability, facial anomalies (ICF) syndrome. *PLoS One* 6:e19464. doi: 10.1371/journal.pone.0019464

Bühler, M., and Moazed, D. (2007). Transcription and RNAi in heterochromatic gene silencing. *Nat. Struct. Mol. Biol.* 14, 1041–1048. doi: 10.1038/nsmb1315

Cam, H. P., Sugiyama, T., Chen, E. S., Chen, X., FitzGerald, P. C., and Grewal, S. I. S. (2005). Comprehensive analysis of heterochromatin- and RNAi-mediated epigenetic control of the fission yeast genome. *Nat. Genet.* 37, 809–819. doi: 10.1038/ng1602

Carone, D. M., Longo, M. S., Ferreri, G. C., Hall, L., Harris, M., Shook, N., et al. (2009). A new class of retroviral and satellite encoded small RNAs emanates from mammalian centromeres. *Chromosoma* 118, 113–125. doi: 10.1007/s00412-008-0181-5

Carroll, C. W., Milks, K. J., and Straight, A. F. (2010). Dual recognition of CENP-A nucleosomes is required for centromere assembly. *J. Cell Biol.* 189, 1143–1155. doi: 10.1083/jcb.201001013

Carroll, C. W., Silva, M. C. C., Godek, K. M., Jansen, L. E. T., and Straight, A. F. (2009). Centromere assembly requires the direct recognition of CENP-A nucleosomes by CENP-N. *Nat. Cell Biol.* 11, 896–902. doi: 10.1038/ncb1899

Castel, S. E., and Martienssen, R. A. (2013). RNA interference in the nucleus: roles for small RNAs in transcription, epigenetics and beyond. *Nat. Rev. Genet.* 14, 100–112. doi: 10.1038/nrg3355

Castellano-Pozo, M., Santos-Pereira, J. M., Rondón, A. G., Barroso, S., Andújar, E., Pérez-Alegre, M., et al. (2013). R loops are linked to histone H3 S10 phosphorylation and chromatin condensation. *Mol. Cell* 52, 583–590. doi: 10.1016/J.MOLCEL.2013.10.006

Catania, S., Pidoux, A. L., and Allshire, R. C. (2015). Sequence features and transcriptional stalling within centromere DNA promote establishment of CENP-A chromatin. *PLoS Genet.* 11:e1004986. doi: 10.1371/journal.pgen.1004986

Chan, F. L., Marshall, O. J., Saffery, R., Won Kim, B., Earle, E., Choo, K. H. A., et al. (2012). Active transcription and essential role of RNA polymerase II at the centromere during mitosis. *Proc. Natl. Acad. Sci.* 109, 1979–1984. doi: 10.1073/pnas.1108705109

Chen, A., Kleiman, F. E., Manley, J. L., Ouchi, T., and Pan, Z.-Q. (2002). Autoubiquitination of the BRCA1*BARD1 RING ubiquitin ligase. *J. Biol. Chem.* 277, 22085–22092. doi: 10.1074/jbc.M201252200

Chen, C.-C., Bowers, S., Lipinszki, Z., Palladino, J., Trusiak, S., Bettini, E., et al. (2015). Establishment of centromeric chromatin by the CENP-A assembly factor CAL1 requires FACT-mediated transcription. *Dev. Cell* 34, 73–84. doi: 10.1016/J.DEVCEL.2015.05.012

Chen, C. C., Dechassa, M. L., Bettini, E., Ledoux, M. B., Belisario, C., Heun, P., et al. (2014). CAL1 is the *Drosophila* CENP-A assembly factor. *J. Cell Biol.* 204, 313–329. doi: 10.1083/jcb.201305036

Chen, E. S., Zhang, K., Nicolas, E., Cam, H. P., Zofall, M., and Grewal, S. I. S. (2008). Cell cycle control of centromeric repeat transcription and heterochromatin assembly. *Nature* 451, 734–737. doi: 10.1038/nature06561

Chen, Y., Baker, R. E., Keith, K. C., Harris, K., Stoler, S., and Fitzgerald-Hayes, M. (2000). The N terminus of the centromere H3-like protein Cse4p performs an essential function distinct from that of the histone fold domain. *Mol. Cell. Biol.* 20, 7037–7048. doi: 10.1128/MCB.20.18.7037-7048.2000

Chiodi, I., Corioni, M., Giordano, M., Valgardsdottir, R., Ghigna, C., Cobianchi, F., et al. (2004). RNA recognition motif 2 directs the recruitment of SF2/ASF to nuclear stress bodies. *Nucleic Acids Res.* 32, 4127–4136. doi: 10.1093/nar/gkh759

Choi, E. S., Strålfors, A., Castillo, A. G., Durand-Dubief, M., Ekwall, K., and Allshire, R. C. (2011). Identification of noncoding transcripts from within CENP-A chromatin at fission yeast centromeres. *J. Biol. Chem.* 286, 23600–23607. doi: 10.1074/jbc.M111.228510

Chueh, A. C., Northrop, E. L., Brettingham-Moore, K. H., Choo, K. H. A., and Wong, L. H. (2009). LINE retrotransposon RNA is an essential structural and functional epigenetic component of a core neocentromeric chromatin. *PLoS Genet.* 5:e1000354. doi: 10.1371/journal.pgen.1000354

Clarke, L., and Carbon, J. (1980). Isolation of a yeast centromere and construction of functional small circular chromosomes. *Nature* 287, 504–509. doi: 10.1038/287504a0

Cohen, R. L., Espelin, C. W., De Wulf, P., Sorger, P. K., Harrison, S. C., and Simons, K. T. (2008). Structural and functional dissection of Mif2p, a conserved DNA-binding kinetochore protein. *Mol. Biol. Cell* 19, 4480–4491. doi: 10.1091/mbc.E08-03-0297

Dambacher, S., Deng, W., Hahn, M., Sadic, D., Fröhlich, J. J., Nuber, A., et al. (2012). CENP-C facilitates the recruitment of M18BP1 to centromeric chromatin. *Nucleus* 3, 101–110. doi: 10.4161/nucl.18955

David, C. J., Boyne, A. R., Millhouse, S. R., and Manley, J. L. (2011). The RNA polymerase II C-terminal domain promotes splicing activation through recruitment of a U2AF65-Prp19 complex. *Genes Dev.* 25, 972–983. doi: 10.1101/gad.2038011

Denegri, M., Moralli, D., Rocchi, M., Biggiogera, M., Raimondi, E., Cobianchi, F., et al. (2002). Human chromosomes 9, 12, and 15 contain the nucleation sites of stress-induced nuclear bodies. *Mol. Biol. Cell* 13, 2069–2079. doi: 10.1091/mbc.01-12-0569

Deyter, G. M. R., and Biggins, S. (2014). The FACT complex interacts with the E3 ubiquitin ligase Psh1 to prevent ectopic localization of CENP-A. *Genes Dev.* 28, 1815–1826. doi: 10.1101/gad.243113.114

Di Paolo, A., Racca, C., Calsou, P., and Larminat, F. (2014). Loss of BRCA1 impairs centromeric cohesion and triggers chromosomal instability. *FASEB J.* 28, 5250–5261. doi: 10.1096/fj.14-250266

Djupedal, I., Portoso, M., Spåhr, H., Bonilla, C., Gustafsson, C. M., Allshire, R. C., et al. (2005). RNA Pol II subunit Rpb7 promotes centromeric transcription and RNAi-directed chromatin silencing. *Genes Dev.* 19, 2301–2306. doi: 10.1101/gad.344205

Drané, P., Ouararhni, K., Depaux, A., Shuaib, M., and Hamiche, A. (2010). The death-associated protein DAXX is a novel histone chaperone involved in the replication-independent deposition of H3.3. *Genes Dev.* 24, 1253–1265. doi: 10.1101/gad.566910

Drinnenberg, I. A., DeYoung, D., Henikoff, S., and Malik, H. S. (2014). Recurrent loss of CenH3 is associated with independent transitions to holocentricity in insects. *eLife* 3:e03676. doi: 10.7554/eLife.03676

Du, Y., Topp, C. N., and Dawe, R. K. (2010). DNA binding of centromere protein C (CENPC) is stabilized by single-stranded RNA. *PLoS Genet.* 6:e1000835. doi: 10.1371/journal.pgen.1000835

Duda, Z., Trusiak, S., and O'Neill, R. (2017). Centromere transcription: means and motive. *Prog. Mol. Subcell. Biol.* 56, 257–281. doi: 10.1007/978-3-319-58592-5_11

Dunleavy, E. M., Almouzni, G., and Karpen, G. H. (2011). H3.3 is deposited at centromeres in S phase as a placeholder for newly assembled CENP-A in G 1 phase. *Nucleus* 2, 146–157. doi: 10.4161/nucl.2.2.15211

Dunleavy, E. M., Roche, D., Tagami, H., Lacoste, N., Ray-Gallet, D., Nakamura, Y., et al. (2009). HJURP is a cell-cycle-dependent maintenance and deposition factor of CENP-A at centromeres. *Cell* 137, 485–497. doi: 10.1016/j.cell.2009.02.040

Ebert, A., Lein, S., Schotta, G., and Reuter, G. (2006). Histone modification and the control of heterochromatic gene silencing in *Drosophila*. *Chromosome Res.* 14, 377–392. doi: 10.1007/s10577-006-1066-1

Ehrlich, M. (2009). DNA hypomethylation in cancer cells. *Epigenomics* 1, 239–259. doi: 10.2217/epi.09.33

Enukashvily, N. I., Donev, R., Waisertreiger, I. S.-R., and Podgornaya, O. I. (2007). Human chromosome 1 satellite 3 DNA is decondensed, demethylated and transcribed in senescent cells and in A431 epithelial carcinoma cells. *Cytogenet. Genome Res.* 118, 42–54. doi: 10.1159/000106440

Epstein, L. M., and Gall, J. G. (1987). Self-cleaving transcripts of satellite DNA from the newt. *Cell* 48, 535–543. doi: 10.1016/0092-8674(87)90204-2

Erhardt, S., Mellone, B. G., Betts, C. M., Zhang, W., Karpen, G. H., and Straight, A. F. (2008). Genome-wide analysis reveals a cell cycle-dependent mechanism controlling centromere propagation. *J. Cell Biol.* 183, 805–818. doi: 10.1083/jcb.200806038

Eymery, A., Callanan, M., and Vourc'h, C. (2009). The secret message of heterochromatin: new insights into the mechanisms and function of centromeric and pericentric repeat sequence transcription. *Int. J. Dev. Biol.* 53, 259–268. doi: 10.1387/ijdb.082673ae

Fachinetti, D., Diego Folco, H., Nechemia-Arbely, Y., Valente, L. P., Nguyen, K., Wong, A. J., et al. (2013). A two-step mechanism for epigenetic specification of centromere identity and function. *Nat. Cell Biol.* 15, 1056–1066. doi: 10.1038/ncb2805

Fachinetti, D., Han, J. S., McMahon, M. A., Ly, P., Abdullah, A., Wong, A. J., et al. (2015). DNA sequence-specific binding of CENP-B enhances the fidelity of human centromere function. *Dev. Cell* 33, 314–327. doi: 10.1016/j.devcel.2015.03.020

Fachinetti, D., Logsdon, G. A., Abdullah, A., Selzer, E. B., Cleveland, D. W., and Black, B. E. (2017). CENP-A modifications on Ser68 and Lys124 are dispensable for establishment, maintenance, and long-term function of human centromeres. *Dev. Cell* 40, 104–113. doi: 10.1016/j.devcel.2016.12.014

Fagegaltier, D., Bougé, A.-L., Berry, B., Poisot, E., Sismeiro, O., Coppée, J.-Y., et al. (2009). The endogenous siRNA pathway is involved in heterochromatin formation in *Drosophila*. *Proc. Natl. Acad. Sci. U.S.A.* 106, 21258–21263. doi: 10.1073/pnas.0809208105

Falk, S. J., Guo, L. Y., Sekulic, N., Smoak, E. M., Mani, T., Logsdon, G. A., et al. (2015). CENP-C reshapes and stabilizes CENP-A nucleosomes at the centromere. *Science* 348, 699–703. doi: 10.1126/science.1259308

Feliciello, I., Chinali, G., and Ugarković, Đ. (2011). Structure and population dynamics of the major satellite DNA in the red flour beetle *Tribolium castaneum*. *Genetica* 139, 999–1008. doi: 10.1007/s10709-011-9601-1

Ferbeyre, G., Smith, J. M., and Cedergren, R. (1998). Schistosome satellite DNA encodes active hammerhead ribozymes. *Mol. Cell. Biol.* 18, 3880–3888. doi: 10.1128/MCB.18.7.3880

Ferreri, G. C., Brown, J. D., Obergfell, C., Jue, N., Finn, C. E., O'Neill, M. J., et al. (2011). Recent amplification of the kangaroo endogenous retrovirus, KERV, limited to the centromere. *J. Virol.* 85, 4761–4771. doi: 10.1128/JVI.01604-10

Ferri, F., Bouzinba-Segard, H., Velasco, G., Hubé, F., and Francastel, C. (2009). Non-coding murine centromeric transcripts associate with and potentiate Aurora B kinase. *Nucleic Acids Res.* 37, 5071–5080. doi: 10.1093/nar/gkp529

Fischle, W., Tseng, B. S., Dormann, H. L., Ueberheide, B. M., Garcia, B. A., Shabanowitz, J., et al. (2005). Regulation of HP1–chromatin binding by histone H3 methylation and phosphorylation. *Nature* 438, 1116–1122. doi: 10.1038/nature04219

Flemming, W. (1880). Beitrage zur kenntniss der zelle und ihrer lebenserscheinungen. *Arch. Mikroskop. Anat.* 1879, 302–436.

Folco, H. D., Campbell, C. S., May, K. M., Espinoza, C. A., Oegema, K., Hardwick, K. G., et al. (2015). The CENP-A N-tail confers epigenetic stability to centromeres via the CENP-T branch of the CCAN in fission yeast. *Curr. Biol.* 25, 348–356. doi: 10.1016/J.CUB.2014.11.060

Foltz, D. R., Jansen, L. E. T., Bailey, A. O., Yates, J. R., Bassett, E. A., Wood, S., et al. (2009). Centromere-specific assembly of CENP-A nucleosomes is mediated by HJURP. *Cell* 137, 472–484. doi: 10.1016/j.cell.2009.02.039

Foltz, D. R., Jansen, L. E. T., Black, B. E., Bailey, A. O., Yates, J. R., and Cleveland, D. W. (2006). The human CENP-A centromeric nucleosome-associated complex. *Nat. Cell Biol.* 8, 458–469. doi: 10.1038/ncb1397

Frescas, D., Guardavaccaro, D., Kuchay, S. M., Kato, H., Poleshko, A., Basrur, V., et al. (2008). KDM2A represses transcription of centromeric satellite repeats and maintains the heterochromatic state. *Cell Cycle* 7, 3539–3547. doi: 10.4161/cc.7.22.7062

Frost, B., Hemberg, M., Lewis, J., and Feany, M. B. (2014). Tau promotes neurodegeneration through global chromatin relaxation. *Nat. Neurosci.* 17, 357–366. doi: 10.1038/nn.3639

Fujita, Y., Hayashi, T., Kiyomitsu, T., Toyoda, Y., Kokubu, A., Obuse, C., et al. (2007). Priming of centromere for CENP-A recruitment by human hMis18α, hMis18β, and M18BP1. *Dev. Cell* 12, 17–30. doi: 10.1016/j.devcel.2006.11.002

Fukagawa, T., and Earnshaw, W. C. (2014). The centromere: chromatin foundation for the kinetochore machinery. *Dev. Cell* 30, 496–508. doi: 10.1016/j.devcel.2014.08.016

Fukagawa, T., Nogami, M., Yoshikawa, M., Ikeno, M., Okazaki, T., Takami, Y., et al. (2004). Dicer is essential for formation of the heterochromatin structure in vertebrate cells. *Nat. Cell Biol.* 6, 784–791. doi: 10.1038/ncb1155

Garavís, M., Escaja, N., Gabelica, V., Villasante, A., and González, C. (2015a). Centromeric alpha-satellite DNA adopts dimeric I-motif structures capped by AT hoogsteen base pairs. *Chemistry* 21, 9816–9824. doi: 10.1002/chem.201500448

Garavís, M., Méndez-Lago, M., Gabelica, V., Whitehead, S. L., González, C., and Villasante, A. (2015b). The structure of an endogenous *Drosophila* centromere reveals the prevalence of tandemly repeated sequences able to form I-motifs. *Sci. Rep.* 5:13307. doi: 10.1038/srep13307

Gassmann, R., Rechtsteiner, A., Yuen, K. W., Muroyama, A., Egelhofer, T., Gaydos, L., et al. (2012). An inverse relationship to germline transcription defines centromeric chromatin in *C. elegans*. *Nature* 484, 534–537. doi: 10.1038/nature10973

Gaubatz, J. W., and Cutler, R. G. (1990). Mouse satellite DNA is transcribed in senescent cardiac muscle. *J. Biol. Chem.* 265, 17753–17758.

Gilbert, L. A., Horlbeck, M. A., Adamson, B., Villalta, J. E., Chen, Y., Whitehead, E. H., et al. (2014). Genome-scale CRISPR-mediated control of gene repression and activation. *Cell* 159, 647–661. doi: 10.1016/j.cell.2014.09.029

Gopalakrishnan, S., Sullivan, B. A., Trazzi, S., Della Valle, G., and Robertson, K. D. (2009). DNMT3B interacts with constitutive centromere protein CENP-C to modulate DNA methylation and the histone code at centromeric regions. *Hum. Mol. Genet.* 18, 3178–3193. doi: 10.1093/hmg/ddp256

Goshima, G., Wollman, R., Goodwin, S. S., Zhang, N., Scholey, J. M., Vale, R. D., et al. (2007). Genes required for mitotic spindle assembly in *Drosophila* S2 cells. *Science* 316, 417–421. doi: 10.1126/science.1141314

Grenfell, A. W., Heald, R., and Strzelecka, M. (2016). Mitotic noncoding RNA processing promotes kinetochore and spindle assembly in *Xenopus*. *J. Cell Biol.* 214, 133–141. doi: 10.1083/jcb.201604029

Gurel, Z., Ronni, T., Ho, S., Kuchar, J., Payne, K. J., Turk, C. W., et al. (2008). Recruitment of ikaros to pericentromeric heterochromatin is regulated by phosphorylation. *J. Biol. Chem.* 283, 8291–8300. doi: 10.1074/jbc.M707906200

Guse, A., Carroll, C. W., Moree, B., Fuller, C. J., and Straight, A. F. (2011). In vitro centromere and kinetochore assembly on defined chromatin templates. *Nature* 477, 354–358. doi: 10.1038/nature10379

Hall, L. E., Mitchell, S. E., and O'Neill, R. J. (2012). Pericentric and centromeric transcription: a perfect balance required. *Chromosome Res.* 20, 535–546. doi: 10.1007/s10577-012-9297-9

Hall, L. L., Byron, M., Carone, D. M., Whitfield, T. W., Pouliot, G. P., Fischer, A., et al. (2017). Demethylated HSATII DNA and HSATII RNA foci sequester PRC1 and MeCP2 into cancer-specific nuclear bodies. *Cell Rep.* 18, 2943–2956. doi: 10.1016/J.CELREP.2017.02.072

Hasson, D., Panchenko, T., Salimian, K. J., Salman, M. U., Sekulic, N., Alonso, A., et al. (2013). The octamer is the major form of CENP-A nucleosomes at human centromeres. *Nat. Struct. Mol. Biol.* 20, 687–695. doi: 10.1038/nsmb.2562

Hayashi, T., Fujita, Y., Iwasaki, O., Adachi, Y., Takahashi, K., and Yanagida, M. (2004). Mis16 and Mis18 are required for CENP-A loading and histone deacetylation at centromeres. *Cell* 118, 715–729. doi: 10.1016/j.cell.2004.09.002

Heckmann, S., Schroeder-Reiter, E., Kumke, K., Ma, L., Nagaki, K., Murata, M., et al. (2011). Holocentric chromosomes of *Luzula elegans* are characterized by a longitudinal centromere groove, chromosome bending, and a terminal nucleolus organizer region. *Cytogenet. Genome Res.* 134, 220–228. doi: 10.1159/000327713

Hédouin, S., Grillo, G., Ivkovic, I., Velasco, G., and Francastel, C. (2017). CENP-A chromatin disassembly in stressed and senescent murine cells. *Sci. Rep.* 7:42520. doi: 10.1038/srep42520

Henikoff, S., Ahmad, K., and Malik, H. S. (2001). The centromere paradox: stable inheritance with rapidly evolving DNA. *Science* 293, 1098–1102. doi: 10.1126/science.1062939

Herrera-Moyano, E., Mergui, X., García-Rubio, M. L., Barroso, S., and Aguilera, A. (2014). The yeast and human FACT chromatin reorganizing complexes solve R-loop mediated transcription-replication conflicts. *Genes Dev.* 28, 735–748. doi: 10.1101/gad.234070.113

Hetrr, E., and Allis, C. D. (2005). RNA meets chromatin. *Genes Dev.* 19, 1635–1655. doi: 10.1101/gad.1324305

Hill, A., and Bloom, K. (1987). Genetic manipulation of centromere function. *Mol. Cell. Biol.* 7, 2397–2405. doi: 10.1128/MCB.7.7.2397.Updated

Hillier, L. W., Miller, R. D., Baird, S. E., Chinwalla, A., Fulton, L. A., Koboldt, D. C., et al. (2007). Comparison of *C. elegans* and *C. briggsae* genome sequences reveals extensive conservation of chromosome organization and synteny. *PLoS Biol.* 5:e167. doi: 10.1371/journal.pbio.0050167

Hindriksen, S., Lens, S. M. A., and Hadders, M. A. (2017). The ins and outs of aurora B inner centromere localization. *Front. Cell Dev. Biol.* 5:112. doi: 10.3389/fcell.2017.00112

Holland, A. J., and Cleveland, D. W. (2009). Boveri revisited: chromosomal instability, aneuploidy and tumorigenesis. *Nat. Rev. Mol. Cell Biol.* 10, 478–487. doi: 10.1038/nrm2718

Holoch, D., and Moazed, D. (2015). RNA-mediated epigenetic regulation of gene expression. *Nat. Rev. Genet.* 16, 71–84. doi: 10.1038/nrg3863

Hori, T., Shang, W.-H., Toyoda, A., Misu, S., Monma, N., Ikeo, K., et al. (2014). Histone H4 Lys 20 monomethylation of the CENP-A nucleosome is essential for kinetochore assembly. *Dev. Cell* 29, 740–749. doi: 10.1016/J.DEVCEL.2014.05.001

Houseley, J., Kotovic, K., El Hage, A., and Tollervey, D. (2007). Trf4 targets ncRNAs from telomeric and rDNA spacer regions and functions in rDNA copy number control. *EMBO J.* 26, 4996–5006. doi: 10.1038/sj.emboj.7601921

Howe, J. A., Wang, H., Fischmann, T. O., Balibar, C. J., Xiao, L., Galgoci, A. M., et al. (2015). Selective small-molecule inhibition of an RNA structural element. *Nature* 526, 672–677. doi: 10.1038/nature15542

Hsieh, C.-L., Lin, C.-L., Liu, H., Chang, Y.-J., Shih, C.-J., Zhong, C. Z., et al. (2011). WDHD1 modulates the post-transcriptional step of the centromeric silencing pathway. *Nucleic Acids Res.* 39, 4048–4062. doi: 10.1093/nar/gkq1338

Huisinga, K. L., and Elgin, S. C. R. (2009). Small RNA-directed heterochromatin formation in the context of development: what flies might learn from fission yeast. *Biochim. Biophys. Acta* 1789, 3–16. doi: 10.1016/j.bbagrm.2008.08.002

Ichida, K., Suzuki, K., Fukui, T., Takayama, Y., Kakizawa, N., Watanabe, F., et al. (2018). Overexpression of satellite alpha transcripts leads to chromosomal instability via segregation errors at specific chromosomes. *Int. J. Oncol.* 52, 1685–1693. doi: 10.3892/ijo.2018.4321

Ideue, T., Cho, Y., Nishimura, K., and Tani, T. (2014). Involvement of satellite I noncoding RNA in regulation of chromosome segregation. *Genes Cells* 19, 528–538. doi: 10.1111/gtc.12149

Iotti, G., Longobardi, E., Masella, S., Dardaei, L., De Santis, F., Micali, N., et al. (2011). Homeodomain transcription factor and tumor suppressor Prep1 is required to maintain genomic stability. *Proc. Natl. Acad. Sci. U.S.A.* 108, E314–E322. doi: 10.1073/pnas.1105216108

Ishak, C. A., Marshall, A. E., Passos, D. T., White, C. R., Kim, S. J., Cecchini, M. J., et al. (2016). An RB-EZH2 complex mediates silencing of repetitive

DNA sequences. *Mol. Cell* 64, 1074–1087. doi: 10.1016/J.MOLCEL.2016.10.021

Jambhekar, A., Emerman, A. B., Schweidenback, C. T. H., and Blower, M. D. (2014). RNA stimulates aurora B kinase activity during mitosis. *PLoS One* 9:e100748. doi: 10.1371/journal.pone.0100748

Jeanpierre, M., Turleau, C., Aurias, A., Prieur, M., Ledeist, F., Fischer, A., et al. (1993). An embryonic-like methylation pattern of classical satellite DNA is observed in ICF syndrome. *Hum. Mol. Genet.* 2, 731–735. doi: 10.1093/hmg/2.6.731

Johnson, W. L., Yewdell, W. T., Bell, J. C., McNulty, S. M., Duda, Z., O'Neill, R. J., et al. (2017). RNA-dependent stabilization of SUV39H1 at constitutive heterochromatin. *eLife* 6:e25299. doi: 10.7554/eLife.25299

Jolly, C., Metz, A., Govin, J., Vigneron, M., Turner, B. M., Khochbin, S., et al. (2004). Stress-induced transcription of satellite III repeats. *J. Cell Biol.* 164, 25–33. doi: 10.1083/jcb.200306104

Jonstrup, A. T., Thomsen, T., Wang, Y., Knudsen, B. R., Koch, J., and Andersen, A. H. (2008). Hairpin structures formed by alpha satellite DNA of human centromeres are cleaved by human topoisomerase II. *Nucleic Acids Res.* 36, 6165–6174. doi: 10.1093/nar/gkn640

Joseph, A., Mitchell, A. R., and Miller, O. J. (1989). The organization of the mouse satellite DNA at centromeres. *Exp. Cell Res.* 183, 494–500. doi: 10.1016/0014-4827(89)90408-4

Kabeche, L., Nguyen, H. D., Buisson, R., and Zou, L. (2018). A mitosis-specific and R loop-driven ATR pathway promotes faithful chromosome segregation. *Science* 359, 108–114. doi: 10.1126/science.aan6490

Kagansky, A., Folco, H. D., Almeida, R., Pidoux, A. L., Boukaba, A., Simmer, F., et al. (2009). Synthetic heterochromatin bypasses RNAi and centromeric repeats to establish functional centromeres. *Science* 324, 1716–1719. doi: 10.1126/science.1172026

Kanellopoulou, C., Muljo, S. A., Kung, A. L., Ganesan, S., Drapkin, R., Jenuwein, T., et al. (2005). Dicer-deficient mouse embryonic stem cells are defective in differentiation and centromeric silencing. *Genes Dev.* 19, 489–501. doi: 10.1101/gad.1248505

Kapoor, M., Montes De Oca Luna, R., Liu, G., Lozano, G., Cummings, C., Mancini, M., et al. (1998). The cenpB gene is not essential in mice. *Chromosoma* 107, 570–576. doi: 10.1007/s004120050343

Kasinathan, S., and Henikoff, S. (2018). Non-B-form DNA is enriched at centromeres. *Mol. Biol. Evol.* 35, 949–962. doi: 10.1093/molbev/msy010

Kato, H., Goto, D. B., Martienssen, R. A., Urano, T., Furukawa, K., and Murakami, Y. (2005). RNA polymerase II is required for RNAi-dependent heterochromatin assembly. *Science* 309, 467–469. doi: 10.1126/science.1114955

Kato, H., Jiang, J., Zhou, B. R., Rozendaal, M., Feng, H., Ghirlando, R., et al. (2013). A conserved mechanism for centromeric nucleosome recognition by centromere protein CENP-C. *Science* 340, 1110–1113. doi: 10.1126/science.1235532

Kim, I. S., Lee, M., Park, K. C., Jeon, Y., Park, J. H., Hwang, E. J., et al. (2012). Roles of Mis18α in epigenetic regulation of centromeric chromatin and CENP-A loading. *Mol. Cell* 46, 260–273. doi: 10.1016/j.molcel.2012.03.021

Kishikawa, T., Otsuka, M., Suzuki, T., Seimiya, T., Sekiba, K., Ishibashi, R., et al. (2018). Satellite RNA increases DNA damage and accelerates tumor formation in mouse models of pancreatic cancer. *Mol. Cancer Res.* 16, 1255–1262. doi: 10.1158/1541-7786.MCR-18-0139

Kishikawa, T., Otsuka, M., Yoshikawa, T., Ohno, M., Ijichi, H., and Koike, K. (2016a). Satellite RNAs promote pancreatic oncogenic processes via the dysfunction of YBX1. *Nat. Commun.* 7:13006. doi: 10.1038/ncomms13006

Kishikawa, T., Otsuka, M., Yoshikawa, T., Ohno, M., Yamamoto, K., Yamamoto, N., et al. (2016b). Quantitation of circulating satellite RNAs in pancreatic cancer patients. *JCI Insight* 1:e86646. doi: 10.1172/jci.insight.86646

Kitamura, E., Tanaka, K., Kitamura, Y., and Tanaka, T. U. (2007). Kinetochore microtubule interaction during S phase in *Saccharomyces cerevisiae*. *Genes Dev.* 21, 3319–3330. doi: 10.1101/gad.449407

Kittler, R., Pelletier, L., Heninger, A. K., Slabicki, M., Theis, M., Miroslaw, L., et al. (2007). Genome-scale RNAi profiling of cell division in human tissue culture cells. *Nat. Cell Biol.* 9, 1401–1412. doi: 10.1038/ncb1659

Kloc, A., Zaratiegui, M., Nora, E., and Martienssen, R. (2008). RNA interference guides histone modification during the s phase of chromosomal replication. *Curr. Biol.* 18, 490–495. doi: 10.1016/j.cub.2008.03.016

Koch, L. (2017). Functional genomics: screening for lncRNA function. *Nat. Rev. Genet.* 18:70. doi: 10.1038/nrg.2016.168

Kumekawa, N., Hosouchi, T., Tsuruoka, H., and Kotani, H. (2001). The size and sequence organization of the centromeric region of *Arabidopsis thaliana* chromosome 4. *DNA Res.* 7, 315–321. doi: 10.1093/dnares/8.6.285

Lagana, A., Dorn, J. F., De Rop, V., Ladouceur, A. M., Maddox, A. S., and Maddox, P. S. (2010). A small GTPase molecular switch regulates epigenetic centromere maintenance by stabilizing newly incorporated CENP-A. *Nat. Cell Biol.* 12, 1186–1193. doi: 10.1038/ncb2129

Larson, K., Yan, S. J., Tsurumi, A., Liu, J., Zhou, J., Gaur, K., et al. (2012). Heterochromatin formation promotes longevity and represses ribosomal RNA synthesis. *PLoS Genet.* 8:e1002473. doi: 10.1371/journal.pgen.1002473

Lee, H.-R., Neumann, P., Macas, J., and Jiang, J. (2006). Transcription and evolutionary dynamics of the centromeric satellite repeat CentO in rice. *Mol. Biol. Evol.* 23, 2505–2520. doi: 10.1093/molbev/msl127

Lehnertz, B., Ueda, Y., Derijck, A. A. H. A., Braunschweig, U., Perez-Burgos, L., Kubicek, S., et al. (2003). Suv39h-mediated histone H3 lysine 9 methylation directs DNA methylation to major satellite repeats at pericentric heterochromatin. *Curr. Biol.* 13, 1192–1200. doi: 10.1016/S0960-9822(03)00432-9

Leonova, K. I., Brodsky, L., Lipchick, B., Pal, M., Novototskaya, L., Chenchik, A. A., et al. (2013). p53 cooperates with DNA methylation and a suicidal interferon response to maintain epigenetic silencing of repeats and noncoding RNAs. *Proc. Natl. Acad. Sci. U.S.A.* 110, E89–E98. doi: 10.1073/pnas.1216922110

Leung, W., Shaffer, C. D., Reed, L. K., Smith, S. T., Barshop, W., Dirkes, W., et al. (2015). *Drosophila* muller f elements maintain a distinct set of genomic properties over 40 million years of evolution. *G3* 5, 719–740. doi: 10.1534/g3.114.015966

Li, F., Sonbuchner, L., Kyes, S. A., Epp, C., and Deitsch, K. W. (2008). Nuclear non-coding RNAs are transcribed from the centromeres of *Plasmodium falciparum* and are associated with centromeric chromatin. *J. Biol. Chem.* 283, 5692–5698. doi: 10.1074/jbc.M707344200

Li, Y.-X., and Kirby, M. L. (2003). Coordinated and conserved expression of alphoid repeat and alphoid repeat-tagged coding sequences. *Dev. Dyn.* 228, 72–81. doi: 10.1002/dvdy.10355

Lindsay, J., Carone, D. M., Brown, J., Hall, L., Qureshi, S., Mitchell, S. E., et al. (2012). Unique small RNA signatures uncovered in the tammar wallaby genome. *BMC Genomics* 13:559. doi: 10.1186/1471-2164-13-559

Listerman, I., Sapra, A. K., and Neugebauer, K. M. (2006). Cotranscriptional coupling of splicing factor recruitment and precursor messenger RNA splicing in mammalian cells. *Nat. Struct. Mol. Biol.* 13, 815–822. doi: 10.1038/nsmb1135

Liu, H., Qu, Q., Warrington, R., Rice, A., Cheng, N., and Yu, H. (2015). Mitotic transcription installs Sgo1 at centromeres to coordinate chromosome segregation. *Mol. Cell* 59, 426–436. doi: 10.1016/j.molcel.2015.06.018

Liu, S. J., Horlbeck, M. A., Cho, S. W., Birk, H. S., Malatesta, M., He, D., et al. (2017). CRISPRi-based genome-scale identification of functional long noncoding RNA loci in human cells. *Science* 355:aah7111. doi: 10.1126/science.aah7111

Liu, S. T., Rattner, J. B., Jablonski, S. A., and Yen, T. J. (2006). Mapping the assembly pathways that specify formation of the trilaminar kinetochore plates in human cells. *J. Cell Biol.* 175, 41–53. doi: 10.1083/jcb.200606020

Logsdon, G. A., Barrey, E. J., Bassett, E. A., DeNizio, J. E., Guo, L. Y., Panchenko, T., et al. (2015). Both tails and the centromere targeting domain of CENP-A are required for centromere establishment. *J. Cell Biol.* 208, 521–531. doi: 10.1083/jcb.201412011

Lopes Novo, C., and Rugg-Gunn, P. (2016). Crosstalk between pluripotency factors and higher-order chromatin organization. *Nucleus* 7, 447–452. doi: 10.1080/19491034.2016.1248013

Lu, J., and Gilbert, D. M. (2007). Proliferation-dependent and cell cycle regulated transcription of mouse pericentric heterochromatin. *J. Cell Biol.* 179, 411–421. doi: 10.1083/jcb.200706176

Lu, Z., Zhang, Q. C., Lee, B., Flynn, R. A., Smith, M. A., Robinson, J. T., et al. (2016). RNA duplex map in living cells reveals higher-order transcriptome structure. *Cell* 165, 1267–1279. doi: 10.1016/j.cell.2016.04.028

Lunyak, V. V., Prefontaine, G. G., Núñez, E., Cramer, T., Ju, B. G., Ohgi, K. A., et al. (2007). Developmentally regulated activation of a SINE B2 repeat as a domain boundary in organogenesis. *Science* 317, 248–251. doi: 10.1126/science.1140871

Lyn Chan, F., and Wong, L. H. (2012). Transcription in the maintenance of centromere chromatin identity. *Nucleic Acids Res.* 40, 11178–11188. doi: 10.1093/nar/gks921

Maddox, P. S., Oegema, K., Desai, A., and Cheeseman, I. M. (2004). "Holo"er than thou: chromosome segregation and kinetochore function in *C. elegans*. *Chromosome Res.* 12, 641–653. doi: 10.1023/B:CHRO.0000036588.42225.2f

Maison, C., Bailly, D., Peters, A. H. F. M., Quivy, J.-P., Roche, D., Taddei, A., et al. (2002). Higher-order structure in pericentric heterochromatin involves a distinct pattern of histone modification and an RNA component. *Nat. Genet.* 30, 329–334. doi: 10.1038/ng843

Maison, C., Bailly, D., Roche, D., de Oca, R. M., Probst, A. V., Vassias, I., et al. (2011). SUMOylation promotes de novo targeting of HP1α to pericentric heterochromatin. *Nat. Genet.* 43, 220–227. doi: 10.1038/ng.765

Makarov, E. M., Makarova, O. V., Urlaub, H., Gentzel, M., Will, C. L., Wilm, M., et al. (2002). Small nuclear ribonucleoprotein remodeling during catalytic activation of the spliceosome. *Science* 298, 2205–2208. doi: 10.1126/science.1077783

Malik, H. S., and Henikoff, S. (2001). Adaptive evolution of cid, a centromere-specific histone in Drosophila. *Genetics* 157, 1293–1298.

Maloney, K. A., Sullivan, L. L., Matheny, J. E., Strome, E. D., Merrett, S. L., Ferris, A., et al. (2012). Functional epialleles at an endogenous human centromere. *Proc. Natl. Acad. Sci. U.S.A.* 109, 13704–13709. doi: 10.1073/pnas.1203126109

Mandal, S. S., Cho, H., Kim, S., Cabane, K., and Reinberg, D. (2002). FCP1, a phosphatase specific for the heptapeptide repeat of the largest subunit of RNA polymerase II, stimulates transcription elongation. *Mol. Cell. Biol.* 22, 7543–7552. doi: 10.1128/MCB.22.21.7543-7552.2002

Manuelidis, L., and Wu, J. C. (1978). Homology between human and simian repeated DNA. *Nature* 276, 92–94. doi: 10.1038/276092a0

Marshall, O. J., Chueh, A. C., Wong, L. H., and Choo, K. H. A. (2008). Neocentromeres: new insights into centromere structure, disease development, and karyotype evolution. *Am. J. Hum. Genet.* 82, 261–282. doi: 10.1016/j.ajhg.2007.11.009

Martens, J. H. A., O'Sullivan, R. J., Braunschweig, U., Opravil, S., Radolf, M., Steinlein, P., et al. (2005). The profile of repeat-associated histone lysine methylation states in the mouse epigenome. *EMBO J.* 24, 800–812. doi: 10.1038/sj.emboj.7600545

Martienssen, R. A., Zaratiegui, M., and Goto, D. B. (2005). RNA interference and heterochromatin in the fission yeast *Schizosaccharomyces pombe*. *Trends Genet.* 21, 450–456. doi: 10.1016/J.TIG.2005.06.005

Masumoto, H., Masukata, H., Muro, Y., Nozaki, N., and Okazaki, T. (1989). A human centromere antigen (CENP-B) interacts with a short specific sequence in alphoid DNA, a human centromeric satellite. *J. Cell Biol.* 109, 1963–1973. doi: 10.1083/jcb.109.5.1963

May, B. P., Lippman, Z. B., Fang, Y., Spector, D. L., and Martienssen, R. A. (2005). Differential regulation of strand-specific transcripts from *Arabidopsis* centromeric satellite repeats. *PLoS Genet.* 1:e79. doi: 10.1371/journal.pgen.0010079

McFarlane, R. J., Mian, S., and Dalgaard, J. Z. (2010). The many facets of the Tim-Tipin protein families' roles in chromosome biology. *Cell Cycle* 9, 700–705. doi: 10.4161/cc.9.4.10676

McKinley, K. L., and Cheeseman, I. M. (2014). Polo-like kinase 1 licenses CENP-a deposition at centromeres. *Cell* 158, 397–411. doi: 10.1016/j.cell.2014.06.016

McKinley, K. L., and Cheeseman, I. M. (2016). The molecular basis for centromere identity and function. *Nat. Rev. Mol. Cell Biol.* 17, 16–29. doi: 10.1038/nrm.2015.5

McNulty, S. M., Sullivan, L. L., and Sullivan, B. A. (2017). Human centromeres produce chromosome-specific and array-specific alpha satellite transcripts that are complexed with CENP-A and CENP-C. *Dev. Cell* 42, 226–240.e6. doi: 10.1016/j.devcel.2017.07.001

Mellone, B. G., Grive, K. J., Shteyn, V., Bowers, S. R., Oderberg, I., and Karpen, G. H. (2011). Assembly of Drosophila centromeric chromatin proteins during mitosis. *PLoS Genet.* 7:e1002068. doi: 10.1371/journal.pgen.1002068

Metz, A., Soret, J., Vourc'h, C., Tazi, J., and Jolly, C. (2004). A key role for stress-induced satellite III transcripts in the relocalization of splicing factors into nuclear stress granules. *J. Cell Sci.* 117, 4551–4558. doi: 10.1242/jcs.01329

Miniou, P., Jeanpierre, M., Bourc'his, D., Barbosa, A. C. C., Blanquet, V., and Viegas-Péquignot, E. (1997). α-Satellite DNA methylation in normal individuals and in ICF patients: heterogeneous methylation of constitutive heterochromatin in adult and fetal tissues. *Hum. Genet.* 99, 738–745. doi: 10.1007/s004390050441

Montembault, E., Dutertre, S., Prigent, C., and Giet, R. (2007). PRP4 is a spindle assembly checkpoint protein required for MPS1, MAD1, and MAD2 localization to the kinetochores. *J. Cell Biol.* 179, 601–609. doi: 10.1083/jcb.200703133

Moree, B., Meyer, C. B., Fuller, C. J., and Straight, A. F. (2011). CENP-C recruits M18BP1 to centromeres to promote CENP-A chromatin assembly. *J. Cell Biol.* 194, 855–871. doi: 10.1083/jcb.201106079

Morozov, V. M., Gavrilova, E. V., Ogryzko, V. V., and Ishov, A. M. (2012). Dualistic function of DAXX at centromeric and pericentromeric heterochromatin in normal and stress conditions. *Nucleus* 3, 276–285. doi: 10.4161/nucl.20180

Muchardt, C., Guillleme, M., Seeler, J. S., Trouche, D., Dejean, A., and Yaniv, M. (2002). Coordinated methyl and RNA binding is required for heterochromatin localization of mammalian HP1α. *EMBO Rep.* 3, 975–981. doi: 10.1093/embo-reports/kvf194

Mukarami, H., Goto, D. B., Toda, T., Chen, E. S., Grewal, S. I., Martienssen, R. A., et al. (2007). Ribonuclease activity of Dis3 is required for mitotic progression and provides a possible link between heterochromatin and kinetochore function. *PLoS One* 2:e317. doi: 10.1371/journal.pone.0000317

Müller, S., MontesdeOca, R., Lacoste, N., Dingli, F., Loew, D., and Almouzni, G. (2014). Phosphorylation and DNA binding of HJURP determine its centromeric recruitment and function in CenH3(CENP-A) loading. *Cell Rep.* 8, 190–203. doi: 10.1016/j.celrep.2014.06.002

Musacchio, A., and Desai, A. (2017). A molecular view of kinetochore assembly and function. *Biology* 6:E5. doi: 10.3390/biology6010005

Nagaki, K., Talbert, P. B., Zhong, C. X., Dawe, R. K., Henikoff, S., and Jiang, J. (2003). Chromatin immunoprecipitation reveals that the 180-bp satellite repeat is the key functional DNA element of *Arabidopsis thaliana* centromeres. *Genetics* 163, 1221–1225.

Nakaseko, Y., Kinoshita, N., and Yanagida, M. (1987). A novel sequence common to the centromere regions of *Schizosaccharomyces pombe* chromosomes. *Nucleic Acids Res.* 15, 4705–4715. doi: 10.1093/nar/15.12.4705

Nardi, I. K., Zasadzińska, E., Stellfox, M. E., Knippler, C. M., and Foltz, D. R. (2016). Licensing of centromeric chromatin assembly through the Mis18α-Mis18β heterotetramer. *Mol. Cell* 61, 774–787. doi: 10.1016/j.molcel.2016.02.014

Neumann, B., Walter, T., Hériché, J. K., Bulkescher, J., Erfle, H., Conrad, C., et al. (2010). Phenotypic profiling of the human genome by time-lapse microscopy reveals cell division genes. *Nature* 464, 721–727. doi: 10.1038/nature08869

Niedenthal, R., Stoll, R., and Hegemann, J. H. (1991). In vivo characterization of the *Saccharomyces cerevisiae* centromere DNA element I, a binding site for the helix-loop-helix protein CPF1. *Mol. Cell. Biol.* 11, 3545–3553. doi: 10.1128/MCB.11.7.3545

Niikura, Y., Kitagawa, R., and Kitagawa, K. (2017). CENP-A ubiquitylation is required for CENP-A deposition at the centromere. *Dev. Cell* 40, 7–8. doi: 10.1016/j.devcel.2016.12.020

Niikura, Y., Kitagawa, R., Ogi, H., Abdulle, R., Pagala, V., and Kitagawa, K. (2015). CENP-A K124 ubiquitylation is required for CENP-A deposition at the centromere. *Dev. Cell* 32, 589–603. doi: 10.1016/J.DEVCEL.2015.01.024

Novikova, I. V., Dharap, A., Hennelly, S. P., and Sanbonmatsu, K. Y. (2013). 3S: shotgun secondary structure determination of long non-coding RNAs. *Methods* 63, 170–177. doi: 10.1016/j.ymeth.2013.07.030

O'Brien, S. L., Fagan, A., Fox, E. J. P., Millikan, R. C., Culhane, A. C., Brennan, D. J., et al. (2007). CENP-F expression is associated with poor prognosis and chromosomal instability in patients with primary breast cancer. *Int. J. Cancer* 120, 1434–1443. doi: 10.1002/ijc.22413

Oestergaard, V. H., and Lisby, M. (2016). TopBP1 makes the final call for repair on the verge of cell division. *Mol. Cell. Oncol.* 3:e1093066. doi: 10.1080/23723556.2015.1093066

Ohkuni, K., and Kitagawa, K. (2011). Endogenous transcription at the centromere facilitates centromere activity in budding yeast. *Curr. Biol.* 21, 1695–1703. doi: 10.1016/j.cub.2011.08.056

Ohno, M., Fukagawa, T., Lee, J. S., and Ikemura, T. (2002). Triplex-forming DNAs in the human interphase nucleus visualized in situ

by polypurine/polypyrimidine DNA probes and antitriplex antibodies. *Chromosoma* 111, 201–213. doi: 10.1007/s00412-002-0198-0

Ohzeki, J., Nakano, M., Okada, T., and Masumoto, H. (2002). CENP-B box is required for de novo centromere chromatin assembly on human alphoid DNA. *J. Cell Biol.* 159, 765–775. doi: 10.1083/jcb.200207112

Ohzeki, J., Shono, N., Otake, K., Martins, N. M. C., Kugou, K., Kimura, H., et al. (2016). KAT7/HBO1/MYST2 regulates CENP-A chromatin assembly by antagonizing Suv39h1-mediated centromere inactivation. *Dev. Cell* 37, 413–427. doi: 10.1016/j.devcel.2016.05.006

Okada, M., Okawa, K., Isobe, T., and Fukagawa, T. (2009). CENP-H–containing complex facilitates centromere deposition of CENP-A in cooperation with FACT and CHD1. *Mol. Biol. Cell* 20, 3986–3995. doi: 10.1091/mbc.e09-01-0065

Panchenko, T., Sorensen, T. C., Woodcock, C. L., Kan, Z.-Y., Wood, S., Resch, M. G., et al. (2011). Replacement of histone H3 with CENP-A directs global nucleosome array condensation and loosening of nucleosome superhelical termini. *Proc. Natl. Acad. Sci. U.S.A.* 108, 16588–16593. doi: 10.1073/pnas.1113621108

Partridge, J. F., Borgstrøm, B., and Allshire, R. C. (2000). Distinct protein interaction domains and protein spreading in a complex centromere. *Genes Dev.* 14, 783–791. doi: 10.1101/GAD.14.7.783

Perea-Resa, C., and Blower, M. D. (2018). Centromere biology: transcription goes on stage. *Mol. Cell. Biol.* 38:e00263-18. doi: 10.1128/MCB.00263-18

Perpelescu, M., Nozaki, N., Obuse, C., Yang, H., and Yoda, K. (2009). Active establishment of centromeric CENP-A chromatin by RSF complex. *J. Cell Biol.* 185, 397–407. doi: 10.1083/jcb.200903088

Pezer, Z., Brajković, J., Feliciello, I., and Ugarković, D. (2012). Satellite DNA-mediated effects on genome regulation. *Genome Dyn.* 7, 153–169. doi: 10.1159/000337116

Pezer, Ž., and Ugarković, Đ. (2008). Role of non-coding RNA and heterochromatin in aneuploidy and cancer. *Semin. Cancer Biol.* 18, 123–130. doi: 10.1016/J.SEMCANCER.2008.01.003

Pfister, S. X., and Ashworth, A. (2017). Marked for death: targeting epigenetic changes in cancer. *Nat. Rev. Drug Discov.* 16, 241–263. doi: 10.1038/nrd.2016.256

Prendergast, L., Müller, S., Liu, Y., Huang, H., Dingli, F., Loew, D., et al. (2016). The CENP-T/-W complex is a binding partner of the histone chaperone FACT. *Genes Dev.* 30, 1313–1326. doi: 10.1101/gad.275073.115

Quénet, D., and Dalal, Y. (2014). A long non-coding RNA is required for targeting centromeric protein A to the human centromere. *eLife* 3:e03254. doi: 10.7554/eLife.03254

Reddy, K., Tam, M., Bowater, R. P., Barber, M., Tomlinson, M., Nichol Edamura, K., et al. (2011). Determinants of R-loop formation at convergent bidirectionally transcribed trinucleotide repeats. *Nucleic Acids Res.* 39, 1749–1762. doi: 10.1093/nar/gkq935

Regnier, V., Vagnarelli, P., Fukagawa, T., Zerjal, T., Burns, E., Trouche, D., et al. (2005). CENP-A is required for accurate chromosome segregation and sustained kinetochore association of BubR1. *Mol. Cell. Biol.* 25, 3967–3981. doi: 10.1128/MCB.25.10.3967-3981.2005

Reinhart, B. J., and Bartel, D. P. (2002). Small RNAs correspond to centromere heterochromatic repeats. *Science* 297:1831. doi: 10.1126/science.1077183

Rieder, C. L. (1979). Ribonucleoprotein staining of centrioles and kinetochores in newt lung cell spindles. *J. Cell Biol.* 80, 1–9. doi: 10.1083/jcb.80.1.1

Rizzi, N., Denegri, M., Chiodi, I., Corioni, M., Valgardsdottir, R., Cobianchi, F., et al. (2004). Transcriptional activation of a constitutive heterochromatic domain of the human genome in response to heat shock. *Mol. Biol. Cell* 15, 543–551. doi: 10.1091/mbc.E03-07-0487

Rojas, A. A., Vazquez-Tello, A., Ferbeyre, G., Venanzetti, F., Bachmann, L., Paquin, B., et al. (2000). Hammerhead-mediated processing of satellite pDo500 family transcripts from *Dolichopoda* cave crickets. *Nucleic Acids Res.* 28, 4037–4043. doi: 10.1093/nar/28.20.4037

Román, A. C., González-Rico, F. J., and Fernandez-Salguero, P. M. (2011). B1-SINE retrotransposons. *Mob. Genet. Elements* 1, 66–70. doi: 10.4161/mge.1.1.15455

Rose, N. R., and Klose, R. J. (2014). Understanding the relationship between DNA methylation and histone lysine methylation. *Biochim. Biophys. Acta Gene Regul. Mech.* 1839, 1362–1372. doi: 10.1016/J.BBAGRM.2014.02.007

Rošić, S., Köhler, F., and Erhardt, S. (2014). Repetitive centromeric satellite RNA is essential for kinetochore formation and cell division. *J. Cell Biol.* 207, 335–349. doi: 10.1083/jcb.201404097

Rudert, F., Bronner, S., Garnier, J. M., and Dollé, P. (1995). Transcripts from opposite strands of gamma satellite DNA are differentially expressed during mouse development. *Mamm. Genome* 6, 76–83.

Sadeghi, L., Siggens, L., Svensson, J. P., and Ekwall, K. (2014). Centromeric histone H2B monoubiquitination promotes noncoding transcription and chromatin integrity. *Nat. Struct. Mol. Biol.* 21, 236–243. doi: 10.1038/nsmb.2776

Saksouk, N., Simboeck, E., and Déjardin, J. (2015). Constitutive heterochromatin formation and transcription in mammals. *Epigenetics Chromatin* 8:3. doi: 10.1186/1756-8935-8-3

Sakuno, T., Tada, K., and Watanabe, Y. (2009). Kinetochore geometry defined by cohesion within the centromere. *Nature* 458, 852–858. doi: 10.1038/nature07876

Sanchez-Pulido, L., Pidoux, A. L., Ponting, C. P., and Allshire, R. C. (2009). Common ancestry of the CENP-A chaperones Scm3 and HJURP. *Cell* 137, 1173–1174. doi: 10.1016/j.cell.2009.06.010

Santaguida, S., and Amon, A. (2015). Short- and long-term effects of chromosome mis-segregation and aneuploidy. *Nat. Rev. Mol. Cell Biol.* 16, 473–485. doi: 10.1038/nrm4025

Santenard, A., Ziegler-Birling, C., Koch, M., Tora, L., Bannister, A. J., and Torres-Padilla, M.-E. (2010). Heterochromatin formation in the mouse embryo requires critical residues of the histone variant H3.3. *Nat. Cell Biol.* 12, 853–862. doi: 10.1038/ncb2089

Sathyan, K. M., Fachinetti, D., and Foltz, D. R. (2017). α-amino trimethylation of CENP-A by NRMT is required for full recruitment of the centromere. *Nat. Commun.* 8:14678. doi: 10.1038/ncomms14678

Scaffidi, P., and Misteli, T. (2006). Lamin A-dependent nuclear defects in human aging. *Science* 312, 1059–1063. doi: 10.1126/science.1127168

Schueler, M. G., Swanson, W., Thomas, P. J., and Green, E. D. (2010). Adaptive evolution of foundation kinetochore proteins in primates. *Mol. Biol. Evol.* 27, 1585–1597. doi: 10.1093/molbev/msq043

Scott, K. C., Merrett, S. L., and Willard, H. F. (2006). A heterochromatin barrier partitions the fission yeast centromere into discrete chromatin domains. *Curr. Biol.* 16, 119–129. doi: 10.1016/J.CUB.2005.11.065

Scott, K. C., White, C. V., and Willard, H. F. (2007). An RNA polymerase III-dependent heterochromatin barrier at fission yeast centromere 1. *PLoS One* 2:e1099. doi: 10.1371/journal.pone.0001099

Shandilya, J., Senapati, P., Hans, F., Menoni, H., Bouvet, P., Dimitrov, S., et al. (2014). Centromeric histone variant CENP-A represses acetylation-dependent chromatin transcription that is relieved by histone chaperone NPM1. *J. Biochem.* 156, 221–227. doi: 10.1093/jb/mvu034

Shang, W.-H., Hori, T., Westhorpe, F. G., Godek, K. M., Toyoda, A., Misu, S., et al. (2016). Acetylation of histone H4 lysine 5 and 12 is required for CENP-A deposition into centromeres. *Nat. Commun.* 7:13465. doi: 10.1038/ncomms13465

Shestakova, E. A., Mansuroglu, Z., Mokrani, H., Ghinea, N., and Bonnefoy, E. (2004). Transcription factor YY1 associates with pericentromeric γ -satellite DNA in cycling but not in quiescent (G0) cells. *Nucleic Acids Res.* 32, 4390–4399. doi: 10.1093/nar/gkh737

Shumaker, D. K., Dechat, T., Kohlmaier, A., Adam, S. A., Bozovsky, M. R., Erdos, M. R., et al. (2006). Mutant nuclear lamin A leads to progressive alterations of epigenetic control in premature aging. *Proc. Natl. Acad. Sci. U.S.A.* 103, 8703–8708. doi: 10.1073/pnas.0602569103

Silva, M. C. C., Bodor, D. L., Stellfox, M. E., Martins, N. M. C., Hochegger, H., Foltz, D. R., et al. (2012). CDK activity couples epigenetic centromere inheritance to cell cycle progression. *Dev. Cell* 22, 52–63. doi: 10.1016/j.devcel.2011.10.014

Slee, R. B., Steiner, C. M., Herbert, B.-S., Vance, G. H., Hickey, R. J., Schwarz, T., et al. (2012). Cancer-associated alteration of pericentromeric heterochromatin may contribute to chromosome instability. *Oncogene* 31, 3244–3253. doi: 10.1038/onc.2011.502

Solovei, I., Wang, A. S., Thanisch, K., Schmidt, C. S., Krebs, S., Zwerger, M., et al. (2013). LBR and lamin A/C sequentially tether peripheral heterochromatin and

inversely regulate differentiation. *Cell* 152, 584–598. doi: 10.1016/j.cell.2013.01.009

Somma, M. P., Ceprani, F., Bucciarelli, E., Naim, V., De Arcangelis, V., Piergentili, R., et al. (2008). Identification of *Drosophila* mitotic genes by combining co-expression analysis and RNA interference. *PLoS Genet.* 4:e1000126. doi: 10.1371/journal.pgen.1000126

Srivastava, S., Zasadzińska, E., and Foltz, D. R. (2018). Posttranslational mechanisms controlling centromere function and assembly. *Curr. Opin. Cell Biol.* 52, 126–135. doi: 10.1016/J.CEB.2018.03.003

Steiner, F. A., and Henikoff, S. (2014). Holocentromeres are dispersed point centromeres localized at transcription factor hotspots. *eLife* 3:e02025. doi: 10.7554/ELIFE.02025

Sugimoto, K., Kuriyama, K., Shibata, A., and Himeno, M. (1997). Characterization of internal DNA-binding and C-terminal dimerization domains of human centromere/kinetochore autoantigen CEN P-C in vitro: role of DNA-binding and self-associating activities in kinetochore organization. *Chromosome Res.* 5, 132–141. doi: 10.1023/A:1018422325569

Sullivan, B. A., and Karpen, G. H. (2004). Centromeric chromatin exhibits a histone modification pattern that is distinct from both euchromatin and heterochromatin. *Nat. Struct. Mol. Biol.* 11, 1076–1083. doi: 10.1038/nsmb845

Sun, D., and Hurley, L. H. (2009). The importance of negative superhelicity in inducing the formation of G-quadruplex and I-motif structures in the c-Myc promoter: implications for drug targeting and control of gene expression. *J. Med. Chem.* 52, 2863–2874. doi: 10.1021/jm900055s

Sun, X., Clermont, P. L., Jiao, W., Helgason, C. D., Gout, P. W., Wang, Y., et al. (2016). Elevated expression of the centromere protein-A(CENP-A)-encoding gene as a prognostic and predictive biomarker in human cancers. *Int. J. Cancer* 139, 899–907. doi: 10.1002/ijc.30133

Tachiwana, H., Müller, S., Blümer, J., Klare, K., Musacchio, A., and Almouzni, G. (2015). HJURP involvement in de novo CenH3(CENP-A) and CENP-C recruitment. *Cell Rep.* 11, 22–32. doi: 10.1016/j.celrep.2015.03.013

Takada, M., Zhang, W., Suzuki, A., Kuroda, T. S., Yu, Z., Inuzuka, H., et al. (2017). FBW7 loss promotes chromosomal instability and tumorigenesis via cyclin E1/CDK2–mediated phosphorylation of CENP-A. *Cancer Res.* 77, 4881–4893. doi: 10.1158/0008-5472.CAN-17-1240

Talbert, P. B., Bryson, T. D., and Henikoff, S. (2004). Adaptive evolution of centromere proteins in plants and animals. *J. Biol.* 3:18. doi: 10.1186/jbiol11

Tanaka, K., Mukae, N., Dewar, H., Van Breugel, M., James, E. K., Prescott, A. R., et al. (2005). Molecular mechanisms of kinetochore capture by spindle microtubules. *Nature* 434, 987–994. doi: 10.1038/nature03483

Tasselli, L., Xi, Y., Zheng, W., Tennen, R. I., Odrowaz, Z., Simeoni, F., et al. (2016). SIRT6 deacetylates H3K18ac at pericentric chromatin to prevent mitotic errors and cellular senescence. *Nat. Struct. Mol. Biol.* 23, 434–440. doi: 10.1038/nsmb.3202

Thiru, P., Kern, D. M., McKinley, K. L., Monda, J. K., Rago, F., Su, K.-C., et al. (2014). Kinetochore genes are coordinately up-regulated in human tumors as part of a FoxM1-related cell division program. *Mol. Biol. Cell* 25, 1983–1994. doi: 10.1091/mbc.e14-03-0837

Ting, D. T., Lipson, D., Paul, S., Brannigan, B. W., Akhavanfard, S., Coffman, E. J., et al. (2011). Aberrant overexpression of satellite repeats in pancreatic and other epithelial cancers. *Science* 331, 593–596. doi: 10.1126/science.1200801

Tittel-Elmer, M., Bucher, E., Broger, L., Mathieu, O., Paszkowski, J., and Vaillant, I. (2010). Stress-induced activation of heterochromatic transcription. *PLoS Genet.* 6:e1001175. doi: 10.1371/journal.pgen.1001175

Tomoyasu, Y., Miller, S. C., Tomita, S., Schoppmeier, M., Grossmann, D., and Bucher, G. (2008). Exploring systemic RNA interference in insects: a genome-wide survey for RNAi genes in *Tribolium*. *Genome Biol.* 9:R10. doi: 10.1186/gb-2008-9-1-r10

Topp, C. N., Zhong, C. X., and Dawe, R. K. (2004). Centromere-encoded RNAs are integral components of the maize kinetochore. *Proc. Natl. Acad. Sci. U.S.A.* 101, 15986–15991. doi: 10.1073/pnas.0407154101

Tyler-Smith, C., and Brown, W. R. A. (1987). Structure of the major block of alphoid satellite DNA on the human Y chromosome. *J. Mol. Biol.* 195, 457–470. doi: 10.1016/0022-2836(87)90175-6

Ugarković, Đ., Podnar, M., and Plohl, M. (1996). Satellite DNA of the red flour beetle *Tribolium castaneum*–comparative study of satellites from the genus Tribolium. *Mol. Biol. Evol.* 13, 1059–1066. doi: 10.1093/oxfordjournals.molbev.a025668

Vafa, O., and Sullivan, K. F. (1997). Chromatin containing CENP-A and alpha-satellite DNA is a major component of the inner kinetochore plate. *Curr. Biol.* 7, 897–900. doi: 10.1016/S0960-9822(06)00381-2

Vakoc, C. R., Sachdeva, M. M., Wang, H., and Blobel, G. A. (2006). Profile of histone lysine methylation across transcribed mammalian chromatin. *Mol. Cell. Biol.* 26, 9185–9195. doi: 10.1128/MCB.01529-06

Valgardsdottir, R., Chiodi, I., Giordano, M., Rossi, A., Bazzini, S., Ghigna, C., et al. (2008). Transcription of satellite III non-coding RNAs is a general stress response in human cells. *Nucleic Acids Res.* 36, 423–434. doi: 10.1093/nar/gkm1056

van Hooser, A. A., Ouspenski, I. I., Gregson, H. C., Starr, D. A., Yen, T. J., Goldberg, M. L., et al. (2001). Specification of kinetochore-forming chromatin by the histone H3 variant CENP-A. *J. Cell Sci.* 114, 3529–3542. doi: 10.1007/bf00332792

Velazquez Camacho, O., Galan, C., Swist-Rosowska, K., Ching, R., Gamalinda, M., Karabiber, F., et al. (2017). Major satellite repeat RNA stabilize heterochromatin retention of Suv39h enzymes by RNA-nucleosome association and RNA:DNA hybrid formation. *eLife* 6:e25293. doi: 10.7554/eLife.25293

Vissel, B., Nagy, A., and Choo, K. H. (1992). A satellite III sequence shared by human chromosomes 13, 14, and 21 that is contiguous with alpha satellite DNA. *Cytogenet. Cell Genet.* 61, 81–86. doi: 10.1159/000133374

Volpe, T. A., Kidner, C., Hall, I. M., Teng, G., Grewal, S. I. S., and Martienssen, R. A. (2002). Regulation of heterochromatic silencing and histone H3 lysine-9 methylation by RNAi. *Science* 297, 1833–1837. doi: 10.1126/science.1074973

Wang, F., Ulyanova, N. P., van der Waal, M. S., Patnaik, D., Lens, S. M. A., and Higgins, J. M. G. (2011). A positive feedback loop involving haspin and aurora B promotes CPC accumulation at centromeres in mitosis. *Curr. Biol.* 21, 1061–1069. doi: 10.1016/J.CUB.2011.05.016

Wang, Z., Zang, C., Rosenfeld, J. A., Schones, D. E., Barski, A., Cuddapah, S., et al. (2008). Combinatorial patterns of histone acetylations and methylations in the human genome. *Nat. Genet.* 40, 897–903. doi: 10.1038/ng.154

Warburton, P. E., Cooke, C. A., Bourassa, S., Vafa, O., Sullivan, B. A., Stetten, G., et al. (1997). Immunolocalization of CENP-A suggests a distinct nucleosome structure at the inner kinetochore plate of active centromeres. *Curr. Biol.* 7, 901–904. doi: 10.1016/S0960-9822(06)00382-4

Warecki, B., and Sullivan, W. (2018). Micronuclei formation is prevented by aurora B-mediated exclusion of HP1a from late-segregating chromatin in *Drosophila*. *Genetics* 210, 171–187. doi: 10.1534/genetics.118.301031

Westhorpe, F. G., Fuller, C. J., and Straight, A. F. (2015). A cell-free CENP-A assembly system defines the chromatin requirements for centromere maintenance. *J. Cell Biol.* 209, 789–801. doi: 10.1083/jcb.201503132

Wilkinson, K. A., Merino, E. J., and Weeks, K. M. (2006). Selective 2′-hydroxyl acylation analyzed by primer extension (SHAPE): quantitative RNA structure analysis at single nucleotide resolution. *Nat. Protoc.* 1, 1610–1616. doi: 10.1038/nprot.2006.249

Willard, H. F. (1985). Chromosome-specific organization of human alpha satellite DNA. *Am. J. Hum. Genet.* 37, 524–532.

Wisniewski, J., Hajj, B., Chen, J., Mizuguchi, G., Xiao, H., Wei, D., et al. (2014). Imaging the fate of histone CSE4 reveals de novo replacement in S phase and subsequent stable residence at centromeres. *eLife* 3:e02203. doi: 10.7554/eLife.02203

Wong, L. H., Brettingham-Moore, K. H., Chan, L., Quach, J. M., Anderson, M. A., Northrop, E. L., et al. (2007). Centromere RNA is a key component for the assembly of nucleoproteins at the nucleolus and centromere. *Genome Res.* 17, 1146–1160. doi: 10.1101/gr.6022807

Wu, R., Singh, P. B., and Gilbert, D. M. (2006). Uncoupling global and fine-tuning replication timing determinants for mouse pericentric heterochromatin. *J. Cell Biol.* 174, 185–194. doi: 10.1083/jcb.200601113

Yamagishi, Y., Honda, T., Tanno, Y., and Watanabe, Y. (2010). Two histone marks establish the inner centromere and chromosome bi-orientation. *Science* 330, 239–243. doi: 10.1126/science.1194498

Yang, C. H., Tomkiel, J., Saitoh, H., Johnson, D. H., and Earnshaw, W. C. (1996). Identification of overlapping DNA-binding and centromere-targeting domains

in the human kinetochore protein CENP-C. *Mol. Cell. Biol.* 16, 3576–3586. doi: 10.1128/MCB.16.7.3576

Yi, Q., Chen, Q., Liang, C., Yan, H., Zhang, Z., Xiang, X., et al. (2018). HP1 links centromeric heterochromatin to centromere cohesion in mammals. *EMBO Rep.* 19:e45484. doi: 10.15252/embr.201745484

Zakrzewski, F., Weisshaar, B., Fuchs, J., Bannack, E., Minoche, A. E., Dohm, J. C., et al. (2011). Epigenetic profiling of heterochromatic satellite DNA. *Chromosoma* 120, 409–422. doi: 10.1007/s00412-011-0325-x

Zaratiegui, M., Castel, S. E., Irvine, D. V., Kloc, A., Ren, J., Li, F., et al. (2011). RNAi promotes heterochromatic silencing through replication-coupled release of RNA Pol II. *Nature* 479, 135–138. doi: 10.1038/nature10501

Zeitlin, S. G., Shelby, R. D., and Sullivan, K. F. (2001). CENP-A is phosphorylated by aurora B kinase and plays an unexpected role in completion of cytokinesis. *J. Cell Biol.* 155, 1147–1158. doi: 10.1083/jcb.200108125

Zhang, T., Talbert, P. B., Zhang, W., Wu, Y., Yang, Z., Henikoff, J. G., et al. (2013). The CentO satellite confers translational and rotational phasing on CENH3 nucleosomes in rice centromeres. *Proc. Natl. Acad. Sci. U.S.A.* 110, E4875–E4883. doi: 10.1073/pnas.1319548110

Zhang, W., Mao, J.-H., Zhu, W., Jain, A. K., Liu, K., Brown, J. B., et al. (2016). Centromere and kinetochore gene misexpression predicts cancer patient survival and response to radiotherapy and chemotherapy. *Nat. Commun.* 7:12619. doi: 10.1038/ncomms12619

Zhang, W., Yeung, C. H. L., Wu, L., and Yuen, K. W. Y. (2017). E3 ubiquitin ligase Bre1 couples sister chromatid cohesion establishment to DNA replication in *Saccharomyces cerevisiae*. *eLife* 6:e28231. doi: 10.7554/eLife.28231

Zhu, L., Chou, S. H., and Reid, B. R. (1996). A single G-to-C change causes human centromere TGGAA repeats to fold back into hairpins. *Proc. Natl. Acad. Sci. U.S.A.* 93, 12159–12164. doi: 10.1073/PNAS.93.22.12159

Zhu, Q., Hoong, N., Aslanian, A., Hara, T., Benner, C., Heinz, S., et al. (2018). Heterochromatin-encoded satellite RNAs induce breast cancer. *Mol. Cell* 70, 842–853.e7. doi: 10.1016/J.MOLCEL.2018.04.023

Zhu, Q., Pao, G. M., Huynh, A. M., Suh, H., Tonnu, N., Nederlof, P. M., et al. (2011). BRCA1 tumour suppression occurs via heterochromatin-mediated silencing. *Nature* 477, 179–184. doi: 10.1038/nature10371

Conflict of Interest Statement: The authors declare that the research was conducted in the absence of any commercial or financial relationships that could be construed as a potential conflict of interest.

frontiers in Genetics

ORIGINAL RESEARCH
published: 19 December 2018
doi: 10.3389/fgene.2018.00676

Altered Expression of Mitochondrial NAD$^+$ Carriers Influences Yeast Chronological Lifespan by Modulating Cytosolic and Mitochondrial Metabolism

Ivan Orlandi[1,2], *Giulia Stamerra*[2] *and Marina Vai*[2]*

[1] SYSBIO Centre for Systems Biology, Milan, Italy, [2] Dipartimento di Biotecnologie e Bioscienze, Università di Milano-Bicocca, Milan, Italy

Nicotinamide adenine dinucleotide (NAD$^+$) represents an essential cofactor in sustaining cellular bioenergetics and maintaining cellular fitness, and has emerged as a therapeutic target to counteract aging and age-related diseases. Besides NAD$^+$ involvement in multiple redox reactions, it is also required as co-substrate for the activity of Sirtuins, a family of evolutionary conserved NAD$^+$-dependent deacetylases that regulate both metabolism and aging. The founding member of this family is Sir2 of *Saccharomyces cerevisiae*, a well-established model system for studying aging of post-mitotic mammalian cells. In this context, it refers to chronological aging, in which the chronological lifespan (CLS) is measured. In this paper, we investigated the effects of changes in the cellular content of NAD$^+$ on CLS by altering the expression of mitochondrial NAD$^+$ carriers, namely Ndt1 and Ndt2. We found that the deletion or overexpression of these carriers alters the intracellular levels of NAD$^+$ with opposite outcomes on CLS. In particular, lack of both carriers decreases NAD$^+$ content and extends CLS, whereas *NDT1* overexpression increases NAD$^+$ content and reduces CLS. This correlates with opposite cytosolic and mitochondrial metabolic assets shown by the two types of mutants. In the former, an increase in the efficiency of oxidative phosphorylation is observed together with an enhancement of a pro-longevity anabolic metabolism toward gluconeogenesis and trehalose storage. On the contrary, *NDT1* overexpression brings about on the one hand, a decrease in the respiratory efficiency generating harmful superoxide anions, and on the other, a decrease in gluconeogenesis and trehalose stores: all this is reflected into a time-dependent loss of mitochondrial functionality during chronological aging.

Keywords: NAD$^+$, chronological lifespan, Ndt1, Ndt2, *Saccharomyces cerevisiae*

OPEN ACCESS

Edited by:
Maria Grazia Giansanti, Istituto di Biologia e Patologia Molecolari (IBPM), Italy

Reviewed by:
Sergio Giannattasio, Istituto di Biomembrane, Bioenergetica e Biotecnologie Molecolari (IBIOM), Italy
Manuela Côrte-Real, University of Minho, Portugal

***Correspondence:**
Marina Vai
marina.vai@unimib.it

Specialty section:
This article was submitted to Genetic Disorders, a section of the journal Frontiers in Genetics

Received: *04 September 2018*
Accepted: *04 December 2018*
Published: *19 December 2018*

Citation:
Orlandi I, Stamerra G and Vai M (2018) Altered Expression of Mitochondrial NAD$^+$ Carriers Influences Yeast Chronological Lifespan by Modulating Cytosolic and Mitochondrial Metabolism. Front. Genet. 9:676. doi: 10.3389/fgene.2018.00676

INTRODUCTION

Significant progress has been made in elucidating fundamental processes such as human aging/longevity as a result of studies performed in the budding yeast *Saccharomyces cerevisiae*. In this single-celled yeast, replicative aging and chronological aging are two complementary models that are used to simulate cellular aging of mitotically active and post-mitotic mammalian cells,

respectively (MacLean et al., 2001; Longo and Kennedy, 2006; Longo et al., 2012). The former cell type is exemplified by fibroblasts and the latter by myocytes.

In the presence of nutrients, *S.cerevisiae* divides asymmetrically (budding) resulting in a large mother cell and a smaller daughter (bud). In this context, the replicative lifespan (RLS), namely the number of buds generated by a mother cell before senescence, indicates the reproductive potential of individual yeast cells (Steinkraus et al., 2008). The chronological lifespan (CLS), instead, refers to the rate of post-mitotic survival of a non-dividing quiescent yeast culture; viability is assessed by measuring the percentage of cells able to resume growth and form a colony after transfer from the depleted medium to the rich fresh one (Fabrizio and Longo, 2007). In a standard CLS experiment, yeast cells are grown in synthetic media with 2% glucose. When glucose becomes limiting, the diauxic shift occurs and cells shift from glucose-driven fermentation to ethanol-driven respiration. This shift determines a metabolic reprogramming, the outcomes of which influence the CLS. Afterwards cell proliferation stops and the yeast culture enters a quiescent stationary phase (Gray et al., 2004; Wanichthanarak et al., 2015). CLS is determined starting 72 h after the diauxic shift (Fabrizio and Longo, 2007).

The signaling pathways and regulators controlling RLS and CLS are evolutionary conserved (Fontana et al., 2010; Swinnen et al., 2014; Bitto et al., 2015; Baccolo et al., 2018). In particular, nicotinamide adenine dinucleotide (NAD^+) homeostasis has emerged as a critical element in the regulation of aging/longevity (Imai, 2010, 2016) and accumulating evidence suggests that a reduction of NAD^+ levels in diverse organisms contributes to the development of age-associated metabolic decline (Imai and Guarente, 2014, 2016; Verdin, 2015). Indeed, in addition to its central role in cellular metabolism participating as essential coenzyme in many redox reactions, NAD^+ is absolutely required as a co-substrate by Sirtuins, a family of NAD^+-dependent deacetylases, the founding member of which is Sir2 of *S.cerevisiae* (Houtkooper et al., 2012; Imai and Guarente, 2014). In mammals, there are seven Sirtuin isoforms (SIRT1-7) and among them SIRT1 is a key component of the systemic regulatory network called "the NAD world," a comprehensive concept that connects NAD^+ metabolism and aging/longevity control in mammals (Imai, 2009, 2010, 2016). The nutrient-sensing SIRT1 is the closest mammalian ortholog of Sir2 (Frye, 2000). Sir2 activity is involved in both replicative and chronological aging: in the former Sir2 extends RLS (Kaeberlein et al., 1999; Imai et al., 2000), whilst in the latter it has a pro-aging role (Fabrizio et al., 2005; Smith et al., 2007; Casatta et al., 2013; Orlandi et al., 2017a).

The other key component of the NAD world is represented by NAD^+ biosynthesis (Imai, 2009, 2010). From yeast to mammalian cells, NAD^+ synthesis occurs either *de novo* from L- tryptophan or through *salvage* pathway(s) from its precursors, namely nicotinamide riboside, nicotinic acid, and its amide form, nicotinamide (Bogan and Brenner, 2008; Canto et al., 2015). Cells mainly rely on the *salvage* pathway(s) for the correct maintenance of NAD^+ levels and it has been observed that the supplementation of NAD^+ precursors is sufficient to attenuate several metabolic defects common to the aging process (Johnson and Imai, 2018; Mitchell et al., 2018; Rajman et al., 2018). However, NAD^+ levels, as well as those of its precursors, are different depending on the type of tissue and cellular compartment (Dolle et al., 2010; Houtkooper et al., 2010; Cambronne et al., 2016) and it remains unclear in which cellular compartment(s) NAD^+ decrease can be relevant to aging. This has increased the interest on the role, on the one hand, of inter-tissue communications (Imai, 2016) and, on the other hand, of the relative subcellular localization of NAD^+ and its precursors during the aging process (Koch-Nolte et al., 2011; Rajman et al., 2018).

In yeast, NAD^+ is synthesized in the cytosol and can be imported across the inner mitochondrial membrane by two specific mitochondrial NAD^+ carriers, namely Ndt1 and Ndt2, which share 70% homology (Todisco et al., 2006). The physiological effects linked to an *NDT1* and *NDT2* double deletion and to the overexpression of *NDT1*, which encodes the main isoform of the NAD^+ transporter (Todisco et al., 2006), have been examined on cells growing with an oxidative or respiro-fermentative metabolism in batch and glucose-limited chemostat cultures (Agrimi et al., 2011).

Here, we show that during chronological aging an altered expression of the specific mitochondrial NAD^+ carriers deeply influences the metabolic reprogramming that enables cells to acquire features required to maintain viability during chronological aging. In particular, lack of *NDT1* and *NDT2* extends CLS, whereas *NDT1* overexpression determines a CLS reduction. This opposite effect on CLS correlates with opposite metabolic features displayed by the two mutants.

MATERIALS AND METHODS

Yeast Strains, Growth Conditions and CLS Determination

The *ndt1*Δ*ntd2*Δ strain and the strain overexpressing *NDT1* (*NDT1*-over strain) were constructed in a previous work (Agrimi et al., 2011) and were derivatives of CEN.PK113-7D (*MAT*a, *MAL2*-8c, *SUC2*). A null mutant *ndt1*Δ*ntd2*Δ (*ndt1*Δ::*URA3 ntd2*Δ::*KlLEU2*) was generated by PCR-based methods in a W303-1A background (*MAT*a *ade2-1 his3-11,15 leu2-3,112 trp1-1 ura3-1 can1-100*). The accurancy of gene replacements was verified by PCR with flanking and internal primers. Cells were grown in batches at 30°C in minimal medium (Difco Yeast Nitrogen Base without amino acids, 6.7 g/L) with 2% w/v glucose. Auxotrophies were compensated for with supplements added in excess (Orlandi et al., 2014). Cell number and cellular volumes were determined using a Coulter Counter-Particle Count and Size Analyser (Vanoni et al., 1983). Duplication time (Td) was obtained by linear regression of the cell number increase over time on a semi-logarithmic plot. For CLS experiments, cells were grown in 2% glucose and the extracellular concentration of glucose and ethanol were measured in medium samples collected at different time-points in order to define the growth profile [exponential phase, diauxic shift (Day 0), post-diauxic phase and stationary phase of the cultures] (Orlandi et al., 2013). CLS was

measured according to (Fabrizio et al., 2005) by counting colony-forming units (CFU) starting with 72 h (Day 3, first age-point) after Day 0. The number of CFU on Day 3 was considered the initial survival (100%).

Isolation of Mitochondria

Mitochondria were prepared from chronologically aging cells essentially as described by Meisinger et al. (2006) with minor modifications. At each time-point, 10^9 cells were collected by centrifugation and spheroplasts were obtained by digestion with Zymolyase 20T. Then, spheroplasts were homogenized by 20 strokes using a Dounce homogenizer and mitochondria collected after differential centrifugation (Meisinger et al., 2006). Fresh crude mitochondrial pellets were used for measurements of NAD^+, NADH, and protein contents.

Metabolite Measurements and Enzymatic Assays

At designated time-points, aliquots of the yeast cultures were centrifuged, and both pellets (washed twice) and supernatants were collected and frozen at −80°C until used. Rapid sampling for intracellular metabolite measurements was performed as previously described (Orlandi et al., 2014). The concentrations of glucose, ethanol, citrate, succinate, and malate were determined using enzymatic assays (K-HKGLU, K-ETOH, K-SUCC, K-CITR, and K-LMALR kits from Megazyme).

To measure NADH and NAD^+ contents, alkali, and acid extractions were performed essentially as described (Lin et al., 2001), except that before incubation of both the alkali extract and the acid one at for 30 min, an additional step was performed in order to improve cells lysis. Alkali or acid-washed glass beads were added to the two types of extracts and cells broken by vortexing (3 cycles of 1 min, interspersed with cooling on ice). NAD^+ and NADH concentrations were determined using the EnzyChrom™ NAD^+/NADH assay kit (BioAssay Systems). The rate of dye formation (formazan) at 565 nm correlates with the level of pyridine nucleotides. Duplicate reactions were performed in multi-well plates or in cuvettes. Different amounts of each sample were used in cycling reactions to obtain values within the linear portion of a standard curve that was prepared every time.

Immediately after preparation of cell-free extracts (Orlandi et al., 2014), the activities of cytosolic and mitochondrial aldehyde dehydrogenase (Ald) were assayed according to Aranda and del Olmo (2003), of phosphoenolpyruvate carboxykinase (Pck1) and isocitrate lyase (Icl1) as described in de Jong-Gubbels et al. (1995). Total protein concentration was estimated using the BCA™ Protein Assay Kit (Pierce).

Fluorescence Microscopy

Dihydroethidium (DHE, Sigma-Aldrich) staining was performed as reported in Madeo et al. (1999) to detect superoxide anion (O_2^-). A Nikon Eclipse E600 fluorescence microscope equipped with a Nikon Digital Sight DS Qi1 camera was used. Digital images were acquired and processed using Nikon software NIS-Elements.

Estimation of Oxygen Consumption Rates and Index of Respiratory Competence

The basal oxygen consumption of intact cells was measured at 30°C using a "Clark-type" oxygen electrode (Oxygraph System, Hansatech Instruments, Nortfolk, UK) as reported (Orlandi et al., 2013). The non-phosphorylating respiration and the maximal/uncoupled respiratory capacity were measured in the presence of 37.5 mM triethyltin bromide (TET, Sigma-Aldrich) and 10 μM of the uncoupler carbonyl cyanide 3-chlorophenylhydrazone (CCCP, Sigma-Aldrich), respectively (Orlandi et al., 2017a). The addition of 2 M antimycin A (Sigma-Aldrich) accounted for non-mitochondrial oxygen consumption. Respiratory rates for the basal oxygen consumption (J_R), the maximal/uncoupled oxygen consumption (J_{MAX}) and the non-phosphorylating oxygen consumption (J_{TET}) were determined from the slope of a plot of O_2 concentration against time, divided by the cellular concentration.

Index of respiratory competence (IRC) was measured according to Parrella and Longo (2008) by plating identical cell samples on YEP (1% w/v yeast extract, 2% w/v bacto peptone)/2% glucose (YEPD) plates and on rich medium/3% glycerol (YEPG) plates. IRC was calculated as colonies on YEPG divided by colonies on YEPD times 100%.

Statistical Analysis of Data

All values are presented as the mean of three independent experiments ± Standard Deviation (SD). Three technical replicates were analyzed in each independent experiment. Statistical significance was assessed by one-way ANOVA test. The level of statistical significance was set at a P value of ≤ 0.05.

RESULTS AND DISCUSSION

Altered Expression of the Specific Mitochondrial NAD+ Carriers Affects CLS

Due to the importance of NAD^+ homeostasis in the aging process from yeast to humans (Baccolo et al., 2018; Rajman et al., 2018; Yaku et al., 2018), we wished to test whether changes in the cellular content of this dinucleotide would cause any effects on CLS. To this end we chose to use the *ndt1*Δ*ndt2*Δ and *NDT1*-over mutant strains: the former lacking the two mitochondrial NAD^+ carriers, Ndt1 and Ndt2, identified so far and the latter overexpressing Ndt1, which is the main isoform of the carrier (Todisco et al., 2006; Agrimi et al., 2011). These strains have been previously characterized as far as NAD content is concerned (Agrimi et al., 2011). In particular, under a fully respiratory metabolism such as growth on ethanol, Ndt1 overexpression determined an increase in cellular and mitochondrial NAD^+ levels without affecting growth. On the contrary, on ethanol the *ndt1*Δ*ndt2*Δ mutant displayed a lower cellular and mitochondrial NAD^+ content and a decrease in the growth rate (Agrimi et al., 2011). Here, an *ndt1*Δ*ndt2*Δ double mutant generated in the W303-1A background was also included. Indeed, the W303-1A strain is commonly used in chronological aging research due to its robust respiratory capacity (Ocampo et al., 2012).

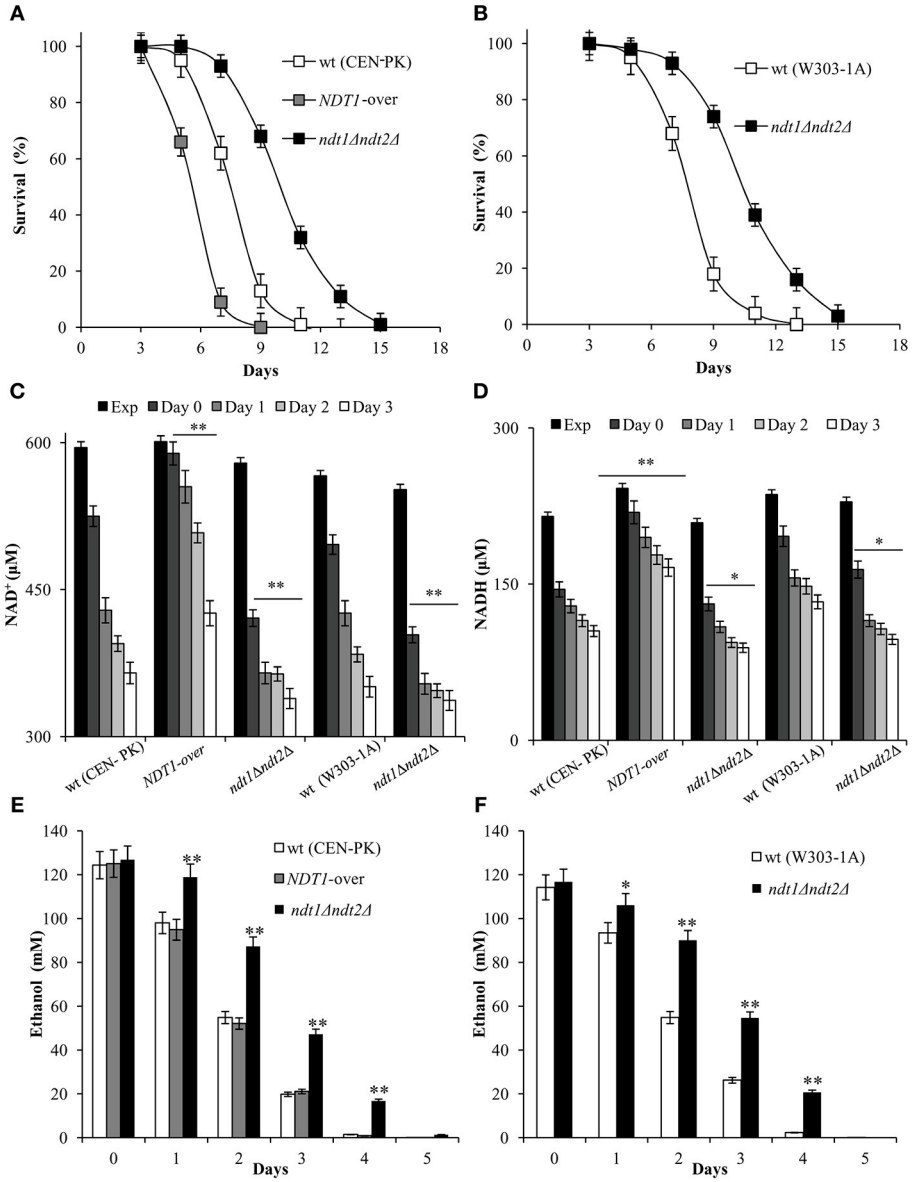

FIGURE 1 | The *NDT1*-over mutant and the *ndt1* Δ*ndt2*Δ one have a short-lived and a long-lived phenotype, respectively. The indicated strains were grown in minimal medium/2% glucose and the required supplements in excess (see section Materials and Methods) and followed up to stationary phase. **(A,B)** CLS was determined by assessing clonogenicity on YEPD plates. 72 h after the diauxic shift (Day 3) was considered the first age-point (100% survival). Day 0, diauxic shift. In parallel, intracellular NAD^+ **(C)**, NADH **(D)** and extracellular ethanol **(E,F)** concentrations were determined at the indicated time-points. Exp, exponential growth phase. All data refer to mean values of three independent experiments with three technical replicates each. Standard deviation (SD) is indicated. Statistical significance as assessed by one-way ANOVA test is indicated (*$P \leq 0.05$ and **$P \leq 0.01$).

Initially, in the context of a standard CLS experiment (Fabrizio and Longo, 2007), we measured CLS and NAD content. As shown in **Figure 1A**, Ndt1 overexpression significantly reduced CLS, whilst the strain devoid of the two mitochondrial NAD^+ carriers lived longer than the prototrophic wild type (wt) CEN.PK 113-7D. The same long-lived phenotype was observed in the auxotrophic background W303-1A (**Figure 1B**) indicating that the different composition of amino acids in the medium does not influence the results. Measurements of intracellular NAD^+ and NADH contents indicated that in the wt, they decreased progressively after the diauxic shift (**Figures 1C,D**). We calculated values of NAD^+ and NADH estimating cell size with a Coulter Counter-Particle Count and Size Analyser: cell size that changes according to the yeast strain and the growth phase of the cell cycle. If we assume a yeast cell size of 70 μm^3 (Sherman, 2002) our measurements of 595 μM NAD^+ (**Figure 1C**) and 215 μM NADH for CEN.PK 113-7D in exponential phase (**Figure 1D**) correspond to 1.42 mM NAD^+

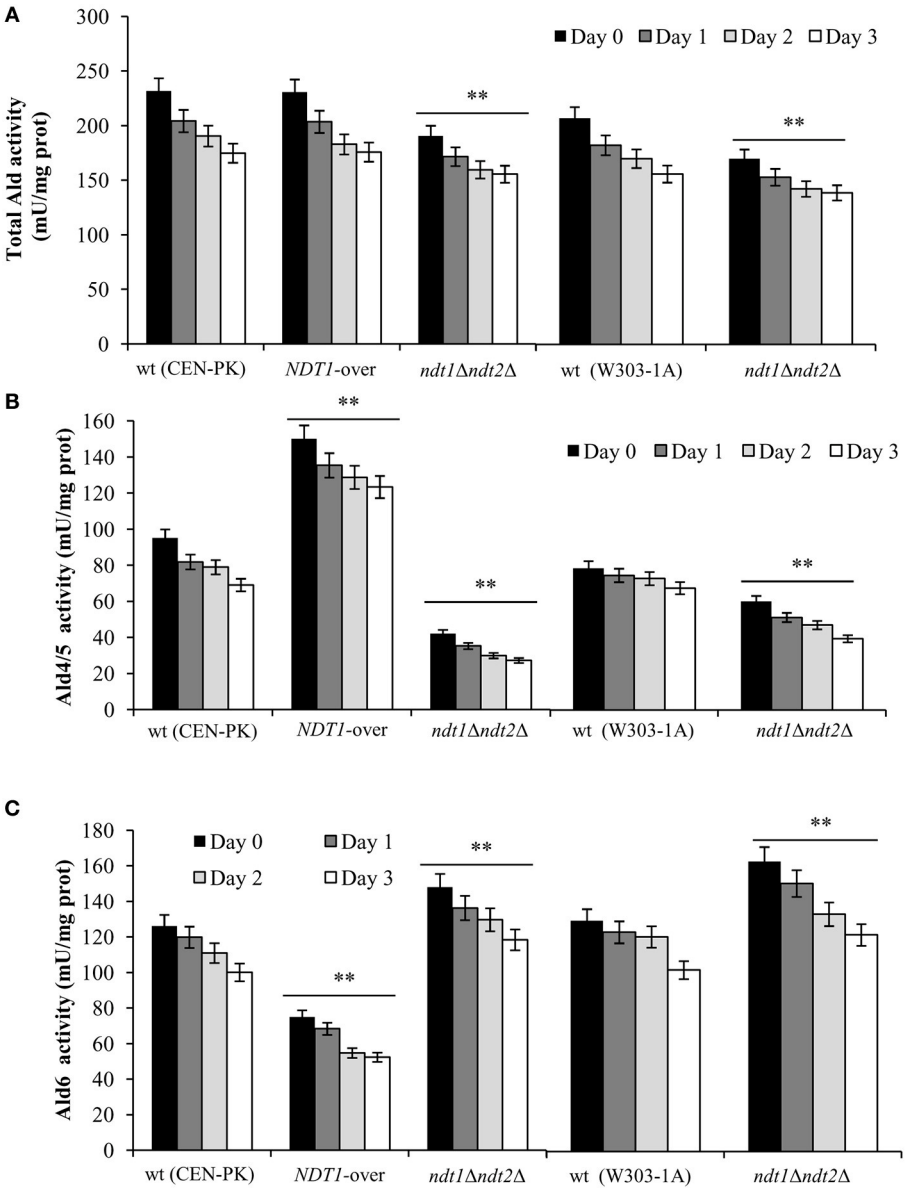

FIGURE 2 | Altered expression of mitochondrial NAD$^+$ carriers influences Ald enzymatic activities. In the context of CLS experiments of **Figure 1**, total Ald **(A)**, Ald4/5 **(B)**, and Ald6 **(C)** enzymatic activities were measured at the indicated time-points. Day 0, diauxic shift. All data are the mean ± SD obtained from three independent experiments with three technical replicates each. Statistical significance as in **Figure 1** (**$P \leq 0.01$).

and 0.82 mM NADH, in reasonable agreement with values of previous reports (Lin et al., 2004). In the context of the CLS experimental set-up, as the diauxic shift occurs and cells utilize the excreted fermentation by-product, ethanol, in the *ndt1*Δ*ndt2*Δ mutant, and in the *NDT1*-over one NAD$^+$ and NADH levels decreased, but both remained constantly lower in the *ndt1*Δ*ndt2*Δ mutant and higher in the *NDT1*-over mutant than those measured in the wt (**Figures 1C,D**). This opposite trend of the dinucleotide contents observed in the two different types of mutants is in line with that detected during exponential growth on ethanol (Agrimi et al., 2011).

It is well known that NAD$^+$ is an essential coenzyme for oxidoreductases of both cytosolic and mitochondrial redox reactions, many of which are involved in the metabolic remodeling that takes place at the diauxic shift. Indeed, at the diauxic shift carbon metabolism shifts from fermentation to mitochondrial respiration and gluconeogenesis allowing cells to be better primed for survival during chronological aging. Thus, we analyzed the metabolic features of the short-lived *NDT1*-over strain and those of the long-lived *ndt1*Δ*ndt2*Δ one. Since the respiration-based metabolism is due to the utilization of ethanol, we initially measured the consumption of this C2

TABLE 1 | Effects of altered expression of mitochondrial NAD^+ carriers on the enzymatic activity of Ald isoforms.

	Day 0	Day 1	Day 2	Day 3
wt (CEN-PK 113-7D)				
Total Ald	227.8 ± 8.7	202.2 ± 3.9	188.3 ± 4.1	170.8 ± 6.9
% Ald6	57	59	58	59
% Ald4/5	43	41	42	41
***NDT1*-OVER**				
Total Ald	231.3 ± 4.2	203.6 ± 6.5	182.1 ± 2.7	176.2 ± 1.4
% Ald6	32**	33**	30**	29**
% Ald4/5	68**	67**	70**	71**
***ndt1*Δ*ndt2*Δ**				
Total Ald	190.4** ± 5.6	171.6** ± 7.2	159.5** ± 4.3	155.6** ± 8.1
% Ald6	78**	79**	81**	77**
% Ald4/5	22**	21**	19**	23**
wt (W303-1A)				
Total Ald	202.9 ± 6.4	185.6 ± 3.8	172.4 ± 7.6	156.2 ± 4.7
% Ald6	59	61	55	63
% Ald4/5	41	39	45	37
***ndt1*Δ*ndt2*Δ**				
Total Ald	174.3** ± 2.9	157.8** ± 8.3	146.1** ± 6.1	128.9** ± 7.7
% Ald6	83**	78**	84**	79**
% Ald4/5	17**	22**	16**	21**

For each time-point total Ald, Ald6, and Ald4/5 enzymatic activities were determined as in ***Figure 2*** *and the percentage of the different Ald isoforms was calculated. Day 0, diauxic shift. Data refer to mean values determined in three independent experiments with three technical replicates each. SD is indicated. Values obtained for wt strains were used as reference for comparisons with NDT1-over and ndt1Δ ndt2Δ cells. (**$P \leq 0.01$, one-way ANOVA test).*

compound. At the diauxic shift (Day 0), the maximal amount of the extracellular ethanol was not affected either by the lack of Ndt1 and Ndt2 or by the Ndt1 overexpression (**Figures 1E,F**). Differently, during the post-diauxic phase in the *ndt1*Δ*ndt2*Δ mutant ethanol decreased more slowly (**Figures 1C,D**). This is indicative of an impairment in ethanol utilization in line with the slow growth rate on medium containing ethanol as carbon source (Agrimi et al., 2011). Consequently, starting from Day 0, we determined the enzymatic activities of the acetaldehyde dehydrogenases (Alds). These enzymes are implicated in the ethanol utilization: they oxidize the acetaldehyde generated from ethanol oxidation producing acetate, which is subsequently converted to acetyl-CoA. In addition, Alds require NAD^+ or $NADP^+$. No difference was detected between the wt and the *NDT1*-over strain in the total Ald activity levels (**Figure 2A**). On the contrary, in the *ndt1*Δ*ndt2*Δ strain a significant decrease was observed (**Figure 2A**) consistent with the reduced ethanol utilization. Notably, interesting results were obtained by measuring the different isoforms of Alds, namely the mitochondrial Ald4/5, and the primary cytosolic counterpart Ald6 (Saint-Prix et al., 2004). Indeed, the activity levels of Ald4/5 were higher and those of Ald6 lower in the *NDT1*-over strain compared with the wt ones, whilst in the *ndt1*Δ*ndt2*Δ strain the Ald6 activity prevailed (**Figures 2B,C**). Since, alterations of the mitochondrial NAD^+ transport are accompanied by a different prevalent subcellular localization of Ald enzymatic activities (**Table 1**), it is reasonable to speculate that in the two different mutants the metabolic pathways that are fed by mitochondrial or cytosolic acetate/acetyl-CoA could be affected. In this context, we initially measured the enzymatic activity of one of the unique enzymes of the glyoxylate shunt, such as isocitrate lyase (Icl1), and that of phosphoenolpyruvate carboxykinase (Pck1), which catalyzes the rate-limiting step in gluconeogenesis. Indeed, starting from the diauxic shift, the glyoxylate shunt becomes operative. It is an anaplerotic device of the TCA cycle, is fed by the cytosolic acetyl-CoA and is the sole possible provider for the Pck1 substrate, namely oxaloacetate (Lee et al., 2011). In the *NDT1*-over strain a decrease in the enzymatic activities of Icl1 and Pck1 was observed, whilst in the *ndt1*Δ*ndt2*Δ mutant both activities strongly increased (**Figures 3A,B**). Since glucose-6-phosphate produced by gluconeogenesis is used for the synthesis of threalose during the post-diauxic phase, we also examined the accumulation of this disaccharide, the intracellular stores of which are advantageous for survival during chronological aging (Shi et al., 2010). In the *NDT1*-over strain a reduction in trehalose levels took place (**Figure 3C**), consistent with the decrease of the Pck1 activity. On the contrary, the *ndt1*Δ*ndt2*Δ cells accumulated more trehalose (**Figure 3C**), consistent with the increase of the Pck1 activity. Taken together, these results indicate that the lack of the two mitochondrial NAD^+ carriers elicits an enhancement along the cytosolic Ald6/glyoxylate/gluconeogenesis axis, whereas Ndt1 overexpression elicits a down-regulation.

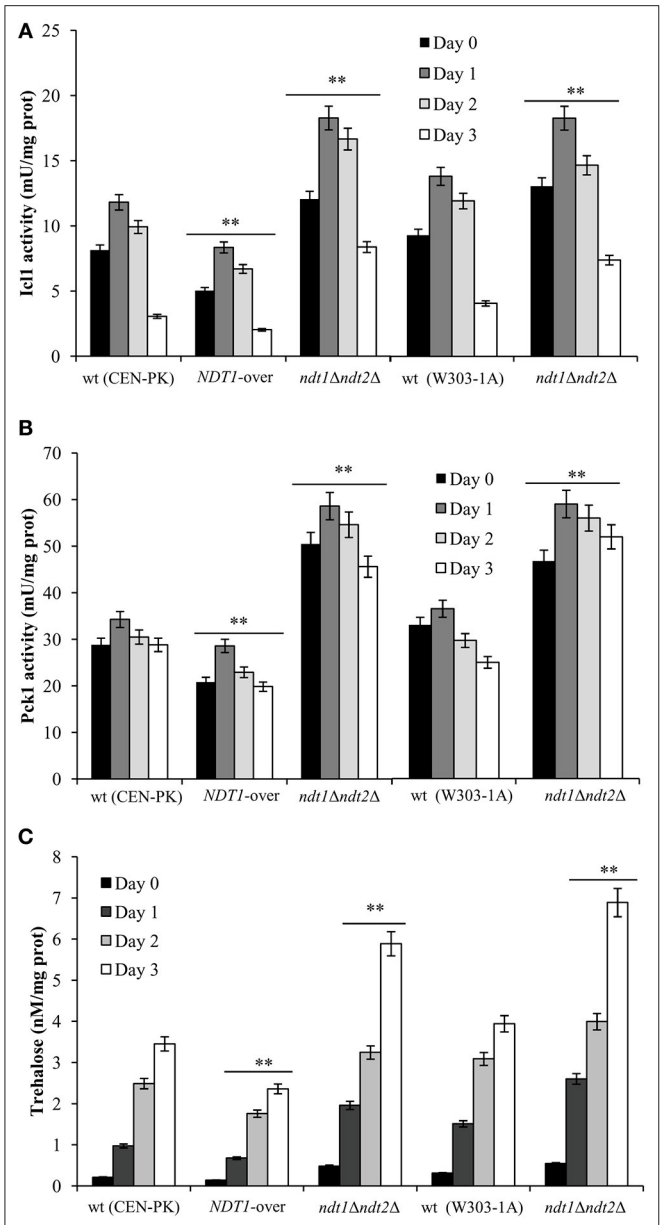

FIGURE 3 | Altered expression of mitochondrial NAD+ carriers influences gluconeogenesis and threalose levels. Bar charts of Icl1 **(A)** and Pck1 **(B)** enzymatic activities and intracellular trehalose concentrations **(C)** determined for the indicated strains grown as in **Figure 1**. Day 0, diauxic shift. All data refer to mean values of three independent experiments with three technical replicates each. SD is indicated (**$P \leq 0.01$).

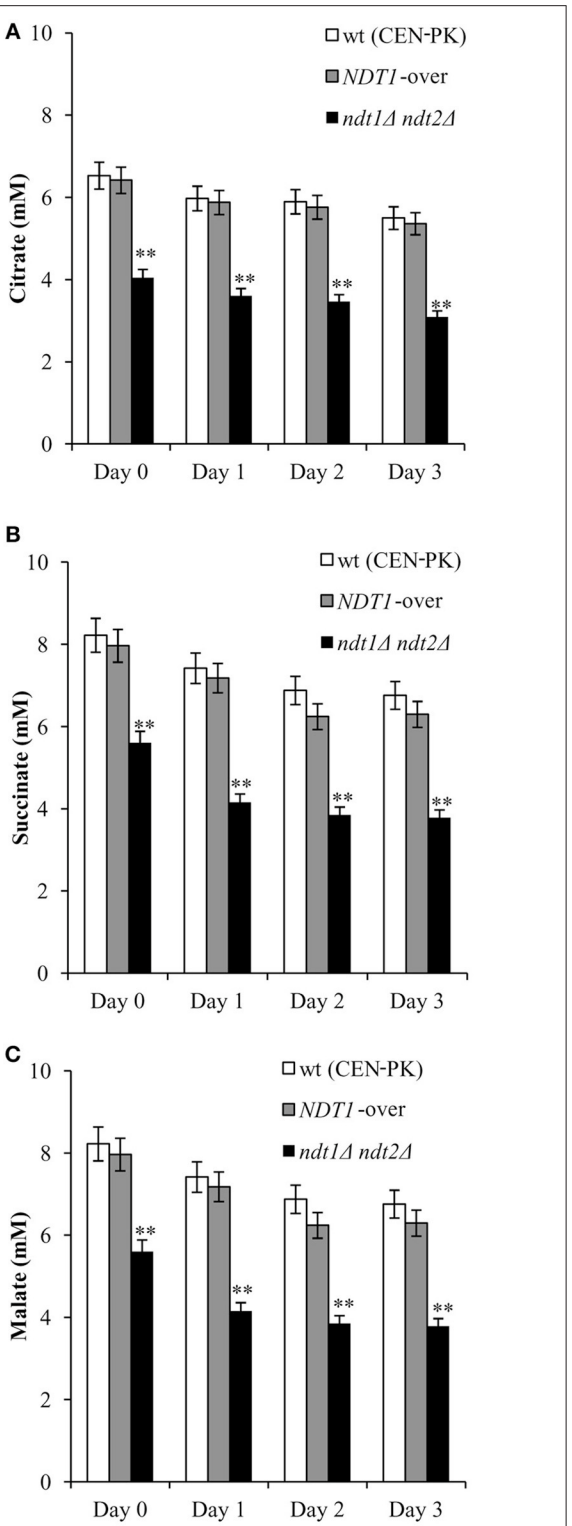

FIGURE 4 | The *ndt1*Δ*ndt2*Δ mutant displays decreased levels of TCA intermediates. The indicated strains were grown as in **Figure 1** and intracellular concentrations of citrate **(A)**, succinate **(B)** and malate **(C)** were measured. Day 0, diauxic shift. Bar charts show the mean values determined in three independent experiments with three technical replicates each. SD is indicated (**$P \leq 0.01$).

Following on, since the TCA cycle is fed by the mitochondrial acetyl-CoA, we assessed the levels of some of its intermediates, such as citrate, malate, and succinate. Starting from the diauxic shift, the levels of these C4 dicarboxylic acids in the *NDT1*-over strain mirrored those measured in the wt (**Figure 4**). On the contrary, in the *ndt1*Δ*ndt2*Δ mutant all these metabolites significantly decreased (**Figure 4**) suggesting an impairment in the TCA cycle.

The *ndt1*Δ*ndt2*Δ Mutant Preserves Functional Mitochondria During Chronological Aging

Considering that during respiration the TCA cycle provides the electron transport chain (ETC) with reducing equivalents through redox reactions and that respiration affects the CLS (Bonawitz et al., 2006; Ocampo et al., 2012; Baccolo et al., 2018), we measured next the respiratory activity in the *NDT1*-over and *ndt1*Δ*ndt2*Δ strains. During the exponential phase, the respiratory parameters for the *NDT1*-over and *ndt1*Δ*ndt2*Δ strains were very similar to those of the wt (**Table 2**) in good agreement with (Agrimi et al., 2011). Differences were observed starting from the diauxic shift (respiratory metabolism). Indeed, in the double deleted mutant, basal oxygen consumption (J_R) was lower than the wt one (**Table 2**). This can be ascribed to a depletion/limitation of reducing equivalents since in the presence of the uncoupler CCCP, which dissipates the proton gradient across the mitochondrial membrane, the maximal oxygen consumption rate (J_{MAX}) of the *ndt1*Δ*ndt2*Δ cells was always lower than that of the wt (**Table 2**). Interestingly, the *ndt1*Δ*ndt2*Δ cells displayed a non-phosphorylating respiration (J_{TET}) strongly reduced compared with that of the wt, the levels of which increased as a function of time in culture (**Table 2**) as expected (Orlandi et al., 2017a,b). As a consequence, in the double deleted mutant the net respiration, which estimates the coupled respiration, was close to the wt one (**Table 2**) indicating that, despite a reduced J_R, during the post-diauxic phase the *ndt1*Δ*ndt2*Δ strain has a better coupling between electron transport and ATP synthesis. On the contrary, the *NDT1*-over strain had a J_R similar to the wt one and a J_{MAX} higher (**Table 2**). Nevertheless, in this strain the net respiration was lower due to a J_{TET} significantly higher than that of the wt (**Table 2**) indicative of an increase of uncoupled respiration. These differences in both the level and in the state of the respiration of the two mutants were accompanied by differences in mitochondrial NAD^+ and NADH contents: in the *ndt1*Δ*ndt2*Δ mutant and in the *NDT1*-over one a decrease and an increase of NAD^+ and NADH contents, respectively, were observed compared with those of the wt (**Figures 5A,B**). This opposite trend in the mitochondrial dinucleotide contents, as well as the different respiratory efficiency, of the two types of mutants are in line with those detected during exponential growth on ethanol (Agrimi et al., 2011).

To the best of our knowledge, Ndt1 and Ndt2 are the only mitochondrial NAD^+ carriers described so far in *S.cerevisiae* (Todisco et al., 2006) and their transport activity for NAD^+ is also consistent with the cellular localization of the enzymes involved in NAD^+ biosynthesis, which are outside the mitochondria, and with the lack of NAD^+- synthesizing enzymes in the yeast mitochondria (Kato and Lin, 2014). However, since in the mitochondria of the *ndt1*Δ*ndt2*Δ mutant, NAD^+ is present, albeit at low levels, it cannot be excluded that this dinucleotide can be imported in the mitochondria with lower efficiency by other carrier systems. Indeed, many mitochondrial transporters often exhibit some overlapping of the transported substrates

TABLE 2 | Respiratory parameters determined for *NDT1*-over *and ndt1*Δ *ndt2*Δ strains.

Genetic Background	Strain	J_R					J_{MAX}				
		Exp	Day 0	Day 1	Day 2	Day 3	Exp	Day 0	Day 1	Day 2	Day 3
CEN-PK 113-7D	wt	**7.12** ± 0.29	**11.23** ± 0.29	**14.24** ± 0.32	**10.63** ± 0.16	**7.59** ± 0.12	**17.32** ± 0.32	**21.76** ± 0.59	**27.65** ± 0.13	**25.11** ± 0.26	**21.31** ± 0.31
	NDT1-over	**7.28** ± 0.31	**11.98** ± 0.17	**13.88** ± 0.32	**10.25** ± 0.24	**7.38** ± 0.17	**17.48** ± 0.21	**26.29**** ± 0.19	**30.15**** ± 0.37	**28.26**** ± 0.25	**23.67**** ± 0.31
	*ndt1*Δ*ndt2*Δ	**7.09** ± 0.22	**9.66**** ± 0.41	**10.77**** ± 0.27	**8.52**** ± 0.17	**6.53**** ± 0.26	**16.76** ± 0.16	**18.12**** ± 013	**21.35**** ± 0.47	**19.57**** ± 0.14	**17.73**** ± 0.09
W303-1A	wt	**7.76** ± 0.07	**9.47** ± 0.13	**14.41** ± 0.25	**11.69** ± 0.15	**7.52** ± 0.21	**16.23** ± 0.37	**19.97** ± 0.27	**26.33** ± 0.26	**25.41** ± 0.17	**24.28** ± 0.24
	*ndt1*Δ*ndt2*Δ	**7.55** ± 0.35	**8.42**** ± 0.17	**11.83**** ± 0.28	**9.64**** ± 0.36	**6.38**** ± 0.24	**15.97** ± 0.25	**17.34*** ± 0.27	**20.13**** ± 0.19	**18.99**** ± 0.31	**16.54**** ± 0.26
Genetic Background	**Strain**	J_{TET}					net_R				
		Exp	Day 0	Day 1	Day 2	Day 3	Exp	Day 0	Day 1	Day 2	Day 3
CEN-PK 113-7D	wt	**1.43** ± 0.41	**2.13** ± 0.19	**2.80** ± 0.45	**3.30** ± 0.29	**3.89** ± 0.19	**5.32** ± 0.27	**9.12** ± 0.16	**11.44** ± 0.26	**7.26** ± 0.16	**3.69** ± 0.23
	NDT1-over	**1.72** ± 0.09	**3.47**** ± 0.26	**3.97**** ± 0.27	**4.22**** ± 0.37	**5.58**** ± 0.33	**5.55** ± 0.09	**8.51** ± 0.17	**9.91** ± 0.32	**5.93**** ± 0.24	**1.82**** ± 0.17
	*ndt1*Δ*ndt2*Δ	**1.24** ± 0.38	**1.31**** ± 0.12	**1.43**** ± 0.38	**1.51**** ± 0.18	**1.84**** ± 0.26	**5.61** ± 0.13	**8.35** ± 026	**9.37** ± 0.16	**7.12** ± 0.17	**4.73**** ± 0.26
W303-1A	wt	**1.24** ± 0.38	**1.58** ± 0.38	**3.23** ± 0.44	**3.55** ± 0.22	**3.98** ± 0.19	**6.52** ± 0.23	**7.87** ± 0.26	**11.18** ± 0.11	**8.14** ± 0.31	**3.54** ± 0.13
	*ndt1*Δ*ndt2*Δ	**1.04** ± 0.26	**1.18**** ± 0.09	**1.27**** ± 0. 32	**1.46**** ± 0.29	**1.59**** ± 0.27	**6.14** ± 0.19	**7.23** ± 0.08	**10.59*** ± 0.14	**8.06** ± 0.23	**4.53*** ± 0.21

*Oxygen consumption rates (J) are expressed as pmol/10^6 cells/s. Basal respiration rate (J_R), uncoupled respiration rate (J_{MAX}), non-phosphorylating respiration (J_{TET}), and net respiration ($net_R = J_R$-J_{TET}). Substrates and inhibitors used in the measurements of the respiratory parameters are detailed in the text. Exp, exponential growth phase; Day 0, diauxic shift. Data refer to mean values determined in three independent experiments with three technical replicates each. SD is indicated. Values obtained for wt were used as reference for comparisons with NDT1-over and ndt1*Δ*ndt2*Δ *cells. (*$P \leq 0.05$ *and* **$P \leq 0.01$, *one-way ANOVA test). Mean values are provided in bold.*

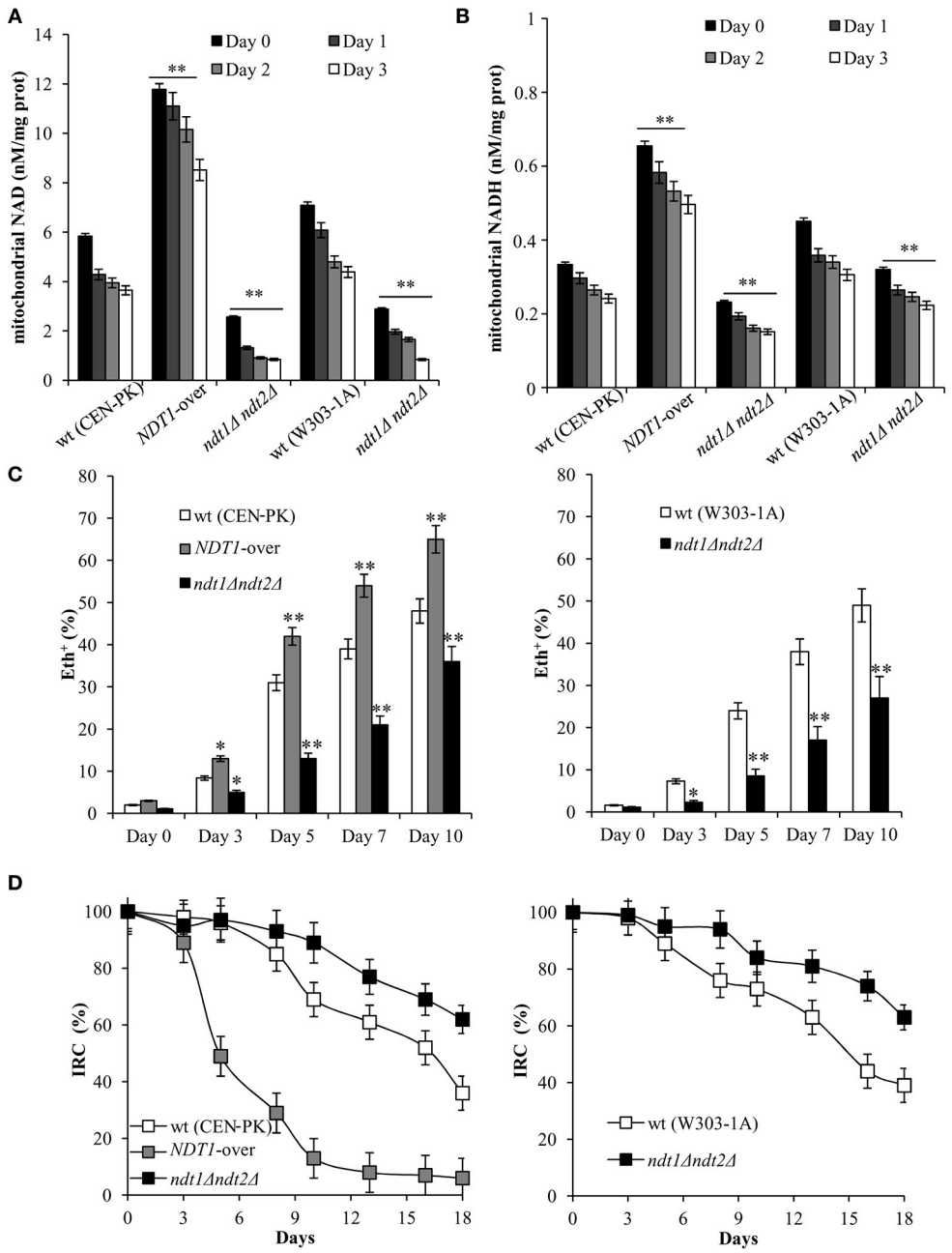

FIGURE 5 | Lack of Ndt1 and Ndt2 has a positive effect on mitochondrial functionality during chronological aging. Cells were grown as in **Figure 1**. Mitochondrial NAD^+ **(A)** and NADH **(B)** contents were determined at the indicated time-points. Day 0, diauxic shift. Bar charts show the mean values determined in three independent experiments with three technical replicates each. SD is indicated (**$P \leq 0.01$). **(C)** Bar charts of the percentage of fluorescent/superoxide positive cells assessed by the superoxide-driven conversion of non-fluorescent dihydroethidium into fluorescent ethidium (Eth). Day 0, diauxic shift. About 1,000 cells for each sample (three technical replicates) in three independent experiments were examined. SD is indicated (*$P \leq 0.05$ and **$P \leq 0.01$). **(D)** Starting from the diauxic shift (Day 0), at indicated time-points aliquots of wt, *NDT1*-over, and *ndt1*Δ*ndt2*Δ cultures were serially diluted and plated onto YEPD and YEPG plates in order to determine the index of respiratory competence (IRC). SD is indicated.

(Palmieri et al., 2006). In addition, other systems contribute to the homeostasis of the intramitochondrial NAD pool, as well as to balance dinucleotide pools between mitochondria and cytosol/nucleus. They include, among others, two NADH dehydrogenases (Nde1 and Nde2) distributed on the external surface of the inner mitochondrial membrane and the glycerol-3-phosphate shuttle (Bakker et al., 2001). Nde1 and Nde2 directly catalyze the transfer of electrons from cytosolic NADH

to ubiquinone without the translocation of protons across the membrane. In such a way, the ETC is supplied with electrons (Baccolo et al., 2018). The expression of *NDE1* and *NDE2* is induced after the diauxic shift (Bakker et al., 2001). With regard to the glycerol-3-phosphate shuttle, it is a system of crucial importance under conditions where the availability of energy is limited (Rigoulet et al., 2004). In the glycerol-3-phosphate shuttle, cytosolic glycerol-3-phosphate dehydrogenase oxidizes cytosolic NADH catalyzing the reduction of dihydroxyacetone phosphate to glycerol-3-phosphate. Subsequently, into the mitochondrial matrix, glycerol-3-phosphate delivers its electrons to ubiquinone via the FAD-dependent glycerol-3-phosphate dehydrogenase, Gut2 (Bakker et al., 2001). The result is a stepwise transfer of electrons from the cytosol to the respiratory chain. Consequently, despite the low mitochondrial dinucleotide contents, the *ndt1*Δ*ndt2*Δ mutant might feed the oxidative phosphorylation with the NADH produced in the cytosol.

Afterward, given the differences in the state of respiration, we decided to analyze the content of superoxide anion (O_2^-), which is the primary mitochondrial reactive oxygen species (ROS) produced by electron leakage from the respiratory chain. It is known that O_2^-/ROS accumulation limits the long-term survival of yeast cells during CLS (Pan, 2011; Breitenbach et al., 2014; Baccolo et al., 2018). In the *ndt1*Δ*ndt2*Δ chronologically cells and in the *NDT1*-over ones, a strong decrease and increase in O_2^- content was observed, respectively, compared to that of the wt (**Figure 5C**) consistent with non-phosphorylating respiration data (**Table 2**). Indeed, it is a state of non-phosphorylating respiration prone to generate O_2^- (Hlavata et al., 2003; Guerrero-Castillo et al., 2011). In addition, we analyzed the mitochondrial functionality by measuring the IRC, which defines the percentage of viable cells competent to respire (Parrella and Longo, 2008). Starting from the diauxic shift where all the strains were respiration-competent, a different trend of the IRC was observed for the *ndt1*Δ*ndt2*Δ strain and in the *NDT1*-over one. In the former, a lower decrease in the mitochondrial functionality was detected and at Day 18 the IRC was still about 60% against about 40% in the wt (**Figure 5D**). In the *NDT1*-over chronologically aging cells, a dramatic time-dependent loss of mitochondrial functionality was observed reaching at Day 18 values close to zero (**Figure 5D**). This is in line with the increased O_2^- formation because it is known that ROS levels influence mitochondrial fitness and mitochondrial dysfunctions, in turn, lead to a higher propensity to produce ROS (Breitenbach et al., 2014).

Thus, taken together all the results clearly indicate that, in the context of a standard CLS experiment, alterations in the expression of the specific mitochondrial NAD^+ carriers determined by *NDT1* and *NDT2* double deletion and *NDT1* overexpression deeply influence the metabolism with opposite outcomes on chronological longevity (**Figure 6**). We found that the former extends CLS, whereas the latter shortens it. This is a direct consequence, on the one hand, of the participation of NAD^+ together with its reduced counterpart, NADH, in a wide range of metabolic reactions modulating the activity of compartment-specific pathways among which the TCA cycle and the ETC in the mitochondria and the glycolysis/gluconeogenesis in the cytosol. On the other hand, the CLS is regulated by signaling pathways that coordinate the metabolic reprogramming required to ensure longevity (Breitenbach et al., 2014; Zhang and Cao, 2017). On the whole, in the *ndt1*Δ*ndt2*Δ chronologically aging cells and in the *NDT1*-over ones an opposite metabolic remodeling is observed, involving both cytosolic (gluconeogenesis), and mitochondrial (TCA and respiration) metabolic pathways (**Figure 6**), which are operative during chronological aging. Lack of the mitochondrial NAD^+ carriers results in a reduced oxygen consumption that does not depend upon dysfunctional mitochondria but most likely upon a decreased amount of reducing equivalents provided by a TCA cycle, the activity of which is reduced. Nevertheless, this mutant maintains a net respiration close to that of the wt indicating that in the mutant the respiration, albeit reduced, is more efficient. This confirms previous data on *ndt1*Δ*ndt2*Δ cells exponentially growing on ethanol that show a better coupling of respiration and phosphorylation (Agrimi et al., 2011). Such a state of more coupled respiration is less prone to generate hazardous O_2^- decreasing the risk of inducing oxidative stress and its detrimental effects on cell survival of non-dividing cells during chronological aging: in agreement with this, *ndt1*Δ*ndt2*Δ cells are long-lived. In agreement with a short-lived phenotype accompanied by O_2^- accumulation and severe mitochondrial damage, *NDT1*-over chronologically aging cells display an enhanced uncoupled respiration and a lower respiratory efficiency. As in the case of the *ndt1*Δ*ndt2*Δ cells, changes in the state of respiration have been already observed in *NDT1*-over cells exponentially growing on ethanol (Agrimi et al., 2011). In this context of fully respiratory metabolism, the *NDT1* overexpression determines a decrease in the respiratory efficiency similar to that described here when cells have exhausted glucose and shift to ethanol-driven respiration. These results further underline how the mitochondrial NAD^+ carriers and, consequently, the availability of mitochondrial NAD^+, and/or NADH is important to achieve an efficient respiration and how this aspect can influence the CLS.

Concerning gluconeogenesis, the enzymatic activity of Pck1 is generally considered the main flux-controlling step in the pathway. The gluconeogenic activity of this enzyme depends on its de/acetylation state (Lin et al., 2009; Casatta et al., 2013). Indeed, an increase in the enzymatic activity of Pck1 correlates with an increase in its acetylated active form promoting gluconeogenesis and CLS (Lin et al., 2009; Casatta et al., 2013; Orlandi et al., 2017a,b). The enzyme responsible for Pck1 deacetylation (inactive form) is the NAD^+-dependent deacetylase Sir2 (Lin et al., 2009). During chronological aging, lack of Sir2 correlates with an increase of the acetylated Pck1 and with a carbohydrate metabolism shift toward glyoxylate-requiring gluconeogenesis increasing CLS (Casatta et al., 2013; Orlandi et al., 2017a,b). It is conceivable that, as the deacetylase activity of Sir2 relies on NAD^+, the low level of this dinucleotide in the *ndt1*Δ*ndt2*Δ mutant might decrease Sir2-mediated deacetylation of Pck1 and consequently increase gluconeogenesis and CLS. Differently, in the *NDT1*-over mutant, a different

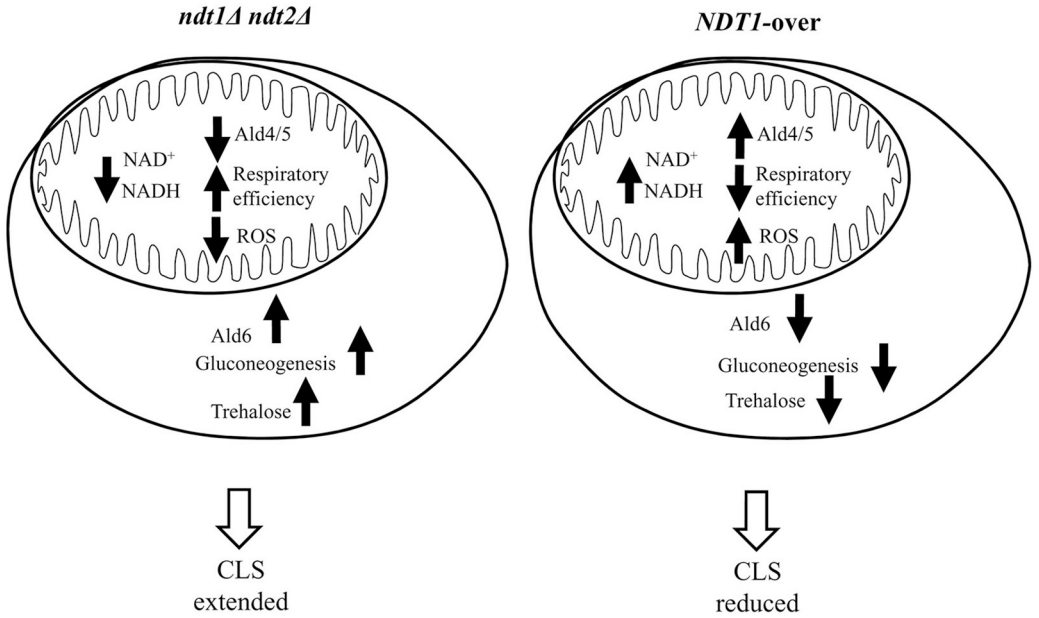

FIGURE 6 | Simplified scheme summarizing the effects of the altered expression of mitochondrial NAD$^+$ carriers during chronological aging.

availability of NAD$^+$ might favor Sir2 enzymatic activity leading to an increase of the deacetylated inactive form of Pck1 and to the observed decrease of gluconeogenesis and CLS.

Furthermore, in the *ndt1*Δ*ndt2*Δ mutant and the *NDT1*-over one, other metabolic traits that result from an enhancement and a down-regulation, respectively, of the cytosolic Ald6/glyoxylate/gluconeogenesis axis fit-well with their CLS. Indeed, Ald6 activity requires NADP$^+$ providing NADPH, which is also provided by the pentose phosphate pathway fueled by the gluconeogenesis with glucose-6 phosphate. NADPH is a source of reducing energy and an essential cofactor for glutathione/thioredoxin-dependent enzymes that are essential for protecting cells from oxidative stress (Pollak et al., 2007). Thus, NADPH availability can contribute to influence the physiological state of the cells and consequently their survival. In this context, the *ndt1*Δ*ndt2*Δ mutant might be further favored by an enhanced gluconeogenic activity that leading also to increased intracellular trehalose stores, ensures viability during chronological aging. On the contrary the down-regulation of the Ald6/glyoxylate/gluconeogenesis axis observed in the *NDT1*-over mutant decreasing cellular protection systems, might contribute to affect negatively the CLS.

To date, substantial number of evidence points out that lowering NAD$^+$ levels can decrease Sirtuin activities and affect the aging process both in *S.cerevisiae* and mammalian cells (Imai and Guarente, 2016). In particular, in yeast lack of the nicotinic acid phosphoribosyltransferase, Npt1, which in the salvage pathway generates NAD$^+$ from nicotinic acid (NA), reduces NAD$^+$ content. This is accompanied by loss of silencing and decrease in RLS (Smith et al., 2000), as NAD$^+$ levels are not sufficient for Sir2 to function (Ondracek et al., 2017). Addition of nicotinamide riboside (an NAD$^+$ precursor) corrects the deficit in NAD$^+$ content of the *npt1*Δ mutant, promotes Sir2-dependent silencing and extends RLS (Belenky et al., 2007). Furthermore, yeast cells grown in media lacking NA has a short RLS and low NAD$^+$ levels; supplementation of isonicotinamide extends RLS in a Sir2-dependent manner by restoring NAD$^+$ content and alleviating the nicotinamide (NAM) inhibition on Sir2 (McClure et al., 2012). Indeed, NAM is an NAD$^+$ precursor that is also an endogenous non-competitive inhibitor of Sir2 (Sauve et al., 2005). Yeast cells grown in the presence of NAM have the same phenotype of *sir2*Δ ones such as silencing defects and a short RLS (Sauve et al., 2005). In the context of chronological aging, NAM supplementation at the diauxic shift results in a phenocopy of chronologically aging *sir2*Δ cells: due to the inhibition of Sir2, Pck1 enzymatic activity, and gluconeogenesis are promoted and CLS is extended (Orlandi et al., 2017a). On the opposite, resveratrol, a Sirtuin activating compound, restricts CLS by enhancing Sir2 activity, in particular Sir2-mediated deacetylation of Pck1, and consequently gluconeogenesis is decreased (Orlandi et al., 2017b).

In conclusion, taken together all our results show that affecting the cellular distribution and the content of NAD$^+$ has a deep impact on both metabolism and chronological aging and that a critical functional role is played by the Sir2 activity. In addition, our data indicate that in order to elucidate the intimate interplay between NAD$^+$, Sirtuins and aging, it will be important to determine how NAD$^+$ levels change in different compartments during aging and the tissue-specific regulation of NAD metabolism and Sirtuin activity.

AUTHOR CONTRIBUTIONS

MV conceived the project. MV and IO designed the experiments. IO and GS performed the experiments. MV wrote the manuscript. All authors have read and approved the final version of the manuscript.

ACKNOWLEDGMENTS

The authors are grateful to Neil Campbell for English editing. This work was supported by CARIPLO Foundation 2015-0641 to MV and GS was supported by fellowships from SYSBIONET, Italian roadmap of ESFRI.

REFERENCES

Agrimi, G., Brambilla, L., Frascotti, G., Pisano, I., Porro, D., Vai, M., et al. (2011). Deletion or overexpression of mitochondrial NAD+ carriers in *Saccharomyces cerevisiae* alters cellular NAD and ATP contents and affects mitochondrial metabolism and the rate of glycolysis. *Appl. Environ. Microbiol.* 77, 2239–2246. doi: 10.1128/AEM.01703-10

Aranda, A., and del Olmo, M. (2003). Response to acetaldehyde stress in the yeast *Saccharomyces cerevisiae* involves a strain-dependent regulation of several *ALD* genes and is mediated by the general stress response pathway. *Yeast* 20, 747–759. doi: 10.1002/yea.991

Baccolo, G., Stamerra, G., Pellegrino Coppola, D., Orlandi, I., and Vai, M. (2018). Mitochondrial metabolism and aging in yeast. *Int. Rev. Cell Mol. Biol.* 340, 1–33. doi: 10.1016/bs.ircmb.2018.05.001

Bakker, B. M., Overkamp, K. M., van Maris, A. J., Kotter, P., Luttik, M. A., van Dijken, J. P., et al. (2001). Stoichiometry and compartmentation of NADH metabolism in *Saccharomyces cerevisiae*. *FEMS Microbiol. Rev.* 25, 15–37. doi: 10.1111/j.1574-6976.2001.tb00570.x

Belenky, P., Racette, F. G., Bogan, K. L., McClure, J. M., Smith, J. S., and Brenner, C. (2007). Nicotinamide riboside promotes Sir2 silencing and extends lifespan via Nrk and Urh1/Pnp1/Meu1 pathways to NAD+. *Cell* 129, 473–484. doi: 10.1016/j.cell.2007.03.024

Bitto, A., Wang, A., Bennett, C., and Kaeberlein, M. (2015). Biochemical genetic pathways that modulate aging in multiple species. *Cold Spring Harb. Perspect. Med.* 5:a025114. doi: 10.1101/cshperspect.a025114

Bogan, K. L., and Brenner, C. (2008). Nicotinic acid, nicotinamide, and nicotinamide riboside: a molecular evaluation of NAD+ precursor vitamins in human nutrition. *Annu. Rev. Nutr.* 28, 115–130. doi: 10.1146/annurev.nutr.28.061807.155443

Bonawitz, N. D., Rodeheffer, M. S., and Shadel, G. S. (2006). Defective mitochondrial gene expression results in reactive oxygen species-mediated inhibition of respiration and reduction of yeast life span. *Mol. Cell. Biol.* 26, 4818–4829. doi: 10.1128/MCB.02360-05

Breitenbach, M., Rinnerthaler, M., Hartl, J., Stincone, A., Vowinckel, J., Breitenbach-Koller, H., et al. (2014). Mitochondria in ageing: there is metabolism beyond the ROS. *FEMS Yeast Res.* 14, 198–212. doi: 10.1111/1567-1364.12134

Cambronne, X. A., Stewart, M. L., Kim, D., Jones-Brunette, A. M., Morgan, R. K., Farrens, D. L., et al. (2016). Biosensor reveals multiple sources for mitochondrial NAD(+). *Science* 352, 1474–1477. doi: 10.1126/science.aad5168

Canto, C., Menzies, K. J., and Auwerx, J. (2015). NAD(+) metabolism and the control of energy homeostasis: a balancing act between mitochondria and the nucleus. *Cell Metab.* 22, 31–53. doi: 10.1016/j.cmet.2015.05.023

Casatta, N., Porro, A., Orlandi, I., Brambilla, L., and Vai, M. (2013). Lack of Sir2 increases acetate consumption and decreases extracellular pro-aging factors. *Biochim. Biophys. Acta* 1833, 593–601. doi: 10.1016/j.bbamcr.2012.11.008

de Jong-Gubbels, P., Vanrolleghem, P., Heijnen, S., van Dijken, J. P., and Pronk, J. T. (1995). Regulation of carbon metabolism in chemostat cultures of *Saccharomyces cerevisiae* grown on mixtures of glucose and ethanol. *Yeast* 11, 407–418. doi: 10.1002/yea.320110503

Dolle, C., Niere, M., Lohndal, E., and Ziegler, M. (2010). Visualization of subcellular NAD pools and intra-organellar protein localization by poly-ADP-ribose formation. *Cell. Mol. Life Sci.* 67, 433–443. doi: 10.1007/s00018-009-0190-4

Fabrizio, P., Gattazzo, C., Battistella, L., Wei, M., Cheng, C., McGrew, K., et al. (2005). Sir2 blocks extreme life-span extension. *Cell* 123, 655–667. doi: 10.1016/j.cell.2005.08.042

Fabrizio, P., and Longo, V. D. (2007). The chronological life span of *Saccharomyces cerevisiae*. *Methods Mol. Biol.* 371, 89–95. doi: 10.1007/978-1-59745-361-5_8

Fontana, L., Partridge, L., and Longo, V. D. (2010). Extending healthy life span - from yeast to humans. *Science* 328, 321–326. doi: 10.1126/science.1172539

Frye, R. A. (2000). Phylogenetic classification of prokaryotic and eukaryotic Sir2-like proteins. *Biochem. Biophys. Res. Commun.* 273, 793–798. doi: 10.1006/bbrc.2000.3000

Gray, J. V., Petsko, G. A., Johnston, G. C., Ringe, D., Singer, R. A., and Werner-Washburne, M. (2004). "Sleeping beauty": quiescence in *Saccharomyces cerevisiae*. *Microbiol. Mol. Biol. Rev.* 68, 187–206. doi: 10.1128/MMBR.68.2.187-206.2004

Guerrero-Castillo, S., Araiza-Olivera, D., Cabrera-Orefice, A., Espinasa-Jaramillo, J., Gutierrez-Aguilar, M., Luevano-Martinez, L. A., et al. (2011). Physiological uncoupling of mitochondrial oxidative phosphorylation. Studies in different yeast species. *J. Bioenerg. Biomembr.* 43, 323–331. doi: 10.1007/s10863-011-9356-5

Hlavata, L., Aguilaniu, H., Pichova, A., and Nystrom, T. (2003). The oncogenic $RAS2^{val19}$ mutation locks respiration, independently of PKA, in a mode prone to generate ROS. *EMBO J.* 22, 3337–3345. doi: 10.1093/emboj/cdg314

Houtkooper, R. H., Canto, C., Wanders, R. J., and Auwerx, J. (2010). The secret life of NAD+: an old metabolite controlling new metabolic signaling pathways. *Endocr. Rev.* 31, 194–223. doi: 10.1210/er.2009-0026

Houtkooper, R. H., Pirinen, E., and Auwerx, J. (2012). Sirtuins as regulators of metabolism and healthspan. *Nat. Rev. Mol. Cell Biol.* 13, 225–238. doi: 10.1038/nrm3293

Imai, S. (2009). From heterochromatin islands to the NAD World: a hierarchical view of aging through the functions of mammalian Sirt1 and systemic NAD biosynthesis. *Biochim. Biophys.* 1790, 997–1004. doi: 10.1016/j.bbagen.2009.03.005

Imai, S. (2010). "Clocks" in the NAD World: NAD as a metabolic oscillator for the regulation of metabolism and aging. *Biochim. Biophys. Acta* 1804, 1584–1590. doi: 10.1016/j.bbapap.2009.10.024

Imai, S., Armstrong, C. M., Kaeberlein, M., and Guarente, L. (2000). Transcriptional silencing and longevity protein Sir2 is an NAD-dependent histone deacetylase. *Nature* 403, 795–800. doi: 10.1038/35001622

Imai, S., and Guarente, L. (2014). NAD+ and sirtuins in aging and disease. *Trends Cell Biol.* 24, 464–471. doi: 10.1016/j.tcb.2014.04.002

Imai, S. I. (2016). The NAD World 2.0: the importance of the inter-tissue communication mediated by NAMPT/NAD(+)/SIRT1 in mammalian aging and longevity control. *NPJ Syst. Biol. Appl.* 2:16018. doi: 10.1038/npjsba.2016.18

Imai, S. I., and Guarente, L. (2016). It takes two to tango: NAD(+) and sirtuins in aging/longevity control. *NPJ Aging Mech. Dis.* 2:16017. doi: 10.1038/npjamd.2016.17

Johnson, S., and Imai, S. I. (2018). NAD (+) biosynthesis, aging, and disease. *F1000 Res.* 7:132. doi: 10.12688/f1000research.12120.1

Kaeberlein, M., McVey, M., and Guarente, L. (1999). The SIR2/3/4 complex and SIR2 alone promote longevity in *Saccharomyces cerevisiae* by two different mechanisms. *Genes Dev.* 13, 2570–2580. doi: 10.1101/gad.13.19.2570

Kato, M., and Lin, S. J. (2014). Regulation of NAD+ metabolism, signaling and compartmentalization in the yeast *Saccharomyces cerevisiae*. *DNA Repair* 23, 49–58. doi: 10.1016/j.dnarep.2014.07.009

Koch-Nolte, F., Fischer, S., Haag, F., and Ziegler, M. (2011). Compartmentation of NAD+-dependent signalling. *FEBS Lett.* 585, 1651–1656. doi: 10.1016/j.febslet.2011.03.045

Lee, Y. J., Jang, J. W., Kim, K. J., and Maeng, P. J. (2011). TCA cycle-independent acetate metabolism via the glyoxylate cycle in *Saccharomyces cerevisiae*. *Yeast* 28, 153–166. doi: 10.1002/yea.1828

Lin, S. J., Ford, E., Haigis, M., Liszt, G., and Guarente, L. (2004). Calorie restriction extends yeast life span by lowering the level of NADH. *Genes Dev.* 18, 12–16. doi: 10.1101/gad.1164804

Lin, S. S., Manchester, J. K., and Gordon, J. I. (2001). Enhanced gluconeogenesis and increased energy storage as hallmarks of aging in *Saccharomyces cerevisiae*. *J. Biol. Chem.* 276, 36000–36007. doi: 10.1074/jbc.M103509200

Lin, Y. Y., Lu, J. Y., Zhang, J., Walter, W., Dang, W., Wan, J., et al. (2009). Protein acetylation microarray reveals that NuA4 controls key metabolic target regulating gluconeogenesis. *Cell* 136, 1073–1084. doi: 10.1016/j.cell.2009.01.033

Longo, V. D., and Kennedy, B. K. (2006). Sirtuins in aging and age-related disease. *Cell* 126, 257–268. doi: 10.1016/j.cell.2006.07.002

Longo, V. D., Shadel, G. S., Kaeberlein, M., and Kennedy, B. (2012). Replicative and chronological aging in *Saccharomyces cerevisiae*. *Cell Metab.* 16, 18–31. doi: 10.1016/j.cmet.2012.06.002

MacLean, M., Harris, N., and Piper, P. W. (2001). Chronological lifespan of stationary phase yeast cells; a model for investigating the factors that might influence the ageing of postmitotic tissues in higher organisms. *Yeast* 18, 499–509. doi: 10.1002/yea.701

Madeo, F., Frohlich, E., Ligr, M., Grey, M., Sigrist, S. J., Wolf, D. H., et al. (1999). Oxygen stress: a regulator of apoptosis in yeast. *J. Cell Biol.* 145, 757–767. doi: 10.1083/jcb.145.4.757

McClure, J. M., Wierman, M. B., Maqani, N., and Smith, J. S. (2012). Isonicotinamide enhances Sir2 protein-mediated silencing and longevity in yeast by raising intracellular NAD^+ concentration. *J. Biol. Chem.* 287, 20957–20966. doi: 10.1074/jbc.M112.367524

Meisinger, C., Pfanner, N., and Truscott, K. N. (2006). Isolation of yeast mitochondria. *Methods Mol. Biol.* 313, 33–39. doi: 10.1385/1-59259-958-3:033

Mitchell, S. J., Bernier, M., Aon, M. A., Cortassa, S., Kim, E. Y., Fang, E. F., et al. (2018). Nicotinamide improves aspects of healthspan, but not lifespan, in mice. *Cell Metab.* 27, 667–676. doi: 10.1016/j.cmet.2018.02.001

Ocampo, A., Liu, J., Schroeder, E. A., Shadel, G. S., and Barrientos, A. (2012). Mitochondrial respiratory thresholds regulate yeast chronological life span and its extension by caloric restriction. *Cell Metab.* 16, 55–67. doi: 10.1016/j.cmet.2012.05.013

Ondracek, C. R., Frappier, V., Ringel, A. E., Wolberger, C., and Guarente, L. (2017). Mutations that allow *SIR2* orthologs to function in a $NAD(^+)$-depleted environment. *Cell Rep.* 18, 2310–2319. doi: 10.1016/j.celrep.2017.02.031

Orlandi, I., Pellegrino Coppola, D., Strippoli, M., Ronzulli, R., and Vai, M. (2017a). Nicotinamide supplementation phenocopies *SIR2* inactivation by modulating carbon metabolism and respiration during yeast chronological aging. *Mech. Ageing Dev.* 161, 277–287. doi: 10.1016/j.mad.2016.06.006

Orlandi, I., Pellegrino Coppola, D., and Vai, M. (2014). Rewiring yeast acetate metabolism through MPC1 loss of function leads to mitochondrial damage and decreases chronological lifespan. *Microb. Cell* 1, 393–405. doi: 10.15698/mic2014.12.178

Orlandi, I., Ronzulli, R., Casatta, N., and Vai, M. (2013). Ethanol and acetate acting as carbon/energy sources negatively affect yeast chronological aging. *Oxid. Med. Cell. Longev.* 2013:802870. doi: 10.1155/2013/802870

Orlandi, I., Stamerra, G., Strippoli, M., and Vai, M. (2017b). During yeast chronological aging resveratrol supplementation results in a short-lived phenotype Sir2-dependent. *Redox Biol.* 12, 745–754. doi: 10.1016/j.redox.2017.04.015

Palmieri, F., Agrimi, G., Blanco, E., Castegna, A., Di Noia, M. A., Iacobazzi, V., et al. (2006). Identification of mitochondrial carriers in *Saccharomyces cerevisiae* by transport assay of reconstituted recombinant proteins. *Biochim. Biophys. Acta* 1757, 1249–1262. doi: 10.1016/j.bbabio.2006.05.023

Pan, Y. (2011). Mitochondria, reactive oxygen species, and chronological aging: a message from yeast. *Exp. Gerontol.* 46, 847–852. doi: 10.1016/j.exger.2011.08.007

Parrella, E., and Longo, V. D. (2008). The chronological life span of *Saccharomyces cerevisiae* to study mitochondrial dysfunction and disease. *Methods* 46, 256–262. doi: 10.1016/j.ymeth.2008.10.004

Pollak, N., Dolle, C., and Ziegler, M. (2007). The power to reduce: pyridine nucleotides - small molecules with a multitude of functions. *Biochem. J.* 402, 205–218. doi: 10.1042/BJ20061638

Rajman, L., Chwalek, K., and Sinclair, D. A. (2018). Therapeutic potential of NAD-boosting molecules: the *in vivo* evidence. *Cell Metab.* 27, 529–547. doi: 10.1016/j.cmet.2018.02.011

Rigoulet, M., Aguilaniu, H., Averet, N., Bunoust, O., Camougrand, N., Grandier-Vazeille, X., et al. (2004). Organization and regulation of the cytosolic NADH metabolism in the yeast *Saccharomyces cerevisiae*. *Mol. Cell. Biochem.* 256–257, 73–81. doi: 10.1023/B:MCBI.0000009888.79484.fd

Saint-Prix, F., Bonquist, L., and Dequin, S. (2004). Functional analysis of the *ALD* gene family of *Saccharomyces cerevisiae* during anaerobic growth on glucose: the $NADP^+$-dependent Ald6p and Ald5p isoforms play a major role in acetate formation. *Microbiology* 150, 2209–2220. doi: 10.1099/mic.0.26999-0

Sauve, A. A., Moir, R. D., Schramm, V. L., and Willis, I. M. (2005). Chemical activation of Sir2-dependent silencing by relief of nicotinamide inhibition. *Mol. Cell* 17, 595–601. doi: 10.1016/j.molcel.2004.12.032

Sherman, F. (2002). Getting started with yeast. *Meth. Enzymol.* 350, 3–41. doi: 10.1016/S0076-6879(02)50954-X

Shi, L., Sutter, B. M., Ye, X., and Tu, B. P. (2010). Trehalose is a key determinant of the quiescent metabolic state that fuels cell cycle progression upon return to growth. *Mol. Biol. Cell* 21, 1982–1990. doi: 10.1091/mbc.e10-01-0056

Smith, D. L. Jr., McClure, J. M., Matecic, M., and Smith, J. S. (2007). Calorie restriction extends the chronological lifespan of *Saccharomyces cerevisiae* independently of the Sirtuins. *Aging Cell* 6, 649–662. doi: 10.1111/j.1474-9726.2007.00326.x

Smith, J. S., Brachmann, C. B., Celic, I., Kenna, M. A., Muhammad, S., Starai, V. J., et al. (2000). A phylogenetically conserved NAD^+-dependent protein deacetylase activity in the Sir2 protein family. *Proc. Natl. Acad. Sci. U.S.A.* 97, 6658–6663. doi: 10.1073/pnas.97.12.6658

Steinkraus, K. A., Kaeberlein, M., and Kennedy, B. K. (2008). Replicative aging in yeast: the means to the end. *Annu. Rev. Cell Dev. Biol.* 24, 29–54. doi: 10.1146/annurev.cellbio.23.090506.123509

Swinnen, E., Ghillebert, R., Wilms, T., and Winderickx, J. (2014). Molecular mechanisms linking the evolutionary conserved TORC1-Sch9 nutrient signalling branch to lifespan regulation in *Saccharomyces cerevisiae*. *FEMS Yeast Res.* 14, 17–32. doi: 10.1111/1567-1364.12097

Todisco, S., Agrimi, G., Castegna, A., and Palmieri, F. (2006). Identification of the mitochondrial NAD^+ transporter in *Saccharomyces cerevisiae*. *J. Biol. Chem.* 281, 1524–1531. doi: 10.1074/jbc.M510425200

Vanoni, M., Vai, M., Popolo, L., and Alberghina, L. (1983). Structural heterogeneity in populations of the budding yeast *Saccharomyces cerevisiae*. *J. Bacteriol.* 156, 1282–1291.

Verdin, E. (2015). $NAD(^+)$ in aging, metabolism, and neurodegeneration. *Science* 350, 1208–1213. doi: 10.1126/science.aac4854

Wanichthanarak, K., Wongtosrad, N., and Petranovic, D. (2015). Genome-wide expression analyses of the stationary phase model of ageing in yeast. *Mech. Ageing Dev.* 149, 65–74. doi: 10.1016/j.mad.2015.05.008

Yaku, K., Okabe, K., and Nakagawa, T. (2018). NAD metabolism: implications in aging and longevity. *Ageing Res. Rev.* 47, 1–17. doi: 10.1016/j.arr.2018.05.006

Zhang, N., and Cao, L. (2017). Starvation signals in yeast are integrated to coordinate metabolic reprogramming and stress response to ensure longevity. *Curr. Genet.* 63, 839–843. doi: 10.1007/s00294-017-0697-4

Conflict of Interest Statement: The authors declare that the research was conducted in the absence of any commercial or financial relationships that could be construed as a potential conflict of interest.

frontiers in Genetics

ORIGINAL RESEARCH
published: 18 December 2018
doi: 10.3389/fgene.2018.00675

Ras-Induced miR-146a and 193a Target Jmjd6 to Regulate Melanoma Progression

*Viviana Anelli[1], Anita Ordas[2], Susanne Kneitz[3], Leonel Munoz Sagredo[4,5], Victor Gourain[4], Manfred Schartl[3,6,7], Annemarie H. Meijer[2] and Marina Mione[1]**

[1] Cibio, University of Trento, Trento, Italy, [2] Institute of Biology, Leiden University, Leiden, Netherlands, [3] Physiological Chemistry, Biocenter, University of Würzburg, Würzburg, Germany, [4] Institute of Toxicology and Genetics, Karlsruhe Institute of Technology, Karlsruhe, Germany, [5] Faculty of Medicine, University of Valparaiso, Valparaíso, Chile, [6] Comprehensive Cancer Center, University Clinic Würzburg, Würzburg, Germany, [7] Hagler Institute for Advanced Study and Department of Biology, Texas A&M University, College Station, TX, United States

Ras genes are among the most commonly mutated genes in human cancer; yet our understanding of their oncogenic activity at the molecular mechanistic level is incomplete. To identify downstream events that mediate ras-induced cellular transformation *in vivo*, we analyzed global microRNA expression in three different models of Ras-induction and tumor formation in zebrafish. Six microRNAs were found increased in Ras-induced melanoma, glioma and in an inducible model of ubiquitous Ras expression. The upregulation of the microRNAs depended on the activation of the ERK and AKT pathways and to a lesser extent, on mTOR signaling. Two Ras-induced microRNAs (miR-146a and 193a) target Jmjd6, inducing downregulation of its mRNA and protein levels at the onset of Ras expression during melanoma development. However, at later stages of melanoma progression, *jmjd6* levels were found elevated. The dynamic of Jmjd6 levels during progression of melanoma in the zebrafish model suggests that upregulation of the microRNAs targeting Jmjd6 may be part of an anti-cancer response. Indeed, triple transgenic fish engineered to express a microRNA-resistant Jmjd6 from the onset of melanoma have increased tumor burden, higher infiltration of leukocytes and shorter melanoma-free survival. Increased *JMJD6* expression is found in several human cancers, including melanoma, suggesting that the up-regulation of Jmjd6 is a critical event in tumor progression.

The following link has been created to allow review of record GSE37015: http://www.ncbi.nlm.nih.gov/geo/query/acc.cgi?token=jjcrbiuicyyqgpc&acc=GSE37015.

Keywords: zebrafish, cancer models, microRNA, Jmjd6, ras, melanoma, miR-146a, miR-193a

OPEN ACCESS

Edited by:
Maria Grazia Giansanti, Consiglio Nazionale delle Ricerche (CNR), Italy

Reviewed by:
Victoriano Mulero, University of Murcia, Spain
Theodora Katsila, University of Patras, Greece

****Correspondence:***
Marina Mione
mariacaterina.mione@unitn.it

Specialty section:
This article was submitted to Genetic Disorders, a section of the journal Frontiers in Genetics

Received: *28 September 2018*
Accepted: *04 December 2018*
Published: *18 December 2018*

Citation:
Anelli V, Ordas A, Kneitz S, Sagredo LM, Gourain V, Schartl M, Meijer AH and Mione M (2018) Ras-Induced miR-146a and 193a Target Jmjd6 to Regulate Melanoma Progression. Front. Genet. 9:675. doi: 10.3389/fgene.2018.00675

INTRODUCTION

Activating mutations in the *RAS* genes or in other members of the ras-signaling pathways are very common in cancer[1] and recent deep sequencing data of cancer genomes[2] suggest that these mutations are important primers of malignancies. Still, the initial molecular events following activation of the pathways downstream of Ras are extremely difficult to study *in vivo*.

[1]http://www.sanger.ac.uk/genetics/CGP/cosmic/
[2]http://cancergenome.nih.gov/

Transgenic models, where the expression of the oncogene leads to cancer development in a reproducible manner provide a suitable experimental system for addressing the complexity of cellular transformation in live animals. The oncogenic versions of the human RAS genes (KRAS, HRAS, and NRAS) have been the first and most successful drivers of cancer in transgenic mice (Chin et al., 1999a,b; Johnson et al., 2001; Malumbres and Barbacid, 2003). This ability of ras oncogenes to initiate and maintain cancer has been related to global molecular and epigenetic changes at early stages of transformation. Among the targets of oncogenes, microRNAs are well-suited to sustain global changes of cellular functions. Changes in several protein levels may be regulated by a single or just a few microRNAs and a number of microRNAs have been found deregulated in cancer (Harrandah et al., 2018). Yet, very few studies have investigated their roles at the onset of transformation as possible "global effectors" of oncogenesis. In this study we have investigated the link between Ras-induced transformation and microRNA expression, using genetically tractable zebrafish models where the expression of a constitutively active *HRAS*^{G12V} allele leads to the development of different cancer types. We found that activated Ras signaling promotes the rapid increase of six microRNAS. Interestingly, two of these microRNAs target the same gene, Jmjd6, a jumonjiC domain protein with at least two reported functions: histone arginine demethylation (Chang et al., 2007) and mRNA splicing regulation (Webby et al., 2009). Results reported here indicate that Jmjd6 is a critical player in zebrafish melanoma development and that at least two Ras-induced microRNAs antagonize Jmjd6 activation.

RESULTS

Dynamic Regulation of MicroRNAs by RAS Activation

To identify miRNAs that are regulated by oncogenic Ras from the earliest stages of transformation, we used a custom Agilent microarray (see M&M). We profiled miRNA expression in transgenic zebrafish overexpressing *HRAS*^{G12V} in melanocytes (Santoriello et al., 2010), in brain cells (Mayrhofer et al., 2017) and ubiquitously (Santoriello et al., 2009) (**Figure 1A**). Six miRNAs (miR-21.1, miR- 21.2, miR-146a, miR-146b-1, miR-193a, miR-193a-1) were up-regulated (log2FC $>$ 1.2 and p-value $<$ 0.01, see **Supplementary Table S1**) in all three transgenic models at 3 day post-fertilization (dpf) and in 7 dpf melanoma, whereas no commonly down-regulated miRNAs were found (**Figure 1B** and **Supplementary Table S1**, highlighted rows).

This study, we focused on the melanoma model, and to clarify the potential roles of the upregulated microRNAs in melanoma progression, we analyzed microRNA expression levels at four time points (3, 7, and 14 dpf and in adult tumors, **Supplementary Table S1**) during melanoma progression. Next, we designed Taqman probes for the active strand (−5p) of miR21, miR-146a and miR-146b and for the active strand (−3p) of miR-193a and validated the expression levels of the six upregulated miRNAs by qPCR in the melanoma model (**Figure 1C**). The expression of the six microRNA genes showed dynamic patterns: one was upregulated up to 7 dpf (miR-146b-1-5p), while the others were upregulated to different extents up to adult melanoma (**Figure 1D** and **Supplementary Table S1**). To further validate the dependence of these microRNAs on ras we used drugs that target different pathways downstream of ras. Next, expression levels of miR-21-5p (including both mir21-1 and miR21-2), miR-146a-5p, miR-146b-1-5p, and miR-193a-3p (including also mir193a-1-3p) were quantified through qPCR, after induction of ras expression and in the presence of drugs. For simplicity, the microRNAs under study are named miR-21, miR-146a, miR-146b, miR-193a from now on.

The Increase of miR-21, miR-146a, and miR-193a Is Ras-Dependent

To investigate whether miR-21, miR-146a, miR-146b, and miR-193a are direct targets of ras, we analyzed their expression profiles using an inducible model, *Tg(hsp70l:EGFP-HRASV12)*^{io3}, called HS-RAS, that expresses oncogenic ras upon heat shock. RNA was extracted from 3 dpf HS-RAS embryos, 6 h after a 30 min heat shock treatment at 37°C, when robust ras activation occurs (Santoriello et al., 2009). QPCR data show that miR-21 and miR-146a are significantly upregulated in Ras overexpressing larvae (**Figure 2A**), thus supporting the hypothesis that miR-21 and miR-146a represents early-response targets, likely to be directly induced by oncogenic Ras. MiR-193a and miR-146b did not show significant upregulation in response to ras; however, we performed the inhibitor experiments also on these two microRNAs as they had shown to be upregulated in the melanoma model (**Figure 1C**).

xs To identifying which signaling pathway(s) downstream of Ras induces overexpression of these microRNAs, we blocked specific pathways in HS-RAS larvae using small chemical inhibitors of ERK, AKT and mTor phosphorylation (**Figure 2B**). To check the efficacy of the inhibitors, we collected treated larvae at 3 dpf and performed western blot analysis for known targets of the three inhibitors. As shown in **Figure 2C** PD98059, rapamycin and LY29004 were able to decrease ERK-P, AKT-P and S6-P levels, respectively. Next we checked the levels of microRNAs in inhibitor treated larvae using qPCR. As shown in **Figures 2D,E**, induction of miR-21 and -146a expression was greatly attenuated by all three inhibitors and most robustly by the ERK inhibitor. MiR-146b levels were not affected by the drug treatments (**Figure 2F**) and miR-193a levels were reduced to statistically significant levels only when larvae were treated with rapamycin (**Figure 2G**). These data suggest that miR-21, miR-146a and to a less extent, miR-193a, are ras-responsive genes and their activation is regulated mostly by the MAPK/ERK and mTOR (for miR-193a) branches of ras signaling.

Predicted Target of MicroRNAs 146a and 193a

As the function of miR-21 is widely studied in cancer (Frezzetti et al., 2011), and miR-146b was found not to respond to Ras signaling, in this study we focused on miR-146a and -193a, to clarify whether they have a role in melanomagenesis.

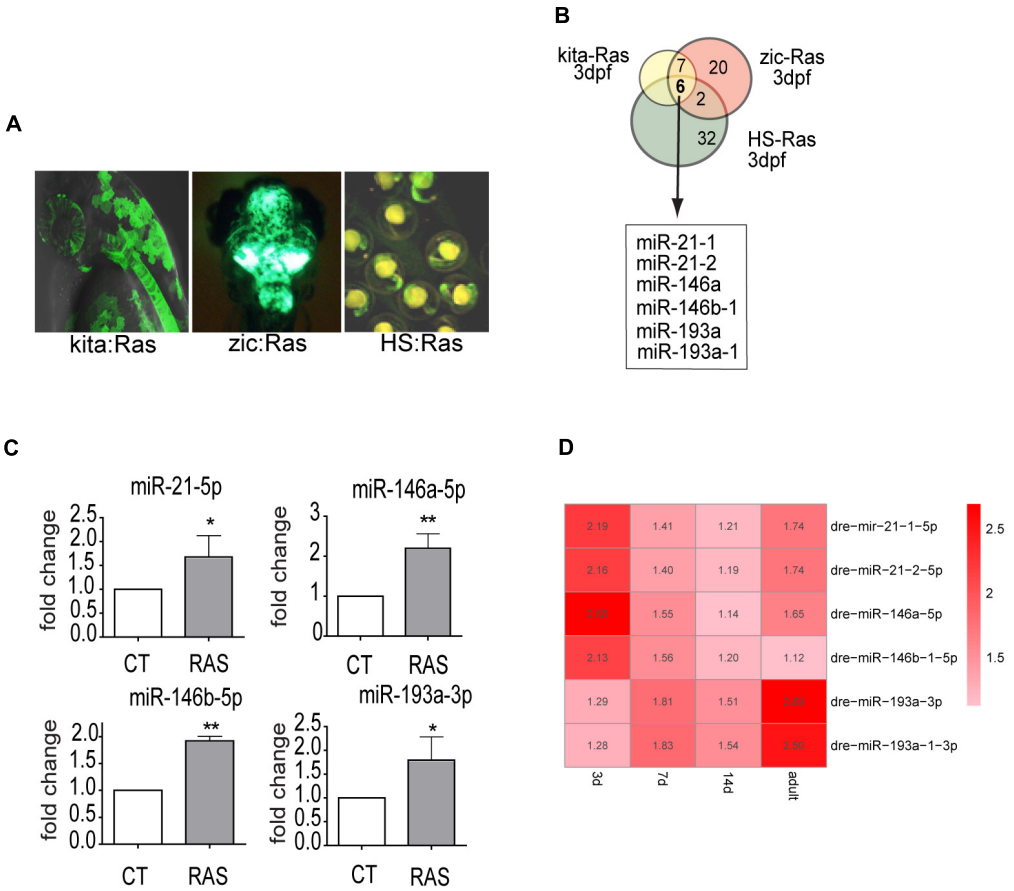

FIGURE 1 | miR-21, miR-146a/b, and miR-193a are upregulated by oncogenic RAS in transgenic cancer models. **(A)** Zebrafish models used in the study of Ras-dependent microRNAs. Green fluorescence denotes the expression of the eGFP-fused oncogene. In Kita:Ras GFP labels transformed melanocytes and notochord; in zic:Ras GFP marks ras-expressing brain cells; in HS-Ras, eGFP-Ras is expressed in whole embryos. For full description of transgenic lines, see text. **(B)** Diagram depicting the overlap between the three sets of upregulated microRNAs. **(C)** Taqman QPCR analysis of miR-21, miR-146a/b, and miR-193a expression levels in 3 dpf kita-RAS larvae compared to control (CT) larvae. The error bar represents the SEM of a triplicate experiment. **(D)** Heatmap representation of microarray analysis of miR-21, miR-146a/b, and miR-193a expression at different stages of melanoma progression. Distinct precursor sequences and genomic loci that express identical mature sequences are named on the form miR-21-1 and miR-21-2. Lettered suffixes denote closely related mature sequences. –5p and –3p indicate the 5′ and 3′ arm respectively. $*P \leq 0.05$ and $**P \leq 0.01$.

A web-based target prediction algorithm [MicroCosmTargets, now incorporated in www.tools4mirs.org (Lukasik et al., 2016)], was used to identify potential targets of zebrafish miR-146a and miR-193a. The tool is based on the genome assembly ZV9[3] and returned a few targets that were selected to contain seed sequences for miR- 146a, miR-193a or both, this last category included only *jmjd6*. We then used a web-based interaction-prediction algorithm for RNA molecules, IntaRNA[4] (Mann et al., 2017) for the fast and accurate prediction of interactions between miR-146a and/or 193a with *jmjd6* mRNAs using the newest genome assembly, GRCz11[5]. This search confirmed the presence of seed sequences for miR-146a and -193a (see **Supplementary Figures S1A,B**).

[3]http://mar2015.archive.ensembl.org/Danio_rerio/Info/Index

[4]http://rna.informatik.uni-freiburg.de/IntaRNA/Input.jsp

[5]https://www.ensembl.org/Danio_rerio/Info/Index

Jmjd6 Is a Target of miR-193a and miR-146a

Danio rerio jmjd6 has 1 transcript (*Ensemble, ENSDAR G00000102896*). The 3′ UTR region of *Jmjd6* contains miRNA recognition elements (MREs) for miR-146a (**Supplementary Figure S1A**), and MREs for miR-193a (**Supplementary Figure S1B**). To determine whether Jmjd6 is a bona fide target of miR-193a and miR-146a, we tested whether miR-193a and miR-146a expression affects *jmjd6* levels using an *in vivo* GFP reporter assay. The entire *jmjd6- 3′ UTR* was cloned downstream of green fluorescent protein (GFP) open reading frame (**Figure 3A**). *In vitro* synthesized mRNA from this construct was then injected into single-cell zebrafish embryos with or without miR-193a or mir-146a duplexes (**Figure 3A**), which mimic microRNA overexpression. The injection of the microRNA duplexes resulted in increased levels of microRNA (**Supplementary Figure S2A**) and caused mild

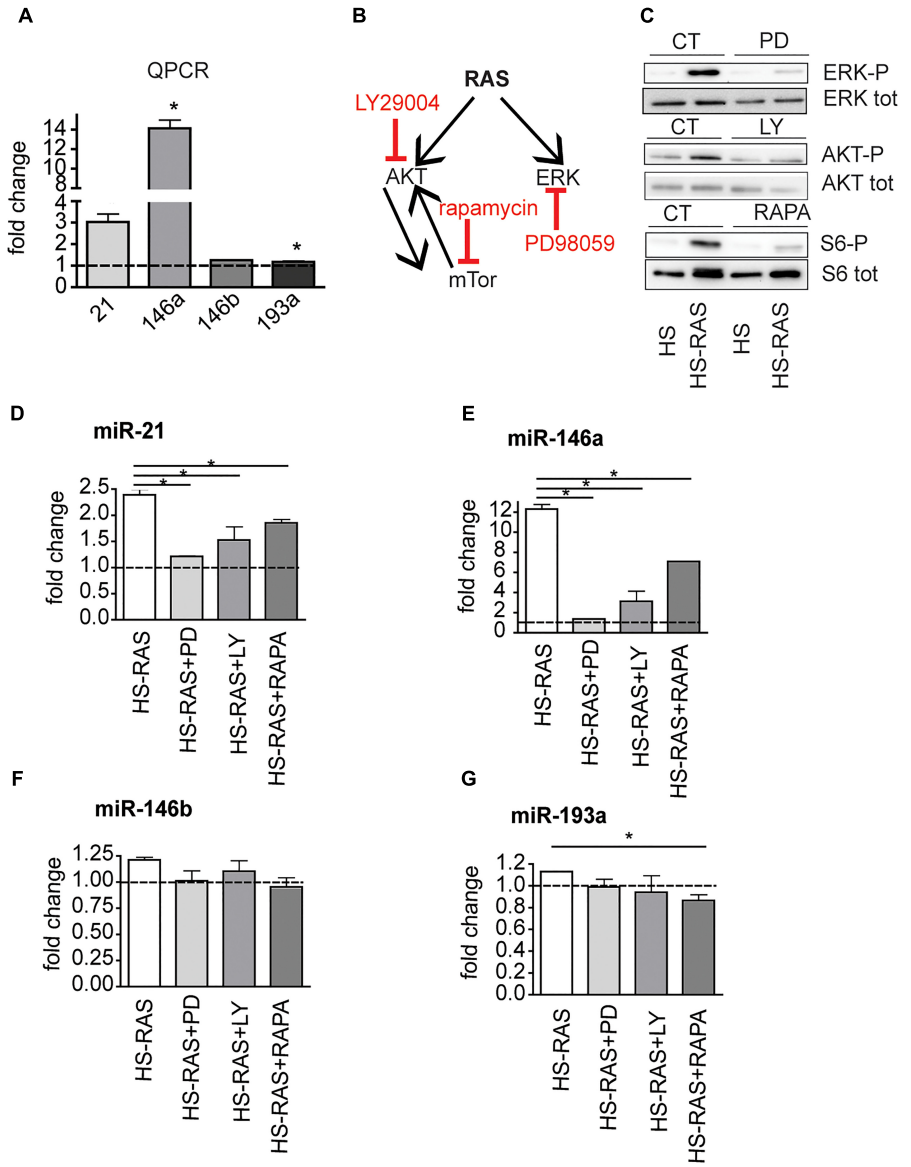

FIGURE 2 | The increase of miR-21, miR-146a/b, and miR-193a is RAS-dependent. **(A)** Taqman QPCR analysis of miR-21, 146a, 146b, and 193a expression following ras upregulation (6 h after heat-shock induction), $*p < 0.05$. **(B)** Diagram showing the ras pathway inhibitors used and their targets. **(C)** Western Blot analysis of ERK-P, AKT-P, and S6-P ribosomal protein levels after the inhibitors treatment. **(D–G)** Taqman qPCR analysis in 3 dpf HS-RAS zebrafish treated with PD98059, LY29004 and rapamycin. The error bars represent the SEM of a triplicate experiment; two tailed Student's test was used for analysis. $*p < 0.05$.

or no phenotypes (**Supplementary Figure S2B**). The following day, GFP expression levels were monitored by fluorescence microscopy (**Figure 3B**) and by western blot analysis with an antibody against GFP (**Figures 3C,D**). In both assays, GFP levels were reduced in embryos injected with miR-193a or miR-146a duplexes. Duplex injection of either miR-146a or miR-193a also resulted in reduction of Jmjd6 protein levels (**Figures 3E,F**).

To validate the direct interaction between miR-146a and miR-193a with *jmjd6* mRNA, we performed RNA immunoprecipitation (RIP, **Figure 3G**). After immunoprecipitation (IP) with Ago2 antibody, which selectively enriched for RISC complex components (Ikeda et al., 2006), *jmjd6* transcripts were readily found in embryos injected with miR-146a and miR-193a duplexes (**Figure 3H**) suggesting that a physical interaction between *jmjd6* transcripts and specific microRNAs occurs in the RISC complex. These data confirmed the interaction between miR-146a and miR-193a with *jmjd6* mRNA.

As we found that *jmjd6* is a target of miR-146a and -193a, we investigated whether the level of jmjd6 was lower in Ras expressing larvae compared to controls. As shown in **Supplementary Figures S3A,B** heat-shock induced Ras overexpression results in down-regulation of *jmjd6* RNA level

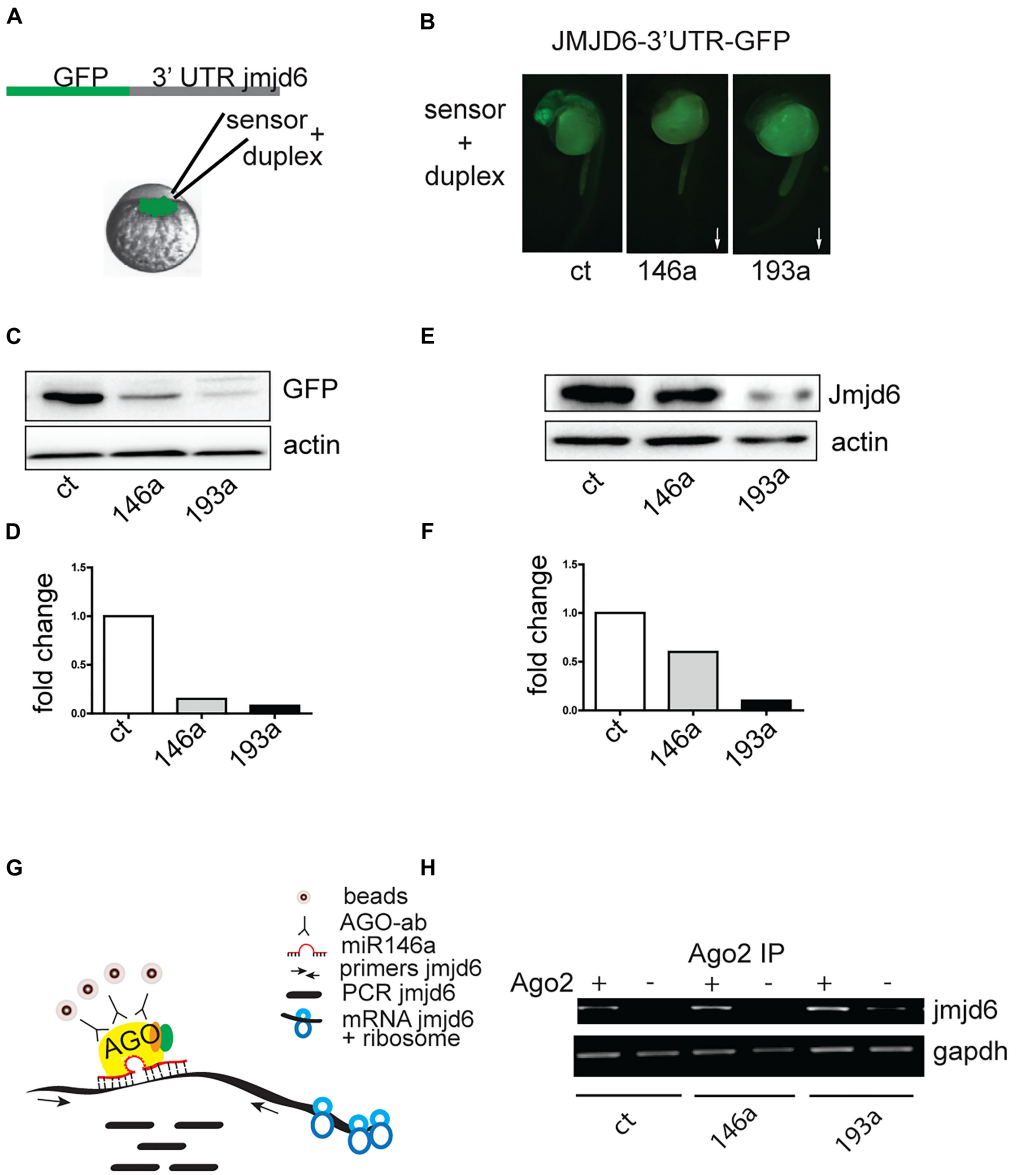

FIGURE 3 | Jmjd6 is a target of miR-146a and miR-193a. **(A)** Effects of increasing microRNA levels on a Jmjd6-GFP sensor expression. Diagram of the construct used as sensor. **(B)** Representative images of 24 hpf zebrafish embryos injected with the Jmjd6-3′ UTR GFP sensor and the microRNA duplexes as indicated. Arrows illustrate the direction of the changes in expression. **(C)** Western blot analysis of GFP expression and **(D)** quantification of the changes in Jmjd6-3′ UTR GFP sensor levels upon microRNA overexpression. **(E)** Reduction of *Jmjd6* protein levels following miR-146a, and miR-193a duplex injection in 3 dpf embryos shown by Western Blot analysis. **(F)** Quantification of the Western Blot shown in **(E)**. **(G)** RIP (RNA immuno precipitation) diagram and **(H)** analysis of *jmjd6* transcripts in the RISC complex following duplex injections in 3 dpf embryos.

(**Supplementary Figure S3A**, column 2) and *jmjd6* protein levels (**Supplementary Figure S3B**, lane 2). To test if *jmjd6* down-regulation was due to increased expression of miR-146a and/or miR-193a, we reduced microRNA expression by injecting morpholinos (MO) specific to miR-146a or miR-193a and measured *jmjd6* mRNA and protein levels in morpholino injected HS-Ras embryos. All morpholinos were able to reduce expression levels of their targets (data not shown) and to increase the levels of *jmjd6* transcripts, repressed by ras, to levels similar to controls (**Supplementary Figure S3A**, columns 3–4) and protein levels (**Supplementary Figure S3B**, lanes 3–4), suggesting that ras-induced miRs are responsible for the downregulation of *jmjd6* levels observed in response to ras expression.

Jmjd6 in Melanoma

In our model of melanoma progression, where ras is overexpressed in melanocytes, *jmjd6* levels are reduced compared to control larvae at 3 and 7 dpf (**Figure 4A**). However, at 14 dpf, there is no significant difference in *jmjd6* levels between kita:Ras

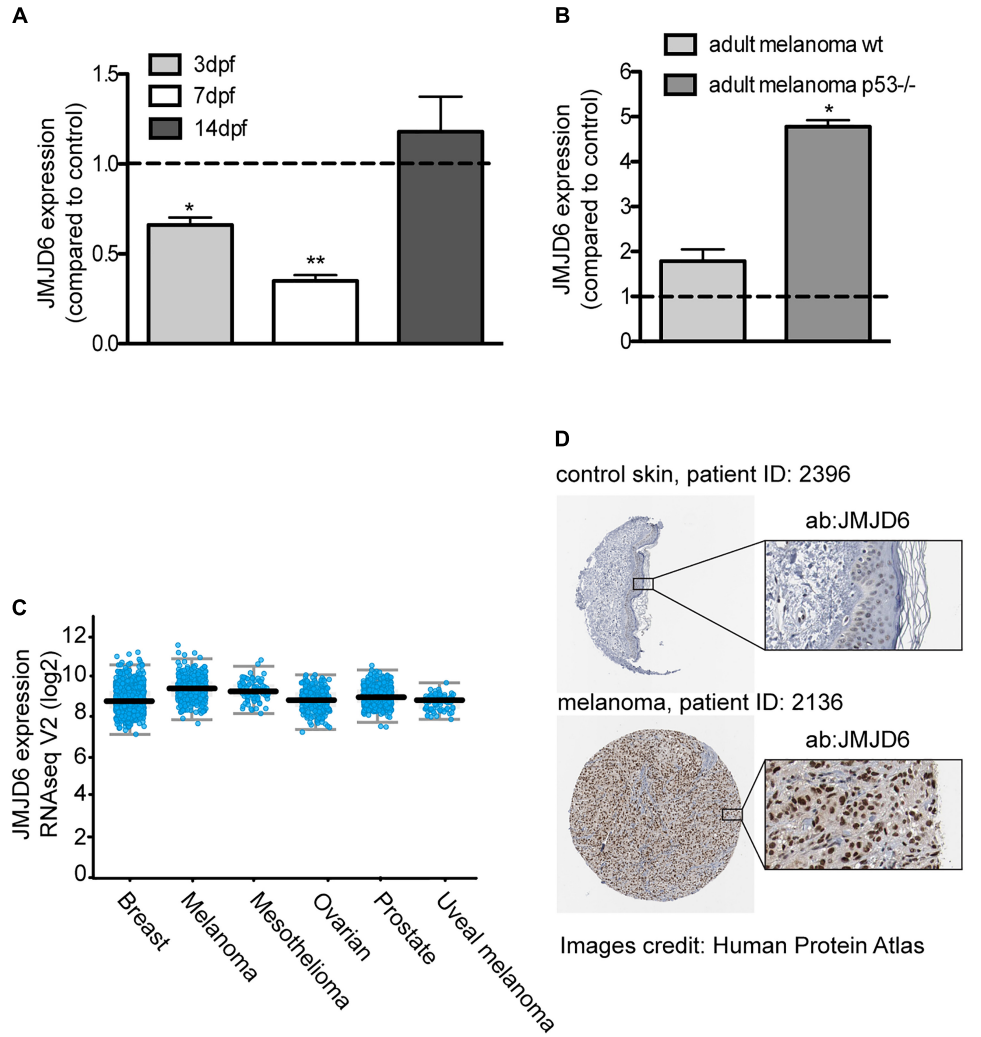

FIGURE 4 | JMJD6 is up-regulated in zebrafish and human melanoma. **(A)** *Jmjd6* mRNA levels in 3, 7, 14 days kita-RAS zebrafish and **(B)** in adult melanoma developing in two different genetic backgrounds, as shown. The error bars represent the SEM of triplicate experiments; two tailed Student's test was used for analysis. $*p < 0.01$. **(C)** Analysis of *JMJD6* expression in a variety of cancers from the cBioPortal database; every spot represents a case. **(D)** Expression of JMJD6 (brown nuclear staining) in control skin and in a malignant melanoma from the Protein Atlas website (https://www.proteinatlas.org/ENSG00000070495-JMJD6).

and controls. We then analyzed the levels of *jmjd6* expression in full-blown melanoma in two different genotypes: wild type (p53+/+) and p53−/−. In the latter background, melanomas developed earlier and were highly invasive from the earliest stages (Santoriello et al., 2010). QPCR analysis of *jmjd6* levels in six wild type and in three p53−/− cases showed significantly higher levels of expression of *jmjd6* in melanoma, especially in tumors developing in a p53−/− genetic background (**Figure 4B**).

Given the unexpected increase of *jmjd6* expression in melanoma, and its correlation with a more aggressive phenotype (Liu et al., 2017), to understand the clinical relevance of our findings, we queried online databases to investigate the expression levels of miR-146a, miR-193a and JMJD6 in melanoma samples from human patients. Data reported here on human melanoma are derived from publicly available resources, as stated in the following text and in the figure's legend. While no changes in miR-193a expression were reported in melanoma, a couple of studies (GSE18509 and GSE31568, see dbDEMC at www.picb.ac.cn/dbDEMC/index.html) reported an increase of miR-146a in melanoma (not shown). Next, we analyzed the expression levels of JMJD6 in different types of cancers, including melanoma, using the website cBioPortal for Cancer Genomics[6] (Cerami et al., 2012). As shown in **Figure 4C**, we found that JMJD6 is upregulated in different cancers, with melanoma being one of the cancer having higher levels of JMJD6 expression and high genomic alteration frequency (with amplification in almost 3% of cases, **Supplementary Figure S4A**). Looking carefully into the skin cutaneous melanoma TCGA dataset we found that the levels of *JMJD6* are upregulated in 16% of human cutaneous melanoma (72 out of 469 patients, **Supplementary Figure S4B**).

[6]http://www.cbioportal.org/

Moreover, *JMJD6* expression levels are higher in the samples with HRAS and BRAF mutations compared to samples with *wild type* HRAS and BRAF (**Supplementary Figures S4C,D**), suggesting that *JMJD6* is upregulated by RAS signaling in these melanomas. Patients with alteration of *JMJD6* (mutations, amplifications, deep deletions, or multiple alterations) have a worse overall survival and disease/progression-free survival compared with patients with wild type JMJD6 (**Supplementary Figures S4E,F**), suggesting a key role of JMJD6 in disease progression.

Next, we investigated the levels of JMJD6 protein in human melanoma using the website Protein Atlas[7] (Uhlen et al., 2017). The website reported medium (in three patients) or high (in nine patients) nuclear JMJD6 immunostaining in malignant melanoma. An example of a high JMJD6 immunostaining in melanoma is shown in comparison to control skin (where JMJD6 is not expressed) (**Figure 4D**) (Uhlen et al., 2017). These data suggest that the microRNA-mediated downregulation of *jmjd6* in the zebrafish progressive melanoma model is a transient event and at later stages of melanoma development or in more aggressive melanomas in fish and in human, *Jmjd6* is overexpressed.

Expression of miR-Resistant Jmjd6 Promotes Ras-Induced Melanoma

Given the dynamic changes in *Jmjd6* expression in the Ras-induced melanoma model in zebrafish, and the overall increase in expression in human melanoma, we wanted to clarify the role of Jmjd6 in melanoma with a gain of function approach. Therefore, we produced a transgenic line that expresses miR (146a and 193a) -resistant *jmjd6* in melanocytes. This was achieved by replacing the 3′ UTR of *jmjd6* in the transgenic construct with an artificial sequence (SV40 polyA, **Figure 5A**). With this construct, we generated a *tg(UAS:eGFP-jmjd6)* transgenic line using standard Tol2 transposase methods (Kawakami, 2004), and crossed it to kita:Gal4 fish. The double transgenic fish, designated as *kita:Jmjd6,* have no phenotype; however *eGFP-Jmjd6* expression was confirmed by kita driven GFP nuclear localization in melanocytes and notochord cells (**Figures 5B–D**). To study the effects of combined expression of oncogenic ras and Jmjd6 in melanoma we generated triple transgenic fish, *Et(kita:Gal4TA, UAS:mCherry)*^{hmz1}*;Tg(UAS:eGFP-HRASV12)*^{io006}; *Tg(UAS:eGFP-JMJD6)*^{ka202} (designated as *kita/Ras/Jmjd6*, **Figure 5E**) and observe the fish for the development of melanoma at regular intervals, from 7 days to 1 month. As shown in the disease-free survival curve, 60% of double transgenic kita-ras fish show melanoma at 1 month (**Figure 5F**). However, triple transgenic fish *kita/Ras/Jmjd6* developed melanoma at an earlier stage (**Figures 5E,F**) and by 1 month of age, penetrance of melanoma was 95% (**Figure 5F**). The tumors appeared in multiple locations in the same fish (**Figure 5E**) and were more invasive, as judged by the body surface showing melanoma lesions and by histological analysis (**Figures 5G,H**).

We also noticed that Kita/Ras/Jmjd6 melanomas have massive infiltration of leukocytes (L-plastin+ cells), resembling macrophages and neutrophils for their shape, much higher than in to Kita/Ras melanomas (**Figures 5I–L**).

[7]https://www.proteinatlas.org/

DISCUSSION

In this study we used a progressive model of melanoma in zebrafish to study the changes of microRNA expression at the onset of RAS-induced transformation and throughout progression of the disease. We found six microRNAs, which are upregulated as an early response to oncogenic RAS expression in three different models. As two of these microRNAs target Jmjd6 we investigated the significance of these interactions for melanoma progression. To our surprise we discovered that the target of these increased microRNAs, Jmjd6, is overexpressed in aggressive zebrafish melanoma. This suggested that overexpression of Jmjd6 promotes melanoma progression and that the increase of the microRNAs that downregulate Jmjd6 at the onset of Ras expression is part of a defensive response against the pro-oncogenic activity of Jmjd6. We validated this hypothesis by generating triple transgenic zebrafish that express micro-RNA resistant Jmjd6. Melanoma develop faster in the kita/ras/jmjd6 fish, supporting a pro-oncogenic role of Jmjd6. Further work is needed to clarify how Jmjd6 favors melanoma development.

Jmjd6 is a JumanjiC-domain containing protein, which has been endorsed for different functions. It was initially identified as a phosphatidylserine receptor (PSR) on the surface of phagocytes (Fadok et al., 2000). Ablation of Jmjd6 in mice, and morpholino downregulation of Jmjd6/PSR in zebrafish (Hong et al., 2004) causes abnormal development and leads to neonatal lethality in mouse (Böse et al., 2004; Kunisaki et al., 2004). However, many lines of evidence argue against a function of Jmjd6 as a PSR, primarily its nuclear localization (Cui et al., 2004; Tibrewal et al., 2007), and a number of newly reported nuclear activities. Subsequently, Jmjd6 was shown to function as an arginine demethylase, which removes repressive symmetric methylation marks from histone 2 (H2R3me2s) and histone 4 (H4R3me2s) arginines (Chang et al., 2007), but other groups have been unable to confirm the arginine demethylation activity of JMJD6 (Hahn et al., 2010). Webby et al. (2009) reported that JMJD6 acts as a lysyl-5-hydroxylase of the splice factor subunit U2A65. Silencing of JMJD6 expression in endothelial cells resulted in abnormal splicing of the VEGF receptor 1 (Boeckel et al., 2011). Meanwhile, a structural study suggested that methyl groups on single-stranded RNAs (ssRNAs) might be substrates of JMJD6 (Hong et al., 2010). More recently, a proteomic approach identified JMJD6 as one of a few binding partners of the bromodomain and extraterminal (BET) domain protein Brd4 (Rahman et al., 2011), which regulates gene expression through interaction with the cdk9 subunit of the positive transcription and elongation factor, pTEFb complex (Jang et al., 2005). Further studies lead to the identification of JMJD6 as the partner of BRD4 in binding distal enhancers known as anti-pause enhancers, which regulate release from transcriptional pausing in a large subset of transcriptional units which depend on long-range interactions (Liu et al., 2013). Here, the demethylase activity of JMJD6 on

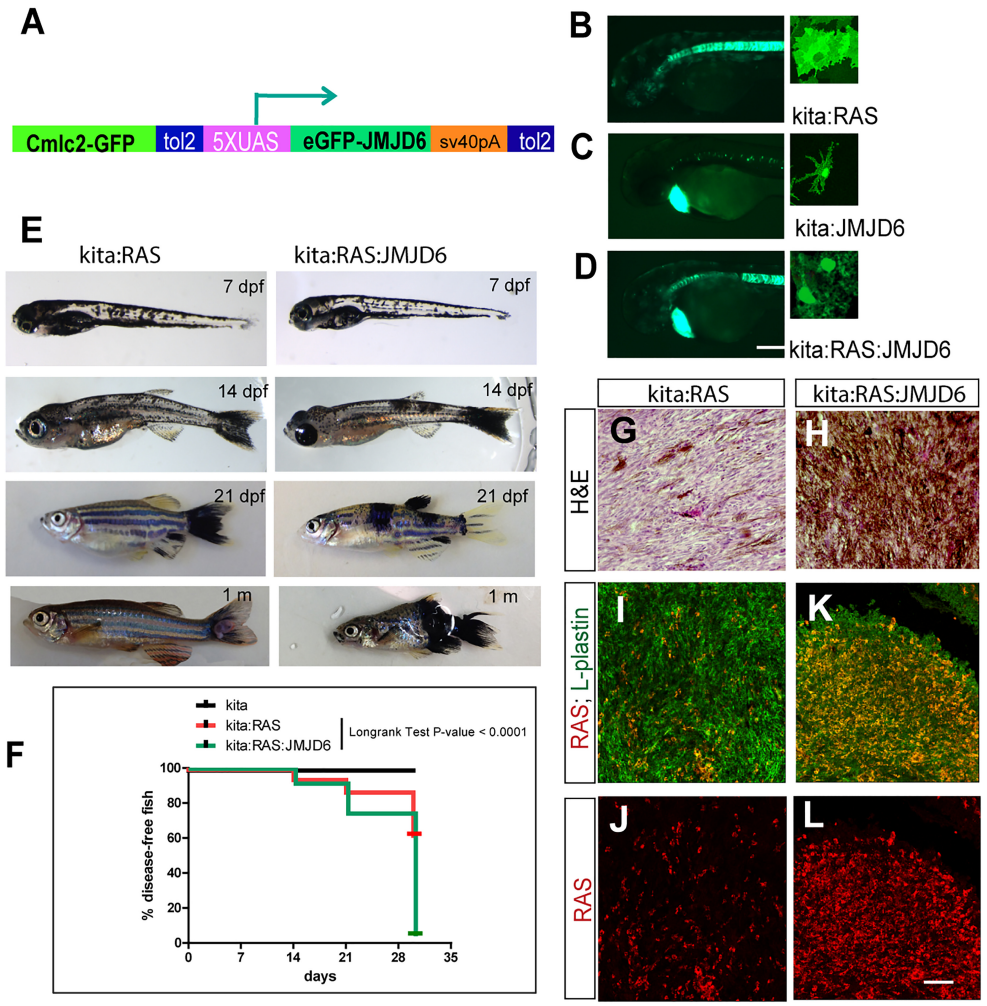

FIGURE 5 | Expression of miR-resistant Jmjd6 promotes Ras-induced melanoma. **(A)** Schematic representation of the construct used to generate a transgenic line expressing microRNA-resistant Jmjd6 under the UAS promoter. Cmlc2-GFP is the cardiac myosin light chain promoter driving GFP expression in the heart as marker of transgenesis. **(B–D)** Examples of GFP staining in crosses between the UAS lines and the kita:Gal4 line (as indicated). Expression is visible in the notochord (Distel et al., 2009) and in melanocytes in all kita crosses **(B–D)**, and in the heart for the UAS:Jmjd6 line, **C,D**) GFP is localized to the nucleus for Jmjd6-GFP or the plasma membrane for eGFP-HRASV12. **(E)** Double or triple transgenic larvae and juveniles at the indicated stages of development. **(F)** Disease- free survival curve of the double or triple transgenic fish. *N* = 100 for kita; 321 for kita:Ras; 211 for kita:Ras:Jmjd6. Long-rank test: *p*-value < 0,0001. **(G,H)** H&E staining of representative melanoma sections from transgenic fish as indicated. **(I–L)** Immunostaining for L-plastin (red florescence) and GFP (only in **I–K**, indicating HRASV12, green fluorescence) in representative melanoma sections from transgenic fish as indicated. Calibration bar: 100 μm for **(B,D)**, 50 μm for **(I–L)**.

the snRNA, 7SK, results in the disassembly of the transcriptional repressive complex HEXIM1-7SK, releasing pTEFb from pausing (Liu et al., 2013). It would be interesting to study whether anti-pause enhancers, which are the substrates of the JMJD6-Brd4 interaction, are associated with pro-oncogenic gene expression in melanoma. Given the robust correlation between Jmjd6 overexpression and aggressive melanoma in different models and in human samples, it would be important to clarify if the pro-oncogenic function of JMJD6 depends on this transcriptional activity. More recently, Liu et al. (2017) have shown that the JMJD6 promotes melanomagenesis through the regulation of the alternative splicing of PAK1, a key MAPK signaling component. In recent years, also RNA binding abilities of Jmjd6 are emerging, perhaps its many functions, linked to arginine methylation of RNA binding proteins in transcription initiation complexes, spliceosome and ribosomes may be mediated by its RNA-binding abilities. Indeed Heim et al. (2014), showed that treatment with RNAse disrupt Jmjd6 nuclear localization.

In our study we found that two microRNAs induced by Ras (miR-146a and miR-193a) behave as tumor suppressors. MiR-146a and b are well-studied for their roles in immune responses. Induced by inflammation and infection through NF-kB signaling (Bhaumik et al., 2008), miR-146a, and to a lesser extent miR-146b, function in a negative feedback loop to downregulate several pro-inflammatory effectors. Indeed miR-146a has been implicated in attenuating pro-inflammatory responses (Saba et al., 2014), which could contribute in cancer to the elimination of early transformed cells by the immune system, and in reducing the

metastatic potential of breast cancer cells (Bhaumik et al., 2008). Increase in expression of miR-146a was reported in unclassified melanoma samples (Philippidou et al., 2010), and found to suppress brain metastasis from melanoma in experimental models (Hwang et al., 2013). These findings support a tumor suppressor role for miR-146a in melanoma. Our study provides evidence that miR-146a is induced by the same MAPK/AKT pathway that sustains melanoma growth at the earliest stages of transformation, when it could exert an anti-melanoma function by repressing Jmjd6 and perhaps also pro-tumoral inflammation. The tumor suppressive activity of miR-193a has been related to its ability to inhibit cell proliferation and to promote apoptosis of cancer cells (Nakano et al., 2013; Mamoori et al., 2018). MiR-193a undergoes epigenetic silencing in acute myeloid leukemia by the AML1/ETO fusion protein (Li et al., 2013), where miR-193 was found to repress several pro-leukemogenic factors, including KIT. Moreover miR193a has been found to participate in a regulatory loop that controls p53 family member levels (Ory et al., 2011) thus further reinforcing the hypothesis that miR193a is a tumor suppressor. The finding that both microRNAs target Jmjd6 and that this regulation is conserved in zebrafish and human melanoma suggests that lowering JMJD6 levels in cancer is another function of the tumor suppressors miR-146a and miR-193a.

The mechanisms through which Jmjd6 promote melanoma progression is still unknown. Different approaches, including transcriptome, epigenome and spliceosome analysis, can help to gain insights into the pro-oncogenic activity of JMJD6. In these studies, the transgenic lines kita:Jmjd6 and kita/Ras/Jmjd6 will provide a source of GFP tagged Jmjd6 proteins expressed specifically in melanocytes. We were puzzled by the massive presence of L-plastin positive cells (leukocytes, possibly including neutrophils and macrophages) within the *kita/Ras/Jmjd6* melanomas, compared to *kita/Ras* melanomas. Neutrophils and eosinophil infiltrations in melanoma predict unfavorable disease outcome (Ding et al., 2018) whereas accumulation of dendritic cells and T-lymphocytes is positively correlated with survival. Therefore, the increase of L-plastin positive neutrophils and macrophages is an index of the aggressiveness of these tumors. It is intriguing that one of the microRNAs targeting Jmjd6 in this progressive model of melanoma is miR-146a, a well-known regulator of inflammatory responses. It would be interesting to investigate whether miR-146a levels differ in melanoma developing in *kita/Ras* (where they are increased according to RNA-Seq data) versus those developing in *kita/Ras/Jmjd6*.

In summary, this study has shown that several microRNAs are induced by RAS signaling in melanoma initiating cells at the onset of transformation. Induced miR-146a and -193a target Jmjd6, which is temporarily downregulated. At later stages of melanoma development, and in human malignant melanoma with unfavorable prognosis, Jmjd6 is overexpressed, and in a zebrafish model where melanocytes express both Ras and Jmjd6, melanomas are more aggressive. Therefore, Jmjd6 has pro-oncogenic activities and the initial downregulation mediated by microRNAs may be part of an anti-oncogenic response, which is induced by the same RAS oncogene.

MATERIALS AND METHODS

Zebrafish Lines

Zebrafish were maintained and staged as described (Kimmel et al., 1995).

In addition to wild type AB fish, we used the following lines:

- *Et(kita:Gal4TA, UAS:mCherry)*^{hmz1}*; Tg(UAS:eGFP-HRASV12)*^{io006} a double transgenic line in which oncogenic ras expression is regulated by the kita promoter and that develop melanoma (Santoriello et al., 2010), also crossed to *ZDF1 (p53*$^{m214k/+}$*)*(Berghmans et al., 2005).
- *Tg(hsp70l:EGFP-HRAS_G12V)*^{io3} an heat-inducible oncogene expressing line (Santoriello et al., 2009).
- *Et(zic4:Gal4TA4, UAS:mCherry)*$^{hzm5;}$ *Tg(UAS:eGFP-HRASV12)*^{io006} a double transgenic line in which oncogenic ras expression is regulated by the zic4 promoter and that develop glioma (Mayrhofer et al., 2017).
- *Et(kita:Gal4TA, UAS:mCherry)*^{hmz1}*; Tg(UAS:eGFP-Jmjd6)*^{ka202}*;* and *Et(kita:Gal4TA, UAS:mCherry)*^{hmz1}*; Tg(UAS:eGFP-HRASV12)*^{io006}*; Tg(UAS:eGFP-Jmjd6)*^{ka202}xs double and triple transgenic lines in which the expression of a microRNA resistant Jmjd6 is regulated by Gal4 expressed under the kita promoter alone (double) or together with HRASV12 (triple), generated in the course of this study. This study was carried out in accordance with the recommendations of the OPBA of the University of Trento on Animal Welfare. Experimental procedures on zebrafish were performed in accordance with the European law on Animal Protection and Authorization No. 75/2017-PR from the Italian Ministry of Health.

miRNA Array

Custom-designed 8 × 15k microarray slides were ordered from Agilent Technologies. The 15k custom design was obtained from Edwin Cuppen and Eugene Berezikov (Hubrecht Institute, Utrecht, Netherlands) and has been submitted into the Gene Expression Omnibus (GEO) database (GPL 15403). The 15k design contained a duplicate of 7604 probes of 60-oligonucleotide length. The probes consisted of 2 × 22 nucleotide sequences antisense to mature miRNAs separated by a spacer of 8 nucleotides (CGATCTTT) and with a second spacer with the same sequence at the end. From 7604 probes 546 were designed for left (5′) and right (3′) arms of the hairpins of zebrafish miRNAs that are known in miRBase, while the remainder 7058 probes corresponded to predicted hairpin structures in the zebrafish genome that might include additional miRNAs but were not considered in this study. Total RNA, including microRNA, were extracted from 3-7-14 dpf wt or UAS-RAS larvae (driven by kita:Gal4, zic:Gal4, or hsp:Gal4), and from adult melanoma or wt fin tissue using miRNeasy Mini Kit®(Qiagen). Three biological replicates were obtained for each condition. For dual color hybridization of the Agilent chips miRNA samples from RAS transgenics were labeled with Hy3 and samples from control fish were labeled with Hy5 with miRCURY^{TM} LNA microRNA, Hy3^{TM}/Hy5^{TM} Power Labeling kit (Exiqon) using 1 microgram of total RNA according to the manufacturer's instructions.

The dual color hybridization of the microarray chips was performed according to Agilent protocol GE2_105_Jan09[8] for two-color microarray-based gene expression analysis except that hybridization and washing was performed at 37°C. The arrays were scanned with DNA Microarray Scanner G2565CA from Agilent Technologies. The arrays were scanned twice with 10% PMT and 100% PMT laser power. Microarray data was processed from raw data image files with Feature Extraction Software 9.5.3.1 (Agilent Technologies). The XDR function was used to extend the dynamic range. Processed data were subsequently imported into Rosetta Resolver 7.1 (Rosetta Biosoftware, Seattle, WA, United States) and subjected to default ratio error modeling. The raw data have been submitted to GEO under accession number GSE 37015. Values above 1.2 log2 Fold Changes and p-values < 0.01 in all three models were used as selection criteria.

QPCR for MicroRNAs

To confirm microarray data, total RNA, including miRNA, were purified from 3 dpf embryos using miRNeasy Mini Kit®(Qiagen). Mature miRNA were reverse transcribed using specific primers mix for each miR to produce different cDNA for TaqMan®MicroRNA assay (30 ng of total mRNA for each reaction) (Applied Biosystems). Taqman probes were designed for the active strand (−5p) of miR-21, miR-146a, and miR-146b and for the active (−3p) strand of miR-193a. Real-time PCR reactions based on TaqMan reagent chemistry were performed in duplicate on ABI PRISM®7900HT Fast Real-Time PCR System (Applied Biosystems). The level of miRNA expression was measured using C_T (cycle threshold). For normalization, miR-133, which was unaffected by RAS overexpression, was taken as reference. Fold change was generated using the equation 2^{-CT}. The list of oligos used and their sequences is provided in **Supplementary Table S2**.

Inhibitor Treatment

Three dpf HS-RAS and AB embryos were incubated in 2ml E3 medium in a 12 well plate in the presence of the following inhibitors: 1 μg/ml PD98059 (Calbiochem), 15 μM LY294002 (Cell Signaling) and 1 μM Rapamycin (Tocris). After 2 h, embryos were heat-shocked at 39°C for 30 min. After 6 h 50 RAS-GFP+ or GFP- embryos were collected in Trizol or sample buffer (2% SDS, 10% glycerol, 60 mM Tris pH 6.8) for miRNA or protein extraction respectively.

Western Blot and Antisera

Ten 3 dpf embryos were homogenized in 200 μl sample buffer (2% SDS, 10% glycerol, 60 mM Tris pH 6.8). 30 μg of total extract were resolved by SDS-PAGE, transferred to nitrocellulose and tested with the following antibodies: phospho-p44/42 (1:1000, Cell Signaling), p44/42 (1:1000, Cell Signaling), Phospho-AKT (1:1000, Cell Signaling), AKT (1:1000, Cell Signaling), Phospho-S6 (1:1000, Cell Signaling), S6 (Cell Signaling 1:1000), jmjd6 (Abcam, 1:1000), GFP (1:1000, Torrey Pines, United States), actin (1:5000, MP Biomedical).

[8]www.Agilent.com

Manual Inspection of 3′ UTR of Candidate MicroRNA Targets

An initial analysis performed with MicroCosm (now incorporated in tools4mirs at https://tools4mirs.org/) which used a previous version of the zebrafish genome identified a few genes as potential targets of both miR146a and 193a. Manual inspection of the 3′ UTR regions of these genes using the GRCz11 release at Ensembl[5] confirmed that only *jmjd6* 3′ UTR region contained sequences that match the seed regions of both microRNAs. We then used a web-based interaction-prediction algorithm for RNA molecules, IntaRNA[4] (Mann et al., 2017) for the fast and accurate prediction of the interactions between miR-146a and/or 193a with *jmjd6* mRNAs (*Ensemble, ENSDARG00000102896*[5]). We followed the web-site instructions and used *jmjd6* and miR-146a-5p and -193a-3p sequences as input. The following parameters were used: minimum number of base pairs in seed: 7; temperature for energy computation: 37°C; energy parameter set (Vienna package), Turner Model 2004 (Lorenz et al., 2011); energy interaction levels < -8.

Morpholino, Duplexes, and Plasmids

Morpholinos, including a standard control morpholino, were obtained from Gene Tools (United States), titrated to non-toxic concentrations and injected in a final volume of 2 nl per 1-cell embryo. A list of all morpholinos, their sequences and the concentration used is provided in **Supplementary Table S3**. Synthetic miR- duplexes controls and 146a were designed and ordered from SIGMA (United States). Synthetic miR- duplexes for miR-193a were purchased from Ambion. Duplexes were dissolved in RNAse free water and diluted using annealing buffer (30 mM HEPES-KOH pH 7.4, 10 mM KCl, 2 mM $MgCl_2$, 50 mM NH_4Ac) to a final concentration of 10 μM for miR-146a 5 μM for miR-193a. The solution was incubated for 1 min at 90°C, cooled down slowly to room temperature and injected in a final volume of 2 nl per 1-cell embryo. A list of all duplexes, their sequences and the concentration used is provided in **Supplementary Table S4**.

For Jmjd6 reporter construct, the whole *Jmjd6* (*Ensemble, ENSDARG00000102896*) 3′ UTRs was PCR amplified from cDNA using specific primers (**Supplementary Table S2**). The PCR product was subcloned into the pCS2:eGFP vector downstream of the GFP open reading frame and confirmed by sequencing.

Generation of a Jmjd6 Transgenic Line

To express a microRNA resistant Jmjd6 in melanocytes, the full coding region excluding the stop codon of *Jmjd6* (*Ensemble, ENSDARG00000102896*) was PCR amplified and cloned into *pEntry5-no stop* (Invitrogen) and then recombined using gateway technology with a *pEnt5-4nrUAS* (generated by cloning four non-repetitive UAS elements into pENT5′ from Invitrogen), a *p3E-EGFPpA* (Tol2Kit clone n.366) + *pDestTol2CG2* (Tol2Kit clone n. 395) using gateway (Kwan and North, 2017). Clone numbers and sequences can be found at: http://chien.neuro.utah.edu/tol2kitwiki/index.php/Main_Page.

Final recombined clones were checked by sequencing. *4nrUAS:eGFP-Jmjd6* plasmid was injected in 1-cell embryos

of the *Et(kita:Gal4TA, UAS:mCherry)*^{hmz1} line to generate a transgenic line using standard Tol2 mediated transgenesis (Kawakami, 2004; Pase and Lieschke, 2009).

Zebrafish Embryo Injections

Zebrafish embryos at the stage of 1–2 cells were injected with morpholinos against miRs or Jmjd6 diluted in double distilled, sterile H_2O. The morpholino oligonucleotides were injected at a concentration of 5 ng/nl, in a volume of 2 nl/embryo. miR duplexes mimicking mature microRNA were injected following a described protocol (Pase and Lieschke, 2009), at a concentration of 10 μM for miR-146a and miR-146b and 5 μM for miR193a in a volume of 2 nl/embryo.

Sensor injections: mRNA encoding for eGFP carrying Jmjd6 3′ UTR was *in vitro* synthesized and injected in 1–2 cell zebrafish embryos at 100 pg/embryo, alone or in combination with duplexes or morpholinos.

Imaging

Photographs of whole larvae were acquired with a Nikon S100 stereomicroscope equipped with epifluorescence and multiple filters. We used a Leica SP5 confocal for analysis of melanocytes expressing Ras-eGFP, Jmjd6-GFP, and L-plastin immunoreactivity.

AGO2 – RIP

One hundred 3 dpf embryos injected or not with miR duplex were homogenized in ice-cold buffer A containing 50 mM Tris-HCl pH 7.5, 5 mM EDTA, 5 mM EGTA, complete proteinase inhibitor (Roche) and 1 U/μl RNAse inhibitor SUPERnase-IN (Ambion). Unbroken cells were removed at 100 g for 5 min at 4°C. NP40 was added at 0.5% (wt/vol) and samples incubated at 4°C for 15 min with rotation and centrifuged at 10000 × *g* for 15 min. SN was the transferred to a new tube and the protein were measured by BCA. 2 mg of protein were diluted with buffer A and incubated overnight at 4°C with 50 μl Dynabeads (Invitrogen) bound with 2 μg Ago2 antibody (Abcam) or IgG (negative control). The next morning beads were washed four times with 1 ml of washing buffer containing 50 mM Tris-HCl pH 7.4, 150 mM NaCl, 1 mM $MgCl_2$ and 0.05% NP40. Beads were then resuspended in 1ml of washing buffer and 200 μl of beads were pelleted and resuspended in 50 ul sample buffer to test Ago2 by western blot (Abcam 1:1000). The remaining 800 ul were resuspend with 500 μl of trizol and RNA was extracted by RNeasy micro Kit (Qiagen). All the RNA was retro-transcribed using Vilo (Invitrogen) and 1 μl of cDNA was used for PCR using specific primers for *jmjd6* or the housekeeping gene, *gapdh*.

Analysis of Data From cBioportal and Protein Atlas

Analysis of JMJD6 expression, correlation with HRAS or BRAF mutations, survival and disease/progression-free survival in patients was done using the dataset Skin Cutaneus Melanoma TCGA dataset in cBioportal[6]. The survival and disease/progression-free survival were done taking into account the following JMJD6 alterations: mutations, amplifications, deep deletions or multiple alterations.

We report here examples of JMJD6 protein localization in control skin (ID: 2396[9]) and in a malignant melanoma (ID: 2136[10]) from the Protein Atlas website.

AUTHOR CONTRIBUTIONS

VA and MM design the study, conducted experiments, and wrote the manuscript. VA, AO and AM performed the microarray analysis. SK, LS, and VG performed bioinformatics analysis. MS and AM provided conceptual insights.

FUNDING

Work in the lab of MCM is supported the European Commission under the Horizon 2020 program (U. M. Cure/Project No. 667787), and by a 5 × 1000 LILT-2016 contribution. AM acknowledges the contribution of the European Commission 6th Framework Project ZF-TOOLS (LSHG-CT-2006-037220).

ACKNOWLEDGMENTS

We would like to thank Cristina Santoriello for help and discussion on the experimental design, Nadine Borel and EZRC personnel for fish care, Reinhard Koester and Martin Distel for sharing the Gal4 lines used in this study, Kyuson Yun for reading and commenting on an earlier version of the manuscript, Erik Dassi for help with the heatmap in **Figure 1**, and Sabrina Burkart for technical support.

SUPPLEMENTARY MATERIAL

The Supplementary Material for this article can be found online at: https://www.frontiersin.org/articles/10.3389/fgene.2018.00675/full#supplementary-material

FIGURE S1 | Output of IntaRNA website, showing interaction of microRNAs 146a **(A)** and 193a **(B)** with the 3′ UTR of jmjd6. An energy of −8 Kcal/mol or less is indicative of a stable interaction.

FIGURE S2 | Injections of duplexes microRNAs cause increase of the corresponding microRNAs and mild developmental defects. **(A)** QPCR analysis of the expression levels of the microRNAs indicated. **(B)** All the other injected embryos developed without visible abnormalities.

FIGURE S3 | Jmjd6 is down-regulated upon Ras expression. Jmjd6 mRNA **(A)** and protein levels **(B)** are downregulated by Ras overexpression (2nd lane) and rescued to normal levels by downregulating the increased microRNAs (lanes 3–4).

[9]https://www.proteinatlas.org/ENSG00000070495-JMJD6/tissue/skin
[10]https://www.proteinatlas.org/ENSG00000070495-JMJD6/pathology/tissue/melanoma#img

FIGURE S4 | cBioPortal data of JMJD6. **(A)** Alteration frequency of JMJD6 in different type of cancers. **(B)** JMJD6 expression in melanoma patients; each bar represents a patient. Red bars: patients with upregulated JMJD6. Blue bars: patients with downregulated JMJD6. JMJD6 expression in HRAS **(C)** and BRAF **(D)** mutated melanoma. Overall survival **(E)** and disease/progression-free survival **(F)** in patients with (red curve) or without (blue curve) JMJD6 alterations.

TABLE S1 | miRNA array results table. Column A: probe ID; column B: sequence of the probe; column C: Gene ID; column D: Gene symbol; Columns E–P: fold change and relative *p*-value of the samples as indicated. Fold change and *p*-value are calculated by comparing the miRNAs expression in kita-Ras larvae at 3, 7, and 14 dpf, HS-Ras, and zic at 3 dpf and adult melanoma with the respective control (AB for all the larvae and skin from adult AB wild type fish for the adult melanoma). MicroRNAs selected for further studies (see text for criteria used) and their expression values (log2FoldChanges and pValues) are highlighted.

TABLE S2 | Oligo sequences. Sequences of the oligos used for qPCR, RIP assay, *jmjd6* 3′-UTR cloning and Gateway cloning of Jmjd6.

TABLE S3 | Morpholino sequences. Sequences of the morpholinos used in the study.

TABLE S4 | microRNA duplexes. Sequences of the miR control (miR-C) and miR-146a_l injected in the embryos. The sequence of miR-193a was not provided by the supplier (Ambion).

REFERENCES

Berghmans, S., Murphey, R. D., Wienholds, E., Neuberg, D., Kutok, J. L., Fletcher, C. D. M., et al. (2005). tp53 mutant zebrafish develop malignant peripheral nerve sheath tumors. *Proc. Natl. Acad. Sci. U.S.A.* 102, 407–412. doi: 10.1073/pnas.0406252102

Bhaumik, D., Scott, G. K., Schokrpur, S., Patil, C. K., Campisi, J., and Benz, C. C. (2008). Expression of microRNA-146 suppresses NF-kappaB activity with reduction of metastatic potential in breast cancer cells. *Oncogene* 27, 5643–5647. doi: 10.1038/onc.2008.171

Boeckel, J.-N., Guarani, V., Koyanagi, M., Roexe, T., Lengeling, A., Schermuly, R. T., et al. (2011). Jumonji domain-containing protein 6 (Jmjd6) is required for angiogenic sprouting and regulates splicing of VEGF-receptor 1. *Proc. Natl. Acad. Sci. U.S.A.* 108, 3276–3281. doi: 10.1073/pnas.1008098108

Böse, J., Gruber, A. D., Helming, L., Schiebe, S., Wegener, I., Hafner, M., et al. (2004). The phosphatidylserine receptor has essential functions during embryogenesis but not in apoptotic cell removal. *J. Biol.* 3:15. doi: 10.1186/jbiol10

Cerami, E., Gao, J., Dogrusoz, U., Gross, B. E., Sumer, S. O., Aksoy, B. A., et al. (2012). The cBio cancer genomics portal: an open platform for exploring multidimensional cancer genomics data. *Cancer Discov.* 2, 401–404. doi: 10.1158/2159-8290.CD-12-0095

Chang, B., Chen, Y., Zhao, Y., and Bruick, R. K. (2007). JMJD6 is a histone arginine demethylase. *Science* 318, 444–447. doi: 10.1126/science.1145801

Chin, L., Artandi, S. E., Shen, Q., Tam, A., Lee, S. L., Gottlieb, G. J., et al. (1999a). deficiency rescues the adverse effects of telomere loss and cooperates with telomere dysfunction to accelerate carcinogenesis. *Cell* 97, 527–538.

Chin, L., Tam, A., Pomerantz, J., Wong, M., Holash, J., Bardeesy, N., et al. (1999b). Essential role for oncogenic Ras in tumour maintenance. *Nature* 400, 468–472. doi: 10.1038/22788

Cui, P., Qin, B., Liu, N., Pan, G., and Pei, D. (2004). Nuclear localization of the phosphatidylserine receptor protein via multiple nuclear localization signals. *Exp. Cell Res.* 293, 154–163. doi: 10.1016/j.yexcr.2003.09.023

Ding, Y., Zhang, S., and Qiao, J. (2018). Prognostic value of neutrophil-to-lymphocyte ratio in melanoma: evidence from a PRISMA-compliant meta-analysis. *Medicine* 97:e11446. doi: 10.1097/MD.0000000000011446

Distel, M., Wullimann, M. F., and Köster, R. W. (2009). Optimized Gal4 genetics for permanent gene expression mapping in zebrafish. *Proc. Natl. Acad. Sci. U.S.A.* 106, 13365–13370. doi: 10.1073/pnas.0903060106

Fadok, V. A., Bratton, D. L., Rose, D. M., Pearson, A., Ezekewitz, R. A., and Henson, P. M. (2000). A receptor for phosphatidylserine-specific clearance of apoptotic cells. *Nature* 405, 85–90. doi: 10.1038/35011084

Frezzetti, D., De Menna, M., Zoppoli, P., Guerra, C., Ferraro, A., Bello, A. M., et al. (2011). Upregulation of miR-21 by Ras *in vivo* and its role in tumor growth. *Oncogene* 30, 275–286. doi: 10.1038/onc.2010.416

Hahn, P., Wegener, I., Burrells, A., Böse, J., Wolf, A., Erck, C., et al. (2010). Analysis of Jmjd6 cellular localization and testing for its involvement in histone demethylation. *PLoS One* 5:e13769. doi: 10.1371/journal.pone.0013769

Harrandah, A. M., Mora, R. A., and Chan, E. K. L. (2018). Emerging microRNAs in cancer diagnosis, progression, and immune surveillance. *Cancer Lett.* 438, 126–132. doi: 10.1016/j.canlet.2018.09.019

Heim, A., Grimm, C., Müller, U., Häußler, S., Mackeen, M. M., Merl, J., et al. (2014). Jumonji domain containing protein 6 (Jmjd6) modulates splicing and specifically interacts with arginine-serine-rich (RS) domains of SR- and SR-like proteins. *Nucleic Acids Res.* 42, 7833–7850. doi: 10.1093/nar/gku488

Hong, J.-R., Lin, G.-H., Lin, C. J.-F., Wang, W.-P., Lee, C.-C., Lin, T.-L., et al. (2004). Phosphatidylserine receptor is required for the engulfment of dead apoptotic cells and for normal embryonic development in zebrafish. *Development* 131, 5417–5427. doi: 10.1242/dev.01409

Hong, X., Zang, J., White, J., Wang, C., Pan, C.-H., Zhao, R., et al. (2010). Interaction of JMJD6 with single-stranded RNA. *Proc. Natl. Acad. Sci. U.S.A.* 107, 14568–14572. doi: 10.1073/pnas.1008832107

Hwang, S. H., Lee, B.-H., Kim, H.-J., Cho, H.-J., Shin, H.-C., Im, K.-S., et al. (2013). Suppression of metastasis of intravenously-inoculated B16/F10 melanoma cells by the novel ginseng-derived ingredient, gintonin: involvement of autotaxin inhibition. *Int. J. Oncol.* 42, 317–326. doi: 10.3892/ijo.2012.1709

Ikeda, K., Satoh, M., Pauley, K. M., Fritzler, M. J., Reeves, W. H., and Chan, E. K. L. (2006). Detection of the argonaute protein Ago2 and microRNAs in the RNA induced silencing complex (RISC) using a monoclonal antibody. *J. Immunol. Methods* 317, 38–44. doi: 10.1016/j.jim.2006.09.010

Jang, M. K., Mochizuki, K., Zhou, M., Jeong, H.-S., Brady, J. N., and Ozato, K. (2005). The bromodomain protein Brd4 is a positive regulatory component of P-TEFb and stimulates RNA polymerase II-dependent transcription. *Mol. Cell* 19, 523–534. doi: 10.1016/j.molcel.2005.06.027

Johnson, L., Mercer, K., Greenbaum, D., Bronson, R. T., Crowley, D., Tuveson, D. A., et al. (2001). Somatic activation of the K-ras oncogene causes early onset lung cancer in mice. *Nature* 410, 1111–1116. doi: 10.1038/35074129

Kawakami, K. (2004). Transgenesis and gene trap methods in zebrafish by using the Tol2 transposable element. *Methods Cell Biol.* 77, 201–222. doi: 10.1016/S0091-679X(04)77011-9

Kimmel, C. B., Ballard, W. W., Kimmel, S. R., Ullmann, B., and Schilling, T. F. (1995). Stages of embryonic development of the zebrafish. *Dev. Dyn.* 203, 253–310. doi: 10.1002/aja.1002030302

Kunisaki, Y., Masuko, S., Noda, M., Inayoshi, A., Sanui, T., Harada, M., et al. (2004). Defective fetal liver erythropoiesis and T lymphopoiesis in mice lacking the phosphatidylserine receptor. *Blood* 103, 3362–3364. doi: 10.1182/blood-2003-09-3245

Kwan, W., and North, T. E. (2017). Netting novel regulators of hematopoiesis and hematologic malignancies in zebrafish. *Curr. Top. Dev. Biol.* 124, 125–160. doi: 10.1016/bs.ctdb.2016.11.005

Li, Y., Gao, L., Luo, X., Wang, L., Gao, X., Wang, W., et al. (2013). Epigenetic silencing of microRNA-193a contributes to leukemogenesis in t(8;21) acute myeloid leukemia by activating the PTEN/PI3K signal pathway. *Blood* 121, 499–509. doi: 10.1182/blood-2012-07-444729

Liu, W., Ma, Q., Wong, K., Li, W., Ohgi, K., Zhang, J., et al. (2013). Brd4 and JMJD6-associated anti-pause enhancers in regulation of transcriptional pause release. *Cell* 155, 1581–1595. doi: 10.1016/j.cell.2013.10.056

Liu, X., Si, W., Liu, X., He, L., Ren, J., Yang, Z., et al. (2017). JMJD6 promotes melanoma carcinogenesis through regulation of the alternative splicing of PAK1, a key MAPK signaling component. *Mol. Cancer* 16:175. doi: 10.1186/s12943-017-0744-2

Lorenz, R., Bernhart, S. H., Höner Zu Siederdissen, C., Tafer, H., Flamm, C., Stadler, P. F., et al. (2011). ViennaRNA Package 2.0. *Algorithms Mol. Biol.* 6:26. doi: 10.1186/1748-7188-6-26

Lukasik, A., Wójcikowski, M., and Zielenkiewicz, P. (2016). Tools4miRs – one place to gather all the tools for miRNA analysis. *Bioinformatics* 32, 2722–2724. doi: 10.1093/bioinformatics/btw189

Malumbres, M., and Barbacid, M. (2003). RAS oncogenes: the first 30 years. *Nat. Rev. Cancer* 3, 459–465. doi: 10.1038/nrc1097

Mamoori, A., Gopalan, V., and Lam, A. K.-Y. (2018). Role of miR-193a in cancer: complexity and factors control the pattern of its expression. *Curr. Cancer Drug Targets* 18, 618–628. doi: 10.2174/1568009618666180308105727

Mann, M., Wright, P. R., and Backofen, R. (2017). IntaRNA 2.0: enhanced and customizable prediction of RNA-RNA interactions. *Nucleic Acids Res.* 45, W435–W439. doi: 10.1093/nar/gkx279

Mayrhofer, M., Gourain, V., Reischl, M., Affaticati, P., Jenett, A., Joly, J.-S., et al. (2017). A novel brain tumour model in zebrafish reveals the role of YAP activation in MAPK- and PI3K-induced malignant growth. *Dis. Model Mech.* 10, 15–28. doi: 10.1242/dmm.026500

Nakano, H., Yamada, Y., Miyazawa, T., and Yoshida, T. (2013). Gain-of-function microRNA screens identify miR-193a regulating proliferation and apoptosis in epithelial ovarian cancer cells. *Int. J. Oncol.* 42, 1875–1882. doi: 10.3892/ijo.2013.1896

Ory, B., Ramsey, M. R., Wilson, C., Vadysirisack, D. D., Forster, N., Rocco, J. W., et al. (2011). A microRNA-dependent program controls p53-independent survival and chemosensitivity in human and murine squamous cell carcinoma. *J. Clin. Invest.* 121, 809–820. doi: 10.1172/JCI43897

Pase, L., and Lieschke, G. J. (2009). Validating microRNA target transcripts using zebrafish assays. *Methods Mol. Biol.* 546, 227–240. doi: 10.1007/978-1-60327-977-2_14

Philippidou, D., Schmitt, M., Moser, D., Margue, C., Nazarov, P. V., Muller, A., et al. (2010). Signatures of microRNAs and selected microRNA target genes in human melanoma. *Cancer Res.* 70, 4163–4173. doi: 10.1158/0008-5472.CAN-09-4512

Rahman, S., Sowa, M. E., Ottinger, M., Smith, J. A., Shi, Y., Harper, J. W., et al. (2011). The Brd4 extraterminal domain confers transcription activation independent of pTEFb by recruiting multiple proteins, including NSD3. *Mol. Cell. Biol.* 31, 2641–2652. doi: 10.1128/MCB.0134110

Saba, R., Sorensen, D. L., and Booth, S. A. (2014). MicroRNA-146a: a dominant, negative regulator of the innate immune response. *Front. Immunol.* 5:578. doi: 10.3389/fimmu.2014.00578

Santoriello, C., Deflorian, G., Pezzimenti, F., Kawakami, K., Lanfrancone, L., d'Adda di Fagagna, F., et al. (2009). Expression of H-RASV12 in a zebrafish model of Costello syndrome causes cellular senescence in adult proliferating cells. *Dis. Model Mech.* 2, 56–67. doi: 10.1242/dmm.001016

Santoriello, C., Gennaro, E., Anelli, V., Distel, M., Kelly, A., Köster, R. W., et al. (2010). Kita driven expression of oncogenic HRAS leads to early onset and highly penetrant melanoma in zebrafish. *PLoS One* 5:e15170. doi: 10.1371/journal.pone.0015170

Tibrewal, N., Liu, T., Li, H., and Birge, R. B. (2007). Characterization of the biochemical and biophysical properties of the phosphatidylserine receptor (PS-R) gene product. *Mol. Cell. Biochem.* 304, 119–125. doi: 10.1007/s11010-007-9492-8

Uhlen, M., Zhang, C., Lee, S., Sjöstedt, E., Fagerberg, L., Bidkhori, G., et al. (2017). A pathology atlas of the human cancer transcriptome. *Science* 357:eaan2507. doi: 10.1126/science.aan2507

Webby, C. J., Wolf, A., Gromak, N., Dreger, M., Kramer, H., Kessler, B., et al. (2009). Jmjd6 catalyses lysyl-hydroxylation of U2AF65, a protein associated with RNA splicing. *Science* 325, 90–93. doi: 10.1126/science.1175865

Conflict of Interest Statement: The authors declare that the research was conducted in the absence of any commercial or financial relationships that could be construed as a potential conflict of interest.

frontiers in Genetics

ORIGINAL RESEARCH
published: 11 December 2018
doi: 10.3389/fgene.2018.00612

High MYC Levels Favour Multifocal Carcinogenesis

Manuela Sollazzo†, China Genchi*†, Simona Paglia, Simone Di Giacomo, Annalisa Pession, Dario de Biase and Daniela Grifoni**

Cancer Evolution Laboratory, Department of Pharmacy and Biotechnology, University of Bologna, Bologna, Italy

OPEN ACCESS

Edited by:
Maria Grazia Giansanti, Consiglio Nazionale delle Ricerche (CNR), Italy

Reviewed by:
Louise Cheng, Peter MacCallum Cancer Centre, Australia
Romain Levayer, Institut Pasteur, France

***Correspondence:**
Manuela Sollazzo
manuela.sollazzo2@unibo.it
Daniela Grifoni
daniela.grifoni@unibo.it

†Present address:
Manuela Sollazzo, Cellular Biochemistry Laboratory, Department of Pharmacy and Biotechnology, University of Bologna, Bologna, Italy
China Genchi, Laboratory of Membrane Trafficking, Signaling and Development, Department of Biosciences, University of Milan, Milan, Italy

Specialty section:
This article was submitted to Genetic Disorders, a section of the journal Frontiers in Genetics

Received: *15 September 2018*
Accepted: *20 November 2018*
Published: *11 December 2018*

Citation:
Sollazzo M, Genchi C, Paglia S, Di Giacomo S, Pession A, de Biase D and Grifoni D (2018) High MYC Levels Favour Multifocal Carcinogenesis. Front. Genet. 9:612. doi: 10.3389/fgene.2018.00612

The term "field cancerisation" describes the formation of tissue sub-areas highly susceptible to multifocal tumourigenesis. In the earlier stages of cancer, cells may indeed display a series of molecular alterations that allow them to proliferate faster, eventually occupying discrete tissue regions with irrelevant morphological anomalies. This behaviour recalls cell competition, a process based on a reciprocal fitness comparison: when cells with a growth advantage arise in a tissue, they are able to commit wild-type neighbours to death and to proliferate at their expense. It is known that cells expressing high MYC levels behave as super-competitors, able to kill and replace less performant adjacent cells; given MYC upregulation in most human cancers, MYC-mediated cell competition is likely to pioneer field cancerisation. Here we show that MYC overexpression in a sub-territory of the larval wing epithelium of *Drosophila* is sufficient to trigger a number of cellular responses specific to mammalian pre-malignant tissues. Moreover, following induction of different second mutations, high MYC-expressing epithelia were found to be susceptible to multifocal growth, a hallmark of mammalian pre-cancerous fields. In summary, our study identified an early molecular alteration implicated in field cancerisation and established a genetically amenable model which may help study the molecular basis of early carcinogenesis.

Keywords: MYC, field cancerisation, multifocality, *Drosophila*, TSGs, cell competition

INTRODUCTION

The molecular events underlying cancer initiation are largely unknown. It is commonly accepted that most cancers are monoclonal in origin, evolving from a single cell whose lineage accumulates in time multiple molecular insults (Michor et al., 2004; Vogelstein et al., 2013; Feinberg et al., 2016). In particular, driver mutations, which provide cells with a growth advantage and are positively selected during lineage evolution, are generally associated with clonal expansion and are frequently found in pre-malignant lesions (Maley et al., 2004; Lawrence et al., 2014; Curtius et al., 2017). In the 1950s, Slaughter introduced the concept of "field cancerisation": while studying oral cancers, he observed that they recurred more frequently adjacent to a resected tumour (Slaughter et al., 1953). Therefore, field cancerisation was defined as the process leading to the formation of a tissue sub-territory which, despite a normal appearance, bears a series of alterations that make cells more susceptible to malignant transformation than wild-type neighbours, giving rise to multifocal cancers (Wodarz et al., 2004). Successive studies, also fostered by the development of post-genomic technologies (Metzker, 2010), have demonstrated that this phenomenon is not specific to the oral mucosa, being rather a common feature of epithelial organs (Braakhuis et al., 2003; Dakubo et al., 2007;

Nonn et al., 2009; Zeki et al., 2011; Jakubek et al., 2016; Lu et al., 2016; Park et al., 2016; Abdalla et al., 2017; Castven et al., 2017).

Although the interest in deciphering cancer's molecular signature is obvious, it may be quite difficult to understand what mutations favour and maintain the malignant phenotype: a surprising number of driver mutations is indeed present in pre-cancerous tissues, also in those that are not likely to evolve into a frank malignancy (Hofstad et al., 1996; Martincorena et al., 2015; Kato et al., 2016). This suggests that several alterations are evolutionarily neutral and do not impact cell's phenotype, maybe depending on their temporal occurrence (de Bruin et al., 2014), the tissue context (Galandiuk et al., 2012; Gagneur et al., 2013; Vermeulen et al., 2013) and the genetic background (Chandler et al., 2013). In human tissues, a number of genetic alterations have been associated with field cancerisation (Papadimitrakopoulou et al., 1996; Braakhuis et al., 2002; Santos-Garcia et al., 2005; Haaland et al., 2009; Trujillo et al., 2011; Mohan and Jagannathan, 2014), and genetic/genomic instability (Ellsworth et al., 2004; Zaky et al., 2008; Giaretti et al., 2012), mitochondrial defects (McDonald et al., 2008; Maggrah et al., 2013; Parr et al., 2013), production of reactive oxygen species (ROS) (Bongers et al., 1995; Jaloszynski et al., 2003; Chan et al., 2017), increased expression of proliferation and apoptosis markers (Birchall et al., 1997; Bascones-Martinez et al., 2013) and epigenetic modifications (Grady, 2005; Lee et al., 2011; Kamiyama et al., 2012; Luo et al., 2014) are also repeatedly found in regions adjacent to malignant tumours from a variety of organs. Whatever the cause of these modifications, from DNA replication errors to mutagenic injuries, the ongoing pre-cancerous field will most likely be composed of a number of genetically different clones, with the fittest one expected to colonise the entire territory over time (Driessens et al., 2012). This process of selection based on fitness comparison is a distinctive trait of cell competition (CC), a phenomenon first observed and characterised in *Drosophila* (Morata and Ripoll, 1975), and then demonstrated to be conserved in mammals (Penzo-Mendez and Stanger, 2014; Di Gregorio et al., 2016).

Competitive interactions are typically triggered when cells with different proliferation rates are found in close proximity: the fittest cells (winners) commit less fit neighbours (losers) to death and overgrow to replace them in the tissue (Levayer and Moreno, 2013, 2016; Tamori and Deng, 2013; Tsuboi et al., 2018). A number of molecules and signalling pathways have to date been found to play a role in CC (Moreno et al., 2002; Tyler et al., 2007; Vincent et al., 2011; Rodrigues et al., 2012; Akai et al., 2018): among these, the MYC protein was shown to be the most powerful inducer of CC (named in this case MYC-Mediated Cell Competition, MMCC) from *Drosophila* to mammals (Johnston, 2014), paving the way to studies that found this process implicated in a number of seemingly distant contexts, from organ development (de la Cova et al., 2004; Moreno and Basler, 2004; Claveria et al., 2013; Sancho et al., 2013; Villa del Campo et al., 2014; Villa Del Campo et al., 2016) to tissue regeneration (Oertel et al., 2006; Gogna et al., 2015; Rosen et al., 2015; Villa Del Campo et al., 2016; Shakiba and Zandstra, 2017), cell stemness (Rhiner et al., 2009; Diaz-Diaz et al., 2017) and cancer (Froldi et al., 2010; Ziosi et al., 2010; Eichenlaub et al., 2016; Suijkerbuijk et al., 2016). Of note, we and others recently demonstrated that MMCC is also active in human cancer cells (Patel et al., 2016; Di Giacomo et al., 2017). MYC upregulation is sufficient as to transform cells into super-competitors (Moreno and Basler, 2004), able to kill and replace suboptimal neighbours, and this capability has opened to speculations about a possible role for MMCC in field cancerisation (Rhiner and Moreno, 2009; Johnston, 2014). MYC family proteins are long investigated for their essential functions in cell physiology and in cancer (Stine et al., 2015); the *Drosophila* genome bears a single *locus* (*diminutive*, *dm*) encoding the MYC protein, which exerts the same functions as the mammalian orthologues (Gallant, 2013). MYC overexpression in wild-type cells may provoke a series of contradictory responses: on the one hand, it supports cell growth by accelerating biosynthesis, cell metabolism and cell cycle (Evan and Littlewood, 1993; Grewal et al., 2005; Meyer and Penn, 2008); on the other hand, it promotes potentially harmful reactions such as ROS production and genetic instability (Vafa et al., 2002; Greer et al., 2013; Kuzyk and Mai, 2014), and increases propensity to apoptotic cell death (Montero et al., 2008; McMahon, 2014). Cancer cells upregulating MYC are contrariwise protected from untimely death, primarily due to relevant changes in metabolic pathways leading to MYC addiction (Gabay et al., 2014). MYC seems thus to elicit in normal cells a number of biological responses similar to those found in mammalian pre-cancerous fields (Mohan and Jagannathan, 2014). Moreover, MYC upregulation is an early event in human prostate cancer (Gurel et al., 2008), and MYC overexpression is sufficient to transform luminal epithelial cells into pre-malignant derivatives in the mouse prostatic gland (Kim et al., 2009; Iwata et al., 2010). MYC upregulation has also been observed in cytologically normal bronchial epithelial cells of mice with pre-neoplastic lung squamous cell carcinoma lesions (Xiong et al., 2017), and it was reported to initiate gastric tumourigenesis following Hippo pathway deregulation in the pyloric stem cell (Choi et al., 2018). These observations led us to speculate that high MYC levels may be sufficient for an epithelial tissue to become responsive to the effect of second mutations that would otherwise be irrelevant when occurring in a wild-type epithelium.

In *Drosophila*, the tumour suppressor genes (TSGs) are historically subdivided into two classes, called "hyperplastic" and "neoplastic" according to the mutant phenotype (Hariharan and Bilder, 2006), most of which have in time been found to encode different components of the Hippo pathway (Grusche et al., 2010), a highly conserved signalling cascade central in cell growth and organ size modulation (Halder and Johnson, 2011). Broadly speaking, loss-of-function (LOF) mutants of these hyperplastic TSGs (*fat*, *ft*; *dachsous*, *ds*; *expanded*, *ex*; *warts*, *wts*; and *hippo*, *hpo*) show a substantial overgrowth of the larval epithelial organs, called imaginal discs (Aldaz and Escudero, 2010), and premature death at the pupal stage (Hariharan and Bilder, 2006), whereas LOF mutants of neoplastic TSGs do not survive beyond embryogenesis (Menut et al., 2007). An exception is made for *scribble* (*scrib*), *discs large* (*dlg*), and *lethal giant larvae* (*lgl*) neoplastic mutants which, given the abundant maternal transcript released into the zygote, survive up to the end of the larval life, showing abnormal growth of the imaginal discs with

a complete loss of the epithelial structure (Bilder et al., 2000; Bilder, 2004). In case single mutant cells are created in a wild-type background through clonal analysis techniques (del Valle et al., 2012), those bearing hyperplastic LOF mutations survive and overgrow in the target tissue (Xu et al., 1995; Buratovich and Bryant, 1997; Udan et al., 2003; Maitra et al., 2006), whereas those bearing neoplastic LOF mutations are usually eliminated during development (Agrawal et al., 1995; Enomoto and Igaki, 2011). We and others demonstrated these opposite behaviours are dictated by MMCC: while hyperplastic mutant cells upregulate MYC and behave like winners in the wild-type tissue, killing the surrounding neighbours and growing at their expense (Neto-Silva et al., 2010; Ziosi et al., 2010), neoplastic mutant cells do not upregulate MYC and behave like losers in the context, being themselves out-competed by adjacent wild-type cells (Froldi et al., 2010; Menendez et al., 2010). We previously showed that a MYC-overexpressing background strengthens the super-competitive behaviour of *ft*, *ds* and *ex* mutant clones, which were found to kill the surrounding cells with increased efficiency and to grow more rapidly, although it did not provide mutant cells with the capability to evolve into a malignant mass (Ziosi et al., 2010).

Here we expanded on previous work by first identifying in *Drosophila* MYC-overexpressing epithelial organs a series of morphological and molecular markers typically found in human pre-cancerous fields. Moreover, we investigated the impact of a MYC-overexpressing background on the cellular phenotypes consequent to mutations in neoplastic TSGs, showing it is in this case sufficient to make mutant cells able to initiate multifocal malignant transformation, a peculiar trait of human pre-neoplastic fields.

MATERIALS AND METHODS

Fly Stocks and Manipulation

The following fly lines were used in the study, built using stocks obtained from the Bloomington Drosophila Stock Center, Indiana: w; UAS-GFP$^{(Bl-6874)}$; hh-Gal4$^{(Bl-67046)}$ – yw, PI3K92E$^{CAAX(Bl-25908)}$ – w; Ubi-GFPnls, FRT40A$^{(Bl-5629)}$/CyO; hh-Gal4$^{(Bl-67046)}$/TM6b – w; l(2)gl^4 P(neo-FRT)40A$^{(Bl-36289)}$/In(2-3)Gla,Bc; UAS-HAdm/TM6b – w; Rab5^{2}P(neo-FRT)40A$^{(Bl-42702)}$/In(2-3)Gla,Bc; UAS-HAdm/TM6b. UAS-HAdm on III is a gift of P. Bellosta. Plain genotypes are given for each experiment in the figure legends. For all experiments, flies were kept at 25°C. Larvae were heat-shocked once at 48 ± 4 h AEL in a water bath at 37°C for 10 min and dissected after additional 72 h development.

Immunofluorescence

Frozen or fresh larvae were prepared for immunofluorescence by standard methods. The following antibodies and dilutions were used: mouse α-MYC (1:5, P. Bellosta); rabbit α-Lgl (1:400, D. Strand); rabbit α-active Caspase 3 (1:100, Cell Signalling Technologies); rabbit α-aPKCζ (1:200, Santa Cruz Biotechnology); rabbit α-pAKT (1:100, Cell Signaling Technologies); rabbit α-PH3 (1:100, Upstate Technology); mouse α-γH2Av (1:30, DSHB); mouse α-dIAP1 (1:100, B. A. Hay); rabbit α-Pc (1:400, Santa Cruz Biotechnology); mouse α-En (1:50, DSHB). Alexa Fluor 555 goat α-mouse and α-rabbit (1:500, Invitrogen) and DyLight 649-conjugated goat α-mouse and α-rabbit (1:750, Jackson ImmunoResearch Laboratories) were used as secondary antibodies. Samples were analysed with a Leica TSC SP2 laser confocal microscope and entire images were processed with Adobe Photoshop software or ImageJ free software from NIH. All the images represent a single confocal stack unless otherwise specified. Image magnification is 400× unless otherwise specified.

ROS Detection

Larvae were dissected in PBS1X and carcasses were incubated for 30 min at room temperature in PBS1X – DHE (Dihydroethidium, Invitrogen Molecular Probes) at a final concentration of 30 μM in gentle shaking before fixation. Wing discs were immediately imaged under a Nikon 90i wide-field fluorescence microscope.

Statistical Analysis

For the experiments shown in **Figures 3–7**, the number of wing discs analysed was 15÷25 from different larvae for each sample. For each experiment, the data presented are the average of three biological replicates. Multifocality was assessed on a total of 346 wing discs for *l*(2)*gl*^{4} clones (see **Figures 9**, **10**), and on a total of 146 wing discs for *Rab5*^{2} (see **Figure 11**). For the experiments shown in **Figures 2**, **8**, **13**, the number of discs analysed is indicated. Mean Fluorescence Intensity (MFI) (**Figures 2**, **5**–**7**), clone area (**Figures 8**, **13**) and positive signals (**Figures 3**, **4**) were calculated by ImageJ free software (NIH) on images captured with a Nikon 90i wide-field fluorescence microscope at a magnification of 200×. All measurements have been taken inside the yellowish area highlighted in **Figure 1A**. *P*-values were as follows: $^{**}p \leq 0.01$ and $^{***}p \leq 0.001$. Mean, SEM and the *t*-Student test *p*-value were calculated by using GraphPad Prism software, San Diego, CA, United States.

RESULTS

MYC-Overexpressing Tissues Show Several Markers Repeatedly Found in Human Pre-cancerous Fields

Pre-cancerous fields are defined as tissue areas composed of histologically normal but genetically altered cells, shown to be more susceptible than wild-type counterparts to the onset of new mutations, promoting in time the development of multifocal tumours (Slaughter et al., 1953; Dotto, 2014). Since these areas are found to surround primary masses in several epithelial malignancies (Nonn et al., 2009; Zeki et al., 2011; Park et al., 2016), a pre-neoplastic field can be considered, borrowing Paget's hypothesis, a soil providing "bad seeds" with the capacity to initiate malignant growth, including those that would normally fail. The wide series of aberrations underlying the process of field cancerisation can hardly be attributed to a single cellular event, but deregulation of a gene piloting a number of cell behaviours may greatly favour its formation.

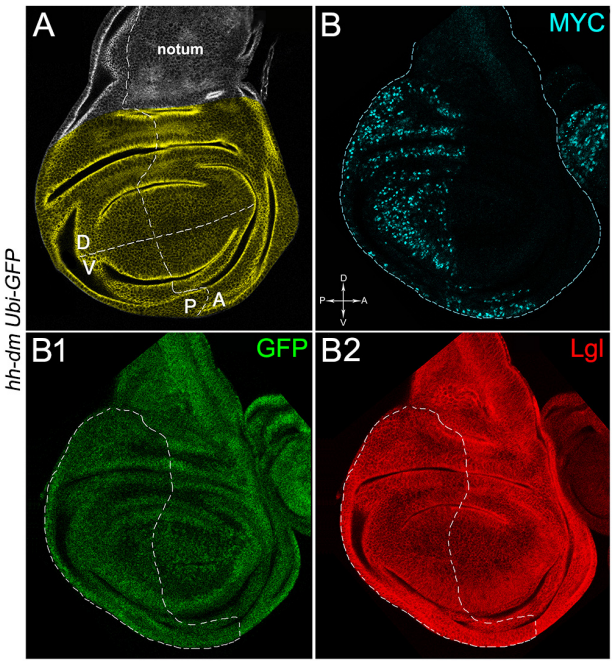

FIGURE 1 | MYC overexpression in the posterior compartment of the wing disc does not cause morphological alterations. **(A)** Representation of an imaginal wing disc from a wild-type late *Drosophila* larva. The Posterior/Anterior (P/A) and the Dorsal/Ventral (D/V) boundaries are indicated by dotted lines. All the measures for this study have been taken in the yellowish area. **(B–B2)** Immunostaining for MYC (**B**, cyan) and Lgl (**B2**, red) on wing discs from late *yw*; *Ubi-GFPnls*, *FRT40A/+*; *hh-Gal4/UAS-dm* larvae. GFP is shown in **B1**. The basic genotype is indicated on the left of the figure panel. P compartments are outlined in **B1,B2**, and disc axes are indicated in **B**. Magnification is 400×.

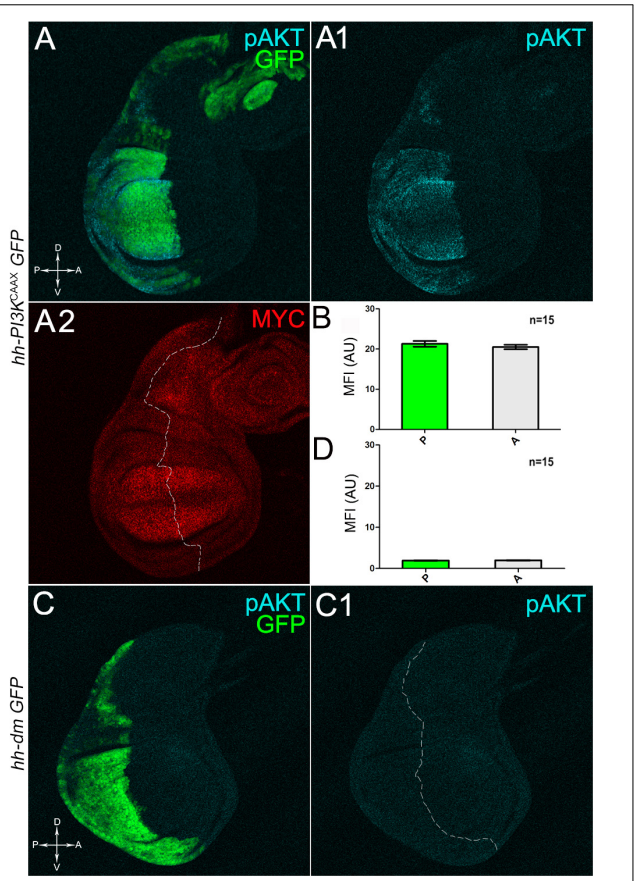

FIGURE 2 | MYC and PI3K^{CAAX} overexpression do not induce reciprocal activation. **(A–A2)** Immunostaining for pAKT (**A,A1**, cyan) and MYC (**A2**, red) on wing discs from late *yw/yw, UAS-PI3K^{CAAX}; hh-Gal4, UAS-GFP/+* larvae. **(B)** Graph comparing the Mean Fluorescence Intensity Arbitrary Units (MFI-AU) of MYC staining measured in the P (green bar) and A (grey bar) compartments of 15 wing discs from different larvae. **(C,C1)** Immunostaining for pAKT (cyan) on wing discs from late *yw*; *hh-Gal4, UAS-GFP/UAS-dm* larvae. **(D)** Graph comparing the Mean Fluorescence Intensity Arbitrary Units (MFI-AU) of pAKT staining measured in the P (green bar) and A (grey bar) compartments of 15 wing discs from different larvae. Basic genotypes are indicated on the left of the figure panel. P compartments are outlined in **A2,C1**, and disc axes are indicated in **A,C**. Magnification is 400×.

MYC represents an excellent candidate, because its misexpression does not account on gene mutation but is rather caused by alterations in many, if not all, signalling pathways (Nussinov et al., 2016). As an example, activated forms of RAS are frequently found in human pre-neoplastic tissues (Braakhuis et al., 2003), and it is known that activated RAS stabilises MYC protein in *Drosophila* (Prober and Edgar, 2002) and mammals (Sears et al., 2000). Stabilised MYC is in turn able to remodulate cell growth and proliferation, metabolism and stress response (Meyer and Penn, 2008). Moreover, a founder cell upregulating MYC could easily expand into a MYC-upregulating field through MMCC (Johnston, 2014). Therefore, MYC could play a causative role both in driving the expansion and in determining the intrinsic characteristics of a pre-cancerous field. To investigate this issue we bypassed field formation, since it is well established that *Drosophila* epithelial cells upregulating MYC eliminate the wild-type neighbours during development and colonise a large fraction of the tissue through MMCC (de la Cova et al., 2004; Moreno and Basler, 2004).

We then took advantage of the UAS-Gal4 binary system (Brand and Perrimon, 1993) to drive MYC overexpression (hereafter referred to as MYC^{OVER}) under the control of the *hedgehog* (*hh*) promoter in the posterior compartment of the wing disc, a *Drosophila* larval epithelial organ (Bryant, 1975). **Figure 1A** shows the Posterior/Anterior (P/A) and the Dorsal/Ventral (D/V) axes of the larval wing disc, while the yellowish region represents the area subjected to measurements and P vs. A comparisons, being the notum mostly composed of anterior cells (see P/A boundary in the notum region). As can be appreciated in **Figure 1B**, MYC^{OVER} is confined to the P compartment (representing the pre-cancerous field), where it does not seem to cause evident alterations in tissue morphology with respect to the A compartment (representing the wild-type field), as noted in **Figures 1B1,B2**, where a Ubi-GFPnls transgene and the Lgl protein mark cell nuclei and cell membranes, respectively. To demonstrate MYC's specificity in providing cells with a complex pre-cancerisation signature, we

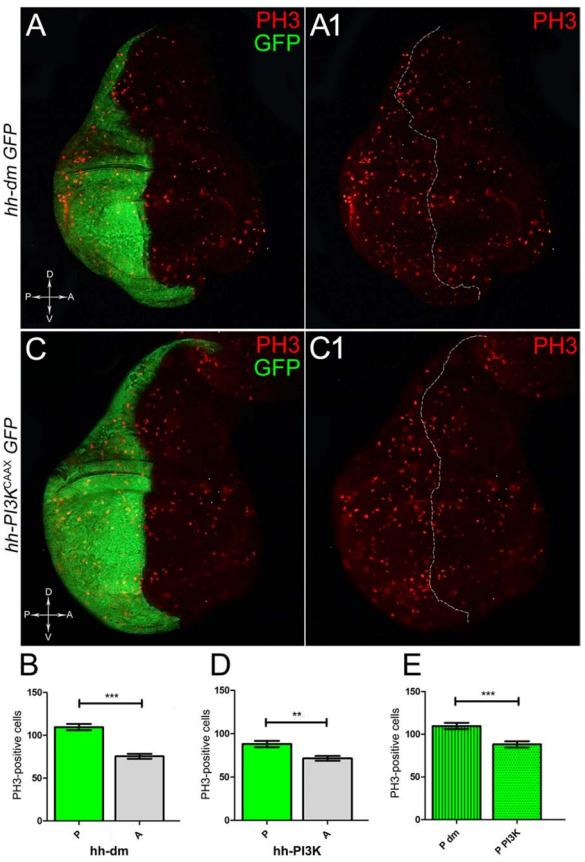

FIGURE 3 | MYC and PI3K^{CAAX} overexpression increases mitotic activity. **(A,A1)** Immunostaining for PH3 (red) on wing discs from late *yw*; *hh-Gal4, UAS-GFP/UAS-dm* larvae. **(B)** Graph comparing the PH3-positive nuclei counted in the P (green bar) and A (grey bar) compartments, $^{***}p \leq 0.001$. **(C,C1)** Immunostaining for PH3 (red) on wing discs from late *yw/yw, UAS-PI3K*^{CAAX}*; hh-Gal4, UAS-GFP/+* larvae. **(D)** Graph comparing the PH3-positive nuclei counted in the P (green bar) and A (grey bar) compartments, $^{**}p \leq 0.01$. **(E)** Graph comparing the PH3-positive nuclei counted in the P compartments of *yw*; *hh-Gal4, UAS-GFP/UAS-dm* (striped green bar) and *yw/yw, UAS-PI3K*^{CAAX}*; hh-Gal4, UAS-GFP/+* (dotted green bar) larvae, $^{***}p \leq 0.001$. Basic genotypes are indicated on the left of the figure panels and under the graphs. P compartments are outlined in **A1,C1**, and disc axes are indicated in **A,C**. Magnification is 400×.

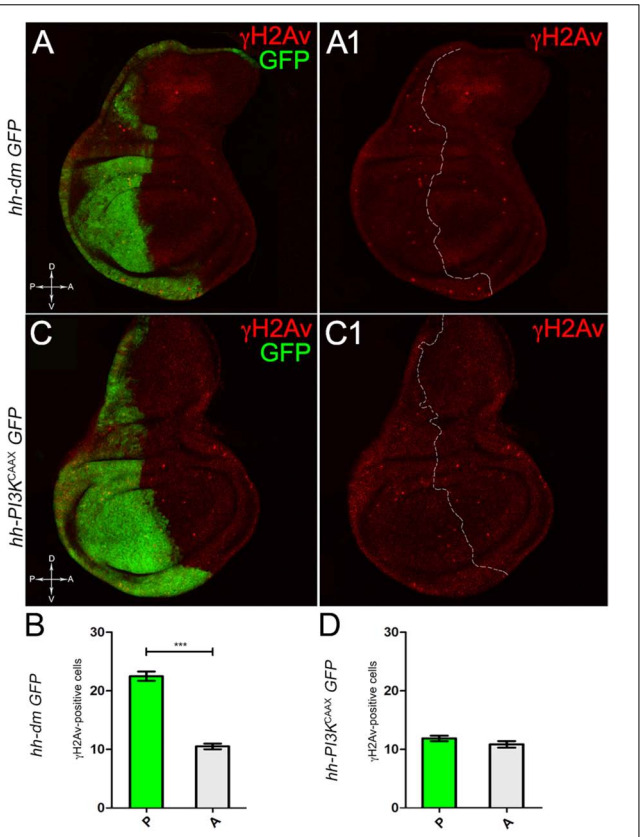

FIGURE 4 | MYC overexpression increases genetic instability. **(A,A1)** Immunostaining for γH2Av (red) on wing discs from late *yw*; *hh-Gal4, UAS-GFP/UAS-dm* larvae. **(B)** Graph comparing the γH2Av-positive foci counted in the P (green bar) and A (grey bar) compartments, $^{***}p \leq 0.001$. **(C,C1)** Immunostaining for γH2Av (red) on wing discs from late *yw/yw, UAS-PI3K*^{CAAX}*; hh-Gal4, UAS-GFP/+* larvae. **(D)** Graph comparing the γH2Av-positive foci counted in the P (green bar) and A (grey bar) compartments. Basic genotypes are indicated on the left of both the figure panels and the graphs. P compartments are outlined in **A1,C1**, and disc axes are indicated in **A,C**. Magnification is 400×.

compared the results of each experiment with those obtained following overexpression of a membrane-tethered form of PI3K (PI3K^{CAAX}), another potent growth inducer (de la Cova et al., 2004). We first verified if overexpression of the PI3K^{CAAX} transgene (PI3K$^{CAAX-OVER}$) caused consistent activation of the PI3K/AKT signalling pathway. As noted in **Figures 2A,A1**, the phosphorylated form of AKT was detected in the P compartment of the wing disc following PI3K$^{CAAX-OVER}$ (GFP^{+} region in **Figure 2A**). Moreover, it did not impact MYC endogenous levels (**Figure 2A2**, the P/A border is outlined), being the MFI of MYC staining statistically comparable in P and A compartments (**Figure 2B**). Following MYC^{OVER}, the levels of phosphorylated AKT in the P compartment (GFP^{+} region, **Figures 2C,C1**, the P/A border is outlined) were also comparable to those observed in the A compartment (**Figure 2D**), confirming that, differently from what has been observed in a previous study (Levayer et al., 2015), in our genetic system and under our working conditions, the two growth inducers do not significantly cross-regulate each other, making it suitable for the successive analyses.

We started by investigating in the MYC^{OVER} tissue a number of markers characteristic of human pre-neoplastic fields. Since it is known that pre-malignant areas may display a higher proliferative index than normal tissues (Mohan and Jagannathan, 2014), we first checked the mitotic activity of MYC^{OVER} cells by immunostaining for the phosphorylated histone H3 (PH3), which is known to play a key role during mitosis both in *Drosophila* and mammals (Kamakaka and Biggins, 2005). A mitotic index analysis highlighted a 32% increase of PH3-positive nuclei in MYC^{OVER} P compartments with respect to their A counterparts (**Figures 3A,A1,B**), and a 20% increase in the PI3K$^{CAAX-OVER}$ P vs. A compartments (**Figures 3C,C1,D**). This result was not unexpected, as PI3K activation plays important

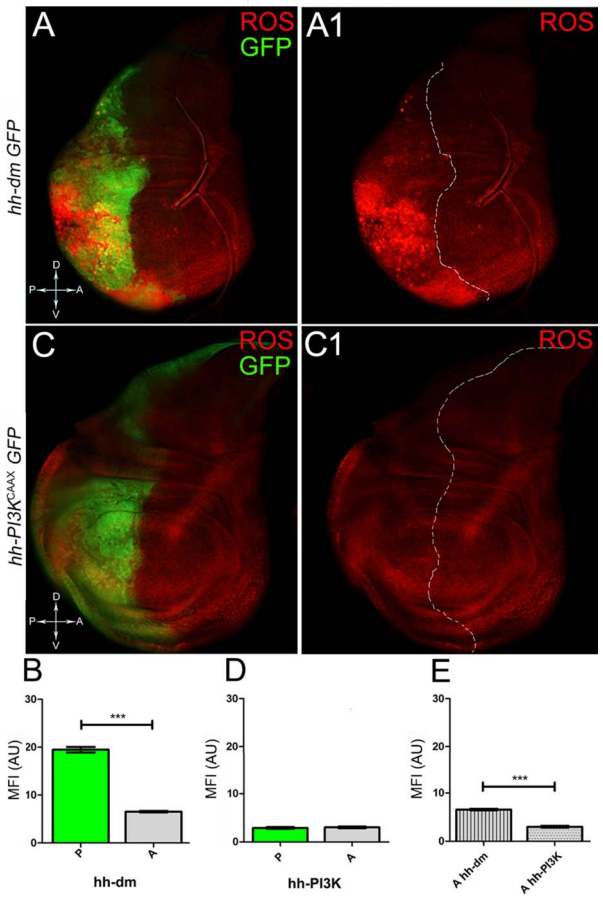

FIGURE 5 | MYC overexpression causes intense ROS production. **(A,A1)** ROS production (red) in wing discs from late *yw*; *hh-Gal4, UAS-GFP/UAS-dm* larvae. **(B)** Graph comparing the Mean Fluorescence Intensity of ROS positivity measured in the P (green bar) and A (grey bar) compartments, $^{***}p \leq 0.001$. **(C,C1)** ROS production (red) in wing discs from late *yw/yw, UAS-PI3K^{CAAX}; hh-Gal4, UAS-GFP/+* larvae. **(D)** Graph comparing the Mean Fluorescence Intensity Arbitrary Units (MFI-AU) of ROS positivity measured in the P (green bar) and A (grey bar) compartments. **(E)** Graph comparing the Mean Fluorescence Intensity Arbitrary Units (MFI-AU) of ROS positivity measured in the A compartments of *yw*; *hh-Gal4, UAS-GFP/UAS-dm* (striped grey bar) and *yw/yw, UAS-PI3K^{CAAX}; hh-Gal4, UAS-GFP/+* (dotted grey bar) larvae, $^{***}p \leq 0.001$. Basic genotypes are indicated on the left of the figure panels and under the graphs. P compartments are outlined in **A1,C1**, and disc axes are indicated in **A,C**. Magnification is 400×.

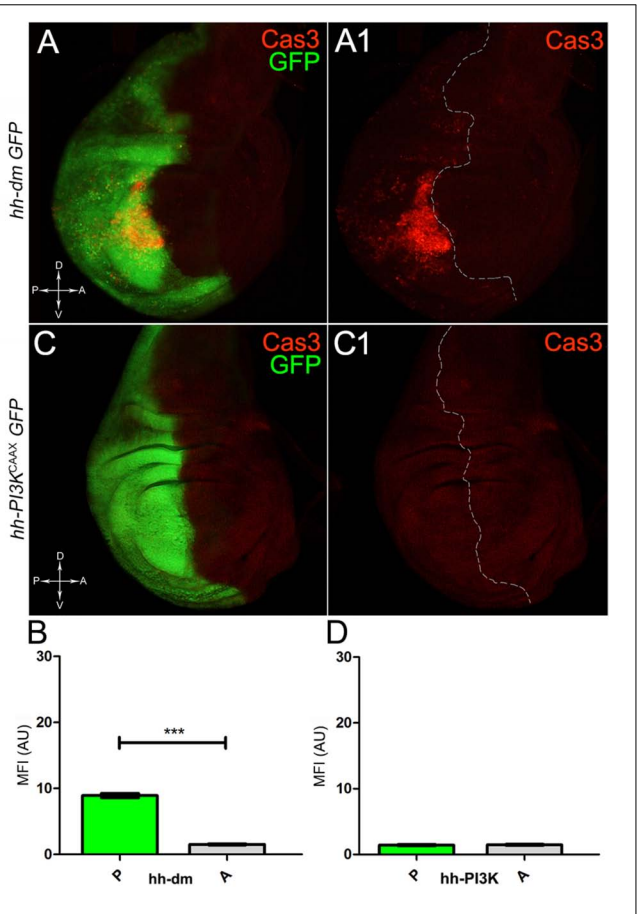

FIGURE 6 | MYC overexpression triggers apoptotic death. **(A,A1)** Immunostaining for Cas3 (red) on wing discs from late *yw*; *hh-Gal4, UAS-GFP/UAS-dm* larvae. **(B)** Graph comparing the Mean Fluorescence Intensity Arbitrary Units (MFI-AU) of Cas3 staining measured in the P (green bar) and A (grey bar) compartments, $^{***}p \leq 0.001$. **(C,C1)** Immunostaining for Cas3 (red) on wing discs from late *yw/yw, UAS-PI3K^{CAAX}; hh-Gal4, UAS-GFP/+* larvae. **(D)** Graph comparing the Mean Fluorescence Intensity Arbitrary Units (MFI-AU) of Cas3 staining measured in the P (green bar) and A (grey bar) compartments. Basic genotypes are indicated on the left of the figure panels and under the graphs. P compartments are outlined in **A1,C1**, and disc axes are indicated in **A,C**. Magnification is 400×.

roles in cell growth and proliferation (Leevers et al., 1996). The mitotic index of the MYC^{OVER} tissue was, however, significantly higher than that observed in the PI3K$^{CAAX-OVER}$ samples, as in the graph reported in **Figure 3E**. To assess genetic instability, another feature of pre-cancerous fields with obvious mutagenic effects (Bhattacharjee and Nandi, 2016), we used an antibody against the γ variant of the phosphorylated histone H2, which is recognised as the first modification occurring following DNA double strand breaks, resulting in the assembling of multi-protein complexes which attempt to repair DNA damage (Dronamraju and Mason, 2011). As can be seen in **Figures 4A,A1**, the γH2Av foci (red) in the MYC^{OVER} P compartment (GFP^{+}, outlined in **Figure 4A1**) were about twice compared to the A compartment (**Figure 4B**), while they resulted comparable in the P and A compartments of the PI3K$^{CAAX-OVER}$ samples (**Figures 4C,C1,D**). Our study continued by evaluating the presence and abundance of ROS in the presumptive pre-cancerous field. As noted in **Figures 5A,A1**, a strong increase in ROS generation (red) was found in the MYC^{OVER} P compartment of the wing disc (GFP^{+}, outlined in **Figure 5A1**), quantified as about 20 arbitrary units (AU) MFI vs. the 6.5 AU found in the A compartment (compare green and grey bars in the graph **Figure 5B**). Contrariwise, no significant differences were found between the P (GFP^{+}, outlined in **Figure 5C1**) and A compartments following PI3K$^{CAAX-OVER}$, as is appreciable in **Figures 5C,C1,D**. As MYC^{OVER} and PI3K$^{CAAX-OVER}$ samples underwent parallel enzymatic reactions, we could also compare

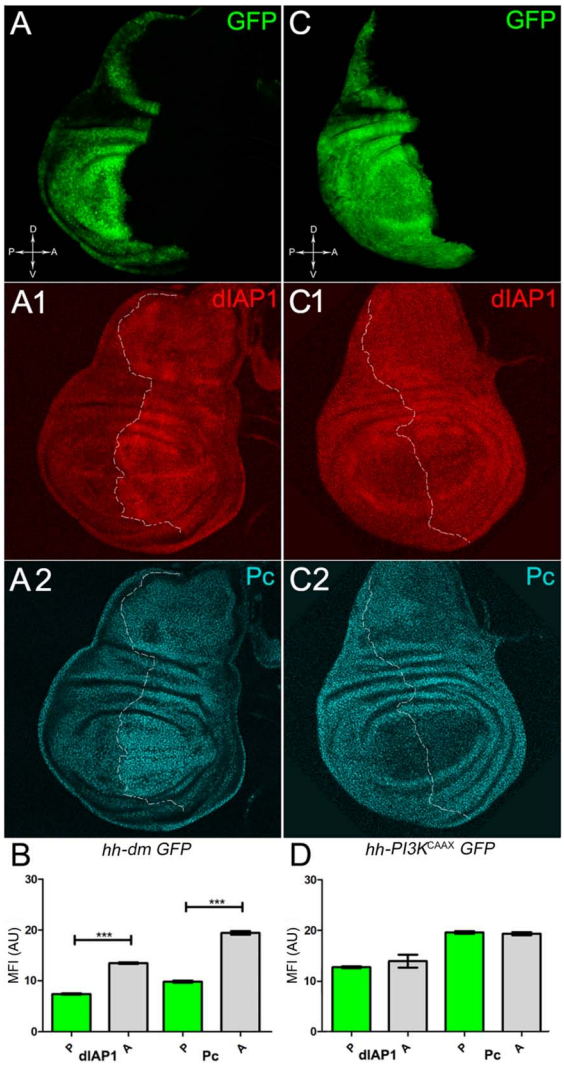

FIGURE 7 | MYC overexpression downregulates survival and epigenetic markers. **(A–A2)** Immunostaining for dIAP1 (**A1**, red) and Pc (**A2**, cyan) on wing discs from late *yw*; *hh-Gal4, UAS-GFP/UAS-dm* larvae. **(B)** Graph comparing the Mean Fluorescence Intensity Arbitrary Units (MFI-AU) of dIAP and Pc staining measured in the P (green bars) and A (grey bars) compartments, $^{***}p \leq 0.001$. **(C–C2)** Immunostaining for dIAP1 (**C1**, red) and Pc (**C2**, cyan) on wing discs from late *yw/yw, UAS-PI3K*^{CAAX}*; hh-Gal4, UAS-GFP/+* larvae. **(D)** Graph comparing the Mean Fluorescence Intensity Arbitrary Units (MFI-AU) of dIAP and Pc staining measured in the P (green bars) and A (grey bars) compartments. Basic genotypes are indicated under the figure panels. P compartments are outlined in **A1,A2,C1,C2**, and disc axes are indicated in **A,C**. Magnification is 400×.

ROS levels in the respective wild-type A compartments, and found that MYC^{OVER} A compartment showed a twofold ROS increase with respect to the PI3K$^{CAAX-OVER}$ A compartment (**Figure 5E**). This was an interesting finding, as ROS are diffusible ions and molecules and they may freely move away from the producing cells, thus expanding MYC's pre-cancerisation effect to adjacent tissues by a non-autonomous mechanism. In this sense, a recent study demonstrated that, in *Drosophila* epithelial tumours, apoptotic caspases enhance tumour malignancy by generating ROS, which in turn recruit immune cells that signal back to the epithelium to activate cancer pathways (Perez et al., 2017). Although MYC^{OVER} tissues cannot be compared to overt cancers, similar cell-cell interactions may be at work that cooperate with MMCC to expand the pre-cancerous field. An analysis of apoptotic cell death carried out by immunostaining for the activated form of the effector Caspase 3 (Cas3) revealed that MYC^{OVER} epithelial cells were highly prone to apoptotic death (see **Figures 6A,A1**), with about 9 MFI AU in the P compartment vs. 1.5 in the A counterpart, as can be noted in **Figure 6B**. By contrast, no significant differences were noticed between P and A compartments overexpressing PI3K^{CAAX} (**Figures 6C,C1,D**). Consistently with Caspase 3 activation, MYC^{OVER} cells downregulated the anti-apoptotic protein dIAP1 (Wang et al., 1999), as shown in **Figure 7A1** (**Figure 7A** shows the GFP^{+} P compartment), with 7.4 MFI AU in the P vs. 13.5 in the A compartment (**Figure 7B**); dIAP1 indeed functions by inhibiting the initiator caspase DRONC (Meier et al., 2000) that, in turn, activates the effector caspases. Also in this case, PI3K$^{CAAX-OVER}$ tissues did not show significant differences in dIAP1 staining between the P and A compartments (**Figures 7C,C1,D**). Finally, with regard to changes in the epigenetic signature of human pre-neoplastic tissues (Grady, 2005; Lee et al., 2011), we analysed the effect of MYC^{OVER} on the chromatin modifier Polycomb (Pc), known to shape cellular plasticity through large-scale epigenetic regulation (Klebes et al., 2005). We previously showed that Pc expression is nearly absent in *Drosophila* epithelial cancers (Grifoni et al., 2015). As it is known that Pc and other proteins of the Pc group (PcG) are necessary to MYC auto-repression in *Drosophila* (Goodliffe et al., 2005; Khan et al., 2009), Pc downregulation in overt cancers may help sustain high MYC cellular levels, so allowing it to impact many different phenotypic traits. As can be observed in **Figure 7A2**, Pc resulted downregulated also in our pre-cancerisation model, with 9.8 vs. 19.4 MFI AU in the P (GFP^{+} in **Figure 7A**, outlined in 7A2), and A compartments, respectively (**Figure 7B**). This is consistent with MYC and PcG proteins *trans*-regulation (Benetatos et al., 2014), and since low Pc levels result in a higher chromatin accessibility, this condition would favour additional mutational insults through inappropriate entrance of DNA cleaving enzymes (Zhang et al., 2008). Also in this case, PI3K$^{CAAX-OVER}$ tissues did not display significant differences compared to the wild-type counterparts (**Figures 7C2,D**).

Altogether, these results support our hypothesis that high levels of MYC are sufficient as to induce a series of molecular changes, which are likely to turn the affected tissue into a pre-malignant field. Moreover, this ability seems to be specific to MYC, as an active form of the growth inducer PI3K failed to promote significant alterations of the markers analysed.

Single-Cell Mutations of Neoplastic TSGs Initiate Multifocal Growth in a MYC^{OVER} Tissue

With the aim to translate the evidence described above into a functional demonstration of MYC^{OVER}'s capacity to establish

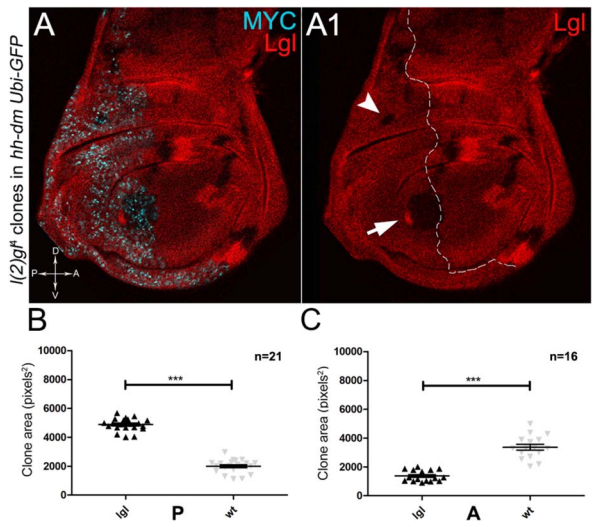

FIGURE 8 | About one/third of lgl^{-} clones overgrows at the expense of the surrounding wild-type tissue in a MYC-overexpressing background. **(A,A1)** Immunostaining for Lgl (red) and MYC (cyan) on wing discs from late *w*; *l(2)gl*^{4}, *FRT40A/Ubi-GFPnls*, *FRT40A*; *hh-Gal4/UAS-dm* larvae. The arrow points to a posterior wild-type twin clone and the arrowhead indicates a scattered $lgl^{-/-}$ clone with no obvious wild-type twin in the posterior hinge region **(A1)**. **(B,C)** Graphs comparing the average clone area of $lgl^{-/-}$ (black triangles, black in the images) and wild-type twins (grey triangles, double red in the images) in the P **(B)** and A **(C)** compartments, $^{***}p \leq 0.001$. The basic genotype is indicated on the left of the figure. The P compartment is outlined in **A1**, and disc axes are indicated in **A**. Magnification is 400×.

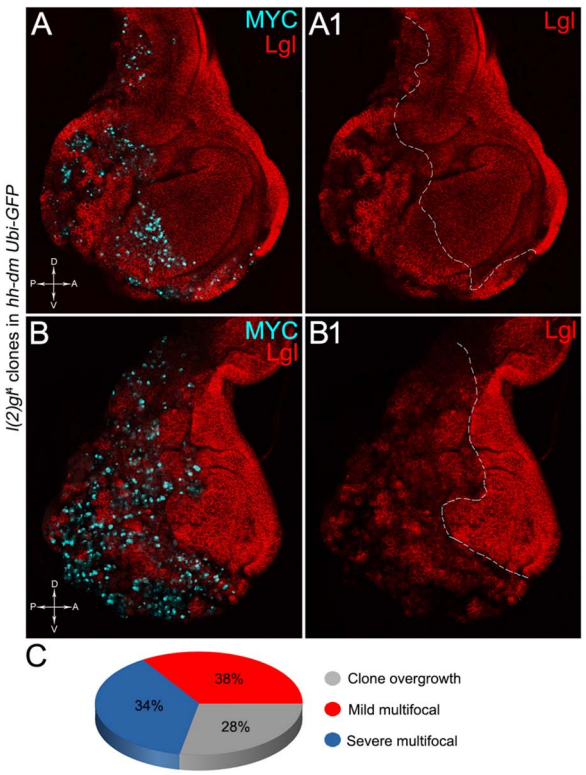

FIGURE 9 | The majority of $lgl^{-/-}$ cells forms multifocal nests which colonise a large fraction of the MYC-overexpressing tissue. **(A–B1)** Immunostaining for Lgl (red) and MYC (cyan) on wing discs from late *w*; *l(2)gl*^{4}, *FRT40A/Ubi-GFPnls*, *FRT40A*; *hh-Gal4/UAS-dm* larvae. **(C)** Pie chart illustrating the numerical proportions of overgrown, mild and severe multifocal $lgl^{-/-}$ clones found in the P compartment of *w*; *l(2)gl*^{4}, *FRT40A/Ubi-GFPnls*, *FRT40A*; *hh-Gal4/UAS-dm* wing discs. The basic genotype is indicated on the left of the figure panel. P compartments are outlined in **A1,B1**, and disc axes are indicated in **A,B**. Magnification is 400×.

a pre-malignant condition, we investigated the phenotypic consequences of the induction of second mutations in a MYC^{OVER} background. We used a genetic model which, through a combination of the UAS-Gal4 (Brand and Perrimon, 1993) and Flp-FRP (Xu and Rubin, 1993) binary systems, allowed us to express MYC in the P compartment and to induce second mutations of interest later in time, so reproducing the temporal sequence that is likely to occur during cancer initiation. The A compartment has been used as a control, to assess the clonal phenotype promoted by the same second mutations in a region carrying endogenous MYC expression.

As described in the Introduction, we previously showed that hyperplastic TSGs (hTSGs) exploit excess MYC to grow more rapidly, but are not able to initiate malignant transformation (Ziosi et al., 2010); we thus aimed at exploring MYC^{OVER}'s effect on the clonal behaviour of neoplastic TSGs (nTSGs). We first analysed the *lethal giant larvae* (*lgl*) mutation. Lgl protein regulates the apical-basal cell polarity in the epithelia (Grifoni et al., 2013); we previously demonstrated its functional conservation from *Drosophila* to humans (Grifoni et al., 2004), and we and others found the human orthologue *HUGL-1* involved in cancers from different organs (Grifoni et al., 2004, 2007; Schimanski et al., 2005; Lu et al., 2009). In the *Drosophila* wing disc, *lgl* mutant cells are unable to grow in a wild-type background, especially in the regions where MYC levels are high, and are eliminated by MMCC (Froldi et al., 2010). In the same wild-type background, MYC^{OVER} in *lgl* mutant clones rescues them from death and transforms $lgl^{-/-}$ cells from losers into super-competitors (Froldi et al., 2010). But what happens to newly formed *lgl*, MYC^{OVER} cells when they are surrounded by MYC^{OVER} neighbours? As can be seen in **Figure 8**, while $lgl^{-/-}$ clones were smaller than wild-type twins in the A control compartment of the disc (**Figures 8A,A1,C**), in the 28% of the wing discs analysed the $lgl^{-/-}$ clones growing in the MYC^{OVER} P compartment appeared significantly larger than the wild-type twins (**Figures 8A,A1,B**). As an example, the arrow in **Figure 8A1** points to a wild-type clone (double red) which appears much smaller than the *lgl* mutant twin (black). In addition, the arrowhead indicates an *lgl* mutant clone in the hinge region of the P compartment with no apparent wild-type twin clone. This suggests that the *lgl* mutant cells have a greater ability to exploit the excess MYC protein than the surrounding neighbours, hence the gain of a competitive advantage over the wild-type tissue. However, the average clone area occupied by the $lgl^{-/-}$ cells in this system was about 5000 px^2, whereas it was found to be around 24000 px^2 in a previous study where $lgl^{-/-}$, MYC^{OVER} cells were induced in a wild-type background (Froldi

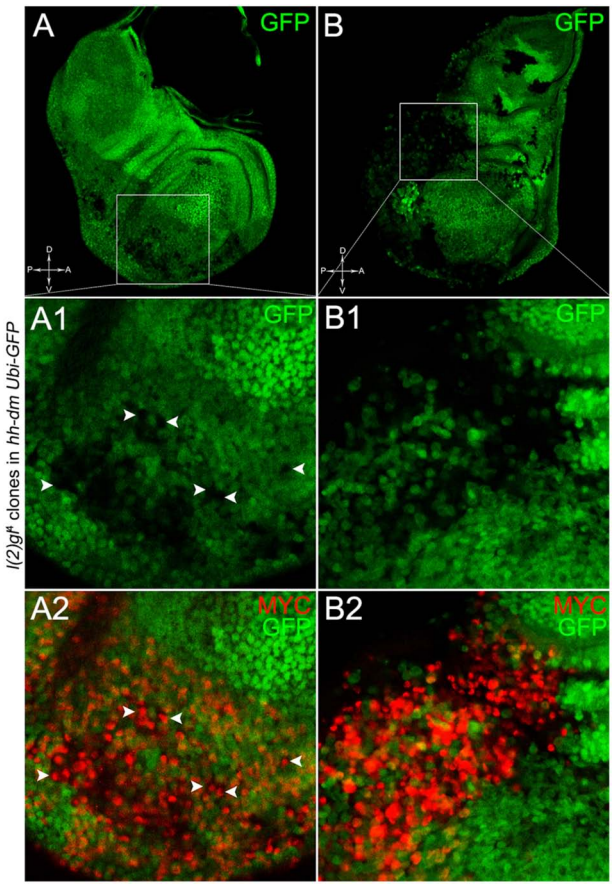

FIGURE 10 | *lgl*$^{-/-}$ cells undergoing severe multifocal growth accumulate MYC protein. Immunostaining for MYC (red) on wing discs from late *w*; *l(2)gl*^{4}, *FRT40A/Ubi-GFPnls*, *FRT40A*; *hh-Gal4/UAS-dm* larvae. In **A1,A2**, arrowheads indicate MYC-accumulating mutant cells. The basic genotype is indicated on the left of the figure panel. Disc axes are indicated in **A,B**. **A1–B2** are magnified views of the squares drawn in **A,B**. Magnification is 400× in **A,B**, 1000× in **A1,A2**, and 1200× in **B1,B2**.

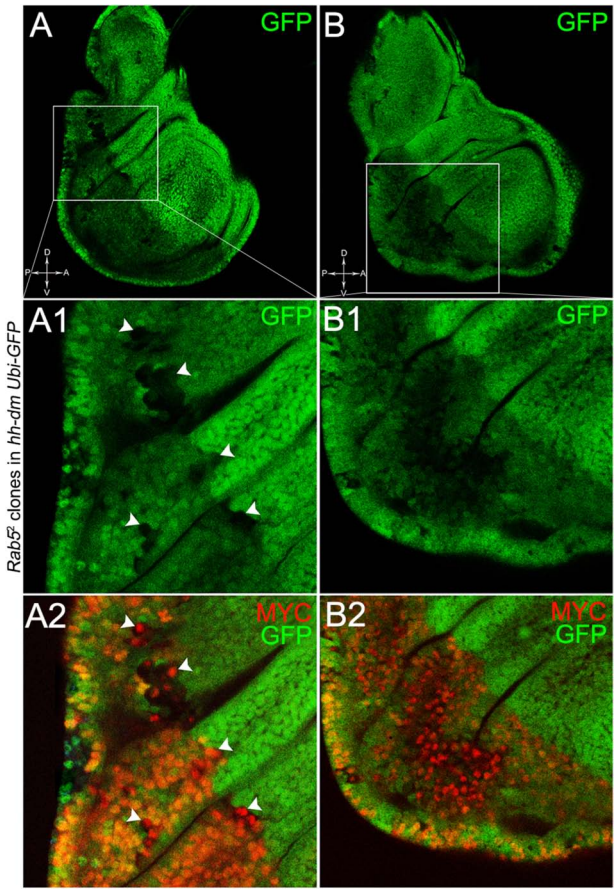

FIGURE 11 | *Rab5*$^{-/-}$ cells show a fully penetrant, multifocal phenotype in a MYC-overexpressing background. Immunostaining for MYC (red) on wing discs from late *w*; *Rab5*^{2}, *FRT40A/Ubi-GFPnls*, *FRT40A*; *hh-Gal4/UAS-dm* larvae. In **A1,A2**, arrowheads indicate MYC-accumulating mutant cells. The basic genotype is indicated on the left of the figure panel. Disc axes are indicated in **A,B**. **A1–B2** are magnified views of the squares drawn in **A,B**. Magnification is 400× in **A,B**, 1000× in **A1,A2**, and 800× in **B1,B2**.

et al., 2010), demonstrating the MYC^{OVER} neighbours exert a competitive pressure against the growth of the *lgl* mutant clones, which translates into a limited capability of *lgl*$^{-/-}$ cells to form large masses in a uniform MYC^{OVER} field.

The remaining 72% of the wing discs analysed displayed a novel phenotype: the *lgl* mutant tissue grew as a multitude of spots scattered all across the MYC^{OVER} P compartment. **Figure 9** shows two typical samples that we classified as "mild multifocal" (**Figure 9A**), which represented the 38% of the total samples (**Figure 9C**), and "severe multifocal" (**Figure 9B**), which represented the 34% of the total samples (**Figure 9C**). We classified multifocality as "mild" when the *lgl* mutant clones (black), though colonising a large fraction of the P compartment, did not alter its width (**Figure 9A1**), and "severe" when the *lgl*$^{-/-}$ cells filled the entire P compartment, which appeared dramatically enlarged (see how the P/A border moved from P to A comparing **Figures 9A1,B1**). This deep organ alteration suggests a locally invasive, malignant behaviour of these mutant cells that may be favoured by clone confluence during growth, as it is with other tumour models in *Drosophila* (Menendez et al., 2010; Ballesteros-Arias et al., 2014), with MYC protein levels that appeared to increase along with phenotype severity (compare **Figures 9A,B**). *lgl* mutant cells displayed preferential MYC accumulation, as can be appreciated in **Figure 10A2**, where arrowheads indicate some of the mutant cells (black, see **Figure 10A1**) accumulating MYC. Again, the organs displaying larger mutant spots (**Figure 10B**, squared area) showed an obvious increase in MYC protein levels (**Figure 10B2**). The most interesting aspect of this model is that it faithfully reproduced a distinctive feature of human pre-cancerous fields, i.e., multifocality (Dotto, 2014). The multifocal phenotype has never been associated with *lgl* mutations in *Drosophila*; therefore, it represents a novel trait acquired by a cell subject to a mutation in the *lgl* nTSG while being part of a MYC^{OVER} field.

To verify that a MYC^{OVER} field represented a *bona fide* pre-cancerous area, and that multifocality did not result from a

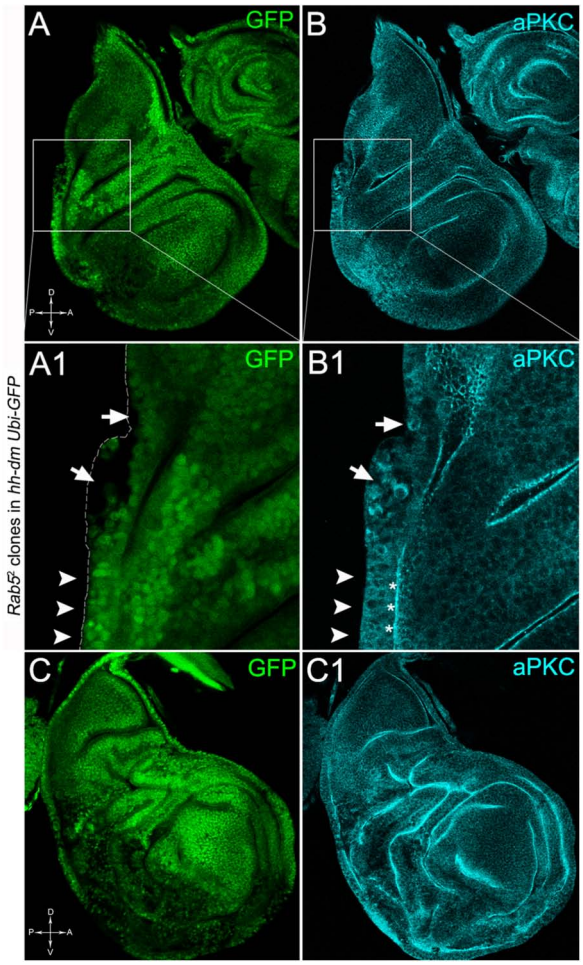

FIGURE 12 | *Rab5*$^{-/-}$ cells show loss of cell polarity in a MYC-overexpressing background. Immunostaining for aPKC (cyan) on wing discs from late *w*; *Rab5*^{2}, *FRT40A*/*Ubi-GFPnls*, *FRT40A*; *hh-Gal4*/*UAS-dm* larvae. In **A1,B1**, arrows indicate mutant cells (black) displaying membrane redistribution of the apical marker aPKC, while the arrowheads point to a normal region of the disc border where the pseudostratified epithelium shows apical aPKC staining (asterisks). The dashed line in **A1** marks the disc outer border. The basic genotype is indicated on the left of the figure panel. Disc axes are indicated in **A,C**. **A1,B1** are magnified views of the squares drawn in **A,B**. Magnification is 400× in **A,B,C,C1** and 1000× in **A1,B1**.

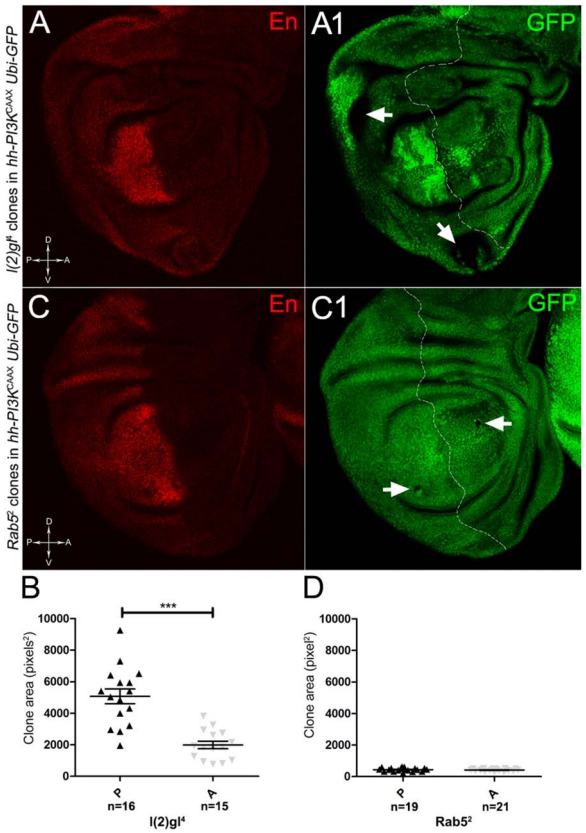

FIGURE 13 | *lgl*$^{-/-}$ and *Rab5*$^{-/-}$ cells do not display multifocal growth in a PI3K^{CAAX}-overexpressing background. **(A,A1)** Immunostaining for En (red) on wing discs from late *w/yw, UAS-PI3K*^{CAAX}*; l(2)gl*^{4}, *FRT40A*/*Ubi-GFPnls; hh-Gal4*/+ larvae. The arrows in **A1** indicate the mutant clones (black). **(B)** Graph comparing the average clone area of *lgl*$^{-/-}$ clones in the P (black triangles) and A (grey triangles) compartments, ***$p \leq 0.001$. **(C,C1)** Immunostaining for En (red) on wing discs from late *w/yw, UAS-PI3K*^{CAAX}*; Rab5*^{2}, *FRT40A*/*Ubi-GFPnls; hh-Gal4*/+ larvae. The arrows in **C1** indicate the mutant clones (black). **(D)** Graph comparing the average clone area of *Rab5*$^{-/-}$ clones in the P (black triangles) and A (grey triangles) compartments. Basic genotypes are indicated on the left of the figure panel. The P compartment is outlined in **A1,C1**, and disc axes are indicated in **A,C**. Magnification is 400×.

specific interaction between *lgl* and MYC, we induced a LOF mutation of a different nTSG in the MYC^{OVER} field. Rab5 is an evolutionarily conserved core component of the vesicle trafficking machinery (Lu and Bilder, 2005), implicated in various aspects of human tumourigenesis (Torres and Stupack, 2011; Mendoza et al., 2014). Like *lgl*, entire fly organs mutated for *Rab5* show neoplastic growth (Lu and Bilder, 2005; Vaccari and Bilder, 2009), and *Rab5* mutant cells induced in a wild-type wing disc suffer from cell competition and are eliminated from the organ (Ballesteros-Arias et al., 2014). Using the same clonal system as above, we induced *Rab5* LOF clones in animals whose P compartments overexpressed MYC. As can be seen in **Figure 11**, the multifocal phenotype was evident also for the *Rab5*$^{-/-}$ cells (**Figures 11A,B** and respective magnifications A1 and B1). Also in this case, mutant cells showed MYC accumulation (**Figures 11A2,B2**, arrowheads in A2 indicate some mutant nests accumulating MYC). The 100% of the organs analysed showed a multifocal phenotype, subdivided in 71% mild and 29% severe. Moreover, *Rab5* mutant cells showed loss of apical-basal cell polarity, a central feature of epithelial cancers (Wodarz and Nathke, 2007): in **Figure 12**, the magnifications in A1 and B1 show a region of the disc outer border where one can appreciate that the normal epithelium (arrowheads in A1 and B1) displays a wild-type localisation of the apical marker atypical PKC (aPKC, cyan, asterisks in B1). On the contrary, the mutant cells in the region indicated by the arrows in A1 and B1 (black in A1) show a redistribution of the polarity marker from the apical side to the entire cell cortex, together with aberrant, three-dimensional

growth. In **Figures 12C,C1**, the impairment of aPKC expression (cyan) is evident across the entire MYC^{OVER} P compartment. This characteristic is consistent with Rab5 function: the endocytic trafficking is indeed essential in the maintenance of cell polarity, and mutations in genes involved in endocytosis provoke the expansion of cell's apical domain (Shivas et al., 2010).

Altogether, this evidence indicated that MYC overexpression in an epithelial tissue is sufficient to promote multifocal malignant lesions following single-cell mutations of different nTSGs.

To assess if multifocality may be considered a trait arising from specific properties conferred by the MYC field to the mutant cells, we repeated the same experiments as above in a $PI3K^{CAAX-OVER}$ territory. Using the same system as above, we first analysed *lgl* mutant behaviour. In **Figures 13A,A1**, we can observe *lgl* mutant clones (GFP^-, indicated by the arrows) in the $PI3K^{CAAX}$ P compartment (marked in red by En staining in A). They are located outside the central region of the disc where, instead, we observed the presence of wild-type clones (GFP^{2+}), indicating that mutant twins were eliminated by MMCC. Therefore, despite the over-expression of $PI3K^{CAAX}$, $lgl^{-/-}$ clones continue to die in this area of the wing discs where MYC is normally highly expressed (see **Figure 2A2**). A statistical analysis of the clone area in the P and A compartments showed that $lgl^{-/-}$ mutant clones were significantly larger in P, with an average size of about 5000 px^2, compared to A, where they displayed an average size of about 2000 px^2 (**Figure 13B**). The most important observation was, however, the total absence of multifocal growth. We then analysed the behaviour of the $Rab5^2$ mutation in a $PI3K^{CAAX}$ background. In **Figures 13C,C1**, a wing disc is shown where small mutant clones of comparable size are present in both compartments (black, arrows in **Figure 13C1**). In **Figure 13D**, the graph indicates that the mutant clones do not show significant differences in size between the P and A compartments. Finally, as it was for *lgl*, no multifocal growth was observed in all the *Rab5* samples analysed.

These latter findings indicate that MYC confers on cells mutant for different nTSGs the ability to grow in multiple foci dispersed all across the modified territory. This seems to be a specific characteristic of MYC, as the growth inducer PI3K did not promote this peculiar phenotype. MYC upregulation emerges from our study as an excellent candidate to foster field cancerisation, by inducing a complex pre-cancerisation molecular signature able to provide cells hit by non-competitive mutations with the ability to initiate carcinogenesis.

DISCUSSION

Field cancerisation is studied in the effort to understand if essential events recur in tumour initiation that may help develop early therapeutic interventions. It is now recognised that many types of cancers start from cells owing some, but not all, phenotypic traits necessary for malignancy, and those traits may result from various mutagenic insults, on the basis of which the most performant cells are selected for clonal expansion (Curtius et al., 2018). This process may be driven by cell competition, which is intensively studied both in *Drosophila* (Merino et al., 2016) and mammals (Di Gregorio et al., 2016). In this context, we focused our attention on MMCC, a process based on steep differences in MYC levels in confronting cells, which ultimately favour the expansion of high MYC-expressing cells at the expense of the less fit neighbours (Grifoni and Bellosta, 2015). Given the broad implication of MYC protein in human cancers (Gabay et al., 2014), its myriad functions inside the cell (Dang et al., 2006) and its regulation at both the transcriptional and post-transcriptional levels by a number of signalling pathways (Nussinov et al., 2016), it seems an excellent candidate to pioneer field cancerisation (Moreno, 2008).

To address this question, we first investigated the cellular responses to MYC overexpression (MYC^{OVER}) in the imaginal wing disc, a *Drosophila* epithelial tissue widely used to model development, cell competition and cancer (Herranz et al., 2016). We found that MYC^{OVER} was *per se* sufficient to activate a series of cellular behaviours consistent with the formation of a pre-neoplastic field, such as ROS production, genetic instability, changes in apoptotic and proliferation activity and alteration of epigenetic markers. Moreover, we showed that these cellular responses were not elicited by a MYC's generic pro-growth function, as an active form of the powerful growth inducer PI3K was not able to induce similar phenotypes, except a mild pro-proliferative effect. High MYC levels seem rather to prime field cancerisation by triggering a cascade of molecular changes that cooperate in taking cells a step closer to malignancy.

This *bona fide* pre-cancerous tissue was then tested for the ability to initiate tumourigenesis following mutations in neoplastic TSGs (nTSGs). We previously studied the effects of MYC^{OVER} on three hyperplastic TSGs (hTSGs) owing to the Hippo signalling pathway: *ds*, *ft* and *ex*, and found that mutant clones grew more rapidly while killing the MYC^{OVER} wild-type neighbours with higher efficiency, but they did not show any signs of malignancy (Ziosi et al., 2010). We and others demonstrated that most hTSGs upregulate MYC (Neto-Silva et al., 2010; Ziosi et al., 2010), hence their competitive capability, while some nTSGs downregulate MYC, hence their elimination from the tissue (Froldi et al., 2010). It is also recognised that the behaviour of both hTSGs and nTSGs depends on tissue's MYC levels (Froldi et al., 2010; Neto-Silva et al., 2010; Ziosi et al., 2010): in a uniform background, as with our model, mutant behaviour should rather be dictated by the intrinsic features of the given mutation.

In the *Drosophila* wing disc, wild-type cells hit by nTSGs mutations are usually irrelevant: they are indeed eliminated rapidly or contribute to the tissue without overgrowing (Froldi et al., 2010; Ballesteros-Arias et al., 2014). The same mutations induced in a MYC^{OVER} field were rather capable to initiate multifocal, three-dimensional growth accompanied by loss of apical-basal cell polarity and aberrant tissue architecture. This was convincing evidence that MYC upregulation was sufficient as to establish a specific, complex pre-cancerisation signature, which predisposes the tissue to undergo malignant multifocal growth following certain second mutations.

Our findings lay the basis for future studies focused on early tumourigenesis. These studies are as essential as difficult: while understanding the very first phases of cancer is mandatory to conceive novel preventive and therapeutic interventions, investigations carried out in complex systems may lead to discouraging results. In this sense, the use of a genetically amenable animal model may greatly help dissect and dismantle the intricate networks implicated in cancer initiation.

AUTHOR CONTRIBUTIONS

MS and DG conceived and designed the study. MS, CG, and SP performed the experiments. DG and DdB analysed the experimental data. SDG performed the statistical analysis. AP and DG wrote the manuscript. All authors contributed to manuscript revision and read and approved the submitted version.

FUNDING

This study was supported by AIRC IG 17252 to AP and Research Fellowships from the University of Bologna to MS, SDG, SP, and DG.

ACKNOWLEDGMENTS

We acknowledge the Bloomington Drosophila Stock Center (NIH P40OD018537) for the fly stocks used in this study, and the Developmental Studies Hybridoma Bank, created by the NICHD of the NIH and maintained at The University of Iowa, for monoclonal antibodies. We thank Paola Bellosta, Bruce Hay, and Dennis Strand for reagents and Silvia Strocchi for manuscript revision.

REFERENCES

Abdalla, M., Tran-Thanh, D., Moreno, J., Iakovlev, V., Nair, R., Kanwar, N., et al. (2017). Mapping genomic and transcriptomic alterations spatially in epithelial cells adjacent to human breast carcinoma. *Nat. Commun.* 8:1245. doi: 10.1038/s41467-017-01357-y

Agrawal, N., Kango, M., Mishra, A., and Sinha, P. (1995). Neoplastic transformation and aberrant cell-cell interactions in genetic mosaics of lethal(2)giant larvae (lgl), a tumor suppressor gene of Drosophila. *Dev. Biol.* 172, 218–229. doi: 10.1006/dbio.1995.0017

Akai, N., Igaki, T., and Ohsawa, S. (2018). Wingless signaling regulates winner/loser status in Minute cell competition. *Genes Cells* 23, 234–240. doi: 10.1111/gtc.12568

Aldaz, S., and Escudero, L. M. (2010). Imaginal discs. *Curr. Biol.* 20, R429–R431. doi: 10.1016/j.cub.2010.03.010

Ballesteros-Arias, L., Saavedra, V., and Morata, G. (2014). Cell competition may function either as tumour-suppressing or as tumour-stimulating factor in *Drosophila*. *Oncogene* 33, 4377–4384. doi: 10.1038/onc.2013.407

Bascones-Martinez, A., Rodriguez-Gutierrez, C., Rodriguez-Gomez, E., Gil-Montoya, J. A., Gomez-Font, R., and Gonzalez-Moles, M. A. (2013). Evaluation of p53, caspase-3, Bcl-2, and Ki-67 markers in oral squamous cell carcinoma and premalignant epithelium in a sample from Alava Province (Spain). *Med. Oral Patol. Oral Cir. Bucal* 18, e846–e850. doi: 10.4317/medoral.18901

Benetatos, L., Vartholomatos, G., and Hatzimichael, E. (2014). Polycomb group proteins and MYC: the cancer connection. *Cell. Mol. Life Sci.* 71, 257–269. doi: 10.1007/s00018-013-1426-x

Bhattacharjee, S., and Nandi, S. (2016). Choices have consequences: the nexus between DNA repair pathways and genomic instability in cancer. *Clin. Transl. Med.* 5:45. doi: 10.1186/s40169-016-0128-z

Bilder, D. (2004). Epithelial polarity and proliferation control: links from the *Drosophila* neoplastic tumor suppressors. *Genes Dev.* 18, 1909–1925. doi: 10.1101/gad.1211604

Bilder, D., Li, M., and Perrimon, N. (2000). Cooperative regulation of cell polarity and growth by *Drosophila* tumor suppressors. *Science* 289, 113–116. doi: 10.1126/science.289.5476.113

Birchall, M. A., Schock, E., Harmon, B. V., and Gobe, G. (1997). Apoptosis, mitosis, PCNA and bcl-2 in normal, leukoplakic and malignant epithelia of the human oral cavity: prospective, in vivo study. *Oral Oncol.* 33, 419–425. doi: 10.1016/S0964-1955(97)00033-X

Bongers, V., Snow, G. B., de Vries, N., Cattan, A. R., Hall, A. G., van der Waal, I., et al. (1995). Second primary head and neck squamous cell carcinoma predicted by the glutathione S-transferase expression in healthy tissue in the direct vicinity of the first tumor. *Lab. Invest.* 73, 503–510.

Braakhuis, B. J., Tabor, M. P., Kummer, J. A., Leemans, C. R., and Brakenhoff, R. H. (2003). A genetic explanation of Slaughter's concept of field cancerization: evidence and clinical implications. *Cancer Res.* 63, 1727–1730.

Braakhuis, B. J., Tabor, M. P., Leemans, C. R., van der Waal, I., Snow, G. B., and Brakenhoff, R. H. (2002). Second primary tumors and field cancerization in oral and oropharyngeal cancer: molecular techniques provide new insights and definitions. *Head Neck* 24, 198–206. doi: 10.1002/hed.10042

Brand, A. H., and Perrimon, N. (1993). Targeted gene expression as a means of altering cell fates and generating dominant phenotypes. *Development* 118, 401–415.

Bryant, P. J. (1975). Pattern formation in the imaginal wing disc of *Drosophila melanogaster*: fate map, regeneration and duplication. *J. Exp. Zool.* 193, 49–77. doi: 10.1002/jez.1401930106

Buratovich, M. A., and Bryant, P. J. (1997). Enhancement of overgrowth by gene interactions in lethal(2)giant discs imaginal discs from *Drosophila melanogaster*. *Genetics* 147, 657–670.

Castven, D., Fischer, M., Becker, D., Heinrich, S., Andersen, J. B., Strand, D., et al. (2017). Adverse genomic alterations and stemness features are induced by field cancerization in the microenvironment of hepatocellular carcinomas. *Oncotarget* 8, 48688–48700. doi: 10.18632/oncotarget.16231

Chan, J. S., Tan, M. J., Sng, M. K., Teo, Z., Phua, T., Choo, C. C., et al. (2017). Cancer-associated fibroblasts enact field cancerization by promoting extratumoral oxidative stress. *Cell Death Dis.* 8:e2562. doi: 10.1038/cddis.2016.492

Chandler, C. H., Chari, S., and Dworkin, I. (2013). Does your gene need a background check? How genetic background impacts the analysis of mutations, genes, and evolution. *Trends Genet.* 29, 358–366. doi: 10.1016/j.tig.2013.01.009

Choi, W., Kim, J., Park, J., Lee, D. H., Hwang, D., Kim, J. H., et al. (2018). YAP/TAZ initiates gastric tumorigenesis via upregulation of MYC. *Cancer Res.* 78, 3306–3320. doi: 10.1158/0008-5472.CAN-17-3487

Claveria, C., Giovinazzo, G., Sierra, R., and Torres, M. (2013). Myc-driven endogenous cell competition in the early mammalian embryo. *Nature* 500, 39–44. doi: 10.1038/nature12389

Curtius, K., Wright, N. A., and Graham, T. A. (2017). Evolution of premalignant disease. *Cold Spring Harb. Perspect. Med.* 7:a026542. doi: 10.1101/cshperspect.a026542

Curtius, K., Wright, N. A., and Graham, T. A. (2018). An evolutionary perspective on field cancerization. *Nat. Rev. Cancer.* 18, 19–32. doi: 10.1038/nrc.2017.102

Dakubo, G. D., Jakupciak, J. P., Birch-Machin, M. A., and Parr, R. L. (2007). Clinical implications and utility of field cancerization. *Cancer Cell Int.* 7:2. doi: 10.1186/1475-2867-7-2

Dang, C. V., O'Donnell, K. A., Zeller, K. I., Nguyen, T., Osthus, R. C., and Li, F. (2006). The c-Myc target gene network. *Semin. Cancer Biol.* 16, 253–264. doi: 10.1016/j.semcancer.2006.07.014

de Bruin, E. C., McGranahan, N., Mitter, R., Salm, M., Wedge, D. C., Yates, L., et al. (2014). Spatial and temporal diversity in genomic instability processes defines lung cancer evolution. *Science* 346, 251–256. doi: 10.1126/science.1253462

de la Cova, C., Abril, M., Bellosta, P., Gallant, P., and Johnston, L. A. (2004). *Drosophila* myc regulates organ size by inducing cell competition. *Cell* 117, 107–116. doi: 10.1016/S0092-8674(04)00214-4

del Valle, Rodriguez, A., Didiano, D., and Desplan, C. (2012). Power tools for gene expression and clonal analysis in *Drosophila*. *Nat. Methods* 9, 47–55. doi: 10.1038/nmeth.1800

Di Giacomo, S., Sollazzo, M., de Biase, D., Ragazzi, M., Bellosta, P., Pession, A., et al. (2017). Human cancer cells signal their competitive fitness through MYC activity. *Sci. Rep.* 7:12568. doi: 10.1038/s41598-017-13002-1

Di Gregorio, A., Bowling, S., and Rodriguez, T. A. (2016). Cell competition and its role in the regulation of cell fitness from development to cancer. *Dev. Cell* 38, 621–634. doi: 10.1016/j.devcel.2016.08.012

Diaz-Diaz, C., Fernandez, de Manuel, L., Jimenez-Carretero, D., Montoya, M. C., Claveria, C., et al. (2017). Pluripotency surveillance by Myc-driven competitive elimination of differentiating cells. *Dev. Cell* 42, 585–599.e4. doi: 10.1016/j.devcel.2017.08.011

Dotto, G. P. (2014). Multifocal epithelial tumors and field cancerization: stroma as a primary determinant. *J. Clin. Investig.* 124, 1446–1453. doi: 10.1172/JCI72589

Driessens, G., Beck, B., Caauwe, A., Simons, B. D., and Blanpain, C. (2012). Defining the mode of tumour growth by clonal analysis. *Nature* 488, 527–530. doi: 10.1038/nature11344

Dronamraju, R., and Mason, J. M. (2011). MU2 and HP1a regulate the recognition of double strand breaks in *Drosophila melanogaster*. *PLoS One* 6:e25439. doi: 10.1371/journal.pone.0025439

Eichenlaub, T., Cohen, S. M., and Herranz, H. (2016). Cell competition drives the formation of metastatic tumors in a *Drosophila* model of epithelial tumor formation. *Curr. Biol.* 26, 419–427. doi: 10.1016/j.cub.2015.12.042

Ellsworth, D. L., Ellsworth, R. E., Love, B., Deyarmin, B., Lubert, S. M., Mittal, V., et al. (2004). Outer breast quadrants demonstrate increased levels of genomic instability. *Ann. Surg. Oncol.* 11, 861–868. doi: 10.1245/ASO.2004.03.024

Enomoto, M., and Igaki, T. (2011). Deciphering tumor-suppressor signaling in flies: genetic link between Scribble/Dlg/Lgl and the Hippo pathways. *J. Genet. Genomics* 38, 461–470. doi: 10.1016/j.jgg.2011.09.005

Evan, G. I., and Littlewood, T. D. (1993). The role of c-myc in cell growth. *Curr. Opin. Genet. Dev.* 3, 44–49. doi: 10.1016/S0959-437X(05)80339-9

Feinberg, A. P., Koldobskiy, M. A., and Gondor, A. (2016). Epigenetic modulators, modifiers and mediators in cancer aetiology and progression. *Nat. Rev. Genet.* 17, 284–299. doi: 10.1038/nrg.2016.13

Froldi, F., Ziosi, M., Garoia, F., Pession, A., Grzeschik, N. A., Bellosta, P., et al. (2010). The lethal giant larvae tumour suppressor mutation requires dMyc oncoprotein to promote clonal malignancy. *BMC Biol.* 8:33. doi: 10.1186/1741-7007-8-33

Gabay, M., Li, Y., and Felsher, D. W. (2014). MYC activation is a hallmark of cancer initiation and maintenance. *Cold Spring Harb. Perspect. Med.* 4:a014241. doi: 10.1101/cshperspect.a014241

Gagneur, J., Stegle, O., Zhu, C., Jakob, P., Tekkedil, M. M., Aiyar, R. S., et al. (2013). Genotype-environment interactions reveal causal pathways that mediate genetic effects on phenotype. *PLoS Genet.* 9:e1003803. doi: 10.1371/journal.pgen.1003803

Galandiuk, S., Rodriguez-Justo, M., Jeffery, R., Nicholson, A. M., Cheng, Y., Oukrif, D., et al. (2012). Field cancerization in the intestinal epithelium of patients with Crohn's ileocolitis. *Gastroenterology* 142, 855–864.e8. doi: 10.1053/j.gastro.2011.12.004

Gallant, P. (2013). Myc function in *Drosophila*. *Cold Spring Harb. Perspect. Med.* 3:a014324. doi: 10.1101/cshperspect.a014324

Giaretti, W., Pentenero, M., Gandolfo, S., and Castagnola, P. (2012). Chromosomal instability, aneuploidy and routine high-resolution DNA content analysis in oral cancer risk evaluation. *Future Oncol.* 8, 1257–1271. doi: 10.2217/fon.12.116

Gogna, R., Shee, K., and Moreno, E. (2015). Cell competition during growth and regeneration. *Annu. Rev. Genet.* 49, 697–718. doi: 10.1146/annurev-genet-112414-055214

Goodliffe, J. M., Wieschaus, E., and Cole, M. D. (2005). Polycomb mediates Myc autorepression and its transcriptional control of many loci in *Drosophila*. *Genes Dev.* 19, 2941–2946. doi: 10.1101/gad.1352305

Grady, W. M. (2005). Epigenetic events in the colorectum and in colon cancer. *Biochem. Soc. Trans.* 33(Pt 4), 684–688. doi: 10.1042/BST0330684

Greer, C., Lee, M., Westerhof, M., Milholland, B., Spokony, R., Vijg, J., et al. (2013). Myc-dependent genome instability and lifespan in Drosophila. *PLoS One* 8:e74641. doi: 10.1371/journal.pone.0074641

Grewal, S. S., Li, L., Orian, A., Eisenman, R. N., and Edgar, B. A. (2005). Myc-dependent regulation of ribosomal RNA synthesis during *Drosophila* development. *Nat. Cell Biol.* 7, 295–302. doi: 10.1038/ncb1223

Grifoni, D., and Bellosta, P. (2015). Drosophila Myc: a master regulator of cellular performance. *Biochim. Biophys. Acta* 1849, 570–581. doi: 10.1016/j.bbagrm.2014.06.021

Grifoni, D., Froldi, F., and Pession, A. (2013). Connecting epithelial polarity, proliferation and cancer in *Drosophila*: the many faces of *lgl* loss of function. *Int. J. Dev. Biol.* 57, 677–687. doi: 10.1387/ijdb.130285dg

Grifoni, D., Garoia, F., Bellosta, P., Parisi, F., De Biase, D., Collina, G., et al. (2007). aPKCzeta cortical loading is associated with Lgl cytoplasmic release and tumor growth in *Drosophila* and human epithelia. *Oncogene* 26, 5960–5965. doi: 10.1038/sj.onc.1210389

Grifoni, D., Garoia, F., Schimanski, C. C., Schmitz, G., Laurenti, E., Galle, P. R., et al. (2004). The human protein Hugl-1 substitutes for *Drosophila* lethal giant larvae tumour suppressor function *in vivo*. *Oncogene* 23, 8688–8694. doi: 10.1038/sj.onc.1208023

Grifoni, D., Sollazzo, M., Fontana, E., Froldi, F., and Pession, A. (2015). Multiple strategies of oxygen supply in *Drosophila* malignancies identify tracheogenesis as a novel cancer hallmark. *Sci. Rep.* 5:9061. doi: 10.1038/srep09061

Grusche, F. A., Richardson, H. E., and Harvey, K. F. (2010). Upstream regulation of the hippo size control pathway. *Curr. Biol.* 20, R574–R582. doi: 10.1016/j.cub.2010.05.023

Gurel, B., Iwata, T., Koh, C. M., Jenkins, R. B., Lan, F., Van Dang, C., et al. (2008). Nuclear MYC protein overexpression is an early alteration in human prostate carcinogenesis. *Mod. Pathol.* 21, 1156–1167. doi: 10.1038/modpathol.2008.111

Haaland, C. M., Heaphy, C. M., Butler, K. S., Fischer, E. G., Griffith, J. K., and Bisoffi, M. (2009). Differential gene expression in tumor adjacent histologically normal prostatic tissue indicates field cancerization. *Int. J. Oncol.* 35, 537–546.

Halder, G., and Johnson, R. L. (2011). Hippo signaling: growth control and beyond. *Development* 138, 9–22. doi: 10.1242/dev.045500

Hariharan, I. K., and Bilder, D. (2006). Regulation of imaginal disc growth by tumor-suppressor genes in *Drosophila*. *Annu. Rev. Genet.* 40, 335–361. doi: 10.1146/annurev.genet.39.073003.100738

Herranz, H., Eichenlaub, T., and Cohen, S. M. (2016). Cancer in *Drosophila*: imaginal discs as a model for epithelial tumor formation. *Curr. Top. Dev. Biol.* 116, 181–199. doi: 10.1016/bs.ctdb.2015.11.037

Hofstad, B., Vatn, M. H., Andersen, S. N., Huitfeldt, H. S., Rognum, T., Larsen, S., et al. (1996). Growth of colorectal polyps: redetection and evaluation of unresected polyps for a period of three years. *Gut* 39, 449–456. doi: 10.1136/gut.39.3.449

Iwata, T., Schultz, D., Hicks, J., Hubbard, G. K., Mutton, L. N., Lotan, T. L., et al. (2010). MYC overexpression induces prostatic intraepithelial neoplasia and loss of Nkx3.1 in mouse luminal epithelial cells. *PLoS One* 5:e9427. doi: 10.1371/journal.pone.0009427

Jakubek, Y., Lang, W., Vattathil, S., Garcia, M., Xu, L., Huang, L., et al. (2016). Genomic landscape established by allelic imbalance in the cancerization field of a normal appearing airway. *Cancer Res.* 76, 3676–3683. doi: 10.1158/0008-5472.CAN-15-3064

Jaloszynski, P., Jaruga, P., Olinski, R., Biczysko, W., Szyfter, W., Nagy, E., et al. (2003). Oxidative DNA base modifications and polycyclic aromatic hydrocarbon DNA adducts in squamous cell carcinoma of larynx. *Free Radic. Res.* 37, 231–240. doi: 10.1080/1071576021000041014

Johnston, L. A. (2014). Socializing with MYC: cell competition in development and as a model for premalignant cancer. *Cold Spring Harb. Perspect. Med.* 4:a014274. doi: 10.1101/cshperspect.a014274

Kamakaka, R. T., and Biggins, S. (2005). Histone variants: deviants? *Genes Dev.* 19, 295–310. doi: 10.1101/gad.1272805

Kamiyama, H., Suzuki, K., Maeda, T., Koizumi, K., Miyaki, Y., Okada, S., et al. (2012). DNA demethylation in normal colon tissue predicts predisposition to multiple cancers. *Oncogene* 31, 5029–5037. doi: 10.1038/onc.2011.652

Kato, S., Lippman, S. M., Flaherty, K. T., and Kurzrock, R. (2016). The conundrum of genetic "Drivers" in benign conditions. *J. Natl. Cancer Inst.* 108:djw036. doi: 10.1093/jnci/djw036

Khan, A., Shover, W., and Goodliffe, J. M. (2009). Su(z)2 antagonizes autorepression of Myc in Drosophila, increasing Myc levels and subsequent transactivation. *PLoS One* 4:e5076. doi: 10.1371/journal.pone.0005076

Kim, J., Eltoum, I. E., Roh, M., Wang, J., and Abdulkadir, S. A. (2009). Interactions between cells with distinct mutations in c-MYC and Pten in prostate cancer. *PLoS Genet.* 5:e1000542. doi: 10.1371/journal.pgen.1000542

Klebes, A., Sustar, A., Kechris, K., Li, H., Schubiger, G., and Kornberg, T. B. (2005). Regulation of cellular plasticity in *Drosophila* imaginal disc cells by the Polycomb group, trithorax group and *lama* genes. *Development* 132, 3753–3765. doi: 10.1242/dev.01927

Kuzyk, A., and Mai, S. (2014). c-MYC-induced genomic instability. *Cold Spring Harb. Perspect. Med.* 4:a014373. doi: 10.1101/cshperspect.a014373

Lawrence, M. S., Stojanov, P., Mermel, C. H., Robinson, J. T., Garraway, L. A., Golub, T. R., et al. (2014). Discovery and saturation analysis of cancer genes across 21 tumour types. *Nature* 505, 495–501. doi: 10.1038/nature12912

Lee, Y. C., Wang, H. P., Wang, C. P., Ko, J. Y., Lee, J. M., Chiu, H. M., et al. (2011). Revisit of field cancerization in squamous cell carcinoma of upper aerodigestive tract: better risk assessment with epigenetic markers. *Cancer Prev. Res.* 4, 1982–1992. doi: 10.1158/1940-6207.CAPR-11-0096

Leevers, S. J., Weinkove, D., MacDougall, L. K., Hafen, E., and Waterfield, M. D. (1996). The Drosophila phosphoinositide 3-kinase Dp110 promotes cell growth. *EMBO J.* 15, 6584–6594. doi: 10.1002/j.1460-2075.1996.tb01049.x

Levayer, R., Hauert, B., and Moreno, E. (2015). Cell mixing induced by myc is required for competitive tissue invasion and destruction. *Nature* 524, 476–480. doi: 10.1038/nature14684

Levayer, R., and Moreno, E. (2013). Mechanisms of cell competition: themes and variations. *J. Cell Biol.* 200, 689–698. doi: 10.1083/jcb.201301051

Levayer, R., and Moreno, E. (2016). How to be in a good shape? The influence of clone morphology on cell competition. *Commun. Integr. Biol.* 9:e1102806. doi: 10.1080/19420889.2015.1102806

Lu, H., and Bilder, D. (2005). Endocytic control of epithelial polarity and proliferation in *Drosophila*. *Nat. Cell Biol.* 7, 1232–1239. doi: 10.1038/ncb1324

Lu, X., Feng, X., Man, X., Yang, G., Tang, L., Du, D., et al. (2009). Aberrant splicing of Hugl-1 is associated with hepatocellular carcinoma progression. *Clin. Cancer Res.* 15, 3287–3296. doi: 10.1158/1078-0432.CCR-08-2078

Lu, Z., Sheng, J., Zhang, Y., Deng, J., Li, Y., Lu, A., et al. (2016). Clonality analysis of multifocal papillary thyroid carcinoma by using genetic profiles. *J. Pathol.* 239, 72–83. doi: 10.1002/path.4696

Luo, Y., Yu, M., and Grady, W. M. (2014). Field cancerization in the colon: a role for aberrant DNA methylation? *Gastroenterol. Rep.* 2, 16–20. doi: 10.1093/gastro/got039

Maggrah, A., Robinson, K., Creed, J., Wittock, R., Gehman, K., Gehman, T., et al. (2013). Paired ductal carcinoma in situ and invasive breast cancer lesions in the D-loop of the mitochondrial genome indicate a cancerization field effect. *Biomed Res. Int.* 2013:379438. doi: 10.1155/2013/379438

Maitra, S., Kulikauskas, R. M., Gavilan, H., and Fehon, R. G. (2006). The tumor suppressors Merlin and Expanded function cooperatively to modulate receptor endocytosis and signaling. *Curr. Biol.* 16, 702–709. doi: 10.1016/j.cub.2006.02.063

Maley, C. C., Galipeau, P. C., Li, X., Sanchez, C. A., Paulson, T. G., and Reid, B. J. (2004). Selectively advantageous mutations and hitchhikers in neoplasms: p16 lesions are selected in Barrett's esophagus. *Cancer Res.* 64, 3414–3427. doi: 10.1158/0008-5472.CAN-03-3249

Martincorena, I., Roshan, A., Gerstung, M., Ellis, P., Van Loo, P., McLaren, S., et al. (2015). Tumor evolution. High burden and pervasive positive selection of somatic mutations in normal human skin. *Science* 348, 880–886. doi: 10.1126/science.aaa6806

McDonald, S. A., Greaves, L. C., Gutierrez-Gonzalez, L., Rodriguez-Justo, M., Deheragoda, M., Leedham, S. J., et al. (2008). Mechanisms of field cancerization in the human stomach: the expansion and spread of mutated gastric stem cells. *Gastroenterology* 134, 500–510. doi: 10.1053/j.gastro.2007.11.035

McMahon, S. B. (2014). MYC and the control of apoptosis. *Cold Spring Harb. Perspect. Med.* 4:a014407. doi: 10.1101/cshperspect.a014407

Meier, P., Silke, J., Leevers, S. J., and Evan, G. I. (2000). The *Drosophila* caspase DRONC is regulated by DIAP1. *EMBO J.* 19, 598–611. doi: 10.1093/emboj/19.4.598

Mendoza, P., Diaz, J., and Torres, V. A. (2014). On the role of Rab5 in cell migration. *Curr. Mol. Med.* 14, 235–245. doi: 10.2174/1566524014666140128111347

Menendez, J., Perez-Garijo, A., Calleja, M., and Morata, G. (2010). A tumor-suppressing mechanism in *Drosophila* involving cell competition and the Hippo pathway. *Proc. Natl. Acad. Sci. U.S.A.* 107, 14651–14656. doi: 10.1073/pnas.1009376107

Menut, L., Vaccari, T., Dionne, H., Hill, J., Wu, G., and Bilder, D. (2007). A mosaic genetic screen for Drosophila neoplastic tumor suppressor genes based on defective pupation. *Genetics* 177, 1667–1677. doi: 10.1534/genetics.107.078360

Merino, M. M., Levayer, R., and Moreno, E. (2016). Survival of the fittest: essential roles of cell competition in development, aging, and cancer. *Trends Cell Biol.* 26, 776–788. doi: 10.1016/j.tcb.2016.05.009

Metzker, M. L. (2010). Sequencing technologies - the next generation. *Nat. Rev. Genet.* 11, 31–46. doi: 10.1038/nrg2626

Meyer, N., and Penn, L. Z. (2008). Reflecting on 25 years with MYC. *Nat. Rev. Cancer* 8, 976–990. doi: 10.1038/nrc2231

Michor, F., Iwasa, Y., and Nowak, M. A. (2004). Dynamics of cancer progression. *Nat. Rev. Cancer* 4, 197–205. doi: 10.1038/nrc1295

Mohan, M., and Jagannathan, N. (2014). Oral field cancerization: an update on current concepts. *Oncol. Rev.* 8:244. doi: 10.4081/oncol.2014.244

Montero, L., Muller, N., and Gallant, P. (2008). Induction of apoptosis by *Drosophila* Myc. *Genesis* 46, 104–111. doi: 10.1002/dvg.20373

Morata, G., and Ripoll, P. (1975). Minutes: mutants of drosophila autonomously affecting cell division rate. *Dev. Biol.* 42, 211–221. doi: 10.1016/0012-1606(75)90330-9

Moreno, E. (2008). Is cell competition relevant to cancer? *Nat. Rev. Cancer* 8, 141–147. doi: 10.1038/nrc2252

Moreno, E., and Basler, K. (2004). dMyc transforms cells into super-competitors. *Cell* 117, 117–129. doi: 10.1016/S0092-8674(04)00262-4

Moreno, E., Basler, K., and Morata, G. (2002). Cells compete for decapentaplegic survival factor to prevent apoptosis in *Drosophila* wing development. *Nature* 416, 755–759. doi: 10.1038/416755a

Neto-Silva, R. M., de Beco, S., and Johnston, L. A. (2010). Evidence for a growth-stabilizing regulatory feedback mechanism between Myc and Yorkie, the *Drosophila* homolog of Yap. *Dev. Cell* 19, 507–520. doi: 10.1016/j.devcel.2010.09.009

Nonn, L., Ananthanarayanan, V., and Gann, P. H. (2009). Evidence for field cancerization of the prostate. *Prostate* 69, 1470–1479. doi: 10.1002/pros.20983

Nussinov, R., Tsai, C. J., Jang, H., Korcsmaros, T., and Csermely, P. (2016). Oncogenic KRAS signaling and YAP1/beta-catenin: similar cell cycle control in tumor initiation. *Semin. Cell Dev. Biol.* 58, 79–85. doi: 10.1016/j.semcdb.2016.04.001

Oertel, M., Menthena, A., Dabeva, M. D., and Shafritz, D. A. (2006). Cell competition leads to a high level of normal liver reconstitution by transplanted fetal liver stem/progenitor cells. *Gastroenterology* 130, 507–520; quiz 590. doi: 10.1053/j.gastro.2005.10.049

Papadimitrakopoulou, V. A., Shin, D. M., and Hong, W. K. (1996). Molecular and cellular biomarkers for field cancerization and multistep process in head and neck tumorigenesis. *Cancer Metastasis Rev.* 15, 53–76. doi: 10.1007/BF00049487

Park, S. K., Song, C. S., Yang, H. J., Jung, Y. S., Choi, K. Y., Koo, D. H., et al. (2016). Field cancerization in sporadic colon cancer. *Gut Liver* 10, 773–780. doi: 10.5009/gnl15334

Parr, R. L., Mills, J., Harbottle, A., Creed, J. M., Crewdson, G., Reguly, B., et al. (2013). Mitochondria, prostate cancer, and biopsy sampling error. *Discov. Med.* 15, 213–220.

Patel, M. S., Shah, H. S., and Shrivastava, N. (2016). c-Myc dependent cell competition in human cancer cells. *J. Cell. Biochem.* 118, 1782–1791. doi: 10.1002/jcb.25846

Penzo-Mendez, A. I., and Stanger, B. Z. (2014). Cell competition in vertebrate organ size regulation. *Wiley Interdiscip. Rev. Dev. Biol.* 3, 419–427. doi: 10.1002/wdev.148

Perez, E., Lindblad, J. L., and Bergmann, A. (2017). Tumor-promoting function of apoptotic caspases by an amplification loop involving ROS, macrophages and JNK in *Drosophila*. *eLife* 6:e26747. doi: 10.7554/eLife.26747

Prober, D. A., and Edgar, B. A. (2002). Interactions between Ras1, dMyc, and dPI3K signaling in the developing *Drosophila* wing. *Genes Dev.* 16, 2286–2299. doi: 10.1101/gad.991102

Rhiner, C., Diaz, B., Portela, M., Poyatos, J. F., Fernandez-Ruiz, I., Lopez-Gay, J. M., et al. (2009). Persistent competition among stem cells and their daughters in the *Drosophila* ovary germline niche. *Development* 136, 995–1006. doi: 10.1242/dev.033340

Rhiner, C., and Moreno, E. (2009). Super competition as a possible mechanism to pioneer precancerous fields. *Carcinogenesis* 30, 723–728. doi: 10.1093/carcin/bgp003

Rodrigues, A. B., Zoranovic, T., Ayala-Camargo, A., Grewal, S., Reyes-Robles, T., Krasny, M., et al. (2012). Activated STAT regulates growth and induces competitive interactions independently of Myc, Yorkie, Wingless and ribosome biogenesis. *Development* 139, 4051–4061. doi: 10.1242/dev.076760

Rosen, C., Shezen, E., Aronovich, A., Klionsky, Y. Z., Yaakov, Y., Assayag, M., et al. (2015). Preconditioning allows engraftment of mouse and human embryonic lung cells, enabling lung repair in mice. *Nat. Med.* 21, 869–879. doi: 10.1038/nm.3889

Sancho, M., Di-Gregorio, A., George, N., Pozzi, S., Sanchez, J. M., Pernaute, B., et al. (2013). Competitive interactions eliminate unfit embryonic stem cells at the onset of differentiation. *Dev. Cell* 26, 19–30. doi: 10.1016/j.devcel.2013.06.012

Santos-Garcia, A., Abad-Hernandez, M. M., Fonseca-Sanchez, E., Cruz-Hernandez, J. J., and Bullon-Sopelana, A. (2005). Proteic expression of p53 and cellular proliferation in oral leukoplakias. *Med. Oral Patol. Oral Cir. Bucal* 10, 5–8; 1–5.

Schimanski, C. C., Schmitz, G., Kashyap, A., Bosserhoff, A. K., Bataille, F., Schafer, S. C., et al. (2005). Reduced expression of *Hugl-1*, the human homologue of *Drosophila* tumour suppressor gene *lgl*, contributes to progression of colorectal cancer. *Oncogene* 24, 3100–3109. doi: 10.1038/sj.onc.1208520

Sears, R., Nuckolls, F., Haura, E., Taya, Y., Tamai, K., and Nevins, J. R. (2000). Multiple Ras-dependent phosphorylation pathways regulate Myc protein stability. *Genes Dev.* 14, 2501–2514. doi: 10.1101/gad.836800

Shakiba, N., and Zandstra, P. W. (2017). Engineering cell fitness: lessons for regenerative medicine. *Curr. Opin. Biotechnol.* 47, 7–15. doi: 10.1016/j.copbio.2017.05.005

Shivas, J. M., Morrison, H. A., Bilder, D., and Skop, A. R. (2010). Polarity and endocytosis: reciprocal regulation. *Trends Cell Biol.* 20, 445–452. doi: 10.1016/j.tcb.2010.04.003

Slaughter, D. P., Southwick, H. W., and Smejkal, W. (1953). Field cancerization in oral stratified squamous epithelium; clinical implications of multicentric origin. *Cancer* 6, 963–968. doi: 10.1002/1097-0142(195309)6:5<963::AID-CNCR2820060515>3.0.CO;2-Q

Stine, Z. E., Walton, Z. E., Altman, B. J., Hsieh, A. L., and Dang, C. V. (2015). MYC, Metabolism, and Cancer. *Cancer Discov.* 5, 1024–1039. doi: 10.1158/2159-8290.CD-15-0507

Suijkerbuijk, S. J., Kolahgar, G., Kucinski, I., and Piddini, E. (2016). Cell competition drives the growth of intestinal adenomas in *Drosophila*. *Curr. Biol.* 26, 428–438. doi: 10.1016/j.cub.2015.12.043

Tamori, Y., and Deng, W. M. (2013). Tissue repair through cell competition and compensatory cellular hypertrophy in postmitotic epithelia. *Dev. Cell* 25, 350–363. doi: 10.1016/j.devcel.2013.04.013

Torres, V. A., and Stupack, D. G. (2011). Rab5 in the regulation of cell motility and invasion. *Curr. Protein Pept. Sci.* 12, 43–51. doi: 10.2174/138920311795659461

Trujillo, K. A., Heaphy, C. M., Mai, M., Vargas, K. M., Jones, A. C., Vo, P., et al. (2011). Markers of fibrosis and epithelial to mesenchymal transition demonstrate field cancerization in histologically normal tissue adjacent to breast tumors. *Int. J. Cancer* 129, 1310–1321. doi: 10.1002/ijc.25788

Tsuboi, A., Ohsawa, S., Umetsu, D., Sando, Y., Kuranaga, E., Igaki, T., et al. (2018). Competition for space is controlled by apoptosis-induced change of local epithelial topology. *Curr. Biol.* 28, 2115–2128.e5. doi: 10.1016/j.cub.2018.05.029

Tyler, D. M., Li, W., Zhuo, N., Pellock, B., and Baker, N. E. (2007). Genes affecting cell competition in Drosophila. *Genetics* 175, 643–657. doi: 10.1534/genetics.106.061929

Udan, R. S., Kango-Singh, M., Nolo, R., Tao, C., and Halder, G. (2003). Hippo promotes proliferation arrest and apoptosis in the Salvador/Warts pathway. *Nat. Cell Biol.* 5, 914–920. doi: 10.1038/ncb1050

Vaccari, T., and Bilder, D. (2009). At the crossroads of polarity, proliferation and apoptosis: the use of Drosophila to unravel the multifaceted role of endocytosis in tumor suppression. *Mol. Oncol.* 3, 354–365. doi: 10.1016/j.molonc.2009.05.005

Vafa, O., Wade, M., Kern, S., Beeche, M., Pandita, T. K., Hampton, G. M., et al. (2002). c-Myc can induce DNA damage, increase reactive oxygen species, and mitigate p53 function: a mechanism for oncogene-induced genetic instability. *Mol. Cell* 9, 1031–1044. doi: 10.1016/S1097-2765(02)00520-8

Vermeulen, L., Morrissey, E., van der Heijden, M., Nicholson, A. M., Sottoriva, A., Buczacki, S., et al. (2013). Defining stem cell dynamics in models of intestinal tumor initiation. *Science* 342, 995–998. doi: 10.1126/science.1243148

Villa Del Campo, C., Claveria, C., Sierra, R., and Torres, M. (2014). Cell competition promotes phenotypically silent cardiomyocyte replacement in the mammalian heart. *Cell Rep.* 8, 1741–1751. doi: 10.1016/j.celrep.2014.08.005

Villa del Campo, C., Lioux, G., Carmona, R., Sierra, R., Munoz-Chapuli, R., et al. (2016). Myc overexpression enhances of epicardial contribution to the developing heart and promotes extensive expansion of the cardiomyocyte population. *Sci. Rep.* 6:35366. doi: 10.1038/srep35366

Vincent, J. P., Kolahgar, G., Gagliardi, M., and Piddini, E. (2011). Steep differences in wingless signaling trigger Myc-independent competitive cell interactions. *Dev. Cell* 21, 366–374. doi: 10.1016/j.devcel.2011.06.021

Vogelstein, B., Papadopoulos, N., Velculescu, V. E., Zhou, S., Diaz, L. A. Jr., and Kinzler, K. W. (2013). Cancer genome landscapes. *Science* 339, 1546–1558. doi: 10.1126/science.1235122

Wang, S. L., Hawkins, C. J., Yoo, S. J., Muller, H. A., and Hay, B. A. (1999). The *Drosophila* caspase inhibitor DIAP1 is essential for cell survival and is negatively regulated by HID. *Cell* 98, 453–463. doi: 10.1016/S0092-8674(00)81974-1

Wodarz, A., and Nathke, I. (2007). Cell polarity in development and cancer. *Nat. Cell Biol.* 9, 1016–1024. doi: 10.1038/ncb433

Wodarz, D., Iwasa, Y., and Komarova, N. L. (2004). On the emergence of multifocal cancers. *J. Carcinog.* 3:13. doi: 10.1186/1477-3163-3-13

Xiong, D., Pan, J., Zhang, Q., Szabo, E., Miller, M. S., Lubet, R. A., et al. (2017). Bronchial airway gene expression signatures in mouse lung squamous cell carcinoma and their modulation by cancer chemopreventive agents. *Oncotarget* 8, 18885–18900. doi: 10.18632/oncotarget.13806

Xu, T., and Rubin, G. M. (1993). Analysis of genetic mosaics in developing and adult Drosophila tissues. *Development* 117, 1223–1237.

Xu, T., Wang, W., Zhang, S., Stewart, R. A., and Yu, W. (1995). Identifying tumor suppressors in genetic mosaics: the Drosophila lats gene encodes a putative protein kinase. *Development* 121, 1053–1063.

Zaky, A. H., Watari, J., Tanabe, H., Sato, R., Moriichi, K., Tanaka, A., et al. (2008). Clinicopathologic implications of genetic instability in intestinal-type gastric cancer and intestinal metaplasia as a precancerous lesion: proof of field cancerization in the stomach. *Am. J. Clin. Pathol.* 129, 613–621. doi: 10.1309/DFLELPGPNV5LK6B1

Zeki, S. S., McDonald, S. A., and Graham, T. A. (2011). Field cancerization in Barrett's esophagus. *Discov. Med.* 12, 371–379.

Zhang, Y., Lin, N., Carroll, P. M., Chan, G., Guan, B., Xiao, H., et al. (2008). Epigenetic blocking of an enhancer region controls irradiation-induced proapoptotic gene expression in *Drosophila* embryos. *Dev. Cell* 14, 481–493. doi: 10.1016/j.devcel.2008.01.018

Ziosi, M., Baena-Lopez, L. A., Grifoni, D., Froldi, F., Pession, A., Garoia, F., et al. (2010). dMyc functions downstream of Yorkie to promote the supercompetitive behavior of hippo pathway mutant cells. *PLoS Genet.* 6:e1001140. doi: 10.1371/journal.pgen.1001140

Conflict of Interest Statement: The authors declare that the research was conducted in the absence of any commercial or financial relationships that could be construed as a potential conflict of interest.

frontiers in Genetics

ORIGINAL RESEARCH
published: 27 November 2018
doi: 10.3389/fgene.2018.00581

p53-Sensitive Epileptic Behavior and Inflammation in *Ft1* Hypomorphic Mice

*Romina Burla[1†], Mattia La Torre[1†], Giorgia Zanetti[1], Alex Bastianelli[1], Chiara Merigliano[1,2], Simona Del Giudice[1], Alessandro Vercelli[3,4], Ferdinando Di Cunto[3,4], Marina Boido[3,4], Fiammetta Vernì[1] and Isabella Saggio[1,2]**

[1] Department of Biology and Biotechnology, Sapienza University of Rome, Rome, Italy, [2] Nanyang Technological University, Singapore, Singapore, [3] Neuroscience Institute Cavalieri Ottolenghi, Torino, Italy, [4] Department of Neuroscience, University of Torino, Piedmont, Italy

OPEN ACCESS

Edited by:
Maria Grazia Giansanti, Consiglio Nazionale Delle Ricerche (CNR), Italy

Reviewed by:
Maria Rosaria D'Apice, Consiglio Nazionale Delle Ricerche (CNR), Italy
Cristina Capanni, Istituto di Genetica Molecolare (IGM), Italy

***Correspondence:**
Isabella Saggio
isabella.saggio@uniroma1.it

[†] These authors share first authorship

Specialty section:
This article was submitted to Genetic Disorders, a section of the journal Frontiers in Genetics

Received: *29 August 2018*
Accepted: *08 November 2018*
Published: *27 November 2018*

Citation:
Burla R, La Torre M, Zanetti G, Bastianelli A, Merigliano C, Del Giudice S, Vercelli A, Di Cunto F, Boido M, Vernì F and Saggio I (2018) p53-Sensitive Epileptic Behavior and Inflammation in Ft1 Hypomorphic Mice. Front. Genet. 9:581. doi: 10.3389/fgene.2018.00581

Epilepsy is a complex clinical condition characterized by repeated spontaneous seizures. Seizures have been linked to multiple drivers including DNA damage accumulation. Investigation of epilepsy physiopathology in humans imposes ethical and practical limitations, for this reason model systems are mostly preferred. Among animal models, mouse mutants are particularly valuable since they allow conjoint behavioral, organismal, and genetic analyses. Along with this, since aging has been associated with higher frequency of seizures, prematurely aging mice, simulating human progeroid diseases, offer a further useful modeling element as they recapitulate aging over a short time-window. Here we report on a mouse mutant with progeroid traits that displays repeated spontaneous seizures. Mutant mice were produced by reducing the expression of the gene *Ft1* (*AKTIP* in humans). *In vitro*, AKTIP/Ft1 depletion causes telomere aberrations, DNA damage, and cell senescence. AKTIP/Ft1 interacts with lamins, which control nuclear architecture and DNA function. Premature aging defects of *Ft1* mutant mice include skeletal alterations and lipodystrophy. The epileptic behavior of *Ft1* mutant animals was age and sex linked. Seizures were observed in 18 mutant mice (23.6% of aged $\geq$ 21 weeks), at an average frequency of 2.33 events/mouse. Time distribution of seizures indicated non-random enrichment of seizures over the follow-up period, with 75% of seizures happening in consecutive weeks. The analysis of epileptic brains did not reveal overt brain morphological alterations or severe neurodegeneration, however, Ft1 reduction induced expression of the inflammatory markers IL-6 and TGF-β. Importantly, *Ft1* mutant mice with concomitant genetic reduction of the guardian of the genome, p53, showed no seizures or inflammatory marker activation, implicating the DNA damage response into these phenotypes. This work adds insights into the connection among DNA damage, brain function, and aging. In addition, it further underscores the importance of model organisms for studying specific phenotypes, along with permitting the analysis of genetic interactions at the organismal level.

Keywords: aging, epilepsy, DNA damage, p53, DNA repair

INTRODUCTION

Epilepsy comprises a family of disorders characterized by enduring predisposition to generate spontaneous seizures (Scharfman, 2007; Fisher et al., 2014). Seizures are underpinned by multiple mechanisms and their clinical outcome varies widely (Scharfman, 2007). Regardless of their outcome, seizures arise from disruption of mechanisms that create a balance between neuronal excitation and inhibition. Factors corrupting this balance result from alterations at different levels of brain function, from ion channels to receptors, and neuronal circuits (Stafstrom and Carmant, 2015). Epilepsies are often associated with morphological brain abnormalities (Bertram, 2013), but at least one-third have non-structural etiologies (Guerrini et al., 2014). In the last years, concomitantly with human population demographic changes, high incidence of epileptic disorders has been associated with aging, whose specific pathophysiology is under investigation (Leppik and Birnbaum, 2010).

Understanding the mechanistic path to disease is complex in humans due to ethical issues, unavailability of controls and high costs of human research. As a result, studies mostly rely on the use of models, including human 3D cultures and stem cell based systems (Riminucci et al., 2006; Simão et al., 2015), or, for organismal analyses, genetically engineered mice (Baraban, 2007; Saggio et al., 2014; Remoli et al., 2015; La Torre et al., 2018). One of the way in which epilepsy has been modeled in mice is via the inactivation of genes implicated in ion channels (Yu et al., 2006; Baraban, 2007; Glasscock et al., 2012), or of genes encoding for neurotransmitter receptors (Fonck et al., 2005). In addition, epileptic phenomena have been observed in mouse models of Alzheimer disease (Vogt et al., 2011; Ziyatdinova et al., 2011). However, no other genetic models of age related epilepsy have been yet described. Prematurely aging mouse mutants, which recapitulate aging traits over a short time-window (Blasco, 2005; Stewart et al., 2007), offer a specific advantage to model diseases caused or exacerbated by aging, including brain pathologies.

An emerging cause for brain disease and for the aging brain is DNA damage (Langie et al., 2017). DNA integrity poses a challenge for the nervous system as its development depends on a complex series of dynamic and adaptive processes associated to DNA damage (Mckinnon, 2013). Unrepaired DNA lesions have detrimental effects on the developing of a functional nervous system and neural progenitor cells rely on DNA repair systems during the developmental program. After completion of neurogenesis, DNA repair is still of paramount importance to safeguard the genome (Madabhushi et al., 2014), especially to protect the neurons against reactive oxygen species (Langie et al., 2017). DNA damage is also direct cause for cell senescence and for a related inflammatory response (Campisi, 2013; López-Otín et al., 2013).

Mouse mutants of DNA damage functions have opened the path to establish a link between DNA damage and the seizure phenotype (Shen et al., 2010; Bianchi et al., 2017). For example, the inactivation of XRCC1, a central factor in the DNA single strand break repair pathway, leads to profound neuropathology involving behavioral phenotypes consistent with epilepsy (Lee et al., 2009). Data based on studies in *Drosophila* suggest that nuclear architecture and lamins could play a role into epilepsy (Frost, 2016). However, the hierarchy and range of events connecting nuclear architecture, molecular DNA function to epileptic behavior is still to be dissected, along with the elements exacerbating this pathology in aging.

DNA damage affects genome near to randomly, but some chromosomal regions, such as telomeres, are more prone to DNA instability. In mammals, telomeric DNA is composed of double-stranded short tandem repeats of TTAGGG sequence forming higher-order DNA structures binding a specialized protein complex, known as shelterin (de Lange, 2005). We identified a telomere-associated protein named AKTIP in humans (and Ft1 in mouse), which interacts with the shelterin members TRF1 and TRF2 (Burla et al., 2015). AKTIP/Ft1 reduction causes telomere aberrations, DNA instability and cell senescence (Burla et al., 2015). *In vivo*, the genetic reduction of *Ft1* causes premature aging defects including skeletal alterations and lipodystrophy (La Torre et al., 2018). AKTIP/Ft1 interacts with lamins (Burla et al., 2016a,b), pivotal elements for the control of nuclear architecture and DNA function, including DNA repair, replication and transcription (Dittmer and Misteli, 2011). Importantly, *Ft1* mutant mice share similarities with lamin mutant animals, which are models of choice for human progeroid syndromes, linking the *Ft1* model to premature aging and progeroid diseases (Burla et al., 2016a,b, 2018).

Here we report that *Ft1* mutant mice are subjected to repeated seizures. We show that this trait is not linked to overt brain morphological alterations, but is age and inflammation linked. We also demonstrate that this phenotype is sensitive to the expression of the guardian of the genome *p53*, pointing to a role of DNA function in the seizure phenotype.

RESULTS

Seizures in Ft1 Mutant Mice

Mice with reduced levels of *Ft1* were generated using the knock out first (kof) strategy based on the insertion into the target gene (referred as kof allele) of the βgeok cassette (Testa et al., 2004), which traps and truncates *Ft1* nascent transcript reducing the expression of the targeted gene (La Torre et al., 2018). Previous observations of $Ft1^{kof/kof}$ mice revealed that mutant animals display significant reduction in body weight and lifespan, compared to controls. Twenty-one percent of the animals show a severe body size reduction and early post-natal death (we refer to these mice as severely affected $Ft1^{kof/kof}$ mice, abbreviated with SA $Ft1^{kof/kof}$ or SA mutant mice). The leftovers, non SA $Ft1^{kof/kof}$ mice have a mild phenotype, with a median survival of 113 weeks, allowing adult phenotype observation (La Torre et al., 2018).

To investigate mutant mouse behavior, we worked on a cohort of animals aged ≥ 21 weeks non SA $Ft1^{kof/kof}$. We recorded spontaneous behavioral abnormalities in non SA $Ft1^{kof/kof}$ mice including episodes of motor tremors and convulsions, fast runs, jumps, and excessive salivation (**Figure 1** and **Supplementary Movies 1–3**). Dissection of video recordings indicated that non SA $Ft1^{kof/kof}$ displayed sudden movements followed by facial twitching, violent hind

limbs shaking and falling, back arching, short jerks in muscles of the hind limbs and forelimbs extension, Straub tail and incontinence, followed by short jerks and fast breathing (**Figure 1A** and **Supplementary Movies 1–3**). Eventually, animals stood up and returned to normal activity; after few minutes switched to post-ictal phase characterized by short periods of complete immobility, interrupted by short intervals of movement (**Supplementary Movies 4–6**). Recording showed moving rhythmical up-down or left-right, stroking mouth with forepaws, in a repetitive motion, and appearing to be chewing and grooming (**Figure 1A** and **Supplementary Movies 4–6**). Temporal evaluation of the data indicated that non SA $Ft1^{kof/kof}$ mice display a behavioral repertoire corresponding in quality and duration to epileptic phenotypes (**Figure 1B**), as described for other mouse models (Chabrol et al., 2010; Robie et al., 2017).

Over a total of 260 animals (including $Ft1^{+/+}$, $Ft1^{+/kof}$, and $Ft1^{kof/kof}$), 18 $Ft1^{kof/kof}$ exhibited at least one seizure manifestation (**Figures 2A,B**). No seizure episodes were observed in heterozygote $Ft1^{+/kof}$ or wt mice (**Figure 2A**). The frequency of seizures reached a maximum of one seizure episode per week. Of 18 seizure positive mutants, 7 exhibited one seizure-like manifestation during their follow-up period, while the leftover displayed more than one seizure. On average, we observed 2.33 ± 0.14 seizures during the entire follow-up period in the seizure positive mutants (**Figure 2B**). Time distribution of seizures for each mutant animal experiencing more than one seizure indicated non-random enrichment of seizures over the follow-up period, with 75% of seizures happening in consecutive weeks (**Figure 2C**).

Seizures of Ft1 Mutant Mice Are Age and Gender Linked

To analyze the distribution of seizures during aging, we subdivided mouse lifespan in three major intervals: young ($3 \leq$ weeks ≤ 20), juvenile ($21 \leq$ weeks ≤ 60), and adult ($61 \leq$ weeks ≤ 100). We monitored, for each age interval, the fraction of mice exhibiting seizures for the first time (**Figure 3A**). None of young non SA $Ft1^{kof/kof}$ mice ($n = 189$) displayed seizures, while seizures were observed in juvenile and adult mice, in 16 out of 68 and 2 out of 8, respectively.

We previously reported that non SA $Ft1^{kof/kof}$ mice display growth defects, which start within the juvenile interval and become prominent through aging (La Torre et al., 2018). We then asked whether the seizure phenotype was paralleled by age-associated growth impairment. We considered the difference between the average body weight of wt ($n = 6$) and sex-matched seizure positive mutant mice ($n = 8$) (Δbody weight), and plotted it against the number of seizures observed in each mutant animal

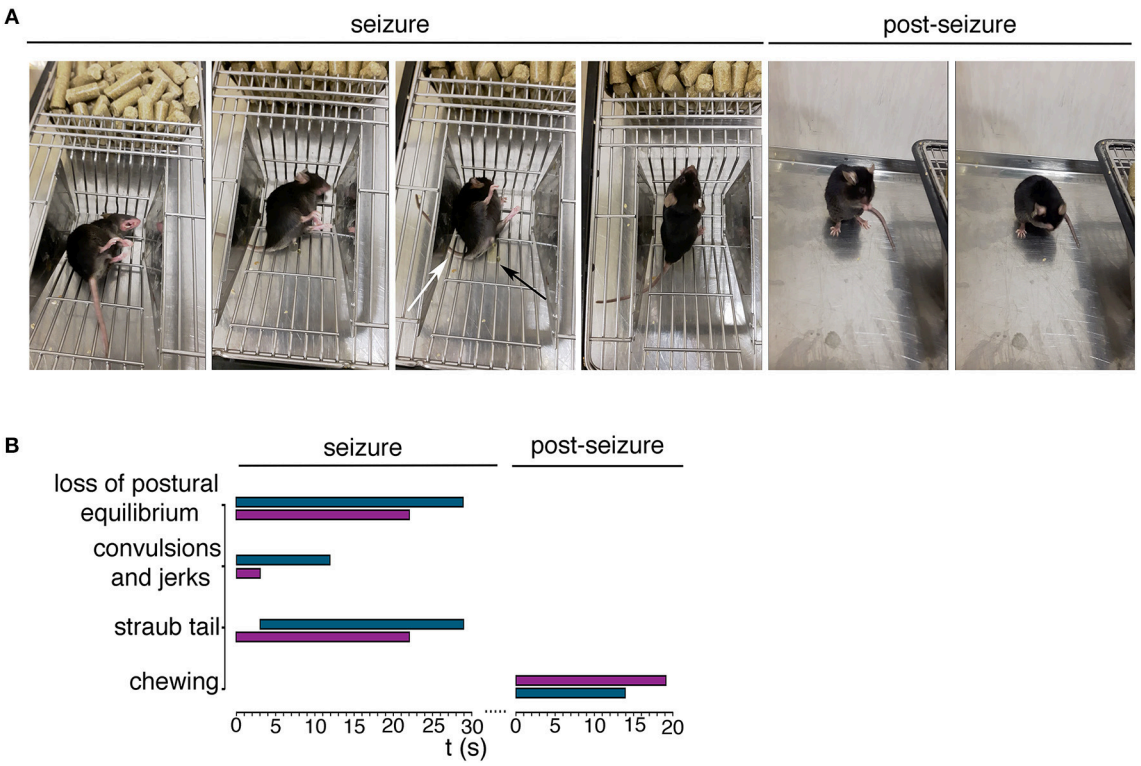

FIGURE 1 | $Ft1^{kof/kof}$ mice exhibit seizures. **(A)** Representative movie frames from non SA $Ft1^{kof/kof}$ mice recording during and post seizure. Starting from left of the seizure panel group: loss of postural equilibrium, arching of the back, Straub tail (third picture, white arrow) and incontinence (third picture, black arrow), recovery of the postural equilibrium. Frames from the movie also show motor automatisms in the post seizure panel group, as chewing (first picture) and grooming (second picture). **(B)** Progression of behavior of two $Ft1^{kof/kof}$ mice, during and post seizure events, each represented by a horizontal bar. The length of each bar indicates the duration of the relative motor type. In turquoise seizure analysis of mouse ID #13489, and in purple the same analysis of mouse ID #16247.

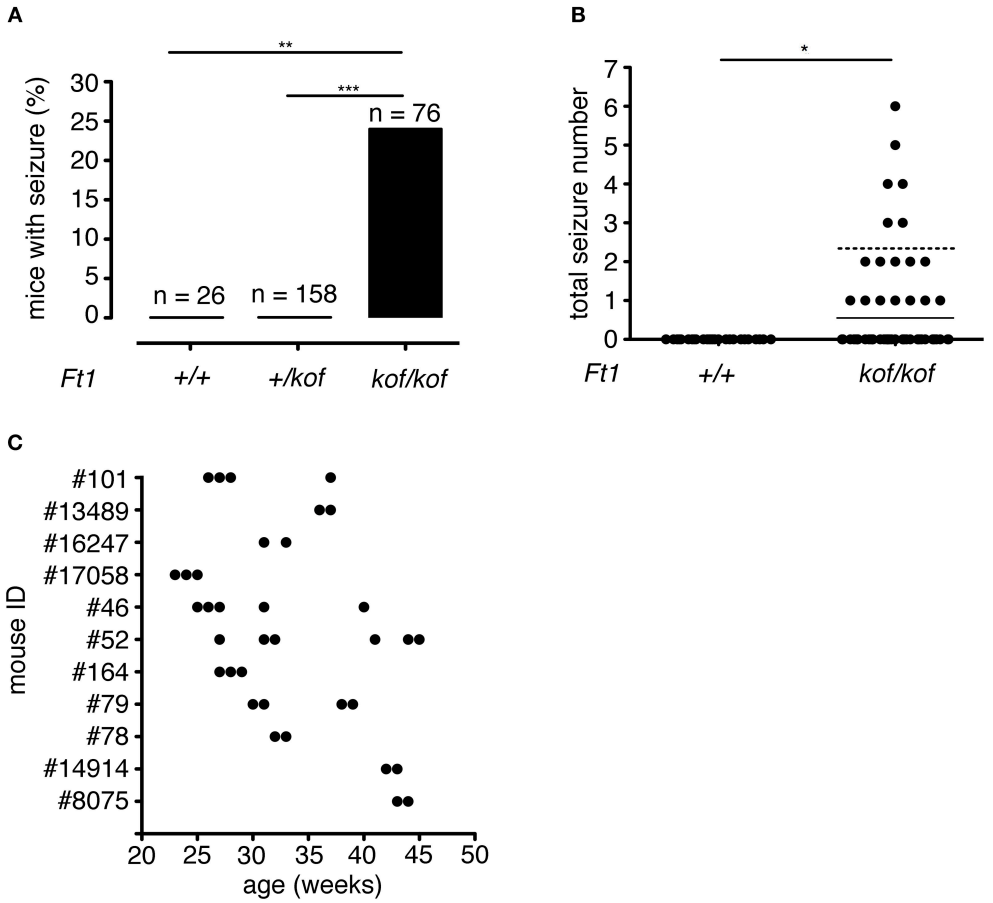

FIGURE 2 | Seizure frequency in $Ft1^{kof/kof}$ mice. **(A)** Percentages of mice that exhibited seizure; no seizures were observed in wt ($^{**}p < 0.01$ χ^2 test) or in heterozygous $Ft1^{+/kof}$ mice ($^{***}p < 0.001$ χ^2 test). **(B)** Total number of seizure experienced by wt and $Ft1^{kof/kof}$ mice, each dot represents one mouse. Line indicates average seizure number considering all $Ft1^{kof/kof}$; dashed line indicates average seizure number (2.33 ± 0.14) considering $Ft1^{kof/kof}$ which experienced seizures ($^{*}p < 0.05$ Student's *t*-test). **(C)** Temporal seizure distribution for each $Ft1^{kof/kof}$ mouse which experienced more than one seizure. Each dot represents a seizure episode. n, total number of analyzed mice.

to generate a regression curve (**Figure 3B**). The two variables were linked by positive correlation ($r^2 = 0.60$; $^{**}p < 0.01$ in Pearson's R test).

Non SA $Ft1^{kof/kof}$ male mice were previously shown to display a stronger phenotype as compared to $Ft1^{kof/kof}$ females (La Torre et al., 2018). We thus decided to explore gender differences in the seizure trait. We analyzed a cohort of non SA $Ft1^{kof/kof}$ animals aged ≥ 21 weeks including 37 males and 39 females. Seizure positive mutants were 37.8% among males and 10.3% among non SA $Ft1^{kof/kof}$ female mice (**Figure 3C**).

In order to verify whether aging would induce variations in Ft1 expression we monitored two cohorts of $Ft1^{+/+}$ mice by QPCR. Results indicate that there are no significant variation in Ft1 expression with aging (**Supplementary Figure 1A**). In addition, the human counterpart of Ft1, AKTIP, is also expressed in brain cells (**Supplementary Figure 1B**).

Altogether these results indicate that *Ft1* reduction causes seizures, and that this phenotype parallels overall organismal alterations characteristic of non SA $Ft1^{kof/kof}$ mice including age dependent growth impairment and sex-linked defects (La Torre et al., 2018).

Structure of Ft1 Mutant Brain

To define whether *Ft1* function impacted on brain structure we firstly measured skull and cranial length of non SA $Ft1^{kof/kof}$ mice by X-ray analysis (**Figure 4**). Mutant and age- and sex-matched wt animals were monitored at 2, 4, 8, and 13 months. Length measures revealed a continuous increase during postnatal development in mutant mice as in controls, with a mild alteration induced by *Ft1* reduction at the age of 8 weeks ($^{*}p < 0.05$ in Student's *t*-test) (**Figures 4A–D**). We then investigated brain morphology by histological analysis. We firstly evaluated the hippocampus, as hippocampal defects are often cause of epilepsy. Nissl-staining of coronal sections of $Ft1^{kof/kof}$ brains did not highlight overt alterations of hippocampal organization or gross lesions, such as cell loss, structural deformation or scars (**Figures 5A–B**). By immunofluorescence, we further analyzed hippocampus cytoarchitecture. Semi-quantitative analysis

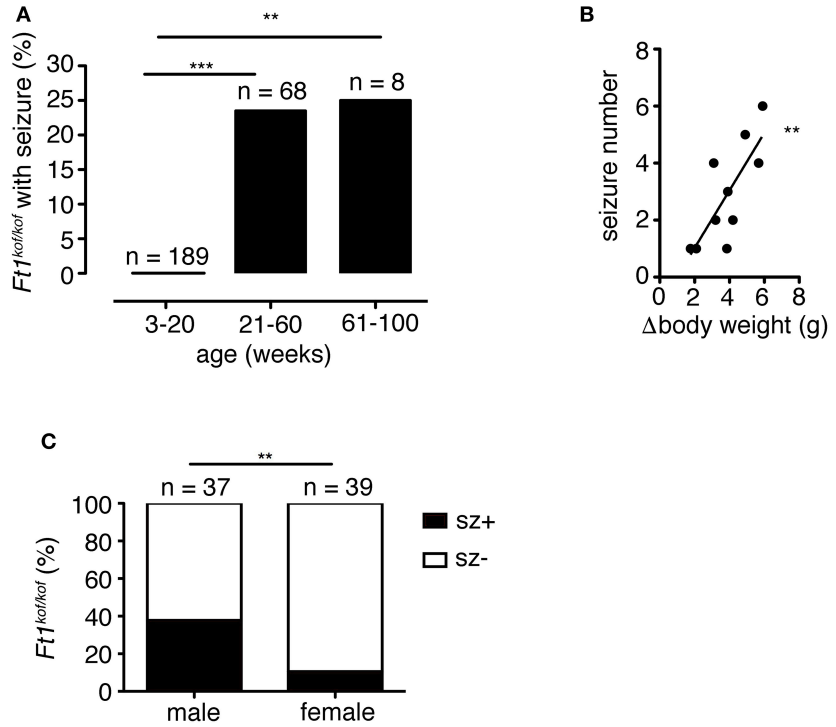

FIGURE 3 | Seizures in $Ft1^{kof/kof}$ mice are age, body weight and sex-linked. **(A)** Percentage of $Ft1^{kof/kof}$ mice exhibiting first seizure clustered in three age intervals (young: $3 \leq$ weeks ≤ 20; juvenile: $21 \leq$ weeks ≤ 60; adult: $61 \leq$ weeks ≤ 100). No seizures were observed in young animals ($^{**}p < 0.01$ and $^{***}p < 0.001$ in χ^2 test). **(B)** Correlation between the severity of growth defect and seizure frequency ($r^2 = 0.60$; $^{**}p < 0.01$ in Pearson's R test). Each dot represents data from an individual animal: body weight differences (Δbody weight) were obtained subtracting average body weight of $Ft1^{kof/kof}$ to the average weight of age and sex-matched wt group. **(C)** Gender related differences in seizure behavior ($^{**}p < 0.01$ in χ^2 test). *n*, total number of analyzed mice.

of Parvalbumin-positive GABAergic interneurons showed a mild reduction in $Ft1^{kof/kof}$ mice as compared to controls (**Figure 5C** and **Supplementary Figure 2**). Then we evaluated the somatosensory cortex cytoarchitecture: by Nissl-staining and MAP2 immunofluorescence, we did not detect evident alterations, including cortical thinning and layering defects in $Ft1^{kof/kof}$ brain compared to wt (**Figures 6A–C**). The density of Parvalbumin-positive GABAergic interneurons in the cortex was non-significantly affected by *Ft1* reduction (**Figure 6D** and **Supplementary Figure 3**). Moreover, we did not observe any evident macroscopic alterations in the whole brain structure, as for example shrinkage of specific cerebral regions, ventricle enlargement, corpus callosum thinning (data not shown), or in brain volume (wt 177.95 mm^3, $Ft1^{kof/kof}$ 189.46 mm^3; **Supplementary Figure 4**). Overall, these analyses did not reveal robust differences between non SA $Ft1^{kof/kof}$ and control mice, thus in principle excluding the presence of severe brain degenerative processes.

p53-Sensitive Inflammatory Response in Ft1 Mutant Brain

To investigate on molecular drivers for the seizure phenotype observed in $Ft1^{kof/kof}$ mice we reasoned on studies in aging and progeroid models which link DNA damage to systemic inflammation and neurodegeneration (Campisi, 2013; López-Otín et al., 2013). Given the progeroid traits observed in non SA $Ft1^{kof/kof}$ mice and the implication of *Ft1* in telomere metabolism and DNA function we decided to monitor the level of two canonical, interrelated, inflammatory cytokines: IL-6 and TGF-β. To get a full picture also on the connection with DNA damage, we explored this aspect in non SA $Ft1^{kof/kof}$ mice, expressing normal levels of the guardian of the genome *p53* and in mice defective for *p53* expression due to heterozygous *p53* inactivation ($Ft1^{kof/kof}$; $p53^{+/ko}$). QPCR analysis showed significant higher levels of both IL-6 and TGF-β in $Ft1^{kof/kof}$ brains as compared to age matched control mice (**Figures 7A,B**; $^{**}p < 0.01$). Indeed, in $Ft1^{kof/kof}$; $p53^{+/ko}$ mutant mice IL-6 and TGF-β activation was reversed. These results suggest that the activation of the DNA damage response pivotal player, *p53*, is a crucial event in the organismal response to *Ft1* reduction (**Figures 7A,B**). As expected, *p53* reduction did not impact on *Ft1* expression, which remained significantly reduced in $Ft1^{kof/kof}$; $p53^{+/ko}$ as in $Ft1^{kof/kof}$ animals (**Figure 7C**).

Given the activation of the inflammatory cytokines and its rescue by p53 reduction, we decided to explore the link between p53, as an element directly associated with DNA function, to the seizure phenotype of $Ft1^{kof/kof}$ mice. To this purpose, we analyzed three cohorts of $\geq$ 21 weeks mice including $Ft1^{+/+}$;$p53^{+/ko}$, $Ft1^{+/kof}$;$p53^{+/ko}$ and $Ft1^{kof/kof}$;$p53^{+/ko}$ mice, as

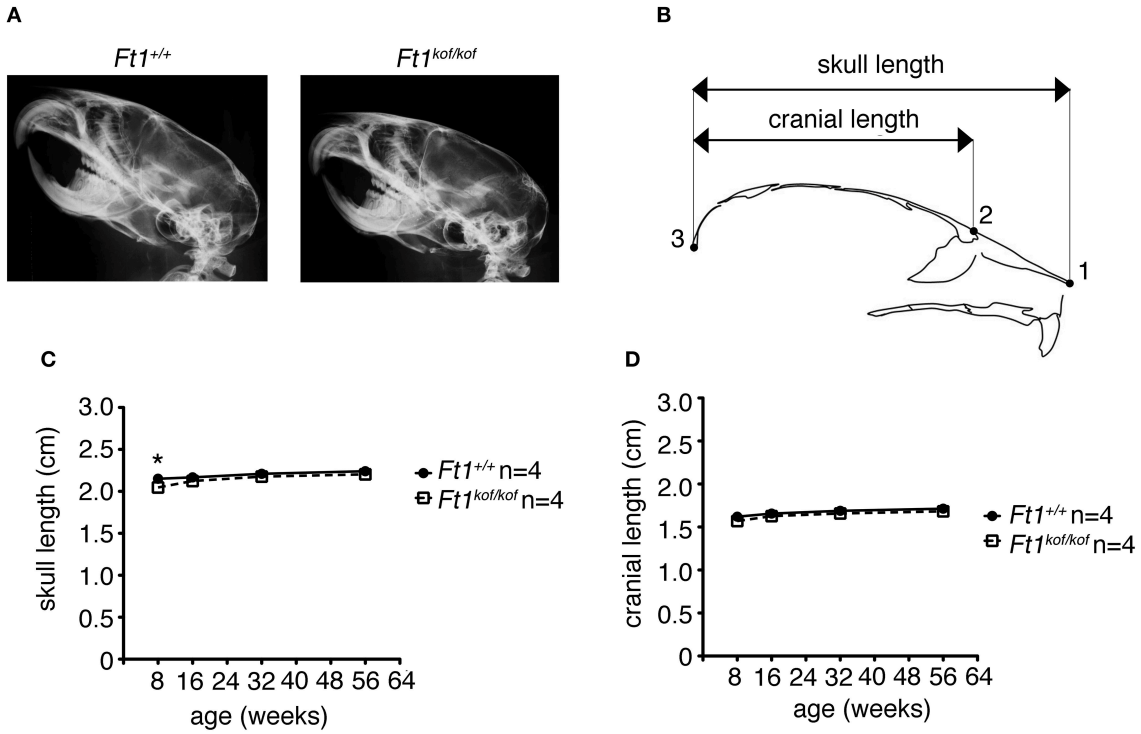

FIGURE 4 | *Ft1* reduction does not affect skull development. **(A)** X-ray analysis of craniofacial skeleton of wt and $Ft1^{kof/kof}$ mice. **(B)** Schematic view of mouse skull and description of landmarks used for the anterior-posterior craniofacial skeleton length analysis. **(C,D)** Skull and cranium length analysis of $Ft1^{kof/kof}$ animals and age-matched wt controls. Curves are not overall significantly different in Student's *t*-test ($p = 0.225$), the difference of the skull length between $Ft1^{kof/kof}$ and $Ft1^{+/+}$ animals is significantly different at the age of 8 weeks (*$p < 0.05$ in Student's *t*-test). n, total number of analyzed mice.

compared to genetically and age matched controls. None of the mice with the $p53^{+/ko}$ mutation displayed seizures, suggesting on one side that *p53* reduction alone does not cause seizures, and, on the other side, that it rescues the seizure phenotype of our *Ft1* mutant mice (**Figure 7D**).

Altogether these results establish a link among *Ft1*, *p53*, inflammatory parameters and seizure behavior.

DISCUSSION

Epilepsy is a complex disorder codified by the concept of predisposition to generate spontaneous seizures. Studies to interpret seizure etiology are complex in humans, indeed many open questions remain about its causes and mechanisms. An important tool to understand and interpret epileptic phenomena comes from model systems. Mutant mice in particular have been instrumental for the identification of genes and gene-determined molecular processes generating brain dysfunction and epileptic phenotypes (Fonck et al., 2005; Yu et al., 2006; Baraban, 2007; Löscher, 2011; Glasscock et al., 2012). In this work we report on the epileptic behavior of a mouse mutant obtained by genetically reducing the expression of the telomeric gene *Ft1* (AKTIP in humans) and present data supportive of a link between DNA damage and epileptic behavior.

As a consequence to its biological function, AKTIP/*Ft1* mutant cells display DNA replication defects, DNA and telomere damage, along with cell senescence (Burla et al., 2015, 2016a). AKTIP/*Ft1* is linked to nuclear architecture through the biochemical interaction occurring with A- and B-type lamins, the main components of the nucleoskeleton, which, in turn, is a pivotal element for the control of DNA function (Dittmer and Misteli, 2011; Burla et al., 2018). Mice with reduced *Ft1* expression display a segmental phenotype including reduced subcutaneous fat, growth and skeletal defects. These traits partly recapitulate the premature aging phenotypes observed in progeroid mice generated by mutations of lamins or DNA maintenance genes (Blasco, 2005; Stewart et al., 2007; Burla et al., 2018), and are exacerbated in adult individuals as compared to juvenile. Given the connection of AKTIP/*Ft1* with both lamins and DNA function, *Ft1* mutant mice represent an attractive model for investigating how these connections may impact on the organismal phenotype and on different tissues and organs.

We report here that *Ft1* mutant mice exhibit spontaneous seizures. Digital movies document the seizure manifestation highlighting typical traits, as loss of postural equilibrium, limb jerks, and convulsions, as in other epileptic mouse models (Yang et al., 2007; Minkeviciene et al., 2009; Chabrol et al., 2010; Glasscock et al., 2012; Simeone et al., 2018). Seizures were observed after the 20th week of age suggesting age-dependent degenerative changes. Seizures also correlated with growth impairment, which, in $Ft1^{kof/kof}$ mice, is exacerbated with aging (La Torre et al., 2018). The frequency of seizures was higher

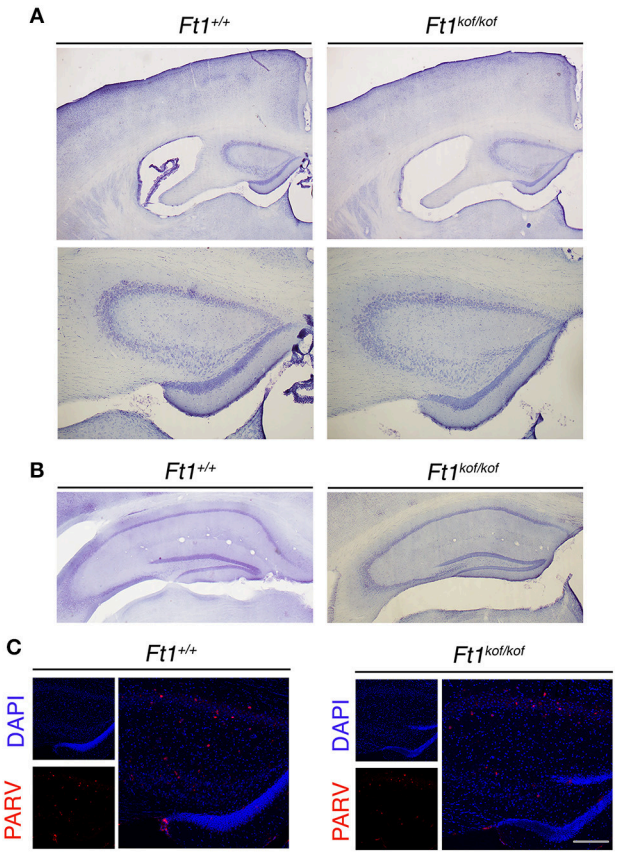

FIGURE 5 | *Ft1* reduction does not overtly affect hippocampal organization. **(A)** Nissl-stained coronal sections of $Ft1^{+/+}$ and $Ft1^{kof/kof}$ mouse brains (upper panels), and higher magnification of the anterior hippocampus (bottom panels), at about Bregma −1.22 mm. **(B)** Nissl-stained hippocampus of $Ft1^{+/+}$ and $Ft1^{kof/kof}$ mice, at about Bregma −2.18 mm. **(C)** Confocal images showing parvalbumin-positive interneurons (PARV, in red) at the hippocampal level; cell nuclei are labeled by DAPI staining (in blue). Scale bars: **(A)** 500 μm (upper panel), **(A)** 200 μm (bottom panel), **(B)** 400 μm, **(C)** (merge) 160 μm, **(C)** (DAPI/PARV) 200 μm.

in male mice, in line with the overall impact of *Ft1* reduction observed in our model (La Torre et al., 2018).

Along with behavioral descriptions, the importance of mouse models resides in the fact that they allow investigating upstream events to behavioral phenotypes, which, in humans, is complex to explore. We thus exploited these animals to analyze the pathophysiological path to seizures in an attempt to contribute to establish experimentally proven links between DNA function and brain alterations.

The analysis of brain morphology and cytoarchitecture in non SA epileptic $Ft1^{kof/kof}$ mice did not highlight overt defects nor macroscopic neurodegeneration. These results were obtained by analyzing restricted brain areas and cell subtypes, and we do not exclude the possibility of other or more subtle brain alterations escaping our analysis. However, given the data, we hypothesized that molecular, rather than overt structural aberrations would underpin the epileptic behavior. This interpretation would be in line with the fact that many types of epilepsy have been associated with molecular alterations, rather than with macroscopic brain structure defects (Guerrini et al., 2014).

On the basis of this hypothesis, we investigated on putative molecular culprits for the seizure phenotype. Telomeres and cell senescence have been implicated in disease and aging. In particular, the secretion of a panel of inflammatory signals (Senescence Associated Secretory Phenotype, SASP) is considered a pivotal element in the alteration of tissue homeostasis contributing to pathological status (Campisi et al., 2001; Campisi, 2013). Given the function of AKTIP/*Ft1* in telomere protection along with its importance in preventing cell senescence and DNA damage (Burla et al., 2015; La Torre et al., 2018), we hypothesized that in *Ft1* mutant mice accumulation of damage and consequent senescence would provoke inflammatory cytokine production, which, in turn, could be implicated into the epileptic phenotype.

We thus measured inflammatory factors in the brain along with exploring the implication of DNA function in inflammation. In the brain of *Ft1* mutant mice we detected the activation of IL-6 and TGF-β. Both these factors are related with inflammation (Coppe et al., 2010). IL-6 activation is assigned to the SASP group of factors linked to cell senescence and has been defined as a senescence biomarker in mice (Coppe et al., 2010; Hudgins et al., 2018). The cytokine TGF-β, in association with IL-6, is a further inflammatory stimulus (Sanjabi et al., 2009). Altogether these data suggested a connection between seizures and inflammation in the brain of $Ft1^{kof/kof}$ mice.

To further investigate on the causative cascade of pathologic events occurring in mice from *Ft1* mutation to seizures, we generated *Ft1* mutant mice with a heterozygous ko mutation in *p53*. p53 is a pivotal element in the DNA damage response and we have demonstrated that p53 is activated in AKTIP reduced primary human cells, which contributes to blocking cell proliferation and inducing senescence (Burla et al., 2015; La Torre et al., 2018). Interestingly *p53* loss was shown to rescue aging traits *in vivo*, by releasing DNA damage-induced checkpoints and cell senescence (Varela et al., 2005). In addition, p53 regulated senescence has been defined as a pivotal element in generating the SASP phenotype. Consistently, reduction of p53 expression rescues SASP related aging traits (Baar et al., 2017). In *Ft1* mutant mice, p53 reduction not only reversed back the expression of IL-6 and TGF-β, but also rescued the seizure phenotype. These results, taken together, induce to speculate that the path to seizures generated by Ft1 reduction could start with DNA damage, including telomere dysfunction, followed by p53 activation, cell senescence, and SASP. The latter could eventually induce brain seizures, through a mechanism that remains to be elucidated.

This interpretation of the data is interesting for investigating on seizure causative events in basal physiological conditions, but also in aging. In fact, aging is characterized by the exacerbation of the alteration of the biological pathways which we have taken into consideration, including senescence, genomic instability and telomere fragility (López-Otín et al., 2013). These factors act on aging in a cell intrinsic way and through extrinsic mechanisms

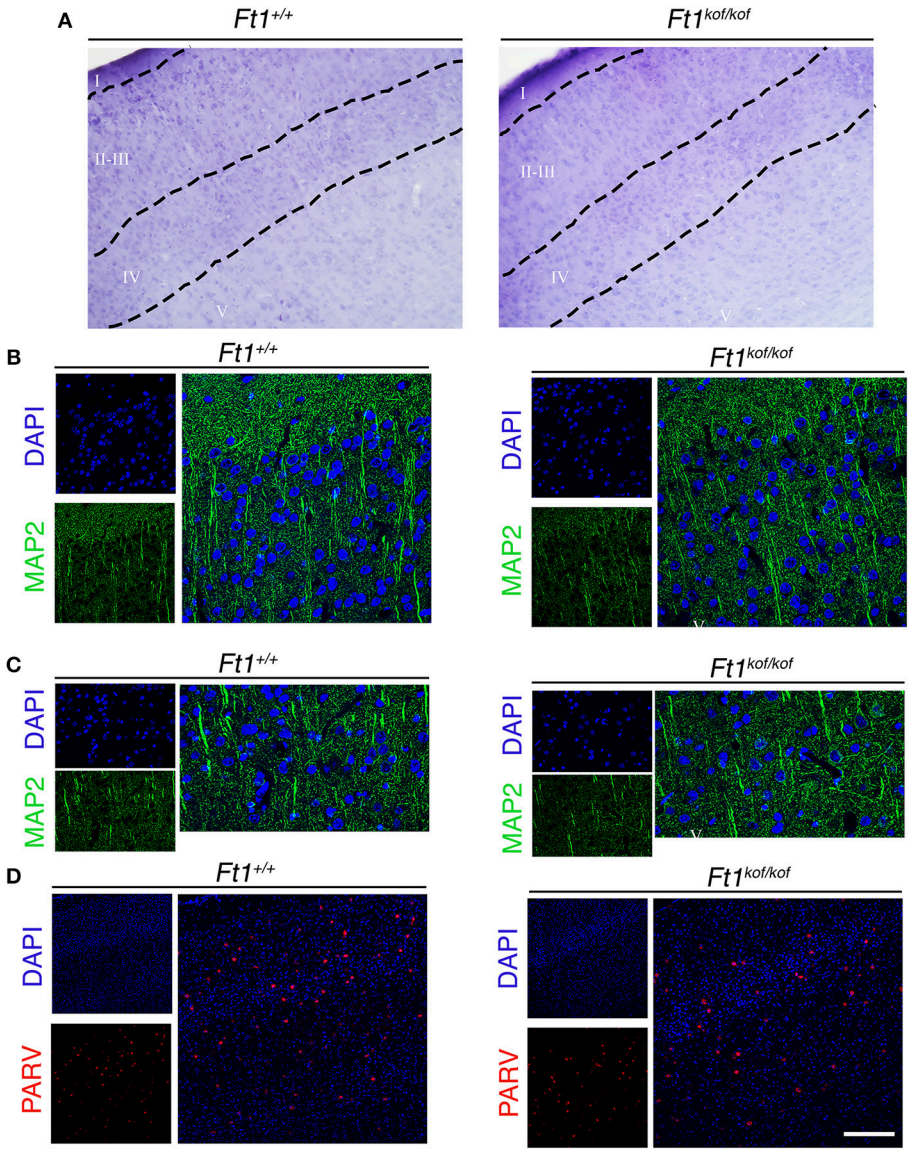

FIGURE 6 | *Ft1* reduction does not affect somatosensory cortex cytoarchitecture. **(A)** Nissl-stained coronal sections, showing somatosensory cortex of $Ft1^{+/+}$ and $Ft1^{kof/kof}$ mice brains. **(B)** MAP2-positive neurons (green) located in the cortical supragranular layers I-II-III and **(C)** in the infragranular layer V; cell nuclei are labeled by DAPI staining (in blue). **(D)** Confocal images showing parvalbumin-positive interneurons (PARV, in red) and DAPI-positive nuclei (in blue). Scale bars: **(A)** 100 μm, **(B,C)** 55 μm, **(D)** 160 μm.

(Lopez-Otin et al., 2016), as secretion of SASP factors (Coppe et al., 2010) and chronic inflammation, profoundly altering tissue microenvironment (Fulop et al., 2017), which, we would suggest, could impact also on brain function.

In conclusion, this work adds new insights into the connection among DNA damage, brain function, and inflammation. In addition, it further underscores the importance of model organisms for studying molecular path to specific phenotypes, along with permitting the study of genetic interactions at the organismal level. These aspects are even more relevant in aging and brain research studies for which work in humans is inaccessible due to time, ethical and sample accessibility issues.

MATERIALS AND METHODS

Mice and Ethical Statements

Mice were maintained and bred in a 12 h light/12 h dark cycle, in a pathogen free unit of the animal house at Biology and Biotechnology Department, Sapienza University. Animals were housed and treated in accordance with protocol 355/2017-PR approved by the Italian Ministry of Health. Animals carrying the knockout first mutations in the *Ft1* gene (*Ft1 kof*) were obtained as previously described (La Torre et al., 2018). In order to obtain *Ft1* and *p53* mutant animals $Ft1^{+/kof}$ were crossed with $p53^{+/ko}$ animals [kindly provided by G. Piaggio and S. Soddu IFO, Italy;

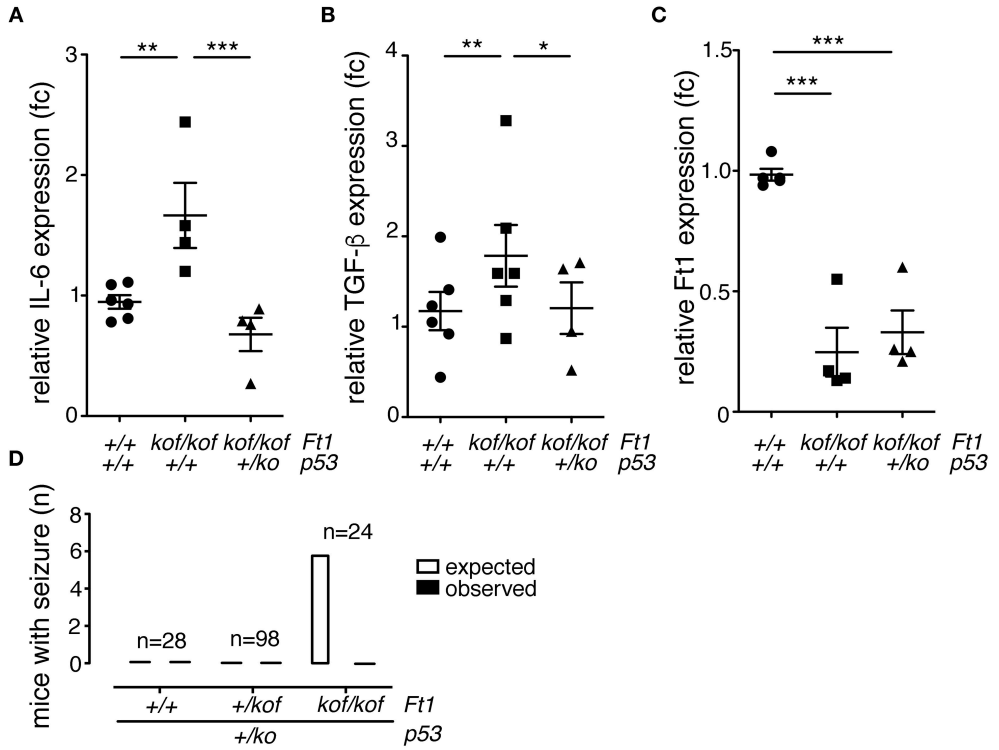

FIGURE 7 | p53 reduction reverses inflammation and seizures in $Ft1^{kof/kof}$ mice. **(A–C)** QPCR expression quantification of IL-6, TGF-β and *Ft1* in $Ft1^{kof/kof}$; $Ft1^{+/kof}$ $Ft1^{kof/kof}$ in a wt or $p53^{+/ko}$ background (*$p < 0.05$; **$p < 0.01$; ***$p < 0.001$ Student's *t*-test). **(D)** Expected versus observed number of mice with seizures in $Ft1^{kof/kof}$; $Ft1^{+/kof}$ $Ft1^{kof/kof}$ in a wt or $p53^{+/ko}$ background. Expected seizure number was calculated considering the seizure frequency in $Ft1^{kof/kof}$ age matched cohort (see **Figure 2A**). To note that none of $Ft1^{kof/kof}$ mice with the $p53^{+/ko}$ mutation displayed seizures. n, total number of analyzed mice.

(Jacks et al., 1994)]; subsequently doubly heterozygous mice were intercrossed to obtain the desired genotypes. Offspring were weaned at 3 weeks and tail biopsies were used for genotyping. When needed, mice were anesthetized by intramuscular Zoletil 20 (Virbac S.A., France), or euthanized by asphyxiation with carbon dioxide or cervical dislocation.

Genotyping

Mice were genotyped as previously described (La Torre et al., 2018). Briefly genomic DNA was extracted from tail biopsies digested 50°C with a proteinase K/SDS solution using the blackPREP Rodent Tail DNA Kit (Analytik Jena, Jena, Germany) following manufacturer's instructions.

Mice were PCR genotyped using the following primers:

Ft1 E4 F: 5′-GTGAAGCAGAAGCTGCCAGGAGT−3′;
Ft1 E6 R: 5′-AGCTCACCCGAGGTGGGATCAA−3′;
p53-X6 F: 5′-AGCGTGGTGGTACCTTATGAGC−3′;
p53-Neo19 F: 5′-GCTATCAGGACATAGCGTTGGC−3′;
p53-X7 R: 5′-GGATGGTGGTATACTCAGAGCC−3′

Seizure Observation

Seizures were observed during routine mouse handling. Where indicated seizure and post-seizure events were video recorded. The movies were then analyzed for specific behavioral signs as previously described (Chabrol et al., 2010).

X-ray and Cephalometric Measurements

X-ray images were taken using Faxitron MX-20 (Faxitron X-ray Corp.) at 24 kV for 6 s; images captured with Medical Imaging Film HM Plus (Ferrania). Skull length and cranial length were measured by Image J software as previously described (Rueden et al., 2017).

Histological Analysis

Eight month-old mice were euthanized and brains were removed and postfixed in 4% PFA for 2 h at 4°C. Samples were then immersed in a solution containing 30% sucrose in phosphate buffer 0.1 M at 4°C for cryoprotection, embedded in cryostat medium (Killik; Bio-Optica, Milan, Italy), and cut on the cryostat (HM 550; Microm) in serial transverse 50 μm thick sections. Some brain sections (one section every 600 μm) were Nissl-stained to evaluate the gross cerebral morphology: briefly sections were mounted on 2% gelatin-coated Superfrost slides and air-dried overnight; slides were hydrated in distilled water for 1 min before staining in 0.1% Cresyl violet acetate (Sigma Aldrich, St. Louis, MO) for 10 min, dehydrated in an ascending series of ethanol, cleared in xylene and cover-slipped with Eukitt (Bioptica, Milan, Italy). Sections were examined at a Nikon Eclipse 80i microscope Equipped with a Nikon DS-Fi1 camera. Brain volume of wt and $Ft1^{kof/kof}$ mice was calculated considering Bregma 2.10 mm to Bregma −2.54 mm segments

in Nissl-stained serial sections reconstructed by Neurolucida software (MicroBrightField, Williston, VT, USA) and the volume (expressed in mm^3) was obtained by NeuroExplorer software (MicroBrightField). For immunofluorescence, brain sections were permeabilized with in PBS 0.3% Triton X-100 at RT on a tilting plate for 20 min; then, to block unspecific binding of the antibody, sections were incubated for 30 min at RT with 0.3% Triton X-100 and 10% normal donkey serum or normal goat serum (Sigma-Aldrich) in PBS (pH 7.4). Sections were then incubated at 4°C overnight with the following antibodies: 1:7,500 anti-Parvalbumin (rabbit; Swant); 1:200 anti-MAP2 (mouse; Chemicon). Then, sections were incubated with appropriate fluorochrome-conjugated secondary antibodies, for 1h at RT: 1:400 Alexa Fluor 647, goat anti mouse (Jackson ImmunoResearch Laboratories); 1:200 cyanine 3-conjugated secondary antibody, donkey anti-rabbit (Jackson ImmunoResearch Laboratories); 1:200 cyanine 2-conjugated secondary antibody, donkey anti-mouse (Jackson ImmunoResearch Laboratories). Finally sections were incubated with 4,6 Diamino-2 phenyindole Dilactate (DAPI; Sigma Aldrich) in PBS 1:50 for 3 min. Samples were washed and coverslips were mounted with the anti-fade mounting medium Mowiol. For double staining and 3D reconstructions, slides were examined with a Leica TCS SP5 confocal laser scanning microscope.

Cell Culture

Human foreskin primary fibroblasts (HPFs), HeLa (ATCC CCL-2) and 293T (ATCC CRL-11268) cells were cultured in DMEM with 10% FBS. SH-SY5Y (ATCC CRL-2266) cells were cultured in EMEM supplemented with 10% FBS.

RNA Extraction and QPCR Analysis

Cells were lysed using the TRIzol reagent (Invitrogen). Brains were removed from euthanized mice and frozen in liquid nitrogen. RNA was extracted using the TRIzol reagent (Invitrogen) according to manufacturer. After DNaseI treatment (Invitrogen) RNA from cells and brains was reverse transcribed into cDNA with oligo d(T) primer and OMNISCRIPT RT KIT (Qiagen). QPCRs were performed as described (Piersanti et al., 2015) using the following primers:

Ft1 E3 F: AACCAGTCCTCCACGAAGTGCA;
Ft1 E3 R: TAGGGCTTCGCTATGGGTAGAGCA;
Ft1 E6 F: CCGTCTTTCACCCACTAGTTGAT;
Ft1 E6 R: TTGCGAACGCTCTTTTCACA;
mGAPDH F: GTGGCAAAGTGGAGATTGTTGCC;
mGAPDH R: TGTGCCGTTGAATTTGCCGT;
IL-6 F: CTCTGGGAAATCGTGGAAAT;
IL-6 R: CCAGTTTGGTAGCATCCATC
TGF-β F: CCCTATATTTGGAGCCTGGA;
TGF-β R: CTTGCGACCCACGTAGTAGA;
AKTIP F: TCCACGCTTGGTGTTCGAT;
AKTIP R: TCACCTGAGGTGGGATCAACT
GAPDH F: TGGGCTACACTGAGCACCAG
GAPDH R: GGGTGTCGCTGTTGAAGTCA

Statistics

χ^2 test was applied for comparisons of the mouse cohorts. Independent data sets were analyzed with the Student's *t*-test (unpaired, two-tailed). Correlation analyses were performed via Pearson's R test.

ETHICS STATEMENT

This study was carried out in accordance with the recommendations of the European Directive 2010/63/EU on the protection of animals used for scientific purposes. The protocol was approved by the Italian Ministry of Health (Ministero della Salute) with protocol number 355/2017-PR.

AUTHOR CONTRIBUTIONS

RB, MLT, FDC, AV, and FV contributed to the design of the experiments and to the writing of the manuscript. MLT, GZ, AB, SDG, MB, and CM performed the experiments and analyzed the data. IS designed the experiments, analyzed the data and wrote the manuscript.

FUNDING

This work has been supported by Sapienza Ateneo grants to FV, IS, MLT, and RB; by grants EU FP7 Brainvectors (n. 286071), Telethon GEP15033 and PRF 2016-67 to IS. This work is in the memory of P. Bianco.

ACKNOWLEDGMENTS

This work has been supported by Sapienza Ateneo grants to FV, IS, ML, and RB; by grants EU FP7 Brainvectors (n. 286071), Telethon GEP15033 and PRF 2016-67 to IS. This work is in the memory of P. Bianco.

SUPPLEMENTARY MATERIAL

The Supplementary Material for this article can be found online at: https://www.frontiersin.org/articles/10.3389/fgene.2018.00581/full#supplementary-material

REFERENCES

Baar, M. P., Brandt, R. M. C., Putavet, D. A., Klein, J. D. D., Derks, K. W. J., Bourgeois, B. R. M., et al. (2017). Targeted apoptosis of senescent cells restores tissue homeostasis in response to chemotoxicity and aging. *Cell* 169, 132–147 e116. doi: 10.1016/j.cell.2017.02.031

Baraban, S. C. (2007). Emerging epilepsy models: insights from mice, flies, worms and fish. *Curr. Opin. Neurol.* 20, 164–168. doi: 10.1097/WCO.0b013e328042bae0

Bertram, E. H. (2013). Neuronal circuits in epilepsy: do they matter? *Exp. Neurol.* 244, 67–74. doi: 10.1016/j.expneurol.2012.01.028

Bianchi, F. T., Tocco, C., Pallavicini, G., Liu, Y., Vernì, F., Merigliano, C., et al. (2017). Citron kinase deficiency leads to chromosomal instability and TP53-sensitive microcephaly. *Cell Rep.* 18, 1674–1686. doi: 10.1016/j.celrep.2017.01.054

Blasco, M. A. (2005). Mice with bad ends: mouse models for the study of telomeres and telomerase in cancer and aging. *EMBO J.* 24, 1095–1103. doi: 10.1038/sj.emboj.7600598

Burla, R., Carcuro, M., Raffa, G. D., Galati, A., Raimondo, D., Rizzo, A., et al. (2015). AKTIP/Ft1, a new shelterin-interacting factor required for telomere maintenance. *PLoS Genet.* 11:e1005167. doi: 10.1371/journal.pgen.1005167

Burla, R., Carcuro, M., Torre, M. L., Fratini, F., Crescenzi, M., D'apice, M. R., et al. (2016a). The telomeric protein AKTIP interacts with A- and B-type lamins and is involved in regulation of cellular senescence. *Open Biol.* 6:160103. doi: 10.1098/rsob.160103

Burla, R., La Torre, M., Merigliano, C., Verni, F., and Saggio, I. (2018). Genomic instability and DNA replication defects in progeroid syndromes. *Nucleus* 9, 368–379. doi: 10.1080/19491034.2018.1476793

Burla, R., La Torre, M., and Saggio, I. (2016b). Mammalian telomeres and their partnership with lamins. *Nucleus* 7, 187–202. doi: 10.1080/19491034.2016.1179409

Campisi, J. (2013). Aging, cellular senescence, and cancer. *Annu. Rev. Physiol.* 75, 685–705. doi: 10.1146/annurev-physiol-030212-183653

Campisi, J., Kim, S. H., Lim, C. S., and Rubio, M. (2001). Cellular senescence, cancer and aging: the telomere connection. *Exp. Gerontol.* 36, 1619–1637. doi: 10.1016/S0531-5565(01)00160-7

Chabrol, E., Navarro, V., Provenzano, G., Cohen, I., Dinocourt, C., Rivaud-Péchoux, S., et al. (2010). Electroclinical characterization of epileptic seizures in leucine-rich, glioma-inactivated 1-deficient mice. *Brain* 133, 2749–2762. doi: 10.1093/brain/awq171

Coppe, J. P., Desprez, P. Y., Krtolica, A., and Campisi, J. (2010). The senescence-associated secretory phenotype: the dark side of tumor suppression. *Annu. Rev. Pathol.* 5, 99–118. doi: 10.1146/annurev-pathol-121808-102144

de Lange, T. (2005). Shelterin: the protein complex that shapes and safeguards human telomeres. *Genes Dev.* 19, 2100–2110. doi: 10.1101/gad.1346005

Dittmer, T. A., and Misteli, T. (2011). The lamin protein family. *Genome Biol.* 12:222. doi: 10.1186/gb-2011-12-5-222

Fisher, R. S., Acevedo, C., Arzimanoglou, A., Bogacz, A., Cross, J. H., Elger, C. E., et al. (2014). ILAE official report: a practical clinical definition of epilepsy. *Epilepsia* 55, 475–482. doi: 10.1111/epi.12550

Fonck, C., Cohen, B. N., Nashmi, R., Whiteaker, P., Wagenaar, D. A., Rodrigues-Pinguet, N., et al. (2005). Novel seizure phenotype and sleep disruptions in knock-in mice with hypersensitive alpha 4* nicotinic receptors. *J. Neurosci.* 25, 11396–11411. doi: 10.1523/JNEUROSCI.3597-05.2005

Frost, B. (2016). Alzheimer's disease: an acquired neurodegenerative laminopathy. *Nucleus* 7, 275–283. doi: 10.1080/19491034.2016.1183859

Fulop, T., Larbi, A., Dupuis, G., Le Page, A., Frost, E. H., Cohen, A. A., et al. (2017). Immunosenescence and inflamm-aging as two sides of the same coin: friends or foes? *Front. Immunol.* 8:1960. doi: 10.3389/fimmu.2017.01960.

Glasscock, E., Qian, J., Kole, M. J., and Noebels, J. L. (2012). Transcompartmental reversal of single fibre hyperexcitability in juxtaparanodal Kv1.1-deficient vagus nerve axons by activation of nodal KCNQ channels. *J. Physiol.* 590, 3913–3926. doi: 10.1113/jphysiol.2012.235606

Guerrini, R., Marini, C., and Mantegazza, M. (2014). Genetic epilepsy syndromes without structural brain abnormalities: clinical features and experimental models. *Neurotherapeutics* 11, 269–285. doi: 10.1007/s13311-014-0267-0

Hudgins, A. D., Tazearslan, C., Tare, A., Zhu, Y., Huffman, D., and Suh, Y. (2018). Age- and tissue-specific expression of senescence biomarkers in mice. *Front. Genet.* 9:59. doi: 10.3389/fgene.2018.00059

Jacks, T., Remington, L., Williams, B. O., Schmitt, E. M., Halachmi, S., Bronson, R. T., et al. (1994). Tumor spectrum analysis in p53-mutant mice. *Curr. Biol.* 4, 1–7. doi: 10.1016/S0960-9822(00)00002-6

La Torre, M., Merigliano, C., Burla, R., Mottini, C., Zanetti, G., Del Giudice, S., et al. (2018). Mice with reduced expression of the telomere-associated protein Ft1 develop p53-sensitive progeroid traits. *Aging Cell*, 17:e12730. doi: 10.1111/acel.12730

Langie, S. A., Cameron, K. M., Ficz, G., Oxley, D., Tomaszewski, B., Gorniak, J. P., et al. (2017). The ageing brain: effects on DNA repair and DNA methylation in mice. *Genes* 8:E75 doi: 10.3390/genes8020075

Lee, Y., Katyal, S., Li, Y., El-Khamisy, S. F., Russell, H. R., Caldecott, K. W., et al. (2009). The genesis of cerebellar interneurons and the prevention of neural DNA damage require XRCC1. *Nat. Neurosci.* 12, 973–980. doi: 10.1038/nn.2375

Leppik, I. E., and Birnbaum, A. K. (2010). Epilepsy in the elderly. *Ann. N. Y. Acad. Sci.* 1184, 208–224. doi: 10.1111/j.1749-6632.2009.05113.x

López-Otín, C., Blasco, M. A., Partridge, L., Serrano, M., and Kroemer, G. (2013). The hallmarks of aging. *Cell* 153, 1194–1217. doi: 10.1016/j.cell.2013.05.039

Lopez-Otin, C., Galluzzi, L., Freije, J. M. P., Madeo, F., and Kroemer, G. (2016). Metabolic control of longevity. *Cell* 166, 802–821. doi: 10.1016/j.cell.2016.07.031

Löscher, W. (2011). Critical review of current animal models of seizures and epilepsy used in the discovery and development of new antiepileptic drugs. *Seizure* 20, 359–368. doi: 10.1016/j.seizure.2011.01.003

Madabhushi, R., Pan, L., and Tsai, L. H. (2014). DNA damage and its links to neurodegeneration. *Neuron* 83, 266–282. doi: 10.1016/j.neuron.2014.06.034

Mckinnon, P. J. (2013). Maintaining genome stability in the nervous system. *Nat. Neurosci.* 16, 1523–1529. doi: 10.1038/nn.3537

Minkeviciene, R., Rheims, S., Dobszay, M. B., Zilberter, M., Hartikainen, J., Fulop, L., et al. (2009). Amyloid beta-induced neuronal hyperexcitability triggers progressive epilepsy. *J. Neurosci.* 29, 3453–3462. doi: 10.1523/JNEUROSCI.5215-08.2009

Piersanti, S., Burla, R., Licursi, V., Brito, C., La Torre, M., Alves, P. M., et al. (2015). Transcriptional response of human neurospheres to helper-dependent CAV-2 vectors involves the modulation of DNA damage response, microtubule and centromere gene groups. *PLoS ONE* 10:e0133607. doi: 10.1371/journal.pone.0133607

Remoli, C., Michienzi, S., Sacchetti, B., Consiglio, A. D., Cersosimo, S., Spica, E., et al. (2015). Osteoblast-specific expression of the fibrous dysplasia (FD)-causing mutation Gsalpha(R201C) produces a high bone mass phenotype but does not reproduce FD in the mouse. *J. Bone Miner. Res.* 30, 1030–1043. doi: 10.1002/jbmr.2425

Riminucci, M., Saggio, I., Robey, P. G., and Bianco, P. (2006). Fibrous dysplasia as a stem cell disease. *J. Bone Miner. Res.* 21 (Suppl. 2), P125–131. doi: 10.1359/jbmr.06s224

Robie, A. A., Seagraves, K. M., Egnor, S. E., and Branson, K. (2017). Machine vision methods for analyzing social interactions. *J. Exp. Biol.* 220, 25–34. doi: 10.1242/jeb.142281

Rueden, C. T., Schindelin, J., Hiner, M. C., Dezonia, B. E., Walter, A. E., Arena, E. T., et al. (2017). ImageJ2: ImageJ for the next generation of scientific image data. *BMC Bioinformatics* 18:529. doi: 10.1186/s12859-017-1934-z

Saggio, I., Remoli, C., Spica, E., Cersosimo, S., Sacchetti, B., Robey, P. G., et al. (2014). Constitutive expression of Gsalpha(R201C) in mice produces a heritable, direct replica of human fibrous dysplasia bone pathology and demonstrates its natural history. *J. Bone Miner. Res.* 29, 2357–2368. doi: 10.1002/jbmr.2267

Sanjabi, S., Zenewicz, L. A., Kamanaka, M., and Flavell, R. A. (2009). Anti-inflammatory and pro-inflammatory roles of TGF-beta, IL-10, and IL-22 in immunity and autoimmunity. *Curr. Opin. Pharmacol.* 9, 447–453. doi: 10.1016/j.coph.2009.04.008

Scharfman, H. E. (2007). The neurobiology of epilepsy. *Curr. Neurol. Neurosci. Rep.* 7, 348–354. doi: 10.1007/s11910-007-0053-z

Shen, J., Gilmore, E. C., Marshall, C. A., Haddadin, M., Reynolds, J. J., Eyaid, W., et al. (2010). Mutations in PNKP cause microcephaly, seizures and defects in DNA repair. *Nat. Genet.* 42, 245–249. doi: 10.1038/ng.526

Simão, D., Pinto, C., Piersanti, S., Weston, A., Peddie, C. J., Bastos, A. E., et al. (2015). Modeling human neural functionality *in vitro*: three-dimensional culture for dopaminergic differentiation. *Tissue Eng. Part A* 21, 654–668. doi: 10.1089/ten.tea.2014.0079

Simeone, K. A., Hallgren, J., Bockman, C. S., Aggarwal, A., Kansal, V., Netzel, L., et al. (2018). Respiratory dysfunction progresses with age in Kcna1-null mice, a model of sudden unexpected death in epilepsy. *Epilepsia* 59, 345–357. doi: 10.1111/epi.13971

Stafstrom, C. E., and Carmant, L. (2015). Seizures and epilepsy: an overview for neuroscientists. *Cold Spring Harb. Perspect. Med.* 5:a022426. doi: 10.1101/cshperspect.a022426

Stewart, C. L., Kozlov, S., Fong, L. G., and Young, S. G. (2007). Mouse models of the laminopathies. *Exp. Cell Res.* 313, 2144–2156. doi: 10.1016/j.yexcr.2007.03.026

Testa, G., Schaft, J., Van Der Hoeven, F., Glaser, S., Anastassiadis, K., Zhang, Y., et al. (2004). A reliable lacZ expression reporter cassette for multipurpose, knockout-first alleles. *Genesis* 38, 151–158. doi: 10.1002/gene.20012

Varela, I., Cadiñanos, J., Pendás, A. M., Gutiérrez-Fernández, A., Folgueras, A. R., Sánchez, L. M., et al. (2005). Accelerated ageing in mice deficient in Zmpste24 protease is linked to p53 signalling activation. *Nature* 437, 564–568. doi: 10.1038/nature04019

Vogt, D. L., Thomas, D., Galvan, V., Bredesen, D. E., Lamb, B. T., and Pimplikar, S. W. (2011). Abnormal neuronal networks and seizure susceptibility in mice overexpressing the APP intracellular domain. *Neurobiol. Aging* 32, 1725–1729. doi: 10.1016/j.neurobiolaging.2009.09.002

Yang, Y., Mahaffey, C. L., Bérubé, N., Maddatu, T. P., Cox, G. A., and Frankel, W. N. (2007). Complex seizure disorder caused by Brunol4 deficiency in mice. *PLoS Genet.* 3:e124. doi: 10.1371/journal.pgen.0030124

Yu, F. H., Mantegazza, M., Westenbroek, R. E., Robbins, C. A., Kalume, F., Burton, K. A., et al. (2006). Reduced sodium current in GABAergic interneurons in a mouse model of severe myoclonic epilepsy in infancy. *Nat. Neurosci.* 9, 1142–1149. doi: 10.1038/nn1754

Ziyatdinova, S., Gurevicius, K., Kutchiashvili, N., Bolkvadze, T., Nissinen, J., Tanila, H., et al. (2011). Spontaneous epileptiform discharges in a mouse model of Alzheimer's disease are suppressed by antiepileptic drugs that block sodium channels. *Epilepsy Res.* 94, 75–85. doi: 10.1016/j.eplepsyres.2011.01.003

Conflict of Interest Statement: The authors declare that the research was conducted in the absence of any commercial or financial relationships that could be construed as a potential conflict of interest.

frontiers in Genetics

MINI REVIEW
published: 02 October 2018
doi: 10.3389/fgene.2018.00436

Modeling Congenital Disorders of N-Linked Glycoprotein Glycosylation in *Drosophila melanogaster*

Anna Frappaolo[1†], Stefano Sechi[1†], Tadahiro Kumagai[2†], Angela Karimpour-Ghahnavieh[1], Michael Tiemeyer[2,3] and Maria Grazia Giansanti[1]**

[1] Istituto di Biologia e Patologia Molecolari del CNR, Dipartimento di Biologia e Biotecnologie, Sapienza - Università di Roma, Rome, Italy, [2] Complex Carbohydrate Research Center, University of Georgia, Athens, GA, United States, [3] Department of Biochemistry and Molecular Biology, University of Georgia, Athens, GA, United States

Protein glycosylation, the enzymatic addition of N-linked or O-linked glycans to proteins, serves crucial functions in animal cells and requires the action of glycosyltransferases, glycosidases and nucleotide-sugar transporters, localized in the endoplasmic reticulum and Golgi apparatus. Congenital Disorders of Glycosylation (CDGs) comprise a family of multisystemic diseases caused by mutations in genes encoding proteins involved in glycosylation pathways. CDGs are classified into two large groups. Type I CDGs affect the synthesis of the dolichol-linked $Glc_3Man_9GlcNac_2$ precursor of N-linked glycosylation or its transfer to acceptor proteins. Type II CDG (CDG-II) diseases impair either the trimming of the N-linked oligosaccharide, the addition of terminal glycans or the biosynthesis of O-linked oligosaccharides, which occur in the Golgi apparatus. So far, over 100 distinct forms of CDGs are known, with the majority of them characterized by neurological defects including mental retardation, seizures and hypotonia. Yet, it is unclear how defective glycosylation causes the pathology of CDGs. This issue can be only addressed by developing animal models of specific CDGs. *Drosophila melanogaster* is emerging as a highly suitable organism for analyzing glycan-dependent functions in the central nervous system (CNS) and the involvement of N-glycosylation in neuropathologies. In this review we illustrate recent work that highlights the genetic and neurobiologic advantages offered by *D. melanogaster* for dissecting glycosylation pathways and modeling CDG pathophysiology.

Keywords: Drosophila, glycosylation, congenital disorders, Golgi, model organism

OPEN ACCESS

Edited by:
Roberta Fraschini, Università degli Studi Milano-Bicocca, Italy

Reviewed by:
Vladimir Lupashin, University of Arkansas for Medical Sciences, United States
Giuliano Callaini, Università degli Studi di Siena, Italy

***Correspondence:**
Michael Tiemeyer
mtiemeyer@ccrc.uga.edu
Maria Grazia Giansanti
mariagrazia.giansanti@uniroma1.it

† These authors have contributed equally to this work

Specialty section:
This article was submitted to Genetic Disorders, a section of the journal Frontiers in Genetics

Received: *10 July 2018*
Accepted: *14 September 2018*
Published: *02 October 2018*

Citation:
Frappaolo A, Sechi S, Kumagai T, Karimpour-Ghahnavieh A, Tiemeyer M and Giansanti MG (2018) Modeling Congenital Disorders of N-Linked Glycoprotein Glycosylation in Drosophila melanogaster. Front. Genet. 9:436. doi: 10.3389/fgene.2018.00436

INTRODUCTION

Protein glycosylation is one of the most frequent post-translational modifications in eukaryotes; approximately one fifth of all proteins in protein structural databases are glycosylated (Ohtsubo and Marth, 2006; Freeze and Ng, 2011; Khoury et al., 2011). The oligosaccharide moieties added to glycoproteins impact their structure and biological function by contributing to protein folding, stability, and transport to appropriate sub-cellular locations. Glycans also mediate cell–cell interactions, modulate signal transduction, and regulate molecular trafficking and endocytosis. The two main types of protein glycosylation are N-linked and O-linked glycosylation. The biosynthesis and elaboration of glycoprotein N-linked or O-linked glycans, require the coordinated action

of hundreds of glycogenes, primarily glycosyltransferases and glycosidases, which are trafficked to specific locations within the endoplasmic reticulum (ER) and Golgi apparatus (Ohtsubo and Marth, 2006). Cytoplasmic and nuclear proteins are frequently modified with O-linked N-acetylglucosamine (GlcNAc) which regulates many biological processes but is beyond the scope of this review. N- and O-linked glycosylation of secreted and membrane protein starts in the ER or early *cis*-Golgi and is completed in later Golgi compartments. Major animal glycans contain ten monosaccharides: glucose (Glc), Galactose (Gal), N-acetylglucosamine (GlcNAc), N-acetylgalactosamine (GalNAc), fucose (Fuc), mannose (Man), xylose (Xyl), glucuronic acid (GlcA), iduronic acid (IdoA), and sialic acid (SA, either as 5-N-acetylneuraminic acid, Neu5Ac, or as 5-N-acetylglycolylneuraminic acid, Neu5Gc).

The N-glycosylation pathway starts at the ER membrane where a precursor glycan is built upon a dolichol isoprenoid lipid (**Figure 1**). This precursor glycan, with the composition $Glc_3Man_9GlcNAc_2$, is transferred *en bloc* onto asparagine residues located within glycosylation sequons of nascent polypeptide chains either co-translationally or shortly after translation by multi-subunit oligosaccharyltransferase (OST) complexes within the lumen of the ER (Li et al., 2008; Zielinska et al., 2010; Shwartz and Aebi, 2011). The transferred $Glc_3Man_9GlcNAc_2$ glycan is subsequently trimmed by sequential action of ER glucosidases. Glc-trimming is an essential component of the folding process for most secretory pathway glycoproteins (Helenius and Aebi, 2004). Thus, human diseases that arise from altered biosynthesis or trimming of the N-linked precursor glycan, or ineffective transfer of the precursor to protein will impact the folding and stability of many glycoproteins and, consequently, manifest with multi-systemic and broadly severe clinical phenotypes.

Glycoproteins arrive at the *cis*-Golgi carrying high-Man glycans (**Figure 1**). Mannose trimming in the *cis*-Golgi by Golgi α-mannosidases removes Man residues to generate the $Man_5GlcNAc_2$ intermediate. In medial Golgi compartments, $Man_5GlcNAc_2$ is the substrate for GlcNAcT-1, a glycosyltransferase that transfers a GlcNAc residue to a terminal Man residue on the α3-arm of the $Man_5GlcNAc_2$ structure, thereby initiating the synthesis of hybrid and complex N-linked glycans (Stanley, 2011; Moremen et al., 2012). The product of GlcNAcT-1 is also a substrate for core fucosylation, the addition of one or more Fuc residues (depending on the species) to the most proximal core GlcNAc residues attached to Asn. The α3-arm initiated by GlcNAT-1 can be extended with Gal, Sia and/or other residues, resulting in the production of hybrid structures. Removal of the remaining Man residues from the α6-arm allows branching with additional GlcNAc residues catalyzed by specific GlcNAcT enzymes and subsequent extension to generate fully elaborated multiantennary complex glycans in late medial and *trans* Golgi compartments (Stanley, 2011). The vectorial nature of N-glycan processing is facilitated by enzyme specificity and by the spatial distribution of processing steps across the Golgi apparatus. Therefore, human diseases that impact N-glycan fine structure may arise from genes that encode for processing enzymes or for proteins that regulate Golgi architecture and trafficking. Such diseases may be characterized by relatively restricted phenotypes associated with altered function, half-life, or targeting of specific glycoproteins.

In contrast to N-linked glycosylation, O-linked glycosylation does not rely on a precursor core that is transferred *en bloc* to the nascent polypeptide. Instead, O-glycosylation is initiated on folding or folded proteins and involves the formation of a glycosidic linkage between serine or threonine and GalNAc, GlcNAc, Man, Glc, Xyl, or Fuc residues (Stanley, 2011). Some *O*-glycans are specifically elaborated on well-defined protein domains and contribute to protein folding, stability, protease sensitivity, and protein function. The biosynthesis of *O*-glycans in the secretory pathway is initiated in the early *cis*-Golgi or in a transitional compartment that retains characteristics of the ER and is completed in subsequent processing steps distributed across the Golgi apparatus. Therefore, human diseases arising from genes that regulate Golgi dynamics may impact both N-linked and O-linked glycoprotein glycosylation.

Congenital disorders of glycosylation (CDGs) are inborn errors in protein and lipid glycosylation that arise from mutations in genes controlling steps in glycan addition (Freeze and Ng, 2011; Jaeken, 2013). More than 100 distinct forms of CDGs have been discovered, many of which display multisystemic defects including severe neurological impairment, highlighting the important role of regulated glycosylation in central nervous system (CNS) functions (Barone et al., 2014; Freeze et al., 2015). Because 1–2% of the genome encodes for glyco-enzymes and glycan transporters, it is likely that many other CDGs remain to be discovered (Freeze et al., 2015). CDGs have been traditionally divided into two large groups (Goreta et al., 2012; Freeze et al., 2014). Type I CDGs impair the synthesis of the dolichol pyrophosphate oligosaccharide precursor of N-linked glycoproteins or its transfer to acceptor proteins (Freeze and Ng, 2011) resulting in decreased efficiency of protein N-glycosylation. Type II CDGs (CDG-II) are characterized by defects in the processing of N-linked glycans or the biosynthesis of O-linked oligosaccharides (Freeze and Ng, 2011; Goreta et al., 2012; Freeze et al., 2014). Although most CDGs exhibit neurological impairment (Freeze et al., 2015), there are no comprehensive studies, aimed at elucidating the molecular mechanisms that link defective glycosylation to the neuropathological aspects of the disease. Animal models that faithfully recapitulate the pathological aspects of the disease, including the neurological defects, provide a valuable resource to study the molecular mechanisms underlying pathology in CDGs. In this review we focus our attention on the advantages offered by the use of *Drosophila melanogaster* for understanding and modeling the glycobiology of CDGs.

Drosophila melanogaster AS A MODEL SYSTEM FOR STUDYING CDGs

Drosophila models offer many advantages for studying CDGs as well as other human diseases (Moulton and Letsou, 2016). Fundamental biological processes are highly conserved between *Drosophila* and humans; approximately 75% of human-disease

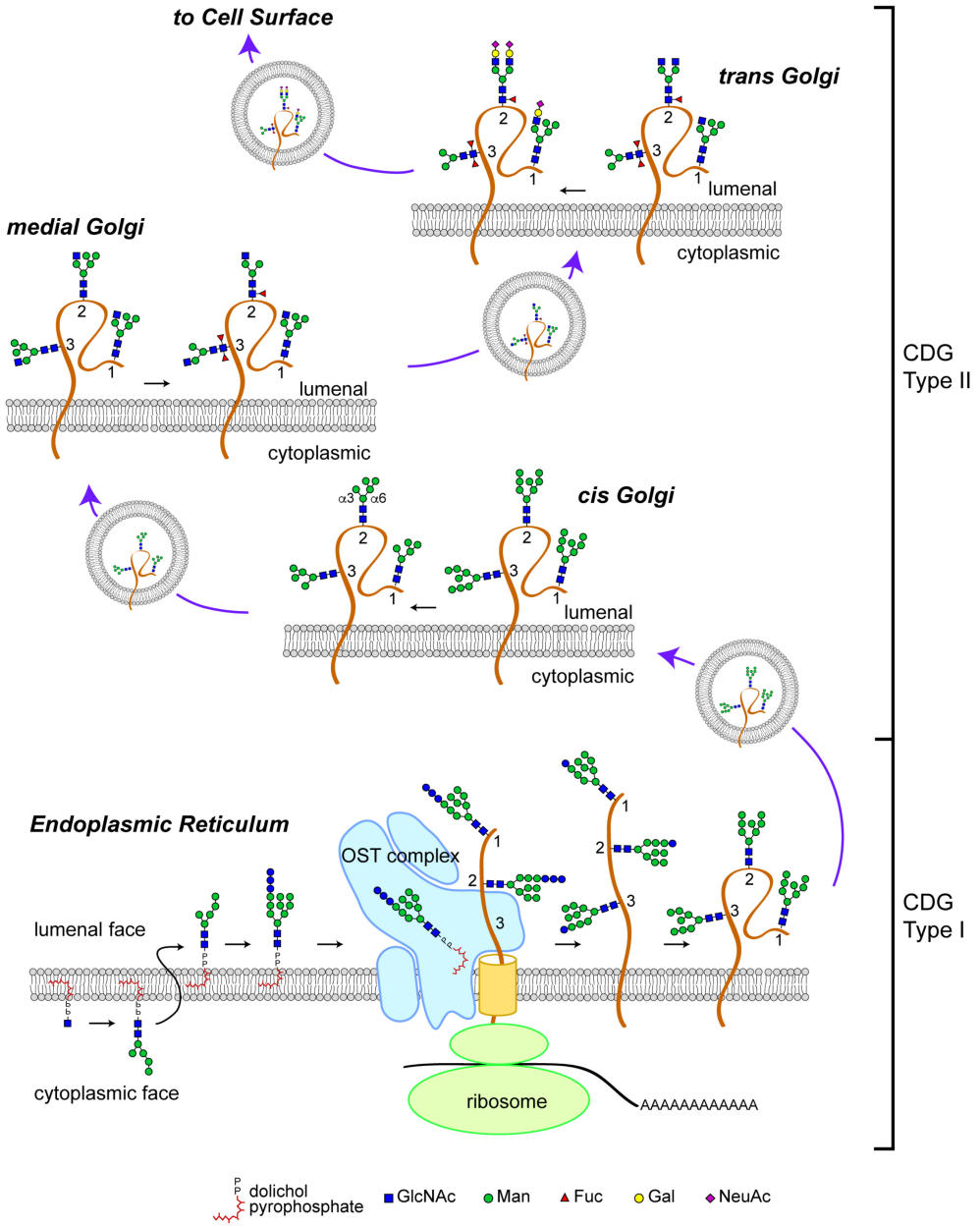

FIGURE 1 | N-linked glycosylation pathway. Biosynthesis of the N-linked precursor glycan begins on the cytoplasmic face of the ER where a GlcNAc residue is added in a pyrophosphate linkage to dolichol, an isoprenoid lipid. The GlcNAc-P-P-Dol is extended to form $Man_5GlcNAc_2$-P-P-Dol which is then flipped so that the glycan moiety is within the lumen of the ER. Further extension produces a $Glc_3Man_9GlcNAc_2$-P-P-Dol that is a substrate for the oligosaccharyltransferase (*OST*) complex, which transfers the precursor glycan *en bloc* to a nascent polypeptide. This figure depicts the glycosylation of a glycoprotein (brown) with 3 N-linked glycosylation sites (labeled *1, 2, and 3*). Once transfered to protein, the glycan precursor is trimmed of its Glc residues during folding as part of the calnexin/calreticulin quality control cycle. CDG Type I mutations affect the biosynthesis of the precursor glycan, its transfer to protein, and early trimming steps. Once successfully folded, glycoproteins bearing high-Man glycans are transported to the Golgi apparatus where Man trimming occurs. In the early *cis* Golgi, high-Man glycans can be trimmed to $Man_5GlcNAc_2$ by complete removal of Man residues on the α3 arm and partial removal of Man residues on the α6 arm. In the medial Golgi, the first committed step toward production of a complex glycan is taken; GlcNAcT1 adds a GlcNAc to the α3 Man residue to form a hybrid type glycan (*site 1* retains this structure). The GlcNAc-extended $Man_5GlcNAc_2$ glycan can be core fucosylated by the addition of a Fuc residue to the internal GlcNAc (*site 2*). In *Drosophila* and other arthropods, a second Fuc residue can be added (*site 3*). Additional Man trimming by Golgi mannosidases provide substrates for branching in the medial and *trans* Golgi (*site 2*). Subsequent extention with Gal and capping with sialic acid (shown here, as N-acetylneuraminic acid, NeuAc) completes the maturation of complex N-linked glycans. Hybrid glycans can also be extended on the α3 arm (*site 1*). The abundance of hybrid and complex glycans is reduced in *Drosophila* compared to vertebrate species due to the presence of an hexosaminidase that removes the GlcNAc added by GlcNAcT1, thereby blocking additional branching/extension and producing a paucimanose glycan (*site 3*). CDG Type II mutations impact the availability of substrates and the activity of enzymes that process N-glycans in the Golgi apparatus. Graphical representation of monosaccharide residues and glycan structures is consistent with the Symbol Nomenclature For Glycans (SNFG), which has been broadly adopted by the glycobiology community (Varki et al., 2015).

related genes have a homolog in *Drosophila* (Reiter et al., 2001; Chien et al., 2002). Moreover the genome of *D. melanogaster* is far less complex than the human genome and exhibits fewer gene duplications (Hartl, 2000). All of these characteristics, and its extraordinary repertoire of readily available genetic tools, have combined to make *Drosophila* a valuable, emerging model system for investigating glycan-dependent functions *in vivo* and for understanding the link between CDG neuropathology and glycan changes (Katoh and Tiemeyer, 2013; Scott and Panin, 2014). Such studies are extremely challenging in vertebrates due to the complexity of the nervous system and the redundancy of glycosylation pathways and enzymes (Freeze et al., 2014; Scott and Panin, 2014). *Drosophila* combines the advantages of a well-characterized glycome and the availability of electrophysiological and behavioral assays to test neurological impairment in the whole organism (Gatto and Broadie, 2011; Dani et al., 2014; Scott and Panin, 2014). Moreover, larval neuromuscular junction (NMJ) synapses use ionotropic glutamate receptors (GluRs), providing an excellent model system for excitatory synapses in the mammalian CNS.

Various analytic techniques have revealed that the most abundant N-linked glycans on *Drosophila* glycoproteins are of the high-Man or paucimannosidic type. However, hybrid and complex glycans are also present, although they represent a lower fraction of the total glycan profile when compared with vertebrates (Katoh and Tiemeyer, 2013). The relative paucity of complex glycans in *Drosophila* is a result of an arthropod-specific glycan processing enzyme encoded by a gene named Fused Lobes (*Fdl*) that removes the GlcNAc residue added by GlcNAcT-1, thereby blocking further glycan elaboration (**Figures 1**, **2**). The presence of Fdl in the secretory pathway means that *Drosophila* glycan profiles are skewed away from the highly abundant complex profiles found in most vertebrates. Nonetheless, the glycans that escape the activity of Fdl in *Drosophila* are readily processed to complexity, indicating common logic underlies glycan maturation in vertebrates and *Drosophila*. The resulting low content of complex glycans also provides a benefit for this system because it generates a simpler profile to analyze and a larger dynamic range for detecting shifts induced by mutations. Additionally, unlike mammalian organisms, the *Drosophila* genome contains only a single sialyltransferase (*DSiaT*), which greatly simplifies *in vivo* analysis of glycoprotein sialylation (Aoki et al., 2007; Koles et al., 2007; Repnikova et al., 2010).

In this section we describe *Drosophila* mutants that offer functional models for characterized human CDGs (**Figure 2**). We discuss the phenotypic characteristics that recapitulate the pathological aspects of the human disease and the translational impact of modeling the CDG in this organism. Many other *Drosophila* mutants have been shown to impact glycoprotein or glycolipid glycosylation and it is likely that the impact of many others is underappreciated (Seppo et al., 2003; Baas et al., 2011; Daenzer et al., 2016; Jumbo-Lucioni et al., 2016). But here, we focus on those mutations that have immediate parallels with human type I and II CDGs.

PMM2-CDG (CDG-Ia)

The most prevalent CDG is known as CDG-1a or PMM2-CDG, accounting for around 80% of all diagnosed cases. PMM2-CDG is inherited as an autosomal-recessive trait resulting from mutations in human *PMM2*, which encodes phosphomannomutase-2, that converts mannose-6-phosphate to mannose-1-phosphate, the precursor of GDP-mannose (Freeze et al., 2014, 2015). Because GDP-mannose is the donor for the addition of the first 5 Man residues to the dolichol-linked precursor, synthesis of N-linked glycans is impacted, as is *O*-mannosylation. The defect results in hypoglycosylation of many types of glycoproteins including serum glycoproteins, plasma membrane glycoproteins, and lysosomal enzymes. Pediatric patients suffering with CDG-Ia present with variable clinical features that affect nearly all systems and include failure to thrive, hypotonia, psychomotor retardation, ataxia, dysmorphia and coagulopathy (Freeze, 2009; Grünewald, 2009; Jaeken, 2013). Most adult CDG-Ia patients are wheelchair bound and display peripheral neuropathy and mental retardation (Grünewald, 2009).

Overall, the *Drosophila* PMM2 protein displays 56% amino acid identity with human PMM2 (Parkinson et al., 2016). Parkinson et al. (2016) generated *Drosophila pmm2* mutants. Similar to CDG-1a patients, *pmm2* mutants displayed uncoordinated movement and reduced lifespan. Analysis of the N-linked glycome of the *pmm2*-null mutant larval body demonstrated a global suppression of N-linked glycosylation. Furthermore, the N-linked glycome of adult heads with neurally targeted *pmm2* RNAi revealed increased abundance of pauci-mannose glycans. Analysis of the larval NMJs revealed altered glycan composition within the heavily glycosylated synaptomatrix which correlated with striking NMJ structural overgrowth and increased neurotransmission strength. Since NMJ synaptogenesis requires *trans*-synaptic Wnt/Wingless signaling, which in turn depends on expression of Dally-like protein (Dlp, a heparan sulfate proteoglycan) and matrix metalloproteinases (MMPs). Because knockdown of *PMM2* resulted in loss of MMP2, reduced synaptic levels of Wingless, Dlp co-receptor and downstream *trans*-synaptic signaling, the authors propose that the matrix metalloproteome and Wnt signaling pathway might provide potential new targets for developing CDG-1a treatments.

SLC35-CDG (CDG-IIc)

Also known as CDG-IIc and leukocyte adhesion deficiency type II syndrome (LAD II), this disorder is caused by mutations in a GDP-Fuc transporter (GFR). SLC35-CDG patients show craniofacial dysmorphism, severe retardation and chronic infections with unusually high leukocytosis. Importantly neutrophils of these patients lack the ability to synthesize the fucosylated glycan sialyl-Lewis X, a ligand of the selectin family of cell adhesion molecules, that is necessary for their recruitment to infection sites (Yakubenia et al., 2008). Several mutations in SLC35 nucleotide sugar transporters have been identified in *Drosophila*, including the ER Fuc transporter (*Efr*), fringe connection (*frc*), slalom (*sll*) and neurally altered carbohydrate

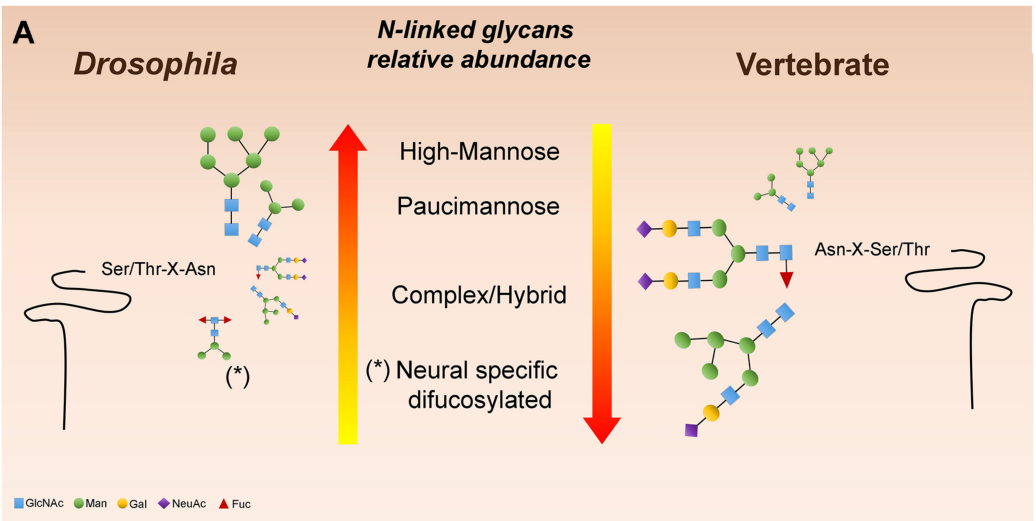

B

Human disorder	Human gene	*Drosophila* gene	*Drosophila* disease model	References
PMM2-CDG	*PMM2*	*pmm2*	➢ Reduced lifespan ➢ Severe postural and locomotor defects ➢ Global loss of N-linked glycoprotein glycosylation ➢ NMJ structural overgrowth, increased neurotransmission strength	Parkinson et al., 2016
SLC35-CDG	*SLC35C*	*Gfr*	➢ Abolished GDP-fucose transport *in vivo* and *in vitro* ➢ Decreased levels of fucosylated N-glycans.	Geisler et al., 2012
COG7-CDG	*COG7*	*Cog7*	➢ Reduced lifespan ➢ Severe postural and locomotor defects ➢ Temperature sensitive paralysis ➢ Altered NMJ architecture, reduced bouton number ➢ Increased abundance of high mannose type glycans, increase of HRP-epitopes, hyposialylation	Frappaolo et al., 2017
COG5-CDG	*COG5*	*fws*	➢ Failures of cytokinesis in male meiotic cells ➢ Defective spermatid elongation and sperm maturation	Farkas et al., 2003; Fári et al., 2016
ATP6AP2-CDG	*ATP6AP2*	*VhaM9.8/VhaPRR*	➢ Reduced lifespan ➢ Locomotor defects ➢ Suppressed or decreased courtship ➢ Defects in short- and long-term memory ➢ Altered presynaptic transmission, defects of synapse morphology and axonal transport	Rujano et al., 2018

FIGURE 2 | *Drosophila melanogaster* as a model system to study glycoprotein N-glycosylation **(A)** Representation of *Drosophila* and vertebrate N-glycome characteristics. N-linked glycans are scaled proportionally to their relative abundance. The major reason for the high-mannose and pauci-mannose dominance in the *Drosophila* N-linked glycan profile is the existence of an arthropod-specific, N-acetylhexosaminidase known as Fused lobes (Fdl), which converts the precursor for complex glycans ($GlcNAc_1Man_{3-5}GlcNAc_2$-Protein) to a paucimannose structure ($Man_{3-5}GlcNAc_2$-Protein) that cannot be extended further. Glycoprotein glycans that escape Fdl are fully capable of being processed into complex structures. **(B)** Human glycosylation disorders and phenotypic characteristics of the *Drosophila* model.

(*nac*). In *nac*^{1} mutant, a conserved serine at position 29 of the Golgi GFR is replaced by a leucine, which abolishes GDP-Fuc transport *in vivo* and *in vitro*. Mass spectrometry and HPLC analysis demonstrated reduced core α1,3-and α1,6-fucosylation in *nac*^{1} (Geisler et al., 2012). While Lewis-type glycans have not yet been identified in *Drosophila*, the commonality of altered fucosylation in SLC35 CDG-IIc and in select *Drosophila* mutants provides opportunities to investigate the regulation of protein fucosylation in a whole organism.

COG-CDG (CDG-IIe and CDG-IIi)

The eight-subunit Conserved Oligomeric Golgi (COG) complex is a Golgi tether required for intra Golgi trafficking of vesicles that recycle Golgi resident proteins and is essential for proper localization of Golgi-localized glycosylation enzymes including glycosyltransferases (Ungar et al., 2002; Kranz et al., 2007; Miller and Ungar, 2012; Willett et al., 2013; Climer et al., 2015). Mutations in the genes encoding human COG1, COG2, and COG4–COG8 are associated with monogenic forms of

inherited, autosomal recessive, CDGs-II (Freeze and Ng, 2011; Climer et al., 2015). Common features of patients carrying mutations in COG proteins (COG-CDG) are feeding problems and developmental defects, including microcephaly and growth retardation associated with dysmorphic features, hypotonia and cerebral atrophy (Wu et al., 2004; Spaapen et al., 2005; Foulquier et al., 2006; Kranz et al., 2007; Morava et al., 2007; Ng et al., 2007; Paesold-Burda et al., 2009; Reynders et al., 2009; Zeevaert et al., 2009; Lübbehusen et al., 2010; Fung et al., 2012; Kodera et al., 2015). COG7–CDG patients had the highest mortality within the first year of life and presented with dysmorphic facial features, generalized hypotonia, skeletal anomalies, hepatomegaly, progressive jaundice, cardiac insufficiency, microcephaly, and severe epilepsy (Wu et al., 2004; Spaapen et al., 2005; Morava et al., 2007; Ng et al., 2007; Zeevaert et al., 2009). Defects in COG proteins have been linked to glycosylation alterations in mammalian cultured cells and in COG–CDG patients, including hyposialylation of serum proteins, abnormal synthesis of N- and O-linked glycans and altered glycolipid glycosylation (Kingsley et al., 1986; Suvorova et al., 2002; Wu et al., 2004; Spaapen et al., 2005; Morava et al., 2007; Ng et al., 2007; Zeevaert et al., 2009; Struwe and Reinhold, 2012).

Analysis of phenotypes associated with mutations in *Drosophila* homologs of human COG complex members highlights both the value and also the limitations of modeling COG-complex disorders in this organism. The *Drosophila* homolog of human COG5, Four way stop (Fws), is not essential for adult survival but is required for male fertility. Mutations in *fws* impair spermatocyte cytokinesis, acroblast structure and elongation and individualization of differentiating spermatids (Farkas et al., 2003; Fári et al., 2016). Thus, the *Drosophila COG5* mutant presents less severe involvement than the presently known human COG-complex CDGs. On the other hand, loss of COG7 in COG7–CDG patients and in *Drosophila* mutants results in reduced life span and severe psychomotor defects (Frappaolo et al., 2017). Analysis of N-glycans from heads of *Drosophila Cog7* mutants, revealed increased abundance of high-Man type glycans compared to wild type, accompanied by a disproportionate increase of the $Man_5GlcNAc_2$ glycan, which is the precursor for all complex glycans. Additionally, a substantial increase in the abundance of a family of neural-specific, difucosylated N-glycans known as HRP-epitopes, was detected. However, not all N-glycans were increased in *Cog7* mutants. A single sialylated N-glycan was detected among the glycans harvested from adult heads and quantification relative to standard indicated that it was decreased in two mutant allelic combinations compared to wild type (Frappaolo et al., 2017). Moreover, like *DSiaT* mutants, *Cog7* mutant flies exhibit temperature sensitive (TS) paralysis, coordination defects, and altered architecture of larval NMJ. Thus the phenotypic characteristics of our *Drosophila* COG7–CDG model closely parallel the pathological characteristics of COG7–CDG patients including N-linked glycome defects with hyposialylation. Ongoing analysis of the COG protein interactome is beginning to highlight molecular hierarchies and trafficking paradigms that may underlie altered protein glycosylation (Belloni et al., 2012; Miller et al., 2012; Willett et al., 2013; Hong and Lev, 2014; Climer et al., 2015; Bailey Blackburn et al., 2016; Frappaolo et al., 2017; Sechi et al., 2017).

ATP6AP2-CDG

The multi-subunit vacuolar-type proton ATPase (V-ATPase) is a highly conserved proton pump, which acidifies intracellular compartments and is essential for endocytosis and vesicular trafficking. Rujano et al. (2018) identified missense mutations in the extracellular domain of the accessory V-ATPase subunit ATP6AP2 that cause a novel glycosylation disorder associated with hepatopathy, immunodeficiency, cutis laxa, muscular hypotonia, dysmorphic features, and psychomotor impairment. Analysis of ATP6AP2-CDG patients' serum proteins revealed hypoglycosylation, a defect that could be recapitulated by *ATP6AP2* deficiency in the mouse. Null alleles of the *Drosophila* ortholog of *ATP6AP2* cause an early lethal phenotype in *Drosophila*. The introduction of an ATP6AP2 transgene carrying the p.L98S mutation in the background of *Drosophila ATP6AP2* null mutants, reduced viability and affected the developing optic lobes in larval brains by expanding the pool of optic lobe neuroblasts, a phenotype associated with altered Notch signaling (Vaccari et al., 2010). In agreement with the role of V-ATPase-mediated acidification in autophagic degradation (Mauvezin et al., 2015), p.L98S mutation leads to lipid accumulation and autophagic dysregulation in the liver-like fat body, associated with defects of lysosomal acidification and mTOR signaling. Thus the *Drosophila* ATP6AP2-CDG model has allowed the elucidation of molecular mechanisms underlying pathological aspects of the human disease.

CONCLUSION AND PERSPECTIVES

Many impactful studies utilizing model systems (Zebrafish, flies, *C. elegans,* mice, etc.,) have enhanced our understanding of the underlying biochemical and phenotypic consequences of altered glycan biosynthesis associated with human CDG subtypes. Clinical phenotypes of human CDGs have parallels in these model systems. For the growing subset of CDGs modeled in *Drosophila*, specific phenotypes related to neural function, lifespan, viability, and glycomic diversity are replicated across these highly divergent species. This phenotypic reproducibility across species should not be surprising since the core biosynthetic pathways for protein glycosylation as well as the basic mechanisms that regulate Golgi trafficking are shared across broad swaths of evolutionary space. This conservation will allow mechanistic questions to be effectively answered in CDG models. One of these key questions is whether phenotypes arise from altered glycosylation of broad sets of glycoproteins or whether aberrant glycosylation of small subsets of glycoproteins can be linked to underlying pathologies. Once candidate proteins, whose glycosylation is altered in a given CDG, are identified by cutting edge glycoproteomics, the genetic tools offered by model systems such as *Drosophila* will allow unprecedented

targeted investigations of the cell- and tissue-specific impacts of glycosylation deficiencies.

AUTHOR CONTRIBUTIONS

All authors edited and critically revised the manuscript.

FUNDING

The Research in MG lab was supported by a grant from Associazione Italiana per la Ricerca sul Cancro (AIRC), grant IG 2017, Id 20779 and a grant from Fondazione Telethon Italy (grant number GEP 14076). Work in the MT laboratory was supported by a grant from the NIGMS/NIH, P41GM103490.

REFERENCES

Aoki, K., Perlman, M., Lim, J. M., Cantu, R., Wells, L., and Tiemeyer, M. (2007). Dynamic developmental elaboration of N-linked glycan complexity in the *Drosophila melanogaster* embryo. *J. Biol. Chem.* 282, 9127–9142. doi: 10.1074/jbc.M606711200

Baas, S., Sharrow, M., Kotu, V., Middleton, M., Nguyen, K., Flanagan-Steet, H., et al. (2011). Sugar-free frosting, a homolog of SAD kinase, drives neural-specific glycan expression in the *Drosophila* embryo. *Development* 138, 553–563. doi: 10.1242/dev.055376

Bailey Blackburn, J. B., Pokrovskaya, I., Fisher, P., Ungar, D., and Lupashin, V. V. (2016). COG complex complexities: detailed characterization of a complete set of HEK293T cells lacking individual COG subunits. *Front. Cell Dev. Biol.* 4:23. doi: 10.3389/fcell.2016.00023

Barone, R., Fiumara, A., and Jaeken, J. (2014). Congenital disorders of glycosylation with emphasis on cerebellar involvement. *Semin. Neurol.* 34, 357–366. doi: 10.1055/s-0034-1387197

Belloni, G., Sechi, S., Riparbelli, M. G., Fuller, M. T., Callaini, G., and Giansanti, M. G. (2012). Mutations in *Cog7* affect Golgi structure, meiotic cytokinesis and sperm development during *Drosophila* spermatogenesis. *J. Cell Sci.* 125, 5441–5452. doi: 10.1242/jcs.108878

Chien, S., Reiter, L. T., Bier, E., and Gribskov, M. (2002). Homophila: human disease gene cognates in *Drosophila*. *Nucleic Acid Res.* 30, 149–151. doi: 10.1093/nar/30.1.149

Climer, L. K., Dobretsov, M., and Lupashin, V. (2015). Defects in the COG complex and COG-related trafficking regulators affect neuronal Golgi function. *Front. Neurosci.* 9:405. doi: 10.3389/fnins.2015.00405

Daenzer, J. M., Jumbo-Lucioni, P. P., Hopson, M. L., Garza, K. R., Ryan, E. L., and Fridovich-Keil, J. L. (2016). Acute and long-term outcomes in a *Drosophila* melanogaster model of classic galactosemia occur independently of galactose-1-phosphate accumulation. *Dis. Model Mech.* 9, 1375–1382. doi: 10.1242/dmm.022988

Dani, N., Zhu, H., and Broadie, K. (2014). Two protein N-acetylgalactosaminyl transferases regulate synaptic plasticity by activity-dependent regulation of integrin signaling. *J. Neurosci.* 34, 13047–13065. doi: 10.1523/JNEUROSCI.1484-14.2014

Fári, K., Takács, S., Ungár, D., and Sinka, R. (2016). The role of acroblast formation during *Drosophila* spermatogenesis. *Biol. Open* 5, 1102–1110. doi: 10.1242/bio.018275

Farkas, R. M., Giansanti, M. G., Gatti, M., and Fuller, M. T. (2003). The *Drosophila Cog5* homologue is required for cytokinesis, cell elongation, and assembly of specialized Golgi architecture during spermatogenesis. *Mol. Biol. Cell* 14, 190–200. doi: 10.1091/mbc.e02-06-0343

Foulquier, F., Vasile, E., Schollen, E., Callewaert, N., Raemaekers, T., Quelhas, D., et al. (2006). Conserved oligomeric Golgi complex subunit 1 deficiency reveals a previously uncharacterized congenital disorder of glycosylation type II. *Proc. Natl. Acad. Sci. U.S.A.* 103, 3764–3769. doi: 10.1073/pnas.0507685103

Frappaolo, A., Sechi, S., Kumagai, T., Robinson, S., Fraschini, R., Karimpour-Ghahnavieh, A., et al. (2017). COG7 deficiency in *Drosophila* generates multifaceted developmental, behavioral and protein glycosylation phenotypes. *J. Cell Sci.* 130, 3637–3649. doi: 10.1242/jcs.209049

Freeze, H. H. (2009). Towards a therapy for phosphomannomutase 2 deficiency, the defect in CDG-Ia patients. *Biochim. Biophys. Acta* 1792, 835–840. doi: 10.1016/j.bbadis.2009.01.004

Freeze, H. H., Chong, J. X., Bamshad, M. J., and Ng, B. G. (2014). Solving glycosylation disorders: fundamental approaches reveal complicated pathways. *Am. J. Hum. Genet.* 94, 161–175. doi: 10.1016/j.ajhg.2013.10.024

Freeze, H. H., Eklund, E. A., Ng, B. G., and Patterson, M. C. (2015). Neurological aspects of human glycosylation disorders. *Annu. Rev. Neurosci.* 38, 105–125. doi: 10.1146/annurev-neuro-071714-034019

Freeze, H. H., and Ng, B. G. (2011). Golgi glycosylation and human inherited diseases. *Cold Spring Harb. Perspect. Biol.* 3:a005371. doi: 10.1101/cshperspect.a005371

Fung, C. W., Matthijs, G., Sturiale, L., Garozzo, D., Wong, K. Y., Wong, R., et al. (2012). COG5-CDG with a mild neurohepatic presentation. *JIMD Rep.* 3, 67–70. doi: 10.1007/8904_2011_61

Gatto, C. L., and Broadie, K. (2011). Fragile X mental retardation protein is required for programmed cell death and clearance of developmentally-transient peptidergic neurons. *Dev. Biol.* 356, 291–317. doi: 10.1016/j.ydbio.2011.05.001

Geisler, C., Kotu, V., Sharrow, M., Rendić, D., Pöltl, G., Tiemeyer, M., et al. (2012). The *Drosophila* neurally altered carbohydrate mutant has a defective Golgi GDP-fucose transporter. *J. Biol. Chem.* 287, 29599–29609. doi: 10.1074/jbc.M112.379313

Goreta, S. S., Dabelic, S., and Dumic, J. (2012). Insights into complexity of congenital disorders of glycosylation. *Biochem. Med.* 22, 156–170. doi: 10.11613/BM.2012.019

Grünewald, S. (2009). The clinical spectrum of phosphomannomutase 2 deficiency (CDG-Ia). *Biochim. Biophys. Acta* 1792, 827–834. doi: 10.1016/j.bbadis.2009.01.003

Hartl, D. L. (2000). Molecular melodies in high and low C. *Nat. Rev. Genet.* 1, 145–149. doi: 10.1038/35038580

Helenius, A., and Aebi, M. (2004). Roles of N-linked glycans in the endoplasmic reticulum. *Annu. Rev. Biochem.* 73, 1019–1049. doi: 10.1146/annurev.biochem.73.011303.073752

Hong, W., and Lev, S. (2014). Tethering the assembly of SNARE complexes. *Trends Cell Biol.* 24, 35–43. doi: 10.1016/j.tcb.2013.09.006

Jaeken, J. (2013). Congenital disorders of glycosylation. *Handb. Clin. Neurol.* 113, 1737–1743. doi: 10.1016/B978-0-444-59565-2.00044-7

Jumbo-Lucioni, P. P., Parkinson, W. M., Kopke, D. L., and Broadie, K. (2016). Coordinated movement, neuromuscular synaptogenesis and trans-synaptic signaling defects in *Drosophila* galactosemia models. *Hum. Mol. Genet.* 25, 3699–3714. doi: 10.1093/hmg/ddw217

Katoh, T., and Tiemeyer, M. (2013). The N's and O's of *Drosophila* glycoprotein glycobiology. *Glycoconj. J.* 30, 57–66. doi: 10.1007/s10719-012-9442-x

Khoury, G. A., Baliban, R. C., and Floudas, C. A. (2011). Proteome-wide post-translational modification statistics: frequency analysis and curation of the swiss-prot database. *Sci. Rep.* 1:90. doi: 10.1038/srep00090

Kingsley, D. M., Kozarsky, K. F., Segal, M., and Krieger, M. (1986). Three types of low density lipoprotein receptor-deficient mutant have pleiotropic defects in the synthesis of N-linked, O-linked, and lipid-linked carbohydrate chains. *J. Cell Biol.* 102, 1576–1585. doi: 10.1083/jcb.102.5.1576

Kodera, H., Ando, N., Yuasa, I., Wada, Y., Tsurusaki, Y., Nakashima, M., et al. (2015). Mutations in COG2 encoding a subunit of the conserved oligomeric golgi complex cause a congenital disorder of glycosylation. *Clin. Genet.* 87, 455–460. doi: 10.1111/cge.12417

Koles, K., Lim, J. M., Aoki, K., Porterfield, M., Tiemeyer, M., Wells, L., et al. (2007). Identification of N-glycosylated proteins from the central nervous system of *Drosophila melanogaster*. *Glycobiology* 17, 1388–1403. doi: 10.1093/glycob/cwm097

Kranz, C., Ng, B. G., Sun, L., Sharma, V., Eklund, E. A., Miura, Y., et al. (2007). COG8 deficiency causes new congenital disorder of glycosylation type IIh. *Hum. Mol. Genet.* 16, 731–741. doi: 10.1093/hmg/ddm028

Li, H., Chavan, M., Schindelin, H., Lennarz, W. J., and Li, H. (2008). Structure of the oligosaccharyl transferase complex at 12 A resolution. *Structure* 16, 432–440. doi: 10.1016/j.str.2007.12.013

Lübbehusen, J., Thiel, C., Rind, N., Ungar, D., Prinsen, B. H., de Koning, T. J., et al. (2010). Fatal outcome due to deficiency of subunit 6 of the conserved oligomeric Golgi complex leading to a new type of congenital disorders of glycosylation. *Hum. Mol. Genet.* 19, 3623–3633. doi: 10.1093/hmg/ddq278

Mauvezin, C., Nagy, P., Juhász, G., and Neufeld, T. P. (2015). Autophagosome-lysosome fusion is independent of V-ATPase-mediated acidification. *Nat. Commun.* 6:7007. doi: 10.1038/ncomms8007

Miller, V. J., Sharma, P., Kudlyk, T. A., Frost, L., Rofe, A. P., Watson, I. J., et al. (2012). Molecular insights into vesicle tethering at the Golgi by the conserved oligomeric Golgi (COG) complex and the golgin TATA element modulatory factor (TMF). *J. Biol. Chem.* 288, 4229–4240. doi: 10.1074/jbc.M112.426767

Miller, V. J., and Ungar, D. (2012). Re'COG'nition at the Golgi. *Traffic* 13, 891–897. doi: 10.1111/j.1600-0854.2012.01338.x

Morava, E., Zeevaert, R., Korsch, E., Huijben, K., Wopereis, S., Matthijs, G., et al. (2007). A common mutation in the COG7 gene with a consistent phenotype including microcephaly, adducted thumbs, growth retardation, VSD and episodes of hyperthermia. *Eur. J. Hum. Genet.* 15, 638–645. doi: 10.1038/sj.ejhg.5201813

Moremen, K. W., Tiemeyer, M., and Nairn, A. V. (2012). Vertebrate protein glycosylation: diversity, synthesis and function. *Nat. Rev. Mol. Cell Biol.* 13, 448–462. doi: 10.1038/nrm3383

Moulton, M. J., and Letsou, A. (2016). Modeling congenital disease and inborn errors of development in *Drosophila* melanogaster. *Dis. Model Mech.* 9, 253–269. doi: 10.1242/dmm.023564

Ng, B. G., Kranz, C., Hagebeuk, E. E., Duran, M., Abeling, N. G., Wuyts, B., et al. (2007). Molecular and clinical characterization of a Moroccan Cog7 deficient patient. *Mol. Genet. Metab.* 91, 201–214. doi: 10.1016/j.ymgme.2007.02.011

Ohtsubo, K., and Marth, J. D. (2006). Glycosylation in cellular mechanisms of health and disease. *Cell* 126, 855–867. doi: 10.1016/j.cell.2006.08.019

Paesold-Burda, P., Maag, C., Troxler, H., Foulquier, F., Kleinert, P., Schnabel, S., et al. (2009). Deficiency in COG5 causes a moderate form of congenital disorders of glycosylation. *Hum. Mol. Genet.* 18, 4350–4356. doi: 10.1093/hmg/ddp389

Parkinson, W. M., Dookwah, M., Dear, M. L., Gatto, C. L., Aoki, K., Tiemeyer, M., et al. (2016). Synaptic roles for phosphomannomutase type 2 in a new *Drosophila* congenital disorder of glycosylation disease model. *Dis. Model Mech.* 9, 513–527. doi: 10.1242/dmm.022939

Reiter, L. T., Potocki, L., Chien, S., Gribskov, M., and Bier, E. (2001). A systematic analysis of human disease-associated gene sequences in *Drosophila* melanogaster. *Genome Res.* 11, 1114–1125. doi: 10.1101/gr.169101

Repnikova, E., Koles, K., Nakamura, M., Pitts, J., Li, H., Ambavane, A., et al. (2010). Sialyltransferase regulates nervous system function in *Drosophila*. *J. Neurosci.* 30, 6466–6476. doi: 10.1523/JNEUROSCI.5253-09.2010

Reynders, E., Foulquier, F., Leão Teles, E., Quelhas, D., Morelle, W., Rabouille, C., et al. (2009). Golgi function and dysfunction in the first COG4-deficient CDG type II patient. *Hum. Mol. Genet.* 18, 3244–3256. doi: 10.1093/hmg/ddp262

Rujano, M. A., Cannata Serio, M., Panasyuk, G., Péanne, R., Reunert, J., Rymen, D., et al. (2018). Mutations in the X-linked ATP6AP2 cause a glycosylation disorder with autophagic defects. *J. Exp. Med.* 214, 3707–3729. doi: 10.1084/jem.20170453

Scott, H., and Panin, V. M. (2014). N-glycosylation in regulation of the nervous system. *Adv. Neurobiol.* 9, 367–394. doi: 10.1007/978-1-4939-1154-7_17

Sechi, S., Frappaolo, A., Fraschini, R., Capalbo, L., Gottardo, M., Belloni, G., et al. (2017). Rab1 interacts with GOLPH3 and controls Golgi structure and contractile ring constriction during cytokinesis in *Drosophila* melanogaster. *Open Biol.* 7:160257. doi: 10.1098/rsob.160257

Seppo, A., Matani, P., Sharrow, M., and Tiemeyer, M. (2003). Induction of neuron-specific glycosylation by Tollo/Toll-8, a *Drosophila* toll-like receptor expressed in non-neural cells. *Development* 130, 1439–1448. doi: 10.1242/dev.00347

Shwartz, F., and Aebi, M. (2011). Mechanisms and principles of N-linked protein glycosylation. *Curr. Opin. Struct. Biol.* 21, 576–582. doi: 10.1016/j.sbi.2011.08.005

Spaapen, L. J., Bakker, J. A., van der Meer, S. B., Sijstermans, H. J., Steet, R. A., Wevers, R. A., et al. (2005). Clinical and biochemical presentation of siblings with COG-7 deficiency, a lethal multiple O- and N-glycosylation disorder. *J. Inherit. Metab. Dis.* 28, 707–714. doi: 10.1007/s10545-005-0015-z

Stanley, P. (2011). Golgi glycosylation. *Cold Spring Harb. Perspect. Biol.* 3:a005199. doi: 10.1101/cshperspect.a005199

Struwe, W. B., and Reinhold, V. N. (2012). The conserved oligomeric Golgi complex is required for fucosylation of N-glycans in *Caenorhabditis elegans*. *Glycobiology* 22, 863–875. doi: 10.1093/glycob/cws053

Suvorova, E. S., Duden, R., and Lupashin, V. V. (2002). The Sec34/Sec35p complex, a Ypt1p effector required for retrograde intra-Golgi trafficking, interacts with Golgi SNAREs and COPI vesicle coat proteins. *J. Cell Biol.* 157, 631–643. doi: 10.1083/jcb.200111081

Ungar, D., Oka, T., Brittle, E. E., Vasile, E., Lupashin, V. V., Chatterton, J. E., et al. (2002). Characterization of a mammalian Golgi-localized protein complex, COG, that is required for normal Golgi morphology and function. *J. Cell Biol.* 157, 405–415. doi: 10.1083/jcb.200202016

Vaccari, T., Duchi, S., Cortese, K., Tacchetti, C., and Bilder, D. (2010). The vacuolar ATPase is required for physiological as well as pathological activation of the Notch receptor. *Development* 137, 1825–1832. doi: 10.1242/dev.045484

Varki, A., Cummings, R. D., Aebi, M., Packer, N. H., Seeberger, P. H., Esko, J. D., et al. (2015). Symbol nomenclature for graphical representations of glycans. *Glycobiology* 25, 1323–1324. doi: 10.1093/glycob/cwv091

Willett, R., Ungar, D., and Lupashin, V. (2013). The Golgi puppet master: COG complex at center stage of membrane trafficking interactions. *Histochem. Cell Biol.* 140, 271–283. doi: 10.1007/s00418-013-1117-6

Wu, X., Steet, R. A., Bohorov, O., Bakker, J., Newell, J., Krieger, M., et al. (2004). Mutation of the COG complex subunit gene COG7 causes a lethal congenital disorder. *Nat. Med.* 10, 518–523. doi: 10.1038/nm1041

Yakubenia, S., Frommhold, D., Schölch, D., Hellbusch, C. C., Körner, C., Petri, B., et al. (2008). Leukocyte trafficking in a mouse model for leukocyte adhesion deficiency II/congenital disorder of glycosylation IIc. *Blood* 112, 1472–1481. doi: 10.1182/blood-2008-01-132035

Zeevaert, R., Foulquier, F., Cheillan, D., Cloix, I., Guffon, N., Sturiale, L., et al. (2009). A new mutation in COG7 extends the spectrum of COG subunit deficiencies. *Eur. J. Med. Genet.* 52, 303–305. doi: 10.1016/j.ejmg.2009.06.006

Zielinska, D. F., Gnad, F., Wiśniewski, J. R., and Mann, M. (2010). Precision mapping of an in vivo N-glycoproteome reveals rigid topological and sequence constraints. *Cell* 141, 897–907. doi: 10.1016/j.cell.2010.04.012

Conflict of Interest Statement: The authors declare that the research was conducted in the absence of any commercial or financial relationships that could be construed as a potential conflict of interest.

The handling Editor and author MG declared their involvement as co-editors in the Research Topic, and confirm the absence of any other collaboration.

frontiers in Genetics

ORIGINAL RESEARCH
published: 18 September 2018
doi: 10.3389/fgene.2018.00379

SUMO-Targeted Ubiquitin Ligases (STUbLs) Reduce the Toxicity and Abnormal Transcriptional Activity Associated With a Mutant, Aggregation-Prone Fragment of Huntingtin

*Kentaro Ohkuni[1†], Nagesh Pasupala[2†‡], Jennifer Peek[2], Grace Lauren Holloway[2], Gloria D. Sclar[2], Reuben Levy-Myers[2], Richard E. Baker[3], Munira A. Basrai[1] and Oliver Kerscher[2]**

[1] Genetics Branch, Center for Cancer Research, National Cancer Institute, National Institutes of Health, Bethesda, MD, United States, [2] Biology Department, College of William & Mary, Williamsburg, VA, United States, [3] Department of Microbiology and Physiological Systems, University of Massachusetts Medical School, Worcester, MA, United States

Cell viability and gene expression profiles are altered in cellular models of neurodegenerative disorders such as Huntington's Disease (HD). Using the yeast model system, we show that the SUMO-targeted ubiquitin ligase (STUbL) Slx5 reduces the toxicity and abnormal transcriptional activity associated with a mutant, aggregation-prone fragment of huntingtin (Htt), the causative agent of HD. We demonstrate that expression of an aggregation-prone Htt construct with 103 glutamine residues (103Q), but not the non-expanded form (25Q), results in severe growth defects in *slx5*Δ and *slx8*Δ cells. Since Slx5 is a nuclear protein and because Htt expression affects gene transcription, we assessed the effect of STUbLs on the transcriptional properties of aggregation-prone Htt. Expression of Htt 25Q and 55Q fused to the Gal4 activation domain (AD) resulted in reporter gene auto-activation. Remarkably, the auto-activation of Htt constructs was abolished by expression of Slx5 fused to the Gal4 DNA-binding domain (BD-Slx5). In support of these observations, RNF4, the human ortholog of Slx5, curbs the aberrant transcriptional activity of aggregation-prone Htt in yeast and a variety of cultured human cell lines. Functionally, we find that an extra copy of *SLX5* specifically reduces Htt aggregates in the cytosol as well as chromatin-associated Htt aggregates in the nucleus. Finally, using RNA sequencing, we identified and confirmed specific targets of Htt's transcriptional activity that are modulated by Slx5. In summary, this study of STUbLs uncovers a conserved pathway that counteracts the accumulation of aggregating, transcriptionally active Htt (and possibly other poly-glutamine expanded proteins) on chromatin in both yeast and in mammalian cells.

Keywords: Slx5, STUbL, SUMO, ubiquitin, Htt

OPEN ACCESS

Edited by:
Roberta Fraschini, Università degli Studi Milano-Bicocca, Italy

Reviewed by:
Eric M. Rubenstein, Ball State University, United States
Hansen Wang, University of Toronto, Canada

***Correspondence:**
Oliver Kerscher
opkers@wm.edu

†Joint first authors

*‡**Present address:***
Nagesh Pasupala, Biophysics and Biophysical Chemistry, Johns Hopkins School of Medicine, Baltimore, MD, United States

Specialty section:
This article was submitted to Genetic Disorders, a section of the journal Frontiers in Genetics

Received: *21 June 2018*
Accepted: *27 August 2018*
Published: *18 September 2018*

Citation:
Ohkuni K, Pasupala N, Peek J, Holloway GL, Sclar GD, Levy-Myers R, Baker RE, Basrai MA and Kerscher O (2018) SUMO-Targeted Ubiquitin Ligases (STUbLs) Reduce the Toxicity and Abnormal Transcriptional Activity Associated With a Mutant, Aggregation-Prone Fragment of Huntingtin. Front. Genet. 9:379. doi: 10.3389/fgene.2018.00379

INTRODUCTION

Ubiquitin and SUMO are members of a conserved family of small ubiquitin-like modifier proteins (UBLs) that can be conjugated to lysine residues of target proteins to modulate their activity, function, localization, and half-life. The conjugation of both SUMO and ubiquitin to numerous target proteins is a multi-step process and involves a cascade of similar, yet distinct E1 activating enzymes, E2 conjugating enzymes, and E3 ligases. Additionally, dedicated SUMO or ubiquitin-specific proteases render these protein modifiers conjugation competent and also aid in their deconjugation from modified proteins. As such, the dynamic conjugation and deconjugation of UBLs has key roles in cell growth and the maintenance of genome integrity and has been implicated in disease-related processes including cancer, inflammation, and neurodegeneration (Hoeller et al., 2006; Kerscher et al., 2006; Dorval and Fraser, 2007; Dasso, 2008; Liu and Shuai, 2008; Sarge and Park-Sarge, 2009; van Wijk et al., 2011; Cubeñas-Potts and Matunis, 2013). Mammalian cells express one form of ubiquitin and three forms of conjugatable SUMO (SUMO-1, SUMO-2, and SUMO-3), while budding yeast only expresses one form each of ubiquitin and SUMO (Smt3). Chains of ubiquitin can be formed through conjugation of internal lysines. Analogously, Smt3, SUMO-2, and SUMO-3 can form SUMO chains on the proteins they modify, a property not shared by SUMO-1, which lacks the internal lysines required for polymerization (Ulrich, 2008; Vertegaal, 2010). The majority of proteins that are modified with ubiquitin chains are targeted to the proteasome. In contrast, SUMO chains and hybrid SUMO-ubiquitin chains do not play a direct role in proteolytic targeting but play an important but poorly understood role in SUMO-dependent signaling and the regulation of chromatin (Guzzo et al., 2012).

STUbLs, including the heterodimeric Slx5/Slx8 in budding yeast and the RNF4 homodimer in mammalian cells, are ubiquitin E3 ligases that can specifically target and bind sumoylated proteins and facilitate their ubiquitylation. Members of this unusual subfamily of ubiquitin ligases are well conserved, contain a RING domain required for their ubiquitylation activity, and use multiple SIMs (SUMO-interacting motifs) to target sumoylated substrates (Wang et al., 2006; Kerscher, 2007; Sun et al., 2007; Uzunova et al., 2007; Xie et al., 2007; Mullen and Brill, 2008; Tatham et al., 2008; Prudden et al., 2011; Alonso et al., 2012). Not surprisingly, STUbLs play an important role in the cross-regulation of proteins that can be modified with both SUMO and ubiquitin (Perry et al., 2008; Geoffroy and Hay, 2009). Deletion of *SLX5* and *SLX8* results in the accumulation of high-molecular weight SUMO adducts and renders cells hypersensitive to DNA damage and perturbed DNA replication (Zhang et al., 2006; Prudden et al., 2007). Similarly, depletion of RNF4 sensitizes cells to DNA damage (Tatham et al., 2008; Geoffroy and Hay, 2009; Yin et al., 2012). However, several lines of evidence suggest that STUbLs also play a critical role in protein quality control. For example, Slx5/Slx8 plays a role in degrading a mutant yeast transcriptional regulator, *mot1-103*, the nuclear degradation of the SUMO E3 ligase Siz1 in mitosis, and proteolysis of centromeric histone H3 variant Cse4, and also a transcription factor, Mat α2, that is not modified with SUMO (Wang and Prelich, 2009; Westerbeck et al., 2014; Hickey and Hochstrasser, 2015; Ohkuni et al., 2016). Similarly, RNF4 has been shown to regulate the SUMO- and ubiquitin-mediated proteasomal degradation of a mutant cystic fibrosis transmembrane conductance regulator (F508del CFTR), mutant attaxin (Atxn1 82Q), and possibly the reduction of SDS-resistant aggregates of mutant huntingtin (Htt, 97QP) in the cytosol of mammalian cells (Ahner et al., 2013; Guo et al., 2014).

Mutant Htt is the causative agent of Huntington's disease (HD), a hereditary neurodegenerative illness that affects 2.71 per 100,000 people worldwide (Pringsheim et al., 2012). The IT15 gene, first discovered in 1993, encodes the huntingtin protein (Htt) which is essential for normal development of mammals and interacts with a variety of proteins implicated in transcription, intracellular transport, and cell signaling. However, the complete extent of Htt function remains unknown (Cattaneo et al., 2005). The amino-terminus of Htt normally contains a stretch of 17–28 glutamine (Q) residues, that is expanded to more than 36Q (and sometimes over 100) in patients with HD. These amino-terminal poly-glutamine expansions form aggregates of mutant Htt that visibly accumulate in neurons and in cell culture models, including budding yeast.

It has been suggested that Htt aggregates may be neuroprotective in that they incorporate cytotoxic Htt monomers into inert cellular inclusions (Arrasate et al., 2004). However, there is also ample evidence that cellular aggregates of Htt sequester a variety of other proteins required for vesicle trafficking, cell cycle regulation, transcriptional regulation, cytoskeletal functions, cell signaling, and protein turnover, thus contributing to the demise of cells expressing these aggregation-prone proteins (Suhr et al., 2001; Bauer et al., 2012).

The majority of Htt aggregates occur in the cytosol, but there is considerable evidence that the accumulation of Htt in the nucleus enhances its toxicity [reviewed in Davies et al. (1997), Lunkes and Mandel (1997), and Benn et al. (2008)]. For example, it has recently been found that a poly-glutamine expanded Htt protein fused with a nuclear localization signal (Htt-103Q-NLS), unlike Htt-103Q, is highly toxic to Wild-type (WT) budding yeast (Wolfe et al., 2014). Interestingly, the authors of this study found that toxicity of Htt-103Q-NLS can be suppressed by overexpression of other poly-Q rich proteins including Nab3, an RNA binding protein (Wolfe et al., 2014). The poly-Q tract on Htt is known to sequester other naturally occurring proteins with poly-Q tracts. For example, there are 14 proteins with poly-Q tracts of at least 20 glutamines encoded in the yeast genome, and at least 66 genes in the human genome that have been classified as encoding poly-Q proteins (Butland et al., 2007). Proteins with poly-Q tracts are involved in a variety of functions, but the majority are classified as transcription cofactors, coactivators, and DNA-binding proteins, or regulators of metabolic processes (Butland et al., 2007). In mammalian cells, poly-Q expanded Htt globally disrupts transcriptional regulation (Steffan et al., 2000; Dunah et al., 2002; Schaffar et al., 2015). In a yeast two-hybrid assay, transcriptional activity of aggregation-prone

Htt was dependent on the length of the poly-Q tract (Gerber et al., 1994; Benn et al., 2008; Atanesyan et al., 2012). These observations underscore the importance of understanding the functional role that Htt has in the nucleus.

We reasoned that Slx5, owing to it's protein quality-control functions, may alter the aggregation or distribution of Htt aggregates in WT cells. Therefore, we investigated whether STUbLs, Slx5, and Slx8 play a role in preventing the toxicity of poly-Q expanded Htt in budding yeast cells. We found that expression of Htt-103Q elicited a severe growth defect and was toxic in *slx5*Δ and *slx8*Δ mutants. The genetic interaction of Htt with STUbLs led us to examine the functional role of STUbLs in counteracting the toxic effects of Htt-103Q. For this we assessed the interaction of STUbLs with various Htt constructs using a reporter gene assay. Using this assay, we established that both Slx5 and RNF4, the human STUbL ortholog, reduced the transcriptional activity of Htt in yeast and human cells. Functionally, we determined that a plasmid-borne copy of *SLX5* reduced the levels of both cytosolic and nuclear Htt aggregates but did not affect the levels of monomeric Htt protein in the nucleus. Finally, we completed a global RNA sequencing study to identify transcripts that are affected by Htt-103Q and modulated by an extra copy of *SLX5*. Therefore, our data implicates STUbLs in a conserved mechanism that prevents the accumulation of aggregating proteins such as Htt on chromatin and curbs their promiscuous transcriptional activity both in yeast and in mammalian cells.

MATERIALS AND METHODS

Yeast Strains, Plasmids, Mammalian Tissue Culture, and Media

All strains and plasmids used in this study are listed in **Supplementary Table S1**. Unless noted otherwise, preparation of yeast media and manipulation of yeast strains were performed as previously reported (Guthrie and Fink, 2002). Unless otherwise noted, all yeast strains were grown at 30°C. Yeast plasmids expressing 25Q and 103Q Htt were purchased from Addgene.org (Addgene plasmid # 1177 (GPD-25Q-GFP Htt in p416), # 1180 (GPD-103Q-GFP Htt in p416)). These plasmids were used for growth assays and microscopy. For Htt localization and auto-activation assays, Htt with 25Q, 55Q, and 97Q were PCR-amplified using NEB Q5 hot start high-fidelity polymerase 2× master mix (Cat # M0494S) and cloned into the pCR8/GW/TOPO entry vector (Life Technologies) and then recombined into either pAG414GAL-ccdB-DsRed (Addgene #14359) forming GAL-97QHtt-DsRed/TRP1/CEN (BOK 1213) or pACT2.2gtwy (Addgene # 11346) forming ADH1-GAL4AD-25QHtt/LEU2/2μ (BOK 1207), ADH1-GAL4AD-55QHtt/LEU2/2μ (BOK1209) and ADH1-GAL4AD-97QHtt/LEU2/2μ (BOK 1215). All plasmids expressing Htt encode exon I (17 amino acids) followed by poly-Q and proline-rich regions. NEBase Changer v1.2.1 software at NEB website was used for designing mutagenesis 5′-phospho primers and NEB Q5 hot start high-fidelity polymerase 2x master mix was used for PCR amplification. After PCR, template plasmid DNA in the reaction mixture was digested by treatment with DpnI enzyme (cat # R0176S) and PCR amplicon was ligated using T4 DNA Ligase enzyme (Cat # M0202S). All primer sequences used for cloning and mutagenesis are available upon request. Yeast cells were transformed as previously described (Amberg et al., 2005) or using the frozen-EZ yeast transformation II kit (Zymo research corporation, Irvine CA). For mammalian 2-hybrid assays, the Matchmaker Mammalian Assay Kit 2 (Clontech.com Cat. No. 630305) was used as per suppliers instructions. The pVP16 Activation Domain (AD) Htt constructs were designed in the Kerscher lab and synthesized by Genewiz (South Plainville, NJ, United States) to produce pVP16-Htt25Q-AD and pVP16-Htt55Q-AD. RNF4 was PCR amplified and cloned into *EcoR*1 and *Hind*III sites in the pM-BD plasmid to produce pM-BD-RNF4.

PC3 (Prostate Adenocarcinoma), PNT2 (Prostate Epithelium), and LNCaP (Prostate Carcinoma) cells were grown in RPMI media with 10% heat inactivated FBS (Thermo Fisher Scientific #10438018) and 1% antifungal/antibiotic (anti/anti) (Thermo Fisher Scientific #15240062). PC12 (Rat pheochromocytoma) cells were grown as above but also contained 10% horse serum. HEK 293 (Embryonic Kidney) cells were grown in DMEM media with 10% heat inactivated FBS and 1% anti-anti. Cells were transfected using Lipofectamine 2000 or 3000 reagents using supplier instruction (Thermo Fisher Scientific, Cat. No. 11668-019 or L3000-015).

Growth Curves

Yeast strains YOK2206-2207, YOK2209-2210, YOK2824-2828 were grown overnight in 5 ml selective media with 2% dextrose. OD readings were recorded every hour from OD_{600} ∼ 0.15 to OD_{600} ∼2.0 for up to 10 h (Thermo Fisher Scientific Spectronic 200). Readings were averaged and graphed in Microsoft Excel. Error bars represent the standard error of four independent cultures for each strain listed. Doubling times were calculated as previously published (Murakami and Kaeberlein, 2009).

Spotting Assays

Yeast strains were grown overnight in 5 ml selective media with 2% dextrose. When cultures reached mid-log phase (OD_{600} 0.8–1.0), 1 OD of cells was harvested. Cultures were 10-fold serially diluted and 5 μl was spotted onto selective medium containing 2% dextrose. Plates were dried at ambient temperature and incubated at 30°C for up to 3 days.

Ortho-Nitrophenyl-β-Galactoside (ONPG) and SEAP Assays

Yeast cultures of pJ694alpha containing the appropriate AD and BD constructs were grown until cells reached mid-log phase (OD_{600} of 1 ml = 0.5–0.8) and lac-Z reporter gene expression was determined as outlined in the Clontech Yeast Methods protocols handbook (PT3024-1). Briefly, the exact OD_{600} was recorded when the cultures were harvested. Cells

were then washed in Z-buffer (16.1 g/L of $Na_2HPO_4{\cdot}7H_2O$, 5.50 g/L of $NaH_2PO_4{\cdot}H_2O$, 0.75 g/L of KCl, and 0.246 g/L of $MgSO_4{\cdot}7H_2O$. pH 7.0). Cell pellets were resuspended in 100 µl of Z-buffer and three cycles of freeze/thaw each for 30 s was done to break open the cells. Cells were then incubated in the presence of ONPG (4 mg/ml) in Z-buffer at 30°C until yellow color developed. Reactions were stopped using 1 M Na_2CO_3 and cell debris was removed by centrifugation. The OD_{420} was determined using a spectrophotometer and β-galactosidase units were calculated using the formula [β-gal units = $1000 \times OD_{420}/(t \times V \times OD_{600})$] where t is elapsed time (in minutes) of incubation, V is 0.1 ml times 5 (concentration factor) (Miller, 1972). The β-galactosidase units reported were average values of at least three independent experiments and values were graphed including +/−*SD*. The Great EscAPe Chemiluminescence kit (Clontech #631737) was used to detect SEAP levels in the mammalian 2-hybrid assay. Twenty-five microliters of culture media were obtained and spun for 1 min at 12,000 rpm to remove cells. The supernatant was transferred to black 96-well plates with clear, flat well bottoms (Corning #353219) and after addition of SEAP substrate solution, Chemiluminescent signals were visualized and analyzed using a Li-COR C-Digit Blot Scanner and also autoradiography film. Student's *t*-tests were used to analyze statistical significance of SEAP transcriptional levels.

Fluorescence Microscopy

Images of live cells were collected using a Zeiss Axioscope two plus microscope (Carl Zeiss Microscopy, LLC, Thornwood, NY, United States) fitted with a Qimaging Retiga™ SRV charge-coupled device digital camera (Qimaging, Surrey, BC, Canada), i-Vision software for macintosh (Bio Vision Technologies, Exton, PA, United States) and a Uniblitz shutter assembly (Vincent Associates/ UNIBLITZ, Rochester, NY, United States). Pertinent filter sets for the above applications include CZ909 (GFP), XF114-2 (CFP), Filter set 15 (DsRed1), and 49 (DAPI and Hoechst 33258) (Chroma Technology Group, Bellows Falls, VT, United States). Where applicable, images were normalized using i-vision software and pseudo-colored and adjusted using Adobe Photoshop software (vs13.0 × 64, Adobe Systems, San Jose, CA, United States).

Subcellular Fractionation Assay

Cells were grown in a 2% raffinose synthetic complete medium at 25°C until reaching mid-log phase. Then, galactose was added to the media to a final concentration of 2% to induce Htt-25Q-NLS-GFP or Htt-103Q-NLS-GFP expression from the *GAL* promoter for 4 h at 25°C. Whole cell extract (WCE) was purified from 50 OD_{600} equivalent cells. Subcellular fractionation was performed as described previously (Au et al., 2008). Western blot analysis of WCE, soluble, and chromatin fraction was carried out to monitor the Htt25Q-NLS or Htt103Q-NLS levels. Tub2 and histone H3 were used as markers for soluble and chromatin fractions, respectively. Protein levels were quantified using Gene Tools software (version 3.8.8.0) from SynGene (Frederick, MD, United States). Primary antibodies were anti-GFP mouse (1:3000, 11814460001, Roche), anti-Tub2 rabbit (1:3000, Basrai laboratory), and anti-H3 rabbit (1:7500, ab1791, Abcam).

Total RNA Isolation

Cells were grown in a 2% raffinose synthetic complete medium at 25°C until reaching mid-log phase. Then, galactose was added to the media to a final concentration of 2% to induce Htt-25Q-NLS or Htt103Q-NLS expression from the *GAL* promoter for 4 h at 25°C. Total RNAs were isolated from 3 OD_{600} equivalent cells using MasterPure™ Yeast RNA purification kit with DNase I treatment as indicated by the manufacturer (Epicentre). All RNA samples had an RNA integrity number (RIN) of 8 and above, indicative of high sample quality. Half of the sample is used for RNA sequencing, and another half is for RT-PCR for a validation of the RNA sequencing.

Reverse Transcription-PCR (RT-PCR)

Total RNAs (100 ng for *HBT1*, 10 ng for *UIP4* and *UBC11*, and 1 ng for *ACT1*) were analyzed by AccessQuick™ RT-PCR system (Promega). Primer sets and PCR conditions are available upon request. PCR products were loaded onto Ethidium Bromide-stained 1.5% agarose gels in TBE (KD Medical) and band intensities were quantified with Gene Tools software (version 3.8.8.0) from SynGene (Frederick, MD, United States). Expression levels were calculated based on the standard curve on the same gel and relative values were determined when level of the NLS-Htt25Q-GFP [Vector] was defined as 100.

mRNA-Seq and Analysis

Three independent RNA-seq libraries for each of 4 samples were prepared from total RNA using the Illumina TruSeq Stranded Total RNA Kit RS-122-2201. They were pooled and sequenced in a single 150 cycle paired end HiSeq run at the Frederick National Laboratory for Cancer Research (FNLCR) at the CCR Sequencing Facility, NCI, NIH, Frederick, MD 21701. Fifty-six to 81 million pass-filter reads were obtained with > 95% base calling quality of Q30. Reads were adapter-trimmed with low-quality calls removed using Trimmomatic v0.36 and aligned using STAR 2.5.1. The transcriptome reference was annotated transcripts from *Saccharomyces cerevisiae* S288C, assembly EF4 (Ensembl). One library (YMB10544_c) contained 45% rRNA sequences and was removed from further analysis (all other libraries contained < 2% rRNA reads). Genewise read counts were quantitated using RSEM 1.2.22, and differential expression analysis was performed using edgeR version 3.20.9 utilizing the tool's GLM functionality. An F-like test was performed first to identify genes showing a statistically significant difference in at least one condition (3961 of 7126 total), and only these genes were included in subsequent pairwise comparisons. Analysis of identified transcripts was completed using the online Panther classification system[1] (Mi et al., 2013) and the Saccharomyces Genome Database[2].

[1] www.pantherdb.org

[2] www.yeastgenome.org

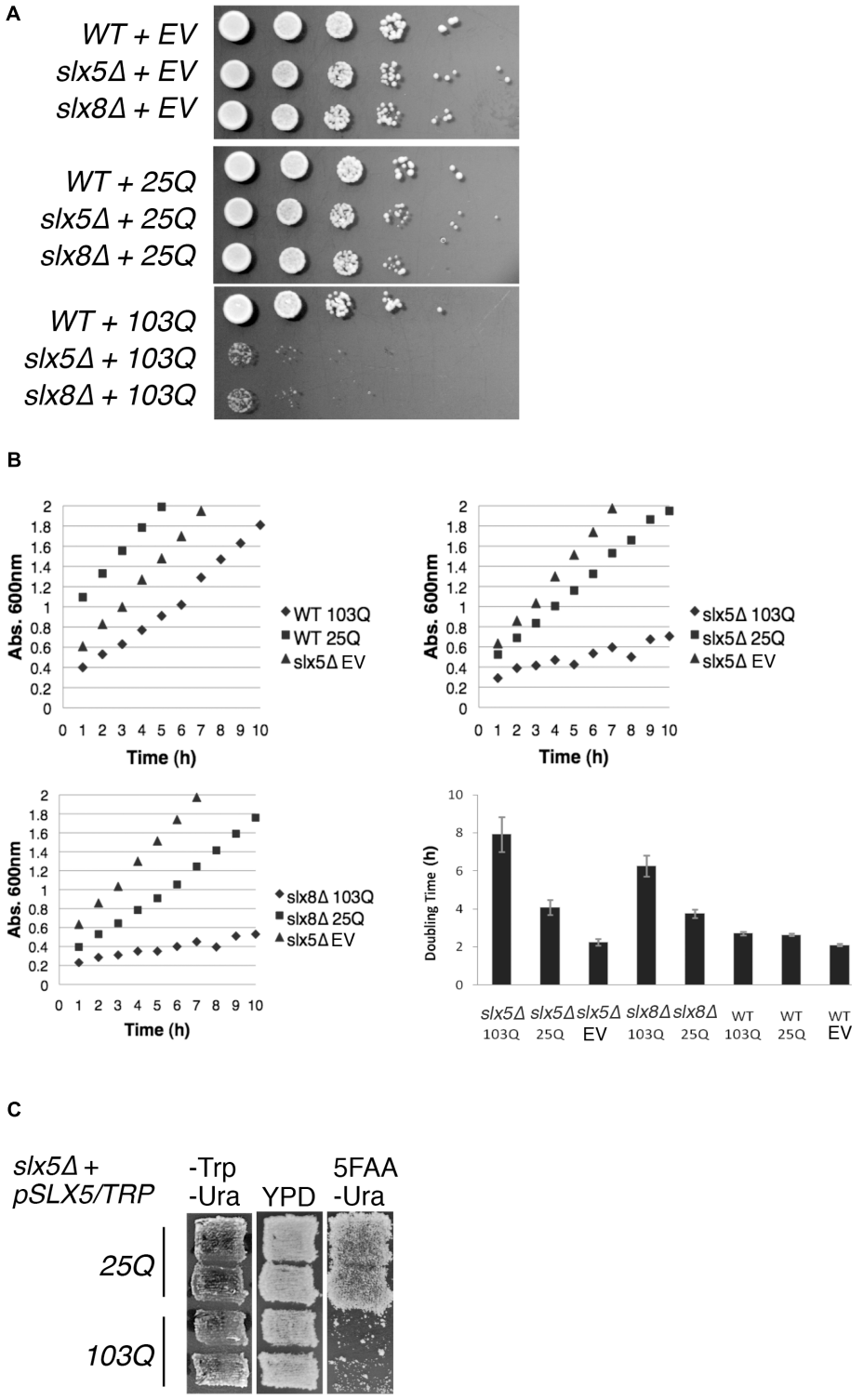

FIGURE 1 | STUbL subunits Slx5 and Slx8 alleviate toxicity of poly-Q expanded Htt. **(A)** WT, *slx5*Δ, and *slx8*Δ strains expressing Htt-25Q, Htt-103Q, or empty vector (EV) were grown to mid-logarithmic phase and 5 μl of 10-fold serial dilutions of each culture were spotted on SC-URA medium. Plates were incubated at 30°C for 3 days. **(B)** Yeast transformants in **A** and the indicated controls were grown overnight in 5 ml of SC-URA medium. Ten OD_{600} readings of cultures were recorded every hour until the OD_{600} reached ∼2.0. The average doubling times of four independent experiments were graphed with +/– standard error. EV (empty vector) **(C)** A shuffle strain, *slx5*Δ with *SLX5/TRP* plasmid (YOK 2990), was transformed with either Htt-25Q or Htt-103Q constructs. Transformants were patched in duplicate on selective medium (SC-TRP URA) and rich medium (YPD). Patches were then replica plated on SC-URA medium with 5FAA to counter-select against the *TRP1* marked plasmid.

RESULTS

Expression of Poly-Q Expanded Huntingtin Causes a Growth Defect in STUbL Mutants

STUbLs play an important role in the quality control of both SUMO-modified and non-sumoylated proteins (Wang et al., 2006; Xie et al., 2010; Westerbeck et al., 2014). Therefore, we tested our hypothesis that Slx5 and Slx8 are required for growth in the presence of a toxic, aggregation-prone model protein: exon 1 of poly-Q expanded Htt. Budding yeast is established as an exquisite model system for the study of poly-Q expanded proteins (Krobitsch and Lindquist, 2000) and hence we compared the effect of expression of Htt with either a 25-glutamine residue tract (Htt-25Q or 25Q) or an abnormal, aggregation-prone 103-glutamine tract (Htt-103Q or 103Q) on the growth properties of WT, *slx5*Δ, and *slx8*Δ cells. Isogenic WT, *slx5*Δ, and *slx8*Δ cells were transformed with low-copy (*CEN*) plasmids expressing GFP-tagged Htt-25Q or Htt-103Q under control of the constitutive GPD promoter (Krobitsch and Lindquist, 2000). The resulting transformants, or an empty vector control, were grown to mid-log phase and equal numbers of cells were serially diluted and spotted on selective media (**Figure 1A**). Though *slx5*Δ and *slx8*Δ cells initially formed smaller colonies than WT cells, no severe growth defect or lethality was apparent after 2–3 days of growth at 30°C for both the vector and Htt-25Q transformants (**Figure 1A** top and middle panel). In contrast, *slx5*Δ and *slx8*Δ cells transformed with the Htt-103Q construct showed a severe growth defect (**Figure 1A** bottom panel), supporting our hypothesis that STUbLs are required to relieve the growth-inhibiting properties of aggregation-prone poly-Q expanded Htt in budding yeast.

Next, we used liquid cultures to investigate the effect of Htt-25Q and Htt-103Q constructs on the growth of WT, *slx5*Δ, and *slx8*Δ. For this analysis, we compared the slopes of growth curves for WT, *slx5*Δ, and *slx8*Δ cells that were transformed with either Htt-25Q or Htt-103Q constructs. First, we found that WT cells transformed with Htt-25Q or Htt-103Q grew equally well as *slx5*Δ cells once established in logarithmic phase of growth (**Figure 1B** top left). Similarly, *slx5*Δ and *slx8*Δ cells transformed with either an empty vector or the Htt-25Q construct displayed similar growth characteristics (**Figure 1B**, top right and bottom left). In sharp contrast, the growth curves for *slx5*Δ and *slx8*Δ cells transformed with 103Q constructs revealed a significant growth delay with two- to four-fold increases in doubling times from 2 to 8 h (**Figure 1B** bottom right).

Further support that STUbL subunits, Slx5, and Slx8, have a role in preventing the Htt-103Q induced growth delay or toxicity was derived from a shuffle assay used to examine the ability of a *slx5*Δ STUbL mutant to grow in the presence of Htt-25Q or Htt-103Q. For this assay, a *slx5*Δ shuffle strain (*slx5*Δ*; SLX5/TRP1/CEN*) was transformed with Htt-25Q or Htt-103Q. All transformants showed similar growth characteristics and were patched in duplicate onto selective (-TRP -URA) media. Once patches grew in, cells were replica-plated on rich media (YPD) and then onto 5FAA media to counter-select against the *TRP*-marked WT *SLX5* plasmid (Toyn et al., 2000). After two successive replicas onto fresh 5FAA media, the majority of cells with the Htt-103Q construct failed to grow into colonies because they had lost *SLX5*. In stark contrast, *slx5*Δ cells harboring Htt-25Q grew unimpeded because growth of these cells did not depend on *SLX5* (**Figure 1C**). In summary, our results show that STUbLs provide an essential function for yeast cells growing in the presence of aggregation-prone, poly-Q expanded proteins.

Slx5 Reduces the Number of Poly-Q Expanded Huntingtin Aggregates

Intrigued by the poly-Q-induced growth defect in both STUbL mutants, we decided to compare the phenotypic manifestations of aggregation-prone Htt in WT, *slx5*Δ, and *slx8*Δ cells. We used a fluorescence microscope to collect images of WT, *slx5*Δ, and *slx8*Δ cells transformed with either the GFP-tagged 25Q construct or a GFP-tagged 103Q construct. We predicted, based on the results of our growth assays (**Figure 1**), that STUbL mutants would affect the localization of 103Q construct but not the 25Q construct. Consistent with previous results (Krobitsch and Lindquist, 2000), the Htt-25Q-GFP construct was evenly distributed across the nucleus and cytosol of WT, *slx5*Δ and *slx8*Δ cells (data not shown). In contrast, WT cells expressing Htt-103Q-GFP revealed a mixture of speckles, aggregates, and diffuse-staining cells (see **Supplementary Figure S1**). However, the majority of *slx5*Δ and *slx8*Δ cells expressing 103Q did not reveal a GFP signal as these cells were dead, as determined by a vital stain that differentiates live and dead cells (**Supplementary Figure S1**). By comparison, WT cells expressing 103Q contained less than 5% of dead or dying cells in the culture. These results also show that constitutive expression of 103Q, unlike 25Q, results in lethality of STUbL mutants. These data are consistent with our growth assays (**Figures 1A–C**) and support our conclusion that STUbLs fulfill an essential role in preventing cytotoxicity due to poly-Q expanded proteins such as Htt-103Q.

The Htt-103Q-induced lethality in *slx5*Δ strain impeded our microscopic analysis of Htt toxicity in STUbL mutants and hence we assayed the effect of plasmid-borne *SLX5* on the phenotype of 103Q aggregates in WT cells. We reasoned that Slx5, owing to it's quality-control functions, may alter the aggregation or distribution of Htt aggregates in WT cells. WT cells were transformed with GFP-tagged 103Q and either a *SLX5 CEN* plasmid (under control of its own promoter on a low-copy *CEN* vector) or an empty control vector. The transformants were grown to mid-logarithmic phase in selective media and 103Q aggregates were analyzed using fluorescence microscopy (**Figure 2A**). We determined that the incidence of 103Q aggregates was reduced by almost 14-fold while the number of diffuse-staining cells increased by at least twofold with plasmid borne *SLX5* (**Figure 2B**).

Htt has been reported to reside both in the cytosol as well as the nucleus, but the majority of Htt aggregates are observed to form in the cytosol (Davies et al., 1997; Krobitsch and Lindquist, 2000). The nuclear localization of Slx5 and Slx8 (Cook et al., 2009) and the lethality of Htt103Q in *slx5*Δ and *slx8*Δ strains prompted us to further investigate the role

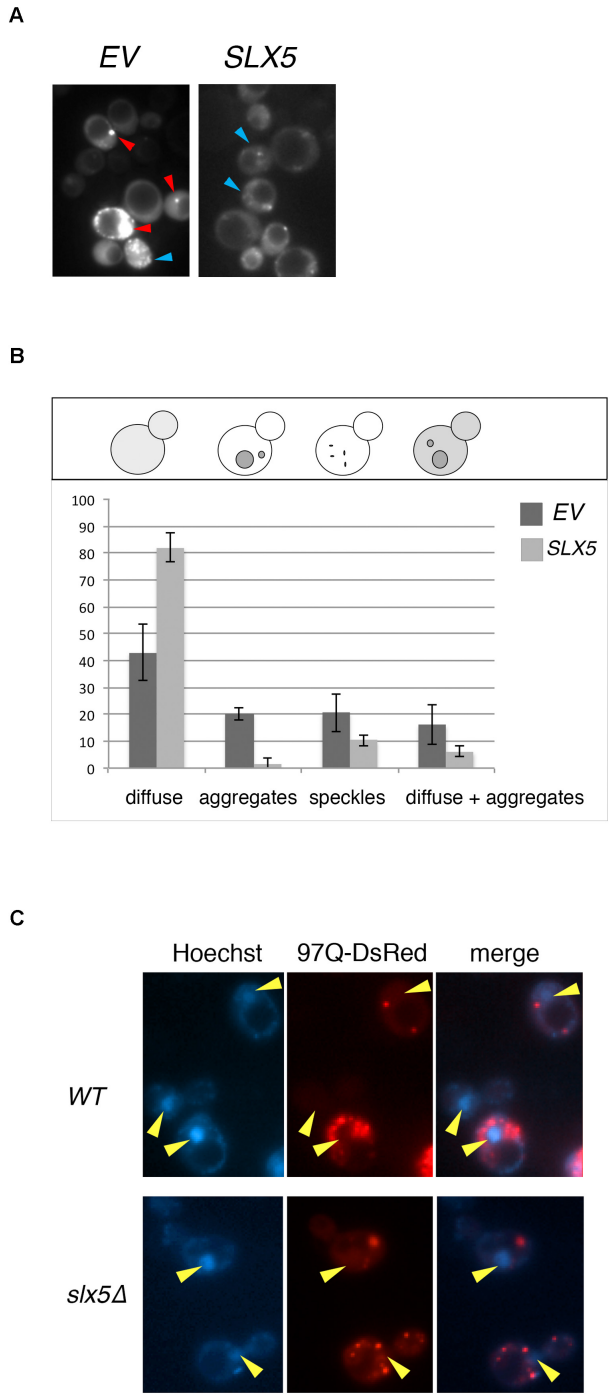

FIGURE 2 | Plasmid-borne SLX5 reduces aggregates of poly-Q expanded huntingtin. **(A)** Representative images of Htt-103Q in WT cells with and without an *SLX5/CEN* plasmid. Example of aggregates (clearly defined, bright cytoplasmic structures – red arrow-heads) and speckles (multiple small, not clearly defined cytoplasmic granules – blue arrow-heads) **(B)** Quantitation of phenotypes observed in 2A. WT strain expressing Htt-103Q-GFP alone (YOK 2842) or Htt-103Q-GFP with *SLX5* (YOK 2843) were grown to mid-logarithmic phase in selective medium. Images of 103Q diffuse staining, aggregates, and speckles in the indicated strains were recorded and then quantitated. Average counts for three independent experiments were graphed +/– standard

(Continued)

FIGURE 2 | Continued

deviation. Y-axis: percent of cells (n = 100/experiment). Y-axis: phenotypes scored **(C)** Aggregates of poly-Q expanded Htt are localized in the cytoplasm. WT and *slx5*Δ strains transformed with GAL-Htt-97Q-DsRed (YOK 3112 and YOK 3114) were grown overnight in SC-TRP medium with 2% raffinose. Cultures were diluted to ∼0.2 OD in a fresh medium with 2% galactose and incubated for an additional 16 h for expression of Htt-97Q-DsRed prior to imaging Htt aggregates using a fluorescence microscope. Nuclei were stained with Hoechst dye. Merged images indicate the absence of Htt-97Q aggregates in nuclei (yellow arrow-heads).

of STUbLs in the localization of Htt. For this analysis, we transiently expressed 97Q-DsRed under control of the strong inducible *GAL promoter* in WT and the *slx5*Δ mutant. This transient expression prevented the cytotoxicity associated with constitutive expression of aggregation-prone Htt in *slx5*Δ strains. After galactose induction, we imaged the nuclei of live WT and *slx5*Δ cells were stained with Hoechst dye (33342). In both WT and *slx5*Δ cells (n > 200), Htt aggregates or speckles were solely observed in the cytosol. A low level of diffusely staining 97Q-DsRed was evenly distributed between the cytosol and the nucleus of WT and did not appear to be enriched in either compartment. A similar localization pattern for 97Q-DsRed to that in WT cells was observed in the *slx5*Δ cells (**Figure 2C**). Based on these results we propose that 97Q, under the conditions employed, does not readily form large aggregates in the nuclei of yeast cells.

Regulation of Transcriptional Activity of Htt by Slx5 and RNF4

It was previously reported that poly-Q expanded Htt, in the absence of a Gal4-DNA-binding fusion (BD), induces the expression of reporter genes in a two-hybrid reporter assay (Atanesyan et al., 2012). This transcriptional auto-activation was directly related to the length of the poly-glutamine tract in Htt (Atanesyan et al., 2012). Therefore, we determined the effect of Slx5 on this poly-Q dependent transcriptional activity. Htt-25Q and Htt-55Q were fused to the Gal4 activation domain (AD) and assayed for the auto-activation of each construct in the presence or absence of BD-Slx5 or just BD. Consistent with published data (Atanesyan et al., 2012), all AD fusions of Htt, by themselves, induced expression of both a *HIS3* and a *lacZ* reporter gene, indicating that both 25Q and 55Q associate with the Gal4-UAS independent of a BD (**Figure 3A**). We used AD-Htt-25Q and AD-Htt-55Q to avoid the potential toxicity associated with AD-Htt-97Q. Auto-activation of the *HIS3* reporter gene was scored using a growth assay, transformed cells where diluted and spotted on media with (*SD*-Trp-Leu) or without histidine (*SD*-Trp-Leu-His). Concomitantly, auto-activation of the *lacZ* reporter was quantitated using ONPG assays that were performed in triplicate. Intriguingly, when the AD-Htt constructs were paired with BD-Slx5, the Htt-induced auto-activation was reduced to background levels (**Figure 3A**). To confirm that the reduction of the Htt-induced transcriptional auto-activation is not due to the decreased expression of Htt 25Q and Htt 55Q in the presence of

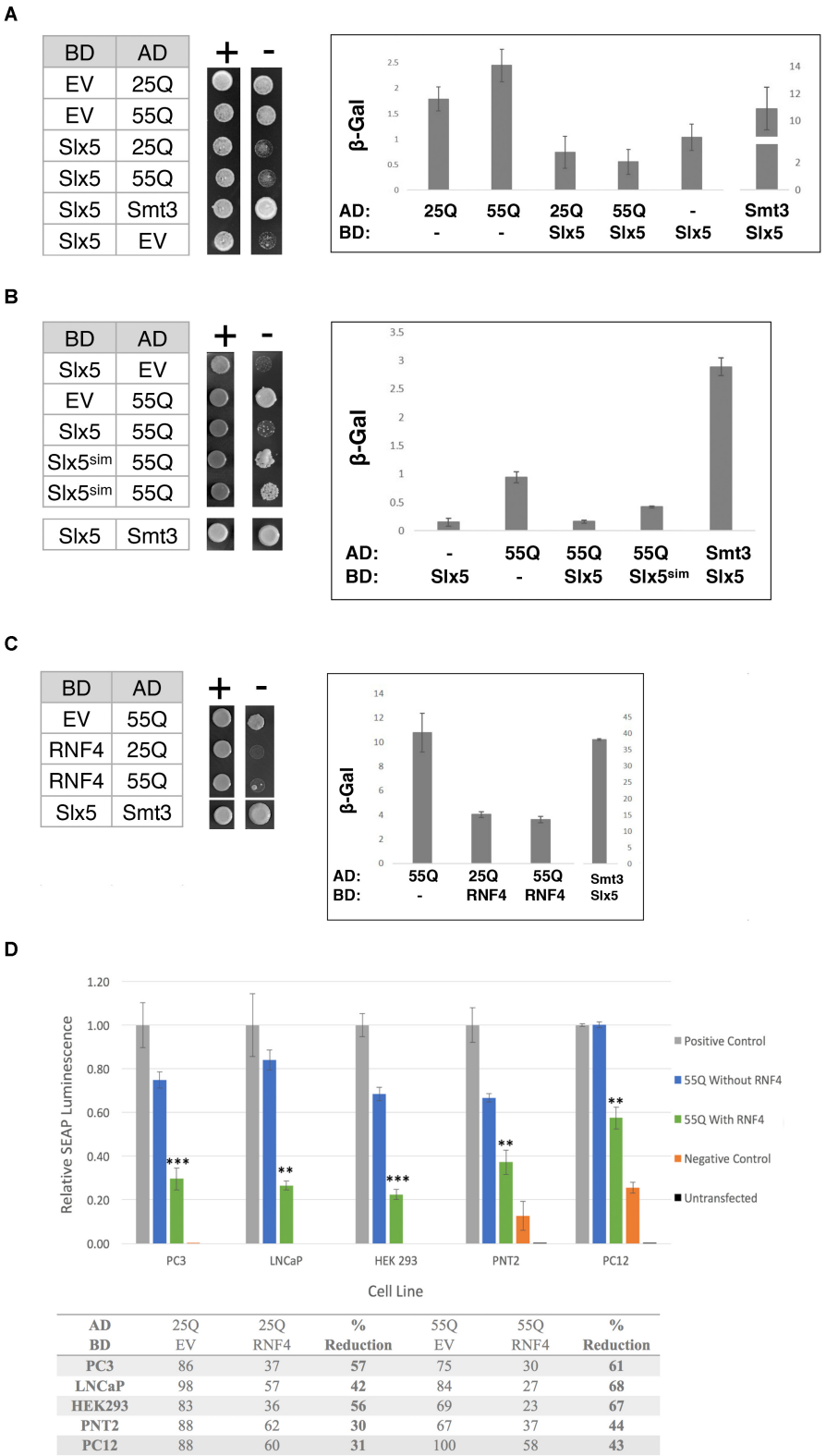

AD / BD	25Q EV	25Q RNF4	% Reduction	55Q EV	55Q RNF4	% Reduction
PC3	86	37	57	75	30	61
LNCaP	98	57	42	84	27	68
HEK293	83	36	56	69	23	67
PNT2	88	62	30	67	37	44
PC12	88	60	31	100	58	43

FIGURE 3 | The STUbL subunit Slx5 reduces the transcriptional auto-activation of poly-Q expanded Htt. **(A)** Yeast two-hybrid strain pJ694α was co-transformed with the indicated AD and BD plasmids. 1 OD of overnight-grown cells were diluted 100-fold and 5 μl of each cell suspension was spotted on SC-TRP LEU for growth control and SC-TRP LEU HIS to assess activation of the *HIS3* reporter gene. Transcriptional activation was also scored by quantification of β-galactosidase

(Continued)

FIGURE 3 | Continued
activity using ONPG assays (error bar – *SD*). **(B)** Effect of $Slx5^{sim}$ expression on the repression of poly-Q expanded Htt auto-activation as indicated by growth on SC-TRP LEU HIS medium and β-galactosidase assays. **(C)** Expression of the human *SLX5* ortholog RNF4 represses the transcriptional activity of poly-Q expanded Htt. To assess activation of the *lacZ* reporter gene in the indicated strains β-galactosidase units of strains were determined and graphed +/– standard deviation. **(D)** RNF4 significantly reduces the transcriptional activation of Htt in mammalian cells. Mammalian two hybrid analysis of PC3, LNCaP, HEK 293, PNT2, and PC12 cells [$n = 3$]. Reporter gene auto-activation of 25Q and 55Q Htt was assessed by transfection of pM-EV (empty vector) and pVP16-Htt. Where indicated, pM-RNF4 was cotransfected with 25Q or 55Q Htt to measure RNF4's inhibitory function. Values of relative SEAP luminescence for 55Q are graphed as shown and values for both 25Q and 55Q are shown in the table below the graph. Assay results were normalized to the positive control. Error bars represent standard deviation. $^{**}p < 0.01$, $^{***}p < 0.001$.

BD-SLX5, we tested the expression of AD-Htt 25Q and AD-Htt-55Q by Western blotting (**Supplementary Figure S3**). The result shows that the steady state levels of both Htt-25Q and Htt-55Q were not affected by *BD-SLX5*.

Next we asked if the suppression of AD-Htt reporter gene activation was dependent on the SIMs in Slx5. We combined a SIM mutant of Slx5 that fails to interact with SUMO (BD-$Slx5^{sim}$) with AD-55Q and assessed the auto-activation properties of our poly-Q Htt constructs on the two reporters using growth and quantitative ONPG assays. We found that $Slx5^{sim}$ reduced the auto-activation of the AD-55Q construct significantly less than WT Slx5 (**Figure 3B**, ONPG assay). This data suggests that SUMO-binding may support the ability of Slx5 to suppress the transcriptional activity of AD-Htt. However, SUMO-binding of Slx5 may not be a steadfast requirement to reduce Htt toxicity because the $Slx5^{sim}$ mutant can still suppress the Htt-103Q growth phenotype (**Supplementary Figure S2**).

To determine whether ability of Slx5 to repress auto-activation of poly-Q expanded Htt is evolutionarily conserved, we tested mammalian BD-RNF4 in combination with AD-25Q and AD-55Q. Consistent with results for Slx5, RNF4 also repressed the auto-activation activity of AD-25Q and AD-55Q constructs in our reporter assay (**Figure 3C**). In the presence of RNF4, the auto-activation activity of AD-25Q and AD-55Q was reduced threefold, when compared to AD-55Q alone. These results strongly support a role for RNF4, and other STUbLs, in counteracting the aggregation of transcriptionally active Htt and possibly other poly-Q expanded proteins associated with neurodegenerative diseases.

Finally, we tested whether RNF4 curbs the transcriptional activity of aggregation-prone proteins in a mammalian tissue culture model of Huntington's disease, employing a mammalian Matchmaker (2-hybrid) assay. For this approach, both Htt-25Q and Htt-55Q were cloned into the pVP16AD Gal4-activation domain vector and co-transformed with the reporter plasmid pG5SEAP into 5 separate cell lines (PC3, LNCaP, HEK293, PNT2, and PC12). Consistent with our finding in yeast, all mammalian cell lines recapitulated the Htt-dependent transcription of the pG5SEAP reporter (**Figure 3D** – blue bars). Next, reporter gene activation was assayed in the presence of BD-RNF4. Mammalian two-hybrid analysis in all cell lines displayed a significant decrease in the transcriptional activation of 25Q and 55Q Htt upon addition of RNF4 BD (**Figure 3D** green bars and table). The strength of RNF4's inhibitory effect ranged from 30–60% reduction on 25Q but was statistically significant for all 5 cell lines (Student's *T*-test), indicating that RNF4's inhibitory effect is consistent and reproducible. In all cell lines, 55Q mHtt displayed greater transcriptional reduction (40–70%), suggesting that this poly-Q expanded 55Q Htt is more amenable to RNF4's activity. Due to their neuronal origin, results from the PC12 cell two-hybrid are the most physiologically relevant model of Huntington's Disease. As an important indicator of specificity, reporter gene activation by a positive control construct (pM-pVP16), was not affected by transfection of RNF4 (data not shown). In summary, we have now shown that both in yeast and mammalian cells auto-activation of Htt can be significantly modulated due to the activity of STUbLs.

Slx5 Reduces Chromatin-Associated Htt Aggregates in Budding Yeast

To study the physiological relevance of our assays for transcriptional activity, we examined whether Htt-103Q associates with chromatin using subcellular fractionation of whole-cell lysates after overexpression of nuclear targeted Htt-25Q-NLS-GFP or Htt-103Q-NLS-GFP. We assayed levels of Htt in whole-cell extracts, soluble fractions, and chromatin (**Figure 4A**). As expected, both aggregated (high-molecular weight) and non-aggregated (53 kD, monomer) forms of Htt-103Q, but not Htt-25Q, were clearly detectable in the chromatin fraction, indicating that both aggregated and non-aggregated Htt-103Q associate with chromatin.

To examine the role of *SLX5* in modulating chromatin bound Htt-103Q, we assayed levels of Htt-103Q-NLS-GFP in the presence or absence of plasmid-borne *SLX5* (**Figures 4B–E**). Consistent with the microscopy of Htt-103Q-GFP expressing cells (**Figure 2B**), the soluble, monomeric form of Htt-103Q (53 kDa) was increased with plasmid-borne *SLX5* (**Figures 4B,C**). Importantly, aggregated Htt in the chromatin fraction was reduced ∼3-fold ($p = 0.0262$) in the strain with plasmid borne *SLX5* (**Figures 4B,D**). In contrast, monomeric, chromatin-bound Htt-103Q (53 kDa) remained similar in both strains (**Figures 4B,E**). These data show that increased expression of *SLX5* specifically reduces Htt-103Q aggregates in chromatin. We propose that STUbLs contribute to reducing chromatin-associated Htt aggregates.

Identification of Htt-Altered Transcripts Modulated by a STUbL in Yeast

The reduced association of aggregated Htt-103Q-NLS with chromatin in the presence of plasmid-borne *SLX5* (**Figure 4B**) led us to postulate that Slx5 curbs the abnormal transcriptional activities induced by Htt-103Q-NLS. Hence, we performed genome-wide RNA-seq analysis to examine the transcriptome

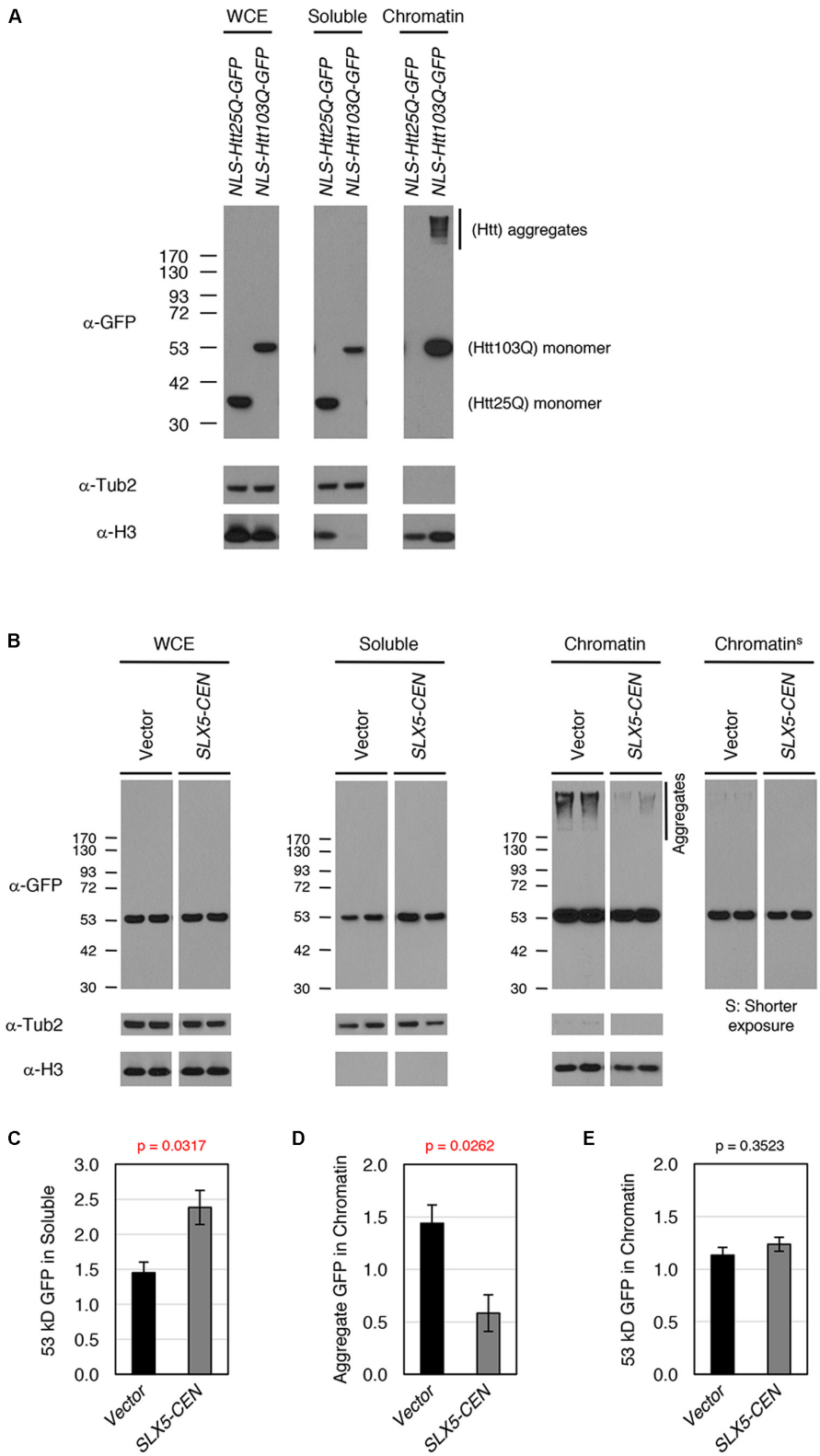

FIGURE 4 | Slx5 reduces the level of chromatin associated Htt103Q aggregates. **(A)** Htt103Q, but not Htt25Q, associates with chromatin. Whole cell extracts (WCEs) prepared from equal numbers of cells expressing GFP-tagged Htt25Q-NLS or Htt103Q-NLS from a *GAL* promoter were fractionated into soluble and chromatin fractions. Htt25Q-NLS-GFP or Htt103Q-NLS-GFP levels in each fraction were monitored by western blot analysis with anti-GFP antibody. Tub2 and

(Continued)

FIGURE 4 | Continued
histone H3 were used as markers for soluble and chromatin fractions, respectively. **(B)** WCEs prepared from equal numbers of cells expressing Htt103Q-NLS-GFP with (*SLX5-CEN*) or without (Vector) were fractionated into soluble and chromatin fractions as described in **A**. Htt103Q-NLS-GFP levels were monitored by western blot analysis with anti-GFP antibody. Three independent transformants were assayed and shown are the results from two of these. **(C)** Quantification of the 53 kD GFP signals in soluble fraction from 4B. The 53 kD GFP was normalized using Tub2 levels in soluble fraction. The graph represents the mean of three independent clones with SEM. *P*-value is 0.0317. **(D)** Quantification of the aggregate GFP signals in chromatin fraction from 4B. The aggregate GFP signal was normalized using H3 levels in chromatin fraction. The graph represents the mean of three independent transformants with SEM. *P*-value is 0.0262. **(E)** Quantification of the 53 kD GFP signals in chromatin fraction from 4B. The 53 kD GFP (shorter exposure) was normalized using H3 levels in chromatin fraction. The graph represents the mean of three independent transformants with SEM. *P*-value is 0.3523.

of four strains expressing either Htt-25Q-NLS or Htt-103Q-NLS with or without plasmid-borne *SLX5*. Consistent with the effect of Htt-103Q on transcription, our results showed that the expression of > 50% of all yeast genes (3438 genes) was altered in the presence of Htt-103Q-NLS when compared to Htt-25Q-NLS with empty vector (**Figure 5A**, 25Q [V] vs. 103Q [V]). Of the 3438 genes affected by Htt-103Q-NLS, 48.6% of the genes were up-regulated and 51.4% were down-regulated. These results show that chromatin associated Htt-103Q-NLS affects global transcription in budding yeast.

We next analyzed the effect of plasmid-borne *SLX5* on the transcriptome of cells expressing Htt-25Q-NLS or Htt-103Q-NLS. Our RNA-seq data showed that *SLX5* had a minimal effect on the transcriptome of cells expressing Htt-25Q-NLS as only 33 genes were differentially expressed (25Q [V] vs. 25Q [*SLX5*]). In contrast to this, plasmid-borne *SLX5* affected the transcription of 398 genes in cells expressing Htt-103Q-NLS when compared to Htt-103Q-NLS without *SLX5* (**Figure 5A**, 103Q [V] vs. 103Q [*SLX5*]). The majority of the 398 genes encode for proteins that reside in the cytoplasm (37%), nucleus (19%), or mitochondria (14%) (**Figure 5B** and **Supplementary Table S4**). Of the 398 genes that were significantly altered by plasmid-borne *SLX5*, 66% (261) genes were upregulated and 34% (137) genes were down-regulated (**Supplementary Table S2**). We observed two distinctive characteristics on the transcriptome of Htt-103Q-NLS with and without plasmid-borne *SLX5* (**Figure 5C**). First, for 99.4% (361 out of 363) of *SLX5*-affected genes, the effect of added Slx5 was inversely correlated with that of 103Q (**Supplementary Table S2** and **Figure 5A**). Plasmid-borne *SLX5* upregulated the expression of 68.0% (247) of the genes that were downregulated by Htt-103Q-NLS, and downregulated the expression of 31.4% (114) of genes that were upregulated by Htt-103Q-NLS (**Figure 5A**). For example, expression of YAL008W was down-regulated by Htt-103Q-NLS, and up-regulated by plasmid-borne *SLX5*. In contrast, expression of YAL014C was up-regulated by Htt-103Q-NLS, and down-regulated by plasmid-borne *SLX5*. Only two genes (YDL182W and YGR092W) were an exception to this pattern (**Supplementary Table S2**). A second distinctive characteristic of the transcription profiles show that about 25% of the genes that are affected by plasmid-borne *SLX5* are neighbors or adjacent to each other on the chromosome (e.g., YBR052C, YBR053C, and YBR054W) (**Supplementary Table S3**). The RNA sequencing data generated in this study have been deposited in NCBI's Gene Expression Omnibus (Barrett et al., 2013) and are accessible through GEO Series accession number GSE115990.

To confirm the transcriptome data from RNA-seq, we performed RT-PCR to assay the transcription of a subset of Htt-103Q-NLS/Slx5 modulated genes such as *YDL223C/HBT1, YPL186C/UIP4,* and *YOR339C/UBC11* (**Figure 5D**). Consistent with our RNA-seq data, we found that expression of *YDL223C/HBT1* and *YPL186C/UIP4* is down-regulated by Htt-103Q-NLS, and up-regulated by plasmid-borne *SLX5* (Down-Up). In contrast, *YOR339C/UBC11* is up-regulated by Htt-103Q-NLS, and down-regulated by plasmid-borne *SLX5* (Up-Down). In agreement with the RNA-seq data the expression of *ACT1* was not significantly affected when assayed by RT-PCR. In summary, our data shows that chromatin-associated Htt-103Q-NLS affects global transcriptional in budding yeast. Most importantly, we define a role for Slx5 in modulating the aberrant transcriptional activity, induced by chromatin-associated Htt-103Q-NLS.

DISCUSSION

In this study we show, for the first time, that STUbLs are required to prevent the toxicity associated with an aggregation-prone protein namely poly-Q expanded Htt and define a functional role for STUbLs in counteracting the toxic effects of Htt-103Q expression. Using reporter gene assays we determined that Slx5 and RNF4 reduce the transcriptional activity of Htt in yeast and human cells, respectively. For example, Htt fused to the Gal4 activation domain (AD) auto-activates Gal4-regulated reporter genes. However, reporter gene activation by Htt-AD is reduced to background levels in the presence of BD-Slx5 or BD-RNF4. Most importantly, our results show that Slx5 reduces cytosolic and chromatin-associated Htt-103Q aggregates and modulates the transcriptome of cells expressing Htt-103Q. Taken together we provide evidence for a conserved role of STUbLs in preventing the accumulation of aggregating proteins such as Htt on chromatin and propose that STUbLs counteract the transcriptional effect of these aggregates in yeast and mammalian cells.

In the initial stages of our analysis of Htt in STUbL mutants, we focused on the cellular distribution and aggregates formed by aggregation-prone Htt in yeast. We detected aggregates, speckles, and diffuse-staining Htt in both WT and a yeast STUbL mutant, *slx5*Δ (**Supplementary Figure S1**). Due to its toxicity in STUbL mutants, we ultimately studied the effect of an extra plasmid-borne copy of *SLX5* in WT cells expressing Htt-103Q. Presence of the *SLX5* plasmids increased diffusely staining Htt in WT cells while reducing the incidence of Htt aggregates

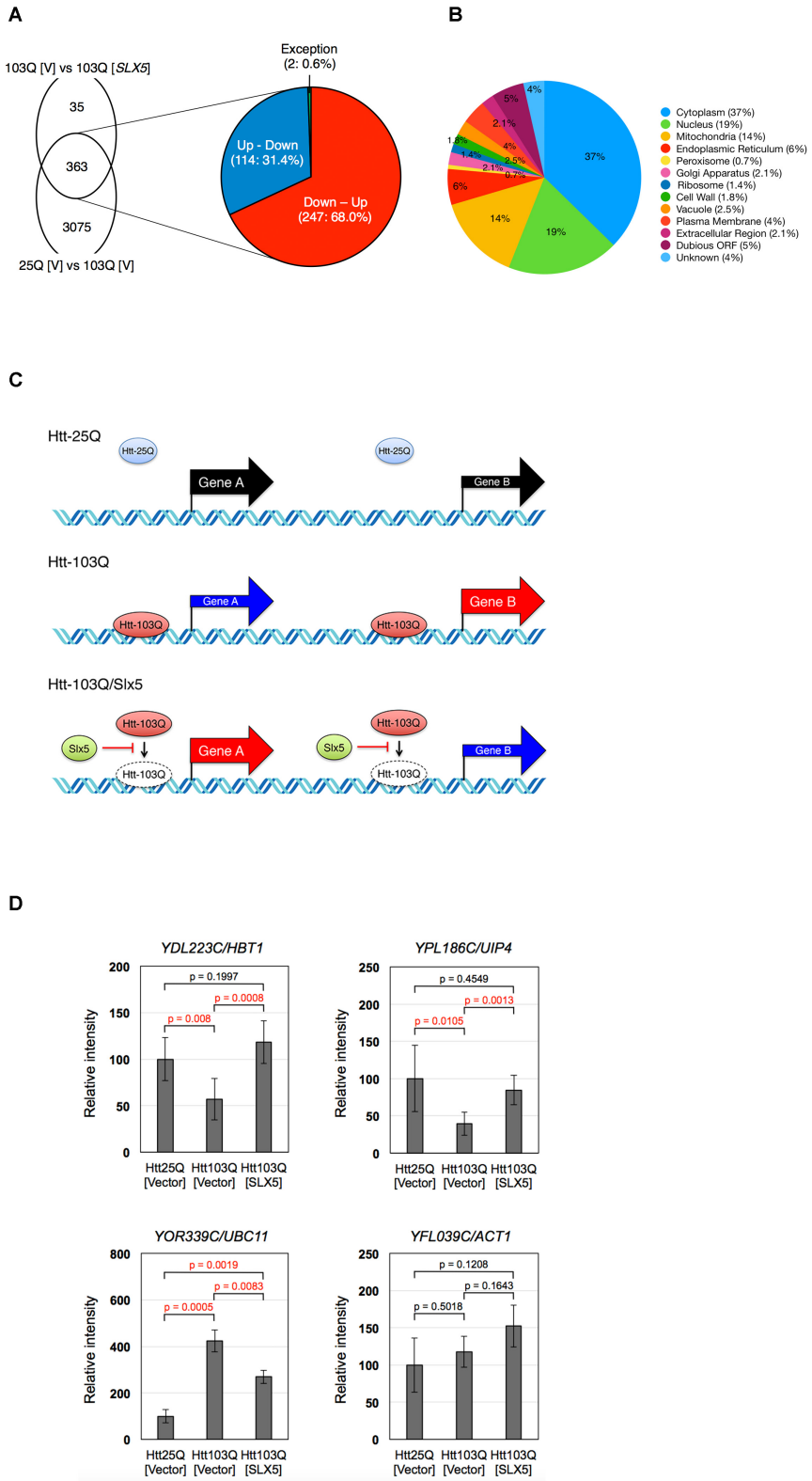

FIGURE 5 | Slx5 modulates the transcriptional activity due to expression of Htt-103Q-NLS. Depiction of 398 *SLX5* modulated genes identified by RNA sequencing. **(A)** RNA-seq analysis shows that Htt103Q-NLS leads to a global effect on the transcriptome as it affects the expression of 3438 genes (25Q [V] vs. 103Q [V]). Plasmid-borne *SLX5* affects the expression of 398 genes in Htt103Q-NLS cells (103Q [V] vs. 103Q [*SLX5*]) as shown in **Supplementary Table S2**. The overlap

(Continued)

FIGURE 5 | Continued
between Htt25Q-NLS and Htt103Q-NLS (25Q [V] vs. 103Q [V]) is 363 genes. The expanded view of **A** shows that expression of most of the 363 genes (99.4%) inversely correlates between 25Q [V] vs. 103Q [V] and 103Q [V] vs. 103Q [*SLX5*]. Expression of 247 of the 363 genes (68.0%) is down-regulated by Htt103Q, and this effect is reversed by plasmid-borne *SLX5* (Down – Up). Expression of 114 of the 363 genes (31.4%) is up-regulated by the Htt103Q, and this effect is reversed by plasmid-borne *SLX5* (Up – Down). **(B)** Subcellular localization of differentially expressed genes. The localization of proteins encoded by the 398 genes indicated in **Supplementary Table S2** was analyzed using cellular components assignment from the PANTHER Classification System and the Saccharomyces Genome Database. Pie chart shows a ratio of the genes placed into cellular component categories. Individual genes are listed in **Supplementary Table S4**. **(C)** Schematic of gene expression in Htt25Q-NLS and Htt103Q-NLS cells and the effect of plasmid-borne *SLX5* on the transcriptome of Htt103Q-NLS cells. Expression of genes A and B are downregulated and upregulated in Htt103Q-NLS cells relative to Htt25Q-NLS cells, respectively. Slx5 reduces the association of Htt with chromatin and this contributes to the reversal in gene expression such that gene A is upregulated and gene B is downregulated. **(D)** RT-PCR validation of gene expression analysis. Total RNAs were purified from strains expressing either Htt25Q-NLS or Htt103Q-NLS from a *GAL* promoter for 4 h with or without plasmid-borne *SLX5*. RT-PCR analyses was performed using the same samples used for the RNA-seq. Relative intensities are reported as the mean ± *SD* of three biological repeats. Reactions for *YDL223C/HBT1* and *YPL186C/UIP4* were performed in duplicate. *N* = 3 for *YOR339C/UBC11* and *YFL039C/ACT1*, *N* = 6 for *YDL223C/HBT1* and *YPL186C/UIP4*.

(**Figures 2A,B**). However, we failed to detect a reproducible, STUbL-dependent, reduction of Htt by western blot analysis (for example **Supplementary Figure S3**). Previously it has been reported that the STUbL RNF4 is involved in the degradation of another poly-Q expanded protein, Atxn1 82Q (Guo et al., 2014). While our data are consistent with a re-distribution of Htt aggregate, we did not observe that Slx5 altered the steady-state levels of this aggregation-prone protein. One explanation for this may be that budding yeast cells do not disassemble the nuclear envelope, making it difficult to observe the effect of nuclear localized STUbLs on aggregates of Htt in the cytosol. We overcame this limitation in our yeast model by using nuclear-targeted Htt-103Q to assess both the transcriptional activity and the chromatin association of Htt in the presence or absence of *SLX5* (**Figure 3** and **Figure 4**).

First, using Gal4-based two-hybrid reporter assays, we were able to show that yeast Slx5 and human RNF4, both nuclear localized proteins, curb the transcriptional activity of Htt. Therefore, we predict that the role of RNF4 in mammalian cells is to dispel transcriptionally active Htt complexes rather than to degrade cytosolic Htt aggregates. However, at this point we cannot entirely exclude the possibility that Slx5 and RNF4 form repressive promotor-associated complexes see (Cubeñas-Potts and Matunis, 2013). Regarding the Gal4-AD-fusion of Htt, similar constructs have proven invaluable in defining the aberrant transcriptional activity of poly-Q expanded proteins. The most important observation in this regard is that the poly-Q domain is necessary and sufficient for both the targeting to the Gal4 UAS and reporter gene activation (Atanesyan et al., 2012). Furthermore, introduction of a poly-Q stretch into transcription factors increases their transcriptional activity. Even though we have not yet observed a direct, physical interaction between Htt and Slx5 (we predict a transient interaction involving Htt-associated proteins), our assays are consistent with an important role of Slx5 in counteracting nuclear activities of aggregation prone, chromatin associated proteins. The finding that a STUbL plays an important role in transcriptional regulation is not entirely surprising. Before it became known as a STUbL, RNF4 had already been identified as a co-regulator of androgen receptor-dependent transcription (Yan et al., 2002). Furthermore, RNF4 can act both as a transcriptional activator or a repressor depending on the proteins it interacts with (Fedele et al., 2000).

Second, using Gal-driven, nuclear-targeted 103Q constructs, we assessed the chromatin association of an aggregation-prone Htt construct. This time we were able to clearly document that an extra plasmid-borne copy of *SLX5* reduced the levels of chromatin-associated Htt (**Figure 4**). The association of Htt with DNA, transcription factor recognition elements, and transcription factors has previously been reported (Benn et al., 2008). STUbLs may provide a mechanism to counteract these inappropriate associations of Htt. For example, it is tempting to speculate that Slx5 recruits Cdc48/Ufd1/Npl4 (Cdc48-UN), a SUMO-targeted STUbL effector, to dislodge Htt from chromatin (Nie et al., 2012; Bergink et al., 2013). Cdc48 has also been identified in association with Htt aggregates and we are now studying the effect that Cdc48-UN plays in Htt-mediated transcriptional activation (Wang et al., 2008).

Finally, we have completed a global RNA sequencing study to identify those transcripts that are affected by nuclear-targeted Htt-103Q and modulated by an extra plasmid-borne copy of *SLX5*. Our transcriptome analysis revealed that *SLX5* counteracts transcriptional abnormalities of 398 genes induced by expression of 103Q-NLS. Dysregulated transcripts encode proteins localized throughout the cells, with the majority enriched in the cytoplasm (263) nucleus (33) and mitochondria (19). Functional categorization of the differentially transcribed genes showed that at least 22 are involved in transcription, transcriptional regulation, and RNA/DNA binding (*RTC3, RPA43, RPB7, BUD27, TFA2, SRB7, YAP7, MCM1, PHO4, MAP1, HSP31, SNF5, RPP1, TMA22, RPS27A, MRPL49, NHP2, RPL7A, RPL7B, MAP1, HST2,* and *CBC2*) (**Supplementary Table S4**). We posit that some of the transcriptionally active and chromatin-associated proteins identified in our study represent genuine STUbL targets. Additionally, several *SLX5*-modulated genes identified here have previously been described in other Htt studies [e.g., Glo2 (human HAGH1), ZTA1 (human zeta crystalline), Msb1, COA2, BUD22, ERG5, and TIR1], supporting a genuine role of STUbLs in counteracting huntingtin-mediated dysregulation (Willingham et al., 2003; Wolfe et al., 2014). We prefer a model in which Htt aggregates may contain both sumoylated and non-sumoylated proteins, including those listed above. STUbL-mediated ubiquitination could then result in the recruitment of the Cdc48-UN desegregase and the subsequent proteasomal degradation of ubiquitylated proteins in the aggregates (reviewed in Kerscher, 2016).

In summary, the STUbL/Htt assay is one of the first of its kind to assess the ability of RNF4 and other STUbLs to modulate the activity of transcriptionally active, aggregation-prone

proteins. This reporter assay should complement other sophisticated genetic tools used to study protein aggregation processes (Newby et al., 2017). Results from our reporter assays are consistent with biochemical and genome-wide transcriptome data and provide evidence for a role of STUbLs in preventing toxicity due to aggregation-prone Htt in the nucleus. Overall, our findings indicate that STUbLs can reduce the chromatin association and abnormal transcriptionally activity of Htt (or other aggregating proteins) and suggest that mammalian STUbLs may play neuroprotective functions in Huntington's Disease.

AUTHOR CONTRIBUTIONS

OK designed the study, drafted, wrote, and revised the manuscript, designed and completed the experiments, collected and interpreted the data, supervised the students and postdoc co-authors, approved the content for publication, and is accountable for all aspects of the work. KO, NP, and JP acquired, analyzed, and interpreted the data for the work, and revised the manuscript. GH analyzed and interpreted the data for the work. GS acquired, analyzed, and interpreted the data for the work. RL-M made substantial contributions to the conception and design of the work, and revised the manuscript. RB made substantial contributions to the analysis and interpretation of data for the work, and revised the manuscript. MB was involved in the study design, helped in writing the manuscript, revised the manuscript, supervised the data collection and interpretation, supervised the postdoc co-authors, approved the content for publication, and is accountable for all aspects of the work.

FUNDING

This research was supported by NSF grant MBC#1051970, Award No. 17-1 from the Commonwealth of Virginia's Alzheimer's and Related Diseases Research Award Fund (ARDRAF), and a Broderick Family/Goldman Sachs TDAP award to OK. KO and MB were supported by the Intramural Research Program of the National Cancer Institute, National Institutes of Health. Research support for W&M students was provided by the Bailey-Huston Research fund, Summer research fellowships and freshman research funds from the HHMI Science Education and Research program at William & Mary to GS, RL-M, GH, and a Charles Center Honors Fellowship to JP.

ACKNOWLEDGMENTS

We would like to thank all current and former members of the OK's and MB's laboratories, Tamara Golden for critical reading of the manuscript, Lidia Epp for assistance with sequencing, the Cyr lab for providing Htt25Q-NLS and Htt103Q-NLS plasmids, Alexis Sedgewick for strain construction, and Andrew Halleran. RNA sequencing was conducted at the Frederick National Laboratory for Cancer Research (FNLCR) at the CCR Sequencing Facility, NCI, NIH, Frederick, MD, United States.

SUPPLEMENTARY MATERIAL

The Supplementary Material for this article can be found online at: https://www.frontiersin.org/articles/10.3389/fgene.2018.00379/full#supplementary-material

FIGURE S1 | WT strain expressing Htt-103Q-GFP alone (YOK 2842) or Htt-103Q-GFP together with *SLX5* (YOK 2843) were grown to mid-logarithmic phase in selective medium. Images of yeast cells with diffuse staining 103Q-GFP, aggregates, and speckles were recorded, counted, and graphed. Additionally, we stained cells with the LIVE/DEAD Yeast Viability Kit (Thermo Fisher) to quantitate dead or dying cells in the culture (dead). Average counts for three independent experiments were graphed +/− standard deviation. Y-axis: percent of cells.

FIGURE S2 | The $slx5^{SIM}$ mutant suppresses lethality of Htt-103Q in *slx5*Δ. *slx5*Δ strain YOK821 expressing 103Q-Htt/URA3 was transformed with *SLX5* plasmid (BOK376), $slx5^{SIM}$ mutant (BOK463), and an empty vector (pRS425). Resulting transformants were struck to appropriate selective media and incubated for 3 days at 30°C.

FIGURE S3 | Steady-state protein levels of AD-25Q and AD-55Q are not grossly affected by expression of BD-Slx5. AD-25Q and AD-55Q were expressed in the presence or absence of BD-Slx5 in the yeast two-hybrid reporter strain. Proteins were extracted, separated by SDS–PAGE and western blotted with an antibody to the Gal4-AD or PGK, a loading control (Szymanski and Kerscher, 2013). EV – empty Gal4-AD vector expressing only Gal4-AD.

TABLE S1 | Strains used in this study.

TABLE S2 | Expression profiles of 398 genes regulated by an extra copy of *SLX5*. An extra copy of *SLX5* alters the expression profiles of 398 genes in the Htt103Q background (Htt103Q-NLS [Vector] vs. Htt103Q-NLS [*SLX5*]). 363 out of these 398 genes are also found to be differently expressed between Htt25Q-NLS and Htt103Q-NLS (Htt25Q[Vector] vs. Htt103Q[Vector]). Expression of most of the 363 genes (99.4%) is inversely correlation between Htt25Q [Vector] vs. Htt103Q [Vector] and Htt103Q [Vector] vs. Htt103Q [*SLX5*]. Only two genes do not exhibit this inverse relationship (Exceptions: YDL182W and YGR092W). Up- and down-regulated transcripts are shown in red and blue, respectively. Green shows 35 genes that are not detected the comparison between Htt-25Q and Htt-103Q (Htt25Q [Vector] vs. Htt103Q [Vector]).

TABLE S3 | List of clustering genes. The 398 genes, differently expressed between Htt103Q [Vector] and Htt103Q [*SLX5*], are analyzed. We used systematic name to search the neighboring genes. Up- and down-regulated profiles are shown in red and blue, respectively.

TABLE S4 | Cellular Components Categories of genes modulated by Slx5. The number of individual genes placed into cellular component categories is listed in the table. Individual genes are colored red (increased expression in cells with Htt103Q-NLS and Slx5) or blue (decreased expression in cells with Htt103Q-NLS and Slx5), black (only one data-point – compare **Supplementary Table S2**). Note that some genes analyzed are part of multiple cellular component categories.

REFERENCES

Ahner, A., Gong, X., Schmidt, B. Z., Peters, K. W., Rabeh, W. M., Thibodeau, P. H., et al. (2013). Small heat shock proteins target mutant cystic fibrosis transmembrane conductance regulator for degradation via a small ubiquitin-like modifier-dependent pathway. *Mol. Biol. Cell* 24, 74–84. doi: 10.1091/mbc.E12-09-0678

Alonso, A., D'Silva, S., Rahman, M., Meluh, P. B., Keeling, J., Meednu, N., et al. (2012). The yeast homologue of the microtubule-associated protein Lis1 interacts with the sumoylation machinery and a SUMO-targeted ubiquitin ligase. *Mol. Biol. Cell* 23, 4552–4566. doi: 10.1091/mbc.E12-03-0195

Amberg, D. C., Burke, D. J., and Strathern, J. N. (2005). *Methods in Yeast Genetics: A Cold Spring Harbor Laboratory Course Manual*. New York, NY: CSHL Press.

Arrasate, M., Mitra, S., Schweitzer, E. S., Segal, M. R., and Finkbeiner, S. (2004). Inclusion body formation reduces levels of mutant huntingtin and the risk of neuronal death. *Nature* 431, 805–810. doi: 10.1038/nature02998

Atanesyan, L., Günther, V., Dichtl, B., Georgiev, O., and Schaffner, W. (2012). Polyglutamine tracts as modulators of transcriptional activation from yeast to mammals. *Biol. Chem.* 393, 63–70. doi: 10.1515/BC-2011-252

Au, W.-C., Crisp, M. J., DeLuca, S. Z., Rando, O. J., and Basrai, M. A. (2008). Altered dosage and mislocalization of histone H3 and Cse4p lead to chromosome loss in *Saccharomyces cerevisiae*. *Genetics* 179, 263–275. doi: 10.1534/genetics.108.088518

Barrett, T., Wilhite, S. E., Ledoux, P., Evangelista, C., Kim, I. F., Tomashevsky, M., et al. (2013). NCBI GEO: archive for functional genomics data sets–update. *Nucleic Acids Res.* 41, D991–D995. doi: 10.1093/nar/gks1193

Bauer, P. O., Hudec, R., Goswami, A., Kurosawa, M., Matsumoto, G., Mikoshiba, K., et al. (2012). ROCK-phosphorylated vimentin modifies mutant huntingtin aggregation via sequestration of IRBIT. *Mol. Neurodegen.* 7:43. doi: 10.1186/1750-1326-7-43

Benn, C. L., Sun, T., Sadri-Vakili, G., McFarland, K. N., DiRocco, D. P., Yohrling, G. J., et al. (2008). Huntingtin modulates transcription, occupies gene promoters in vivo, and binds directly to DNA in a polyglutamine-dependent manner. *J. Neurosci.* 28, 10720–10733. doi: 10.1523/JNEUROSCI.2126-08.2008

Bergink, S., Ammon, T., Kern, M., Schermelleh, L., Leonhardt, H., and Jentsch, S. (2013). Role of Cdc48/p97 as a SUMO-targeted segregase curbing Rad51–Rad52 interaction. *Nat. Cell Biol.* 15, 526–532. doi: 10.1038/ncb2729

Butland, S. L., Devon, R. S., Huang, Y., Mead, C.-L., Meynert, A. M., Neal, S. J., et al. (2007). CAG-encoded polyglutamine length polymorphism in the human genome. *BMC Genomics* 8:126. doi: 10.1186/1471-2164-8-126

Cattaneo, E., Zuccato, C., and Tartari, M. (2005). Normal huntingtin function: an alternative approach to Huntington's disease. *Nat. Rev. Neurosci.* 6, 919–930. doi: 10.1038/nrn1806

Cook, C. E., Hochstrasser, M., and Kerscher, O. (2009). The SUMO-targeted ubiquitin ligase subunit Slx5 resides in nuclear foci and at sites of DNA breaks. *Cell Cycle* 8, 1080–1089. doi: 10.4161/cc.8.7.8123

Cubeñas-Potts, C., and Matunis, M. J. (2013). SUMO: a multifaceted modifier of chromatin structure and function. *Dev. Cell* 24, 1–12. doi: 10.1016/j.devcel.2012.11.020

Dasso, M. (2008). Emerging roles of the SUMO pathway in mitosis. *Cell Div.* 3:5. doi: 10.1186/1747-1028-3-5

Davies, S. W., Turmaine, M., Cozens, B. A., DiFiglia, M., Sharp, A. H., Ross, C. A., et al. (1997). Formation of neuronal intranuclear inclusions underlies the neurological dysfunction in mice transgenic for the HD mutation. *Cell* 90, 537–548. doi: 10.1016/S0092-8674(00)80513-9

Dorval, V., and Fraser, P. E. (2007). SUMO on the road to neurodegeneration. *Biochim. Biophys. Acta* 1773, 694–706. doi: 10.1016/j.bbamcr.2007.03.017

Dunah, A. W., Jeong, H., Griffin, A., Kim, Y. M., Standaert, D. G., Hersch, S. M., et al. (2002). Sp1 and TAFII130 transcriptional activity disrupted in early Huntington's disease. *Science* 296, 2238–2243. doi: 10.1126/science.1072613

Fedele, M., Benvenuto, G., Pero, R., Majello, B., Battista, S., Lembo, F., et al. (2000). A novel member of the BTB/POZ family, PATZ, associates with the RNF4 RING finger protein and acts as a transcriptional repressor. *J. Biol. Chem.* 275, 7894–7901. doi: 10.1074/jbc.275.11.7894

Geoffroy, M.-C., and Hay, R. T. (2009). An additional role for SUMO in ubiquitin-mediated proteolysis. *Nat. Rev. Mol. Cell Biol.* 10, 564–568. doi: 10.1038/nrm2707

Gerber, H. P., Seipel, K., Georgiev, O., Hofferer, M., Hug, M., Rusconi, S., et al. (1994). Transcriptional activation modulated by homopolymeric glutamine and proline stretches. *Science* 263, 808–811. doi: 10.1126/science.8303297

Guo, L., Giasson, B. I., Glavis-Bloom, A., Brewer, M. D., Shorter, J., Gitler, A. D., et al. (2014). A cellular system that degrades misfolded proteins and protects against neurodegeneration. *Mol. Cell* 55, 15–30. doi: 10.1016/j.molcel.2014.04.030

Guthrie, C., and Fink, G. R. (2002). *Guide to Yeast Genetics and Molecular and Cell Biology*. Cambridge, MA: Academic Press.

Guzzo, C. M., Berndsen, C. E., Zhu, J., Gupta, V., Datta, A., Greenberg, R. A., et al. (2012). RNF4-dependent hybrid SUMO-ubiquitin chains are signals for RAP80 and thereby mediate the recruitment of BRCA1 to sites of DNA Damage. *Sci. Signal.* 5:ra88. doi: 10.1126/scisignal.2003485

Hickey, C. M., and Hochstrasser, M. (2015). STUbL-mediated degradation of the transcription factor MATα2 requires degradation elements that coincide with corepressor binding sites. *Mol. Biol. Cell* 26, 3401–3412. doi: 10.1091/mbc.E15-06-0436

Hoeller, D., Hecker, C.-M., and Dikic, I. (2006). Ubiquitin and ubiquitin-like proteins in cancer pathogenesis. *Nat. Rev. Cancer* 6, 776–788. doi: 10.1038/nrc1994

Kerscher, O. (2007). SUMO junction-what's your function? New insights through SUMO-interacting motifs. *EMBO Rep.* 8, 550–555. doi: 10.1038/sj.embor.7400980

Kerscher, O. (2016). *SUMOylation*. Chichester: John Wiley & Sons, Ltd. doi: 10.1002/9780470015902.a0021849.pub2

Kerscher, O., Felberbaum, R., and Hochstrasser, M. (2006). Modification of proteins by ubiquitin and ubiquitin-like proteins. *Annu. Rev. Cell Dev. Biol.* 22, 159–180. doi: 10.1146/annurev.cellbio.22.010605.093503

Krobitsch, S., and Lindquist, S. (2000). Aggregation of huntingtin in yeast varies with the length of the polyglutamine expansion and the expression of chaperone proteins. *Proc. Natl. Acad. Sci. U.S.A.* 97, 1589–1594. doi: 10.1073/pnas.97.4.1589

Liu, B., and Shuai, K. (2008). Targeting the PIAS1 SUMO ligase pathway to control inflammation. *Trends Pharmacol. Sci.* 29, 505–509. doi: 10.1016/j.tips.2008.07.008

Lunkes, A., and Mandel, J. L. (1997). Polyglutamines, nuclear inclusions and neurodegeneration. *Nat. Med.* 16, 1201–1202. doi: 10.1038/nm1197-1201

Mi, H., Muruganujan, A., Casagrande, J. T., and Thomas, P. D. (2013). Large-scale gene function analysis with the PANTHER classification system. *Nat. Protoc.* 8, 1551–1566. doi: 10.1038/nprot.2013.092

Miller, J. H. (1972). *Experiments in Molecular Genetics*. New York, NY: Cold Spring Laboratory Press.

Mullen, J. R., and Brill, S. J. (2008). Activation of the Slx5-Slx8 ubiquitin ligase by poly-small ubiquitin-like modifier conjugates. *J. Biol. Chem.* 283, 19912–19921. doi: 10.1074/jbc.M802690200

Murakami, C., and Kaeberlein, M. (2009). Quantifying yeast chronological life span by outgrowth of aged cells. *J. Vis. Exp.* 27:e1156. doi: 10.3791/1156

Newby, G. A., Kiriakov, S., Hallacli, E., Kayatekin, C., Tsvetkov, P., Mancuso, C. P., et al. (2017). A genetic tool to track protein aggregates and control prion inheritance. *Cell* 171, 966.e18–979.e18. doi: 10.1016/j.cell.2017.09.041

Nie, M., Aslanian, A., Prudden, J., Heideker, J., Vashisht, A. A., Wohlschlegel, J. A., et al. (2012). Dual recruitment of Cdc48 (p97)-Ufd1-Npl4 ubiquitin-selective segregase by small ubiquitin-like modifier protein (SUMO) and ubiquitin in SUMO-targeted ubiquitin ligase-mediated genome stability functions. *J. Biol. Chem.* 287, 29610–29619. doi: 10.1074/jbc.M112.379768

Ohkuni, K., Takahashi, Y., Fulp, A., Lawrimore, J., Au, W.-C., Pasupala, N., et al. (2016). SUMO-targeted ubiquitin ligase (STUbL) Slx5 regulates proteolysis of centromeric histone H3 variant Cse4 and prevents its mislocalization to euchromatin. *Mol. Biol. Cell* 27, 1500–1510. doi: 10.1091/mbc.E15-12-0827

Perry, J. J. P., Tainer, J. A., and Boddy, M. N. (2008). A SIM-ultaneous role for SUMO and ubiquitin. *Trends Biochem. Sci.* 33, 201–208. doi: 10.1016/j.tibs.2008.02.001

Pringsheim, T., Wiltshire, K., Day, L., Dykeman, J., Steeves, T., and Jette, N. (2012). The incidence and prevalence of Huntington's disease: a systematic review and meta-analysis. *Mov. Disord.* 27, 1083–1091. doi: 10.1002/mds.25075

Prudden, J., Pebernard, S., Raffa, G., Slavin, D. A., Perry, J. J. P., Tainer, J. A., et al. (2007). SUMO-targeted ubiquitin ligases in genome stability. *EMBO J.* 26, 4089–4101. doi: 10.1038/sj.emboj.7601838

Prudden, J., Perry, J. J. P., Nie, M., Vashisht, A. A., Arvai, A. S., Hitomi, C., et al. (2011). DNA repair and global sumoylation are regulated by distinct Ubc9 noncovalent complexes. *Mol. Cell. Biol.* 31, 2299–2310. doi: 10.1128/MCB.05188-11

Sarge, K. D., and Park-Sarge, O.-K. (2009). Sumoylation and human disease pathogenesis. *Trends Biochem. Sci.* 34, 200–205. doi: 10.1016/j.tibs.2009.01.004

Schaffar, G., Breuer, P., Boteva, R., Behrends, C., Tzvetkov, N., Strippel, N., et al. (2015). Cellular toxicity of polyglutamine expansion proteins: mechanism of transcription factor deactivation. *Mol. Cell* 15, 95–105. doi: 10.1016/j.molcel.2004.06.029

Steffan, J. S., Kazantsev, A., Spasic-Boskovic, O., Greenwald, M., Zhu, Y. Z., Gohler, H., et al. (2000). The Huntington's disease protein interacts with p53 and CREB-binding protein and represses transcription. *Proc. Natl. Acad. Sci. U.S.A.* 97, 6763–6768. doi: 10.1073/pnas.100110097

Suhr, S. T., Senut, M.-C., Whitelegge, J. P., Faull, K. F., Cuizon, D. B., and Gage, F. H. (2001). Identities of sequestered proteins in aggregates from cells with induced polyglutamine expression. *J. Cell Biol.* 153, 283–294. doi: 10.1083/jcb.153.2.283

Sun, H., Leverson, J. D., and Hunter, T. (2007). Conserved function of RNF4 family proteins in eukaryotes: targeting a ubiquitin ligase to SUMOylated proteins. *EMBO J.* 26, 4102–4112. doi: 10.1038/sj.emboj.7601839

Szymanski, E. P., and Kerscher, O. (2013). Budding yeast protein extraction and purification for the study of function, interactions, and post-translational modifications. *J. Vis. Exp.* 30:e50921. doi: 10.3791/50921

Tatham, M. H., Geoffroy, M.-C., Shen, L., Plechanovová, A., Hattersley, N., Jaffray, E. G., et al. (2008). RNF4 is a poly-SUMO-specific E3 ubiquitin ligase required for arsenic-induced PML degradation. *Nat. Cell Biol.* 10, 538–546. doi: 10.1038/ncb1716

Toyn, J. H., Gunyuzlu, P. L., White, W. H., Thompson, L. A., and Hollis, G. F. (2000). A counterselection for the tryptophan pathway in yeast: 5-fluoroanthranilic acid resistance. *Yeast* 16, 553–560. doi: 10.1002/(SICI)1097-0061(200004)16:6<553::AID-YEA554>3.0.CO;2-7

Ulrich, H. D. (2008). The fast-growing business of SUMO chains. *Mol. Cell* 32, 301–305. doi: 10.1016/j.molcel.2008.10.010

Uzunova, K., Göttsche, K., Miteva, M., Weisshaar, S. R., Glanemann, C., Schnellhardt, M., et al. (2007). Ubiquitin-dependent proteolytic control of SUMO conjugates. *J. Biol. Chem.* 282, 34167–34175. doi: 10.1074/jbc.M706505200

van Wijk, S. J. L., Müller, S., and Dikic, I. (2011). Shared and unique properties of ubiquitin and SUMO interaction networks in DNA repair. *Genes Dev.* 25, 1763–1769. doi: 10.1101/gad.17593511

Vertegaal, A. C. O. (2010). SUMO chains: polymeric signals. *Biochem. Soc. Trans.* 38, 46–49. doi: 10.1042/BST0380046

Wang, Y., Meriin, A. B., Zaarur, N., Romanova, N. V., Chernoff, Y. O., Costello, C. E., et al. (2008). Abnormal proteins can form aggresome in yeast: aggresome-targeting signals and components of the machinery. *FASEB J.* 23, 451–463. doi: 10.1096/fj.08-117614

Wang, Z., Jones, G. M., and Prelich, G. (2006). Genetic analysis connects SLX5 and SLX8 to the SUMO pathway in *Saccharomyces cerevisiae*. *Genetics* 172, 1499–1509. doi: 10.1534/genetics.105.052811

Wang, Z., and Prelich, G. (2009). Quality control of a transcriptional regulator by SUMO-targeted degradation. *Mol. Cell. Biol.* 29, 1694–1706. doi: 10.1128/MCB.01470-08

Westerbeck, J. W., Pasupala, N., Guillotte, M., Szymanski, E., Matson, B. C., Esteban, C., et al. (2014). A SUMO-targeted ubiquitin ligase is involved in the degradation of the nuclear pool of the SUMO E3 ligase Siz1. *Mol. Biol. Cell* 25, 1–16. doi: 10.1091/mbc.E13-05-0291

Willingham, S., Outeiro, T. F., DeVit, M. J., Lindquist, S. L., and Muchowski, P. J. (2003). Yeast genes that enhance the toxicity of a mutant huntingtin fragment or alpha-synuclein. *Science* 302, 1769–1772. doi: 10.1126/science.1090389

Wolfe, K. J., Ren, H. Y., Trepte, P., and Cyr, D. M. (2014). Polyglutamine-rich suppressors of huntingtin toxicity act upstream of Hsp70 and Sti1 in spatial quality control of amyloid-like proteins. *PLoS One* 9:e95914. doi: 10.1371/journal.pone.0095914.s006

Xie, Y., Kerscher, O., Kroetz, M. B., McConchie, H. F., Sung, P., and Hochstrasser, M. (2007). The yeast Hex3.S*lx*8 heterodimer is a ubiquitin ligase stimulated by substrate sumoylation. *J. Biol. Chem.* 282, 34176–34184. doi: 10.1074/jbc.M706025200

Xie, Y., Rubenstein, E. M., Matt, T., and Hochstrasser, M. (2010). SUMO-independent in vivo activity of a SUMO-targeted ubiquitin ligase toward a short-lived transcription factor. *Genes Dev.* 24, 893–903. doi: 10.1101/gad.1906510

Yan, W., Hirvonen-Santti, S. J., Palvimo, J. J., Toppari, J., and Jänne, O. A. (2002). Expression of the nuclear RING finger protein SNURF/RNF4 during rat testis development suggests a role in spermatid maturation. *Mech. Dev.* 118, 247–253. doi: 10.1016/S0925-4773(02)00261-7

Yin, Y., Seifert, A., Chua, J. S., Maure, J.-F., Golebiowski, F., and Hay, R. T. (2012). SUMO-targeted ubiquitin E3 ligase RNF4 is required for the response of human cells to DNA damage. *Genes Dev.* 26, 1196–1208. doi: 10.1101/gad.189274.112

Zhang, C., Roberts, T. M., Yang, J., Desai, R., and Brown, G. W. (2006). Suppression of genomic instability by SLX5 and SLX8 in *Saccharomyces cerevisiae*. *DNA Repair.* 5, 336–346. doi: 10.1016/j.dnarep.2005.10.010

Conflict of Interest Statement: The authors declare that the research was conducted in the absence of any commercial or financial relationships that could be construed as a potential conflict of interest.

frontiers in Genetics

MINI REVIEW
published: 13 September 2018
doi: 10.3389/fgene.2018.00388

The Relationship Between Vitamin B6, Diabetes and Cancer

Chiara Merigliano[1], Elisa Mascolo[1], Romina Burla[1], Isabella Saggio[1,2] and Fiammetta Vernì[1]**

[1] Dipartimento di Biologia e Biotecnologie "C. Darwin," Sapienza Università di Roma, Rome, Italy, [2] Institute of Structural Biology, School of Biological Sciences, Nanyang Technological University, Singapore, Singapore

Pyridoxal 5′-phosphate (PLP), the active form of vitamin B6, works as cofactor in numerous enzymatic reactions and it behaves as antioxidant molecule. PLP deficiency has been associated to many human pathologies including cancer and diabetes and the mechanism behind this connection is now becoming clearer. Inadequate intake of this vitamin increases the risk of many cancers; furthermore, PLP deprivation impairs insulin secretion in rats, whereas PLP supplementation prevents diabetic complications and improves gestational diabetes. Growing evidence shows that diabetes and cancer are correlated not only because they share same risk factors but also because diabetic patients have a higher risk of developing tumors, although the underlying mechanisms remain elusive. In this review, we will explore data obtained in *Drosophila* revealing the existence of a connection between vitamin B6, DNA damage and diabetes, as flies in the past decade turned out to be a promising model also for metabolic diseases including diabetes. We will focus on recent studies that revealed a specific role for PLP in maintaining chromosome integrity and glucose homeostasis, and we will show that these aspects are correlated. In addition, we will discuss recent data identifying PLP as a putative linking factor between diabetes and cancer.

Keywords: vitamin B6, pyridoxal 5′- phosphate, diabetes, chromosome aberrations, *Drosophila*, AGEs

OPEN ACCESS

Edited by:
Maria Grazia Giansanti, Istituto di Biologia e Patologia Molecolari (IBPM), Consiglio Nazionale Delle Ricerche (CNR), Italy

Reviewed by:
Roberto Contestabile, Università degli Studi di Roma La Sapienza, Italy
Fabrizio Barbetti, Università degli Studi di Roma Tor Vergata, Italy

****Correspondence:***
Isabella Saggio
Isabella.saggio@Uniroma1.it
Fiammetta Vernì
Fiammetta.verni@Uniroma1.it

Specialty section:
This article was submitted to Genetic Disorders, a section of the journal Frontiers in Genetics

Received: *12 July 2018*
Accepted: *29 August 2018*
Published: *13 September 2018*

Citation:
Merigliano C, Mascolo E, Burla R, Saggio I and Vernì F (2018) The Relationship Between Vitamin B6, Diabetes and Cancer. Front. Genet. 9:388. doi: 10.3389/fgene.2018.00388

VITAMIN B6

The biologically active form of the vitamin B6, the pyridoxal 5′-phosphate (PLP), acts as coenzyme in about 160 distinct enzymatic activities mainly involved in amino acid, carbohydrate and lipid metabolism, and plays key roles in the synthesis and/or catabolism of certain neurotransmitters (Percudani and Peracchi, 2003; di Salvo et al., 2011). In addition, PLP works as antioxidant molecule by quenching oxygen reactive species (ROS) (Ehrenshaft et al., 1999) and counteracting the formation of Advanced Glycation End products (AGEs), genotoxic compounds associated with senescence and diabetes (Booth et al., 1997). Mammals, differently from microorganisms, are not able to synthesize PLP but they recycle it through a *salvage pathway* from B6 vitamers as pyridoxal (PL), pyridoxamine (PM), and pyridoxine (PN) contained in food (McCormick and Chen, 1999). In the cytoplasm PL, PM, and PN are converted into the 5′-phosphorylated vitamers by pyridoxal kinase (PDXK), while the FMN-dependent pyridoxine 5′-phosphate oxidase (PNPO) converts PNP and PMP into PLP.

Deficiency of vitamin B6 has been implicated in several clinically relevant diseases including autism, schizophrenia, Alzheimer, Parkinson, epilepsy, Down's syndrome, diabetes, and cancer.

In this review we focus on the role of PLP in diabetes and cancer suggesting more specialist readings for the other pathologies (Hellmann and Mooney, 2010; di Salvo et al., 2012).

VITAMIN B6 IN CANCER AND DIABETES

Epidemiological studies and meta-analysis indicate an inverse correlation between vitamin B6 and cancer development. For example, high expression levels of PDXK have been positively correlated with survival of non-small cell lung cancer (NSCLC) patients (Galluzzi et al., 2012). Furthermore, vitamin B6 intake and blood PLP levels were inversely correlated with the colorectal cancer risk (Gylling et al., 2017). PLP has been proposed to influence carcinogenesis through different pathways including those involved in DNA metabolism, suggesting that antitumor properties of vitamin B6 may be in part due to its protective role against DNA damage (Ames and Wakimoto, 2002). Vitamin B6 has also been associated to diabetes. However, it is not clear whether low PLP levels represent a cause or an effect of diabetes or both. Some studies report that low PLP levels can contribute to cause diabetes (Toyota et al., 1981; Rubi, 2012), whereas others show that diabetes decreases PLP levels (Bennink and Schreurs, 1975; Spellacy et al., 1977; Okada et al., 1999). Several groups reported that B6 administration produces beneficial effects on diabetic pathology and its complications (Cohen et al., 1984; Solomon and Cohen, 1989; Ellis et al., 1991; Hayakawa and Shibata, 1991; Jain, 2007), although underlying cellular and molecular mechanisms are not completely understood.

Pyridoxal 5′-phosphate deficiency might impact on diabetes in different ways. For example, it could act on the pathway that converts tryptophan into nicotinic acid as PLP is a cofactor of some enzymes that work in this pathway (Bennink and Schreurs, 1975; Spellacy et al., 1977; Oxenkrug, 2013). It has been shown that metabolites produced when this pathway does not work properly can interfere with biological insulin activity (Kotake et al., 1975) causing insulin resistance, a hallmark of type 2 diabetes. Moreover, it has also been proposed that PLP may impact on insulin resistance by controlling the expression of genes involved in adipogenesis (Moreno-Navarrete et al., 2016). Another hypothesis is that PLP deficiency might cause insulin resistance through an increase of homocysteine due to impairment of enzymes such as cystathionine-β-synthase (CBS) and cystathionine-γ-lyase (CGL), which require PLP as a coenzyme (Liu et al., 2016).

Cancer and diabetes are correlated as they share some risk factors. Growing evidence shows that diabetic patients have an increased risk to develop some malignance throughout multiple, not fully elucidate mechanisms, including DNA damage (Noto et al., 2011; Dankner et al., 2016). Interpret the cause-effect relationships in humans is difficult for unavailability of controls and high costs of human research. Researches in the field thus rely on model organisms as well as human 3D cultures and stem cell based systems (Riminucci et al., 2006; Simao et al., 2016). In this review we show how *Drosophila* has turned out to be a useful model not only to investigate the role of vitamin B6 in cancer and in diabetes but also to connect these two pathologies. Furthermore, we present evidence from flies suggesting that incorrect PLP intake could represent a cancer risk factor for diabetic patients, as it enhances DNA damage.

PLP SAFEGUARDS GENOME INTEGRITY IN *Drosophila*

Using *Drosophila* as a model system we demonstrated that PLP plays a crucial role in genome integrity maintenance (Marzio et al., 2014). *Drosophila dPdxk* gene encodes the ortholog of the PDXK enzyme, which is required for vitamin B6 biosynthesis. Mutations in *dPdxk* gene produce, in larval neuroblasts, chromosome aberrations (CABs) (∼6 vs. 0.5% in controls), which are fully rescued by PLP. Dividing larval neuroblasts represent a suitable system to study CABs in *Drosophila* as they exhibit morphologically well defined chromosomes that can be stained by a variety of procedures (Gatti and Goldberg, 1991). CABs have been previously observed after X-ray treatment (Gatti et al., 1974) and as a consequence of mutations in genes which control chromatin structure (Mengoli et al., 2014) or different steps of DNA repair (Bianchi et al., 2017; Merigliano et al., 2017). Vitamin B6 antagonists, namely 4-deoxypyridoxine hydrochloride (4-DP), penicillamine, cycloserine, or isoniazid, produce high CAB frequencies (ranging from 3 to 19%) in wild type cells, further confirming that PLP plays an essential role in genome integrity maintenance. The aforementioned function is evolutionarily conserved in humans as the depletion of the human *PDXK* counterpart induces CABs and a copy of the human *PDXK* gene inserted in a *Drosophila dPdxk*^{1} background is capable to rescue CABs (Marzio et al., 2014). Also in *Saccharomyces cerevisiae* mutations in *BUD16* gene, encoding PDXK, result in gross chromosomal rearrangements. Altogether these data support the hypothesis that low PLP levels may promote cancer initiation and progression throughout the formation of CABs, which represent a cancer prerequisite (Mitelman et al., 2007; Aguilera and Gomez-Gonzalez, 2008; Bunting and Nussenzweig, 2013).

DNA DAMAGE IS CAUSED BY HIGH GLUCOSE LEVELS IN PLP DEFICIENT CELLS

We obtained evidence that in *Drosophila* PLP is involved in glucose metabolism as *dPdxk*^{1} mutants display, in their hemolymph, higher glucose concentrations compared to wild type individuals. *dPdxk*^{1} mutants have normal insulin levels, but a weakened ability to respond to insulin signaling (Marzio et al., 2014). Remarkably, in *dPdxk*^{1} mutants, high glucose levels and CABs are correlated. In *dPdxk*^{1} mutant brains, indeed, 1% glucose *in vitro* treatment strongly increases CAB frequency (from 6 to 20%); in contrast sugar treatment of wild type larvae and brains did not result in detectable effects on chromosome integrity. The relationship between glucose and CABs, in PLP depleted cells, is evolutionarily conserved as glucose supplementation enhances chromosome damage also in

PDXK depleted HeLa cells (Marzio et al., 2014). In addition, the wild type *PDXK* human gene, inserted in *dPdxk*^{1} flies, is able to reduce hyperglycemia. Hyperglycemia triggers the formation of AGEs that in turn produces ROS, which are harmful for DNA. It has been shown that ROS, even at low levels, can cause DNA damage that further leads to DNA double strands breaks (DSBs) (Sharma et al., 2016) and that CABs are mainly generated by unrepaired or improperly repaired DSBs. Repairing complex DSBs may result in genomic instability that can be involved in the etiology of a wide variety of human diseases including cancer (Khanna and Jackson, 2001; Kasparek and Humphrey, 2011).

dPdxk^{1} mutant cells accumulate AGEs and treatment of *dPdxk*^{1} mutants with alpha lipoic acid (ALA), a known AGE inhibitor, rescues not only AGEs but also CABs, suggesting that PLP protects from DNA damage *Drosophila* cells by counteracting AGE formation (Marzio et al., 2014). To the best of our knowledge only our work (Marzio et al., 2014) showed the cause effect relationship between AGEs and CABs in flies. However, *Drosophila* represents a good model to study AGEs as flies accumulate significant AGEs over their lifespan (Oudes et al., 1998) and, in addition, an AGE-rich diet results in ROS accumulation (Tsakiri et al., 2013). AGE formation is at the basis of many diabetic complications (Thorpe and Baynes, 1996; Brownlee, 2001; Vlassara and Palace, 2002) and it also can contribute to diabetes onset (Vlassara and Uribarri, 2014). Our data are consistent with studies indicating that vitamin B6 is beneficial for diabetes complication as, for example, nephropathy (Hayakawa and Shibata, 1991) and retinopathy (Ellis et al., 1991) and with *in vivo* studies showing that PLP is able to reduce AGE accumulation and protein glycation (Cohen et al., 1984; Solomon and Cohen, 1989). How PLP counteracts AGEs is not completely understood but it has been proposed that it may trap 3 deoxyglucosone (3-DG), an AGE's metabolism intermediate (Nakamura et al., 2007), although other mechanisms are possible. Besides to its antioxidant role, PLP also works as cofactor for serine hydroxymethyltransferase enzyme, which takes part to the thymidylate synthase cycle by converting dUMP in dTMP (Florio et al., 2011). However, whereas PLP depletion in yeast compromises DNA synthesis (Kanellis et al., 2007), in *Drosophila* it does not seems to have the same effect. Although in *dPdxk*^{1} mutants there is an altered dTMP/dUTP ratio DNA syntesis is not the main cause of CABs as *dPdxk*^{1} mutant are only slighty sensitive to Hydroxyurea, a drug that interferes with replication (Marzio et al., 2014). However, considering the wide range of enzymatic reactions regulated by vitamin B6, we cannot exclude that in addition to block AGE formation PLP may prevent CABs also through other mechanisms.

Drosophila AS TYPE 2 DIABETES MODEL

Drosophila represents a good model to study diabetes as flies and humans largely share mechanisms involved in glucose homeostasis maintenance (Graham and Pick, 2017). In addition, fly genome possess well characterized orthologs of most genes working in the insulin signaling pathway that controls the glucose uptake and storage (Garofalo, 2002).

In humans and mice mutations in insulin pathway genes cause severe insulin resistance syndromes and type 2 diabetes (reviewed in Boucher et al., 2014). In *Drosophila* type 2 diabetes models can be generated by two different strategies: by downregulating conserved genes working on insulin pathways as for example the insulin receptor *InR*, the insulin substrate receptor *chico/IRS1, Akt1, PI3K,* and by feeding flies with a high sugar rich diet (Alfa and Kim, 2016). In both cases resulting flies exhibit diabetic hallmarks as hyperglycemia and insulin resistance allowing the study in flies of various aspects of diabetes and related human disorders. In addition, a diabetic fly model also enhances the ability to identify genes and discover functional interactions that can be exploited for disease treatment.

PLP DEPLETION AS NEW CANCER RISK FACTOR IN DIABETIC CELLS

Meta-analysis and epidemiological studies indicate that diabetic patients have an increased risk to develop several solid and hematologic malignancies (including liver, pancreas, colorectal, kidney, bladder, endometrial, and breast cancers, and non-Hodgkin's lymphoma) although the molecular mechanisms are not completely clarified (Vigneri, 2009; Noto et al., 2011; Dankner et al., 2016). However, some risk factors have been identified including hyperinsulinemia and hyperglycemia that might rise cancer risk in diabetic patients by promoting cell growth (Shikata et al., 2013). Besides triggering cell division hyperglycemia also causes oxidative stress as glucose in excess promotes, through different pathways, ROS formation which in turn induces DNA and cellular damage (Rains and Jain, 2011). In addition, in cells from diabetic patients an impaired DNA repair, combined to a weakened antioxidant defense, contributes to enhance DNA damage (Blasiak et al., 2004). Consistently, oxidative damage and DNA strand breaks have been found in both type 1 and type 2 diabetic patients (Goodarzi et al., 2010; Tatsch et al., 2012; Anand et al., 2014). We have recently shown in *Drosophila* that PLP deficiency can further increase DNA damage in cells from diabetic individuals (Merigliano et al., 2018). Using two different type 2 diabetes models, the first obtained by downregulating genes involved in insulin signaling such as *InR*, *chico (IRS1),* and *Akt1,* and the second by feeding wild type flies with a high sugar diet (Musselman et al., 2011), we showed that the treatment of larval neuroblasts with the strong PLP inhibitor 4-DP produced a very high CAB frequency ranging from 60 to 80% (vs. 25% in wild type cells). Accordingly, genetic analysis revealed a synergistic interaction between *Akt1* and *dPdkx*^{1} mutations in CAB formation (Merigliano et al., 2018). AGEs are in part responsible for CABs in *Drosophila* diabetic PLP depleted cells as they accumulate in these cells and, more strikingly, ALA rescues either AGEs and CABs (Merigliano et al., 2018). These findings indicate that, in diabetic cells, low PLP levels heavily impact on genome integrity. Thus, if translated to humans, these data suggest that low PLP levels may contribute to increase cancer risk in diabetic patients. Although PLP deficiency is a rare condition caused by excessive alcohol consumption, unwanted effects of some drugs (i.e., isonyazide, cycloserine penicillamine), or

celiac disease and renal dialysis (Clayton, 2006), it has been demonstrated, in murine models and by epidemiological studies, that it can also be associated to diabetes (Leklem and Hollenbeck, 1990; Okada et al., 1999; Ahn et al., 2011; Nix et al., 2015). All evidence suggests the importance to maintain under strict control PLP levels in diabetic patients to avoid the chance to increase DNA damage, which could in turn contribute to cancer initiation and progression.

CONCLUSION

Several studies have shown that insufficient intake of vitamin B6 is associated with increased cancer risk and growing evidence indicates that diabetes patients have a higher risk of developing various types of cancer. The findings reviewed here, obtained in *Drosophila*, provide a mechanistic link between aforementioned studies by suggesting that PLP deficiency accompanied by hyperglycemia can lead to DNA damage and may contribute to cancerogenesis. Thus, *Drosophila* has proved to be a useful model system to shed light on a novel and important role of vitamin B6 deficiency in the pathogenesis of cancer and diabetes. In addition, this model organism allowed identifying PLP deficiency as one of the risk factors that contribute to correlating diabetes to cancer.

AUTHOR CONTRIBUTIONS

CM contributed to planning and writing the manuscript. EM and RB contributed to planning the study. IS contributed to writing the manuscript. FV planned the study and wrote the manuscript. All authors performed a critical revision of the manuscript.

FUNDING

The work was supported by MIUR Ateneo to FV and MIUR Avvio alla ricerca to CM.

REFERENCES

Aguilera, A., and Gomez-Gonzalez, B. (2008). Genome instability: a mechanistic view of its causes and consequences. *Nat. Rev. Genet.* 9, 204–217. doi: 10.1038/nrg2268

Ahn, H. J., Min, K. W., and Cho, Y. O. (2011). Assessment of vitamin B(6) status in Korean patients with newly diagnosed type 2 diabetes. *Nutr. Res. Pract.* 5, 34–39. doi: 10.4162/nrp.2011.5.1.34

Alfa, R. W., and Kim, S. K. (2016). Using drosophila to discover mechanisms underlying type 2 diabetes. *Dis. Model. Mech.* 9, 365–376. doi: 10.1242/dmm.023887

Ames, B. N., and Wakimoto, P. (2002). Are vitamin and mineral deficiencies a major cancer risk? *Nat. Rev. Cancer* 2, 694–704. doi: 10.1038/nrc886

Anand, S., Nath, B., and Saraswathy, R. (2014). Diabetes–increased risk for cancers through chromosomal aberrations? *Asian Pac. J. Cancer Prev.* 15, 4571–4573.

Bennink, H. J., and Schreurs, W. H. (1975). Improvement of oral glucose tolerance in gestational diabetes by pyridoxine. *Br. Med. J.* 3, 13–15. doi: 10.1136/bmj.3.5974.13

Bianchi, F. T., Tocco, C., Pallavicini, G., Liu, Y., Verni, F., Merigliano, C., et al. (2017). Citron kinase deficiency leads to chromosomal instability and TP53-sensitive microcephaly. *Cell Rep.* 18, 1674–1686. doi: 10.1016/j.celrep.2017.01.054

Blasiak, J., Arabski, M., Krupa, R., Wozniak, K., Zadrozny, M., Kasznicki, J., et al. (2004). DNA damage and repair in type 2 diabetes mellitus. *Mutat. Res.* 554, 297–304. doi: 10.1016/j.mrfmmm.2004.05.011

Booth, A. A., Khalifah, R. G., Todd, P., and Hudson, B. G. (1997). In vitro kinetic studies of formation of antigenic advanced glycation end products (AGEs). novel inhibition of post-amadori glycation pathways. *J. Biol. Chem.* 272, 5430–5437. doi: 10.1074/jbc.272.9.5430

Boucher, J., Kleinridders, A., and Kahn, C. R. (2014). Insulin receptor signaling in normal and insulin-resistant states. *Cold Spring Harb. Perspect. Biol.* 6:a009191. doi: 10.1101/cshperspect.a009191

Brownlee, M. (2001). Biochemistry and molecular cell biology of diabetic complications. *Nature* 414, 813–820. doi: 10.1038/414813a

Bunting, S. F., and Nussenzweig, A. (2013). End-joining, translocations and cancer. *Nat. Rev. Cancer* 13, 443–454. doi: 10.1038/nrc3537

Clayton, P. T. (2006). B6-responsive disorders: a model of vitamin dependency. *J. Inherit. Metab. Dis.* 29, 317–326. doi: 10.1007/s10545-005-0243-2

Cohen, K. L., Gorecki, G. A., Silverstein, S. B., Ebersole, J. S., and Solomon, L. R. (1984). Effect of pyridoxine (vitamin B6) on diabetic patients with peripheral neuropathy. *J. Am. Podiatry Assoc.* 74, 394–397. doi: 10.7547/87507315-74-8-394

Dankner, R., Boffetta, P., Balicer, R. D., Boker, L. K., Sadeh, M., Berlin, A., et al. (2016). Time-Dependent risk of cancer after a diabetes diagnosis in a cohort of 2.3 Million adults. *Am. J. Epidemiol.* 183, 1098–1106. doi: 10.1093/aje/kwv290

di Salvo, M. L., Contestabile, R., and Safo, M. K. (2011). Vitamin B(6) salvage enzymes: mechanism, structure and regulation. *Biochim. Biophys. Acta* 1814, 1597–1608. doi: 10.1016/j.bbapap.2010.12.006

di Salvo, M. L., Safo, M. K., and Contestabile, R. (2012). Biomedical aspects of pyridoxal 5′-phosphate availability. *Front. Biosci.* 4, 897–913.

Ehrenshaft, M., Bilski, P., Li, M. Y., Chignell, C. F., and Daub, M. E. (1999). A highly conserved sequence is a novel gene involved in de novo vitamin B6 biosynthesis. *Proc. Natl. Acad. Sci. U.S.A.* 96, 9374–9378. doi: 10.1073/pnas.96.16.9374

Ellis, J. M., Folkers, K., Minadeo, M., VanBuskirk, R., Xia, L. J., and Tamagawa, H. (1991). A deficiency of vitamin B6 is a plausible molecular basis of the retinopathy of patients with diabetes mellitus. *Biochem. Biophys. Res. Commun.* 179, 615–619. doi: 10.1016/0006-291X(91)91416-A

Florio, R., di Salvo, M. L., Vivoli, M., and Contestabile, R. (2011). Serine hydroxymethyltransferase: a model enzyme for mechanistic, structural, and evolutionary studies. *Biochim. Biophys. Acta* 1814, 1489–1496. doi: 10.1016/j.bbapap.2010.10.010

Galluzzi, L., Vitale, I., Senovilla, L., Olaussen, K. A., Pinna, G., Eisenberg, T., et al. (2012). Prognostic impact of vitamin B6 metabolism in lung cancer. *Cell Rep.* 2, 257–269. doi: 10.1016/j.celrep.2012.06.017

Garofalo, R. S. (2002). Genetic analysis of insulin signaling in Drosophila. *Trends Endocrinol. Metab.* 13, 156–162. doi: 10.1016/S1043-2760(01)00548-3

Gatti, M., and Goldberg, M. L. (1991). Mutations affecting cell division in Drosophila. *Methods Cell Biol.* 35, 543–586. doi: 10.1016/S0091-679X(08)60587-7

Gatti, M., Tanzarella, C., and Olivieri, G. (1974). Variation with sex of irradiation-induced chromosome damage in somatic cells of *Drosophila melanogaster*. *Nature* 247, 151–152. doi: 10.1038/247151a0

Goodarzi, M. T., Navidi, A. A., Rezaei, M., and Babahmadi-Rezaei, H. (2010). Oxidative damage to DNA and lipids: correlation with protein glycation in patients with type 1 diabetes. *J. Clin. Lab. Anal.* 24, 72–76. doi: 10.1002/jcla.20328

Graham, P., and Pick, L. (2017). Drosophila as a Model for diabetes and diseases of insulin resistance. *Curr. Top. Dev. Biol* 121, 397–419. doi: 10.1016/bs.ctdb.2016.07.011

Gylling, B., Myte, R., Schneede, J., Hallmans, G., Haggstrom, J., Johansson, I., et al. (2017). Vitamin B-6 and colorectal cancer risk: a prospective population-based study using 3 distinct plasma markers of vitamin B-6 status. *Am. J. Clin. Nutr.* 105, 897–904. doi: 10.3945/ajcn.116.139337

Hayakawa, M., and Shibata, M. (1991). The in vitro and in vivo inhibition of protein glycosylation and diabetic vascular basement membrane thickening by pyridoxal-5′-phosphate. *J. Nutr. Sci. Vitaminol.* 37, 149–159. doi: 10.3177/jnsv.37.149

Hellmann, H., and Mooney, S. (2010). Vitamin B6: a molecule for human health? *Molecules* 15, 442–459. doi: 10.3390/molecules15010442

Jain, S. K. (2007). Vitamin B6 (pyridoxamine) supplementation and complications of diabetes. *Metabolism* 56, 168–171. doi: 10.1016/j.metabol.2006.09.002

Kanellis, P., Gagliardi, M., Banath, J. P., Szilard, R. K., Nakada, S., Galicia, S., et al. (2007). A screen for suppressors of gross chromosomal rearrangements identifies a conserved role for PLP in preventing DNA lesions. *PLoS Genet.* 3:e134. doi: 10.1371/journal.pgen.0030134

Kasparek, T. R., and Humphrey, T. C. (2011). DNA double-strand break repair pathways, chromosomal rearrangements and cancer. *Semin. Cell Dev. Biol.* 22, 886–897. doi: 10.1016/j.semcdb.2011.10.007

Khanna, K. K., and Jackson, S. P. (2001). DNA double-strand breaks: signaling, repair and the cancer connection. *Nat. Genet.* 27, 247–254. doi: 10.1038/85798

Kotake, Y., Ueda, T., Mori, T., Igaki, S., and Hattori, M. (1975). Abnormal tryptophan metabolism and experimental diabetes by xanthurenic acid (XA). *Acta Vitaminol. Enzymol.* 29, 236–239.

Leklem, J. E., and Hollenbeck, C. B. (1990). Acute ingestion of glucose decreases plasma pyridoxal 5′-phosphate and total vitamin B-6 concentration. *Am. J. Clin. Nutr.* 51, 832–836. doi: 10.1093/ajcn/51.5.832

Liu, Z., Li, P., Zhao, Z. H., Zhang, Y., Ma, Z. M., and Wang, S. X. (2016). Vitamin B6 prevents endothelial dysfunction, insulin resistance, and hepatic lipid accumulation in apoe (-/-) mice fed with high-fat diet. *J. Diabetes Res.* 2016:1748065. doi: 10.1155/2016/1748065

Marzio, A., Merigliano, C., Gatti, M., and Verni, F. (2014). Sugar and chromosome stability: clastogenic effects of sugars in vitamin B6-deficient cells. *PLoS Genet.* 10:e1004199. doi: 10.1371/journal.pgen.1004199

McCormick, D. B., and Chen, H. (1999). Update on interconversions of vitamin B-6 with its coenzyme. *J. Nutr.* 129, 325–327. doi: 10.1093/jn/129.2.325

Mengoli, V., Bucciarelli, E., Lattao, R., Piergentili, R., Gatti, M., and Bonaccorsi, S. (2014). The analysis of mutant alleles of different strength reveals multiple functions of topoisomerase 2 in regulation of *Drosophila* chromosome structure. *PLoS Genet.* 10:e1004739. doi: 10.1371/journal.pgen.1004739

Merigliano, C., Marzio, A., Renda, F., Somma, M. P., Gatti, M., and Verni, F. (2017). A role for the twins protein phosphatase (PP2A-B55) in the maintenance of drosophila genome integrity. *Genetics* 205, 1151–1167. doi: 10.1534/genetics.116.192781

Merigliano, C., Mascolo, E., La Torre, M., Saggio, I., and Verni, F. (2018). Protective role of vitamin B6 (PLP) against DNA damage in *Drosophila* models of type 2 diabetes. *Sci. Rep.* 8:11432. doi: 10.1038/s41598-018-29801-z

Mitelman, F., Johansson, B., and Mertens, F. (2007). The impact of translocations and gene fusions on cancer causation. *Nat. Rev. Cancer* 7, 233–245. doi: 10.1038/nrc2091

Moreno-Navarrete, J. M., Jove, M., Ortega, F., Xifra, G., Ricart, W., Obis, E., et al. (2016). Metabolomics uncovers the role of adipose tissue PDXK in adipogenesis and systemic insulin sensitivity. *Diabetologia* 59, 822–832. doi: 10.1007/s00125-016-3863-1

Musselman, L. P., Fink, J. L., Narzinski, K., Ramachandran, P. V., Hathiramani, S. S., Cagan, R. L., et al. (2011). A high-sugar diet produces obesity and insulin resistance in wild-type *Drosophila*. *Dis. Model. Mech.* 4, 842–849. doi: 10.1242/dmm.007948

Nakamura, S., Li, H., Adijiang, A., Pischetsrieder, M., and Niwa, T. (2007). Pyridoxal phosphate prevents progression of diabetic nephropathy. *Nephrol. Dial. Transplant.* 22, 2165–2174. doi: 10.1093/ndt/gfm166

Nix, W. A., Zirwes, R., Bangert, V., Kaiser, R. P., Schilling, M., Hostalek, U., et al. (2015). Vitamin B status in patients with type 2 diabetes mellitus with and without incipient nephropathy. *Diabetes. Res. Clin. Pract.* 107, 157–165. doi: 10.1016/j.diabres.2014.09.058

Noto, H., Tsujimoto, T., Sasazuki, T., and Noda, M. (2011). Significantly increased risk of cancer in patients with diabetes mellitus: a systematic review and meta-analysis. *Endocr. Pract.* 17, 616–628. doi: 10.4158/EP10357.RA

Okada, M., Shibuya, M., Yamamoto, E., and Murakami, Y. (1999). Effect of diabetes on vitamin B6 requirement in experimental animals. *Diabetes Obes. Metab.* 1, 221–225. doi: 10.1046/j.1463-1326.1999.00028.x

Oudes, A. J., Herr, C. M., Olsen, Y., and Fleming, J. E. (1998). Age-dependent accumulation of advanced glycation end-products in adult Drosophila melanogaster. *Mech. Ageing Dev.* 100, 221–229. doi: 10.1016/S0047-6374(97)00146-2

Oxenkrug, G. (2013). Insulin resistance and dysregulation of tryptophan-kynurenine and kynurenine-nicotinamide adenine dinucleotide metabolic pathways. *Mol. Neurobiol.* 48, 294–301. doi: 10.1007/s12035-013-8497-4

Percudani, R., and Peracchi, A. (2003). A genomic overview of pyridoxal-phosphate-dependent enzymes. *EMBO Rep.* 4, 850–854. doi: 10.1038/sj.embor.embor914

Rains, J. L., and Jain, S. K. (2011). Oxidative stress, insulin signaling, and diabetes. *Free Radic. Biol. Med.* 50, 567–575. doi: 10.1016/j.freeradbiomed.2010.12.006

Riminucci, M., Saggio, I., Robey, P. G., and Bianco, P. (2006). Fibrous dysplasia as a stem cell disease. *J. Bone Miner. Res.* 21(Suppl. 2), 125–131. doi: 10.1359/jbmr.06s224

Rubi, B. (2012). Pyridoxal 5'-phosphate (PLP) deficiency might contribute to the onset of type I diabetes. *Med. Hypotheses* 78, 179–182. doi: 10.1016/j.mehy.2011.10.021

Sharma, V., Collins, L. B., Chen, T., Herr, N., Takeda, S., Sun, W., et al. (2016). Oxidative stress at low levels can induce clustered DNA lesions leading to NHEJ mediated mutations. *Oncotarget* 7, 25377–25390. doi: 10.18632/oncotarget.8298

Shikata, K., Ninomiya, T., and Kiyohara, Y. (2013). Diabetes mellitus and cancer risk: review of the epidemiological evidence. *Cancer Sci.* 104, 9–14. doi: 10.1111/cas.12043

Simao, D., Pinto, C., Fernandes, P., Peddie, C. J., Piersanti, S., Collinson, L. M., et al. (2016). Evaluation of helper-dependent canine adenovirus vectors in a 3D human CNS model. *Gene Ther.* 23, 86–94. doi: 10.1038/gt.2015.75

Solomon, L. R., and Cohen, K. (1989). Erythrocyte O2 transport and metabolism and effects of vitamin B6 therapy in type II diabetes mellitus. *Diabetes Metab. Res. Rev.* 38, 881–886.

Spellacy, W. N., Buhi, W. C., and Birk, S. A. (1977). Vitamin B6 treatment of gestational diabetes mellitus: studies of blood glucose and plasma insulin. *Am. J. Obstet. Gynecol.* 127, 599–602. doi: 10.1016/0002-9378(77)90356-8

Tatsch, E., Bochi, G. V., Piva, S. J., De Carvalho, J. A., Kober, H., Torbitz, V. D., et al. (2012). Association between DNA strand breakage and oxidative, inflammatory and endothelial biomarkers in type 2 diabetes. *Mutat. Res.* 732, 16–20. doi: 10.1016/j.mrfmmm.2012.01.004

Thorpe, S. R., and Baynes, J. W. (1996). Role of the Maillard reaction in diabetes mellitus and diseases of aging. *Drugs Aging* 9, 69–77. doi: 10.2165/00002512-199609020-00001

Toyota, T., Kai, Y., Kakizaki, M., Ohtsuka, H., Shibata, Y., and Goto, Y. (1981). The endocrine pancreas in pyridoxine deficient rats. *Tohoku J. Exp. Med.* 134, 331–336. doi: 10.1620/tjem.134.331

Tsakiri, E. N., Iliaki, K. K., Hohn, A., Grimm, S., Papassideri, I. S., Grune, T., et al. (2013). Diet-derived advanced glycation end products or lipofuscin disrupts proteostasis and reduces life span in *Drosophila melanogaster*. *Free Radic. Biol. Med.* 65, 1155–1163. doi: 10.1016/j.freeradbiomed.2013.08.186

Vigneri, R. (2009). Diabetes: diabetes therapy and cancer risk. *Nat. Rev. Endocrinol.* 5, 651–652. doi: 10.1038/nrendo.2009.219

Vlassara, H., and Palace, M. R. (2002). Diabetes and advanced glycation endproducts. *J. Intern. Med.* 251, 87–101. doi: 10.1046/j.1365-2796.2002.00932.x

Vlassara, H., and Uribarri, J. (2014). Advanced glycation end products (AGE) and diabetes: cause, effect, or both? *Curr. Diab. Rep.* 14:453. doi: 10.1007/s11892-013-0453-1

Conflict of Interest Statement: The authors declare that the research was conducted in the absence of any commercial or financial relationships that could be construed as a potential conflict of interest.

The reviewer RC declared a shared affiliation, with no collaboration, with the authors to the handling Editor at time of review.

frontiers in Genetics

REVIEW
published: 12 September 2018
doi: 10.3389/fgene.2018.00390

Processing of DNA Ends in the Maintenance of Genome Stability

*Diego Bonetti, Chiara Vittoria Colombo, Michela Clerici and Maria Pia Longhese**

Dipartimento di Biotecnologie e Bioscienze, Università di Milano-Bicocca, Milan, Italy

DNA double-strand breaks (DSBs) are particularly hazardous lesions as their inappropriate repair can result in chromosome rearrangements, an important driving force of tumorigenesis. DSBs can be repaired by end joining mechanisms or by homologous recombination (HR). HR requires the action of several nucleases that preferentially remove the 5′-terminated strands at both DSB ends in a process called DNA end resection. The same nucleases are also involved in the processing of replication fork structures. Much of our understanding of these pathways has come from studies in the model organism *Saccharomyces cerevisiae*. Here, we review the current knowledge of the mechanism of resection at DNA DSBs and replication forks.

Keywords: checkpoint, DNA replication, double-strand break, MRX, nucleases, resection

OPEN ACCESS

Edited by:
Maria Grazia Giansanti,
Istituto di Biologia e Patologia Molecolari (IBPM), Consiglio Nazionale Delle Ricerche (CNR), Italy

Reviewed by:
Simonetta Piatti,
Délégation Languedoc Roussillon (CNRS), France
Marcus Smolka,
Cornell University, United States

****Correspondence:***
Maria Pia Longhese
mariapia.longhese@unimib.it

Specialty section:
This article was submitted to Genetic Disorders, a section of the journal Frontiers in Genetics

Received: *29 June 2018*
Accepted: *29 August 2018*
Published: *12 September 2018*

Citation:
Bonetti D, Colombo CV, Clerici M and Longhese MP (2018) Processing of DNA Ends in the Maintenance of Genome Stability. Front. Genet. 9:390. doi: 10.3389/fgene.2018.00390

INTRODUCTION

DNA double-strand breaks (DSBs) are highly cytotoxic forms of DNA damage because their incorrect repair or failure to repair causes chromosome loss and rearrangements that can lead to cell death or transformation (Liu et al., 2012). They can form accidentally during normal cell metabolism or after exposure of cells to ionizing radiations or chemotherapeutic drugs. In addition, DSBs are intermediates in programmed recombination events in eukaryotic cells. Indeed, defects in DSB signaling or repair are associated with developmental, immunological and neurological disorders, and tumorigenesis (O'Driscoll, 2012).

Conserved pathways extensively studied in recent years are devoted to repair DSBs in eukaryotes. The two predominant repair mechanisms are non-homologous end joining (NHEJ) and homologous recombination (HR) and the choice between them is regulated during the cell cycle. NHEJ allows a direct ligation of the DNA ends with very little or no complementary base pairing and it operates predominantly in the G1 phase of the cell cycle (Chiruvella et al., 2013). The initial step involves the binding to DNA ends of the Ku heterodimer, which protects the DNA ends from degradation, followed by ligation of the broken DNA ends by the DNA ligase IV (Dnl4/Lig4 in yeast) complex. By contrast, HR is the predominant repair pathway in the S and G2 phases of the cell cycle and it requires a homologous duplex DNA to direct the repair (Mehta and Haber, 2014). For HR to occur, the 5′-terminated DNA strands on either side of the DSB must first be degraded by a concerted action of nucleases to generate 3′-ended single-stranded DNA (ssDNA) tails in a process referred to as resection (Cejka, 2015; Symington, 2016). These tails are first bound by the ssDNA binding complex Replication Protein A (RPA). RPA is then replaced by the recombination protein Rad51 to form a right-handed helical filament that is used to search and invade the homologous duplex DNA (Mehta and Haber, 2014).

Double-strand break occurrence also triggers the activation of a sophisticated highly conserved pathway, called DNA damage checkpoint, which couples DSB repair with cell cycle progression

(Gobbini et al., 2013; Villa et al., 2016). Apical checkpoint proteins include phosphatidylinositol 3-kinase related protein kinases, such as mammalian ATM (Ataxia-Telangiectasia-Mutated) and ATR (ATM- and Rad3-related), orthologs of *Saccharomyces cerevisiae* Tel1 and Mec1, respectively (Ciccia and Elledge, 2010). Once Mec1/ATR and/or Tel1/ATM are activated, their checkpoint signals are propagated through the *S. cerevisiae* protein kinases Rad53 and Chk1 (CHK2 and CHK1 in mammals, respectively), whose activation requires the conserved protein Rad9 (53BP1 in mammals) (Sweeney et al., 2005). While Tel1/ATM recognizes unprocessed or minimally processed DSBs, Mec1/ATR is recruited to and activated by RPA-coated ssDNA, which arises upon resection of the DSB ends (Zou and Elledge, 2003).

Most of our knowledge of the nucleolytic activities responsible for DSB resection has come from studies in the budding yeast *S. cerevisiae*, where DNA end resection can be monitored physically at sites of endonuclease-induced DSBs. Interestingly, the same nucleases involved in DSB resection are also responsible for the processing of stalled replication forks both in yeast and in mammals. Here we will focus on the work done in *S. cerevisiae* to understand the resection mechanism at DNA DSBs and replication forks and its regulation by Tel1/ATM and Mec1/ATR checkpoint kinases.

NUCLEASE ACTION AT DNA DOUBLE-STRAND BREAKS

Genetic studies in *S. cerevisiae* identified at least three distinct nucleases involved in end-resection: the MRX (Mre11-Rad50-Xrs2 in yeast; MRE11-RAD50-NBS1 in mammals) complex, Dna2 and Exo1 (DNA2 and EXO1 in mammals, respectively). In particular, the Mre11 subunit of MRX has five conserved phosphoesterase motifs in the amino-terminal half of the protein that are required for 3′–5′ double-strand DNA (dsDNA) exonuclease and ssDNA endonuclease activities of the protein *in vitro* (Bressan et al., 1998; Paull and Gellert, 1998; Trujillo et al., 1998; Usui et al., 1998). Rad50 is characterized by Walker A and B ATP binding cassettes located at the amino- and carboxy-terminal regions of the protein, with the intervening sequence forming a long antiparallel coiled-coil. The apex of the coiled-coil domain can interact with other MRX complexes by Zn^{+}-mediated dimerization to tether the bound DNA ends together (de Jager et al., 2001; Hopfner et al., 2002; Wiltzius et al., 2005; Williams et al., 2008). The ATP-bound state of Rad50 inhibits the Mre11 nuclease activity by masking the active site of Mre11 from contacting DNA (Lim et al., 2011). ATP hydrolysis induces conformational changes of both Rad50 and Mre11 that allow the Mre11 nuclease domain to access the DSB ends and to be engaged in DSB resection (Lammens et al., 2011; Lim et al., 2011; Williams et al., 2011; Möckel et al., 2012; Deshpande et al., 2014).

In the current model for resection, the Sae2 protein (CtIP in mammals) activates a latent dsDNA-specific endonuclease activity of Mre11 within the context of the MRX complex to incise the 5′-terminated dsDNA strands at both DNA ends (Cannavo and Cejka, 2014). The resulting nick generates an entry site for the Mre11 exonuclease to degrade back to the DSB end in the 3′–5′ direction, and for Exo1 and Dna2 nucleases to degrade DNA in the 5′–3′ direction away from the DSB end (Mimitou and Symington, 2008; Zhu et al., 2008; Cejka et al., 2010; Niu et al., 2010; Garcia et al., 2011; Nimonkar et al., 2011; Shibata et al., 2014; Reginato et al., 2017; Wang et al., 2017; **Figure 1**). In yeast, inactivation of either Sgs1-Dna2 or Exo1 results in only minor resection defects, whereas resection is severely compromised when the two pathways are simultaneously inactivated, indicating that they play partially overlapping functions (Mimitou and Symington, 2008; Zhu et al., 2008).

The efficiency of 5′ DNA end cleavage *in vitro* by MRX-Sae2 was shown to be strongly enhanced by the presence of protein blocks at DNA ends (Cannavo and Cejka, 2014; Anand et al., 2016; Deshpande et al., 2016). It has been proposed that the endonucleolytic cleavage catalyzed by MRX-Sae2 allows the resection machinery to bypass end-binding factors that can be present at the break end and restrict the accessibility of DNA ends to Exo1 and Sgs1-Dna2. These end-binding factors includes Spo11, which cleaves DNA by a topoisomerase-like transesterase mechanism and remains covalently attached to the 5′ end of meiotic DSBs, trapped topoisomerases, or the Ku complex (see the next paragraph) (Neale et al., 2005; Bonetti et al., 2010; Mimitou and Symington, 2010; Langerak et al., 2011; Chanut et al., 2016).

While Exo1 shows 5′–3′ exonuclease activity capable to release mononucleotide products from a dsDNA end (Tran et al., 2002), Dna2 has an endonuclease activity that can cleave either 3′ or 5′ overhangs adjoining a duplex DNA (Kao et al., 2004). The resection activity of Dna2 relies on the RecQ helicase Sgs1 (BLM in humans) that provides the substrates for Dna2 by unwinding the dsDNA (Zhu et al., 2008; Cejka et al., 2010; Niu et al., 2010; Nimonkar et al., 2011). Furthermore, RPA directs the resection activity of Dna2 to the 5′ strand by binding and protecting the 3′ strand to Dna2 access (Cejka et al., 2010; Niu et al., 2010). In both yeast and humans, Dna2 contains also a helicase domain that can function as a ssDNA translocase to facilitate the degradation of 5′-terminated DNA by the nuclease activity of the enzyme (Levikova et al., 2017; Miller et al., 2017).

In addition to the end-clipping function, the MRX complex also stimulates resection by Exo1 and Sgs1-Dna2 both *in vitro* and *in vivo* (Cejka et al., 2010; Nicolette et al., 2010; Niu et al., 2010; Shim et al., 2010; Nimonkar et al., 2011). Biochemical experiments have shown that MRX enhances the ability of Sgs1 to unwind dsDNA, possibly by increasing Sgs1 association to DNA ends. Furthermore, MRX enhances both the affinity to DNA ends and the processivity of Exo1 (Cejka et al., 2010; Nicolette et al., 2010; Niu et al., 2010; Nimonkar et al., 2011; Cannavo et al., 2013). The MRX function in promoting Sgs1-Dna2 and Exo1 resection activities does not require Mre11 nuclease, suggesting that it does involve the Mre11 end-clipping activity (Shim et al., 2010).

Interestingly, MRX possesses an ATP-dependent unwinding activity capable of releasing a short oligonucleotide from dsDNA (Paull and Gellert, 1999; Cannon et al., 2013) and the recent identification of the hypermorphic *mre11-R10T* mutation has

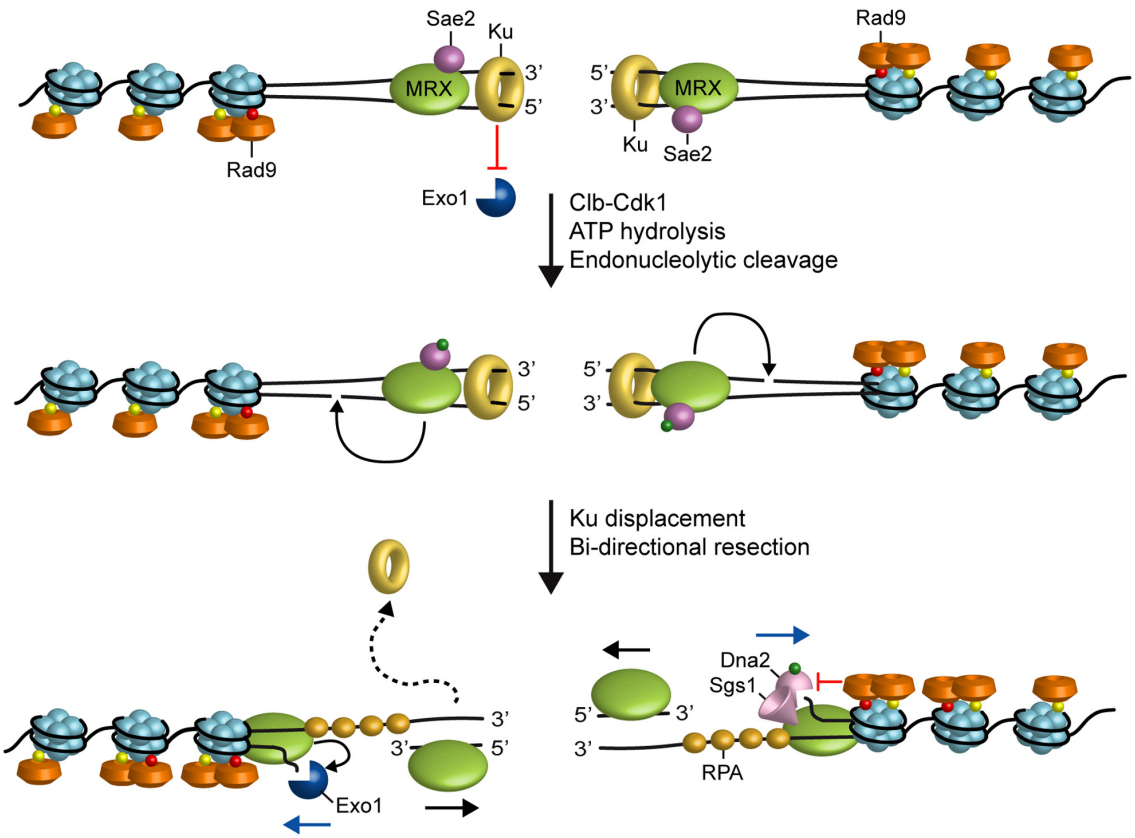

FIGURE 1 | Model for resection of DNA DSBs. MRX, Sae2 and Ku are rapidly recruited to DNA ends. Ku inhibits Exo1 access to DNA ends. In the ATP-bound state, Rad50 blocks the Mre11 nuclease. After ATP hydrolysis by Rad50, Mre11 together with Sae2 phosphorylated by Cdk1 can catalyze an endonucleolytic cleavage of the 5' strand. This incision allows processing by Exo1 and Sgs1-Dna2 in a 5'–3' direction from the nick (blue arrows) and by MRX in a 3'–5' direction toward the DSB ends (black arrows). MRX also promotes the association of Exo1 and Sgs1-Dna2 at DNA ends, whereas Rad9 inhibits the resection activity of Sgs1-Dna2. Red dots indicate phosphorylation events by Mec1 and Tel1, green dots indicate phosphorylation events by Cdk1 and yellow dots indicate methylation of histone H3.

allowed us to demonstrate that this strand-separation function of MRX is important to stimulate Exo1 resection activity (Gobbini et al., 2018). In particular, Mre11-R10T mutant variant, whose single aminoacid substitution is located in the first Mre11 phosphodiesterase domain, accelerates DSB resection compared to wild type Mre11 by potentiating the processing activity of Exo1, whose association to DSBs is increased in *mre11-R10T* cells. Molecular dynamic simulations have shown that the two capping domains of wild type Mre11 dimer rapidly interact with the DNA ends and cause a partial unwinding of the dsDNA molecule. The Mre11-R10T dimer undergoes an abnormal rotation that leads one of the capping domain to wedge in between the two DNA strands and to persistently melt the dsDNA ends (Gobbini et al., 2018). These findings support a model in which MRX can directly stimulate Exo1 activity by promoting local unwinding of the DSB DNA end that facilitates Exo1 persistence on DNA. Although Exo1 is a processive nuclease *in vitro*, single-molecule fluorescence imaging has shown that it is rapidly stripped from DNA by RPA (Myler et al., 2016), suggesting that multiple cycles of Exo1 rebinding at the same DNA end would be required for extensive resection. Therefore, this MRX function in the stimulation of Exo1 activity at DNA ends can be of benefit to increase the processivity of Exo1 in the presence of RPA.

POSITIVE AND NEGATIVE REGULATION OF NUCLEASE ACTION AT DNA DOUBLE-STRAND BREAKS

Homologous recombination is generally restricted to the S and G2 phases of the cell cycle, when a sister chromatid is present as repair template (Aylon et al., 2004; Ira et al., 2004). This restriction is mainly caused by reduced end resection in G1 compared to G2. Reduced resection in G1 is due to both Ku binding to DNA ends and low cyclin-dependent kinase (Cdk1 in *S. cerevisiae*) activity (Aylon et al., 2004; Ira et al., 2004; Clerici et al., 2008; Zierhut and Diffley, 2008). Elimination of Ku in G1 (where Cdk1 activity is low) allows Cdk1-independent DSB resection that is limited to the break-proximal sequence, whereas the absence of Ku does not enhance DSB processing in G2 (where Cdk1 activity is high) (Clerici et al., 2008). Furthermore, inhibition of Cdk1 activity in G2 prevents DSB resection in wild type but not in *ku*Δ cells (Clerici et al., 2008). These

findings suggest that Cdk1 activity is required for resection initiation when Ku is present. However, the finding that Cdk1 inhibition in G2-arrested *ku*Δ cells allows only short but not long-range resection (Clerici et al., 2008) suggests the existence of other Cdk1 targets to allow extensive resection. Consistent with this hypothesis, Cdk1 was shown to promote short- and long-range resection by phosphorylating and activating Sae2 and Dna2, respectively. In fact, substitution of Cdk1-dependent phosphorylation residues in Sae2 causes a delay of DSB resection initiation, while mutations of Cdk1-target sites in Dna2 cause a defect in long-range resection (Huertas et al., 2008; Huertas and Jackson, 2009; Manfrini et al., 2010; Chen et al., 2011).

Subsequent experiments have shown that the Ku complex is rapidly recruited to DSBs and protects the DNA ends from degradation by Exo1 (**Figure 1**). The absence of Ku partially suppresses both the hypersensitivity to DSB-inducing agents and the resection defect of *mre11*Δ and *sae2*Δ cells in an Exo1-dependent fashion (Mimitou and Symington, 2010; Foster et al., 2011; Langerak et al., 2011). This finding suggests that Sae2, once phosphorylated by Cdk1, promotes resection initiation by supporting MRX function in removing Ku from the DSB ends. As Ku preferentially binds dsDNA ends over ssDNA (Griffith et al., 1992), the MRX-Sae2 endonucleolytic activity could limit DSB association of Ku by creating a DNA substrate less suitable for Ku engagement (Mimitou and Symington, 2010; Langerak et al., 2011; Chanut et al., 2016). On the other hand, as the absence of MRX, but not of Sae2 or Mre11 nuclease activity, increases Ku association at DNA ends (Zhang et al., 2007; Wu et al., 2008; Shim et al., 2010), MRX could compete with Ku for end binding. However, the finding that hyperactivation of Exo1 resection activity by the Mre11-R10T mutant variant leads to Ku dissociation from DSB ends and Cdk1-independent DSB resection close to the DSB end suggests that MRX can limit Ku association to DNA ends also indirectly by promoting Exo1 resection activity (Gobbini et al., 2018).

In addition to Ku, the Rad9 protein, originally identified as adaptor for activation of Rad53 checkpoint kinase (Sweeney et al., 2005), inhibits DSB resection (Bonetti et al., 2015; Ferrari et al., 2015; **Figure 1**). The lack of Rad9 suppresses the resection defect of Sae2-deficient cells and increases the resection efficiency also in a wild type context (Bonetti et al., 2015; Ferrari et al., 2015). Both these effects occur in a Sgs1-Dna2-dependent fashion, indicating that Rad9 inhibits mainly the resection activity of Sgs1-Dna2 by limiting Sgs1 association to DSBs. Further support for a role of Rad9 in Sgs1-Dna2 inhibition comes from the identification of the hypermorphic Sgs1-G1298R mutant variant, which potentiates the Dna2 resection activity by escaping the inhibition that Rad9 exerts on Sgs1 (Bonetti et al., 2015).

Recruitment of Rad9 to chromatin involves multiple pathways. The TUDOR domain of Rad9 interacts with histone H3 methylated at K79 (H3-K79me) (Giannattasio et al., 2005; Wysocki et al., 2005; Grenon et al., 2007). Rad9 binding to the sites of damage is strengthened through an interaction of its tandem-BRCT domain with histone H2A phosphorylated at S129 (γH2A) by Mec1 and Tel1 checkpoint kinases (Downs et al., 2000; Shroff et al., 2004; Toh et al., 2006; Hammet et al., 2007). Finally, phosphorylation of Rad9 by Cdk1 leads to Rad9 interaction with the multi-BRCT domain protein Dpb11 (TopBP1 in mammals), which mediates histone−independent Rad9 association to the sites of damage (Granata et al., 2010; Pfander and Diffley, 2011).

Rad9 association to DSB ends is counteracted by the Swr1-like family remodeler Fun30 (SMARCAD1 in mammals) (Chen et al., 2012; Costelloe et al., 2012; Eapen et al., 2012; Bantele et al., 2017) and the scaffold protein complex Slx4-Rtt107 (Dibitetto et al., 2016; Liu et al., 2017), both of which promote DSB resection (Chen et al., 2012; Dibitetto et al., 2016). The Slx4-Rtt107 complex limits Rad9 binding near a DSB possibly by competing with Rad9 for interaction with Dpb11 and γH2A (Ohouo et al., 2013; Dibitetto et al., 2016).

DNA DAMAGE CHECKPOINT REGULATION OF NUCLEASE ACTION AT DOUBLE-STRAND BREAKS

Generation of DNA DSBs triggers the activation of the DNA damage checkpoint, whose key players include the *S. cerevisiae* protein kinases Mec1 (ATR in mammals) and Tel1 (ATM in mammals) (Gobbini et al., 2013). In both yeast and mammals, Tel1/ATM is activated by the MRX/MRN complex, which is required for Tel1/ATM recruitment to the site of damage through direct interaction between Tel1/ATM with the Xrs2 subunit (Nakada et al., 2003; Falck et al., 2005; Lee and Paull, 2005; You et al., 2005). By contrast, Mec1/ATR activation depends on its interactor Ddc2 (ATRIP in mammals) (Paciotti et al., 2000). While blunt or minimally processed DSB ends are preferential substrates for Tel1/ATM (Shiotani and Zou, 2009), RPA−coated ssDNA is the structure that enables Mec1/ATR to recognize DNA (Zou and Elledge, 2003). In both yeast and mammals, as the single−stranded 3′ overhangs increase in length, Mec1/ATR activation is coupled with loss of ATM/Tel1 activation, suggesting that DSB resection promotes a switch from a Tel1/ATM− to a Mec1/ATR−dependent checkpoint (Mantiero et al., 2007; Shiotani and Zou, 2009; **Figure 2**). The substrates for Mec1 and Tel1 are largely overlapping and include H2A, Rad53/CHK2, Chk1, Rad9/53BP1, Sae2/CtIP, Dna2, and RPA (Ciccia and Elledge, 2010).

The DNA damage checkpoint regulates the generation of 3′−ended ssDNA at DNA ends in both positive and negative fashions. Cells lacking Tel1 slightly reduce the efficiency of DSB resection (Mantiero et al., 2007). Tel1, which is loaded at DSBs by MRX, supports MRX persistence at DSBs in a positive feedback loop (Cassani et al., 2016), suggesting that it can facilitates DSB resection by promoting MRX function. Interestingly, Tel1 exerts this role independently of its kinase activity (Cassani et al., 2016), suggesting that it plays a structural role in stabilizing MRX retention to DSBs.

In contrast to *tel1*Δ cells, cells lacking Mec1 accelerate the generation of ssDNA at the DSBs, whereas the same process is impaired by the *mec1-ad* allele (Clerici et al., 2014), indicating that Mec1 inhibits DSB resection. Mec1 exerts this function at least in two ways: (i) it induces Rad53-dependent phosphorylation of Exo1 that leads to the inhibition of Exo1

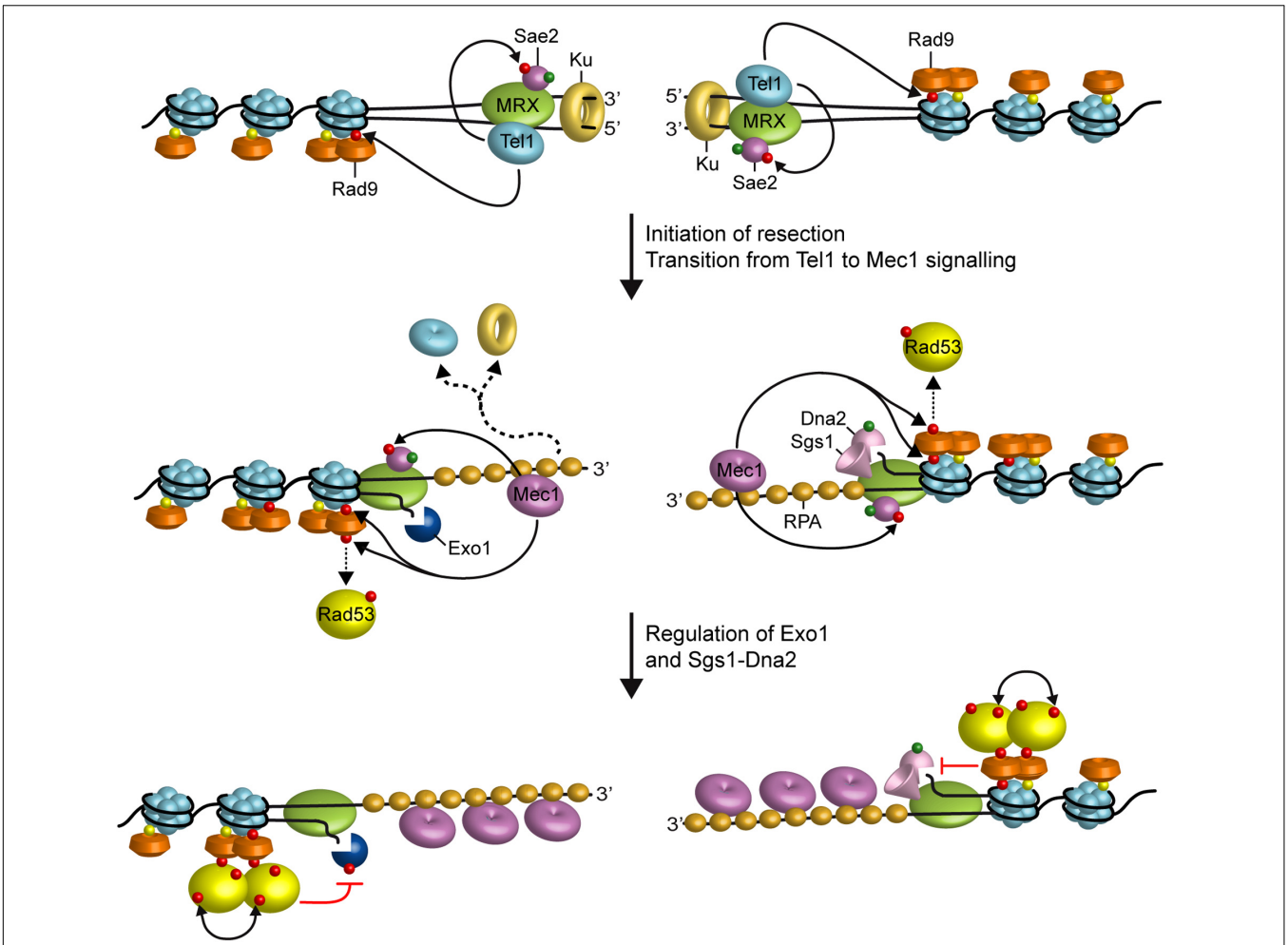

FIGURE 2 | Interplays between end resection and checkpoint. Rad9 is already bound to chromatin via interaction with methylated histone H3 (yellow dots). When a DSB occurs, MRX, Sae2, and Ku localize to the DSB ends. MRX bound to DNA ends recruits and activates Tel1, which in turn promotes DSB resection by phosphorylating Sae2 and stabilizing MRX association to DNA ends. Tel1 also contributes to the recruitment of Rad9 to the DSB ends by phosphorylating H2A. Initiation of DSB resection by MRX-Sae2, Exo1, and Sgs1-Dna2 generate ssDNA tails that promotes a switch from Tel1 to Mec1 signaling. Activated Mec1 contributes to phosphorylate H2A that leads to a further enrichment of Rad9 at DSBs, which counteracts directly Sgs1-Dna2 resection activity. Mec1 also phosphorylates Rad9, which in turn allows Rad53 in-trans autophosphorylation and activation (double black arrows). Activated Rad53 limits DSB resection by phosphorylating and inhibiting Exo1. Phosphorylation events by Mec1 and Tel1 are indicated by red dots, whereas green dots indicate phosphorylation events by Cdk1.

activity (Jia et al., 2004; Morin et al., 2008), (ii) it promotes retention of the resection inhibitor Rad9 at DNA DSBs through phosphorylation of H2A on serine 129 (Eapen et al., 2012; Clerici et al., 2014; Gobbini et al., 2015). The association of Rad9 at DSBs and therefore the inhibition of DSB resection is promoted also by the checkpoint sliding clamp Ddc1-Mec3-Rad17 (9-1-1 in mammals) complex (Ngo and Lydall, 2015), which is required for full Mec1 activation and binds to the ssDNA-dsDNA junction at DNA ends (Gobbini et al., 2013).

Both Mec1 and 9-1-1 have also a positive role in DSB resection. In fact, Mec1 is known to phosphorylate Sae2 and this phosphorylation is important for Sae2 function in resection of both mitotic and meiotic DSBs (Baroni et al., 2004; Cartagena-Lirola et al., 2006). Furthermore, Mec1 also phosphorylates Slx4 and this phosphorylation favors DSB resection by promoting Dpb11-Slx4-Rtt107 complex formation that leads to a destabilization of Rad9 association at DSBs (Smolka et al., 2007; Ohouo et al., 2013; Dibitetto et al., 2016).

Finally, in the absence of Rad9, the 9-1-1 complex facilitates DSB resection by stimulating both Dna2-Sgs1 and Exo1 through an unknown mechanism (Ngo et al., 2014). This effect of 9-1-1 is conserved, as also the human 9-1-1 complex stimulates the activities of DNA2 and EXO1 *in vitro* (Ngo et al., 2014).

In yeast, the checkpoint response to DNA DSBs depends primarily on Mec1. However, if resection initiation is delayed, for example, in the *sae2*Δ mutant, MRX persistence at DSBs is increased, Tel1 is hyperactivated and the *mec1*Δ checkpoint defect is partially bypassed (Usui et al., 2001; Clerici et al., 2006). This persistent checkpoint activation caused by enhanced MRX and Tel1 signaling activity at DSBs contributes to the DNA

damage hypersensitivity and the resection defect of Sae2-deficient cells by increasing Rad9 persistence at DSBs. In fact, *mre11* mutant alleles that reduce MRX binding to DSBs restore DNA damage resistance and resection in *sae2*Δ cells (Chen et al., 2015; Puddu et al., 2015; Cassani et al., 2018). Furthermore, reduction in Tel1 binding to DNA ends or abrogation of its kinase activity restores DNA damage resistance in *sae2*Δ cells (Gobbini et al., 2015). Similarly, impairment of Rad53 activity either by affecting its interaction with Rad9 or by abolishing its kinase activity suppresses the sensitivity to DNA damaging agents and the resection defect of *sae2*Δ cells (Gobbini et al., 2015). The bypass of Sae2 function by Rad53 and Tel1 impairment is due to decreased amount of Rad9 bound at the DSBs (Gobbini et al., 2015). As Rad9 inhibits Sgs1-Dna2 (Bonetti et al., 2015; Ferrari et al., 2015), reduced Rad9 association at DSBs increases the resection efficiency by relieving Sgs1-Dna2 inhibition.

Altogether, these findings support a model whereby the binding of MRX to DNA ends drives the recruitment of Tel1, which facilitates initiation of end resection by phosphorylating Sae2 and promoting MRX association to DNA ends (**Figure 2**). Generation of RPA-coated ssDNA leads to the recruitment of Mec1-Ddc2, which in turn phosphorylates Rad9, Rad53, and H2A. γH2A generation promotes the enrichment of Rad9 to the DSB ends, which limits the resection activity of Dna2-Sgs1. Rad9 association at DSBs also leads to the inhibition of Exo1 activity indirectly by allowing activation of Rad53, which in turn phosphorylates and inhibits Exo1 (**Figure 2**).

This Mec1-mediated inhibition of nuclease action at DSBs avoids excessive generation of ssDNA, which can form secondary structures that can be attacked by structure-selective endonucleases, leading to chromosome fragmentation. Furthermore, since Mec1 is activated by RPA-coated ssDNA, inhibition of end resection by Mec1 keeps under control Mec1 itself. This negative feedback loop may avoid excessive checkpoint activation to ensure a rapid checkpoint turning off to either resume cell cycle progression when the DSB is repaired or adapt to DSBs as a final attempt at survival after cells have exhausted repair options.

NUCLEASE ACTION AT THE REPLICATION FORKS

Accurate and complete DNA replication is essential for the maintenance of genome stability. However, progression of replication forks is constantly challenged by various types of replication stress that generally causes a slowing or stalling of replication forks (Giannattasio and Branzei, 2017; Pasero and Vindigni, 2017). Replication forks can slow or stall at sites containing DNA lesions, chromatin compaction, DNA secondary structures (G-quadruplex, small inverted repeats, trinucleotides repeats), DNA/RNA hybrids and covalent protein-DNA adducts. Furthermore, clashes between transcription and replication machineries can impact genome stability even in unchallenged conditions (Giannattasio and Branzei, 2017; Pasero and Vindigni, 2017). Fork obstacles may result in dysfunctional replication forks, which lack their replication-competent state and necessitate additional mechanisms to resume DNA synthesis. Failure to resume DNA synthesis results in the generation of DNA DSBs, a major source of the genome rearrangements (Liu et al., 2012).

A general feature of stalled replication forks is the accumulation of ssDNA that can originate from physical uncoupling between the polymerase and the replicative helicase or between the leading and the lagging strand polymerases (Pagès and Fuchs, 2003; Byun et al., 2005; Lopes et al., 2006). The accumulation of torsional stress ahead of replication forks (Katou et al., 2003; Bermejo et al., 2011; Gan et al., 2017) can also lead to the annealing of the two newly synthesized strands and the formation of a four-way structure resembling a Holliday junction (i.e., fork reversal), which might expose DNA ends to exonucleolytic processing (Sogo et al., 2002). These tracts of ssDNA coated by the RPA complex recruit the checkpoint kinase Mec1/ATR (Zou and Elledge, 2003), whose activation prevents entry into mitosis, increases the intracellular dNTP pools, represses late origin firing, maintains replisome stability and orchestrates different pathways of replication fork restart/stabilization (Giannattasio and Branzei, 2017; Pasero and Vindigni, 2017).

In both yeast and mammals, the same nucleases involved in DSB resection are emerging as key factors for the processing of replication intermediates to allow repair/restart of stalled replication forks and/or to prevent accumulation of DSBs (Cotta-Ramusino et al., 2005; Segurado and Diffley, 2008; Tsang et al., 2014; Thangavel et al., 2015; Colosio et al., 2016). Indeed, the ability of Mre11, Sae2, Dna2, and Exo1 to resect dsDNA ends is relevant to prevent the accumulation of replication-associated DSBs by promoting DSB repair by HR (Costanzo et al., 2001; Cotta-Ramusino et al., 2005; Segurado and Diffley, 2008; Hashimoto et al., 2012; Tsang et al., 2014; Yeo et al., 2014; Thangavel et al., 2015; Colosio et al., 2016; Ait Saada et al., 2017). In addition, controlled Dna2-mediated degradation of replication forks is a relevant mechanism to mediate reversed fork restart (Thangavel et al., 2015).

Although the nucleolytic processing of nascent strands at stalled replication forks is important to resume DNA synthesis, unrestricted nuclease access can also promote extensive and uncontrolled degradation of stalled replication intermediates and genome instability (Pasero and Vindigni, 2017). In budding yeast, the checkpoint activated by the ssDNA that arise at stalled replication forks plays a role in protecting replication intermediates from aberrant nuclease activity (Tercero and Diffley, 2001; Alabert et al., 2009; Barlow and Rothstein, 2009). In fact, in the absence of the checkpoint, relieve of Exo1 inhibition by Rad53 leads to the formation of long ssDNA gaps and fork collapse (Sogo et al., 2002; Cotta-Ramusino et al., 2005; Segurado and Diffley, 2008). Furthermore, replication stress in ATR-defective *Schizosaccharomyces pombe* and mammalian cells results in MRE11- and EXO1-dependent ssDNA accumulation (Hu et al., 2012; Koundrioukoff et al., 2013; Tsang et al., 2014). Interestingly, in *S. cerevisiae*, Tel1/ATM was recently found to counteract nucleolytic degradation by Mre11 of replication forks that reverse upon treatment with camptothecin (CPT) (Menin et al., 2018), which leads to accumulation of torsional stress by

blocking Top1 on DNA (Postow et al., 2001; Koster et al., 2007; Ray Chaudhuri et al., 2012). Fork reversal in CPT is promoted by the replisome component Mrc1, whose inactivation prevents fork reversal in both wild type and *TEL1* deleted cells (Menin et al., 2018).

Interestingly, the same negative regulators of DSB resection limit nuclease action also at the replication forks. In yeast, Rad9, which is known to counteract the resection activity of Sgs1-Dna2, is important to protect stalled replication forks from detrimental Dna2-mediated degradation when Mec1/ATR is not fully functional (Villa et al., 2018). This Rad9 protective function relies mainly on the interaction of Rad9 with Dpb11, which is recruited to stalled replication forks at origin-proximal regions (Balint et al., 2015). Similarly, human cells lacking 53BP1, the mammalian Rad9 ortholog, are hypersensitive to DNA replication stress and show degradation of nascent replicated DNA (Her et al., 2018). Furthermore, the Ku heterodimer was shown to be recruited to terminally arrested replication forks and to regulate their resection in *S. pombe* (Teixeira-Silva et al., 2017). The lack of Ku leads to extensive Exo1-mediated fork resection, a reduced recruitment of RPA and Rad51 and a delay of fork-restart, suggesting that arrested replication forks undergo fork reversal that provides a substrate for Ku binding.

In addition to the checkpoint, other proteins are devoted to protect replication forks from degradation in mammalian cells. The absence of proteins involved in HR or in the Fanconi anemia network, including FAN1, FANCD2, RAD51, BRCA1, and BRCA2, leads to uncontrolled DNA degradation by MRE11 and EXO1 (Howlett et al., 2005; Hashimoto et al., 2010; Schlacher et al., 2011, 2012; Ying et al., 2012; Chaudhury et al., 2014; Karanja et al., 2014; Chen et al., 2016; Kais et al., 2016; Kolinjivadi et al., 2017; Lemaçon et al., 2017; Mijic et al., 2017; Taglialatela et al., 2017). Furthermore, loss of the WRN exonuclease activity enhances degradation at nascent DNA strands by EXO1 and MRE11 (Su et al., 2014; Iannascoli et al., 2015), whereas cells depleted of the biorientation defect 1-like (BOD1L) protein exhibit a DNA2-dependent degradation of stalled/damaged replication forks (Higgs et al., 2015).

CONCLUSION

Defects in HR and DNA replication underlie a significant proportion of the genomic instability observed in cancer cells. Furthermore, ssDNA formed at DSBs and at replication forks can be source of clustered mutations, frequently occurring during carcinogenesis, and of error-prone repair events that can cause DNA deletions or translocations (Nik-Zainal et al., 2012; Roberts et al., 2012; Alexandrov et al., 2013; Sakofsky et al., 2014). Therefore, there is a growing interest in understanding how ssDNA is generated at both DSBs and replication forks and how its generation is regulated. Mounting evidence indicates that processing of both DSB ends and replication forks is regulated both positively and negatively by several proteins involved also in the DNA damage checkpoint, thus coupling resection with checkpoint activation. Given the importance to maintain genome stability, advancements in delineating the mechanisms that control nuclease action at both DSBs and replication forks will have far-reaching implications for human health.

AUTHOR CONTRIBUTIONS

MPL conceived the idea. DB and MPL wrote the manuscript. CVC and MC revised and edited the manuscript.

FUNDING

This work was supported by the Associazione Italiana per la Ricerca sul Cancro (AIRC) (IG Grant 19783) and Progetti di Ricerca di Interesse Nazionale (PRIN) 2015 to MPL.

ACKNOWLEDGMENTS

We thank all members of the Longhese lab for helpful discussions.

REFERENCES

Ait Saada, A., Teixeira-Silva, A., Iraqui, I., Costes, A., Hardy, J., Paoletti, G., et al. (2017). Unprotected replication forks are converted into mitotic sister chromatid bridges. *Mol. Cell* 66, 398–410.e4. doi: 10.1016/j.molcel.2017.04.002

Alabert, C., Bianco, J. N., and Pasero, P. (2009). Differential regulation of homologous recombination at DNA breaks and replication forks by the Mrc1 branch of the S-phase checkpoint. *EMBO J.* 28, 1131–1141. doi: 10.1038/emboj.2009.75

Alexandrov, L. B., Nik-Zainal, S., Wedge, D. C., Aparicio, S. A., Behjati, S., Biankin, A. V., et al. (2013). Signatures of mutational processes in human cancer. *Nature* 500, 415–421. doi: 10.1038/nature12477

Anand, R., Ranjha, L., Cannavo, E., and Cejka, P. (2016). Phosphorylated CtIP functions as a co-factor of the MRE11-RAD50-NBS1 endonuclease in DNA end resection. *Mol. Cell* 64, 940–950. doi: 10.1016/j.molcel.2016.10.017

Aylon, Y., Liefshitz, B., and Kupiec, M. (2004). The CDK regulates repair of double-strand breaks by homologous recombination during the cell cycle. *EMBO J.* 23, 4868–4875. doi: 10.1038/sj.emboj.7600469

Balint, A., Kim, T., Gallo, D., Cussiol, J. R., Bastos de Oliveira, F. M., Yimit, A., et al. (2015). Assembly of Slx4 signaling complexes behind DNA replication forks. *EMBO J.* 34, 2182–2197. doi: 10.15252/embj.201591190

Bantele, S. C., Ferriera, P., Gritenaite, D., Boos, D., and Pfander, B. (2017). Targeting of the Fun30 nucleosome remodeller by the Dpb11 scaffold facilitates cell cycle-regulated DNA end resection. *eLife* 6:e21687. doi: 10.7554/eLife.21687

Barlow, J. H., and Rothstein, R. (2009). Rad52 recruitment is DNA replication independent and regulated by Cdc28 and the Mec1 kinase. *EMBO J.* 28, 1121–1130. doi: 10.1038/emboj.2009.43

Baroni, E., Viscardi, V., Cartagena-Lirola, H., Lucchini, G., and Longhese, M. P. (2004). The functions of budding yeast Sae2 in the DNA damage response require Mec1- and Tel1-dependent phosphorylation. *Mol. Cell. Biol.* 24, 4151–4165. doi: 10.1128/MCB.24.10.4151-4165.2004

Bermejo, R., Capra, T., Jossen, R., Colosio, A., Frattini, C., Carotenuto, W., et al. (2011). The replication checkpoint protects fork stability by releasing transcribed genes from nuclear pores. *Cell* 146, 233–246. doi: 10.1016/j.cell.2011.06.033

Bonetti, D., Clerici, M., Manfrina, N., Lucchini, G., and Longhese, M. P. (2010). The MRX complex plays multiple functions in resection of Yku- and Rif2-protected DNA ends. *PLoS One* 5:e14142. doi: 10.1371/journal.pone.0014142

Bonetti, D., Villa, M., Gobbini, E., Cassani, C., Tedeschi, G., and Longhese, M. P. (2015). Escape of Sgs1 from Rad9 inhibition reduces the requirement for Sae2 and functional MRX in DNA end resection. *EMBO Rep.* 16, 351–361. doi: 10.15252/embr.201439764

Bressan, D. A., Olivares, H. A., Nelms, B. E., and Petrini, J. H. (1998). Alteration of N-terminal phosphoesterase signature motifs inactivates *Saccharomyces cerevisiae* Mre11. *Genetics* 150, 591–600.

Byun, T. S., Pacek, M., Yee, M. C., Walter, J. C., and Cimprich, K. A. (2005). Functional uncoupling of MCM helicase and DNA polymerase activities activates the ATR-dependent checkpoint. *Genes Dev.* 19, 1040–1052. doi: 10.1101/gad.1301205

Cannavo, E., and Cejka, P. (2014). Sae2 promotes dsDNA endonuclease activity within Mre11-Rad50-Xrs2 to resect DNA breaks. *Nature* 514, 122–125. doi: 10.1038/nature13771

Cannavo, E., Cejka, P., and Kowalczykowski, S. C. (2013). Relationship of DNA degradation by *Saccharomyces cerevisiae* Exonuclease 1 and its stimulation by RPA and Mre11-Rad50Xrs2 to DNA end resection. *Proc. Natl. Acad. Sci. U.S.A.* 110, E1661–E1668. doi: 10.1073/pnas.1305166110

Cannon, B., Kuhnlein, J., Yang, S. H., Cheng, A., Schindler, D., Stark, J. M., et al. (2013). Visualization of local DNA unwinding by Mre11/Rad50/Nbs1 using single-molecule FRET. *Proc. Natl. Acad. Sci. U.S.A.* 110, 18868–18873. doi: 10.1073/pnas.1309816110

Cartagena-Lirola, H., Guerini, I., Viscardi, V., Lucchini, G., and Longhese, M. P. (2006). Budding yeast Sae2 is an in vivo target of the Mec1 and Tel1 checkpoint kinases during meiosis. *Cell Cycle* 5, 1549–1559. doi: 10.4161/cc.5.14.2916

Cassani, C., Gobbini, E., Vertemara, J., Wang, W., Marsella, A., Sung, P., et al. (2018). Structurally distinct Mre11 domains mediate MRX functions in resection, end-tethering and DNA damage resistance. *Nucleic Acids Res.* 46, 2990–3008. doi: 10.1093/nar/gky086

Cassani, C., Gobbini, E., Wang, W., Niu, H., Clerici, M., Sung, P., et al. (2016). Tel1 and Rif2 regulate MRX functions in end-tethering and repair of DNA double-strand breaks. *PLoS Biol.* 14:e1002387. doi: 10.1371/journal.pbio.1002387

Cejka, P. (2015). DNA end resection: nucleases team up with the right partners to initiate homologous recombination. *J. Biol. Chem.* 290, 22931–22938. doi: 10.1074/jbc.R115.675942

Cejka, P., Cannavo, E., Polaczek, P., Masuda-Sasa, T., Pokharel, S., Campbell, J. L., et al. (2010). DNA end resection by Dna2-Sgs1-RPA and its stimulation by Top3-Rmi1 and Mre11-Rad50-Xrs2. *Nature* 467, 112–116. doi: 10.1038/nature09355

Chanut, P., Britton, S., Coates, J., Jackson, S. P., and Calsou, P. (2016). Coordinated nuclease activities counteract Ku at single-ended DNA double-strand breaks. *Nat. Commun.* 7:12889. doi: 10.1038/ncomms12889

Chaudhury, I., Stroik, D. R., and Sobeck, A. (2014). FANCD2-controlled chromatin access of the Fanconi-associated nuclease FAN1 is crucial for the recovery of stalled replication orks. *Mol. Cell. Biol.* 34, 3939–3954. doi: 10.1128/MCB.00457-14

Chen, H., Donnianni, R. A., Handa, N., Deng, S. K., Oh, J., Timashev, L. A., et al. (2015). Sae2 promotes DNA damage resistance by removing the Mre11-Rad50-Xrs2 complex from DNA and attenuating Rad53 signaling. *Proc. Natl. Acad. Sci. U.S.A.* 112, 1880–1887. doi: 10.1073/pnas.1503331112

Chen, X., Bosques, L., Sung, P., and Kupfer, G. M. (2016). A novel role for non-ubiquitinated FANCD2 in response to hydroxyurea-induced DNA damage. *Oncogene* 35, 22–34. doi: 10.1038/onc.2015.68

Chen, X., Cui, D., Papusha, A., Zhang, X., Chu, C. D., Tang, J., et al. (2012). The Fun30 nucleosome remodeller promotes resection of DNA double-strand break ends. *Nature* 489, 576–580. doi: 10.1038/nature11355

Chen, X., Niu, H., Chung, W. H., Zhu, Z., Papusha, A., Shim, E. Y., et al. (2011). Cell cycle regulation of DNA double-strand break end resection by Cdk1-dependent Dna2 phosphorylation. *Nat. Struct. Mol. Biol.* 18, 1015–1019. doi: 10.1038/nsmb.2105

Chiruvella, K. K., Liang, Z., and Wilson, T. E. (2013). Repair of double-strand breaks by end joining. *Cold Spring Harb. Perspect. Biol.* 5:a012757. doi: 10.1101/cshperspect.a012757

Ciccia, A., and Elledge, S. J. (2010). The DNA damage response: making it safe to play with knives. *Mol. Cell* 40, 179–204. doi: 10.1016/j.molcel.2010.09.019

Clerici, M., Mantiero, D., Guerini, I., Lucchini, G., and Longhese, M. P. (2008). The Yku70-Yku80 complex contributes to regulate double-strand break processing and checkpoint activation during the cell cycle. *EMBO Rep.* 9, 810–818. doi: 10.1038/embor.2008.121

Clerici, M., Mantiero, D., Lucchini, G., and Longhese, M. P. (2006). The *Saccharomyces cerevisiae* Sae2 protein negatively regulates DNA damage checkpoint signalling. *EMBO Rep.* 7, 212–218. doi: 10.1038/sj.embor.7400593

Clerici, M., Trovesi, C., Galbiati, A., Lucchini, G., and Longhese, M. P. (2014). Mec1/ATR regulates the generation of single-stranded DNA that attenuates Tel1/ATM signaling at DNA ends. *EMBO J.* 33, 198–216. doi: 10.1002/embj.201386041

Colosio, A., Frattini, C., Pellicanò, G., Villa-Hernández, S., and Bermejo, R. (2016). Nucleolytic processing of aberrant replication intermediates by an Exo1-Dna2-Sae2 axis counteracts fork collapse-driven chromosome instability. *Nucleic Acids Res.* 44, 10676–10690. doi: 10.1093/nar/gkw858

Costanzo, V., Robertson, K., Bibikova, M., Kim, E., Grieco, D., Gottesman, M., et al. (2001). Mre11 protein complex prevents double-strand break accumulation during chromosomal DNA replication. *Mol. Cell* 8, 137–147. doi: 10.1016/S1097-2765(01)00294-5

Costelloe, T., Louge, R., Tomimatsu, N., Mukherjee, B., Martini, E., Khadaroo, B., et al. (2012). The yeast Fun30 and human SMARCAD1 chromatin remodellers promote DNA end resection. *Nature* 489, 581–584. doi: 10.1038/nature11353

Cotta-Ramusino, C., Fachinetti, D., Lucca, C., Doksani, Y., Lopes, M., Sogo, J., et al. (2005). Exo1 processes stalled replication forks and counteracts fork reversal in checkpoint-defective cells. *Mol. Cell* 17, 153–159. doi: 10.1016/j.molcel.2004.11.032

de Jager, M., van Noort, J., van Gent, D. C., Dekker, C., Kanaar, R., and Wyman, C. (2001). Human Rad50/Mre11 is a flexible complex that can tether DNA ends. *Mol. Cell* 8, 1129–1135. doi: 10.1016/S1097-2765(01)00381-1

Deshpande, R. A., Lee, J. H., Arora, S., and Paull, T. T. (2016). Nbs1 converts the human Mre11/Rad50 nuclease complex into an endo/exonuclease machine specific for protein-DNA adducts. *Mol. Cell* 64, 593–606. doi: 10.1016/j.molcel.2016.10.010

Deshpande, R. A., Williams, G. J., Limbo, O., Williams, R. S., Kuhnlein, J., Lee, J. H., et al. (2014). ATP-driven Rad50 conformations regulate DNA tethering, end resection, and ATM checkpoint signaling. *EMBO J.* 33, 482–500. doi: 10.1002/embj.201386100

Dibitetto, D., Ferrari, M., Rawal, C. C., Balint, A., Kim, T. H., Zhang, Z., et al. (2016). Slx4 and Rtt107 control checkpoint signalling and DNA resection at double-strand breaks. *Nucleic Acids Res.* 44, 669–682. doi: 10.1093/nar/gkv1080

Downs, J. A., Lowndes, N. F., and Jackson, S. P. (2000). A role for *Saccharomyces cerevisiae* histone H2A in DNA repair. *Nature* 408, 1001–1004. doi: 10.1038/35050000

Eapen, V. V., Sugawara, N., Tsabar, M., Wu, W. H., and Haber, J. E. (2012). The *Saccharomyces cerevisiae* chromatin remodeler Fun30 regulates DNA end resection and checkpoint deactivation. *Mol. Cell. Biol.* 32, 4727–4740. doi: 10.1128/MCB.00566-12

Falck, J., Coates, J., and Jackson, S. P. (2005). Conserved modes of recruitment of ATM, ATR and DNA-PKcs to sites of DNA damage. *Nature* 434, 605–611. doi: 10.1038/nature03442

Ferrari, M., Dibitetto, D., De Gregorio, G., Eapen, V. V., Rawal, C. C., Lazzaro, F., et al. (2015). Functional interplay between the 53BP1-ortholog Rad9 and the Mre11 complex regulates resection, end-tethering and repair of a double-strand break. *PLoS Genet.* 11:e1004928. doi: 10.1371/journal.pgen.1004928

Foster, S. S., Balestrini, A., and Petrini, J. H. J. (2011). Functional interplay of the Mre11 nuclease and Ku in the response to replication-associated DNA damage. *Mol. Cell. Biol.* 31, 4379–4389. doi: 10.1128/MCB.05854-11

Gan, H., Yu, C., Devbhandari, S., Sharma, S., Han, J., Chabes, A., et al. (2017). Checkpoint kinase Rad53 couples leading- and lagging-strand DNA synthesis under replication stress. *Mol. Cell* 68, 446–455.e3. doi: 10.1016/j.molcel.2017.09.018

Garcia, V., Phelps, S. E. L., Gray, S., and Neale, M. J. (2011). Bidirectional resection of DNA double-strand breaks by Mre11 and Exo1. *Nature* 479, 241–244. doi: 10.1038/nature10515

Giannattasio, M., and Branzei, D. (2017). S-phase checkpoint regulations that preserve replication and chromosome integrity upon dNTP depletion. *Cell. Mol. Life Sci.* 74, 2361–2380. doi: 10.1007/s00018-017-2474-4

Giannattasio, M., Lazzaro, F., Plevani, P., and Muzi-Falconi, M. (2005). The DNA damage checkpoint response requires histone H2B ubiquitination by

Rad6-Bre1 and H3 methylation by Dot1. *J. Biol. Chem.* 280, 9879–9886. doi: 10.1074/jbc.M414453200

Gobbini, E., Cassani, C., Vertemara, J., Wang, W., Mambretti, F., Casari, E., et al. (2018). The MRX complex regulates Exo1 resection activity by altering DNA end structure. *EMBO J.* 37:e98588. doi: 10.15252/embj.201798588

Gobbini, E., Cesena, D., Galbiati, A., Lockhart, A., and Longhese, M. P. (2013). Interplays between ATM/Tel1 and ATR/Mec1 in sensing and signaling DNA double-strand breaks. *DNA Repair.* 12, 791–799. doi: 10.1016/j.dnarep.2013.07.009

Gobbini, E., Villa, M., Gnugnoli, M., Menin, L., Clerici, M., and Longhese, M. P. (2015). Sae2 function at DNA double-strand breaks is bypassed by dampening Tel1 or Rad53 activity. *PLoS Genet.* 11:e1005685. doi: 10.1371/journal.pgen.1005685

Granata, M., Lazzaro, F., Novarina, D., Panigada, D., Puddu, F., Abreu, C. M., et al. (2010). Dynamics of Rad9 chromatin binding and checkpoint function are mediated by its dimerization and are cell cycle-regulated by CDK1 activity. *PLoS Genet.* 6:e1001047. doi: 10.1371/journal.pgen.1001047

Grenon, M., Costelloe, T., Jimeno, S., O'Shaughnessy, A., Fitzgerald, J., Zgheib, O., et al. (2007). Docking onto chromatin via the *Saccharomyces cerevisiae* Rad9 Tudor domain. *Yeast* 24, 105–119. doi: 10.1002/yea.1441

Griffith, A. J., Blier, P. R., Mimori, T., and Hardin, J. A. (1992). Ku polypeptides synthesized in vitro assemble into complexes which recognize ends of double-stranded DNA. *J. Biol. Chem.* 267, 331–338.

Hammet, A., Magill, C., Heierhorst, J., and Jackson, S. P. (2007). Rad9 BRCT domain interaction with phosphorylated H2AX regulates the G1 checkpoint in budding yeast. *EMBO Rep.* 8, 851–857. doi: 10.1038/sj.embor.7401036

Hashimoto, Y., Puddu, F., and Costanzo, V. (2012). RAD51- and MRE11-dependent reassembly of uncoupled CMG helicase complex at collapsed replication forks. *Nat. Struct. Mol. Biol.* 19, 17–24. doi: 10.1038/nsmb.2177

Hashimoto, Y., Ray Chaudhuri, A., Lopes, M., and Costanzo, V. (2010). Rad51 protects nascent DNA from Mre11-dependent degradation and promotes continuous DNA synthesis. *Nat. Struct. Mol. Biol.* 17, 1305–1311. doi: 10.1038/nsmb.1927

Her, J., Ray, C., Altshuler, J., Zheng, H., and Bunting, S. F. (2018). 53BP1 mediates ATR-Chk1 signaling and protects replication forks under conditions of replication stress. *Mol. Cell. Biol* 38:e00472-17. doi: 10.1128/MCB.00472-17

Higgs, M. R., Reynolds, J. J., Winczura, A., Blackford, A. N., Borel, V., Miller, E. S., et al. (2015). BOD1L is required to suppress deleterious resection of stressed replication forks. *Mol. Cell* 59, 462–477. doi: 10.1016/j.molcel.2015.06.007

Hopfner, K. P., Craig, L., Moncalian, G., Zinkel, R. A., Usui, T., Owen, B. A., et al. (2002). The Rad50 zinc-hook is a structure joining Mre11 complexes in DNA recombination and repair. *Nature* 418, 562–566. doi: 10.1038/nature00922

Howlett, N. G., Taniguchi, T., Durkin, S. G., D'Andrea, A. D., and Glover, T. W. (2005). The Fanconi anemia pathway is required for the DNA replication stress response and for the regulation of common fragile site stability. *Hum. Mol. Genet.* 14, 693–701. doi: 10.1093/hmg/ddi065

Hu, J., Sun, L., Shen, F., Chen, Y., Hua, Y., Liu, Y., et al. (2012). The intra-S phase checkpoint targets Dna2 to prevent stalled replication forks from reversing. *Cell* 149, 1221–1232. doi: 10.1016/j.cell.2012.04.030

Huertas, P., Cortés-Ledesma, F., Sartori, A. A., Aguilera, A., and Jackson, S. P. (2008). CDK targets Sae2 to control DNA-end resection and homologous recombination. *Nature* 455, 689–692. doi: 10.1038/nature07215

Huertas, P., and Jackson, S. P. (2009). Human CtIP mediates cell cycle control of DNA end resection and double strand break repair. *J. Biol. Chem.* 284, 9558–9565. doi: 10.1074/jbc.M808906200

Iannascoli, C., Palermo, V., Murfuni, I., Franchitto, A., and Pichierri, P. (2015). The WRN exonuclease domain protects nascent strands from pathological MRE11/EXO1-dependent degradation. *Nucleic Acids Res.* 43, 9788–9803. doi: 10.1093/nar/gkv836

Ira, G., Pellicioli, A., Balijja, A., Wang, X., Fiorani, S., Carotenuto, W., et al. (2004). DNA end resection, homologous recombination and DNA damage checkpoint activation require CDK1. *Nature* 431, 1011–1017. doi: 10.1038/nature02964

Jia, X., Weinert, T., and Lydall, D. (2004). Mec1 and Rad53 inhibit formation of single-stranded DNA at telomeres of *Saccharomyces cerevisiae* cdc13-1 mutants. *Genetics* 166, 753–764. doi: 10.1534/genetics.166.2.753

Kais, Z., Rondinelli, B., Holmes, A., O'Leary, C., Kozono, D., D'Andrea, A. D., et al. (2016). FANCD2 maintains fork stability in BRCA1/2-deficient tumors and promotes alternative end-joining DNA Repair. *Cell Rep.* 15, 2488–2499. doi: 10.1016/j.celrep.2016.05.031

Kao, H. I., Campbell, J. L., and Bambara, R. A. (2004). Dna2p helicase/nuclease is a tracking protein, like FEN1, for flap cleavage during Okazaki fragment maturation. *J. Biol. Chem.* 279, 50840–50849. doi: 10.1074/jbc.M409231200

Karanja, K. K., Lee, E. H., Hendrickson, E. A., and Campbell, J. L. (2014). Preventing over-resection by DNA2 helicase/nuclease suppresses repair defects in Fanconi anemia cells. *Cell Cycle* 13, 1540–1550. doi: 10.4161/cc.28476

Katou, Y., Kanoh, Y., Bando, M., Noguchi, H., Tanaka, H., Ashikari, T., et al. (2003). S-phase checkpoint proteins Tof1 and Mrc1 form a stable replication-pausing complex. *Nature* 424, 1078–1083. doi: 10.1038/nature01900

Kolinjivadi, A. M., Sannino, V., De Antoni, A., Zadorozhny, K., Kilkenny, M., Técher, H., et al. (2017). Smarcal1-mediated fork reversal triggers Mre11-dependent degradation of nascent DNA in the absence of Brca2 and stable Rad51 nucleofilaments. *Mol. Cell* 67, 867–881.e7. doi: 10.1016/j.molcel.2017.07.001

Koster, D. A., Palle, K., Bot, E. S., Bjornsti, M. A., and Dekker, N. H. (2007). Antitumour drugs impede DNA uncoiling by topoisomerase I. *Nature* 448, 213–217. doi: 10.1038/nature05938

Koundrioukoff, S., Carignon, S., Técher, H., Letessier, A., Brison, O., and Debatisse, M. (2013). Stepwise activation of the ATR signaling pathway upon increasing replication stress impacts fragile site integrity. *PLoS Genet.* 9:e1003643. doi: 10.1371/journal.pgen.1003643

Lammens, K., Bemeleit, D. J., Möckel, C., Clausing, E., Schele, A., Hartung, S., et al. (2011). The Mre11:Rad50 structure shows an ATP-dependent molecular clamp in DNA double-strand break repair. *Cell* 145, 54–66. doi: 10.1016/j.cell.2011.02.038

Langerak, P., Mejia-Ramirez, E., Limbo, O., and Russell, P. (2011). Release of Ku and MRN from DNA ends by Mre11 nuclease activity and Ctp1 is required for homologous recombination repair of double-strand breaks. *PLoS Genet.* 7:e1002271. doi: 10.1371/journal.pgen.1002271

Lee, J. H., and Paull, T. T. (2005). ATM activation by DNA double-strand breaks through the Mre11-Rad50-Nbs1 complex. *Science* 308, 551–554. doi: 10.1126/science.1108297

Lemaçon, D., Jackson, J., Quinet, A., Brickner, J. R., Li, S., Yazinski, S., et al. (2017). MRE11 and EXO1 nucleases degrade reversed forks and elicit MUS81-dependent fork rescue in BRCA2-deficient cells. *Nat. Commun.* 8:860. doi: 10.1038/s41467-017-01180-5

Levikova, M., Pinto, C., and Cejka, P. (2017). The motor activity of DNA2 functions as an ssDNA translocase to promote DNA end resection. *Genes Dev.* 31, 493–502. doi: 10.1101/gad.295196.116

Lim, H. S., Kim, J. S., Park, Y. B., Gwon, G. H., and Cho, Y. (2011). Crystal structure of the Mre11-Rad50-ATPγS complex: understanding the interplay between Mre11 and Rad50. *Genes Dev.* 25, 1091–1104. doi: 10.1101/gad.2037811

Liu, P., Carvalho, C. M., Hastings, P. J., and Lupski, J. R. (2012). Mechanisms for recurrent and complex human genomic rearrangements. *Curr. Opin. Genet. Dev.* 22, 211–220. doi: 10.1016/j.gde.2012.02.012

Liu, Y., Cussiol, J. R., Dibitetto, D., Sims, J. R., Twayana, S., Weiss, R. S., et al. (2017). TOPBP1Dpb11 plays a conserved role in homologous recombination DNA repair through the coordinated recruitment of 53BP1Rad9. *J. Cell. Biol.* 216, 623–639. doi: 10.1083/jcb.201607031

Lopes, M., Foiani, M., and Sogo, J. M. (2006). Multiple mechanisms control chromosome integrity after replication fork uncoupling and restart at irreparable UV lesions. *Mol. Cell* 21, 15–27. doi: 10.1016/j.molcel.2005.11.015

Manfrini, N., Guerini, I., Citterio, A., Lucchini, G., and Longhese, M. P. (2010). Processing of meiotic DNA double strand breaks requires cyclin-dependent kinase and multiple nucleases. *J. Biol. Chem.* 285, 11628–11637. doi: 10.1074/jbc.M110.104083

Mantiero, D., Clerici, M., Lucchini, G., and Longhese, M. P. (2007). Dual role for *Saccharomyces cerevisiae* Tel1 in the checkpoint response to double-strand breaks. *EMBO Rep.* 8, 380–387. doi: 10.1038/sj.embor.7400911

Mehta, A., and Haber, J. E. (2014). Sources of DNA double-strand breaks and models of recombinational DNA repair. *Cold Spring Harb. Perspect. Biol.* 6:a016428. doi: 10.1101/cshperspect.a016428

Menin, L., Ursich, S., Trovesi, C., Zellweger, R., Lopes, M., Longhese, M. P., et al. (2018). Tel1/ATM prevents degradation of replication forks that reverse after topoisomerase poisoning. *EMBO Rep.* 19:e45535. doi: 10.15252/embr.201745535

Mijic, S., Zellweger, R., Chappidi, N., Berti, M., Jacobs, K., Mutreja, K., et al. (2017). Replication fork reversal triggers fork degradation in BRCA2-defective cells. *Nat. Commun.* 8:859. doi: 10.1038/s41467-017-01164-5

Miller, A. S., Daley, J. M., Pham, N. T., Niu, H., Xue, X., Ira, G., et al. (2017). A novel role of the Dna2 translocase function in DNA break resection. *Genes Dev.* 31, 503–510. doi: 10.1101/gad.295659.116

Mimitou, E. P., and Symington, L. S. (2008). Sae2, Exo1 and Sgs1 collaborate in DNA double-strand break processing. *Nature* 455, 770–774. doi: 10.1038/nature07312

Mimitou, E. P., and Symington, L. S. (2010). Ku prevents Exo1 and Sgs1-dependent resection of DNA ends in the absence of a functional MRX complex or Sae2. *EMBO J.* 29, 3358–3369. doi: 10.1038/emboj.2010.193

Möckel, C., Lammens, K., Schele, A., and Hopfner, K. P. (2012). ATP driven structural changes of the bacterial Mre11:Rad50 catalytic head complex. *Nucleic Acids Res.* 40, 914–927. doi: 10.1093/nar/gkr749

Morin, I., Ngo, H. P., Greenall, A., Zubko, M. K., Morrice, N., and Lydall, D. (2008). Checkpoint-dependent phosphorylation of Exo1 modulates the DNA damage response. *EMBO J.* 27, 2400–2410. doi: 10.1038/emboj.2008.171

Myler, L. R., Gallardo, I. F., Zhou, Y., Gong, F., Yang, S. H., Wold, M. S., et al. (2016). Single-molecule imaging reveals the mechanism of Exo1 regulation by single-stranded DNA binding proteins. *Proc. Natl. Acad. Sci. U.S.A.* 113, E1170–E1179. doi: 10.1073/pnas.1516674113

Nakada, D., Matsumoto, K., and Sugimoto, K. (2003). ATM-related Tel1 associates with double-strand breaks through an Xrs2-dependent mechanism. *Genes Dev.* 17, 1957–1962. doi: 10.1101/gad.1099003 x

Neale, M. J., Pan, J., and Keeney, S. (2005). Endonucleolytic processing of covalent protein-linked DNA double-strand breaks. *Nature* 436, 1053–1057. doi: 10.1038/nature03872

Ngo, G. H., Balakrishnan, L., Dubarry, M., Campbell, J. L., and Lydall, D. (2014). The 9-1-1 checkpoint clamp stimulates DNA resection by Dna2-Sgs1 and Exo1. *Nucleic Acids Res.* 42, 10516–10528. doi: 10.1093/nar/gku746

Ngo, G. H., and Lydall, D. (2015). The 9-1-1 checkpoint clamp coordinates resection at DNA double strand breaks. *Nucleic Acids Res.* 43, 5017–5032. doi: 10.1093/nar/gkv409

Nicolette, M. L., Lee, K., Guo, Z., Rani, M., Chow, J. M., Lee, S. E., et al. (2010). Mre11-Rad50-Xrs2 and Sae2 promote 5′ strand resection of DNA double-strand breaks. *Nat. Struct. Mol. Biol.* 17, 1478–1485. doi: 10.1038/nsmb.1957

Nik-Zainal, S., Alexandrov, L. B., Wedge, D. C., Van Loo, P., Greenman, C. D., Raine, K., et al. (2012). Mutational processes molding the genomes of 21 breast cancers. *Cell* 149, 979–993. doi: 10.1016/j.cell.2012.04.024

Nimonkar, A. V., Genschel, J., Kinoshita, E., Polaczek, P., Campbell, J. L., Wyman, C., et al. (2011). BLM-DNA2-RPA-MRN and EXO1-BLM-RPA-MRN constitute two DNA end resection machineries for human DNA break repair. *Genes Dev.* 25, 350–362. doi: 10.1101/gad.2003811

Niu, H., Chung, W. H., Zhu, Z., Kwon, Y., Zhao, W., Chi, P., et al. (2010). Mechanism of the ATP-dependent DNA end-resection machinery from *Saccharomyces cerevisiae*. *Nature* 467, 108–111. doi: 10.1038/nature09318

O'Driscoll, M. (2012). Diseases associated with defective responses to DNA damage. *Cold Spring Harb. Perspect. Biol.* 4:a012773. doi: 10.1101/cshperspect.a012773

Ohouo, P. Y., Bastos de Oliveira, F. M., Liu, Y., Ma, C. J., and Smolka, M. B. (2013). DNA-repair scaffolds dampen checkpoint signalling by counteracting the adaptor Rad9. *Nature* 493, 120–124. doi: 10.1038/nature11658

Paciotti, V., Clerici, M., Lucchini, G., and Longhese, M. P. (2000). The checkpoint protein Ddc2, functionally related to *S. pombe* Rad26, interacts with Mec1 and is regulated by Mec1-dependent phosphorylation in budding yeast. *Genes Dev.* 14, 2046–2059. doi: 10.1101/gad.14.16.2046

Pagès, V., and Fuchs, R. P. (2003). Uncoupling of leading- and lagging-strand DNA replication during lesion bypass in vivo. *Science* 300, 1300–1303. doi: 10.1126/science.1083964

Pasero, P., and Vindigni, A. (2017). Nucleases acting at stalled forks: how to reboot the replication program with a few shortcuts. *Annu. Rev. Genet.* 51, 477–499. doi: 10.1146/annurev-genet-120116-024745

Paull, T. T., and Gellert, M. (1998). The 3′ to 5′ exonuclease activity of Mre11 facilitates repair of DNA double-strand breaks. *Mol. Cell* 1, 969–979. doi: 10.1016/S1097-2765(00)80097-0

Paull, T. T., and Gellert, M. (1999). Nbs1 potentiates ATP-driven DNA unwinding and endonuclease cleavage by the Mre11/Rad50 complex. *Genes Dev.* 13, 1276–1288.

Pfander, B., and Diffley, J. F. (2011). Dpb11 coordinates Mec1 kinase activation with cell cycle-regulated Rad9 recruitment. *EMBO J.* 30, 4897–4907. doi: 10.1038/emboj.2011.345

Postow, L., Ullsperger, C., Keller, R. W., Bustamante, C., Vologodskii, A. V., and Cozzarelli, N. R. (2001). Positive torsional strain causes the formation of a four-way junction at replication forks. *J. Biol. Chem.* 276, 2790–2796.

Puddu, F., Oelschlaegel, T., Guerini, I., Geisler, N. J., Niu, H., Herzog, M., et al. (2015). Synthetic viability genomic screening defines Sae2 function in DNA repair. *EMBO J.* 34, 1509–1522. doi: 10.15252/embj.201590973

Ray Chaudhuri, A., Hashimoto, Y., Herrador, R., Neelsen, K. J., Fachinetti, D., Bermejo, R., et al. (2012). Topoisomerase I poisoning results in PARP-mediated replication fork reversal. *Nat. Struct. Mol. Biol.* 19, 417–423. doi: 10.1038/nsmb.2258

Reginato, G., Cannavo, E., and Cejka, P. (2017). Physiological protein blocks direct the Mre11-Rad50-Xrs2 and Sae2 nuclease complex to initiate DNA end resection. *Genes Dev.* 31, 2325–2330. doi: 10.1101/gad.308254.117

Roberts, S. A., Sterling, J., Thompson, C., Harris, S., Mav, D., Shah, R., et al. (2012). Clustered mutations in yeast and in human cancers can arise from damaged long single-strand DNA regions. *Mol. Cell* 46, 424–435. doi: 10.1016/j.molcel.2012.03.030

Sakofsky, C. J., Roberts, S. A., Malc, E., Mieczkowski, P. A., Resnick, M. A., Gordenin, D. A., et al. (2014). Break-induced replication is a source of mutation clusters underlying kataegis. *Cell Rep.* 7, 1640–1648. doi: 10.1016/j.celrep.2014.04.053

Schlacher, K., Christ, N., Siaud, N., Egashira, A., Wu, H., and Jasin, M. (2011). Double-strand break repair-independent role for BRCA2 in blocking stalled replication fork degradation by MRE11. *Cell* 145, 529–542. doi: 10.1016/j.cell.2011.03.041

Schlacher, K., Wu, H., and Jasin, M. (2012). A distinct replication fork protection pathway connects Fanconi anemia tumor suppressors to RAD51-BRCA1/2. *Cancer Cell* 22, 106–116. doi: 10.1016/j.ccr.2012.05.015

Segurado, M., and Diffley, J. F. (2008). Separate roles for the DNA damage checkpoint protein kinases in stabilizing DNA replication forks. *Genes Dev.* 22, 1816–1827. doi: 10.1101/gad.477208

Shibata, A., Moiani, D., Arvai, A. S., Perry, J., Harding, S. M., Genois, M. M., et al. (2014). DNA double-strand break repair pathway choice is directed by distinct MRE11 nuclease activities. *Mol. Cell* 53, 7–18. doi: 10.1016/j.molcel.2013.11.003

Shim, E. Y., Chung, W. H., Nicolette, M. L., Zhang, Y., Davis, M., and Zhu, Z. (2010). *Saccharomyces cerevisiae* Mre11/Rad50/Xrs2 and Ku proteins regulate association of Exo1 and Dna2 with DNA breaks. *EMBO J.* 29, 3370–3380. doi: 10.1038/emboj.2010.219

Shiotani, B., and Zou, L. (2009). Single-stranded DNA orchestrates an ATM-to-ATR switch at DNA breaks. *Mol. Cell* 33, 547–558. doi: 10.1016/j.molcel.2009.01.024

Shroff, R., Arbel-Eden, A., Pilch, D., Ira, G., Bonner, W. M., Petrini, J. H., et al. (2004). Distribution and dynamics of chromatin modification induced by a defined DNA double-strand break. *Curr. Biol.* 14, 1703–1711. doi: 10.1016/j.cub.2004.09.047

Smolka, M. B., Albuquerque, C. P., Chen, S. H., and Zhou, H. (2007). Proteome-wide identification of in vivo targets of DNA damage checkpoint kinases. *Proc. Natl. Acad. Sci. U.S.A.* 104, 10364–10369. doi: 10.1073/pnas.0701622104

Sogo, J. M., Lopes, M., and Foiani, M. (2002). Fork reversal and ssDNA accumulation at stalled replication forks owing to checkpoint defects. *Science* 297, 599–602. doi: 10.1126/science.1074023

Su, F., Mukherjee, S., Yang, Y., Mori, E., Bhattacharya, S., Kobayashi, J., et al. (2014). Non-enzymatic role for WRN in preserving nascent DNA strands after replication stress. *Cell Rep.* 9, 1387–1401. doi: 10.1016/j.celrep.2014.10.025

Sweeney, F. D., Yang, F., Chi, A., Shabanowitz, J., Hunt, D. F., and Durocher, D. (2005). *Saccharomyces cerevisiae* Rad9 acts as a Mec1 adaptor to allow Rad53 activation. *Curr. Biol.* 15, 1364–1375. doi: 10.1016/j.cub.2005.06.063

Symington, L. S. (2016). Mechanism and regulation of DNA end resection in eukaryotes. *Crit. Rev. Biochem. Mol. Biol.* 51, 195–212. doi: 10.3109/10409238.2016.1172552

Taglialatela, A., Alvarez, S., Leuzzi, G., Sannino, V., Ranjha, L., Huang, J. W., et al. (2017). Restoration of replication fork stability in BRCA1- and BRCA2-deficient cells by inactivation of SNF2-family fork remodelers. *Mol. Cell* 68, 414–430. doi: 10.1016/j.molcel.2017.09.036

Teixeira-Silva, A., Ait Saada, A., Hardy, J., Iraqui, I., Nocente, M. C., Fréon, K., et al. (2017). The end-joining factor Ku acts in the end-resection of double strand break-free arrested replication forks. *Nat. Commun.* 8:1982. doi: 10.1038/s41467-017-02144-5

Tercero, J. A., and Diffley, J. F. (2001). Regulation of DNA replication fork progression through damaged DNA by the Mec1/Rad53 checkpoint. *Nature* 412, 553–557. doi: 10.1038/35087607

Thangavel, S., Berti, M., Levikova, M., Pinto, C., Gomathinayagam, S., Vujanovic, M., et al. (2015). DNA2 drives processing and restart of reversed replication forks in human cells. *J. Cell. Biol.* 208, 545–562. doi: 10.1083/jcb.201406100

Toh, G. W., O'Shaughnessy, A. M., Jimeno, S., Dobbie, I. M., Grenon, M., Maffini, S., et al. (2006). Histone H2A phosphorylation and H3 methylation are required for a novel Rad9 DSB repair function following checkpoint activation. *DNA Repair.* 5, 693–703. doi: 10.1016/j.dnarep.2006.03.005

Tran, P. T., Erdeniz, N., Dudley, S., and Liskay, R. M. (2002). Characterization of nuclease-dependent functions of Exo1p in *Saccharomyces cerevisiae*. *DNA Repair.* 1, 895–912. doi: 10.1016/S1568-7864(02)00114-3

Trujillo, K. M., Yuan, S. S., Lee, E. Y., and Sung, P. (1998). Nuclease activities in a complex of human recombination and DNA repair factors Rad50, Mre11, and p95. *J. Biol. Chem.* 273, 21447–21450. doi: 10.1074/jbc.273.34.21447

Tsang, E., Miyabe, I., Iraqui, I., Zheng, J., Lambert, S. A., and Carr, A. M. (2014). The extent of error-prone replication restart by homologous recombination is controlled by Exo1 and checkpoint proteins. *J. Cell. Sci.* 127, 2983–2994. doi: 10.1242/jcs.152678

Usui, T., Ogawa, H., and Petrini, J. H. J. (2001). A DNA damage response pathway controlled by Tel1 and the Mre11 complex. *Mol. Cell* 7, 1255–1266. doi: 10.1016/S1097-2765(01)00270-2

Usui, T., Ohta, T., Oshiumi, H., Tomizawa, J., Ogawa, H., and Ogawa, T. (1998). Complex formation and functional versatility of Mre11 of budding yeast in recombination. *Cell* 95, 705–716.

Villa, M., Bonetti, D., Carraro, M., and Longhese, M. P. (2018). Rad9/53BP1 protects stalled replication forks from degradation in Mec1/ATR-defective cells. *EMBO Rep.* 19, 351–367. doi: 10.15252/embr.201744910

Villa, M., Cassani, C., Gobbini, E., Bonetti, D., and Longhese, M. P. (2016). Coupling end resection with the checkpoint response at DNA double-strand breaks. *Cell. Mol. Life Sci.* 73, 3655–3663. doi: 10.1007/s00018-016-2262-6

Wang, W., Daley, J. M., Kwon, Y., Krasner, D. S., and Sung, P. (2017). Plasticity of the Mre11-Rad50-Xrs2-Sae2 nuclease ensemble in the processing of DNA-bound obstacles. *Genes Dev.* 31, 2331–2336. doi: 10.1101/gad.307900.117

Williams, G. J., Williams, R. S., Williams, J. S., Moncalian, G., Arvai, A. S., Limbo, O., et al. (2011). ABC ATPase signature helices in Rad50 link nucleotide state to Mre11 interface for DNA repair. *Nat. Struct. Mol. Biol.* 18, 423–431. doi: 10.1038/nsmb.2038

Williams, R. S., Moncalian, G., Williams, J. S., Yamada, Y., Limbo, O., Shin, D. S., et al. (2008). Mre11 dimers coordinate DNA end bridging and nuclease processing in double-strand-break repair. *Cell* 135, 97–109. doi: 10.1016/j.cell.2008.08.017

Wiltzius, J. J., Hohl, M., Fleming, J. C., and Petrini, J. H. (2005). The Rad50 hook domain is a critical determinant of Mre11 complex functions. *Nat. Struct. Mol. Biol.* 12, 403–407. doi: 10.1038/nsmb928

Wu, D., Topper, L. M., and Wilson, T. E. (2008). Recruitment and dissociation of nonhomologous end joining proteins at a DNA double-strand break in *Saccharomyces cerevisiae*. *Genetics* 178, 1237–1249. doi: 10.1534/genetics.107.083535

Wysocki, R., Javaheri, A., Allard, S., Sha, F., Coté, J., and Kron, S. J. (2005). Role of Dot1-dependent histone H3 methylation in G1 and S phase DNA damage checkpoint functions of Rad9. *Mol. Cell. Biol.* 25, 8430–8443. doi: 10.1128/MCB.25.19.8430-8443.2005

Yeo, J. E., Lee, E. H., Hendrickson, E. A., and Sobeck, A. (2014). CtIP mediates replication fork recovery in a FANCD2-regulated manner. *Hum. Mol. Genet.* 23, 3695–3705. doi: 10.1093/hmg/ddu078

Ying, S., Hamdy, F. C., and Helleday, T. (2012). Mre11-dependent degradation of stalled DNA replication forks is prevented by BRCA2 and PARP1. *Cancer Res.* 72, 2814–2821. doi: 10.1158/0008-5472.CAN-11-3417

You, Z., Chahwan, C., Bailis, J., Hunter, T., and Russell, P. (2005). ATM activation and its recruitment to damaged DNA require binding to the C terminus of Nbs1. *Mol. Cell. Biol.* 25, 5363–5379. doi: 10.1128/MCB.25.13.5363-5379.2005

Zhang, Y., Hefferin, M. L., Chen, L., Shim, E. Y., Tseng, H. M., and Kwon, Y. (2007). Role of Dnl4-Lif1 in nonhomologous end-joining repair complex assembly and suppression of homologous recombination. *Nat. Struct. Mol. Biol.* 14, 639–646. doi: 10.1038/nsmb1261

Zhu, Z., Chung, W. H., Shim, E. Y., Lee, S. E., and Ira, G. (2008). Sgs1 helicase and two nucleases Dna2 and Exo1 resect DNA double-strand break ends. *Cell* 134, 981–994. doi: 10.1016/j.cell.2008.08.037

Zierhut, C., and Diffley, J. F. (2008). Break dosage, cell cycle stage and DNA replication influence DNA double strand break response. *EMBO J.* 27, 1875–1885. doi: 10.1038/emboj.2008.111

Zou, L., and Elledge, S. J. (2003). Sensing DNA damage through ATRIP recognition of RPA-ssDNA complexes. *Science* 300, 1542–1548. doi: 10.1126/science.1083430

Conflict of Interest Statement: The authors declare that the research was conducted in the absence of any commercial or financial relationships that could be construed as a potential conflict of interest.

Advantages of publishing in Frontiers

OPEN ACCESS
Articles are free to read for greatest visibility and readership

FAST PUBLICATION
Around 90 days from submission to decision

HIGH QUALITY PEER-REVIEW
Rigorous, collaborative, and constructive peer-review

TRANSPARENT PEER-REVIEW
Editors and reviewers acknowledged by name on published articles

Frontiers
Avenue du Tribunal-Fédéral 34
1005 Lausanne | Switzerland

Visit us: www.frontiersin.org
Contact us: info@frontiersin.org | +41 21 510 17 00

REPRODUCIBILITY OF RESEARCH
Support open data and methods to enhance research reproducibility

DIGITAL PUBLISHING
Articles designed for optimal readership across devices

FOLLOW US
@frontiersin

IMPACT METRICS
Advanced article metrics track visibility across digital media

EXTENSIVE PROMOTION
Marketing and promotion of impactful research

LOOP RESEARCH NETWORK
Our network increases your article's readership